U.S. DEPARTMENT OF COMMERCE
National Technical Information Service

PB-293 336

Proceedings: Third Workshop on Catalytic Combustion, Held at Asheville, North Carolina on October 3-4, 1978

Acurex Corp., Mountain View, CA. Aerotherm Div.

Prepared for

Industrial Environmental Research Lab., Research Triangle Park, NC

Feb 79

PB 293336

United States
Environmental Protection
Agency

Industrial Environmental Research
Laboratory
Research Triangle Park NC 27711

EPA-600/7-79-038
February 1979

EPA

Proceedings: Third Workshop on Catalytic Combustion

(Asheville, NC, October 1978)

Interagency Energy/Environment R&D Program Report

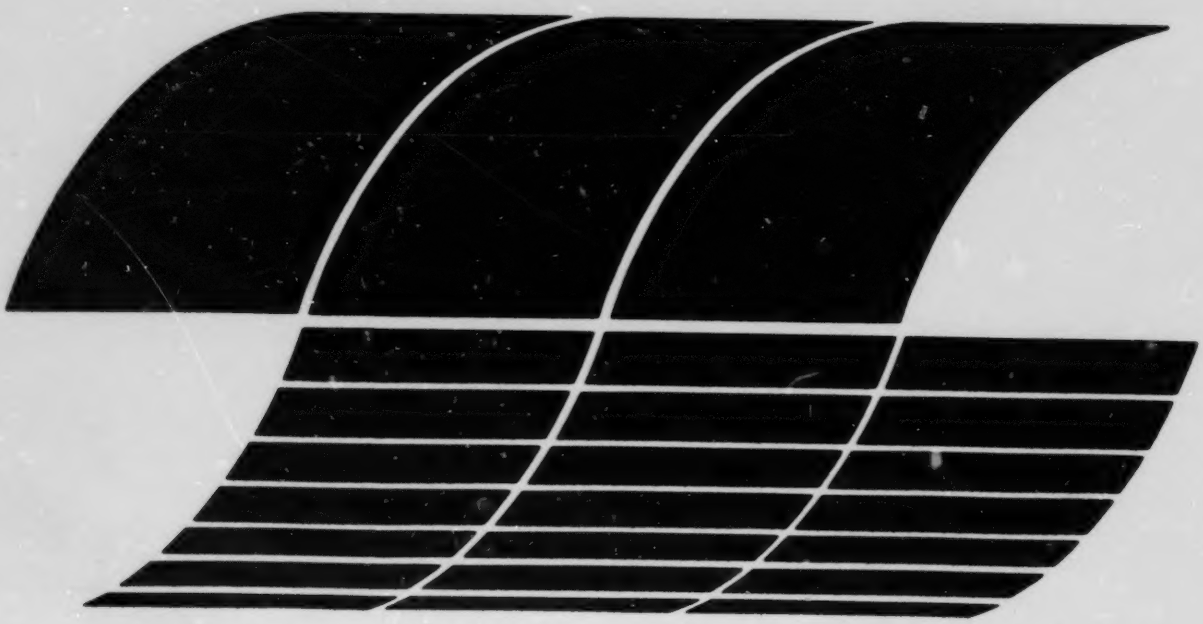

RESEARCH REPORTING SERIES

Research reports of the Office of Research and Development, U.S. Environmental Protection Agency, have been grouped into nine series. These nine broad categories were established to facilitate further development and application of environmental technology. Elimination of traditional grouping was consciously planned to foster technology transfer and a maximum interface in related fields. The nine series are:

1. Environmental Health Effects Research
2. Environmental Protection Technology
3. Ecological Research
4. Environmental Monitoring
5. Socioeconomic Environmental Studies
6. Scientific and Technical Assessment Reports (STAR)
7. Interagency Energy-Environment Research and Development
8. "Special" Reports
9. Miscellaneous Reports

This report has been assigned to the INTERAGENCY ENERGY-ENVIRONMENT RESEARCH AND DEVELOPMENT series. Reports in this series result from the effort funded under the 17-agency Federal Energy/Environment Research and Development Program. These studies relate to EPA's mission to protect the public health and welfare from adverse effects of pollutants associated with energy systems. The goal of the Program is to assure the rapid development of domestic energy supplies in an environmentally-compatible manner by providing the necessary environmental data and control technology. Investigations include analyses of the transport of energy-related pollutants and their health and ecological effects; assessments of, and development of, control technologies for energy systems; and integrated assessments of a wide range of energy-related environmental issues.

EPA REVIEW NOTICE

This report has been reviewed by the participating Federal Agencies, and approved for publication. Approval does not signify that the contents necessarily reflect the views and policies of the Government, nor does mention of trade names or commercial products constitute endorsement or recommendation for use.

This document is available to the public through the National Technical Information Service, Springfield, Virginia 22161.

EPA-600/7-79-038
February 1979

Proceedings: Third Workshop on Catalytic Combustion
(Asheville, NC, October 1978)

John P. Kesselring, Compiler

Acurex Corporation/Aerotherm Division
485 Clyde Avenue
Mountain View, California 94042

Contract No. 68-02-2611
Task No. 30
Program Element No. EHE624A

EPA Project Officer: G. Blair Martin

Industrial Environmental Research Laboratory
Office of Energy, Minerals, and Industry
Research Triangle Park, NC 27711

Prepared for

U.S. ENVIRONMENTAL PROTECTION AGENCY
Office of Research and Development
Washington, DC 20460

PREFACE

This proceedings document covers the major presentations of the Third Workshop on Catalytic Combustion held October 3-4, 1978, at the Grove Park Inn in Asheville, North Carolina. Sponsored by the Combustion Research Branch of the EPA's Industrial Environmental Research Laboratory — Research Triangle Park, the workshop served as a forum for the presentation of results of recent research in the areas of catalyst and catalytic combustion system development. The first Workshop on Catalytic Combustion was held May 25-26, 1976, at the Plantation Inn in Raleigh, North Carolina, and the Second Workshop was held June 21-22, 1977, also at the Plantation Inn. Proceedings documents were not produced for the first and second workshops, but written Summaries were distributed to all attendees. Copies of these Summaries are included in this document as Appendix A. Appendix B lists all attendees of the Third Workshop on Catalytic Combustion.

Dr. John P. Kesselring, Acurex Corporation, acted as Workshop Coordinator, and G. Blair Martin, Combustion Research Branch, Environmental Protection Agency, was the Project Officer.

TABLE OF CONTENTS

Page

"Theoretical Analysis of Temperature and Composition in a Catalytic Monolith Reactor," C. M. Ablow, H. Wise 5

"Progress of Reaction in a Honeycomb Catalyst: CO/Air Combustion," P. M. Walsh, D. A. Santavicca, B. Kim, F. V. Bracco . . 29

"Application of Catalytic Flame Stabilization for Aircraft Afterburners," L. C. Angello, T. J. Rosfjord 61

"EPRI View of Catalytic Combustion," A. C. Dolbec 83

"Overview of Criepi Catalytic Combustion Research Program," Y. Ishihara, H. Fukuzawa 95

"Catalytic Combustion of No. 6 Fuel Oil," J. Pogson, M. N. Mansour. . 111

"Structural Analysis of a Preliminary Catalytic Combustion Ceramic Design," S. M. DeCorso, D. E. Carl 139

"Determination of the Rate of Heterogeneous Reaction on Catalytic Surfaces," P. J. Marteney 157

"Prototype Surface Combustion -- Furnace Evaluation," G. B. Martin . 191

"An Analysis of Catalytic Combustion in Monolithic Honeycomb Beds," R. M. Kendall, J. T. Kelly, E. K. Chu, J. P. Kesselring 215

"The Development of Catalytic Combustors for Stationary Source Applications," W. V. Krill, J. P. Kesselring 259

"Fuel NO_x Control by Catalytic Combustion," E. K. Chu, J. P. Kesselring 291

"Prospects for High-Temperature Catalysts," W. C. Pfefferle 331

"Environmental Aspects of Low Btu Gas-Fired Catalytic Combustion," B. A. Folsom, C. Courtney, M. P. Heap 345

"The Advanced Low-Emissions Catalytic-Combustor Program; Phase I - Description and Status," A. J. Szaniszlo 385

"Catalyst-Coated Flameholder for Lean Stability Improvement," E. J. Szetela, J. B. Mc Vey 389

"Effect of Inlet Temperature on the Performance of a Catalytic Reactor," D. N. Anderson 403

"Performance of Multiple-Venturi Fuel Preparation System," R. R. Tacina 427

"Correlations of Catalytic Combustion Performance Parameters," D. L. Bulzan 431

"Catalyst Design Studies in Low BTU Gas Combustion," R. Carrubba, I. T. Osgerby 435

"Catalyzed Combustion of H_2/Air Mixtures in a Flat Plate Boundary Layer," R. W. Schefer, F. S. Robben, R. K. Cheng. 437

"Application of Rich Catalytic Combustion to Aircraft Engines," G. E. Voecks, D. J. Cerini 477

"Catalytic Combustion in Actual Engines; a Summary of Engine and Rig Tests," G. E. Enga 491

"High Combustion Efficiency and Low Pollutant Emission by Catalytic and Other Means," K. C. Salooja 513

Appendix A - Summaries of First and Second Workshops on Catalytic Combustion A-1

Appendix B - List of Attendees B-1

TECHNICAL REPORT DATA
(Please read Instructions on the reverse before completing)

1. REPORT NO. EPA-600/7-79-038	2.	3. RECIPIENT'S ACCESSION NO. PB293336
4. TITLE AND SUBTITLE Proceedings: Third Workshop on Catalytic Combustion (Asheville, NC, October 1978)		5. REPORT DATE February 1979
		6. PERFORMING ORGANIZATION CODE
7. AUTHOR(S) John P. Kesselring, Compiler		8. PERFORMING ORGANIZATION REPORT NO.
9. PERFORMING ORGANIZATION NAME AND ADDRESS Acurex Corporation/Aerotherm Division 485 Clyde Avenue Mountain View, California 94042		10. PROGRAM ELEMENT NO. EHE624A
		11. CONTRACT/GRANT NO. 68-02-2611, Task 30
12. SPONSORING AGENCY NAME AND ADDRESS EPA, Office of Research and Development Industrial Environmental Research Laboratory Research Triangle Park, NC 27711		13. TYPE OF REPORT AND PERIOD COVERED Proceedings; 5-11/78
		14. SPONSORING AGENCY CODE EPA/600/13

15. SUPPLEMENTARY NOTES IERL-RTP project officer is G. Blair Martin, MD-65, 919/541-2235.

16. ABSTRACT The proceedings document the major presentations at the Third Workshop on Catalytic Combustion, in Asheville, North Carolina, October 3-4, 1978. Sponsored by the Combustion Research Branch of EPA's Industrial Environmental Research Laboratory--Research Triangle Park, the workshop served as a forum for the presentation of results of recent research in the areas of catalyst and catalytic combustion system development. The workshop provided industrial, university, and government representatives with the current state-of-the-art in the application of catalyst systems for pollution control and performance improvement. Applications include firetube and watertube boilers and gas turbines for utility, industrial, automotive, and aircraft systems.

17. KEY WORDS AND DOCUMENT ANALYSIS

a. DESCRIPTORS		b. IDENTIFIERS/OPEN ENDED TERMS	c. COSATI Field/Group	
Pollution	Automotive Engineering	Pollution Control	13B	
Combustion		Stationary Sources	21B	13F
Catalysis	Aircraft Industry	Catalytic Combustion	07D	01C
Catalysts	Utilities			
Boilers	Industries		13A	05C
Gas Turbines			13G	

18. DISTRIBUTION STATEMENT Unlimited	19. SECURITY CLASS *(This Report)* Unclassified	21. NO. OF PAGES ~~590~~ 541
	20. SECURITY CLASS *(This page)* Unclassified	22. PRICE PCA23 / MF A01

EPA Form 2220-1 (9-73)

☆U.S. GOVERNMENT PRINTING OFFICE: 1979-640-013/4189 REGION NO. 4

THIRD WORKSHOP ON CATALYTIC COMBUSTION

G. Blair Martin, Chairman

John P. Kesselring, Workshop Coordinator

THEORETICAL ANALYSIS OF TEMPERATURE AND COMPOSITION IN A CATALYTIC MONOLITH REACTOR

By

C. M. Ablow and H. Wise
SRI International
Menlo Park, California 94025

Preceding page blank

ABSTRACT

A theoretical model of catalytic combustion is developed which allows calculation of temperature and reactant/product distribution in a tubular duct with catalytic walls. Under adiabatic conditions, as prevail in the central ducts of a catalytic monolith combustor, and in the absence of heat conduction along the reactor walls, the model provides an analytic solution. It exhibits the existence of multiple steady states and, for gas mixtures with low Lewis number, temperature excursion in excess of the adiabatic reaction temperature. Gas-phase reactions are shown to increase the fuel consumption in a given length of catalytic duct with corresponding changes in temperature distribution. The model is applied to a series of experimental results obtained with different fuels in tubular reactors. Satisfactory agreement is found between theoretical and experimental data when account is taken of the contribution of heat loss from the reactor to the environment. The theoretical analysis may be employed in optimizing the engineering design of monolith reactors performing over a range of operating conditions.

The research reported here was supported by the U.S. Air Force Office of Scientific Research under contract number F49620-77-C-0123.

Nomenclature

C	specific heat (cal/g-deg)
D	diffusion coefficient (cm/sec^2)
F	Frank-Kamenetskii factor, Eq. (26)
h_M	mass transfer coefficient (cm/sec)
h_T	heat transfer coefficient (cal/cm^2-sec-deg)
$\bar{k}$	nondimensional reaction rate constant
k_G	gas phase reaction rate constant (sec^{-1})
k_S	catalyzed surface reaction rate constant (cm/sec)
Le	Lewis number
m	mass flux (g/cm^2 sec)
Nu	Nusselt number
N_w	ratio of heat transfer coefficients
Pe	Peclet number
Q	heat released by reaction (cal/gm)
R_H	hydraulic radius (cross sectional area divided by perimeter, cm)
R_w	thickness of the duct wall (cm)
Sh	Sherwood number
St	Stanton number
T	temperature (°K)
ΔT_A	temperature rise of adiabatic reaction (°C)
v	flow velocity (cm/sec)
x	distance from duct entry (cm)
Y	fuel mass fraction
y	ratio of Y to Y at duct entry
λ	thermal conductivity (cal/cm-deg-sec)
ρ	density (g/cm^3)
μ	viscosity (poise)
ξ	nondimensional distance
τ	ratio of temperature to ΔT_A

Subscripts

0	at the duct entry
E	exterior of the duct
G	in the gas phase
S	at the solid surface of catalyst
w	in the duct wall

I INTRODUCTION

Catalytic reactors in the form of ceramic monoliths coated with catalytically active metals have been used for the conversion of low concentrations of pollutants to oxidation products. The development of catalytic reactors for the combustion of fuel-air mixtures in thruster applications[1] is receiving attention because the heterogeneous reaction can be initiated over a wide range of fuel-air ratios and can be carried to completion at temperatures sufficiently low to prevent the formation of such pollutants as nitric oxide. During the operation of such combustors, the catalytic monolith effectiveness is generally mass transfer limited,[2] i.e. the reactant species have insufficient time to diffuse to the wall and react before leaving the reactor. Under these conditions it is desirable to increase the degree of reactant conversion by homogeneous, gas-phase reactions promoted by the heat and intermediate chemical species released in a catalyzed reaction.

Theoretical studies[3,4] of monolith combustion have involved computational investigations of mathematical models of reaction and flow including temperature dependent transport and kinetic parameters. In the present work catalyzed combustion is examined by means of a simplified model.

The analysis includes heterogeneous reaction at the tube wall and homogeneous, gas phase reaction. For the low fuel/air ratios under consideration the reaction rates are taken to be of first order in fuel, and of zero order in oxygen concentration. The reaction kinetics involve global reaction rates of the Arrhenius type obtained from separate kinetic studies.

Preceding page blank

The model includes heat transfer by convection in the gas, by diffusion from the tube wall to the gas, by conduction to the surroundings, and by conduction along the tube wall. Conduction to the surroundings is negligible for ducts in the interior of a monolith where uniform conditions prevail.[5] Ducts near the periphery of the monolith are subject to heat transfer through the duct wall. Heat conduction along the tube wall is important near the duct entry where temperature gradients are high.

If heat conduction along the tube wall is neglected, as contrasted to the computer modeling employed in reference 6, the model has analytic solutions in the two cases: (2) temperature independent, diffusion controlled, heterogeneous reaction with heat transfer to the surroundings and (b) temperature dependent reaction without external heat transfer.

II DUCT FLOW MODEL

The steady-state temperature and concentration distributions in each duct cross section are modelled by their average plug flow values in the gas phase, denoted by subscript G, and their values at the catalyst surface, subscript S. The heat balance in a cross section of the fluid reads

$$R_H \frac{d}{dx} (\rho_G v \, C_G T_G) = -h_T (T_G - T_S) + R_H Q k_G \rho_G Y_G \qquad (1)$$

where, for the fuel-lean case, the nearly constant concentration of oxidizer is included in the reaction rate constant k_G. The heat transfer coefficient may be expressed in terms of either the Stanton or Nusselt numbers:

$$h_T = \rho_G v C_G St = (\lambda_G / 4R_H)\ Nu$$

The fuel mass balance in the fluid

$$R_H \frac{d}{dx} (\rho_G v\ Y_G) = -h_M(\rho_G Y_G - \rho_S\ Y_S) - R_H\ k_G \rho_G\ Y_G \quad . \qquad (2)$$

The mass transfer coefficient h_M may be written in terms of the diffusion coefficient D of the fuel through the gas mixture and the Sherwood number Sh:

$$h_M = (D/4\ R_H)\ Sh \quad .$$

The fuel that diffuses to the surface of the catalyst is consumed by the reaction:

$$h_M(\rho_G\ Y_G - \rho_S Y_S) = k_S \rho_S Y_S \quad . \qquad (3)$$

Finally, heat balance in the duct wall may be written as:

$$R_w \lambda_w \frac{d^2 T_S}{dx^2} + h_T(T_G - T_S) + Q\ k_S \rho_S\ Y_S = N_w\ h_T(T_S - T_E) \qquad (4)$$

where N_w is the ratio of the heat transfer coefficients for exterior and interior temperature differences.

III GOVERNING PARAMETERS

The governing parameters are found by a nondimensionalization of the equations. The dimensionless distance and temperature, ξ and τ, are taken to be

$$\xi = x\ St/R_H \quad , \ \tau = T/\Delta T_A \qquad (5)$$

where the adiabatic temperature rise ΔT_A is defined by

$$\Delta T_A = Q\, Y_{G0}/C_G \quad . \tag{6}$$

Since $m = \rho_G v$ is a constant, Eq. (1) may be divided by $m\, C_G\, St\, \Delta T_A$ to obtain

$$\frac{d\tau_G}{d\xi} = -(\tau_G - \tau_S) + R_H Q\, k_G \tau_G\, Y_G/m\, C_G\, St\, \Delta T_A$$

Introduction of the unburned fuel fraction, y, $y = Y/Y_{G0}$, as a dependent variable and use of the constant pressure relation, $\rho_G\, T_G =$ constant, reduces the equation to

$$\frac{d\tau_G}{d\xi} = -(\tau_G - \tau_S) + \bar{k}_G\, y_G/\tau_G \quad , \; \bar{k}_G = k_G\, R_H\, \rho_{G0}\, T_{G0}/m\, St\, \Delta T_A \tag{7}$$

Similar manipulation of Eq. (2) results in

$$\frac{dy_G}{d\xi} = -(Sh/Nu\; Le)\;[y_G - (\rho_S/\rho_G) y_S] - \bar{k}_G\, y_G/\tau_G$$

where Le, the Lewis number, is defined by $Le = \lambda/\rho_G C_G D$. The analogy between heat and mass transfer, Sh = Nu, gives

$$\frac{dy_G}{d\xi} = -[y_G - (\rho_S/\rho_G)\, y_S]/(Le) - \bar{k}_G\, y_G/\tau_G \quad . \tag{8}$$

Eq. (3) reduces by the same method to

$$y_G - (\rho_S/\rho_G)\, y_S = (Le)\, \bar{k}_S\, y_S/\tau_S \quad , \; \bar{k}_S = k_S\, \rho_{G0} T_{G0}/m\, (St)\, \Delta T_A \tag{9}$$

Finally, Eq. (4) becomes

$$(1/\mathrm{Pe})\,\frac{d^2\tau_S}{d\,\xi^2} + \tau_G - \tau_S + \bar{k}_S\, y_S/\tau_S = N_w(\tau_S - \tau_E) \qquad (10)$$

where Pe, the Peclet number, is defined by $\mathrm{Pe} = R_H{}^2\, h_T/R_w\lambda_w(\mathrm{St})^2$.

The fuel fraction y_S at the catalytic surface can be eliminated from Eqs. (7), (8), and (10) by use of Eq. (9). There remain the three following equations for the three variables y_G, τ_G, and τ_S:

$$\frac{d\tau_G}{d\xi} = -(\tau_G - \tau_S) + \bar{k}_G\, y_G/\tau_G \qquad (11)$$

$$\frac{dy_G}{d\xi} = -F\, y_G - \bar{k}_G\, y_G/\tau_G \qquad (12)$$

$$\frac{1}{\mathrm{Pe}}\,\frac{d^2\tau_S}{d\xi^2} + \tau_G - \tau_S + F\, y_G = N_w(\tau_S - \tau_E) \quad ,\; F = 1/(\mathrm{Le} + \tau_G/\bar{k}_S) \qquad (13)$$

Fraction F may be recognized as the factor that indicates the control of the process either by reaction kinetics, if $\bar{k}_S$ is small so that the second term dominates, or by diffusion, if $\bar{k}_S$ is large.[7]

The differential equations are to be solved under the entry conditions:

$$y_G = 1,\; \tau_G = \tau_{G0},\; \frac{d\tau_S}{d\xi} = 0,\; \tau_S = \tau_{G0} \text{ at } \xi = 0. \qquad (14)$$

For a thin ceramic wall the Peclet number, the ratio of the heat transfer coefficients for diffusion into the stream to that for conduction along the wall, will be very large. In this case the term involving Pe may be omitted from Eq. (13). This approximation lowers the order of the differential system so that two of the conditions in Eq. (14) need to be dropped. The conditions on τ_S are the ones omitted on the physical grounds that the temperature of an insulated wall should not be prescribed. As a result of the omission of the wall heat conduction term, the model has solutions where the wall temperature jumps discontinuously from one value to another. The jumps are smoothed over to become intervals of sharp temperature variation[8] if the conduction term is reintroduced.

The equations of the model are then Eqs. (11) and (12) and

$$\tau_G - \tau_S + F\, y_G = N_w(\tau_S - \tau_E) \quad , \tag{15}$$

$$y_G = 1,\ \tau_G = \tau_{G0} \text{ at } \xi = 0 \quad . \tag{16}$$

IV CATALYTIC DUCT REACTOR WITHOUT HEAT TRANSFER TO THE SURROUNDINGS

A duct in the interior of the monolith is likely to be in thermal equilibrium with adjacent ducts. The model is then applicable with $N_w = 0$, the adiabatic case. Eq. (15) becomes

$$\tau_G - \tau_S + F y_G = 0, \tag{17}$$

so that the sum of Eqs. (11) and (12) gives

$$y'_G + \tau_G' = 0$$

Integration of this differential equation gives

$$y_G + \tau_G = 1 + \tau_{G0} \tag{18}$$

where the constant of integration has been fixed by the boundary conditions in Eq. (16).

Equations (17) and (18) relate τ_G, τ_S and y_G to one another and so determine the phase space solution curves. Since either y_G or τ_G is readily eliminated from Eq. (17) by use of Eq. (18), the phase space can be represented as a two-dimensional plane. Figure 1 presents such a phase plane.

The solution curves for positive, non-dimensional reaction rate constants lie between the extremes of kinetic control where $\bar{k}_S = 0$ and diffusion control where $\bar{k}_S = \infty$. Eq. (17) shows that the two conditions correspond to the lines $\tau_S = \tau_G$ and $\tau_S = [\tau_G(Le - 1) + 1 + \tau_{GO}]/Le$, respectively. These lines and the line of the initial condition, $\tau_G = \tau_{GO}$, form a triangle in the phase plane. Points inside the triangle represent positive finite reaction rates and therefore are physically accessible. The vertices of the triangle are points I, K, and D. Point I, $\tau_S = \tau_G = \tau_{GO} + 1$, corresponds to the end of an infinitely long duct where both gas and wall have reached the adiabatic reaction temperature. Point K represents the duct entry temperatures in the absence of exothermic reaction. Point D represents the duct entry temperatures under conditions of diffusion control. A point between K and D indicates an entry condition with finite reaction rate and therefore a wall temperature between those at K and D. At point D, $\tau_S = \tau_{GO} + 1/Le$ so that temperatures above the adiabatic ($\tau_{GO} + 1$) can be attained if $Le < 1$. Such a case is indicated in Figure 1 by point D$'$. The solution curves plotted in Figure 1 are those for propylene/oxygen/nitrogen mixtures at several inlet temperatures, as described below.

Since the unburned fuel fraction y_G can only decrease and, by Eq. (18), τ_G can only increase continuously, conditions producing a solution curve with a maximum point cause a discontinuous wall temperature distribution. For a solution curve such as IV on Figure 1, jumps from the left branch across the middle to the right branch can occur at any point between the local maximum and minimum on the curve. Stability considerations suggest that only the two extreme cases can prevail.

Four different operating conditions can be identified: One producing a phase plane solution curve of type IV which gives rise to wall temperature distributions that may jump in either of two locations; another producing a curve of type III that can cause a jump at the duct entry or at a location downstream (if the part of the solution curve outside of the triangle had been drawn in, one would see that a type III curve is just a type IV curve with its minimum point outside the triangle); a condition (type II) that produces a jump at entry since both the maximum and minimum of the complete solution curve lie outside the triangle; and conditions of type I with no maximum or minimum. Since the jumps in each case are from a branch of the solution curve near side K-I, to one near D-I, the jump may be regarded as a sharp transition of the wall reaction from kinetics to diffusion control. For conditions producing curves of type I without a maximum or minimum, a smooth transition or no transition at all is obtained.

Equation (11) has been integrated under the assumption of no gas phase reaction $\bar{k}_G = 0$, for three cases and the results plotted in Figure 2. A comparison of curves II and III shows the effect of inlet temperature on a given gas mixture. Conditions for curves IA and III differ mainly in fuel concentration.

An interesting deduction from the above analysis is that the phase is independent of the homogeneous reaction. In this adiabatic case, the relation between temperature and concentration is independent of what fraction of the reaction is homogeneous and what is heterogeneous. The gas phase reaction enters the calculations when the distance coordinate for each phase is being obtained, by use of Eq. (11). The importance of gas phase reaction may therefore be gauged by plotting to $\bar{k}_G \, y_G/\tau_G$, a function of τ_G against $(\tau_S - \tau_G)$. Since $(\tau_S - \tau_G)$ can be read directly from Figure 1 as the distance between the solution curve and the line K-I, a convenient function to plot is $\bar{k}_G \, y_{FG}/\tau_G + \tau_G$ as a function of τ_G. Where this latter graph comes near or crosses the solution curve, gas phase reaction makes a major contribution. The homogeneous reaction curve for case IB is plotted in Figure 1. Since quantitative kinetic data on the gas phase oxidation of propylene of the temperatures of interest is not available we have estimated the preexponential factor and activation energy for the homogeneous reaction to be 10^{12} $\sec^{-1}$ and 30 kcal/mol. One sees in the figure that homogeneous reaction does influence the reactive flow beyond the point where 60% of the fuel has been consumed.

The parameter plane of the inlet conditions, the temperature and adiabatic reaction temperature of the gas mixture, has been presented in Figure 3. The plane is divided to show the regions where conditions giving rise to the various types of solution curves are found. In region I the curve of τ_G as a function of τ_S given by Eq. (15) has no inflexion point with zero or negative slope. In the other regions the corresponding phase plane solution curves have such inflexion points along with a local maximum point and a minimum point. Both of these points lie outside the triangle for parameters of region II, the maximum is in the triangle for parameter points in region III, and both extreme points are in the triangle of physically real points for initial conditions in parameter region IV.

V EFFECT OF HEAT TRANSFER BETWEEN DUCT AND SURROUNDINGS

Ducts near the outer periphery of a monolith combustor lose heat to their surroundings. This heat transfer appears in the model as a non-vanishing parameter N_w in Eq. (15).

An analytic solution can be obtained in the diffusion-controlled fast wall reaction limit in the absence of homogeneous reaction. The solution reads

$$\tau_S - \tau_E = Ay_G + By_G^{N_w Le/(1 + N_w)}$$

$$A = (1 - Le)/Le[1 + N_w(1 - Le)]$$

$$B = -A + [1 + Le(\tau_0 - \tau_E)]/Le(1 + N_w) \qquad (19)$$

$$\tau_G - \tau_E = (\tau_S - \tau_E)(1 + N_w) - y_G/Le \qquad (20)$$

$$y_G = e^{-\xi/Le} \qquad (21)$$

Equations (19) and (20) present the phase space solution. Elimination of τ_S from Eq. (20) by use of Eq. (19) gives

$$\tau_G - \tau_E = Cy + (1 + N_w)By^{N_w Le/(1 + N_w} \quad ,$$

$$C = -1/[1 + N_w(1 - Le)] \quad . \qquad (22)$$

The solution is then represented by two curves, one from Eq. (19) for τ_S as a function of y and one from Eq. (22) for τ_G.

The general solution with finite wall reaction rate and with homogeneous reaction may be obtained by numerical integration of the differential equations of the models, Eqs. (11), (12), (15), and (16).

VI APPLICATION

The model has been applied to analyze some experimental results[10] in which the wall and gas temperatures were measured during steady-state catalytic combustion of fuel/oxygen/nitrogen mixtures in monoliths with a small number of ducts with catalytic walls, heated externally to the adiabatic reaction temperatures. Most of the experimental data for propylene combustion were found to fall into the diffusion-controlled reaction regime using the transport and reaction-rate parameters applicable to this system. Consequently the analytic solution given by Eqs. (19), (20), and (21) was employed. The theoretical curves based on the adiabatic model (no heat transfer) were found to be in good agreement with the experimental data when account was taken of conductive heat loss from the reactor to the environment (Figure 4).

With hydrogen as a fuel the reaction system has a small Lewis number (Le $<$ 1). Under these conditions the theoretical analysis predicts wall temperatures that exceed the adiabatic reaction temperature (T_A). Indeed the experimental data (Figure 5) exhibit a temperature maximum, well in excess of T_A. Theoretically, a wall temperature maximum at the reactor entrance is calculated with a monotonic decline along the reactor tube. Again the discrepancy in the temperature profile near the entrance is ascribed to heat conduction along the duct wall.

It is of interest that in calculating the temperature distribution the available kinetic data for catalytic oxidation of hydrogen have a higher degree of uncertainty than for the case of propylene oxidation. In our analysis we increased the Arrhenius preexponential factor by 10^4 over that published in reference 12, to take account of the higher degree of dispersion of Pt on the monolith-washcoat support. With the reaction and transport parameters listed in Table I, the experimental data obtained for this system were found to be in the diffusion-controlled reaction region.

VII CONCLUSIONS

A theoretical model of reactive flow through a duct with catalytic walls has been developed that by means of an analytical solution provides estimates of temperature and fuel product distributions in catalytic combustion in the absence of heat transfer to the environment. The model provides a direct way of assessing the importance of the contributi of the gas phase reaction, and a prediction of the length of duct require to reach a specific temperature and fractional fuel conversion.

The phase space derived from the model relates the concentrations and temperatures at the wall and in the stream that can occur together in each duct cross section. These relations are found to be independent of the homogeneous reaction and of the flow rate. However the distance into the duct where a particular phase is reached depends on the flow rate and degree of homogeneous reaction.

In the adiabatic case, valid for ducts in the interior of a monolith, the analytic solution is found to be confined to a certain triangle in the wall temperature-gas temperature phase plane. The vertex of the triangle is the point where wall and gas reach the adiabatic reaction temperature. The base of the triangle is on the line where the gas temperature has its inlet value and extends from the point of equal wall and gas temperatures to a wall-gas temperature difference inversely proportional to the Lewis number. Thus high wall temperatures are to be expected at the duct entry for gas mixtures with low Lewis number. The surprising fact that temperatures in excess of the adiabatic reaction temperature can be attained is due to this result.

For an adiabatic reacting system with known initial concentration of fuel, oxidizer, and inert diluent, the inlet parameters are the gas inlet temperature and the temperature rise for adiabatic reaction. Different forms of temperature variation along the duct are found for different parameter ranges. Solutions with jump discontinuities downstream of the duct entry are obtained from parameters represented by points in a certain quadrant of the parameter plane (Figure 3). A cold gas mixture with relatively high fuel content (high adiabatic reaction temperature) introduced into the reactor, will favor temperature jumps and multiple steady states. The model also suggests that the contribution of homogeneous relative to heterogeneous reaction will increase with larger monolith tube diameter.

REFERENCES

1. W. C. Pfefferle, R. W. Carrubba, R. M. Heck, and G. W. Roberts, "Catathermal Combustion, A New Process for Low-Emissions Fuel Conversion," ASME paper 75-WA/Fu-1.

2. T. J. Rosfjord, "Catalytic Combustors for Gas Turbine Engines," AIAA paper 76-46.

3. A. E. Cerkanowicz, R. B. Cole, and J. G. Stevens, "Catalytic Combustion Modeling; Comparisons with Experimental Data," ASME paper 77-GT-85.

4. J. T. Kelly, R. M. Kendall, E. Chu, and J. P. Kesselring, "Development and Application of the PROF-HET Catalytic Combustion Code," paper 77-33, Western States Section/The Combustion Institute, Stanford, October 1977.

5. S. M. DeCorso, S. Mumford, R. V. Carrubba, and R. Heck, "Catalysts for Gas Turbine Combustors - Experimental Test Results," J. Eng. for Power, Vol. 99A, 159-167 (1977).

6. J. Votruba, J. Sinkule, V. Hlavacek, and J. Skrivanek, "Heat and Mass Transfer in Monolithic Honeycomb Catalysts - I., Chem. Eng. Sci., Vol. 30, 117-123 (1975).

7. D. A. Frank-Kamenetskii, Diffusion and Heat Transfer in Chemical Kinetics, Plenum Press, New York (1969).

8. G. Eigenberger, "On the Dynamic Behavior of the Catalytic Fixed-Bed Reactor in the Region of Multiple Steady States - I. The Influence of Heat Conduction in Two-Phase Models," Chem. Eng. Sci., Vol. 27, 1909-1916 (1972).

9. R. A. Svehla, "Estimated Viscosities and Thermal Conductivities of Gases at High Temperatures," NASA TR R-132 (1961).

10. L. L. Hegedus, "Temperature Excursions in Catalytic Monoliths", AIChE J., Vol. 21, 849-853 (1975).

11. S. Goldstein, Modern Developments in Fluid Dynamics, Oxford (1938).

12. R. Schefer, R. Cheng, F. Robben, and N. Brown, "Catalyzed Combustion of H_2/Air Mixtures on a Heated Platinum Plate," presented to Western States Section/The Combustion Institute, Boulder (1978).

13. Handbook of Chemistry and Physics (1936).

14. A. Schwartz, L. L. Holbrook, and H. Wise, "Catalytic Oxidation Studies with Platinum and Palladium," J. Catalysis, Vol. 21, 199-207 (1971).

Table I

NUMERICAL VALUES FOR THE CALCULATIONS

Quantity	Propylene	Hydrogen	Reference
Fuel/oxygen/nitrogen (vol%)	0.19/5.08/94.73	1.90/4.60/93.50	10
ΔT_A (°C)	119.	150.	10
T_{G0} (°C)	417.	260	10
T_E (°C)	536	410	
Re	967.	1175.	10
Le	1.554	0.326	10
R_H (cm)	0.0368	0.0368	10
R_W (cm)	0.041	0.041	10
Nu	6.	6.	11
Pr	0.75	0.75	9
St = Nu/Re Pr	8.27×10^{-3}	6.81×10^{-3}	
λ_W (cal/cm-sec-°C)	10^{-3}	10^{-3}	13
λ_G for N_2 at 700°K (cal/cm-sec °C)	1.2×10^{-4}	1.2×10^{-4}	9
μ_G for N_2 at 700°K (poise)	3.2×10^{-6}	3.2×10^{-6}	9
Pe	19.5	23.7	
Preexponential factor A_W (cm/sec)	10^{8*}	1.4	12
Activation energy E_W (kcal/mol)	22.0	3.85	14,12
$m = \mu Re/4R_H$ (gm/cm^2 sec)	0.0210	0.0255	
$\rho_{G0}T_{G0}$ g/cm^3	0.351	0.3395	
$\bar{k}_S$ at 700°K	254	1.16	

---

*Value large enough for diffusion controlled first-order reaction, although negative order reactions were observed.[14]

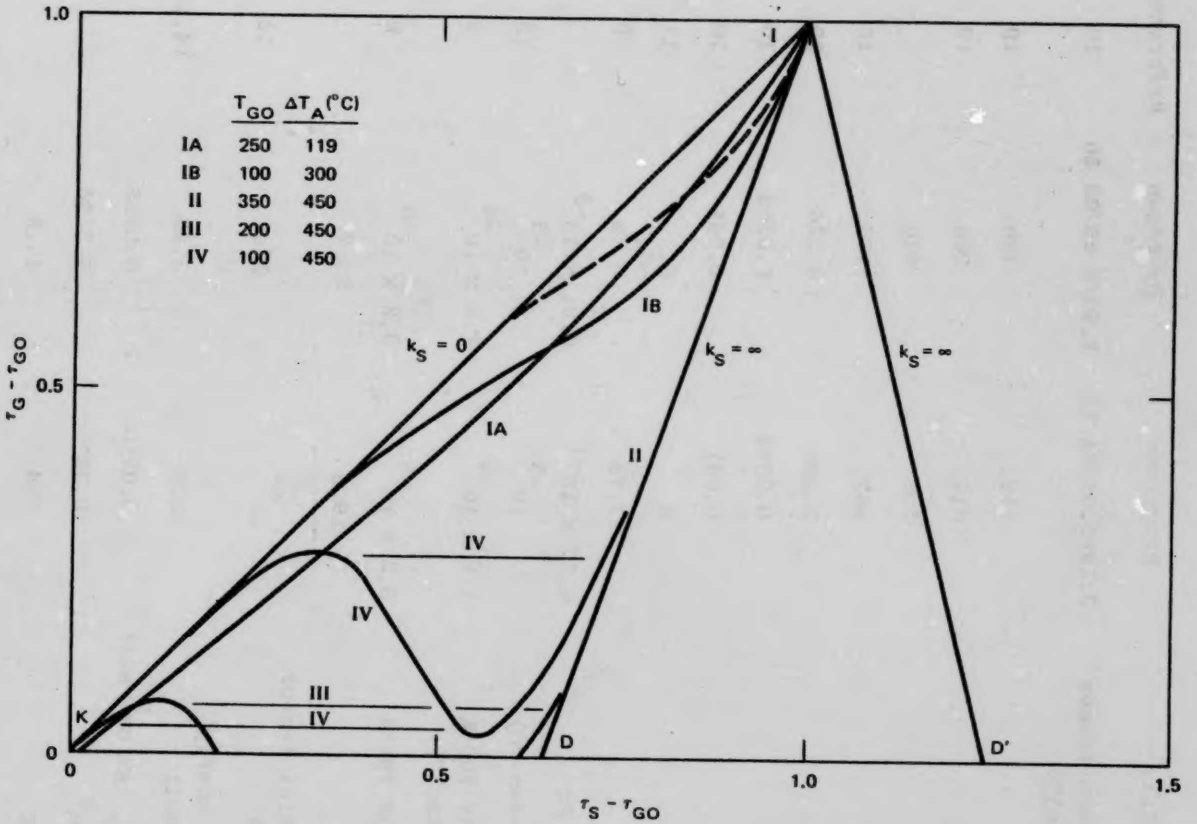

FIGURE 1 PHASE PLANE THEORETICAL CURVES FOR PROPYLENE/OXYGEN/NITROGEN MIXTURES; $y_F = 1 - (\tau_G - \tau_{GO})$; $N_W = 0$; - - - homogeneous reaction for Case IB.

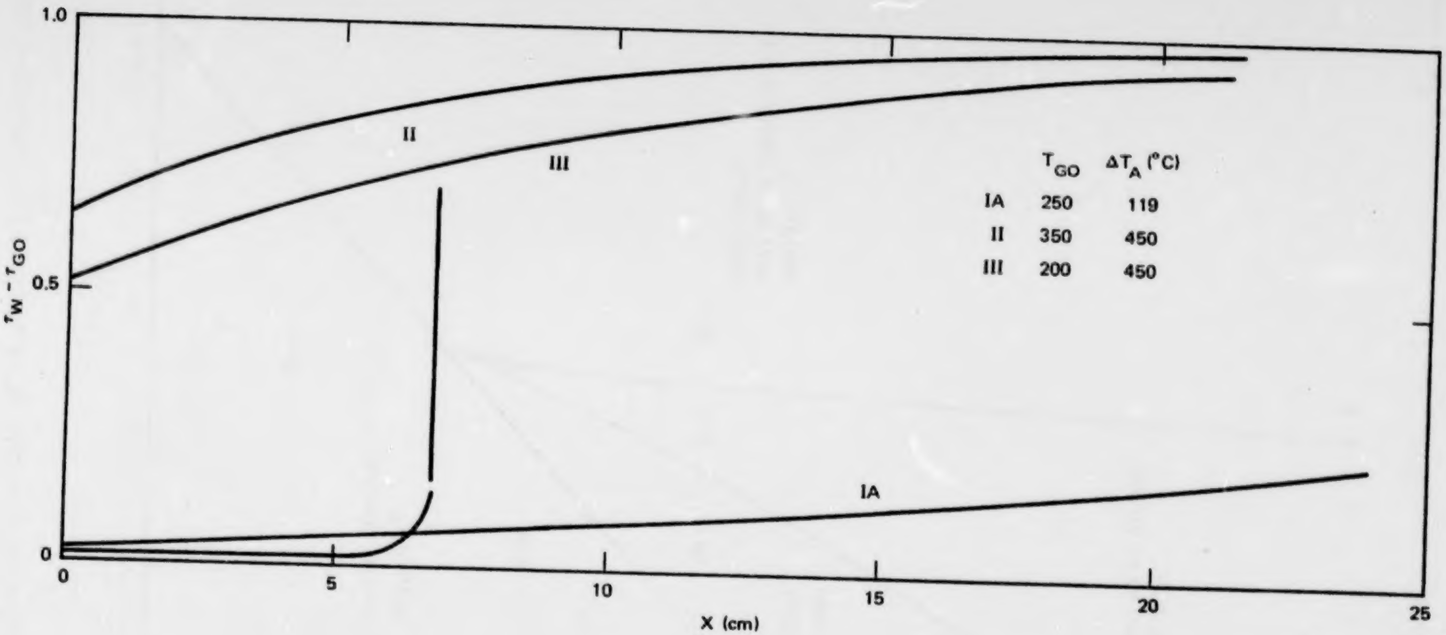

SA-6687-19

FIGURE 2 THEORETICAL NON-DIMENSIONAL WALL TEMPERATURES PLOTTED AGAINST DISTANCE FROM DUCT ENTRY FOR A FEW PROPANE/OXYGEN/NITROGEN MIXTURES FLOWING AT Re = 967 IN A DUCT WITH R_H = 0.0368 CM

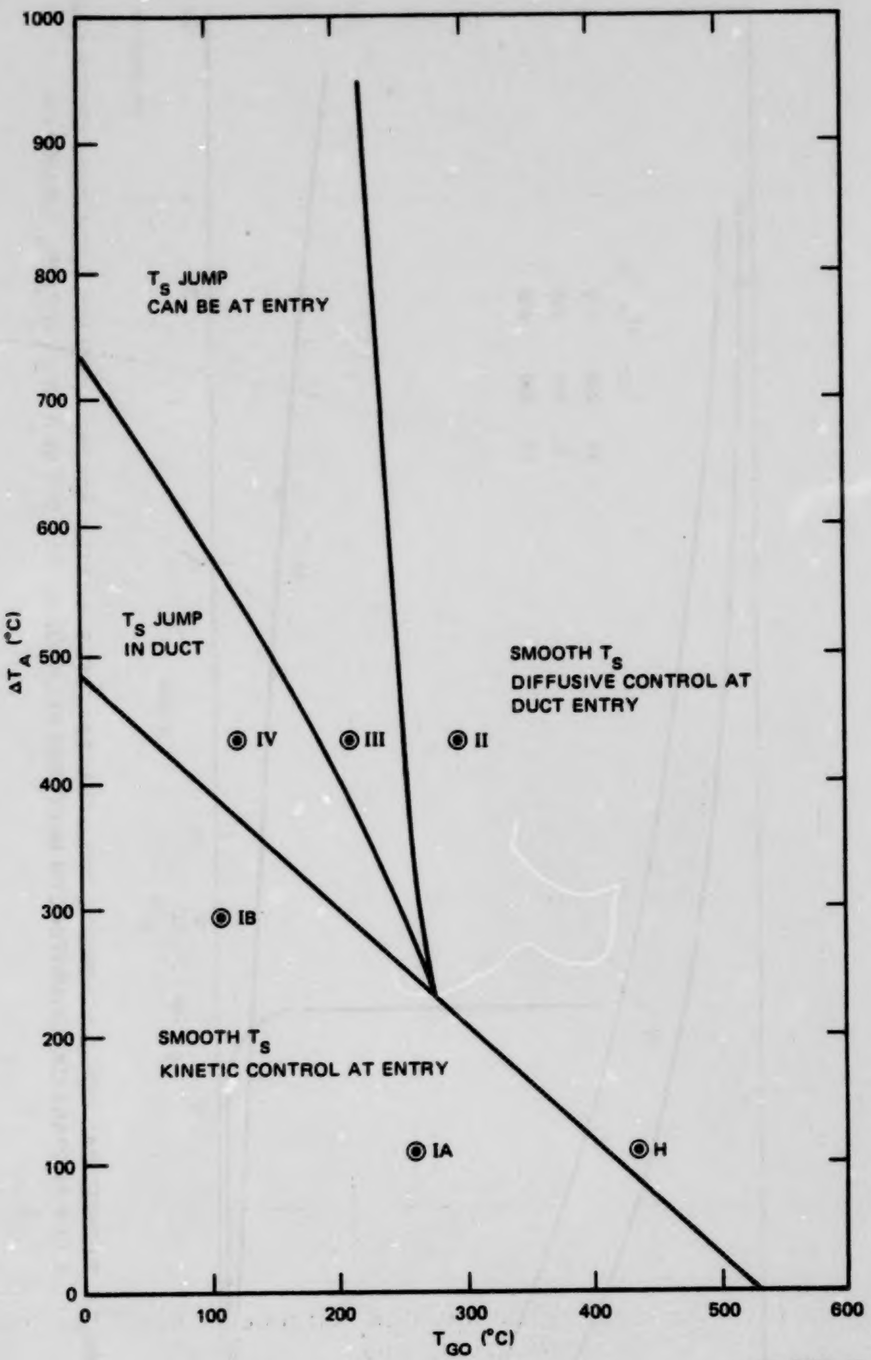

SA-6687-17

FIGURE 3 THEORETICAL REACTIVE FLOW REGIMES FOR PROPYLENE/OXYGEN/NITROGEN MIXTURES. POINT H FOR DATA REF. 10.

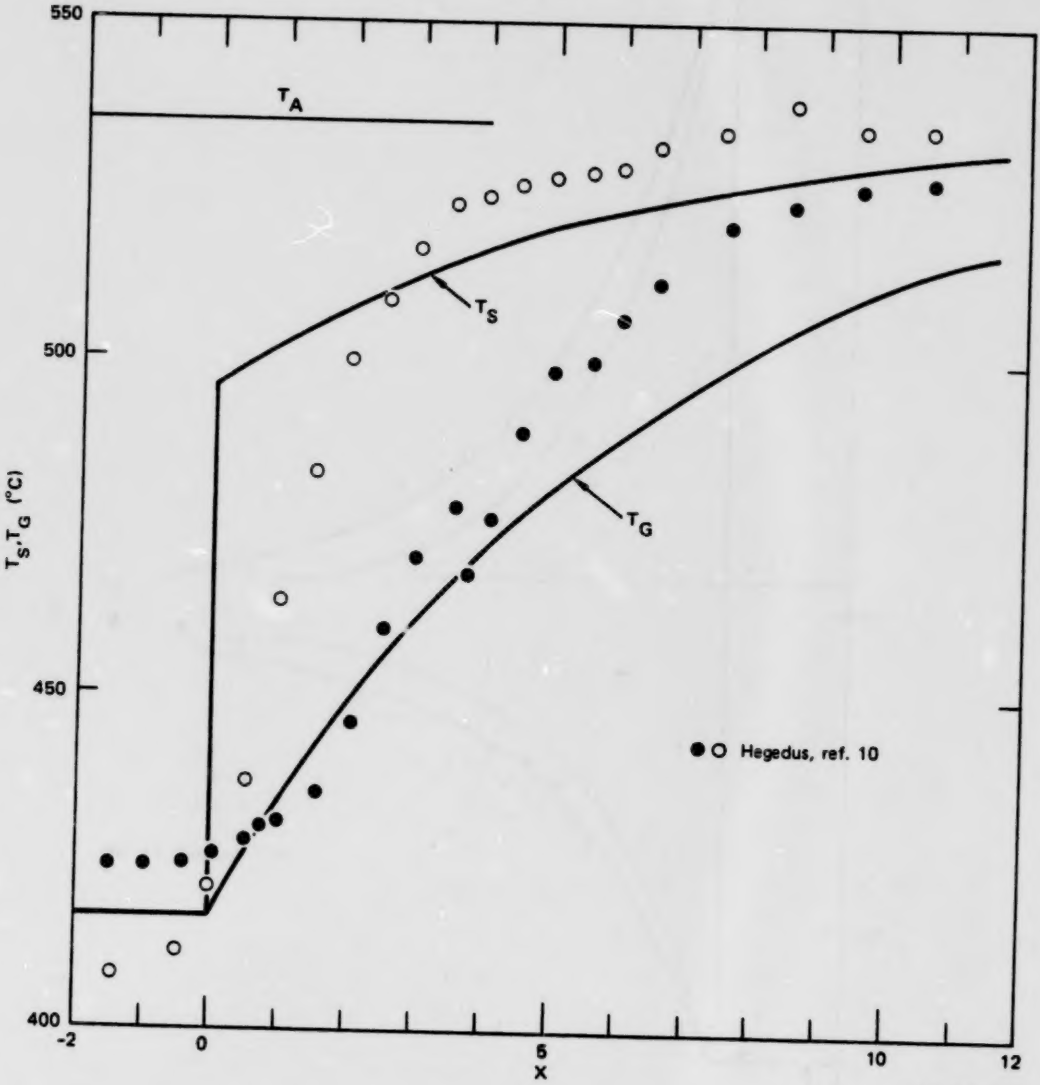

FIGURE 4 PHYSICAL PLANE FOR $C_3H_6/O_2/N_2$ MIXTURE. THEORETICAL CURVES WITH $k = 10^8 \exp(-22{,}000/RT)$, $N_W = 0.2$.

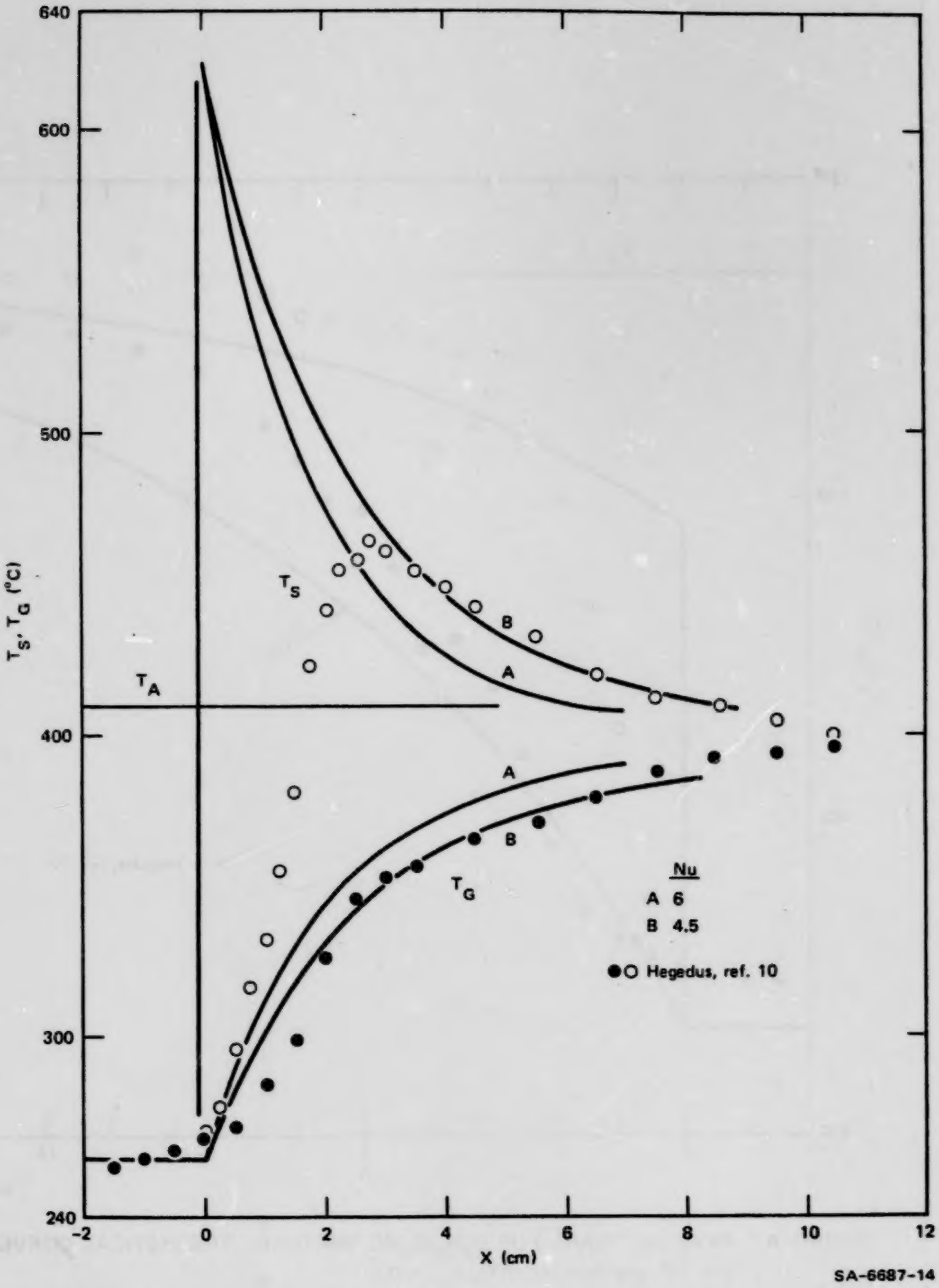

FIGURE 5 PHYSICAL PLANE FOR $H_2/O_2/N_2$ MIXTURE. CURVES COMPUTED WITH $k = 3.2 \times 10^3 \exp(-3850/RT)$ $N_W = 0.2$.

PROGRESS OF REACTION IN A HONEYCOMB CATALYST:

CO/Air Combustion

By:

P. M. Walsh, D. A. Santavicca, B. Kim, and F. V. Bracco
Department of Mechanical and Aerospace Engineering
Princeton University
Princeton, NJ 08540

ABSTRACT

The objective of this program is to collect detailed data within a honeycomb catalyst for the development and testing of a two-dimensional model, and to further current understanding of the fundamental subprocesses which control catalytic combustion. Results of a preliminary study are presented on the combustion of CO/air in a Pt/Al_2O_3/Cordierite honeycomb catalyst. The test conditions were: inlet temperature, 700 ± 8 K; inlet pressure, 109 ± 4 kPa; reference velocity, 5-31 m/s; CO/air equivalence ratio, 0.15 - 0.30; and H_2O concentration, 1.1 - 3.7 mol%. Efforts were made to obtain uniform profiles of temperature, velocity, and CO concentration across the inlet gas stream. Temperature and concentration are uniform within ±1%, but velocity only within ±10%. The philosophy of the program is that a detailed model of the catalytic combustor is necessary to be able to draw consistent conclusions from the experimental data. Since our model has not yet been adequately developed, the following conclusions from the experiment alone are only indicative. Unburned CO at the catalyst outlet can be independent of equivalence ratio in a transitional regime between mass transfer control and homogeneous reaction domination. A relative maximum or shoulder is observed in the substrate temperature near the inlet. Substrate temperature is insensitive to reference velocity at fixed equivalence ratio. Estimates of the rate coefficients for CO oxidation in the catalytic combustor exhaust showed good agreement of the activation energy with published data for homogeneous CO oxidation, indicating that the reaction in the exhaust is not catalyzed by long-lived species generated solely by the catalyst.

Other tasks of this same program include: 1. Substrate and exhaust measurements over a range of inlet temperature and wider ranges of equivalence ratio and reference velocity during combustion of propane, higher hydrocarbons, and coal-derived gases. 2. Measurement of conversion of NH_3 to NO_x during combustion of coal-derived gases. 3. Measurement of gas temperature and composition as functions of axial position inside a monolithic catalyst. All of these tasks are directly related to the application of catalytic combustion to coal-derived gases and aeronautical fuels.

Preceding page blank

CONTENTS

List of Figures
Symbols
Acknowledgments
Introduction
Equipment and Procedure
Data and Discussion
Current Programs
Conclusion
References
Figures

LIST OF FIGURES

1. Inlet gas temperature vs. radial position.

2. Inlet CO concentration vs. radial position.

3. Inlet gas velocity vs. radial position.

4. Substrate temperature vs. radial position.

5. Substrate temperature, exhaust temperature, and exhaust composition vs. axial position at different equivalence ratios.

6. Substrate temperature, exhaust temperature, and exhaust composition vs. axial position at different reference velocities.

7. Ratio of unburned CO to inlet CO vs. reference velocity.

8. Rate coefficient for CO oxidation in the exhaust vs. temperature.

ACKNOWLEDGMENTS

This project is supported by the Air Force Office of Scientific Research under Grant No. AFOSR-76-3052, Dr. B. T. Wolfson, Grant Monitor; and by the Department of Energy under Contract No. EF-77-S-01-2762, Mr. H. G. Jacobson, Technical Project Officer.

The authors are indebted to Dr. W. C. Pfefferle for his many valuable suggestions.

SYMBOLS

C_p	specific heat at constant pressure (J/kg·K)
D	diffusion coefficient (m^2/s)
E	activation energy (J/mol)
k_o	rate constant ($cm^3/mol \cdot s$)
Le	Lewis number = $\lambda/\rho D C_p$
P	pressure (kPa)
R	gas constant = 8.31 J/K·mol
t	time (s)
T	temperature (K)
u	gas velocity (m/s)
λ	thermal conductivity (J/m·s·K)
ρ	density (kg/m^3)
ϕ	equivalence ratio
[ ]	concentration (mol/cm^3)

Subscripts

ad	adiabatic (reaction temperature)
in	condition at catalyst inlet
out	condition at catalyst outlet
ref	reference condition (velocity)

INTRODUCTION

Although many important features of catalytic combustion have been identified, the design of large scale practical devices for heat and power generation could make use of a model which accurately describes the system in terms of fundamental chemical and physical processes, and relates performance to all the relevant design parameters. The goal of our program is to develop a useful model for combustion in monolithic catalysts and to obtain experimental data for testing of the model and the predictions of other investigators. The present work describes experimental results from a preliminary study of CO combustion in Pt/Al_2O_3/Cordierite.

EQUIPMENT AND PROCEDURE

INLET CONDITIONS

Preheated air at a measured flowrate is supplied to a 690 mm long test section with 25.4 mm square channel. A catalyst is placed with its downstream end 90 mm from the test section outlet, and insulated from the wall by Fiberfrax paper. A fuel injector consisting of five 1.6 mm diameter tubes, each containing five 0.3 mm diameter holes, is located 440 mm from the catalyst inlet. A combination pitot tube and thermocouple is mounted 200 mm from the catalyst inlet. In addition to measuring gas velocity and temperature, the pitot tube is used to extract gas samples which are analyzed to determine equivalence ratio. Pressure is regulated by a valve in the exhaust pipe, and taps placed up and downstream of the catalyst are used to measure inlet pressure and pressure drop. The inlet conditions used in the experiments are summarized below.

Inlet temperature (T_{in}) = 700 ± 8 K
Inlet pressure (P_{in}) = 109 ± 4 kPa
Reference velocity (u_{ref}) = 5 - 31 m/s
CO/air equivalence ratio (ϕ) = 0.15 - 0.30
H_2O = 1.1 - 3.7 mol%

A continuous effort has been made to minimize radial gradients in temperature, velocity, and fuel concentration of the inlet stream. The entire test section is insulated so that uniform temperature across the width of the test section is obtained when sufficient time ($\sim$1 hr) has elapsed after startup of the air preheat system. Figure 1 shows temperature profiles obtained by traversing the width of the test section with the pitot/thermocouple probe. These measurements were made with CO being injected and combustion taking place. The uniformity is independent of air flowrate over the range of velocities used. Sufficient fuel/air mixing was obtained only by placing baffles downstream of the fuel injector, and these affect the velocity profile. By trying various configurations, the velocity uniformity is being improved while maintaining an even distribution of fuel. The arrangement used in the present experiments consisted of two screens, each containing four 8 mm diameter holes, placed 30 and 110 mm downstream of the fuel injector. Another screen perforated with 1.6 mm diameter holes was 190 mm from the injector and 50 mm upstream of the pitot tube. The resulting fuel distribution is shown in Figure 2. There is good uniformity over the measured range, however the largest equivalence ratio shown is a factor of 2 to 5 lower than those at which the combustor was run. This is due to the limited range of the CO analyzer (maximum CO = 3 mol%). Velocity profiles, shown in Figure 3, are less satisfactory (range ± 10%). These have recently been improved by replacing the second screen by one containing five 6 mm diameter holes, which gives a range of ± 4%. Average reference velocities were determined using the CO and air flowrates, inlet temperature and pressure, and the cross section area of the catalyst. The catalyst inlet velocity, taking into account the fraction of open monolith area, is $u_{in} \simeq 1.5\ u_{ref}$.

SUBSTRATE AND EXHAUST MEASUREMENTS

Substrate temperatures are measured by a method similar to that described by Kesselring, Krill, and Kendall (1). Ni-Cr/Ni-Al thermocouples are fed through the test section wall and into the ends of catalyst channels. The lengths of wire inside the catalyst are covered by mullite insulator and both ends of the channel sealed with ceramic adhesive. The lifetime of these thermocouples under test conditions is short (5 - 20 hr). A radial temperature distribution in the substrate was measured at the axial position of highest substrate temperature, to determine the effect of heat conduction to the wall of the test section. The measured profile is shown in Figure 4. The variation of substrate temperature at this axial position is ± 20 K over 45% of the sample width.

An expansion quenched, water cooled, stainless steel gas sampling probe is mounted through an elbow in the exhaust pipe and moved along the axis of the test section. Gas samples from the catalyst exhaust were taken at axial positions from 1 to 76 mm downstream of the catalyst outlet. CO and CO_2 were determined using infrared absorption, and O_2 by a paramagnetic analyzer. Exhaust gas temperatures are measured using a thermocouple mounted in the same way as the gas sampling probe. Water concentration is determined using a solid state humidity sensor mounted in the inlet air stream before the heating system.

CATALYST AND FUEL

The catalyst substrate is split cell corrugated Cordierite with approximately 65% open area, and channel cross section area of 1.9 mm^2. The washcoat is alumina with specific area 200 m^2/g. Platinum loading is 4.3 kg/m^3. Catalysts are pretreated to stabilize surface area and platinum concentration by running for several hours at maximum substrate temperatures approximately 100 K higher than those at which exhaust temperature and composition measurements are made. The present data were obtained using two different samples whose dimensions and pretreatment are summarized below.

Sample #8: 24.6 x 24.6 x 76.3 ± 0.2 mm
Pretreatment: run 2.3 hr with propane at maximum substrate temperature 1510 ± 20 K.
Total run time: 9 hr

Sample #10: 24.1 x 24.1 x 76.3 ± 0.2 mm

Pretreatment: run 3.1 hr with propane and 2.1 hr with CO at maximum substrate temperature 1470 ± 20 K.

Total run time: 22 hr

The fuel is carbon monoxide, 99.5 mol%. Natural propane, 96 mol%, is used for pretreatment.

DATA AND DISCUSSION

The combustor was operated over a range of equivalence ratios and reference velocities at fixed inlet temperature and pressure. No attempt was made to minimize unburned fuel, rather the objective was to begin determination of the relationships among operating conditions and performance characteristics. Figure 5 shows substrate temperature, exhaust temperature, and exhaust composition as functions of axial position, obtained at three equivalence ratios with fixed reference velocity. The substrate and gas temperatures increase with increasing equivalence ratio, as expected. Unburned CO is consumed by homogeneous reaction in the exhaust at a rate which increases with increasing average exhaust gas temperature. Gas temperature increases with distance downstream due to heat release from the reaction. The amount of unburned CO at the catalyst outlet is practically independent of inlet equivalence ratio. In a purely mass transfer limited regime, unburned CO is expected to increase with increasing equivalence ratio. If conversion is dominated by homogeneous reaction, unburned CO should decrease as equivalence ratio increases. Under the operating conditions of Figure 5, the system is apparently in an intermediate regime. The substrate temperatures in Figure 5 show a relative maximum at a distance 15-20 mm from the inlet. This may be an example of the effect explained by Pfefferle (2) as resulting from heat recirculation by radiation from the catalyst to the inlet gas stream.

Figures 6a-d show data obtained at various reference velocities with fixed equivalence ratio. The line representing the substrate temperature of Figure 6a is reproduced in Figures 6b and c to show the similarity of the data points. Substrate temperature does not exhibit a sensitive dependence on gas velocity, consistent with the concept that in a system with mass transfer limited surface reaction rate, the substrate temperature depends in a first approximation only on the adiabatic reaction temperature and the local value of the Lewis number ($Le = \lambda/\rho DC_p$). Exhaust composition is shown in Figure 6d. The concentrations of O_2 and CO_2 are nearly the same for the three runs, but unburned CO increases with increasing reference velocity.

Figure 7 shows the ratio of unburned CO to inlet CO as a function of reference velocity for the entire series of runs. The amount of unburned CO is obtained by extrapolating to the catalyst outlet. This figure combines data taken at various equivalence ratios and H_2O concentrations.

Rate coefficients for CO oxidation in the exhaust are estimated from the slopes of the lines through the measured concentrations. The assumed rate expression for homogeneous CO oxidation is taken from Howard, Williams, and Fine (3):

$$\frac{d[CO]}{dt} = -\, k_o [CO] [O_2]^{\frac{1}{2}} [H_2O]^{\frac{1}{2}} \exp(-E/RT)$$

An average measured exhaust temperature was used to determine average exhaust velocity and density. O_2 concentration in the exhaust is assumed constant, and the H_2O concentration is estimated from the measurement in the inlet air. An Arrhenius plot of the calculated rate coefficients, $k_o \exp(-E/RT)$, is shown in Figure 8. The solid line is the fit by Howard et al. (3) to a large number of homogeneous CO oxidation data over the range 840-2360 K:

$$k_o = 1.3 \times 10^{14} \text{ cm}^3/\text{mol}\cdot\text{s}$$
$$E = 126 \text{ kJ/mol}$$

The agreement of the activation energies of the present data and the homogeneous reaction indicates that the oxidation of CO in the exhaust is not being catalyzed by any long-lived species generated solely by the catalyst.

A gradual loss of catalyst activity was observed with increasing total run time. The possibility of gaseous metal carbonyl formation in the inlet stream followed by deposition of elements such as iron and nickel on the catalyst is being investigated.

CURRENT PROGRAMS

The techniques for making detailed measurements of substrate temperature, gas temperature, and gas composition in a catalytic combustor were developed during the experiments with CO. The programs now being pursued include study of propane and low and medium-Btu gases. The measurements will be made over a range of inlet temperature as well as over wider ranges of equivalence ratio and reference velocity. The work on propane is the beginning of a series of experiments on higher hydrocarbons. The behavior of low and medium-Btu gases in catalytic combustion is of special interest because these gases contain fuel components with very different Lewis numbers (H_2, CO, CH_4). This may produce interesting effects in the substrate temperature profile. Measurement of the conversion of fuel nitrogen (NH_3) to NO_x is also included in the study.

A primary objective has been the measurement of gas temperature and composition as functions of axial position inside a catalyst. This is accomplished by drilling an 8 mm diameter hole partway through the catalyst along its axis. The hole is lined with a ceramic sleeve to minimize the activity of the wall. A combination gas sampling and thermocouple probe is moved along the catalyst axis from downstream toward the bottom of the hole If conditions are properly adjusted, the measured gas temperature and composition at the bottom of the hole are equal to their values at the same axial position in a catalyst with no hole. The condition which is most affected by the presence of the hole and probe is the gas velocity in the catalyst channels opening into the hole. The problem of establishing the correct velocity has been solved by feeding pressure taps through the side of the catalyst to measure the pressure at the bottom of the probe hole.

The velocity is adjusted until the pressure is equal to its value at the same axial position in a catalyst without a hole. Measured pressures show a linear decrease with increasing distance from the inlet during propane combustion in the Pt/Al_2O_3/Cordierite catalyst. Another requirement for reliable gas measurement inside a catalyst is that the substrate temperature be unaffected. This condition can also be satisfied despite the changed gas velocity because substrate temperature does not have a strong dependence on velocity. It is the constraint of fixed substrate temperature which distinguishes this experiment from one in which the overall length of catalyst is varied. In a catalyst of given length, the substrate temperature profile is different from the profile in an equivalent section of a longer catalyst. Direct measurements of fuel, oxygen, and product concentrations and gas temperature as functions of axial position inside a catalyst provide data for a rigorous test of a model for combustor operation. Calculations of species concentrations inside monolithic catalytic combustors have been presented by Kelly, Kendall, Chu, and Kesselring (4) and by Cerkanowicz, Cole, and Stevens (5), but an experiment with which to compare these predictions has, to our knowledge, not yet been performed.

CONCLUSION

Improved models and more detailed experimental data are needed to advance the development of catalytic combustors. Preliminary data on CO combustion in Pt/Al_2O_3/Cordierite monoliths exhibit several interesting features. 1. Substrate temperature is only weakly dependent on gas velocity. 2. A relative maximum or shoulder appears in the substrate temperature profile near the inlet. A possible explanation is heat recirculation via radiation (2). 3. The rate of disappearance of unburned CO in the combustor exhaust is consistent with homogeneous reaction data. Thus the exhaust reaction is not catalyzed by species generated by the catalyst.

Pressure measurements inside the catalyst during propane combustion demonstrate a means of compensating for changes in gas velocity caused by the presence of a probe hole.

REFERENCES

1. Kesselring, J. P., W. V. Krill, and R. M. Kendall. Design Criteria for Stationary Source Catalytic Combustors. Presented at the Second EPA Workshop on Catalytic Combustion, Raleigh, NC, June 21-22, 1977.

2. Pfefferle, W. C. The Catalytic Combustor: An Approach to Cleaner Combustion. Journal of Energy, 2(3): 142-146, 1978.

3. Howard, J. B., G. C. Williams, and D. H. Fine. Kinetics of Carbon Monoxide Oxidation in Postflame Gases. Fourteenth Symposium (International) on Combustion, The Combustion Institute, Pittsburgh, PA, 1973. pp. 975-986.

4. Kelly, J. T., R. M. Kendall, E. Chu, and J. P. Kesselring. Development and Application of the PROF-HET Catalytic Combustor Code. Paper 77-33, Presented at the Fall 1977 Meeting, Western States Section, The Combustion Institute, Stanford, CA, October 17-18, 1977.

5. Cerkanowicz, A. E., R. B. Cole, and J. G. Stevens. Catalytic Combustion Modeling: Comparisons with Experimental Data. Presented at the ASME Gas Turbine Conference and Products Show, Philadelphia, PA, March 27-31, 1977.

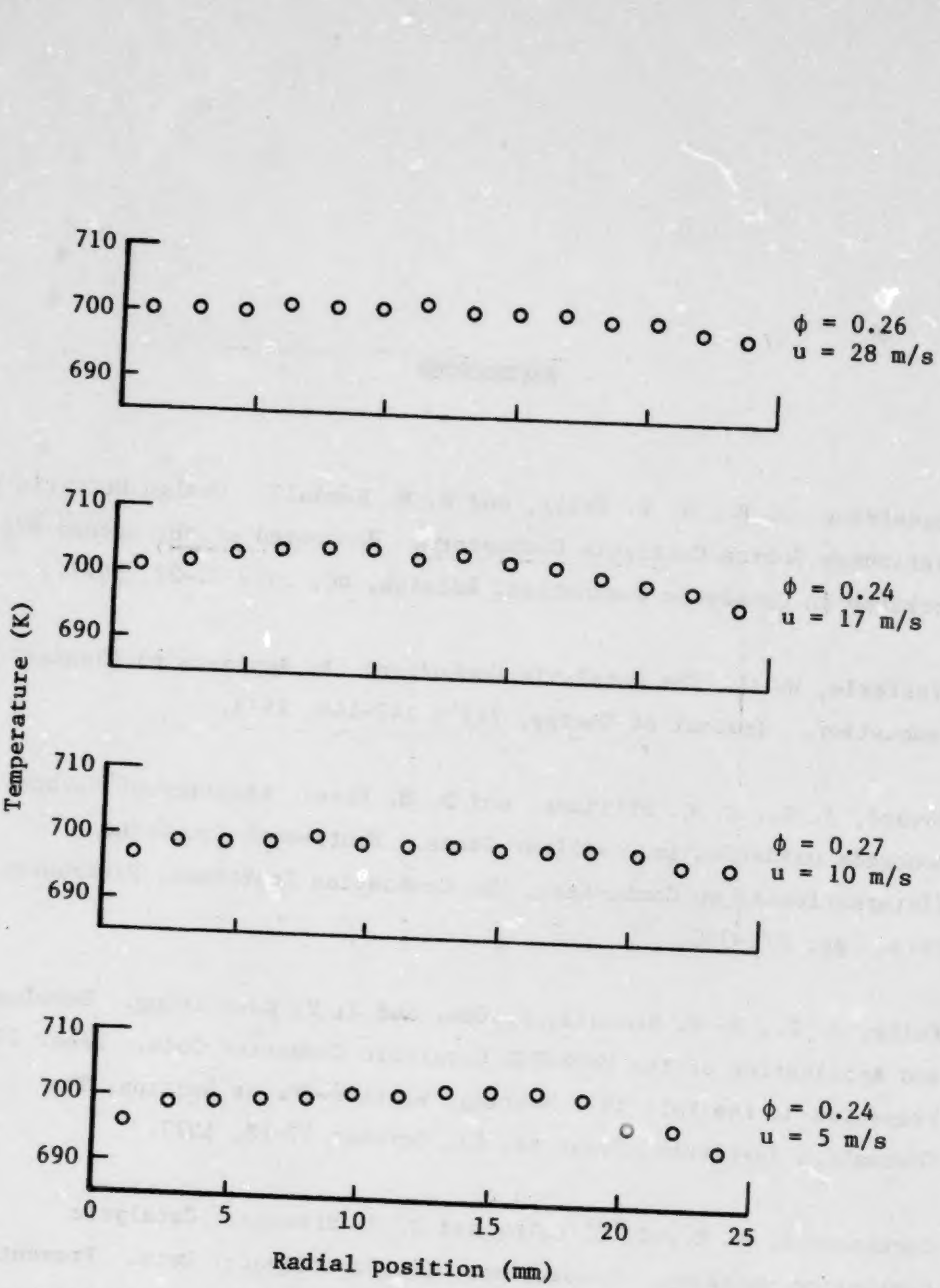

Figure 1. Inlet gas temperature vs. radial position. P_{in} = 112 kPa

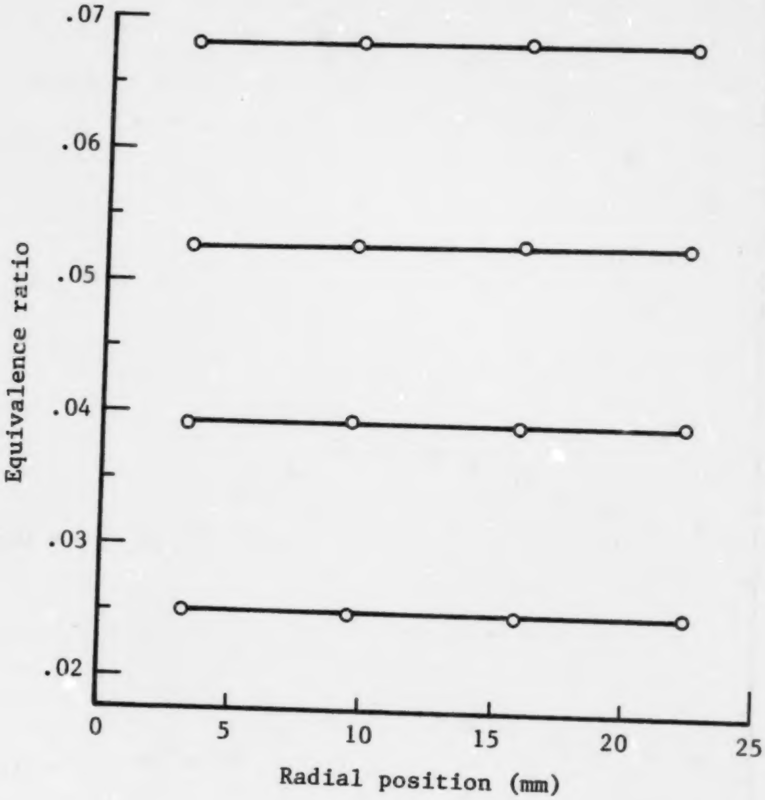

Figure 2. Inlet CO concentration vs. radial position.
P_{in} = 112 kPa
T_{in} = 700 K
u = 60 m/s

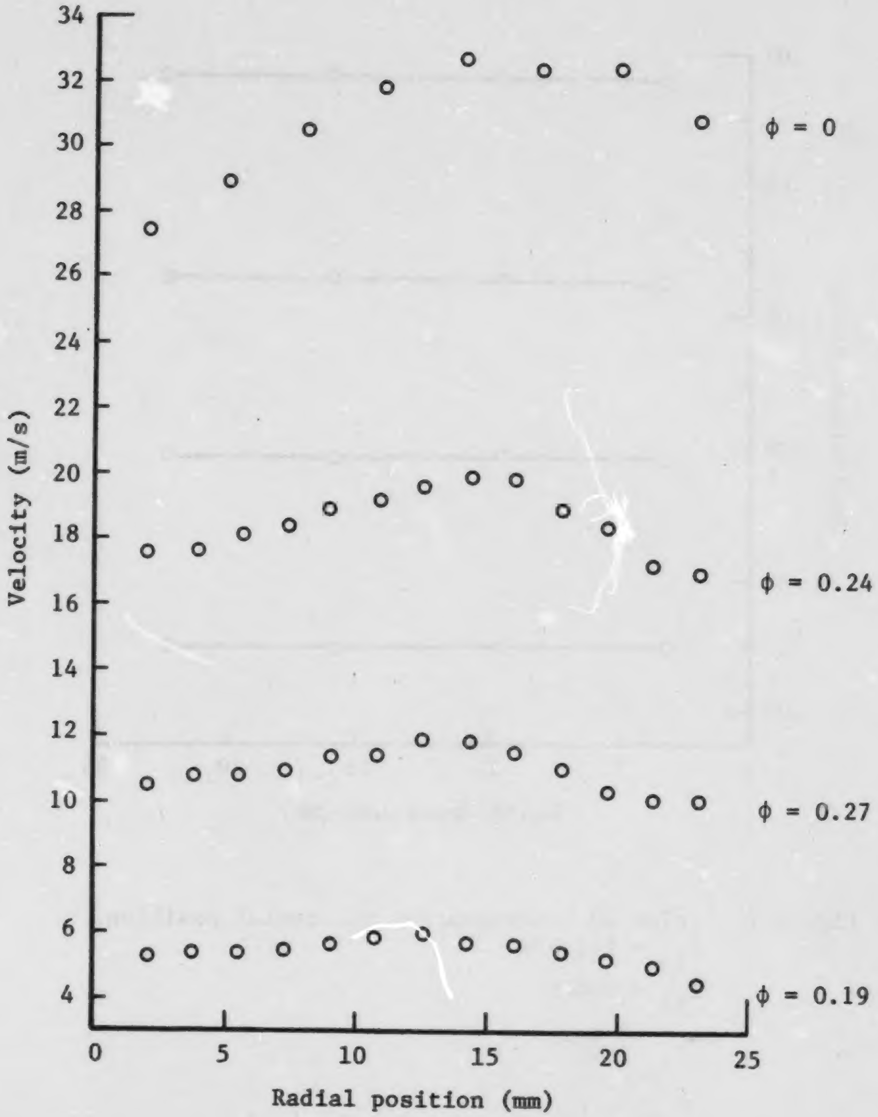

Figure 3. Inlet gas velocity vs. radial position.
P_{in} = 112 kPa
T_{in} = 700 K

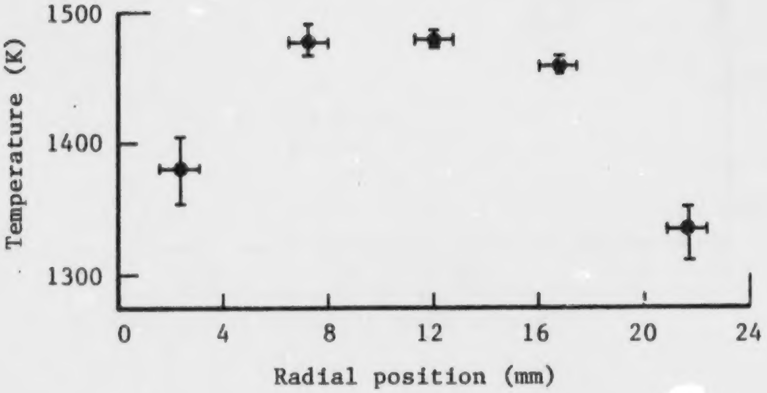

Figure 4. Substrate temperature vs. radial position.
(axial position = 50 mm from catalyst inlet)

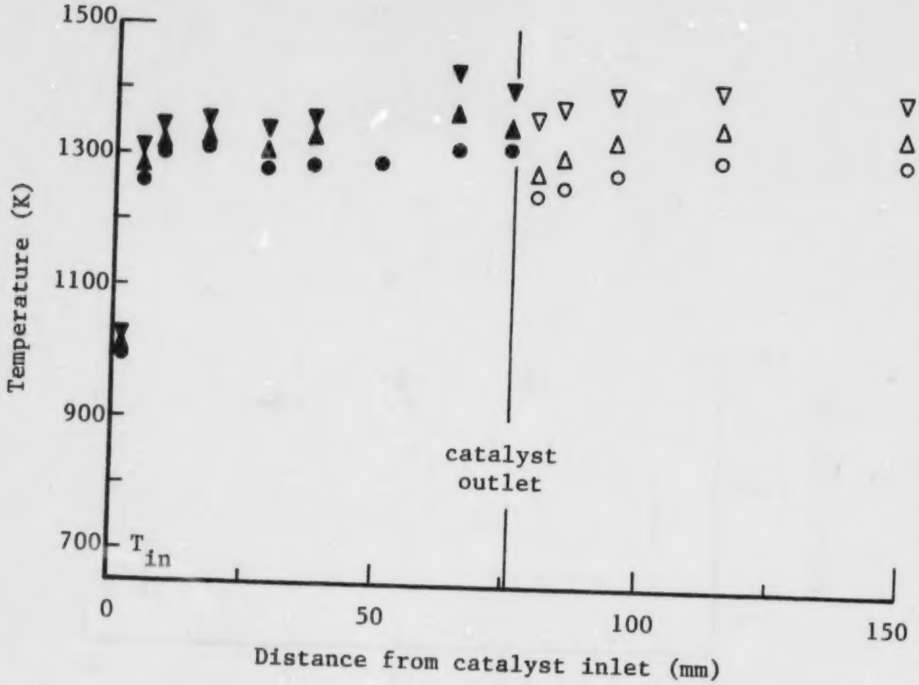

substrate	gas	ϕ	T_{ad}(K)
●	○	$0.24 \pm 0.03 = \phi_1$	1470 ± 80
▲	△	$1.10\ \phi_1$	1540 ± 80
▼	▽	$1.22\ \phi_1$	1610 ± 80

Figure 5a. Substrate temperature and exhaust temperature vs. axial position at different equivalence ratios.

$P_{in} = 112 \pm 2$ kPa

$T_{in} = 700 \pm 8$ K

$u_{ref} = 19 \pm 1$ m/s

$H_2O = 3.0 \pm 0.2$ mol%

$\Delta P/P_{in} = 4.8 \pm 0.3$ %

Catalyst sample #10

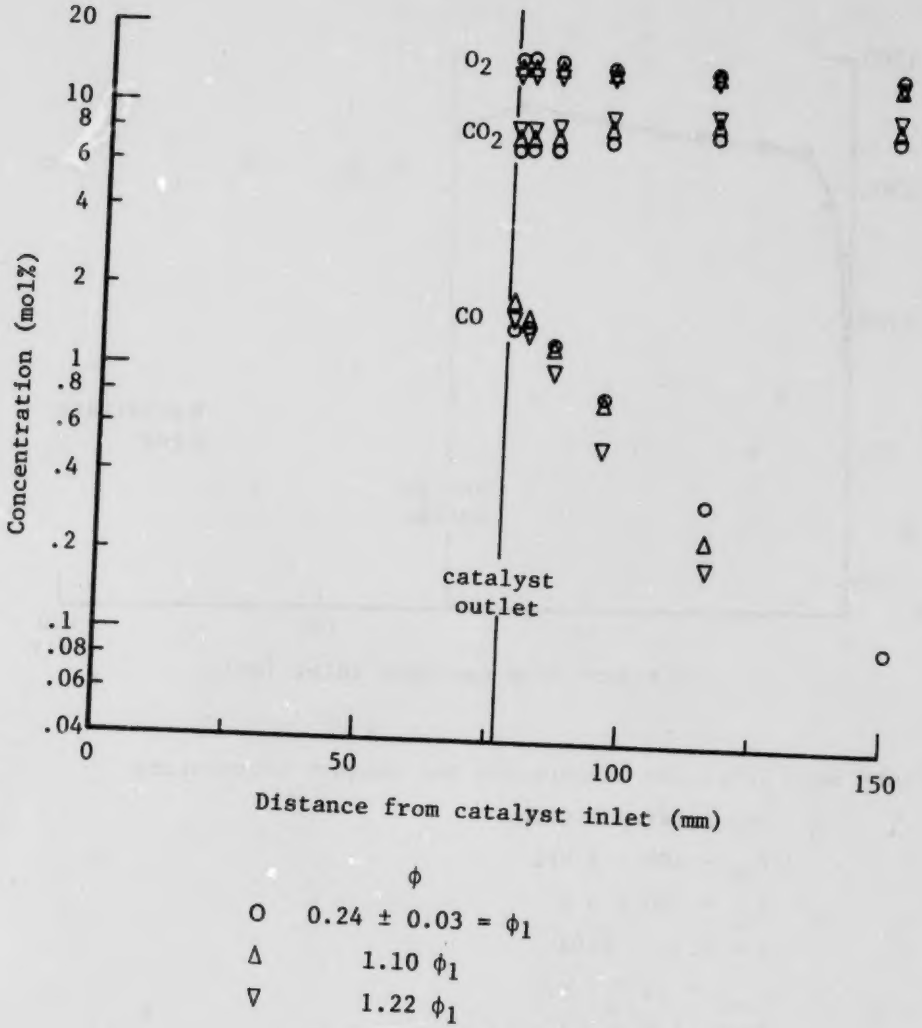

Figure 5b. Exhaust composition vs. axial position at different equivalence ratios.

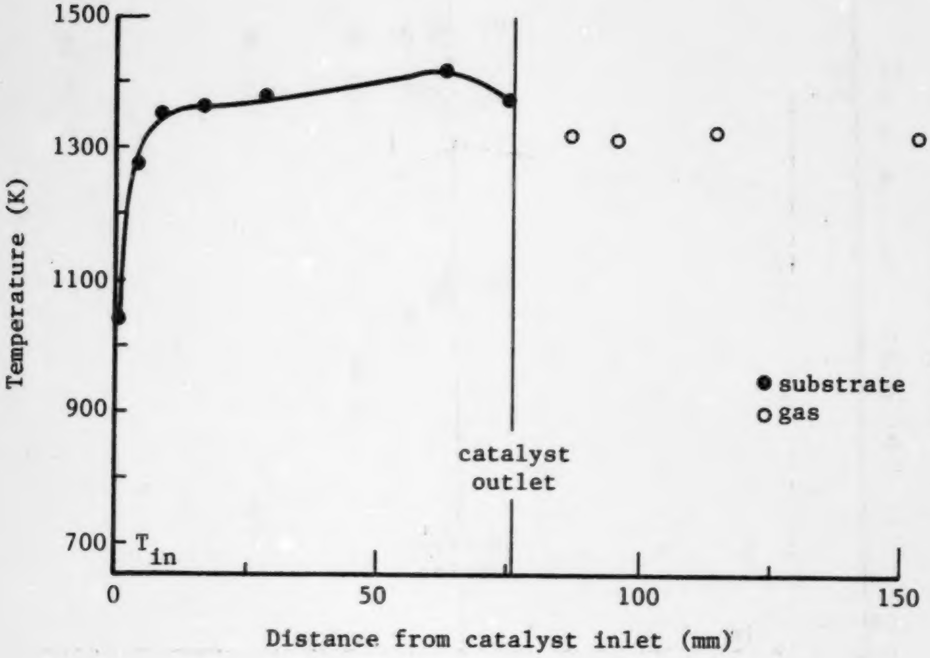

Figure 6a. Substrate temperature and exhaust temperature vs. axial position.

P_{in} = 109 ± 2 kPa
T_{in} = 700 ± 8 K
ϕ = 0.24 ± 0.02
u_{ref} = 15 ± 1 m/s
H_2O = 1.2 ± 0.1 mol%
$\Delta P/P_{in}$ = 3.5 ± 0.1 %
T_{ad} = 1470 ± 50 K
Catalyst sample #8

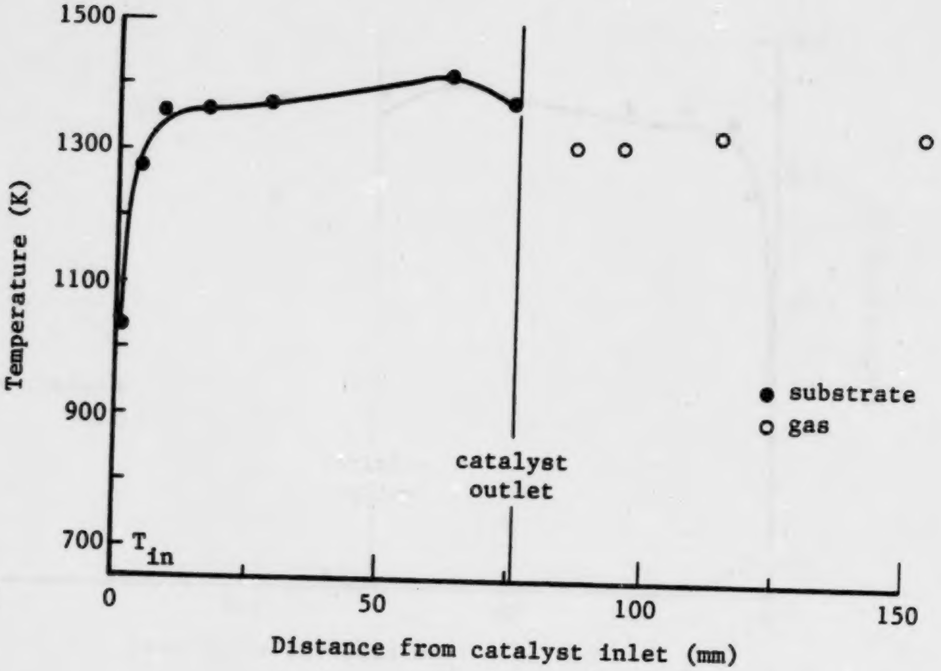

Figure 6b. Substrate temperature and exhaust temperature vs. axial position.

u_{ref} = 21 ± 1 m/s

$\Delta P/P_{in}$ = 5.4 ± 0.1 %

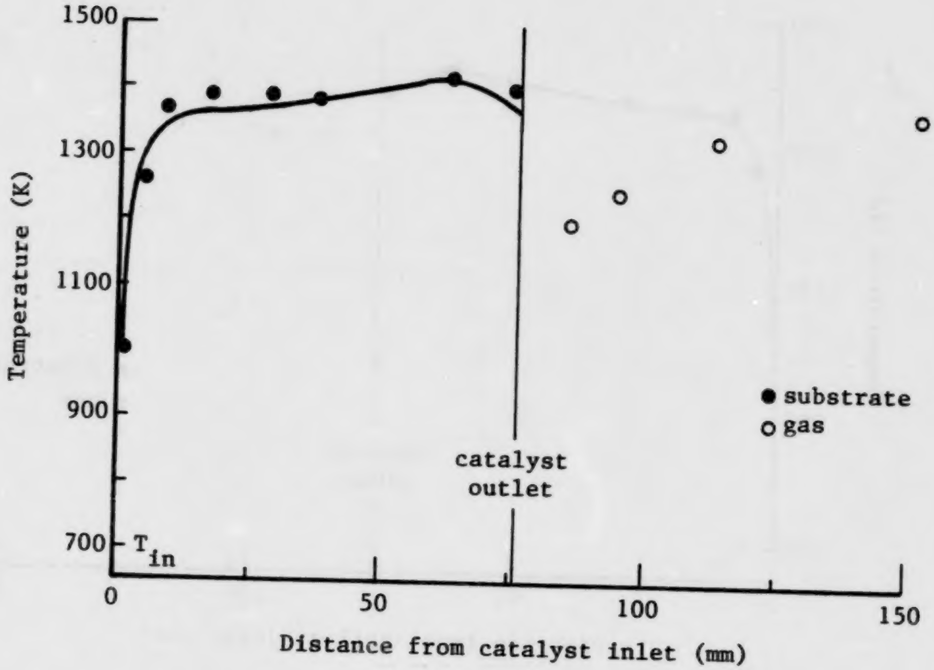

Figure 6c. Substrate temperature and exhaust temperature vs. axial position.

u_{ref} = 30 ± 1 m/s

$\Delta P/P_{in}$ = 8.4 ± 0.1 %

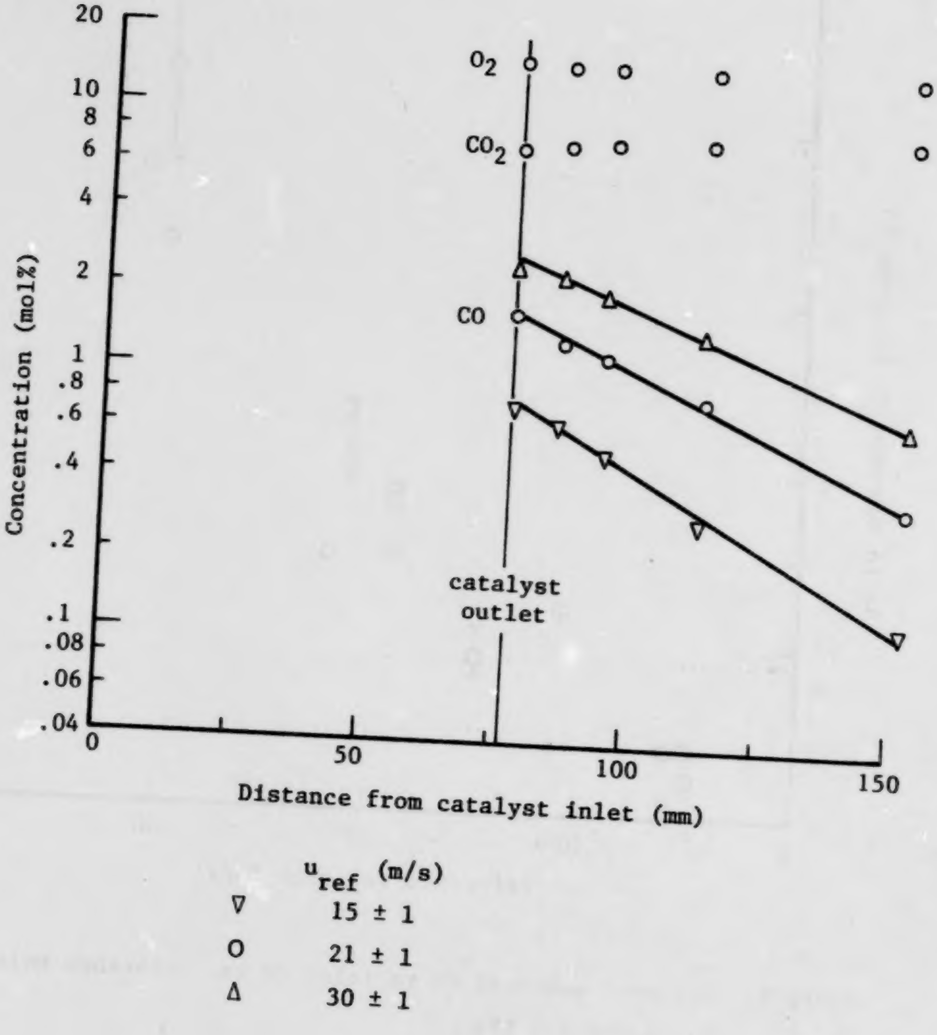

Figure 6d. Exhaust composition vs. axial position at different reference velocities.

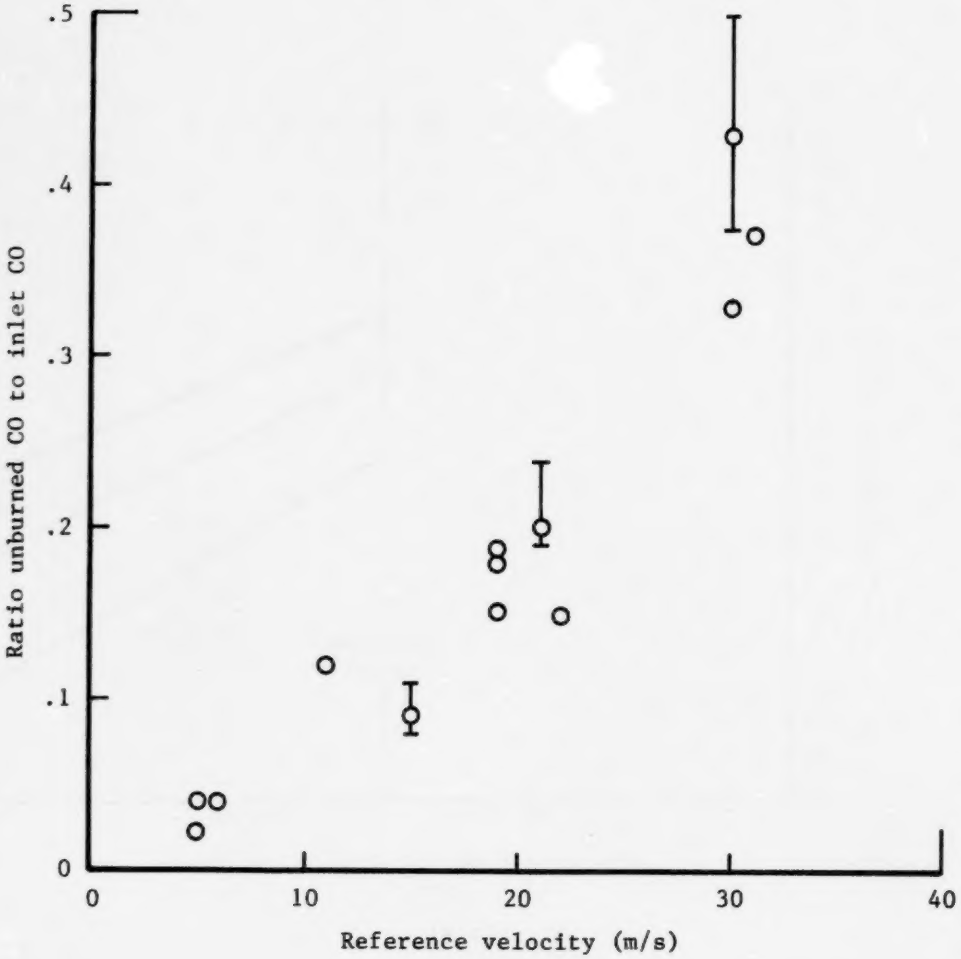

Figure 7. Ratio of unburned CO to inlet CO vs. reference velocity.

P_{in} = 109 ± 4 kPa

T_{in} = 700 ± 8 K

ϕ = 0.19 - 0.30

H_2O = 1.1 - 3.7 mol %

maximum substrate temperature = 1340 ± 90 K

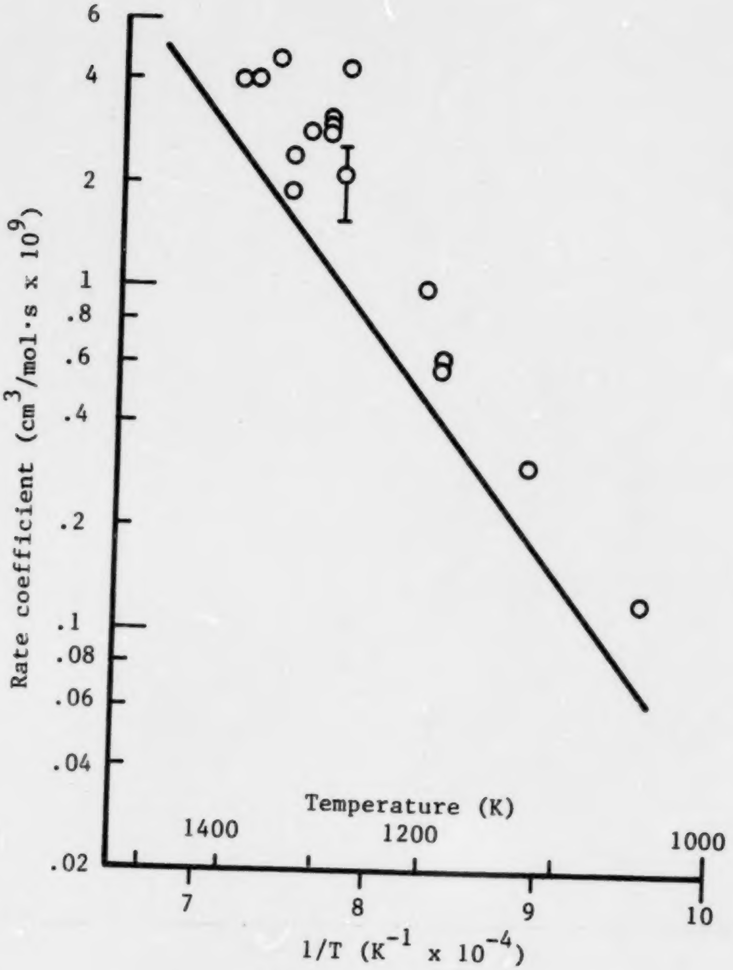

Figure 8. Rate coefficient for CO oxidation in the exhaust vs. temperature.

APPLICATION OF CATALYTIC FLAME STABILIZATION FOR AIRCRAFT AFTERBURNERS

By:

LEONARD C. ANGELLO
AIR FORCE AERO PROPULSION LABORATORY
AIR FORCE WRIGHT AERONAUTICAL LABORATORIES
WRIGHT-PATTERSON AIR FORCE BASE, OHIO 45433

and

DR. THOMAS J. ROSFJORD*
UNITED TECHNOLOGIES RESEARCH CENTER
UNITED TECHNOLOGIES CORPORATION
EAST HARTFORD, CONNECTICUT 06108

---

* Formerly with the Air Force Aero Propulsion Laboratory

INTRODUCTION

Catalytic flame stabilization as applied to aircraft afterburners encompasses the uses of a catalytic surface to initiate, stabilize, and provide a continuous pilot for flame propagation. Catalytic flame stabilization differs from catalytic combustion (a heterogeneous process) in that the catalyst is used only to "boot-strap" the fuel-air mixture to temperature and species conditions such that gas phase reactions can predominate; the balance of energy release is accomplished through homogeneous chemical processes. Previous Air Force Aero Propulsion Laboratory (AFAPL) studies have indicated that an afterburner performance advantage can be realized by employing catalytic flame stabilization in aircraft afterburners. Further, because of the accelerated chemical activity associated with catalysts, an improved ignition capability is expected. Test programs, however, to verify these indications have as yet not been performed.

The purpose of this paper is to outline an experimental test program currently being performed by the Air Force Aero Propulsion Laboratory to investigate the applicability of catalytic flame stabilization for aircraft afterburners. This experimental program shall make use of a J85-5 afterburning turbojet engine to test concept feasibility. The goal of the AFAPL program is to employ catalytic flame stabilization in such a manner that system performance gains result.

Preceding page blank

PROGRAM DESCRIPTION

The AFAPL paper study has considered one application of catalytic materials for aircraft afterburner flameholders -- namely the use of catalytically-active honeycomb devices instead of conventional bluff bodies. The study projects the performance advantages of reduced flameholder pressure drop and/or increased afterburner combustion efficiency. Other potential benefits may include improve ignition capability and reduced acoustic instability (high frequency "screech" and low frequency "rumble").

Based on these indications an experimental test program has been initiated at the Air Force Aero Propulsion Laboratory to evaluate concept employing catalytic flameholders in aircraft afterburners. The AFAPL program shall test catalytically-active flameholder designs in a J85-5 turbojet engine. Candidate stabilizers shall be examined under a full range of afterburner conditions. A conventional flameholder design will also be examined as a data baseline. The performance of the candidate and conventional devices shall be compared to verify and upgrade analytical model predictions.

Data shall be acquired to evaluate the flame stabilization limits, the ignition capability, the imposed total pressure drop and the combustion efficiency associated with each test item. Combustion efficiency shall be determined by integration of point emission measurements. Pressure drop shall be determined by measurement of total pressure upstream and downstream of the flameholder. Flame stabilization limits and ignition capability shall be determined qualitatively.

BACKGROUND

The combustion chamber of a jet engine afterburner is a mechanically simple device: It consists of a straight flow-through duct which contains one or more flameholders to stabilize a reacting fuel/air mixture. The fuel is introduced through several spraybars upstream of the flameholders, resulting in a substantially premixed, prevaporized flow. Conventionally, the flameholders are annular "V" gutters or similar bluff bodies.

The flow conditions of an afterburner differ from the engines main burner in several respects--it operates hotter, at lower pressure and with higher velocities.

An afterburner is not subject to the maximum exit temperature limitations imposed on the main burner. Structual considerations of the turbine blades of current aircraft jet engines restrict the maximum combustor exit temperature to approximately 1650K. The combustion gases produced in an afterburner do not pass through any turbomachinery, and are therefore not similarly limited. For this reason, at the maximum power condition, afterburner combustion occurs at equivalence ratios near unity, while current main burners are confined to values below 0.4.

An afterburner operates operates at significantly lower pressure than a main burner. Typically, the exit nozzle is a variable area, convergent design which actuates to sustain critical conditions. Thus, the afterburner chamber pressure is approximately only twice the ambient pressure. In contrast, current main burner combustors operate up to thirty times the ambient.

A jet engine afterburner functions to augment the maximum thrust that can be produced by the main engine. It becomes operational only after the main engine reaches its maximum power output--termed the "military" condition. In this mode, the engine passes its maximum mass flow. Additionally, the inlet gas temperature is high with typical values of approximately 950K. These two effects, plus the low pressure, result in a typical average inlet velocity of 130 m/s. Such values are more than triple the main burner inlet velocity.

Conventional afterburners do not operate at peak combustion efficiency. Typically, they release only between 85%-95% of the available chemical potential while main burners routinely release 99%. The poorer performance is attributable to the high speed of the flow, which approaches 250 m/s. The practical restriction of reasonable afterburner lengths results in a short residence time and thus incomplete combustion. Faster reaction rates would enhance the axial rate of energy release as depicted in Figure 1. If the accelerated change of combustion efficiency is achieved, the designer could choose either higher performance or decreased hardware length. That is, if current lengths are acceptable, a performance increase associated with an improved efficiency would result ($\Delta\eta_c$). Alternatively, if the current performance level is acceptable, it could be achieved at a shorter length, L_c. It is not possible to precisely predict the length saving without a measurement of the combustion efficiency. However because of the expected asympotic approach to high levels of efficiency, the length reduction should be substantial.

Another implication of the high speed flow in the afterburner is that the flameholder which pilots and establishes the reactions cannot be wide in order to avoid unacceptable pressure drop. Therefore, the combustion originates from a few small sources (one to three flameholder rings) which again because of the high velocity, spread at angles on the order of 7°.

A minimum afterburner length would be the distance necessary to completely fill the cross section with reaction - that is, the distance at which the spreading sources merge. Larger sources would proportionally reduce the required length as shown in Figure 2 and thus provide the designer the option of shorter hardware length. It would also be expected that for a given length, a performance increase would be associated with merging the combustion zones nearer the flameholder, thus representing the option of increased system performance.

One means to achieve the benefits of a larger flameholder, without imposing unacceptable pressure losses, is to consider using a porous body instead of a solid body. This design would permit flow through as well as around the device, producing less pressure drop than a conventional (bluff) body of equal frontal area. Therefore, the porous body could be made wider, reaping the benefits discussed above. In essence, this approach could be termed "toward a flat flame afterburner," for such a design would ensure maximum energy release in minimum lengths. The ideal case of completely filling the combustor cross section with a porous flameholder is not attainable, however, because of the associated pressure loss.

It is recognized that replacing the bluff body stabilizer with a porous device alone is not acceptable. A conventional flameholder successfully stabilizes the overall combustion processes by providing a continuous pilot for the spreading combustion wave. The recirculating wake flow behind the solid body provides gas residence times the same order as the characteristic chemical reaction times, and thus establishes the required piloting phenomenon.

The porous stabilizer does not provide a similar piloting zone. The flow through the body tends to wash out the recirculating, and hence piloting, character. This deficit can be corrected by making the device catalytically active. In this case, the reactants passing through it would be substantially oxidized in a manner similar to a catalytic main burner. Since the afterburner is always accompanied by a military main burner mode, it always receives hot inlet gases. This condition removes the low inlet temperature problem that plagues main burner applications. It also increases the reaction rates, offsetting the problem of decreased catalyst contact time due to the high velocities. Note that complete oxidation of the internal mixture is not a requirement. The degree of reaction would be chosen to produce a stabilizer wake of hot, combustion species similar to that existing behind a bluff body device. Thus, the desired flame stabilization should be achievable using catalytic, porous bodies which would initiate the combustion over a combustor cross section greater than a conventional device of equal pressure loss.

FLAMEHOLDER MODELING STUDIES

An in-house modeling effort was initiated at the Air Force Aero Propulsion Laboratory by T.J. Rosfjord and B. Eresman to investigate the porous, catalytically-active flameholder concept. Experienced gained in other catalytic combustion studies indicated that noble metal catalysts and honeycomb substrates were appropriate flameholder components. The purpose of this modeling effort was to indicate the trade-offs between flameholder blockage and imposed pressure loss for various honeycomb catalyst substrates.

The system analyzed is shown in Figure 3. A uniform, constant density mixture enters the constant area duct, with a portion (Flow II) flowing through a honeycomb blockage while the remaining flow (Flow I) passes around it. The honeycomb is characterized by its fractional blockage area, cell diameter, d, and cell length, ℓ.

The model derived by Rosfjord and Eresman for this system solely incorporated fluid mechanic considerations, and not chemical reactions. To remedy this deficiency, a catalytic reactor model developed at Exxon Research and Engineering (1) was exercised. A JP-4/air mixture at conditions indicated by the fluid mechanic model were input to the kinetic model which sought substrate/catalyst combinations to produce a substrate exit flow temperature of 1350°K: In general, a cell $\ell/d \approx 40$ was required to achieve this condition.

Results of the fluid mechanic modeling performed by Rosfjord and Eresman are plotted in Figure 4. This plot illustrates the trade-off of pressure loss with increasing flameholder blockage, with honeycomb cell ℓ/d as a parameter.

A conventional J85-5 flameholder represents a 36% blockage and imposes a 3.2% pressure loss. The model predicts that similarly sized honeycomb with ℓ/d = 40, would impose only a 2.0% loss. A 45% blockage honeycomb would impose a loss equivalent to the conventional solid body. Considerations such as these guided the design of test hardware as shown in Figure 5.

Figure 6 illustrates the fraction of flow through the honeycomb with increasing flameholder blockage. As expected, the portion of total flow through the honeycomb is significantly less than its fraction of the total area. For a ℓ/d = 40, the 36% blockage device passes 16% of the flow while a device of 45% blockage--the size which imposes a pressure loss equivalent to the conventional flameholder design----passes 25% of the total flow.

PERFORMANCE TRADEOFFS

A study was conducted to quantify performance tradeoffs for the porous, catalytic flameholder design illustrated in Figure 4. The study considered the potential gain in combustor efficiency (η) versus the possible increased flameholder pressure loss (PL) associated with this catalytic flameholder design.

The study was carried out using an existing turbojet/turbofan model (2) capable of predicting the design point performance of a specified system with parametric variations. The propulsion system investigated in this study was a low pressure ratio, turbojet engine of approximately 4000 pounds thrust. Variations in combustion efficiency and flameholder pressure loss were studied while maintaining thrust rating. The net system gain or loss was reflected as changes in specific fuel consumption (SFC).

Figure 7 illustrates the tradeoff as represented by changes in SFC at a maximum afterburner power mode. Assume that the baseline burner operates at $\eta = 90\%$, $PL = 3.2\%$. Increased efficiency to $\eta = 95\%$ at constant PL reduces SFC from 1.81 to 1.75, a 3.3% decrease. Alternatively, a decrease to $PL = 2.0\%$ at constant efficiency translates to a 1.7% SFC reduction. The nearly linear relationship of SFC and η for various PL levels indicates that approximately a two percentage point improvement in efficiency is required to offset each percentage point increase in pressure loss.

The tradeoff depicted in Figure 7 implies that a system gain is achieved for flameholders which result in η improvements which outweigh increased PL. That is, higher pressure losses may be acceptable. This is not true, however, if one considers the total engine operating envelope. The afterburner is utilized for only a small fraction of the total engine life. During AB operation, its efficiency is an important consideration.

However, the flameholder imposes pressure losses at all times.

This situation is depicted in Figure 8. The SFC for various degrees of afterburner operation is plotted with combinations of η and PL as a parameter. The baseline case is $\eta = 90\%$, PL = 3.2%. As shown, increases in PL can be offset with η gains at afterburner modes, but result in an SFC penalty without afterburner operation. As well, decreases in PL will benefit SFC at all power settings.

SUMMARY

In summary, the concept of employing catalytic flame stabilization to the design of flameholder for aircraft afterburners has been developed. Flameholder modeling studies have been presented which show this concept to offer performance benefits in terms of increased efficiency and reduced pressure drop losses. Further benefits may also include increased ignition capability as well as reduced acoustic instability. The feasibility of achieving these advantages can only be evaluated by experimental test programs such as those being currently performed at the Air Force Aero Propulsion Laboratory.

REFERENCES

1. Cerkanowicz, A.E., Cole, R.B., and Stevens, J.G., "Catalytic Combustor Modeling: Comparisons with Experimental Data," ASME Paper 77-GT-85, March 1977.

2. Witherell, Capt. R.E., Design Point Turbine Engine Performance Program, AFAPL TR-68-88, 1968.

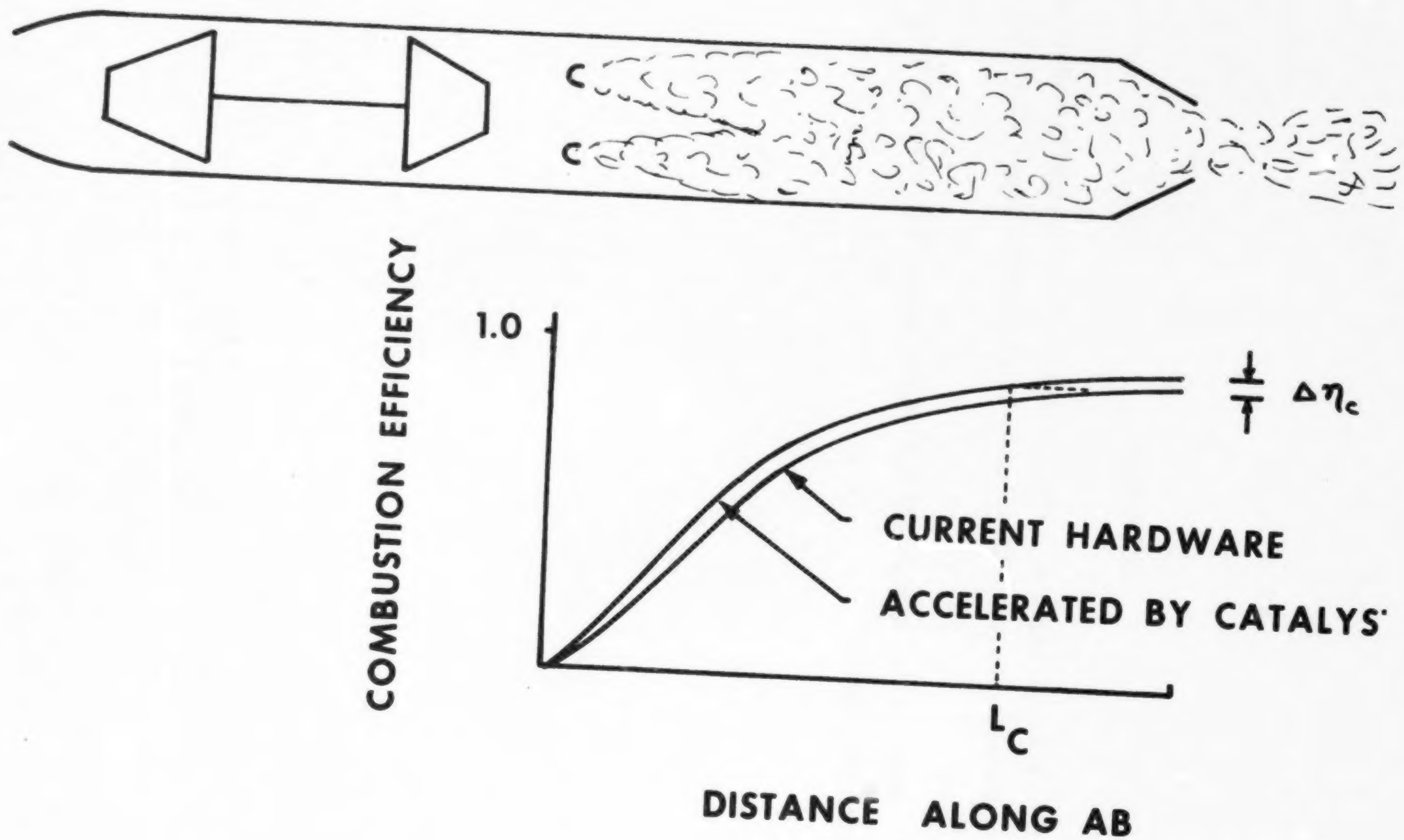
C
C
COMBUSTION EFFICIENCY
1.0
$\Delta\eta_c$
CURRENT HARDWARE
ACCELERATED BY CATALYS'
L_C
DISTANCE ALONG AB

FIGURE 1

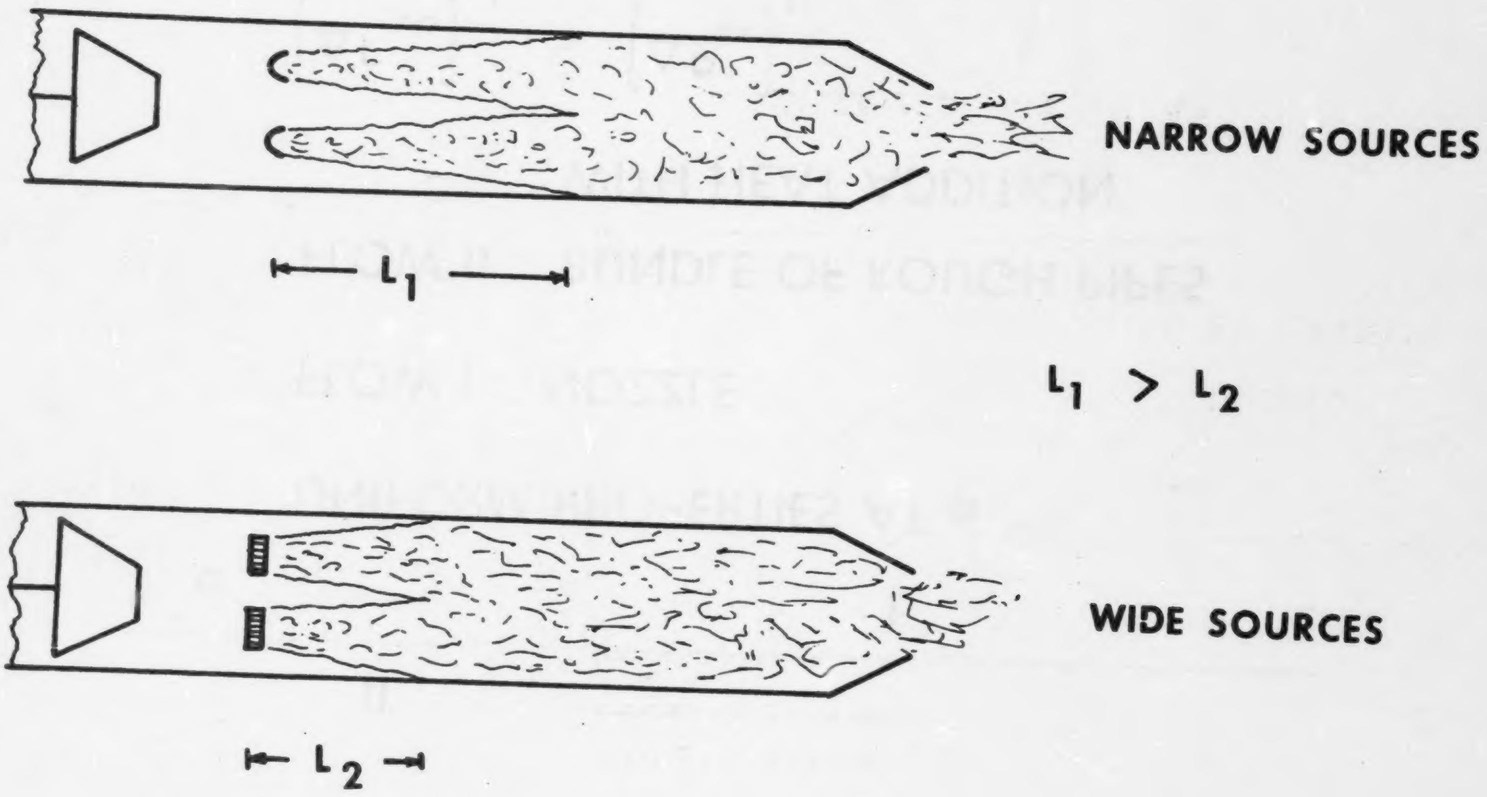

FIGURE 2

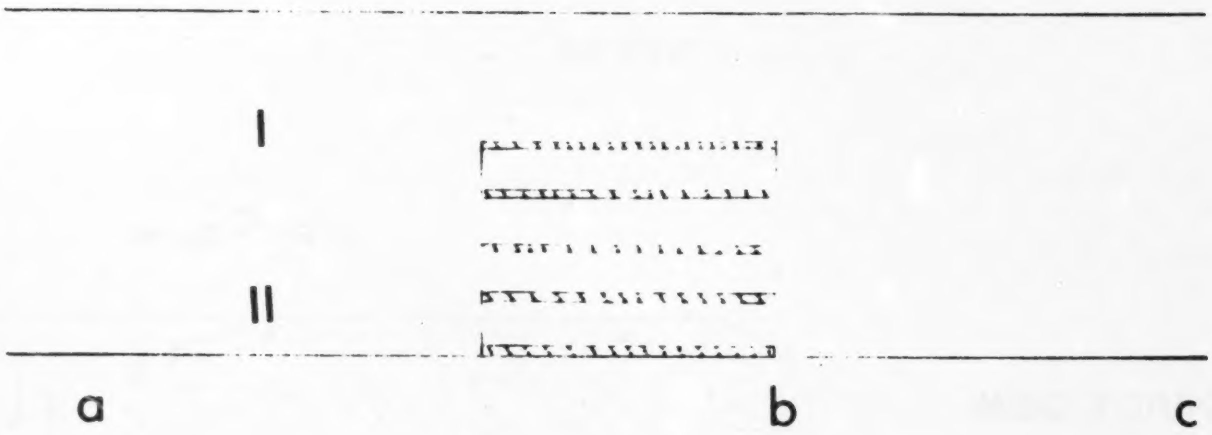

UNIFORM PROPERTIES AT a

FLOW I -- NOZZLE

FLOW II -- BUNDLE OF ROUGH PIPES
WITH HEAT ADDITION

$$\left[\Delta P_{ab}\right]_{I} = \left[\Delta P_{ab}\right]_{II}$$

FIGURE 3

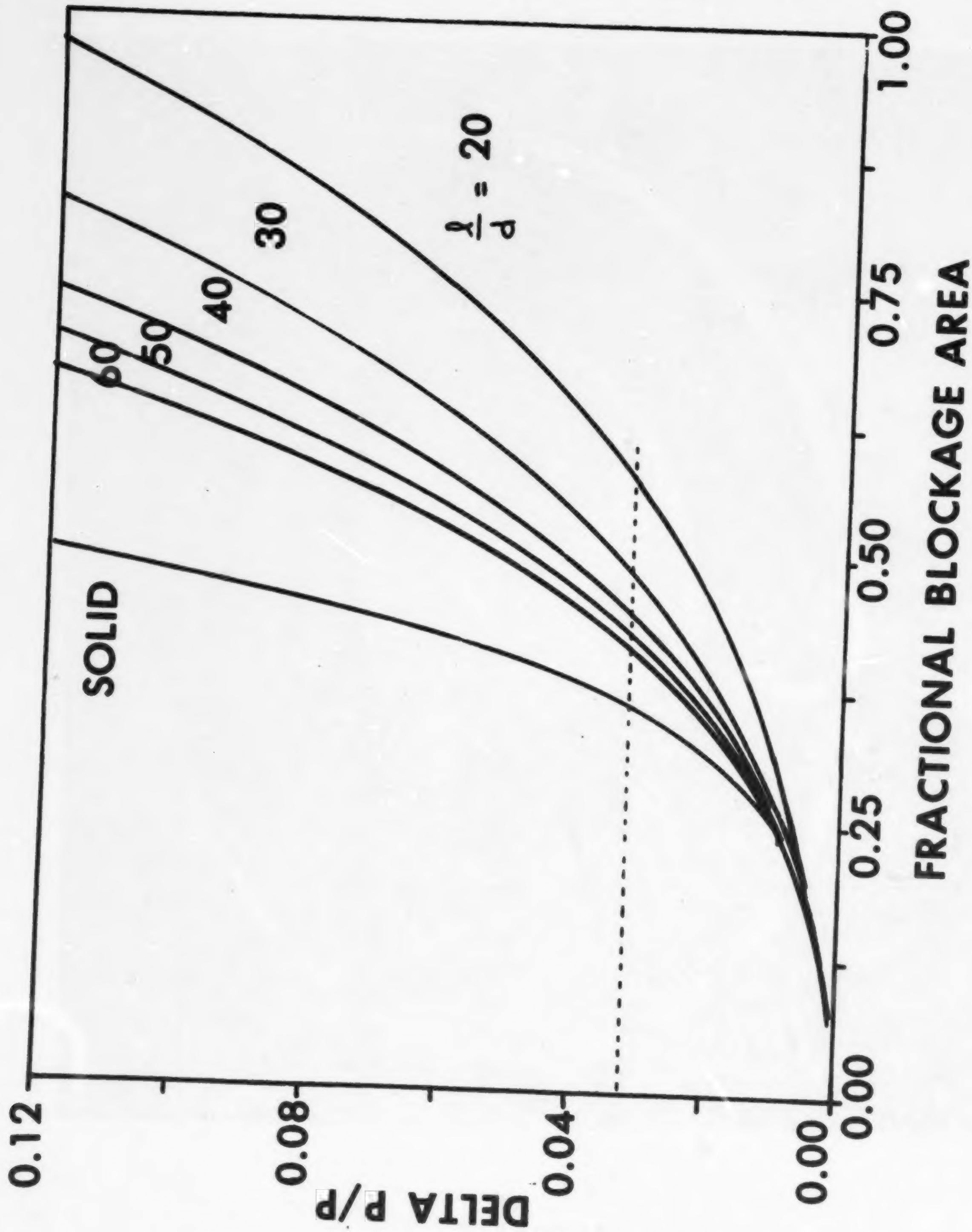
DELTA P/P
0.12
0.08
0.04
0.00
0.00
0.25
0.50
0.75
1.00
FRACTIONAL BLOCKAGE AREA
SOLID
60
50
40
30
$\frac{\ell}{d}$ = 20

FIGURE 4

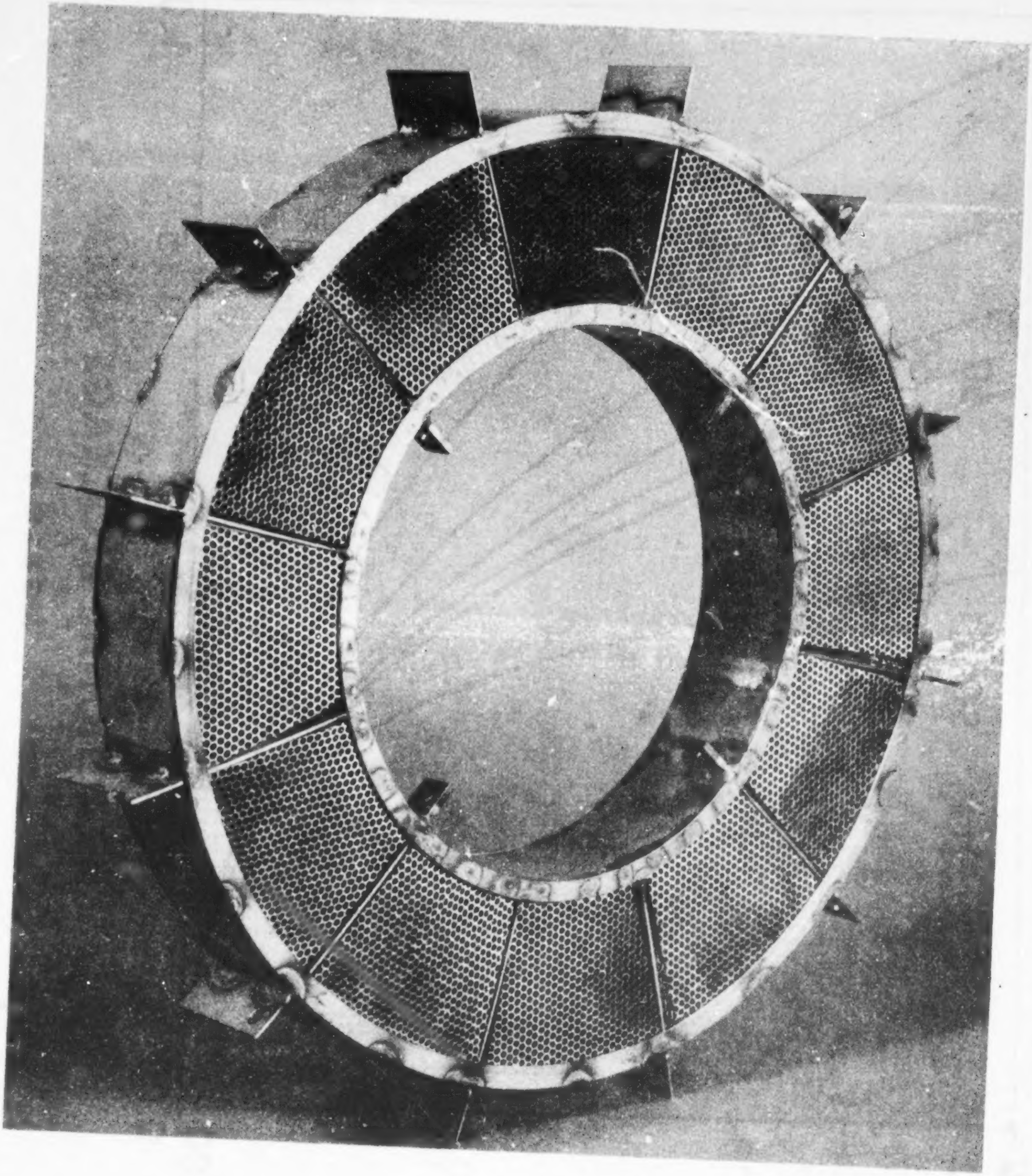

FIGURE 5

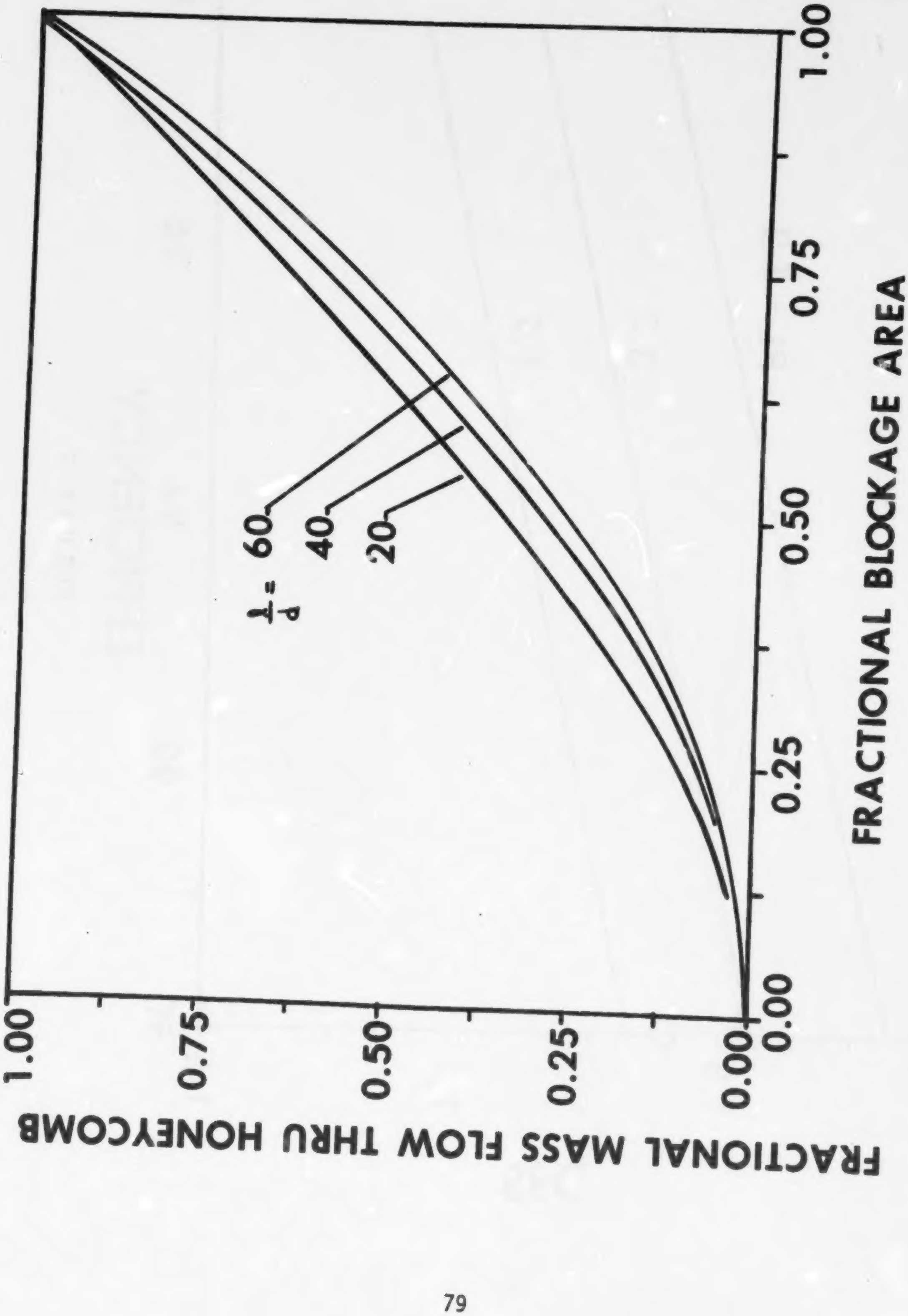
FRACTIONAL MASS FLOW THRU HONEYCOMB
1.00
0.75
0.50
0.25
0.00
FRACTIONAL BLOCKAGE AREA
0.00
0.25
0.50
0.75
1.00
$\frac{l}{d}$ = 60
40
20

FIGURE 6

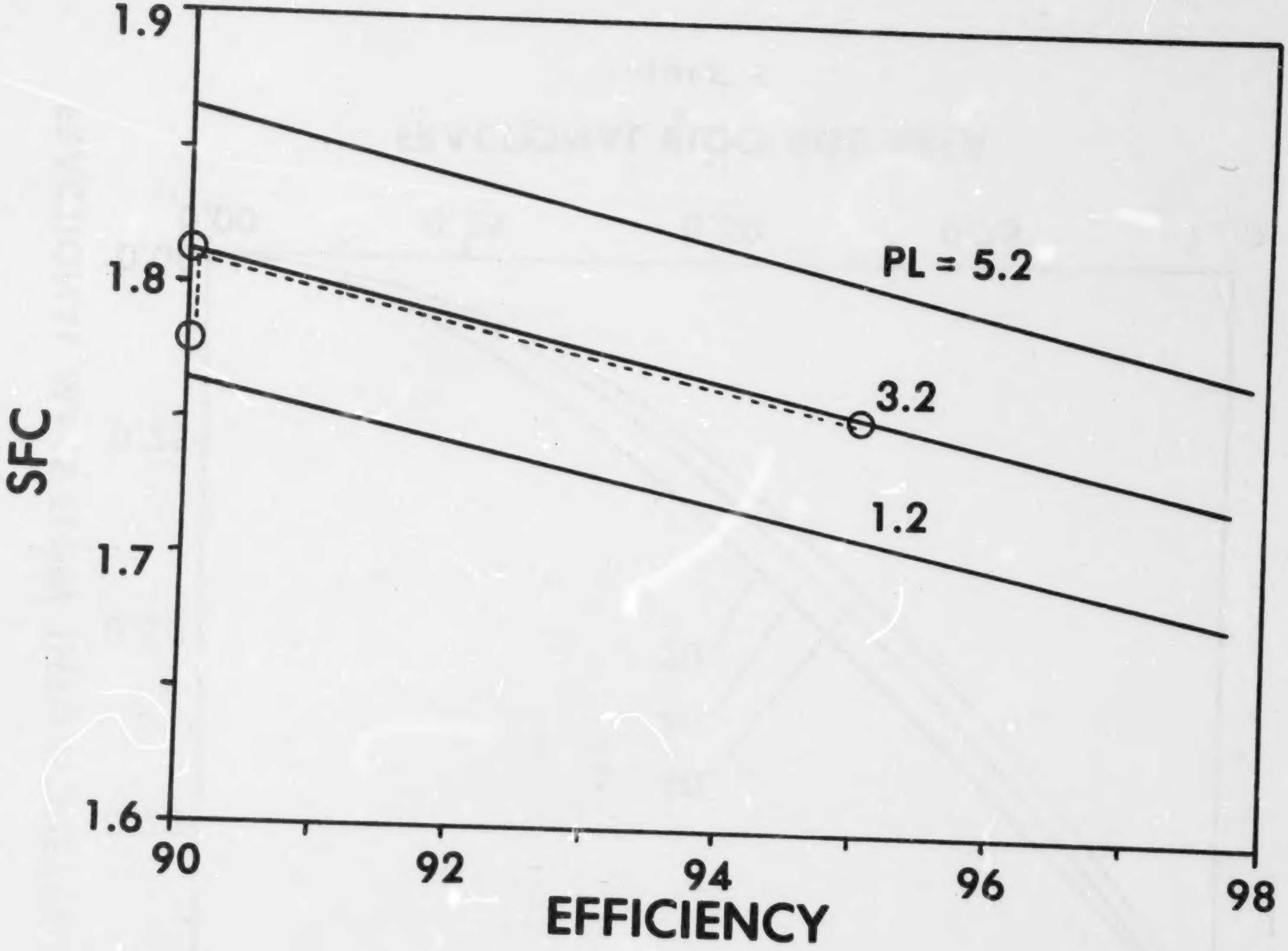

FIGURE 7

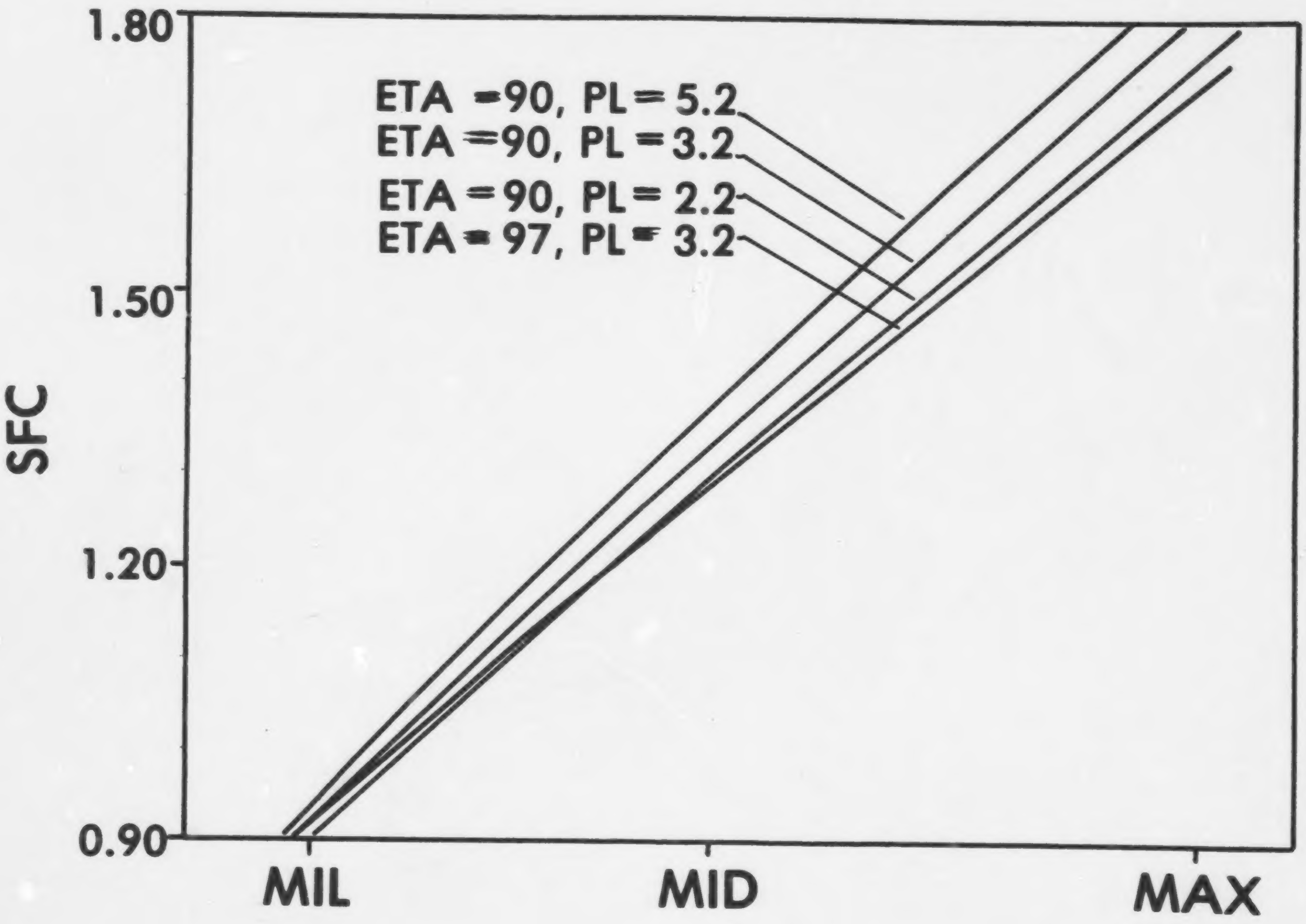
1.80
1.50
1.20
0.90
SFC
ETA =90, PL= 5.2
ETA =90, PL = 3.2
ETA = 90, PL= 2.2
ETA = 97, PL = 3.2
MIL
MID
MAX

FIGURE 8

EPRI VIEW OF CATALYTIC COMBUSTION

by

A. C. Dolbec
Program Manager - Power Generation
Advanced Fossil Power Systems
Electric Power Research Institute, Inc.
Palo Alto, California 94303

ABSTRACT

As current EPRI efforts focus on combustion turbine applications of catalytic combustors, this paper presents the specific turbine duty cycles and general usage. Peaking and baseload applications are discussed.

The expected problems that are apparent at this time are discussed even though the known list is not complete. Apparent catalytic system advantages are discussed in length insofar as they are apparent at this time. Some of these will turn out to be speculative but possibly others real, offering a hope of considerable flexibility for turbine designs in the future. Current work at EPRI regarding catalytic combustion for turbines is outlined, along with those things expected to be done during 1979. Additional work, as yet undefined, is planned.

Preceding page blank

Introduction

Although this paper is titled "EPRI View of Catalytic Combustion," the program and plans presented here represent only the Power Generation/Advanced Fossil Power portion of EPRI. Other portions of EPRI, such as the Fuel Cell Program and Fossil Fuel programs, have followed progress in the catalytic combustion area, and while no major work has been committed, there is a continuous evaluation of the potential of catalytic combustion toward applications other than combustion turbines. Specifically, this paper describes work and plans for the use of catalytic combustion techniques on combustion turbines.

The combustion turbine is considered a vital portion of most advanced fossil power schemes now receiving considerable R&D attention. Several EPRI studies (references 1 and 2) indicate that combustion turbines will figure prominently in intermediate and probably baseload power plant applications in the late 1980's and 1990's. At those times it is expected that environmental requirements will demand considerably lower emission levels than possible with today's technologies. For these reasons certain generation schemes which allow much improved emissions have been favored by EPRI over others that show less promise for great improvement.

Combustion Turbine Applications

Catalytic combustion techniques for combustion turbines need to be explored in two general areas. As there are now some 2000 gas turbines in the United States used for power generation, a "retrofit" market exists for improving the emissions of current turbines where these are located in such areas that improvements would contribute to the overall air quality of the locale. The other basic direction for catalytic combustion is in the design of an improved and more reliable power plant. These prospects appear at this time to be quite exciting. On a retrofit basis, combustion turbines would have to be modified in the field to include a catalytic element within the basic structure of combustion liner and transition piece, as shown in Fig. 1. The objective of this work would be to design a system that could be furnished at minimum cost, which usually means changing the fewest number of existing parts. Most of the some 2000 turbines in commercial use generating power today are used in "peaking" service. This indicates a cycle of some 1500 hours a year with possibly up to 200 starts per year. Thus, catalytic elements in the peaking application need not have an extremely long life but should be able to take significant cycling. As many of these turbines would be at least 10 years old by the time catalytic equipment was available for the market, the cost of such a retrofit would be extremely important.

As the peaking application offers many opportunities for inspection, the ability of the system to be quickly inspected and assure its integrity is highly desirable. These are the general design considerations for a retrofitted system usable on present peaking applications.

New designs of combustion turbines would be used in peaking applications but also in intermediate to baseload duty cycles as new plant technologies become available. This means that for intermediate load use, operation would be between 2000 and 5000 hours per year, whereas baseload applications (probably not significant before the 1990's) would be in excess of 5000 hours a year up to some 7500 to 8000 hours per year. Intermediate and baseload applications would then require a once-a-year minimum time for replacement, and hopefully inspection could be once a year with replacement every three years. This could mean that some 24,000 hours of usage would be required for catalytic elements before they should be replaced. Newly designed machines that might be exposed to this service could benefit in several ways from a catalytic combustion process.

Some Advantages of Catalytic Combustion

Of course, the basic motive of catalytic combustion as perceived now is the potential for emissions reduction. In addition, other features of the catalytic combustor are possible, although at this time very little has been done to analyze how realistic they might be.

Because of the great reduction in peak flame temperature, the amount of heat radiated to metal parts of the machine is greatly reduced. This offers a fewer number of hot parts which should lead towards improved machine reliability. If ways can be found to initiate combustion by catalytic means, then the machine can be lit off in what could only be described as a "soft" manner, taking many seconds to achieve peak flame temperature as contrasted to the present spark ignition and immediate (within a few seconds) light off. The advantage of a soft ignition is that it much reduces the thermal shock to machine parts, particularly when a cold machine is being started. For new turbine designs, the pattern of temperature across the combustor outlet with a catalytic scheme may be considerably less than with the present flame and air supply arrangements. This offers the possibility of reducing the maximum temperature exposure for metal parts while keeping the average temperature the same. In other words, hot spot temperature reduction could offer prolonged life of hot gas path parts downstream of the combustion area. The design of present day combustors is largely an empirical science. Many data points are developed by use of combustion test stands, and these describe the overall temperature, stress, and emission levels that can be expected from a given configuration. An indicated advantage of the catalytic schemes is the ability to predict the temperature and emissions with much more accuracy when scaling from one size of machine to another or one design to another.

This offers the promise that many expensive and time-consuming combustion tests can be eliminated once a secure data base is established that defines the catalytic combustion design approach. By the way, if improving metal temperatures can be turned into a design feature, the amount of cooling air now necessary to keep metal temperatures below roughly 1500°F may be diverted to more efficient use of the cycle.

Problems to be Solved

The turn-down ratio, or region of stable control for a conventional combustor, is roughly 4.5 to 1. Catalytic combustion experiments at this time have demonstrated a turn-down ratio of less than 2 to 1 and potential techniques for improving this characteristic have not been identified. This means that a current design would have to have a conventional combustor for ignition and some portion of the speed and load profile. Such a system is more expensive but, even worse, might have a significant reduction in reliability.

Of great concern to turbine designers is the possibility that a catalytic monolith structure would fracture and be ingested by the turbine. Designs of such structures must be demonstrated that will pass through the turbine without causing damage to the blading. There is a strong feeling among many people in the industry that this can be accomplished.

The premixing required for stable catalytic combustion is not expected to be greatly different from the premixing required for multi-stage combustion now under development by most gas turbine manufacturers. The difficulty with any large volume premixing area is the potential for explosion and the consequent safety hazard it poses. A considerable amount of research should be applied to the area of premixing gas turbine fuel and air to minimize the possibility of an explosion. This data needs to be characterized for a wide range of liquid and some future gas fuels, as each manufacturer will have to have particular design features that address this concern.

One of the design objectives of any combustion system, particularly a catalytic system, is a satisfactory life of the parts. Practical life expectancies must be established for various catalysts as well as system designs that would allow easy access to change the catalyst should the life be shorter than the application requirements. For instance, the peaking application offers opportunities to change parts at frequent intervals. Base and intermediate load operation is much more restrictive and would permit a change-out probably no more often than once every 8000 hours. Catalyst life at the higher turbine temperatures contemplated in the future needs to be established.

The progression of turbine inlet temperatures in the past and the estimated future is shown in Fig. 2. While catalysts can be demonstrated for today's temperatures, work needs to be started now to demonstrate their applicability to the higher temperatures required for gas turbines in the future.

Within the next ten years it is expected that coal-derived liquids will be available for gas turbine fuels in at least a limited sense. The type of coal-derived liquid may vary with the type of coal and change considerably with the process used for conversion. If catalytic elements applied today would not be compatible with future coal-derived liquids, then they would have a very limited application lifetime. Demonstration of the types of contaminants in coal-derived liquids that could affect catalyst lifetime must be shown in order to confidently plan new combustion systems for the future. Coal-derived gases have the same variability, depending on the process, and also must be tested for catalyst compatability.

The potential problems mentioned above are not intended to be a complete list but only some of the more significant problems that have been identified at this time. Many of these are receiving attention at the moment, and it is expected that all will be on some path to solution before the end of 1979. Establishing a data base that will allow people to proceed with the design of catalytic combustion systems is an immediate priority and is being addressed in various areas.

Current EPRI Work

Several groups are working on catalytic combustion, including DOE, EPA, combustion turbine manufacturers, several R&D companies, component manufacturers, and EPRI. Current EPRI concerns and work are directed at several areas. The first, of course, is to develop an overall plan for establishing catalytic combustion in gas turbines. As mentioned previously, this involves one solution to retrofit existing turbines in the field and another solution to create a data base for designing new machines. Since it is considered a significant problem to establish future priorities, a test for catalyst poisoning with coal-derived liquid fuels is being pursued immediately. If special work is to be required for the use of coal-derived liquids, it must be identified now, as a solution could be quite lengthy. Since some future fuels could have significant fuel-bound nitrogen, it is important to establish the ability to convert fuel-bound nitrogen in a combustion turbine using catalytic systems. Work will commence in 1979 to identify the most significant combustion schemes that would enable high fuel-bound nitrogen to be converted to free nitrogen in a catalytic system. The amount of this conversion is important in order to establish the future of fuel economics. Other projects expected to start in 1979 as part of the EPRI program will be a characterization of the premix requirements, with an emphasis on necessary data to minimize explosion potential, and data to establish possible lifetimes of various catalytic elements.

Owing to the great potential exhibited by catalytic combustion experiments to date, a system of this type applied to combustion turbines must be pursued with all possible speed. Since catalytic combustion is the first new type of combustion system applied to turbines since they have been used for power generation, a considerable amount of work needs to be accomplished in order to properly establish a design data base. It is difficult to say when all this work will be done so that turbine designers can confidently proceed to design reliable combustion systems. Hopefully, in five years we would start to see combustion systems being offered for units in the field and the next generation of gas turbine designs that should be commercialized within 10 years would use some form of catalytic combustion, either as a basic combustion system or as an option for the domestic U.S. market.

References

1. Spencer, D., Gildersleeve, O., "Market Potential for New Coal Technologies," EPRI Journal, May 1978, p. 19.

2. "Clean Coal - What Does it Cost at the Busbar?" EPRI Journal, November 1976, p. 6.

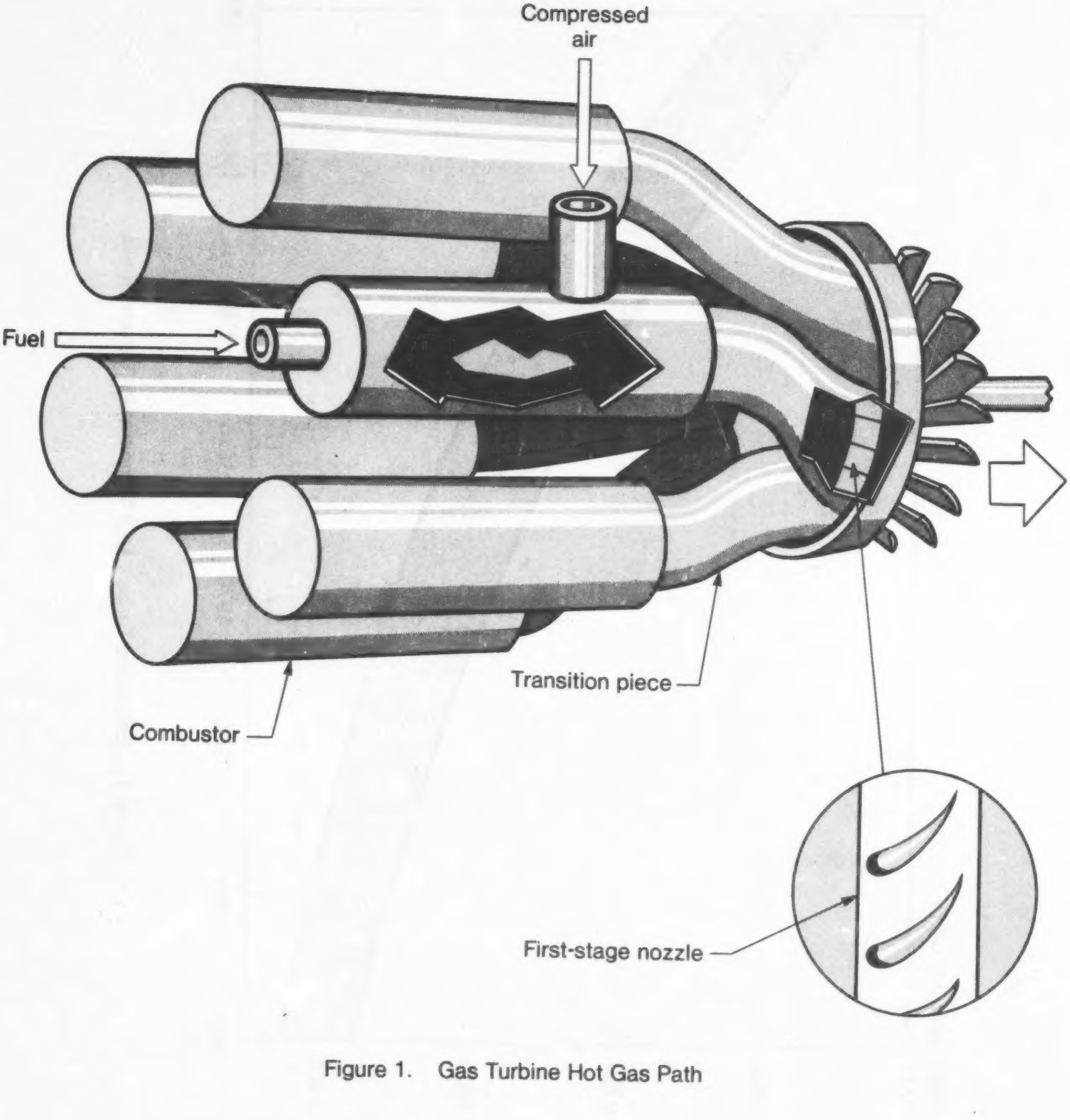

Figure 1. Gas Turbine Hot Gas Path

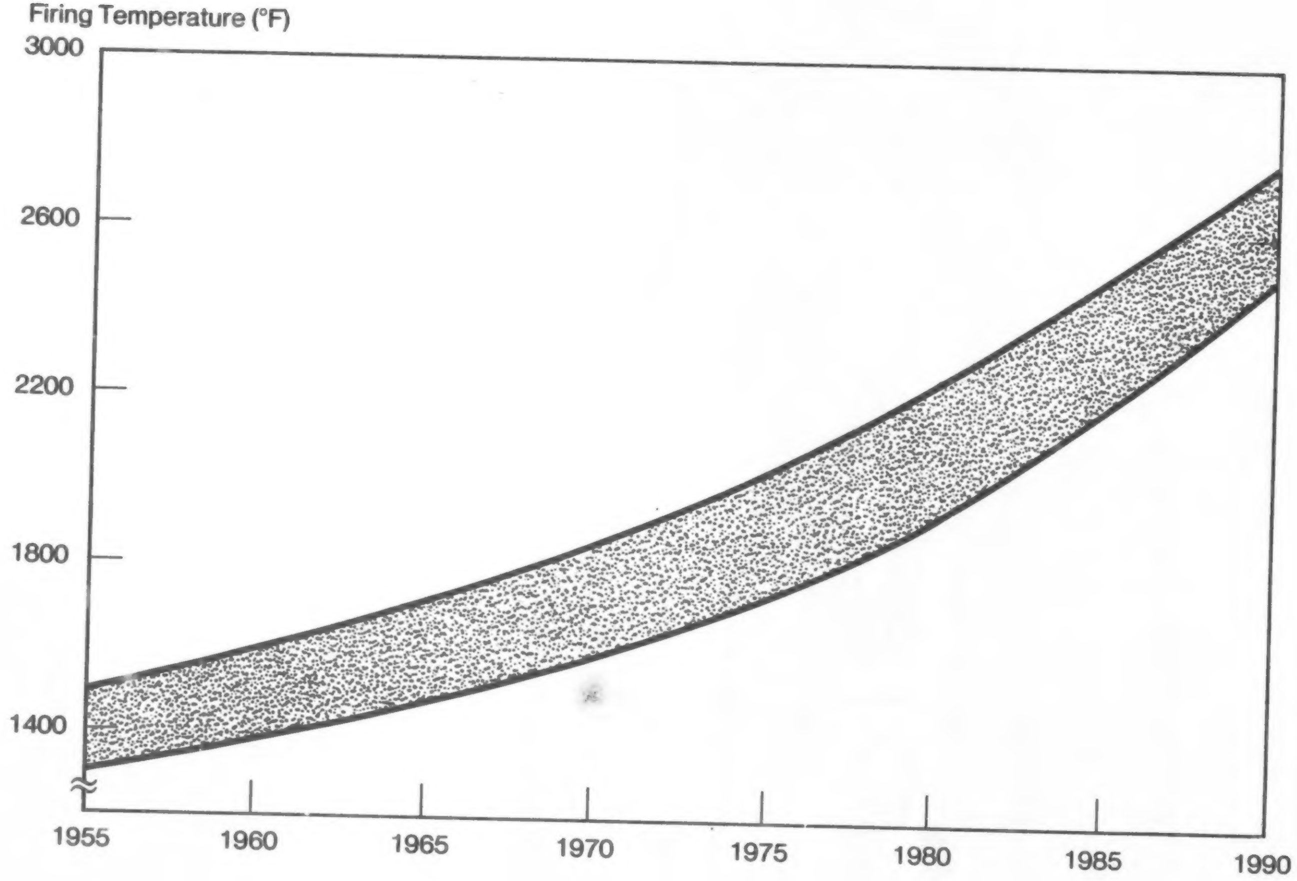

Figure 2. Estimated Turbine Inlet Temperature Versus Years

OVERVIEW OF CRIEPI CATALYTIC COMBUSTION RESEARCH PROGRAM

By:

Yoshimi Ishihara and Hisashi Fukuzawa
Energy and Environment Laboratory
Central Research Institute of Electric Power Industry
Tokyo, Japan 182

ABSTRACT

The objective of this research program is the development of new types of low-NOx-emission utility boilers and high-efficiency gas turbines through the catalytic combustion of light fuel oils, such as naphtha and NGL, or fuel gases.

The steam temperature used in steam power plants is limited to 538°C or 566°C by the thermal fatigue characteristics of the metals used for the steam pipes. Steam at this temperature can easily be obtained by heat transfer with gas at 1000°C, without the need for higher-temperature gas. Fuel can be completely burned at 1000°C through the application of catalytic combustion. Moreover, the catalyst bed can be cooled and the temperature maintained at approximately 1000°C by the use of immersed water tubes and steam tubes. We anticipate that the use of this method of combustion will enable reduction of the NOx concentration to below the level obtainable by flue gas treatment for NOx control (30 ppm or less).

Gas turbine efficiency can be improved by raising the combustion gas temperature, but this has the negative effect of increasing the NOx concentration.

CRIEPI is planning to investigate combustion methods combining two-stage combustion, flue gas recirculation, and catalytic combustion for the maximum reduction of NOx formation.

Preceding page blank

INTRODUCTION

Control of NOx emissions from stationary sources in Japan is prescribed by type of fuel and type and capacity of equipment as shown in Table I. In metropolitan and industrial areas where the environmental standards cannot be met even if the emissions regulations laid down by the government are observed, stationary sources are placed under even tighter controls by agreement with local governments. To restrict total emissions to below current levels, it is necessary to strengthen emission control measures for existing plants. Moreover, the maximum possible reduction is required for the construction of new plants. Thus, for the natural gas boilers in the Chita Thermal Power Plant of the Chubu Electric Power Company, which was constructed in 1977, the NOx concentration was reduced to approximately 50 ppm by combustion control. Then, further reduction to approximately 10 ppm was achieved by the installation of NH_3 catalytic reduction equipment.

Fuels which can be easily gasified are currently being used in Japan for power generation. In 1977, $3,805 \times 10^3$ kℓ of naphtha, $5,586 \times 10^3$ tons of liquid natural gas (LNG), and $2,990 \times 10^3$ kℓ of natural gas liquid (NGL) were used. Consumption of LNG and NGL is tending to increase.

In boilers burning these fuels, NOx in flue gas can be easily reduced to 100 ppm or less by improved combustion control to meet the regulation values set by the government. However, in the installation of new utility boilers, cases in which it is necessary to reduce NOx to the maximum extent possible by flue gas treatment (FGT) for NOx control are anticipated to increase.

Catalytic reduction with NH_3 as an additive is already capable of practical application as an FGT process for NOx control. This process yields clean flue gas containing almost no SO_2 or particulates, equivalent to the combustion gas from the fuels mentioned above. However, consumption of a large quantity of

NH_3, which in itself requires a considerable input of energy, is not desirable from the viewpoint of energy conservation.

If the combustion temperature in the boiler is reduced to approximately 1000°C, it is thought possible to reduce the concentration of NOx to the same level as that enabled by FGT technology. In other words, it is considered possible to develop an energy-conserving, low-NOx boiler.

With this concept, CRIEPI has initiated research in catalytic combustion and will set up experimental equipment this year.

In addition, CRIEPI is cooperating in a government-sponsored project to develop a combined-cycle system employing a steam turbine and a high-temperature gas turbine burning clean fuels such as natural gas, naphtha, or kerosine. It is well known that the NOx concentration is increased by raising the combustion gas temperature in a gas turbine. Thus, NOx countermeasures are required. Although catalytic combustion does not come within the purview of this project, CRIEPI research into catalytic combustion includes the application of NOx control to the burner of high-temperature gas turbines.

This paper describes the current status of catalytic combustion technology in use in Japan and introduces the CRIEPI R&D program on both catalysts and catalytic combustion systems. The aim of this program is the application of catalytic combustion technology to low-NOx, high-efficiency power plants.

CURRENT STATUS OF CATALYTIC COMBUSTION TECHNOLOGY IN JAPAN

Catalytic combustion has been in use for several decades in "platinum pocket heaters" (portable warmers) for the advantages of low temperature in comparison with flame combustion as well as the property of combustability without flame. With this heater, cotton wool in a container is soaked with petroleum benzine or ethyl alcohol as a fuel. This is then covered by glass wool with platinum catalyst. As fuel vapor diffuses to the outside through the platinum catalyst, it gradually oxidizes and generates heat. This is used in cold areas to warm the hands or a part of the body when fishing or playing golf.

Catalytic combustion equipment has recently been installed for deodorization of waste gas from plastic fabrication, printing, and paint factories. Table II shows some examples of major installations (Reference 1).

CRIEPI R&D PROGRAM ON CATALYTIC COMBUSTION

BACKGROUND

The steam temperature of recently-constructed steam power plants has frequently been limited to 566°C (1005°F) or 538°C (1000°F) due to such factors as the strength of the pipe steel at high temperatures, oxidation corrosion, and the cost of materials. Thus, improvement of generation efficiency is being sought by means of raising the steam pressure. To further raise generation efficiency, R&D on a combined-cycle system incorporating gas turbines is being advanced. Steam at 538 - 566°C is easily obtained by heat exchange with gas at 1000°C.

NO formed by the thermal reaction between N_2 and O_2 in the process of combustion, i.e., thermal NO, is controlled by the combustion temperature, fuel/air ratio, and residence time in the combustion zone. The effect of the combustion temperature is particularly large. Hence, if the combustion temperature is reduced to 1000°C, it is thought to be possible to reduce the concentration of NOx to the level obtainable by FGT for NOx control.

Catalytic combustion enables the complete burning of fuel at 1000°C. Since the operating conditions of a catalytic combustor are limited by the critical temperature of the catalyst, development of a catalyst which can be used at 1000°C and a catalyst bed cooling system is necessary.

RESEARCH PROGRAM

Figure 1 shows the boiler being considered by CRIEPI for catalytic combustion at 1000°C. Fuel gas consisting of vaporized fuel and flue gas recirculated from the inlet or outlet of the air preheater is premixed with air and introduced to the catalyst bed and burned. The heat generated by this combustion is cooled and removed by the water tubes of the steam generator, which are arranged over the catalyst bed,and the steam tubes of the steam superheater. The temperature in the catalyst bed is thereby maintained at approximately 1000°C. Exhausting of flue gas which has passed through the catalyst bed from the stack through a heat exchanger such as a steam reheater, economizer, or air preheater is the same as with conventional boilers.

Figure 1 shows catalytic combustion of fuel in a single stage. However, to maintain a uniform temperature distribution in the direction of the gas flow in the catalyst bed, combustion which introduces the fuel/air mixture in multiple stages is required.

Promotion of R&D on a high-efficiency gas turbine by the Agency of Industrial Science Technology of the Ministry of International Trade and Industry began this year. CRIEPI is participating in this project by conducting research on combined-cycle power plant systems and heat-resistant materials and cooling systems.

Although the CRIEPI research on the application of catalytic combustion to gas turbine combustors is separate from the MITI research project, R&D on a low-NOx combustor is being advanced along the lines of the concept shown in Fig. 2.

CRIEPI shaped its approach to research on the control of NOx for power plant boilers employing catalytic combustion three years ago. Research will be promoted after the installation of experimental equipment this year. We are aware that EPA is carrying out research with the same objective. Several of the reports issued by EPA and the Acurex Corporation have been interesting and instructive to us (References 2, 3, 4, 5).

CRIEPI has initiated research in the following three areas.

(1) Development and selection of catalysts
(2) NOx emission control by combustor modifications and manipulation of operating conditions
(3) Cooling systems for catalyst bed temperature control

DEVELOPMENT AND SELECTION OF CATALYSTS

Two types of catalyst are being investigated: catalyst for utility boilers to be used at approximately 1000°C and catalyst for the combustor of high-efficiency gas turbines which can be used at 1300 - 1400°C.

The catalyst for utility boilers must have sufficient catalyst life under operating conditions which not only permit complete combustion of the fuel but also minimize NOx formation. In addition, to improve the heat transfer efficiency of the steam generator or steam superheater installed in the catalyst bed, it is expedient to maintain a uniform temperature distribution in the direction of the gas flow in the catalyst bed. For this purpose, it is necessary to select a catalyst having moderate activity.

Since it is necessary to raise the inlet temperature of a gas turbine to 1300 - 1400°C, the catalyst for a high-temperature gas turbine must be one which can be used at these temperatures. Moreover, since it is desirable to make the catalyst bed small in order to make the combustor compact, the catalyst must have high activity.

CRIEPI has been conducting research on NOx control by catalytic reduction for the past five years, and various types of catalyst have been investigated. In applying these investigations to research on a catalyst for catalytic combustion, the following items were studied in order to clarify the characteristics required of a suitable catalyst.

- High operational temperature capability
- Combustion rate of fuels with each catalyst
- Catalyst life at high temperature

NOx EMISSION CONTROL BY COMBUSTOR MODIFICATIONS AND MANIPULATION OF OPERATING CONDITIONS

NOx formed by combustion of fuels which do not contain nitrogen compounds, such as LNG, NGL, and naphtha, is termed "thermal NOx." Formation of thermal NOx increases as the combustion temperature is raised. In addition, the effects of the fuel/air ratio and residence time in the combustion area are particularly significant. If a fuel rich condition occurs due to an increase in the fuel/air ratio, CO and unburned hydrocarbons will form in the flame, resulting in a reducive atmosphere. Consequently, formation of NOx will reduced. In staged combustion, fuel rich combustion is performed in the first stage and complete combustion can be performed by adding air in the second stage. A remarkable reduction in NOx formation can thereby be achieved. Moreover, since the flame zone is larger in staged combustion and the maximum flame temperature may be lower, NOx formation is reduced. Flue gas recirculation permits reduction of the NOx concentration both by a lower combustion rate due to the reduced oxygen concentration as well as the lower combustion temperature resulting from the addition of low-temperature gas. A remarkable reduction of the NOx concentration, equivalent to that possible with conventional combustion, can be achieved by the application of staged combustion and flue gas recirculation to catalytic combustion.

CRIEPI plans to apply staged combustion and flue gas recirculation to catalytic combustors with the objective of using this technology in both utility boilers and gas turbine combustors.

COOLING SYSTEMS FOR CATALYST BED TEMPERATURE CONTROL

When catalytic combustion takes place at temperatures above 1000°C, the fuel combustion reaction proceeds not only on the surface of the catalyst but also in the gas itself. In order to maintain the temperature of the catalyst bed below the critical temperature of the catalyst, it is necessary to provide for cooling of the catalyst bed.

For catalytic combustion applied to utility boilers, methods of cooling the catalyst bed by the installation of water tubes or steam tubes in the bed are being studied.

Thermal conduction in the catalyst bed is complex, comprising not only conductive transfer between the catalyst and the metal tubes but also convective and radiative heat transfer.

CRIEPI is conducting preparatory experiments with the objective of obtaining basic data for the design of experimental equipment for catalytic combustion. These experiments employ built-in cooling pipes and a device which circulates high-temperature flue gas in a duct filled with catalyst.

Since it is thought that a prototype catalytic combustor is required for the precise investigation of a cooling system for the catalyst bed, this research is concentrated mainly on an investigation of cooling systems which maintain a uniform temperature of the experimental equipment when operating at high temperatures. It is expected that the results of this investigation will provide useful information for the next step of development.

Both the addition of excess air and water injection are being used to lower the gas temperature at the inlet of gas turbines. However, both of these measures are undesirable in that they degrade thermal efficiency.

Our research indicates that it is possible to reduce the combustion temperature to 1300 - 1400°C by flue gas recirculation if the excess air is reduced to near the theoretical values. Further, it appears possible to reduce NOx by means of a lower combustion temperature in combination with staged combustion.

Various problems in connection with the application of catalytic combustion to boilers and gas turbines will be studied this year and next. In addition to model experiments for utility boilers using small-scale catalytic combustion experimental equipment with a built-in cooling system for the catalyst bed, model experiments for gas turbine combustors using pressurized-combustion experimental equipment are planned.

REFERENCES

1. Nakayama, T. Catalytic Combustion Reaction. J, Japan Petroleum Institute, 19(3): 247-251, 1976

2. Thompson, R. E., Pershing, D. W., Berkau, E. E. Catalytic Combustion, A Pollution-Free Means of Energy Conversion ? EPA 650/2-73-081, U.S. Environmental Protection Agency, NTIS No.PB 223-0020, August 1973, 51 pp.

3. Kesselring, J. P. Catalytic Oxidation of Fuel for NOx Control from Area Sources. EPA 600/2-76-037, U.S. Environmental Protection Agency, February 1976, 194 pp.

4. Martin, G. B. Evaluation of a Prototype Surface Combustion Furnace. In: Proceedings of the Second Stationary Sources Combustion Symposium, Volume III New Orleans, LA, August 29 - September 1, 1977, pp. 255 - 278

5. Kesselring, J. P., Krill, W. V., Kendall, R. M. Design Criteria for Stationary Sources Catalytic Combustors. In: Proceedings of the Second Stationary Sources Combustion Symposium, Volume III, New Orleans, LA, August 29 - September 1, 1977. pp. 193 - 228

TABLE 1. EMISSION STANDARDS FOR NITROGEN OXIDES FROM EXISTING AND NEWLY INSTALLED FACILITIES

Kind of facility	Flue gases*1	Standard values Existing facilities (ppm)	Newly installed facilities (ppm)
Boiler			
Gas firing	(a)	130	100
	(b)	130	130
	(c)	150	—
Coal firing	(a)	750	—
	(b)	750	—
	(c)	750	—
Solid-fuel firing	(a)	600	480
	(b)	600	480
	(c)	600	480
Oil-tar firing	(a)	280	—
	(b)	280	—
	(c)	280	—
Other types	(a)	230	150
	(b)	190*2	150
	(c)	—	150
Metal-heating	(a)	220*3	100
	(b)	220*3	150*3
	(c)	220*3	150*3
Oil-heating furnaces*4	(a)	210	100
	(b)	210	100
	(c)	180	150
Cement-sintering furnaces	(a)	—	250
Coking coal furnaces	(a)	—	200

Note: *1 (a) 100,000 normal m^3/h and over. (b) 400,000 normal m^3/h to less than 100,000 normal m^3/h. (c) 100,000 normal m^3/h to less than 40,000 normal m^3/h.

*2 Excluding those incorporated in (or under construction) sulfur oxide treatment facilities.

*3 Heating furnaces for welded steel pipes are excluded.

*4 Excluding cracking furnaces and independent heating furnaces for ammonia production.

TABLE II. EXAMPLES OF CATALYTIC COMBUSTION IN OPERATION

Industry	Flue Gas Components	Gas Concentration as C_6 (ppm)	Flow Rate of Flue Gas (Nm^3/min)	Catalyst Bed Temperature Inlet (°C)	Gas Concentration as C_1 (ppm)
Photogravure printing	Toluene IPA Ethyl acetate Butyl acetate	300 - 1,000	30	270	7
Photogravure printing	Toluene n-Hexane	800 - 1,000	50	305	10
Magnetic printing	Toluene MEK MIBK Chlorine compounds	1,200 - 2,500	60	270	8-10
Metal printing	Toluene Xylene MIBK Butanol	500 - 1,500	30	270	7-10
Synthetic resins	Methanol Formalin Phenol	1,200 - 1,500	100-130 100-130	200 200-250	1-3 10-20
Synthetic resins	Phenol Formalin Toluene Methanol Acetone	1,200 - 1,500	350	250	3-4

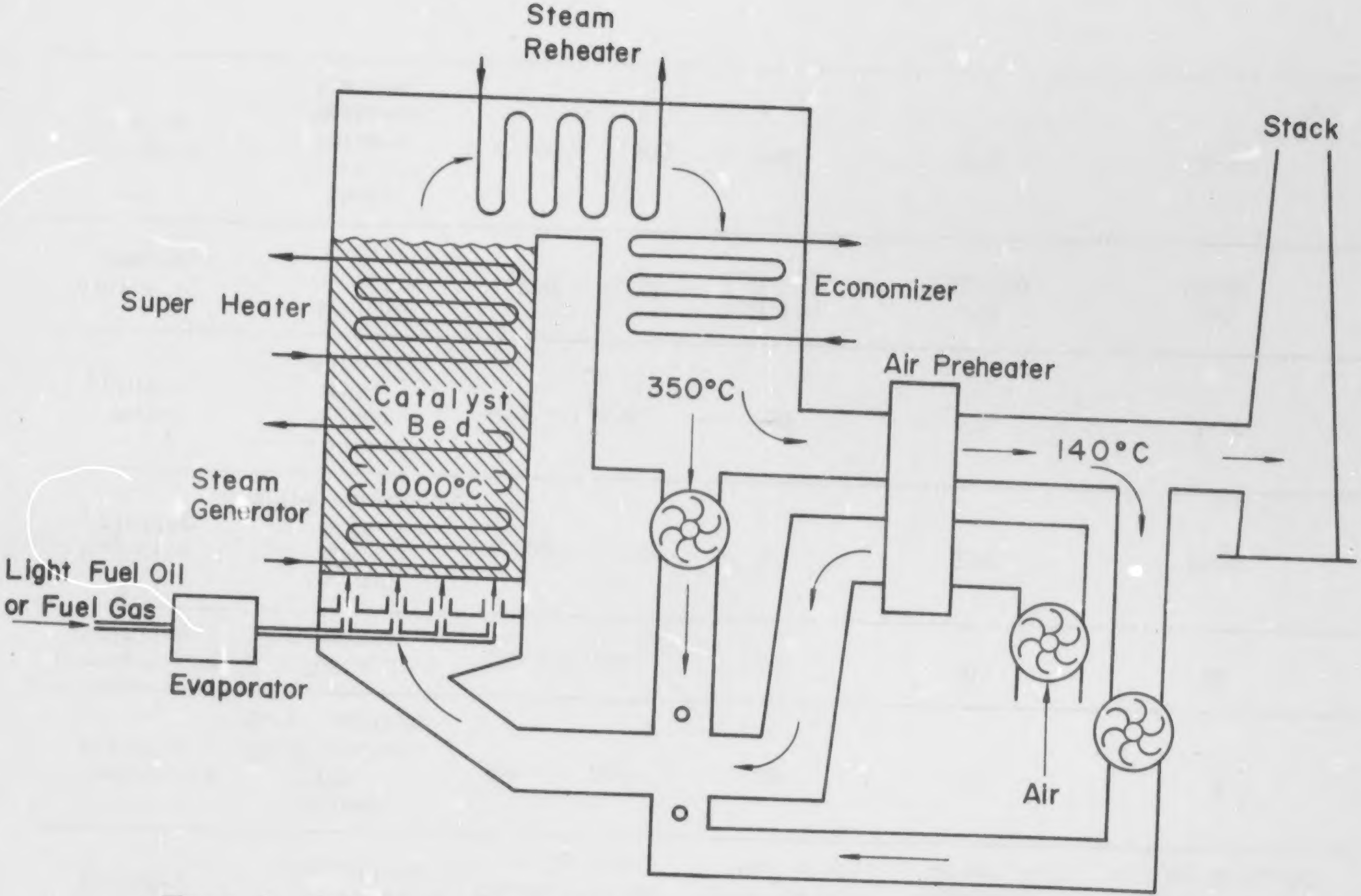

Figure 1 Schematic Figure of Catalytic Combustion Utility Boiler

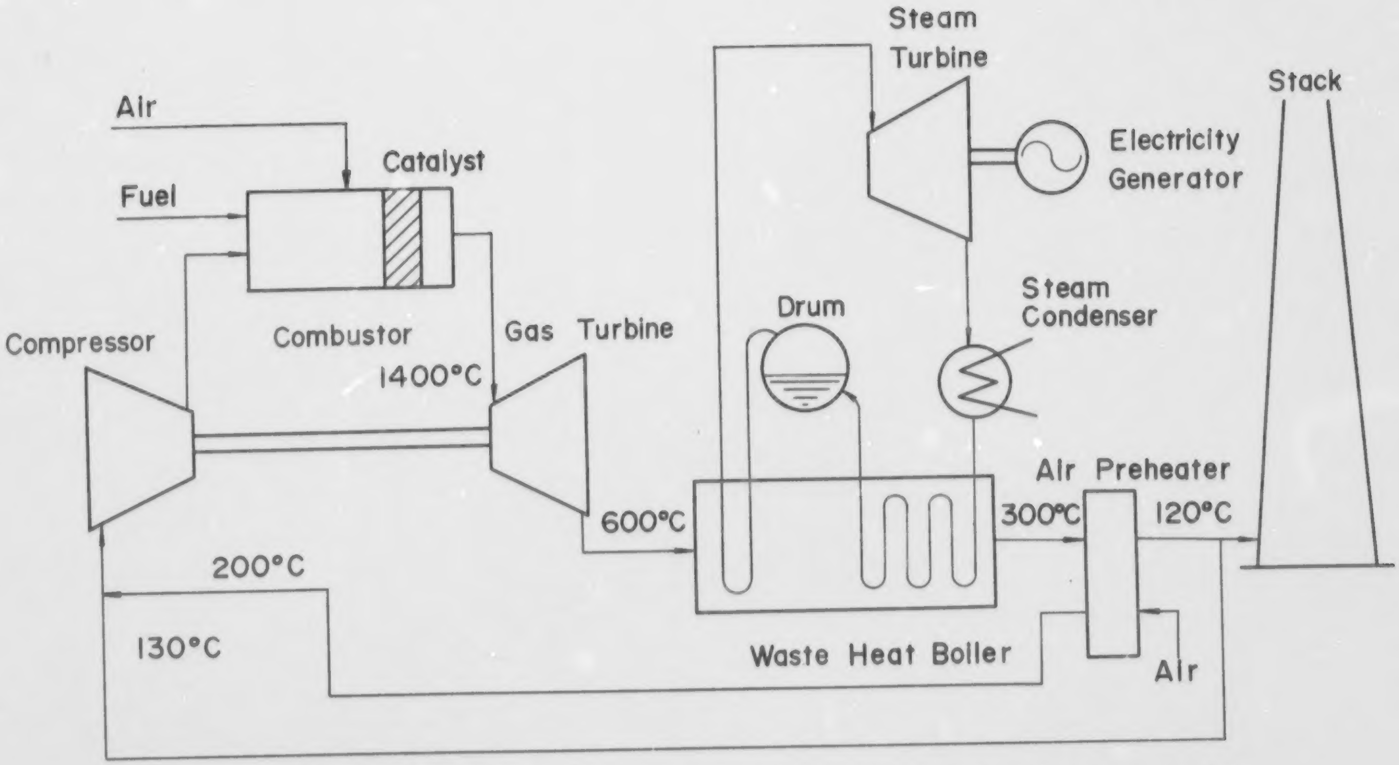

Figure 2 Schematic Figure of a High Efficiency Gas Turbine System Having Low NOx Combustor

#6 FUEL OIL CATALYTIC COMBUSTION

By

J. T. Pogson*

and

M. N. Mansour**

October 1978

*Project Manager, Energy & Environmental Division, Acurex Corporation

**Project Manager, Research & Development Department, Southern California Edison Company

ABSTRACT

A test program to demonstrate the feasibility of burning #6 fuel oil in a catalytic combustor has been completed. Sixteen hours of experimental testing were accomplished, demonstrating that stable catalytic combustion of heavy fuel oils is feasible. Test parameters included an air preheat temperature of 800°F, air/fuel ratios from 11.6 to 15 and 25 to 45, bed heat release rates from 47,500 to 116,675 Btu/hr, and bed temperatures from 1950°F to 2310°F.

While the feasibility test program was successful, considerable design and development testing is required to adapt the catalytic combustor to existing systems. Improved fuel oil delivery and ignition systems and the elimination of flashback potentials must be addressed. At the same time, catalyst and bed materials resistant to thermal shock and capable of long life operation at near stoichiometric air/fuel ratio without the use of large quantities of diluent to moderate flame temperature must also be developed.

Preceding page blank

ACKNOWLEDGEMENTS

This paper describes the work accomplished under Contract V3257907 for the Southern California Edison Company. The authors are grateful to the many individuals of the Acurex/Aerotherm staff who were of assistance during this program. We would particularly like to thank Messrs. Ed Chu, Scott Hagaman, Kerry Seifert, and Patrick Cawley for their operation of the test facility and assistance in the data acquisition.

INTRODUCTION

The primary purpose of the project described in this paper was to demonstrate the feasibility for catalytic combustion of #6 fuel oil. Catalytic combustion offers the potential for an alternate technology to reduce NO_x emissions from the nation's stationary sources. This technology, while still in its research stage, has been recognized and demonstrated in previous programs with gaseous and light distillate fuels oils, (1)*, (2) and (3). Catalytic combustion of very low nitrogen content fuels produces low NO_x, CO, and unburned hydrocarbons due to its inherent temperature control capability and a concurrent promotion of oxidation reactions. Typically, CO and unburned hydrocarbon emissions are less than 5 ppm and thermal NO_x emissions are 10 ppm corrected to 3 percent excess oxygen. Preliminary test results have also indicated that a reduction in the conversion of fuel nitrogen to NO_x may be achieved in a catalytic combustor when gaseous and light fuel oils are doped with nitrogen containing compounds (3). Conversion rates of organic bound nitrogen to NO_x of less than 20 percent have been demonstrated with two-stage rich/lean catalytic burners.

The objective of the present program was to demonstate for a minimum of 10 hours both rich and lean combustion of #6 fuel oil in a graded cell catalytic combustor. During this investigation, preliminary data were acquired to determine the combustor system performance and emissions. The obtained test results were intended to provide a baseline data for further development activities.

Prior to this project catalytic combustion testing had used gaseous or light distillate oil fuels. These fuels require less complex fuel delivery systems and permit the investigator to place his primary attention on the study of the combustion process. Therefore, to examine the type of experimental problems associated with catalytic combustion of #6 fuel oil, several pre-project experiments were conducted. Specific objectives of these pre-project experiments were:

---

*Numbers in parentheses designated references.

1. Develop a #6 fuel oil delivery system that could supply the low flow rates required for this test program
2. Select a fuel oil atomizing nozzle that would not plug or be carbonized by the catalytic combustor radiant heat load
3. Determine the potential for fuel oil build-up on the duct walls upstream of the catalytic combustor
4. Determine the potential for flashbacks and flame holding due to the presence of atomized fuel mist upstream of the combustor bed
5. Test and inspect the catalytic combustor for fuel oil fouling at the combustion surfaces
6. Identify a safe light-off technique.

The initial experimentation was conducted during November 1977 in the Acurex/EPA high pressure catalytic combustion facility. This facility was used only during these pre-project tests because the Acurex-owned atmospheric test facility had not yet been completed.

DESCRIPTION OF HARDWARE

Catalytic Combustor

The demonstration of #6 fuel oil was conducted in a small-scale Acurex experimental test facility. The operational portion of the test facility is shown in Figure 1. The entire combustion apparatus is enclosed within a fume hood to keep all combustion products from the surrounding room. An overview of the lab is shown in Figure 2. Premixed fuel/oxidizer flows vertically downward through an expansion chamber and is encompassed by a chamber heater (Figure 3) that maintains the temperature of the gases entering the system at the desired level.

The gaseous fuel and oxidizer flow is monitored through an external control panel shown in Figure 4. Rotameters are used to set gas flow to the desired rates. Gas pressures are both regulated and monitored from the front panel.

A 36-kilowatt heater is installed on the oxidizer flow line. This heater is designed to allow the mixture of fuel and oxidizer to enter the catalyst bed at temperatures up to 1000°F. The temperatures of both the oxidizer heater and the maintaining heater around the expansion chamber are controlled with solid state controllers. These temperatures are read out with the heater controllers on the front panel.

Twenty-four channels of thermocouple readout are available for instrumenting various combustion systems. The thermocouples (Type K) are fed from the interior of the combustion chamber fume hood through a heavy duty thermocouple junction box (Figure 1, No. 11). These thermocouple readouts are shown in Figure 4 at the bottom of the right-hand console.

Fuel and oxidizer are mixed downstream of the oxidizer heater immediately before entering the expansion chamber. Flame guards are placed in the fuel line to prevent accidental flashbacks. A rupture disk is located in the top of the expansion chamber to allow venting should a major overpressure occur.

Catalyst beds are placed within a quartz reaction chamber (Figure 1, No. 3) so that a window could be cut through the surrounding insulation to view the catalytic reactor during the experiments. Combustion gases move vertically downwards, enter the catalytic reactor, and after reaction enter a watercooled manifold where they make two 90° turns and are exhausted into the top of the fume hood.

A water-cooled sampling probe is available to monitor combustion products. This probe extracts a gas sample from the combustion gas flow and passes it into a heated sample line where it is transmitted to the emissions bench. The emissions bench consists of instrumentation capable of analyzing the concentrations of NO, NO_x, CO, CO_2, O_2 and unburned hydrocarbons in the exhaust system utilized in the facility. Figure 5 illustrates the emissions sampling system utilized in the facility.

At the bottom of the water-cooled manifold there is a viewing port attached to a standoff tube. Through this viewing port, an observer can readily see the catalytic combustor along its axis during operation. The viewing port also allows an optical pyrometer to be used to determine bed temperature.

Fuel Delivery Systems

Since the control panel associated with the Atmospheric Catalytic Combustion Facility is capable of providing only gaseous fuel control, and the program conducted for SCE used #6 fuel oil, a separate fuel delivery system was required to introduce the liquid fuel into the combustion chamber. Figure 6 is a schematic diagram of the fuel delivery system that was fabricated to deliver #6 fuel oil into the preheated oxidizer gases in the expansion chamber of the facility. A 55-gallon drum of oil served as a reservoir. This drum was heated electrically by the use of both blanket heaters and an immersion heater. These heaters were able to provide close temperature control to 200°F, the temperature at which most tests were conducted.

To obtain the degree of fuel atomization required, a gas atomized fuel nozzle was used during the test program. As shown in Figure 6, the atomizing gas line was passed through the drum of oil to be heated to about the same temperature as the oil it was to atomize. This was done to prevent potential oil viscosity increases due to an abrupt temperature drop when the oil came in contact with the atomizing gas as it left the nozzle. Fuel flow was measured by a meter designed to transmit a pulse with each revolution, thus signaling the passage of a discrete volume of liquid. A pulsed digitizer was attached to the output of the flow meter, and the flow rate was determined by averaging the number of pulses over a given period of time, using the calibration factor of the meter. A calibration was conducted on this meter using #6 fuel oil under temperatures and pressures that were encountered during the tests and the volume per pulse was measured to be 5.1 cm^3.

RESULTS AND DISCUSSION

Thirty-two tests were conducted under this project. Air/fuel ratios ranged from 11.6 to 15 and from 25 to 45, with heat release rates from 47,500 to 116,700 Btu/hr, and air preheat held nearly constant at approximately 800°F. Fuel oil was atomized with air, nitrogen, and argon (1 to 1.4 scfm) during the various tests. A total of 16 hours of catalytic combustion demonstration tests were performed.

During the tests, the combustor ceramic surface temperatures varied from 1950°F to 2310°F. Temperatures were limited to less than 2400°F by the quartz enclosure. Temperature control was achieved by the use of either nitrogen or argon diluent to moderate the flame temperature. Diluent volumetric flow rates ranged from zero to twice the air flow rate, depending upon the air/fuel mixutre. As has been shown in previous studies, catalytic combustion at temperatures below 2300°F does not produce significant thermal NO_x. Therefore, the data was examined without parameterizing the combustor bed temperatures to quantify its affect on NO_x formation.

Four different fuel delivery set-ups were used during the test series. Test facility modifications were made following each test series to improve combustion stability. The initial configuration utilized a venturi section with a fuel nozzle mounted approximately 8 inches above the catalyst bed. The oil entrance port was oriented horizontally in the venturi restriction, and an adapter/holder for a Delavan nozzle was used to effect a 90° turn. Tests conducted on this configuration were not stable. Build up of carbonaceous and gummy deposits were experienced on the surface of the catalyst bed, and a significant amount of unburned fuel droplets were noted passing through the bed. Additionally, flashbacks to the tip of the nozzle occurred with such frequency that useful data could not be obtained.

Observation of the combustion process indicated that there was insufficient distance from the nozzle to the catalyst bed for significant vaporization of the oil. Initial calculations had indicated that a distance of only 4 inches should have been sufficient; however, these calculations were based on idealized conditions that were not being met by the configuration.

The distance between the fuel nozzle and the catalytic combustor was then increased. This was accomplished by positioning the nozzle within two coaxial tubes. The largest diameter of the outer tube was three-quarters of an inch, which allowed it to fit down from the top of the expansion chamber. For these tests, the nozzle was positioned about 14 inches from the entrance to the catalyst bed. Operationally, this configuration significantly improved the performance of the system. Although flashbacks still occurred, the frequency of these occurrences was reduced to the extent that data could be easily collected between the flashbacks. A great number of ash particles were generated during this experiment. Subsequent analysis showed that the ash particles were approximately 95 percent carbon or hydrocarbon.

This set of experiments was discontinued when severe catalyst bed degradation was noted. Post-test observation of the catalyst bed indicated that the zircon mullite section had partially melted and the exterior of the fuel delivery nozzle was coated with oil and carbon. This buildup on the exterior of the nozzle indicated that eddies were being formed around the end of the nozzle/fuel delivery tube. Material was being swept up into these eddies and deposited on the nozzle. Configuration modifications to prevent a recurrence of this problem were made. To overcome buildup on the outside of the atomization nozzle, combustion air was forced over the surface by fabricating a flow director that attached around the nozzle. For a test series with this modification, the nozzle was placed 18 inches from the entrance to the catalyst bed. This location allowed a spacing of 1/2 inch between the edge of the flow director and the walls of the conical expansion chamber.

Performance of the system was dramatically improved after the addition of the flow director section to the nozzle. Although flashbacks did occur occasionally, they were much less intense than previous flashbacks. The majority of the data taken on the lean side utilized this configuration and catalyst. Post-test examination of the catalyst indicated that the catalyst was in good shape and that there was no fouling due to oil or ash.

The next test series was directed towards rich combustion in a catalytic bed. Combustion under lean conditions allows high volumes of air to flow through the system. Under rich conditions, however, the amount of air flowing through the system is reduced. It was found that with the nozzle and flow director placed at the location 18 inches from the entrance to the bed, there was insufficient air flow forced through the flow director. Flashbacks again became a problem. Additionally, the presence of the lead-out wires from the thermocouples in the slowly moving, highly loaded rich mixture caused the formation of bridges of carbonaceous material across the wires. This bridging became so severe that the entire 90 mm diameter of the quartz reactor was covered. The combustion taking place in the bed was extremely irregular and unstable. The experiment ended with no data collected. To remedy these problems, the entire nozzle assembly was moved further into the conical expansion chamber to direct the majority of the air flow across the surface of the nozzle. This was accomplished by raising the fuel delivery assembly to 22 inches from the entrance to the catalyst bed. At this location, there was an annulus of 1/4 inch between the walls of the expansion chamber and the flow director.

With this modification, the rich combustion tests were run with little difficulty. The system behaved in a stable manner with few flashbacks. Subsequent examination of the system after the rich combustion test series showed that there was negligible fouling of the walls, or nozzle. Figures 7 and 8 show the catalyst after completing the last series of tests. There also was no visual evidence of oil or ash fouling.

The NO_x levels and nitrogen conversion to NO_x obtained during the test program are shown in Figure 9 as a function of the air/fuel ratio. As indicated in Figure 9, NO_x emission levels, increased from a value of 208 ppm at an air/fuel ratio of 11.8 ($A/F = 14$ at $\phi = 1$) to 1099 ppm at an air/fuel ratio of 30. This corresponded to nitrogen conversion efficiencies of 18 percent and 95 percent, respectively, at the aforementioned air/fuel ratios. Due to the low-catalytic burner flame temperature all measured NO_x was considered to be fuel-nitrogen generated.

The data shown in Figure 9 illustrate that during combustion of rich air/fuel ratios, the conversion of fuel nitrogen is low, while during lean combustion the catalytic burner approaches 100 percent conversion of fuel nitrogen to NO_x. This conversion rate is much greater than that experienced with conventional atomized fuel burners. A possible explanation of this difference may be the fuel stratification which occurs in conventional burners, leading to local rich combustion zones and hence lower nitrogen conversion rates to NO_x.

Also shown in Figure 9 are four data points taken with a separated combustor, which occurred when the zircon mullite test section melted. As illustrated, these correlated data correspond to NO_x levels in the 50 to 100 ppm range, or an order of magnitude lower than that attained with the nonseparated combustor. While several reasons may be advanced to explain this observation, it was felt that the gas phase reduction of NO_x occurred as a result of the bed separation. It was postulated that as the air/fuel mixture passes through the initial section of the combustor there is a partial oxidation of the fuel and a corresponding increase in the mixture temperature and the formation of NO_x precursors (NH_2, HCN, NO). In the subsequent open volume a partial homogeneous reaction occurs at a temperature in the 1000°F to 1500°F range which allows the self-destruction of the NO_x precursors to N_2. Thus, in the remaining section of the catalytic bed, most of the fuel nitrogen has already been destroyed and thus cannot be converted to NO_x.

Figure 10 compares the corrected CO_2 measurements with those predicted from theoretical calculations. The data have been corrected to zero diluent. As shown, fair agreement exists between the data and theory.

The calculated adiabatic flame temperature is compared to the measured thermocouple readings in Figure 11. The measured temperatures were corrected to zero diluent for comparison purposes. Again, the corrected data agree with the predicted temperatures, which indicates that the performance of the combustor system was satisfactory and that the data obtained are reasonable.

Attempts were not made to achieve ignition of heavy fuel oil-air mixtures without the use of gaseous fuels. This decision was made when previous experimentation showed that when the bed temperature dropped below 1800°F the combustor appeared to extinguish itself. That is, the combustor temperature would rapidly drop to the preheat temperature and smoke emissions were visible from the stack. Thus, it was concluded that the 750°F to 800°F preheat would not vaporize the fuel oil sufficiently to permit lightoff.

Table I contains the corrected data for all the data points shown in the previous figures. The NO and CO data are corrected to 3 percent excess O_2. Data for O_2, CO_2, and temperature are corrected to zero diluent. Air/fuel and heat release values are calculated from the measured rotometer and fuel flowrate data.

CONCLUSIONS

The following conclusions may be drawn from the experiments and test data.

- Stable catalytic combustion of heavy fuel oils is feasible using a gaseous fuel lightoff technique and was demonstrated by the series of tests covering 16 hours of experiments.
- Significant vaporization is attained during lean operation with an 850°F preheated air/diluent mixture to provide continuous catalytic combustion of heavy fuel oils without the deposition of significant unburned fuel or ash deposits on the burner.
- Additional design and development of the catalytic burner is required to eliminate unstable combustor operation. Flashbacks occurred when the average velocity of the air/diluent mixture was less than 8 to 9 feet per second.
- Stable burner operation was achieved at air/fuel ratios ranging from 11.6 to 15 and 25 to 45 with diluent to moderate the bed temperature. Even at the lower air/fuel ratios, $\phi > 1.0$, visible smoke emissions were not detected.
- Air/fuel ratios below 15 resulted in low conversion rates of the fuel bound nitrogen to NO_x.
- Catalytic lightoff could not be attained at the lower air/fuel ratios (A/F = 11.6 to 15) because of insufficient fuel vaporization and the tendency for flashbacks to occur.

- Separation of the catalytic combustion support elements, which occurred when the zircon mullite element partially melted, appears to offer a means of reducing nitrogen conversion rates by an order of magnitude below those attained with the standard close packed graded cell combustor.

RECOMMENDATIONS

It is apparent from the tests that additional development efforts are required to provide a reliable heavy fuel oil catalytic burner. One of these activities must be concerned with the development of a higher thermal shock resistant support material.

Other required development efforts are:

- The determination of a fuel atomization system which will require less atomization fluid and permit sufficient vaporization to allow more stable operation at rich conditions. A steam atomization nozzle or a fuel oil prevaporizer may provide such a system.
- Development of a positive heavy fuel oil ignition system to reduce the dependence upon high preheat temperatures.
- Testing of a separated bed combustor to explore the potential for reduced fuel bound nitrogen conversion to NO_x.
- Development of catalytic burner systems which do not require large volumetric flow rates of diluent for temperature control purposes.
- Combined burner system life testing on a subscale combustion rig to establish system reliability and heavy fuel oil contaminate effects.
- Further system characterization to provide scale-up data for greater heat release rates.

REFERENCES

1. Roessler, W. U., et al., "Investigation of Surface Combustion Concepts for NO_x Control in Utility Boilers and Stationary Gas Turbines," Environmental Protection Technology Series Report EPA-650/2-73-014, August 1973.

2. Kesselring, J. P., et al,,"Catalytic Oxidation of Fuels for NO_x Control from Area Sources," Environmental Protection Technology Series Report EPA-600/2/76-037, February 1976.

3. Kesselring, J. P., et al., "Design Criteria for Stationary Source Catalytic Combustion Systems," Acurex Final Report 78-278, March 1978.

TABLE I. DATA CORRECTED TO 3 PERCENT EXCESS O_2

Data Pt. No.	CO_2 0% Diluent	O_2 0% Diluent	PPM CO 3% Excess O_2	NO PPM 3% Excess O_2	UHC PPM 3% Excess O_2	A/F 14.	Q	Corrected Temp °F	Avg VEL Ft/Sec
3-1	13.6%	0.2%	1360	208	--	1.03	49275	3906	14.0
3-2	16.6%	0%	0	221	--	1.0	49275	4075	12.3
3-3	12.1%	0.6%	--	194	--	0.88	49275	3580	8.6
3-5	--	0.03%	--	473	--	0.94	49275	4266	12.0
3-6	14.7%	0%	2708	596	--	1.35	49275	3614	13.6
3-7	10.2%	9.1%	0	749	--	1.8	49275	2838	13.3
3-8	11.7%	0.9%	--	212	--	0.83	49275	3297	7.7
3-9	7.7%	10.4%	0	776	--	2.1	49275	2900	15.1
2-1	5.0%	14.0%	54	797	--	2.95	109217	2080	31.6
2-2	5.4%	13.2%	47	823	--	3.05	111232	NC	33.9
2-3	4.9%	14.1%	94	907	--	2.63	101887	NC	29.5
2-4	6.7%	12.6%	54	894	--	2.2	118562	NC	29.9
2-5	4.4%	15.3%	79	884	--	3.2	69452	1983	22.2
2-6	4.8%	14.7%	89	890	--	2.8	64504	NC	18.2
2-7	4.5%	15.5%	98	906	--	2.2	54334	NC	13.1
2-8	4.9%	14.9%	92	957	--	2.5	47516	NC	13.7
2-9	4.9%	15.0%	72	969	--	2.6	48760	NC	14.9
2-10	4.6%	15.7%	122	977	--	2.9	44041	NC	14.9
2-11	5.5%	14.0%	67	978	--	2.5	47473	NC	15.4
2-12	5.8%	13.3%	63	935	--	2.5	104669	NC	27.6
2-13	4.8%	14.7%	57	943	--	3.1	107528	2089	33.3
2-14	5.0%	14.3%	57	1014	--	2.8	84221	2176	23.2
2-15	5.9%	13.8%	62	1011	--	2.4	84936	NC	23.3
2-16	6.4%	13.2%	61	1015	--	2.2	84936	NC	22.9
2-17	5.1%	14.7%	115	956	--	2.6	47473	NC	13.8
2-18	6.2%	14.1%	92	1099	--	2.0	47759	NC	13.2
1-1	7.0%	16.0%	Unstable	Unstable	--	2.5	116675	NC	28.5
1-2	7.8%	11.6%	64	1052	--	2.2	101374	NC	24.1
1-3	7.7%	12.6%	70.4	32	0	2.3	82078	NC	19.9
1-4	7.5%	13.0%	90	157.5	0	2.5	82500	NC	20.6
1-5	7.0%	13.5%	113	156	0	2.6	80264	NC	20.3
1-6	8.0%	13.0%	113	126	0	2.1	64504	NC	13.6

-- meter inoperable

NC not calculated

H-055b

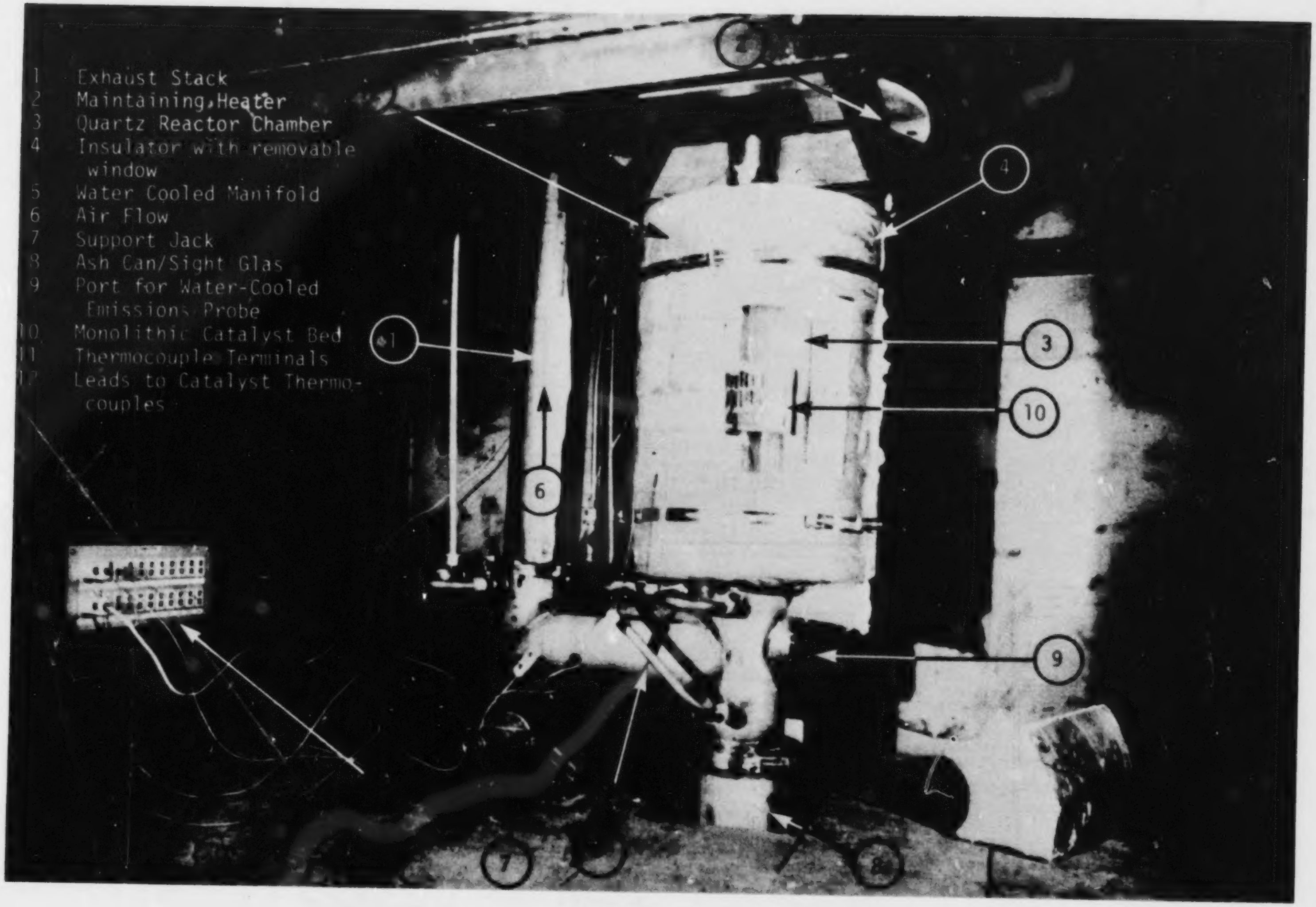
1 Exhaust Stack
2 Maintaining Heater
3 Quartz Reactor Chamber
4 Insulator with removable window
5 Water Cooled Manifold
6 Air Flow
7 Support Jack
8 Ash Can/Sight Glas
9 Port for Water-Cooled Emissions Probe
10 Monolithic Catalyst Bed
11 Thermocouple Terminals
12 Leads to Catalyst Thermocouples
2
4
3
10
6
9
7
8

Figure 1. Atmospheric catalytic combustion facility; view of reactor showing catalyst bed in place within quartz tube.

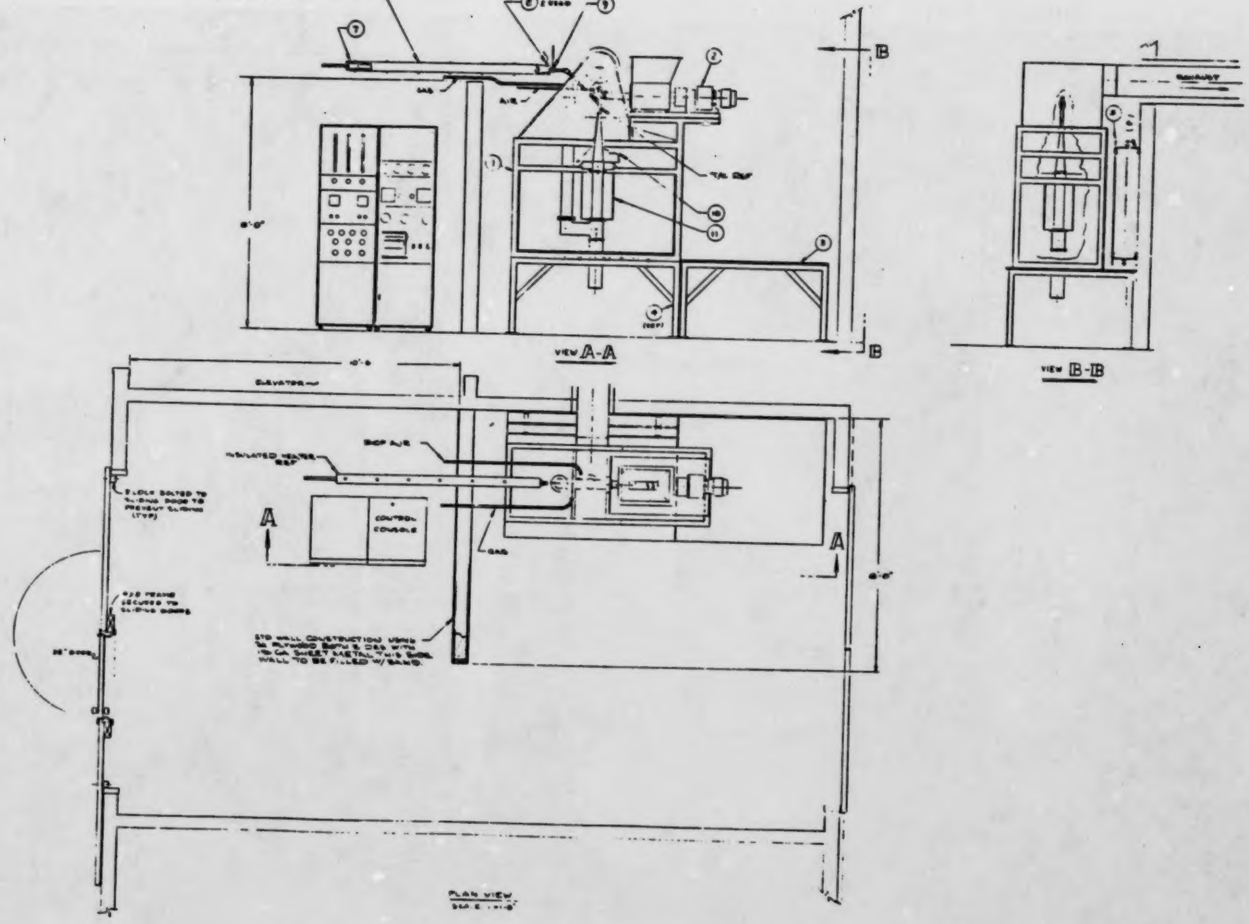

Figure 2. Layout drawing of atmospheric catalytic combustion facility.

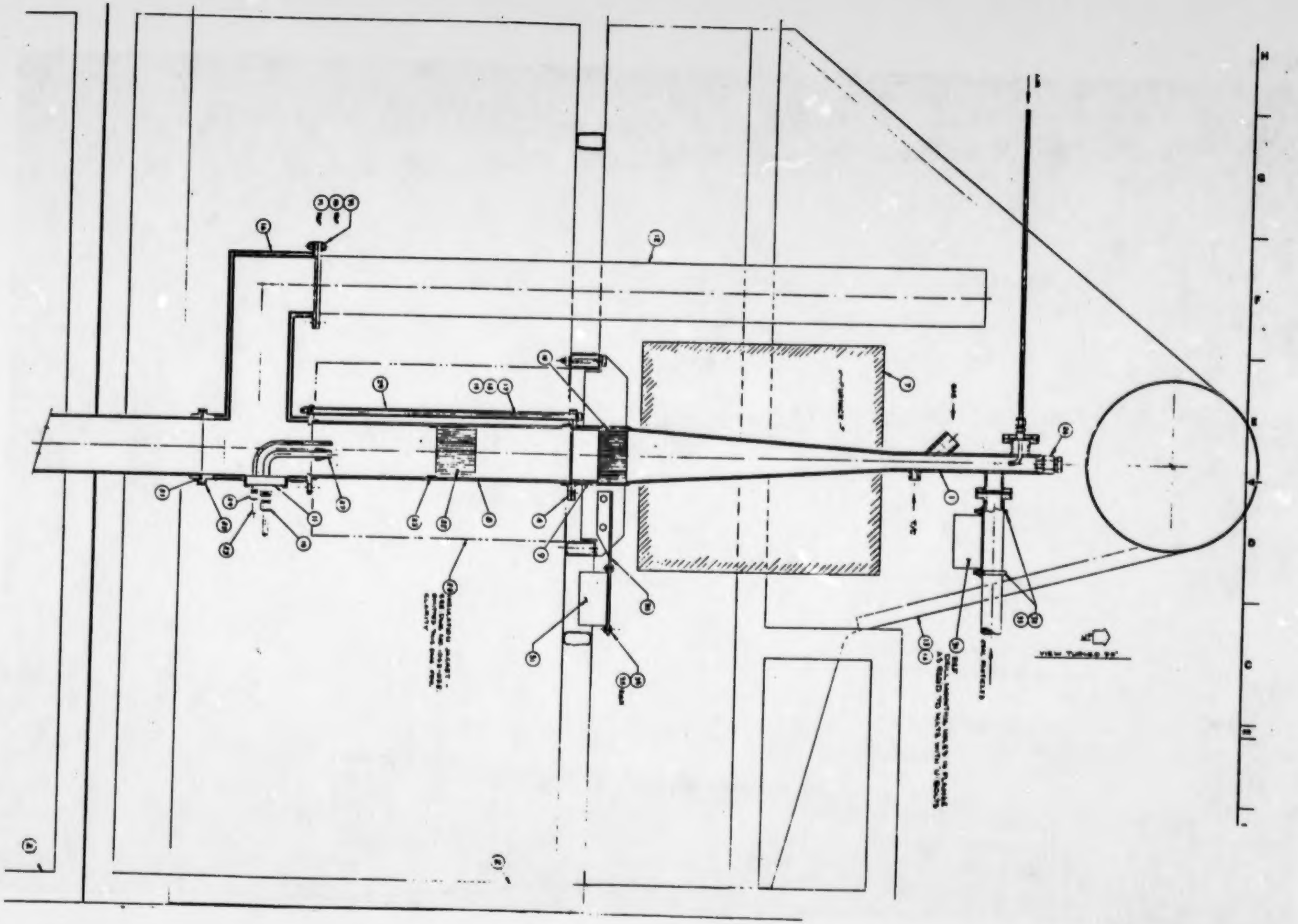

Figure 3. Expansion chamber and other features of the catalytic combustion facility.

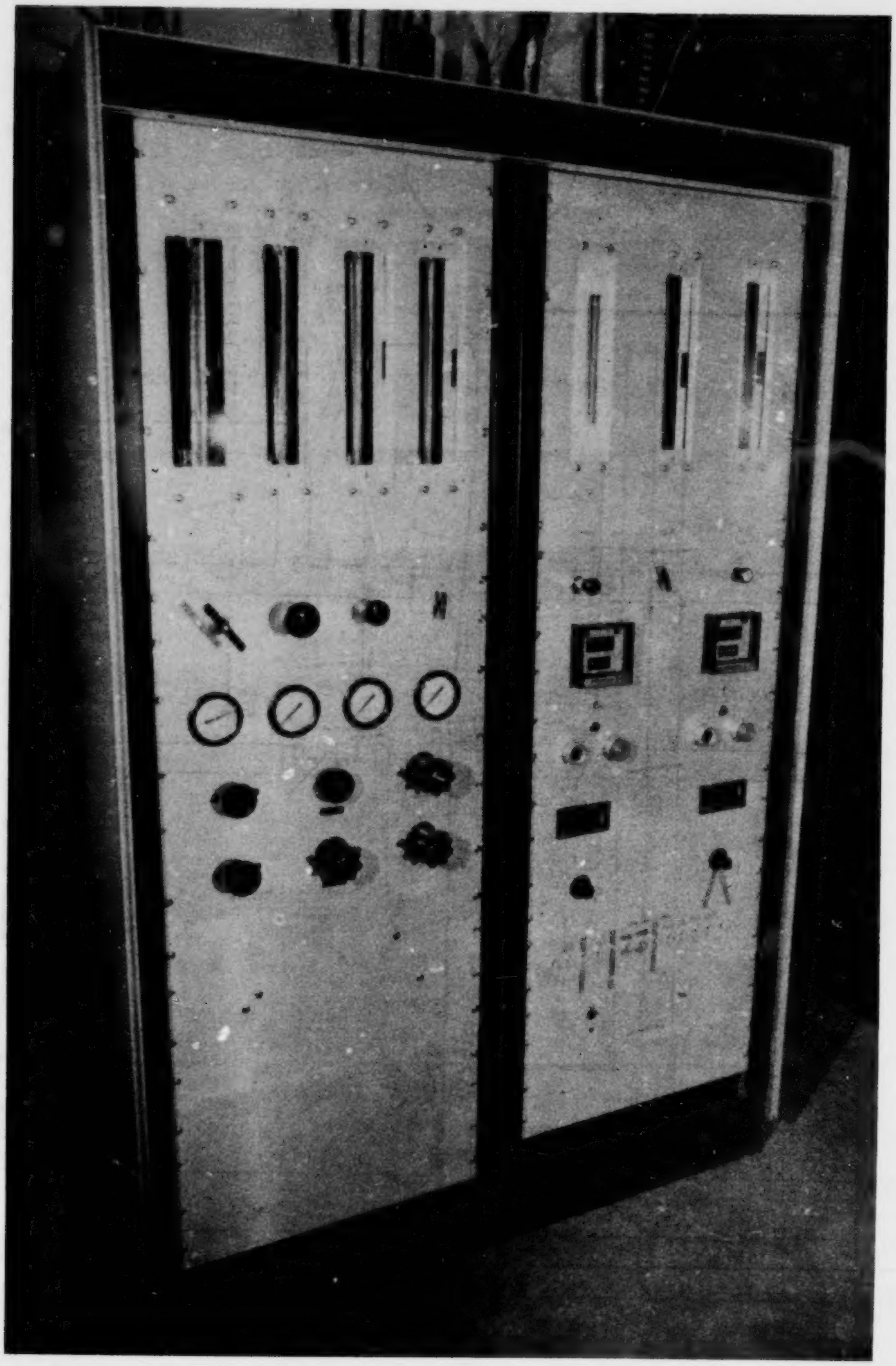

H-086c

Figure 4. Control panel for atmospheric catalytic combustion facility.

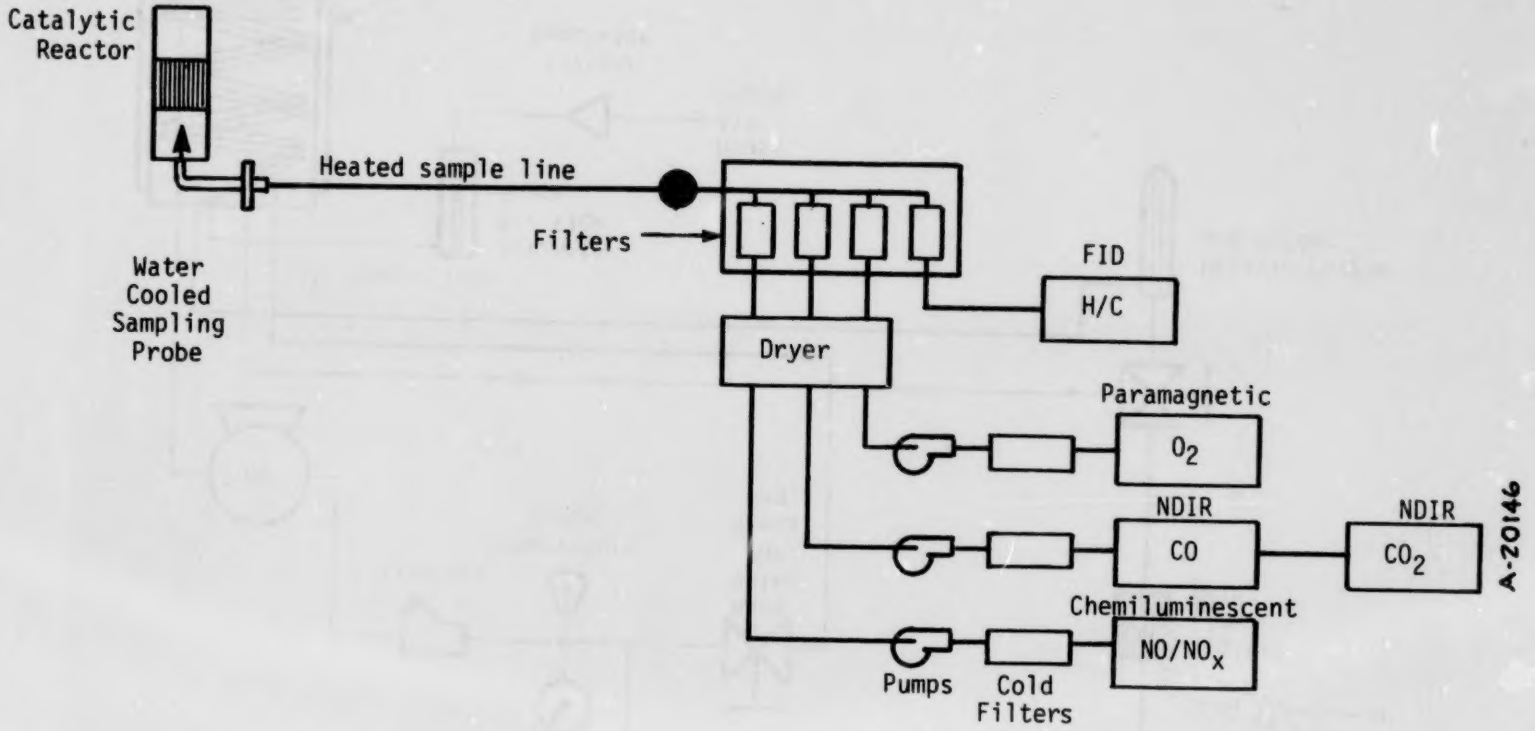

Figure 5. Schematic diagram of emission analysis equipment used with atmospheric catalytic combustion facility.

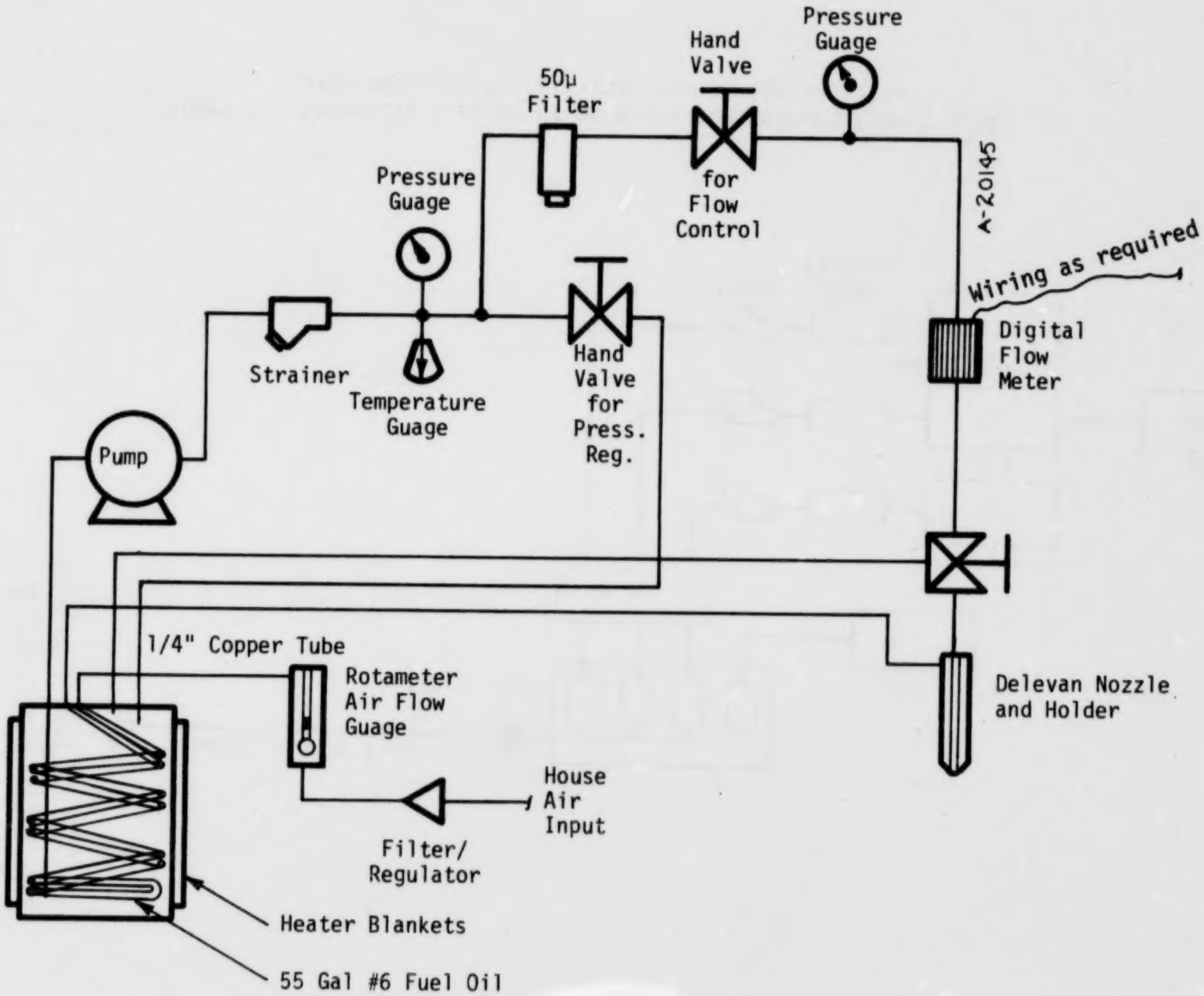

Figure 6. No. 6 fuel oil delivery system.

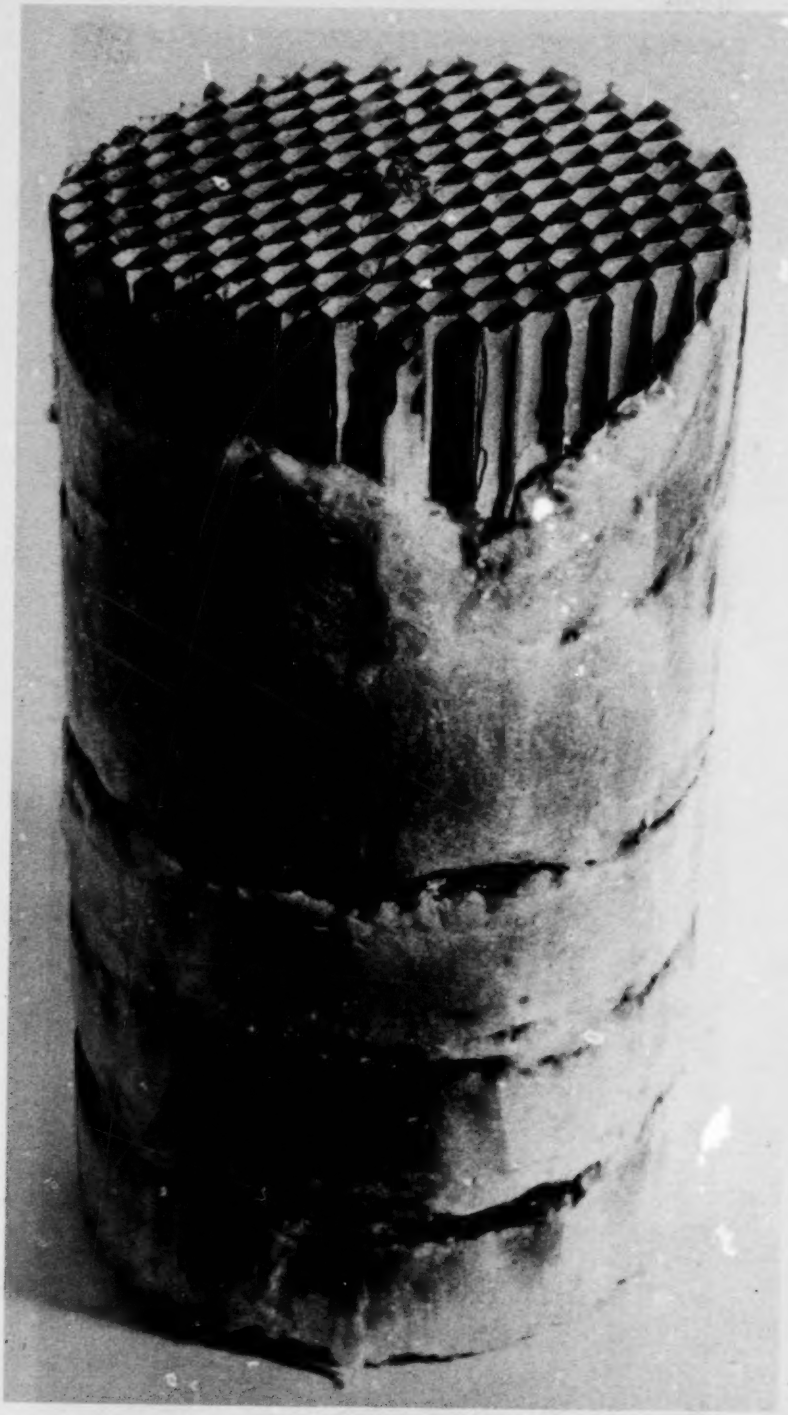

Figure 7. Post-test photograph of catalyst.

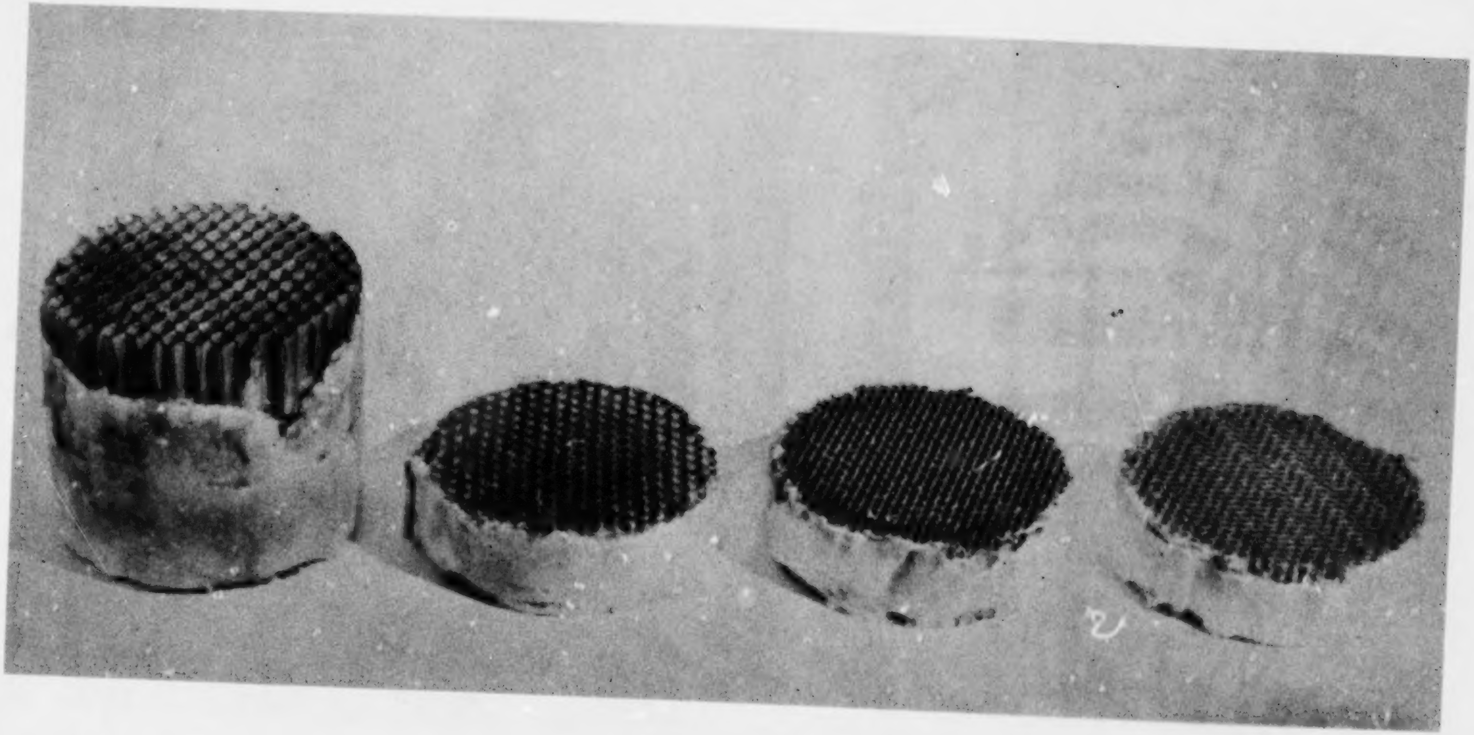

Figure 8. Expanded post-test photograph of catalyst.

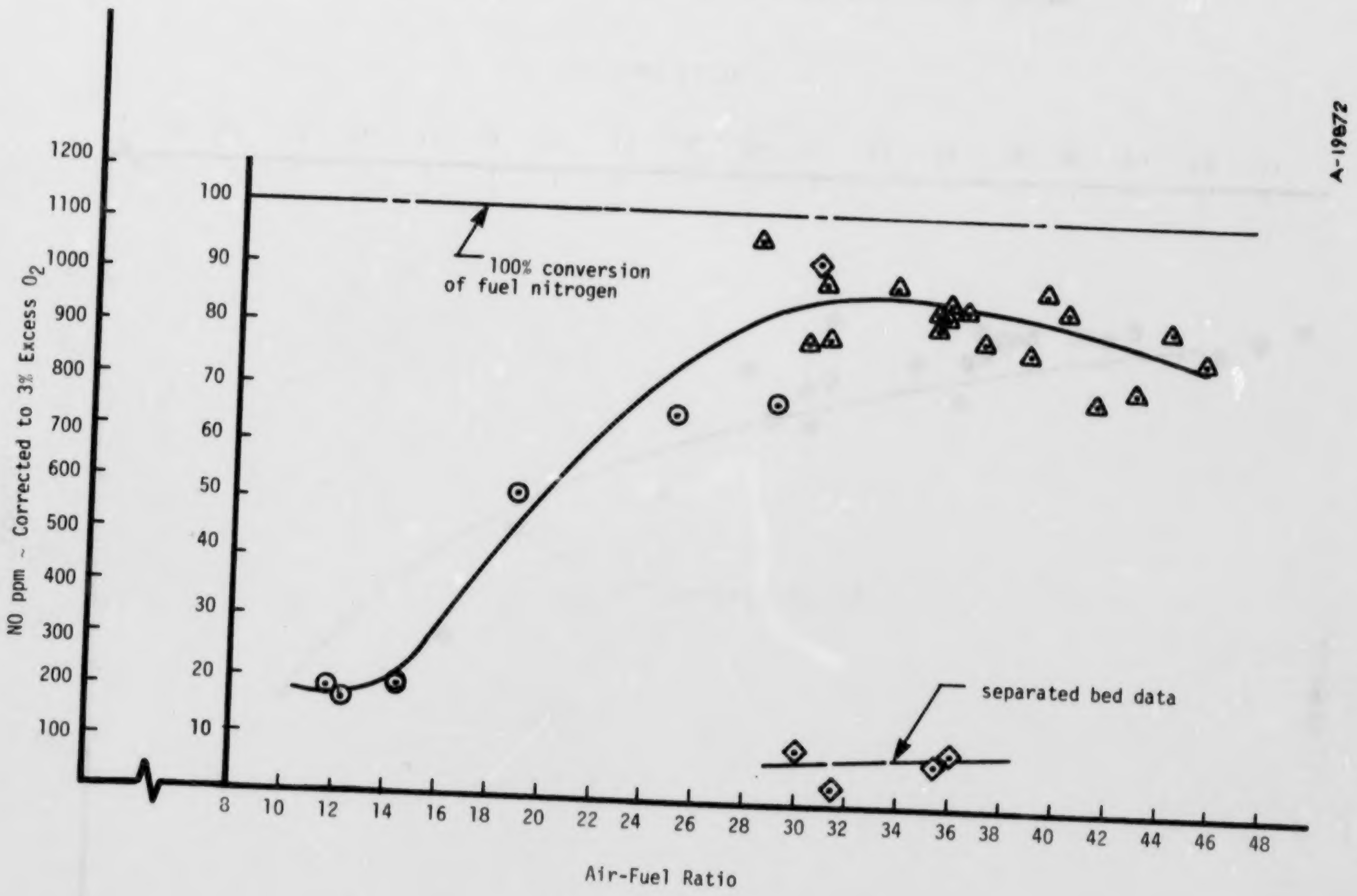

Figure 9. NO and nitrogen conversion -- 3 percent excess O_2

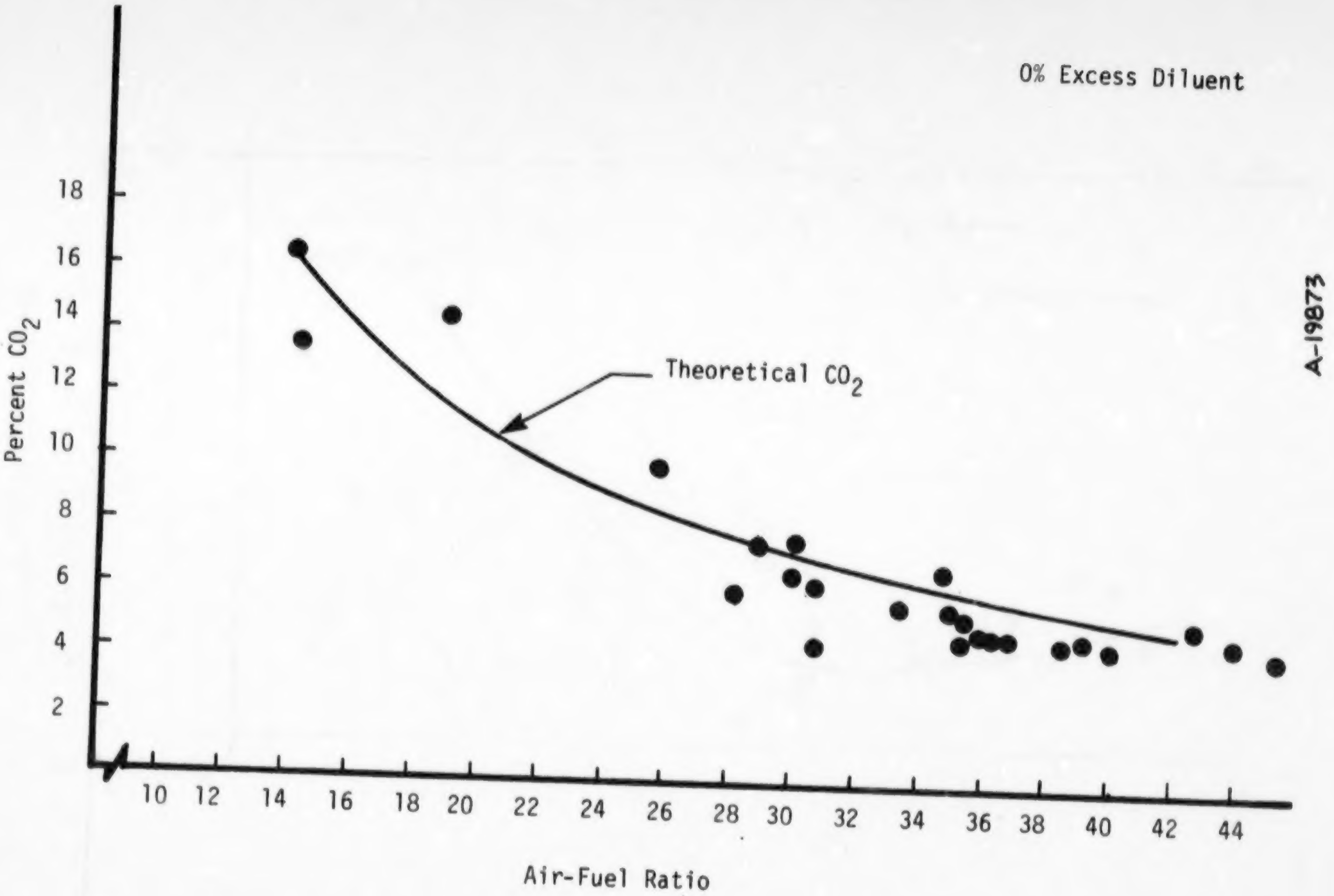

Figure 10. Comparison of corrected CO_2 measurements with theory.

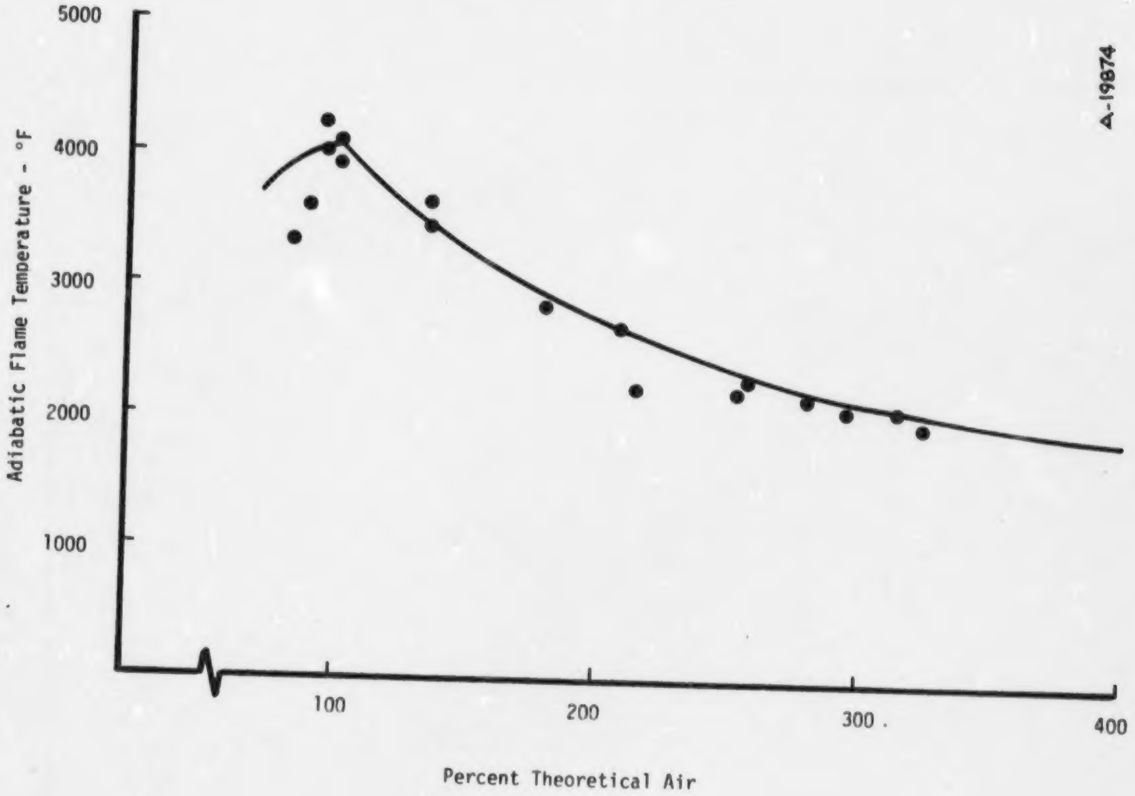

Figure 11. Comparison of combustion product temperature with the adiabatic flame temperature.

STRUCTURAL ANALYSIS OF A PRELIMINARY CATALYTIC CERAMIC DESIGN

By:
S.M. DeCorso
D.E. Carl

Combustion Turbine Systems Division,
Westinghouse Electric Corporation
Lester Branch Box 9175, A-603
Philadelphia, Pa. 19113

Preceding page blank

ABSTRACT

Structural analysis of a preliminary design catalytic ceramic element and its support structure for ultimate use in a low emission application has been performed. A thermo-mechanical analysis of the major components in this conceptual design has been performed for both steady-state and transient (shutdown) situations. Consequently, an arrangement that is thought to be a viable catalytic ceramic combustor element has been identified. Further development is necessary before full scale application.

Preceding page blank

ACKNOWLEDGMENT

This work was performed with the support of the Electric Power Research Institute under Contract No. RP 421-1 with Dr. A. Cohn as Program Manager. The authors wish to thank R. G. Glenn, E. W. Tobery and W. S. Y. Hung for their contributions in performing this task.

INTRODUCTION

In the development of a catalytic combustor for large industrial combustion turbine applications, the problems relating to the structural design of the full size catalytic element and its support structures have to be identified and solved. At this stage of the development, it is necessary to generate a conceptual design of the full size catalytic element and its supporting metal structure. Then thermal, mechanical, and stress analyses must be made to determine its expected structural performance in the combustion turbine transient and steady-state operating environments.

The objectives of this study are to establish a conceptual reference design arrangement for a preliminary catalytic ceramic combustor element to be used in large industrial combustion turbines for low emission application and to evaluate the catalytic reactor structural performance through thermal and mechanical analyses of the catalyst ceramic elements and supporting metal structures over the operating range of the combustion turbine.

CONCEPTUAL DESIGN

Total Combustion System

Based on the small scale test experience in the past (Reference 1), a conceptual design arrangement of a catalytic combustor in an industrial combustion turbine has been envisioned as shown in Figure 1. Adequate mixing in the fuel preparation zone should be provided to produce a faily uniform fuel-air mixture prior to entering the catalytic element. The catalytic element should be sized to provide sufficient contact time for good combustion efficiency and a length short enough to minimize the pressure drop at an acceptable level. Preliminary analyses have indicated that the diameter of the catalytic ceramic element will be larger than that of the conventional combustor currently in production. Downstream of the catalytic element, the reacted products are mixed with dilution air in the "transition section" which leads to the turbine inlet.

Catalytic Ceramic Element

From a preliminary analysis of the available information on contact time, reference velocity, pressure loss, combustor operating conditions and space limitation, including a consideration of the structural integrity, a 7 inch (178 mm) long by 15 inch (381 mm) diameter ceramic substrate has been selected for the present study.

The substrate is to be supported by a metallic cylinder. Preliminary analyses have shown that, if unprotected, the metal cylinder will reach temperatures higher than those allowed for materials currently used. Hence, an intermediate layer between the substrate and the support metal cylinder is required to provide cooling and/or insulation. Further analysis showed that the difference in thermal growth between the ceramic substrate and the metallic cylinder was sufficiently large that some provision must be included in the design to absorb these movements and to hold the substrate.

The recommended conceptual design utilizes an air-cooled coiled wire to provide the flexibility and conformity as shown in Figure 2. The coil is compressed in assembly. A layer of castable ceramic on the outer cylindrical surface of the substrate is required to provide a smooth surface for contact with the coil and to act as a thermal barrier. In the design, two outer layers of cells in the substrate has been made inactive to provide the desired temperature gradient and structural stiffness.

THERMO-MECHANICAL ANALYSIS

The thermo-mechanical analysis was performed for both the steady-state and the transient conditions. One dimensional analogs are utilized in the preliminary steady-state analysis to allow a quick evaluation of the mechanical performance of the catalytic element. The analysis was extended to consider the transient condition in order to determine the effects of different loadings on the structural components over the entire operating cycle. The effects of two dimensionality was introduced in the transient solution which also included the steady-state case.

Steady-State Analysis

In performing the analysis, the catalytic element is divided into its three components: the ceramic substrate, its metal support cylinder and an intermediate compliant layer between them.

Substrate--

Since the conceptual design of the total combustion system is still preliminary at this stage, it is sufficient to select a typical material for analysis. A survey shows that cordierite ($2\ MgO \cdot 2Al_2O_3 \cdot 5\ SiO_2$) is the substrate material used in catalytic converters on automobiles. Most of its material properties are readily available. On this basis, it was selected as the substrate material in the present study.

The ceramic material when used as a support for catalyst takes the form of cellular tubes. It follows that the bulk mechanical properties will depend on such features as cell shape, cell size, cell wall thickness and manufacturing techniques in addition to the mechanical properties due to the pure material. For instance, depending upon cell count, proportions and load direction, the allowable compressive loading on one square inch of bulk surface of the substrate varies considerably (2).

Like most ceramics, cordierite has the capability to withstand thermal shock mainly due to its very low coefficient of thermal expansion (Reference 2) and a low modulus of elasticity, $4 - 18 \times 10^6$ psi (28 - 124 G Pa) depending upon porosity, (3). According to Ref. (2), it can also withstand continuous duties at temperatures of 1350°C (2462°F) and transients as high as 1500°C (2738°F).

For the present analysis, a uniform temperature of 750°F at the inlet and a nominal temperature of 2300°F (1260°C) at the exit of the reactor are assumed. The temperature rise from inlet to discharge is considered linear.

An analysis of the thermal expansions showed that the temperature gradient will cause a thermal distortion to occur in the substrate disk. Hence, it is important that no axial restraints be applied across the face of the disk.

The pressure drop across the substrate is influenced by the size and shape of the cells and the wall thickness used.

For a typical substrate structure such as that used in (Reference 1), the pressure loading is well within the allowable limit.

Support Cylinder--

The metal support system of a catalytic combustor will experience similar pressure and thermal loadings as the secondary dilution zone of a conventional turbine combustor. It is convenient, therefore, to select the material used for the conventional combustor as the material for the support system. There has been extensive experience in the use of Hastelloy X, a nickel base alloy, as the material for combustor components. For the purpose of the present analysis, Hastelloy X is selected as the candidate material for the metal support system. Its mechanical properties are readily available from Ref. (4).

The metals are film cooled by air at the compressor discharge temperature. In the design, adequate film cooling will be provided such that the catalytic combustor shell can be expected to perform its duty, namely, withstand the external loads caused by gravity, airflow, fluid pressure and temperature.

The fundamental stress in the cylindrical elements is the hoop stress due to the pressure differential across the wall. The maximum pressure loading is associated with the pressure drop due to flow losses in the combustor.

Assuming a pressure loss of 5%, the calculated hoop stress for a 0.050 in (1.27 mm) thick wall is at a reasonable stress level. A thicker wall can be used to reduce this stress, if experience deems it necessary.

The cylinder will experience dimensional changes resulting from temperature changes. The differential thermal growth between the cylinder and the substrate will likely be the parameter that defines the design. These differentials must be accommodated if high stresses are to be avoided. The accommodations for these relative movements, either completely or partially, suggest an intermediate layer of high compliancy.

Compliant Layer--

Its primary function is to absorb the relative movements across the layer between the cylinder and the substrate. An additional requirement is that it must distribute the restraints it applies to the substrate uniformly and lightly. This requirement stems from the allowable loading of the substrate, particularly in transverse directions (2).

One promising scheme is to use a metallic mesh layer as possible support of the substrate (see Figure 3). With cooling flow through the wire mesh, the metal temperatures will be low enough for the coils to survive. The wire mesh, of proper wire size and density, could provide flexibility, good capability for conformity and a large number of support points. Therefore, a metallic coiled wire compliant layer will be capable of following the differential growths, conforming to the surface of the substrate, having a multitude of contact points, resisting shearing and operating at high temperatures.

Transient Analysis

In reviewing the operating cycle of a combustion turbine, it has been determined that the most severe transient loading occurs during the shut-down process. Hence, the present analysis is aimed at evaluating the stresses that can be developed during this critical period.

A one-dimensional time dependent analysis of the heat transfer at various stations along the combustor was performed. The change in pressure with time after shut-down was determined based on actual engine data. These calculated temperatures and pressures as a function of time after shut-down are then the input to an existing computer code to perform the stress analysis. In this way, a time history of stresses was developed with temperatures along the combustor at simulated operating conditions at various times following shut-off of the device.

Thermal Analysis of Support Cylinder--

The metal support system must be kept at temperature levels which will result in acceptable life. This temperature was taken to be 1400°F (760°C).

The steady-state temperatures at various stations along the entire metal support structure were calculated. Starting at these levels, transient temperatures for the various stations were calculated to simulate the shut-down process. Actual engine data were used to determine airflows and combustor shell temperatures as a function of time. This information was then used to calculate internal convective heat transfer coefficients as a function of time. The heat transfer coefficients and air temperature were then used to determine the metal temperature at the various stations through the use of an existing transient heat transfer computer code.

Stress Analysis of Support Cylinder--

In order to perform a finite element stress analysis of the metal support cylinder, the structure has been divided into five elements with each element further subdivided into nodes as shown in Figure 4.

The transient stress response at three selected locations are plotted as shown in Figures 5-7. The typical decay of stresses in an initially low stress region is illustrated in Figure 5. In all transient stress plots, it was observed that all initial high stresses tend to decay rapidly to low values with the cool-down as illustrated by the hoop stresses shown in Figure 6. The only stresses that show a temporary increase are those in shell elements C and D. The meridional stresses at node 9, element C increase for about 30 seconds and then start a gradual reduction. The inner hoop stress at node element D increases for about 5 seconds and then decreases in a typical manner as shown in Figure 7. The maximum value reached is less than 30,000 psi (207 MPa) which is low in comparison with the steady-state hoop stresses.

Substrate--

In comparison with the thin walled, flexible shell, the substrate is a three-dimensional device, which can be considered a solid in some aspects.

The most refined elements of a finite element program, namely isoparametric three dimensional solid elements, are recommended for use in the calculation of stresses in bulky structures such as the substrate. There is favorable experience with these elements, but their limitations have to be recognized. The first restraint is associated with modelling which involves a design of the elements to represent the substrate. Since the substrate is supported along the outer surface by the compliant layer, a set of reaction nodes (discrete load points along the outer edges of the outer elements by which loading and/or attachment to adjacent elements is secured) must be specified. The calculation procedure and the characteristics of this element are such that when the reactions at these nodes are developed during the calculation, the stress fields are inaccurate through two or more layers of elements in the model. This makes it necessary to use a larger number of elements and layers. Also, the representation of the contact of the compliant layer with the substrate makes a large number of surface nodes desirable.

In addition, a problem exists in defining the properties of the substrate; usually, when material properties are quoted, such as Young's modulus, density, thermal coefficients of expansion, etc, the values do not recognize the existence of the details, such as holes and cell structure. The results of the stress and other mechanical calculations, therefore, are bulk stresses and deflections, good enough to see if the substrate will fit the space, or be crushed due to the distributed loading on the surface, but not fine enough to determine stresses through or along cell walls. With brittle material, it is these small, local stress details that can cause failure much as flaw details in metallic parts affect performance. Thus, modelling of the cellular construction may be required.

The stress analyses presented thus far have been somewhat simplified. For example, only the pressure loading on the outer contours of the substrate has been considered.

While the substrate is simple in shape and some simple calculations indicate acceptable performance, the device, when considered in more detail, rapidly becomes very complex for the available methods of handling it.

Because of these limitations, the future designs can be better judged only after operational and test procedures are applied.

In summary, detailed stress analysis of a substrate/compliant layer/shell system under the expected thermal and mechanical load situations in a catalytic combustor will be an extremely time consuming task. Consequently, the most cost-effective approach appears to be the testing of the concept described in the paper and the use of the sophisticated finite element methods to investigate the design after the tests provide the necessary thermal and flow input.

From the present study, the following conclusions have been reached:

(1) This preliminary design as currently conceived is expected to perform its functions from the mechanical standpoint. Considerable design & development will be required before full scale application is possible.

(2) At this stage, additional experimental input is needed so that more sophisticated computer analysis can be applied for future designs.

(3) The analyses suggested that a reasonable amount of experimental work in conjunction with analytical methods discussed in the report will provide the necessary design information.

REFERENCES

1. DeCorso, S.M., et al, "Catalysts for Gas Turbine Combustors — Experimental Test Results", ASME Paper No. 76-GT-4, March 1976.

2. Anon., "CELCOR Cellular Ceramics", Corning Glass Works, Corning, N.Y.

3. Boyer, W.A., Corning Glass Works, private communication, December, 1977.

4. Anon., "Hastealloy Alloy X", Haynes Stellite Co., Kokomo, Indiana, August, 1961.

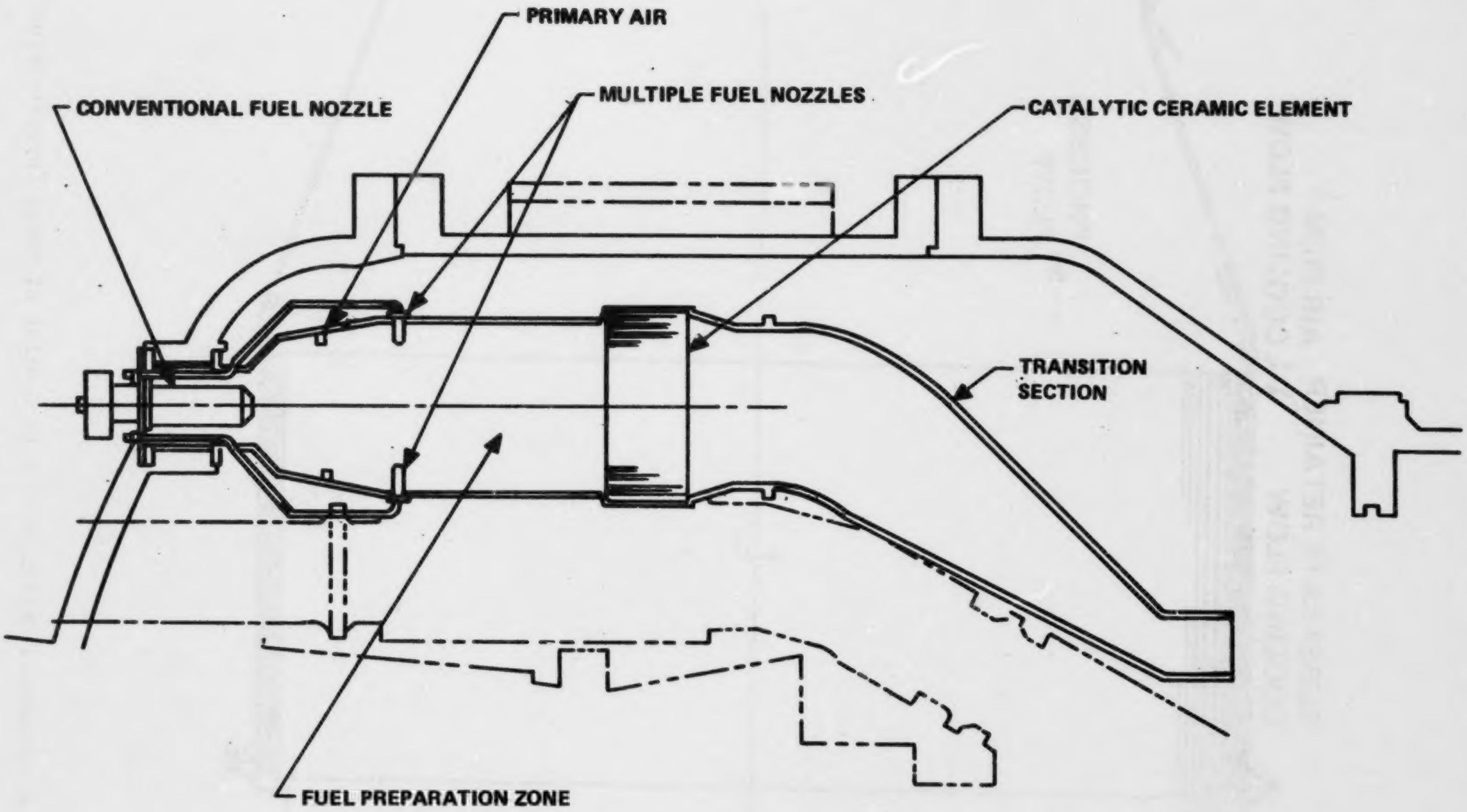

Figure 1. A Conceptual Design Arrangement of a Catalytic Ceramic Element in an Industrial Combustion Turbine

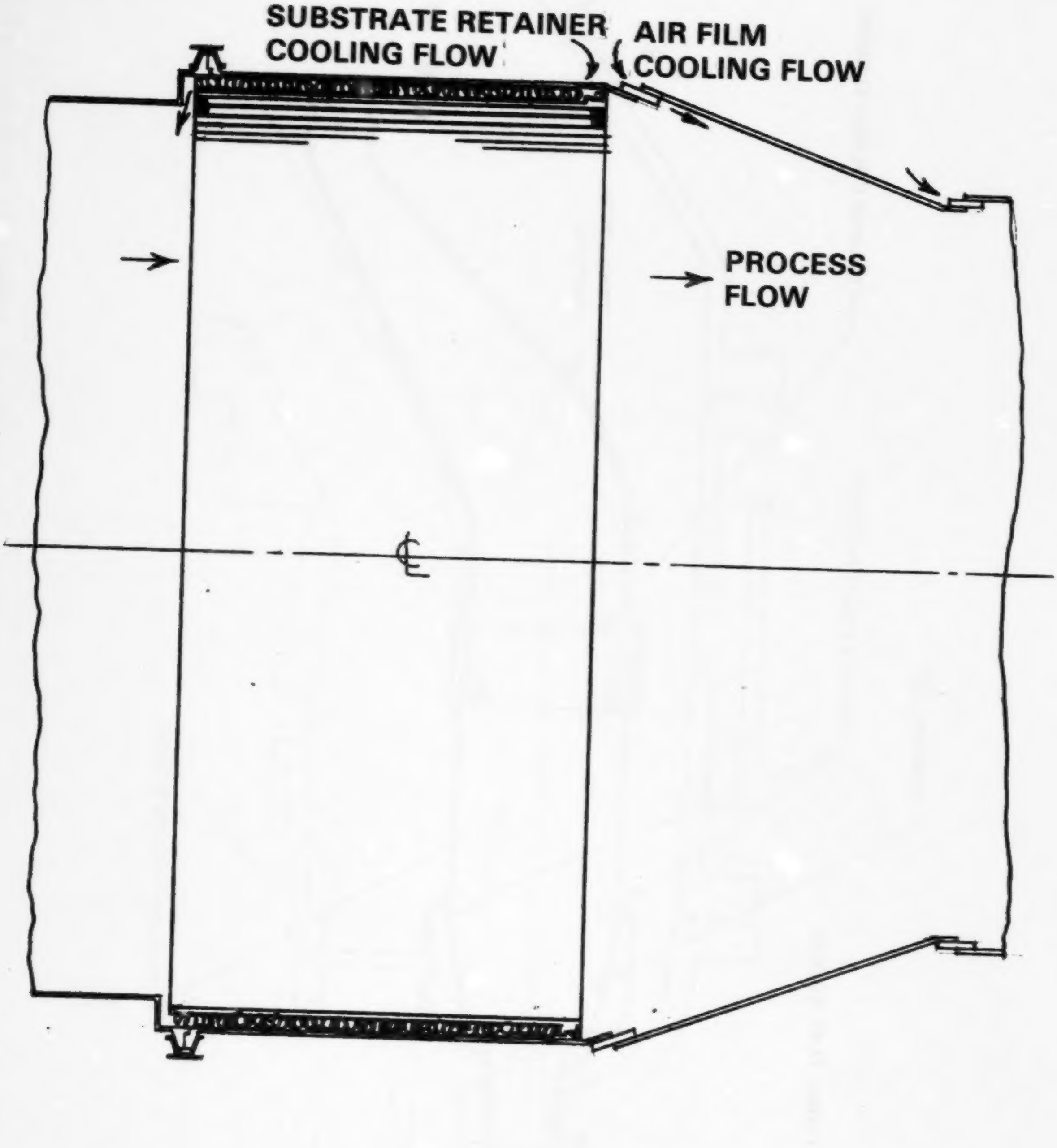

Figure 2. A Conceptual Design with Film Cooling of Metal Support Structure

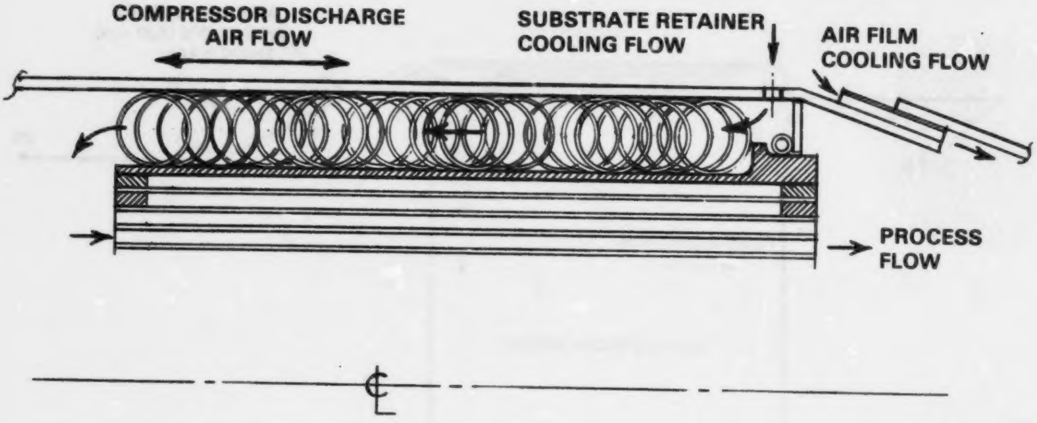
COMPRESSOR DISCHARGE AIR FLOW
SUBSTRATE RETAINER COOLING FLOW
AIR FILM COOLING FLOW
PROCESS FLOW
℄

Figure 3. A Conceptual Coil Wire Design With Cooling

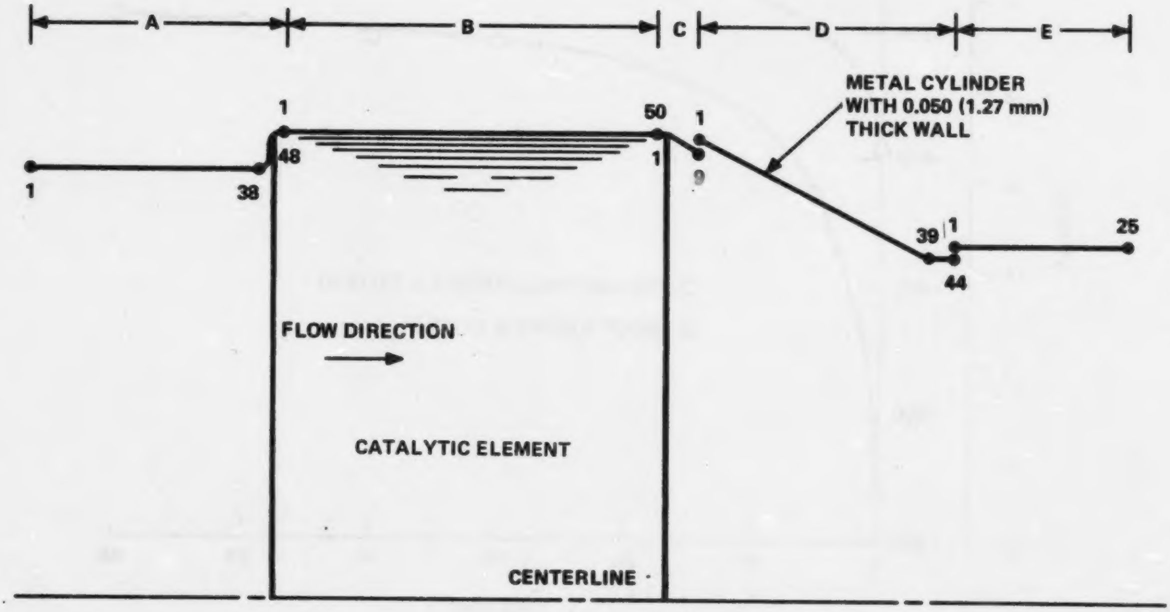

Figure 4. Catalytic Combustor Support Cylinder Model for Finite Element Analysis

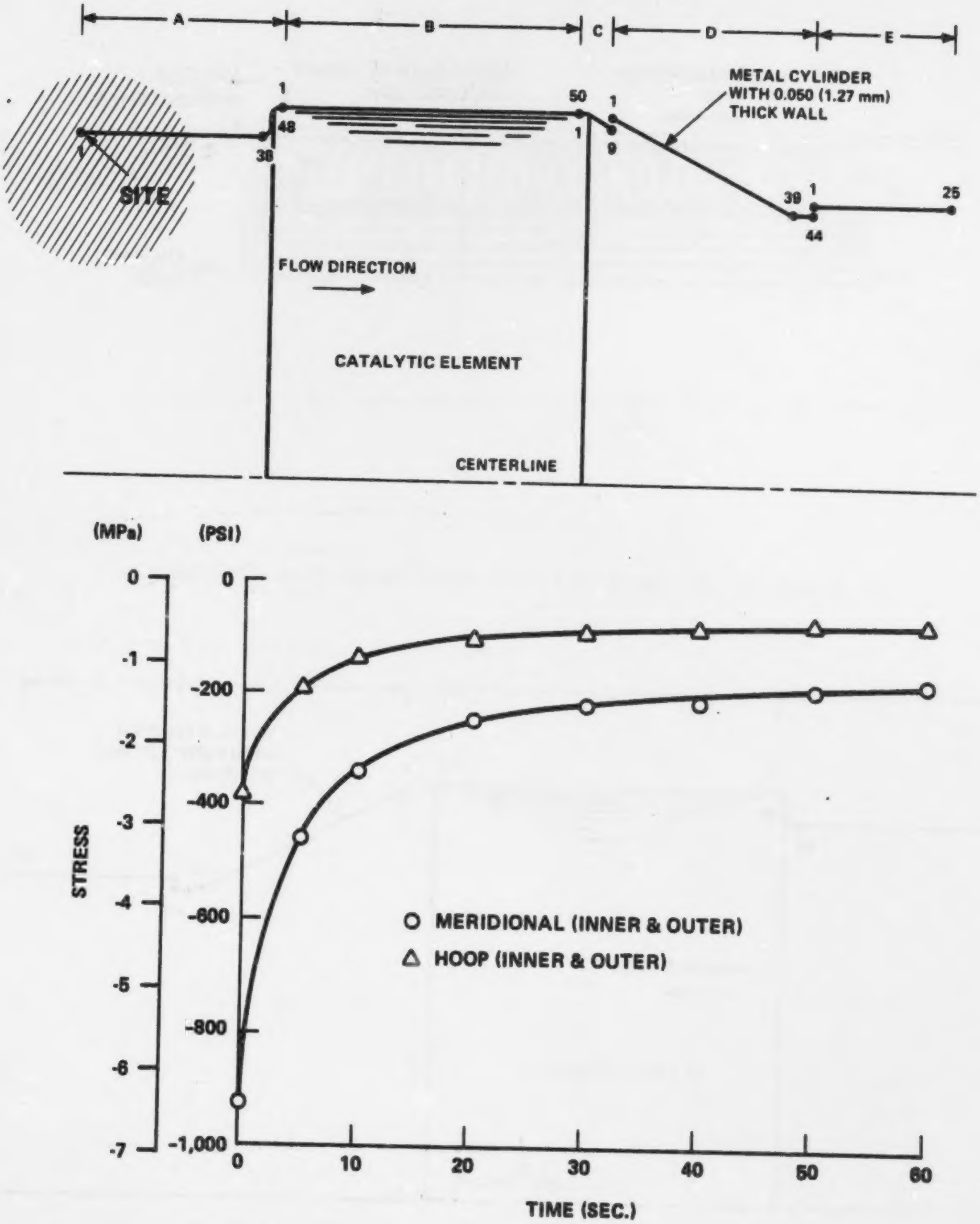

Figure 5. Transient Stress Response - Shell Element A, Node 1

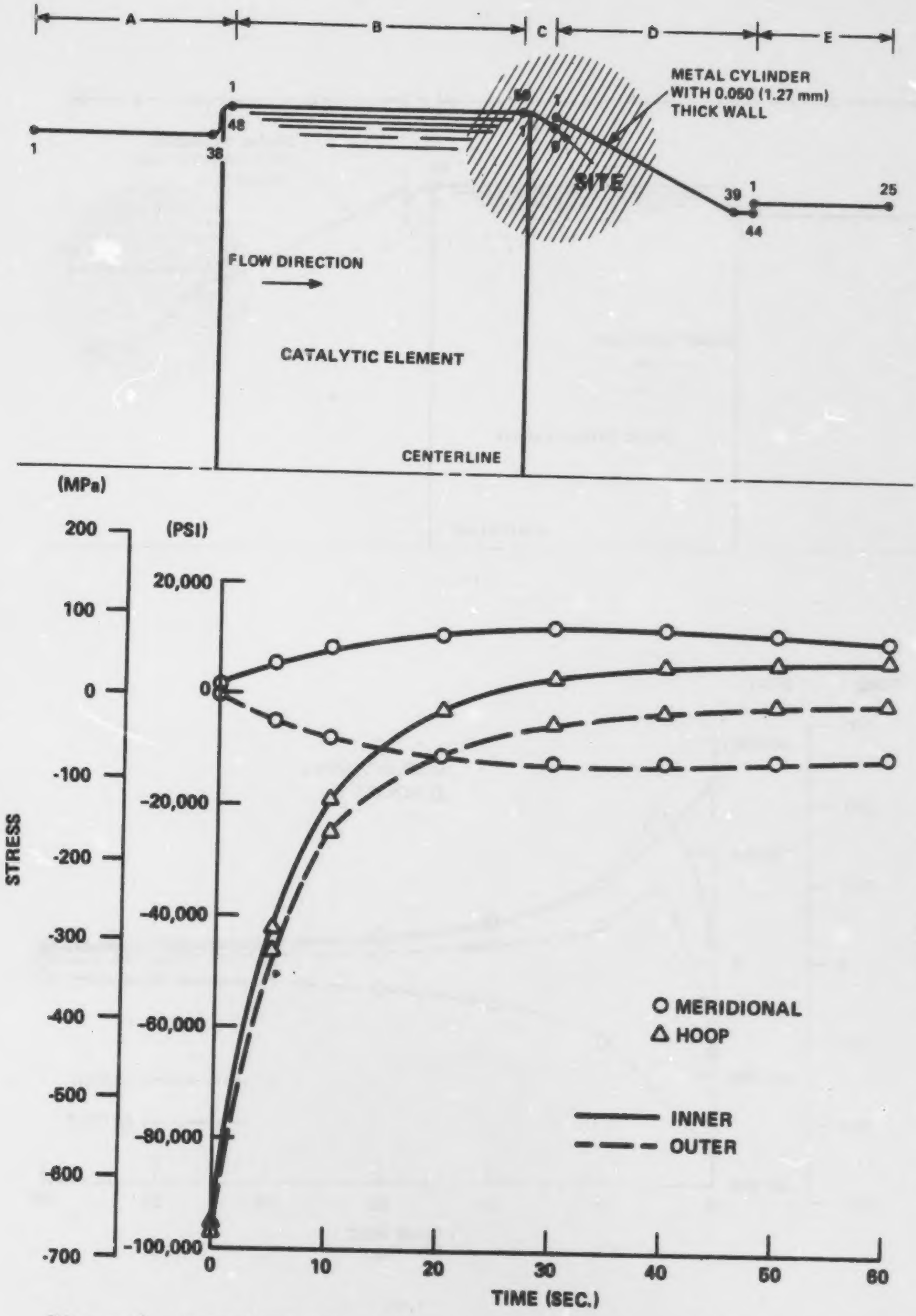

Figure 6. Transient Stress Response - Shell Element C, Node 9

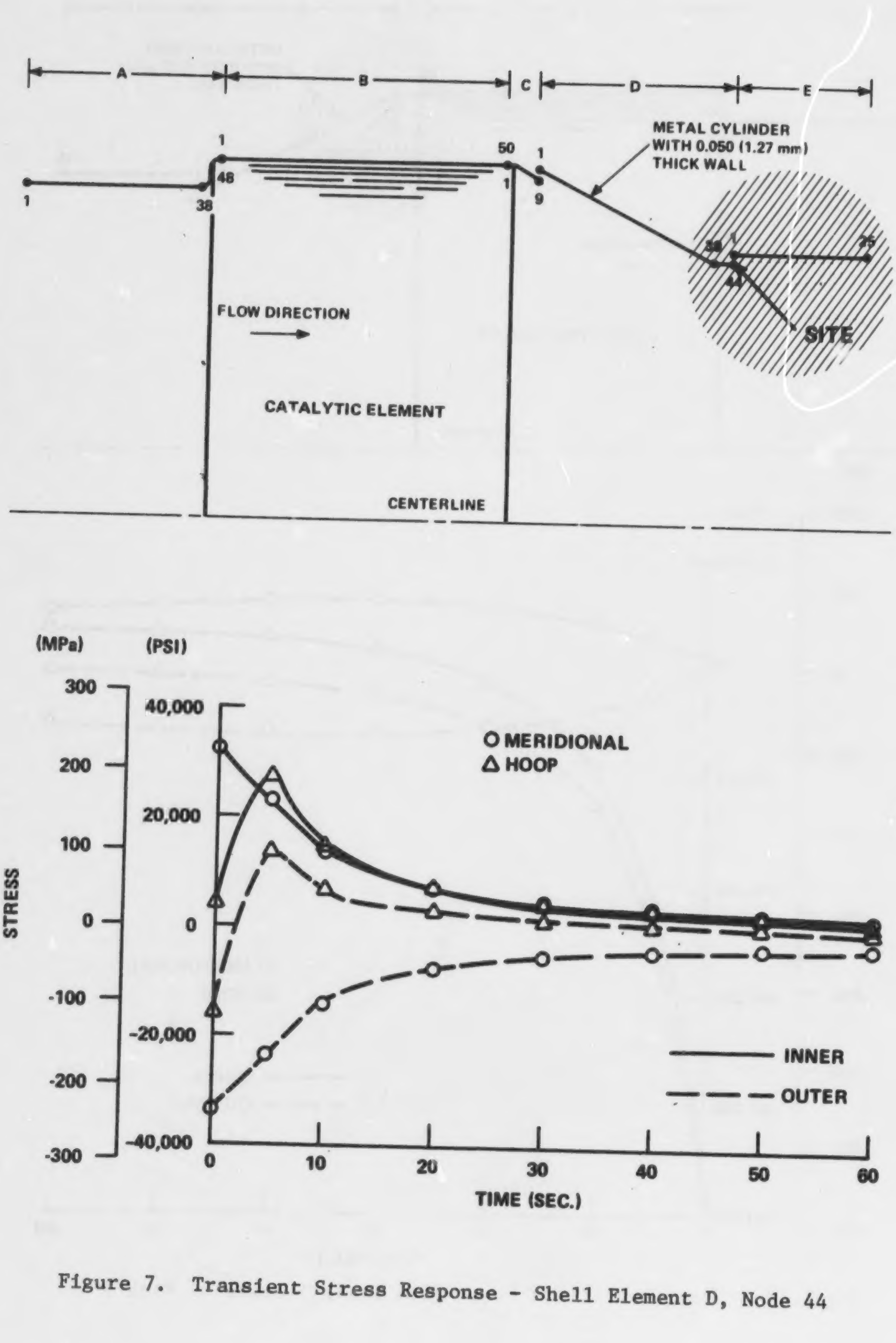

Figure 7. Transient Stress Response - Shell Element D, Node 44

DETERMINATION OF THE RATE OF HETEROGENEOUS REACTION ON CATALYTIC SURFACES

Effects of Surface and Fuel on Observed Performance

By:

Pierre J Marteney
United Technologies Research Center
East Hartford, Conn 06108

ABSTRACT

A program concerned with the fundamentals of catalytic combustion is in progress at UTRC. The ultimate goal is to assess the practicality of catalytic combustion using multicomponent liquid fuels. Experimental observations of catalyst performance are examined using a computer code which considers chemical reaction in the gas and on the surface and heat and mass transport. The reaction rate on the surface is found by estimation, all other processes being known or modelled.

Initial experiments were conducted to verify the approach. A mixture of argon-diluted propane and air in the ratio of 20/1 was used to restrict temperature rise, eliminate or inhibit homogeneous reactions, and expedite chemical analysis of reactants and products with a time of flight mass spectrometer. It has been found that the analytical program correctly predicts ignition temperature, temperature rise and combustion efficiency with a heterogeneous activation energy of 10 to 11 kcal/mole.

Further experiments in the fuel-rich regime have suggested that a two-step reaction model is required for better match of the data. CO_2/CO ratios were found to approach equilibrium with increasing length, indicating that CO_2 is not initially formed. This mechanism is being incorporated into the analytical program.

The effect of fuel and surface variations has also been investigated. Specialty catalyst, having two values of active-surface loading on each of several substrates, have been used with both pure and industrial-grade propane, which contains approximately 35 percent propylene. In addition , the effect of catalyst aging has been examined using samples successively heated in air at higher temperatures. In general, the impure propane is more reactive, but under certain conditions, especially in the fuel-rich regime, the industrial-grade propane appears to inhibit reaction. The variation of reaction rate under these conditions is now being determined.

Preceding page blank

NOMENCLATURE

A_s	Surface area of reactor structure per unit volume of reactor, m^{-1}
A_x	Total cross-sectional area of reactor, m^2
C_s	Specific heat of reactor structure, cal/kg-deg K
G	Green's function or, mass flow rate (based on superficial area), kg/m^2-sec
h	Enthalpy, cal/kg
$\mathscr{h}$	Heat convection coefficient for heat transfer between the interstitial fluid and the reactor bed, cal/m^2-sec-deg K
$\mathscr{h}\ a$	Heat convection coefficient for heat transfer between the interstitial fluid and the surroundings, cal/m^2-sec-deg K
H	Heat of reaction, cal/kg (negative for exothermic reaction)
k	Thermal conductivity of reactor structure, cal/m-sec-deg K
k_c^J	Mass transfer coefficient for species J, m/sec
L	Length of reactor, m
M_J	Molecular weight of species J, kg/kg-mole
$\overline{M}$	Average molecular weight, kg/kg-mole
p	Perimeter of reactor, m
P	Pressure, $Newtons/m^2$
r_{het}	Rate of heterogeneous chemical reaction on catalytic surfaces, kg/m^2-sec
r_{hom}	Rate of homogeneous chemical reaction in the interstitial fluid, kg/m^3-sec
t	Time, sec
T	Temperature, deg K
w_J	Weight fraction of species in interstitial fluid

z	Axial distance, m
γ_J	Moles of species J reacted or formed per mole of fuel reacted
δ	Void fraction of reactor bed
ξ	Dummy variable for z
ρ	Density of interstitial fluid, kg/m^3
ρ_J	Species concentration, kg/m^3
ρ_s	Density of reactor structure, kg/m^3

Subscripts

a	Refers to surroundings
i	Refers to interstitial fluid
o	Refers to reactor inlet condition, or, reference condition
s	Refers to catalytic surface

INTRODUCTION

In hydrocarbon-air combustion systems, off stoichiometric combustion can be used to control pollutants, particularly NO, by limiting the flame temperature rise. Fuel lean combustion can be used effectively with gaseous or prevaporized fuel premixed with excess air. In theory, reduction of emissions would accompany reductions in equivalence ratio. In practice, however, the lean flammability limit must be considered; desired control measures may necessitate a mixture which is nonflammable. The lean mixtures may also require reaction times longer than available residence times to product hydrocarbon burnout. Catalytic combustion provides a means of extending the flammability limit well below the gas phase value, at the same time providing enhancement of the overall reaction rate.

Catalytic combustion may also be applied to the fuel rich regime. Fuel rich combustion may be of value with certain liquid fuels, especially those containing bound nitrogen and sulfur compounds. Rich combustion could be employed with vaporized or partly vaporized residual fuel in order to minimize the production of nitrogen or sulfur oxides; however, the formation of soot or long chain hydrocarbons could limit fuel rich operation. Catalytic combustion may be able to promote oxidation of long chain hydrocarbons and soot precursors. If catalyzed surface reactors are found to be tolerant of liquid fuel, the fuel rich combustion could occur entirely within a catalyst bed.

In assessing the value of catalyzed reactors, it is necessary to be able to determine the kinetics of the heterogeneous reactions. In most cases, however, homogeneous reactions also occur, and often dominate. In the present studies, the gas phase reactions have been eliminated or largely suppressed by dilution of fuel/oxygen mixtures with inert gas, thus reducing the net temperature rise. An analytical program treating both homogenous and heterogeneous processes has been developed; using established values for homogeneous kinetics, coupled with treatment of heat and mass transfer within the catalyst bed, unique solutions of heterogeneous rates are obtained.

A global, Arrhenius-type rate expression, first order with respect to reactants, is used. Details of adsorption, activation, etc. are not explicitly stated in the model. However, changes in physical processes would be evidenced and might appear as changes in the overall rate, for example, as functions of equivalence ratio. In this study, experiments were conducted over a fuel/oxygen equivalence ratio of 1.0 to 3.0 to determine whether apparent changes in mechanism occur, and to determine the relative importance of homogeneous and heterogeneous reactions in practical systems.

During the time in which the analytical model was under development, initial experiments on propane/air ignition and stability were conducted to establish the general features of catalytic combustion. A second line of tests established that reaction in the diluted mixtures was initiated at approximately the same temperatures. The third series of tests focused on obtaining data relating the experimental conditions to combustion efficiency, reaction rate, etc., by means of exhaust gas analysis.

Tests concerning the interaction of fuel and surface have also been conducted. In one series of tests, both surface loading (active surface weight per unit volume of catalyst) and type of catalyst substrate (honeycomb and split-cell ceramic or spiral-rolled, thin-wall metal) were varied. In addition, samples of one batch of catalyst, which had been subject to progressively more severe heating in air, were tested.

EXPERIMENTAL APPARATUS AND PROCEDURE

A general view of the experimental system is shown in Figure 1; a photograph of the burner unit is shown in Figure 2. A cross section of the burner is given in Figure 3. The burner unit was fabricated from 2 inch OD threaded stainless steel pipe and pipe caps. Within the body, several screens were located to promote mixing and prevent flashback. The upper cap was bored to the diameter of the threads; catalyst samples rested on the lip of the body and were retained by the upper cap. Typical mounting of samples is shown in Figure 4. In this instance, a 1 inch diameter sample was mounted in a cored section of untreated substrate.

Gases were taken from cylinders and metered through calibrated flowmeters. Preheating of the system was accomplished by passing the gases through hot watt tubular heaters; the gas/burner system could be preheated to approximately 450°C. Temperatures were monitored by sheathed thermocouples in the gas stream and by the fine wire thermocouples within the bed.

A Bendix time-of-flight mass spectrometer was used for analysis of gases. A fine-tip quartz probe and heated stainless-steel manifold conducted the samples to the TOF. Sample line pressure was maintained at 10 to 15 torr. The mass spectrum from m/e 12 to 44 was scanned for each analysis; concentrations of the species Ar, C_3H_8, O_2, CO_2, CO and H_2O were determined using a reduction program developed at UTRC. Certified standard gases were purchased and used for reference. The prior calibrations of flowmeters and TOF fragmentation and sensitivity factors were validated by the coincidence of stated and analyzed composition of the reference samples.

All experiments were conducted using samples from a single batch of catalyst.* The refractory substrate is in a honeycomb configuration, having eight cells per inch, with a minimum cell wall thickness of .008 inch. The active surface is platinum, and represents approximately 0.1 percent by weight. Samples for test were cut to shape and thickness from 1 inch thick material supplied by the manufacturer.

---

*Matthey-Bishop, Malvern, PA.

For determination of ignition temperature, the system temperature was slowly raised until a measurable temperature difference developed between inlet and outlet gases. For measurements of combustion efficiency, reaction rate, or gas composition, the system was brought to a specific initial temperature with no fuel flowing, after which propane flow was initiated. Preheat then remained unchanged through the run; the data were taken after all temperatures had stablized.

IGNITION TEMPERATURE

The dependence of ignition temperature on stoichiometry in the propane/air system is shown in Figure 5 for reference velocities of 40 and 180 cm/sec. Minimum ignition temperatures of approximately 450K were observed. A moderate effect of equivalence ratio is evident, although the dependence is much weaker than predicted for "normal" ignition. Figure 6 illustrates the relationship between equivalence ratio and ignition temperature given by Burgess and Hertzberg (Reference 1). At 300K the lean limit is $\phi = 0.58$; for $\phi = 0.2$ a minimum ignition temperature of 1223K is indicated. At the lower equivalence ratios, therefore, ignition must be due to heterogenous processes only, since gas phase reactions will not propagate a flame or lead to temperature rise.

Decreased residence time (or increased gas flow) is reflected in increased ignition temperature. A factor of 4.5 in velocity is responsible for a change in ignition temperature of approximately 50K over a broad range of stoichiometries. The space velocities in these tests varied from approximately 30,000 to 350,000 hr^{-1}. Data such as shown in Figure 6, restated in terms of space velocity, are shown in Figure 7. Increase in space velocity simultaneously reduces residence time and promotes transition from laminar to turbulent flow, thus enhancing surface contact. The net effect is a slow change in ignition temperature. At higher space velocities, however, the onset of reaction could be at considerably higher temperatures, since further changes would produce only small increases in turbulence.

The ignition temperature for nitrogen-diluted mixtures was found to be essentially the same as for the normal mixtures, as shown in Figure 8. For the extreme dilution, a factor of 40 to 1, the ignition temperature differed by less than 10K. The substitution of argon for nitrogen produced a slightly lower ignition temperature, with a minimum value of approximately 425K. This is due to the lower heat capacity of argon, allowing greater local retention of heat and quicker bootstrapping into reaction. Except for the higher exhaust temperature however, all features of the argon-diluted mixtures were the same.

REACTION STUDIES

Based upon observations that dilution does not significantly alter the onset or extent of reaction, studies to determine the rate and general course of reaction were undertaken. In order to permit estimation of the heterogenous reaction rate, however, it is necessary to consider the effects of homogenous reaction and heat and mass transfer. An analytical program was developed for this purpose. In brief, for given entrance conditions, the program proceeds stepwise along reactor length, determining the bed temperature, in terms of surface concentrations and interstitial temperature. Iteration proceeds until assumed and calculated profiles agree within specified tolerance. A fuller description of the program is given in the Appendix.

The heterogeneous reaction parameters α and E, used in the Arrhenius rate expression $k_{het} = \alpha \exp{-E/RT}$, can be found by fitting conversion data at different temperatures. These parameters, once fixed, should apply to all situations in which similar kinetics are obeyed. The homogeneous reaction rate is taken from data of Clarke et al. (Reference 3). As illustrated in Figure 9, a large temperature difference is not necessary to capitalize on the temperature sensitivity of the Arrhenius expression for activation energies in the range of 5 to 10 kcal/mole. For example, if conversion at 525K is used as a reference point, predicted conversion at 600K would be twice as great for an activation energy of 10 kcal/mole as for 5 kcal/mole. Thus, temperature differences of only several hundred degrees are adequate to specify activation energy.

In the undiluted propane/oxygen and propane/air systems, however, a temperature rise of 200K would be obtained only for very lean mixtures. Through dilution with argon, the temperature rise can be tailored to desired levels. For example, a stoichiometric mixture of propane in oxygen diluted 20 to 1 by argon has a net temperature rise of only 200K to 250K, depending upon inlet temperature, bed length and velocity. Resulting conditions are thus optimum for determination of activation energy; the parameter α can be determined from the same data once activation energy is known. The result of applying this approach to experimental data is shown in Figure 9, in which the fit to experimental data is shown for an activation energy of 10 kcal/mole.

In addition to providing a reasonable fit to the conversion efficiency, the analytical program also correctly predicts the iginition temperature and temperature rise. However, an unexpected result of the computations is that the system becomes transport-limited rather early, with steady-state fuel concentration on the surface dropping to values orders of magnitude below the oxygen concentration. In the case of propane, the net transport of fuel to the surface, evidenced by the ratio of mass transport coefficient of propane to that of oxygen, is smaller by approximately thirty percent. Especially in the case of fuel lean mixtures, therefore, low surface concentration of fuel restricts the net reaction.

CHANGE IN MECHANISM WITH EQUIVALENCE RATIO

In the development of the reaction model and laboratory experiments, principal emphasis was on fuel lean conditions, since the ability of catalytic combustion to produce low emissions at low equivalence ratios has been demonstrated. However, catalytic combustion schemes using fuel rich mixtures have also been advanced. For instance, a fuel rich preburner operating at an equivalence ratio of 1.4 to 1.8 is attractive if carbon formation can be suppressed. The catalytic combustor, if promoting reaction of fuel to CO or CO_2, could be of great value. To determine the result of rich-mixture operation, tests were conducted at equivalence ratios between 1.0 and 3.0. The results indicate that a two step reaction model may be required.

The concentrations of CO and CO_2 in the reactor exhaust are shown in Figures 11 and 12 for bed lengths of 1 and 0.3 inch, respectively. Inlet conditions were identical for both cases, and exhaust temperatures from the 0.3 inch bed were slightly lower. Consistent with the higher exhaust temperature in the 1 inch reactor, greater conversion to CO_2 was observed. However, the sum of CO_2 and CO produced was essentially constant, as shown in Figure 13. This indicates that the governing step in conversion is an initial reaction on the surface, forming CO. Conversion of CO to CO_2 could then take place either on the surface or in the gas phase.

The effect of bed length or residence time is more strongly illustrated in Figure 14. The ratio of CO_2 to CO is taken from the data of Figures 11 and 12. The curves on Figure 14 represent equilibrium CO_2 to CO ratios at 800K and 900K (References 4 and 5). The concentration of CO_2 in the 1 inch bed is greater by a factor of approximately 1.5 at all equivalence ratios. The CO_2 to CO ratio in the 1 inch bed corresponds to equilibrium at a temperature of approximately 850K which is the measured bed temperature. The CO_2 to CO ratio for the 0.3 in bed would correspond to an equilibrium temperature higher than observed in the bed. In terms of kinetics or equilibrium, no argument could be advanced for destruction of CO_2. The governing step, therefore, must be formation of CO on the surface. The apparent excess of CO in the 0.3 in bed reflects the time-dependent conversion of CO to CO_2, either on the surface or in the gas phase.

Modification of the analytical model to include the two reactions, fuel to CO and CO to CO_2, is in progress. Sufficient data exist for homogeneous rates; the rate for conversion of CO to CO_2 will be determined using CO/oxygen mixtures and ignoring the first reaction step. The rate of the first heterogeneous step can then be found when propane/oxygen mixtures are utilized.

EFFECT OF FUEL AND CATALYST VARIATIONS ON PERFORMANCE

In planning for catalytic combustors, it is desirable to understand the interaction of active surface, configuration, and fuel on the performance. A test matrix, in which these paramters were varied, was developed. Partial results of this series of the test are shown in Table 1. The designations T, Al, and M indicate substrates of Torvex (honeycomb), Alsimag (split-cell) and metal (split-cell) respectively; the second entry indicates the loading of the active surface, platinum, in grams per cubic foot. A third entry, I, indicates the use of industrial rather than pure propane.

Within the precision of the temperature measurements, little difference was found between the two loadings for a given substrate, when pure propane fuel was used. The minimum ignition temperature, although not shown, varied only slightly. Differences between Torvex and Alsimag may be ascribed to the total surface per unit volume; the ratio is aproximately 2 to 1. The gain in performance due to added active metal is essentially negligible. In the case of metal substrate, variation in loading from 20 to 40 g/ft^3 did produce significant differences, probably because the gross surface area is still greater than in the two preceding cases, and additional metal can result in additional active surface.

Variation of fuel produced minor differences; combustion temperatures using industrial propane were slightly higher. However, the minimum ignition temperatures were lower by 25K to 50K, and the ignition was more rapid. Disappearance of propane also tended to be greater; at the same time, the fraction of CO in product gases tended to be larger.

The effect of high-temperature exposure of catalyst to air was also investigated. Samples which had been stabilized in air for 24 hours at 1000 C (OC-1), then treated for an additional 24 hours at 1100 C (OC-2) and an additional 24 hours at 1200 C (OC-3) were tested on the two grades of propane. Results are shown in Table 2.

The effect of air-aging is strong in two important respects. The degree of reaction, as shown in Table 2, is reduced by the successive treatments. Not shown, but a pronounced effect, is the rate at which reaction propagates. Response of sample OC-1 to fuel was rapid; response of sample OC-3 was very sluggish. This was especially true for pure propane. Industrial propane produced a more uniform response time, although performance also decreased with aging.

ACKNOWLEDGEMENT

Thanks are due to Ms. C. J. Hewitt for programming and running the analytical model and to Dr. M. F. Zabielski for assistance in mass spectrometric analysis.

REFERENCES

1. Burgess, D. and M. Hertzberg: The Flammability Limits of Lean Fuel-Air Mixtures. ISA Transactions, Vol. 14, pp. 129-136, (1975).

2. Coward, H. F. and G. W. Jones: Limits of Flammability of Gases and Vapors. Bulletin 503, Bureau of Mines, U.S. Dept. of Interior, Washington, D.C. (1952).

3. Clarke, A. E., A. J. Harrison and J. Odgers: Combustion Stability in a Spherical Combustor. Seventh Symposium (International) on Combustion, pp. 664-673, (1958).

4. Gordon, S. and S. J. McBride: Computer Program for Calculation of Complex Chemical Equilibrium Compositions Rocket Performance, Incident and Reflected Shocks and Chapman-Jouget Detonations. NAS SP-273, (1971).

5. Stull, D. R., et al.: JANAF Thermochemical Tables. Dow Chemical Company, Midland, Michigan, 1960 et seq.

TABLE 1

Combustion Temperatures as a Function of Substrate and Active Surface

All runs at Tin = 400 C

φ	T-19	T-41	Al-41	Al-74	Al74I
.4	625	570	665	695	650
1.0	785	800	930	800	940
1.8	770	760	825	815	830

φ	M-20	M-20I	M-40	M-40I
.4	530	540	645	660
1.0	680	750	885	890
1.8	695	-	815	825

TABLE 2

Effect of Heating on Catalyst Activity

All runs at T_{in} = 400 C

Ø	OC-1 T,K	OC-2 T,K	OC-3 T,K
0.4	605		425
1.0	755		415
1.8	710		430
(C.P. Fuel)			
0.4	465	440	445
1.0	685	535	545
1.8	700	590	490
(Industrial Propane)			

FIG. 1

UTRC CATALYTIC COMBUSTION LABORATORY

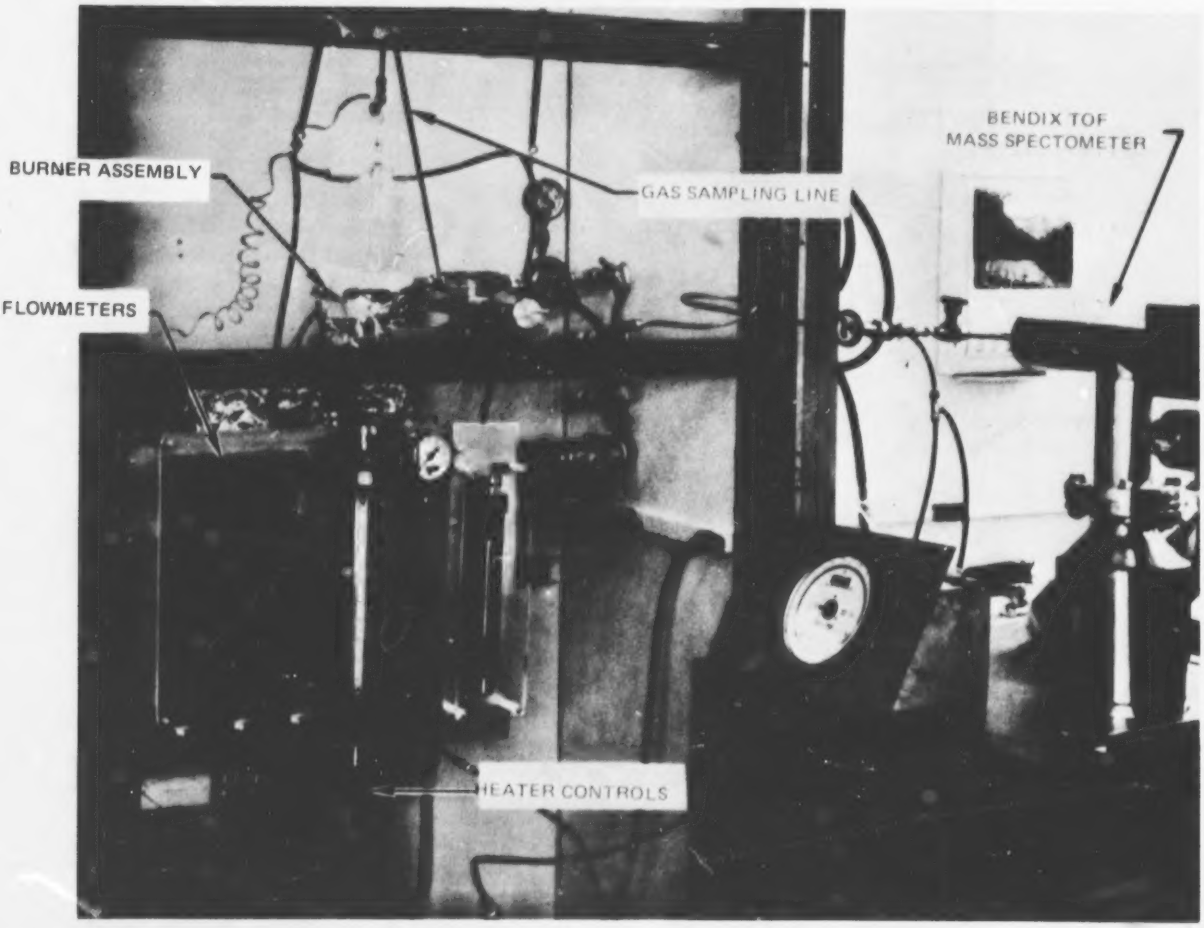

FIG. 2

UTRC CATALYTIC BURNER

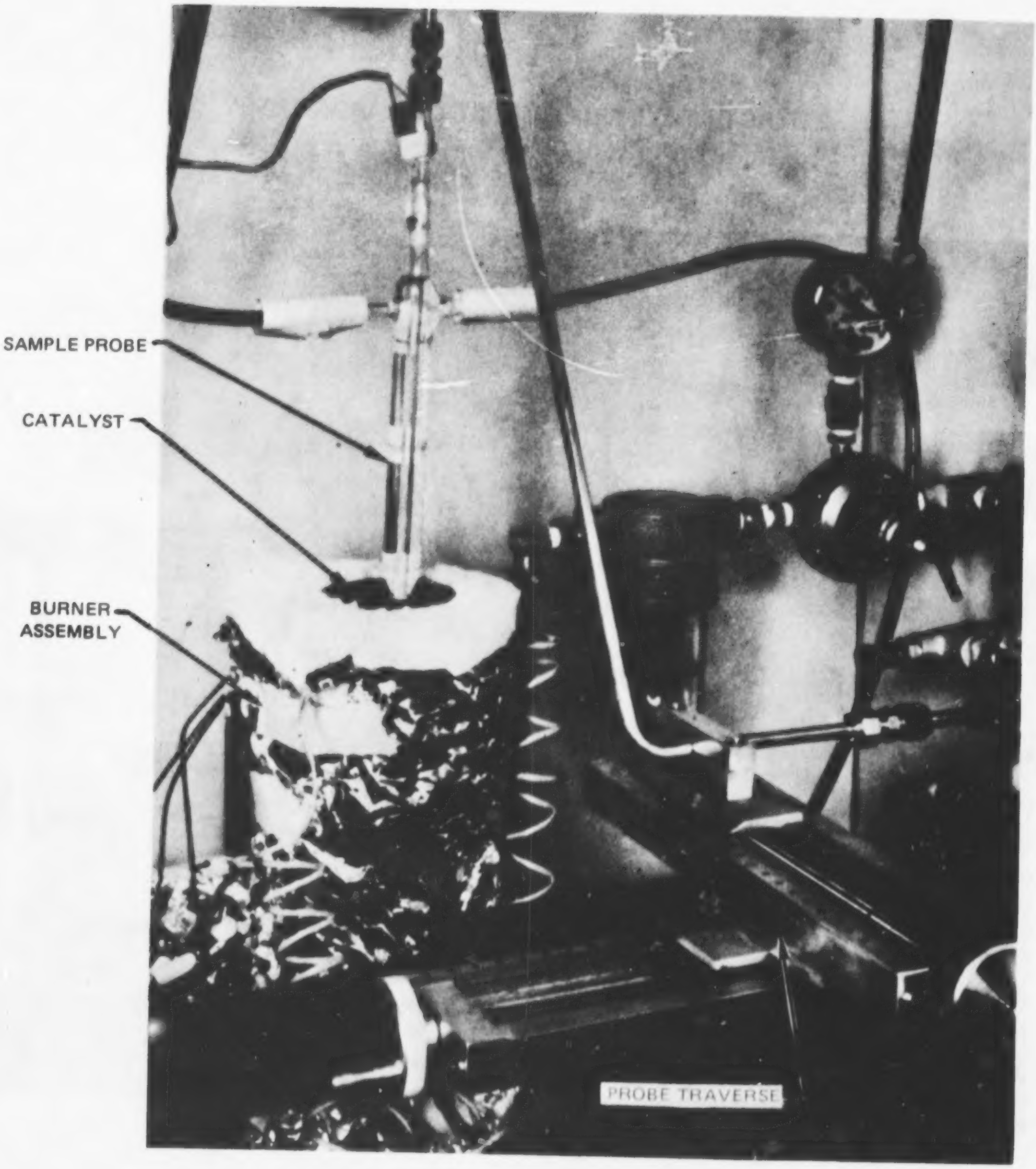

SECTIONAL VIEW OF CATALYTIC BURNER

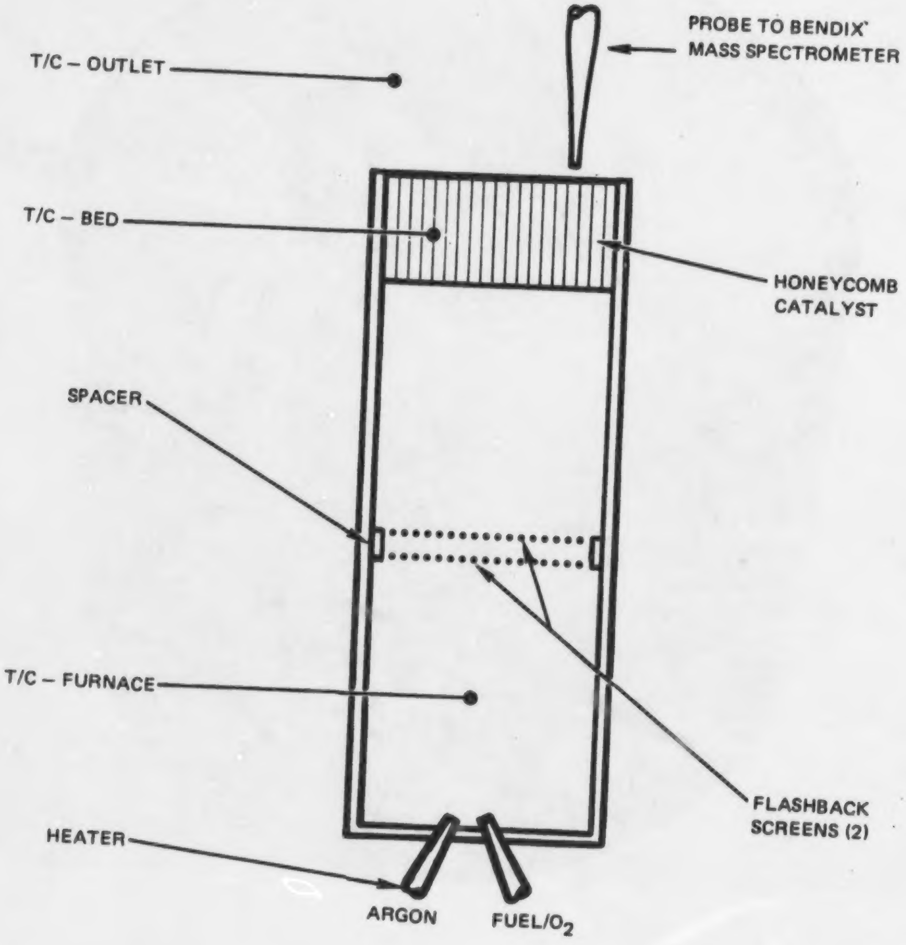

FIG. 4

TYPICAL MOUNTING OF CATALYST SAMPLE

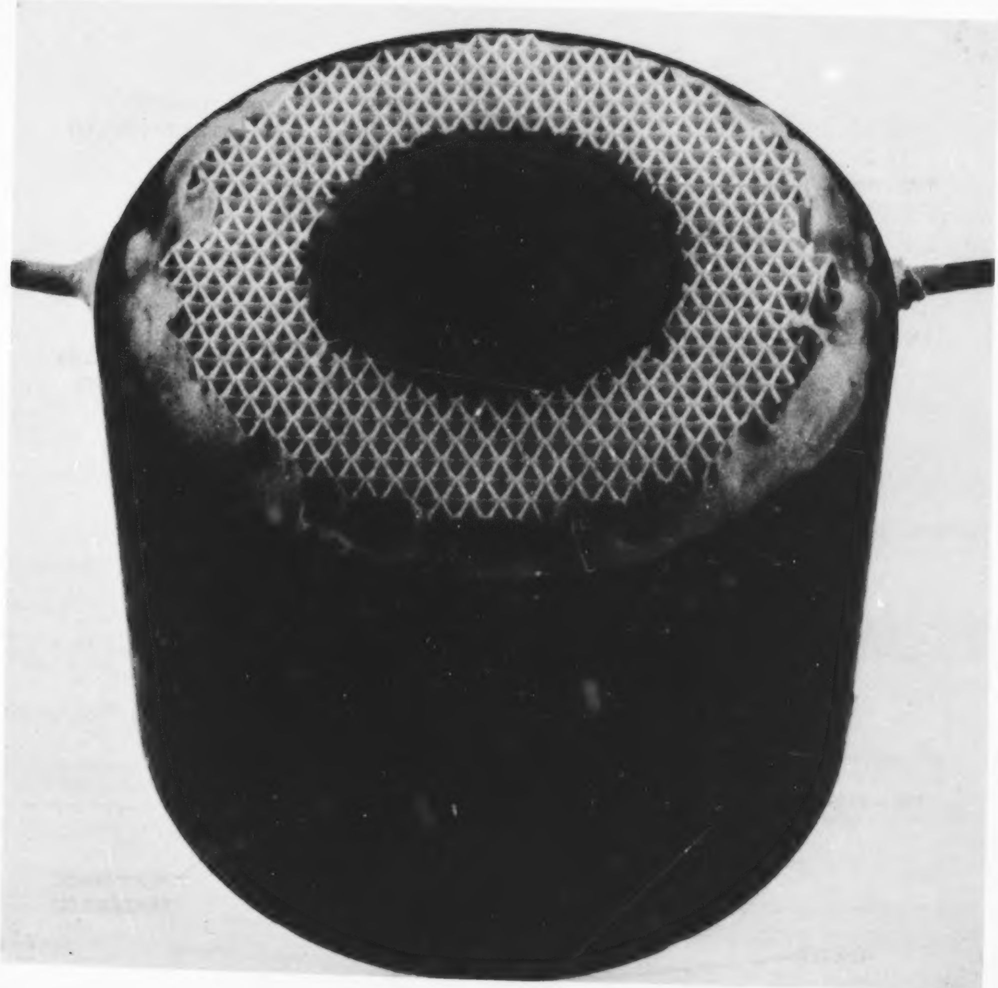

FIG. 5

IGNITION TEMPERATURE OF PROPANE/AIR MIXTURE

C.P. PROPANE

MATTHEY BISHOP CATALYST, 1 IN. THICK

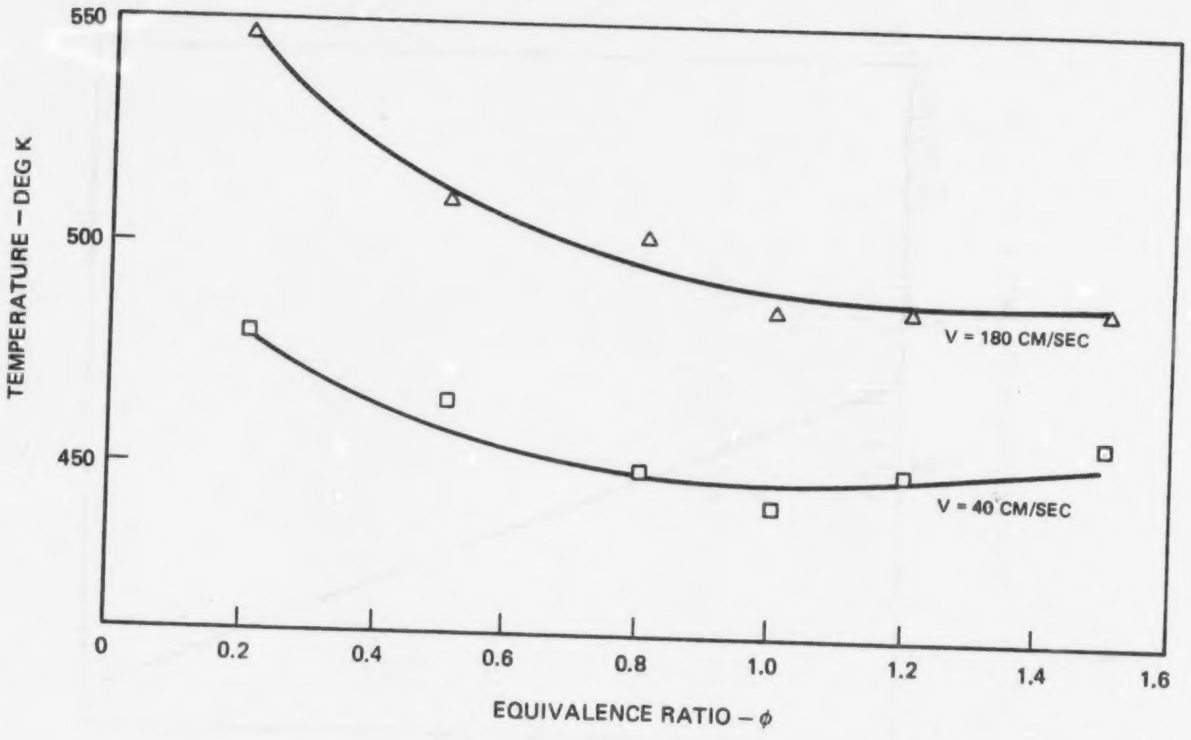

FIG. 6

EFFECT OF TEMPERATURE ON LEAN FLAMMABILITY LIMIT OF PROPANE/AIR MIXTURES

REF: BURGESS AND HERTZBERG

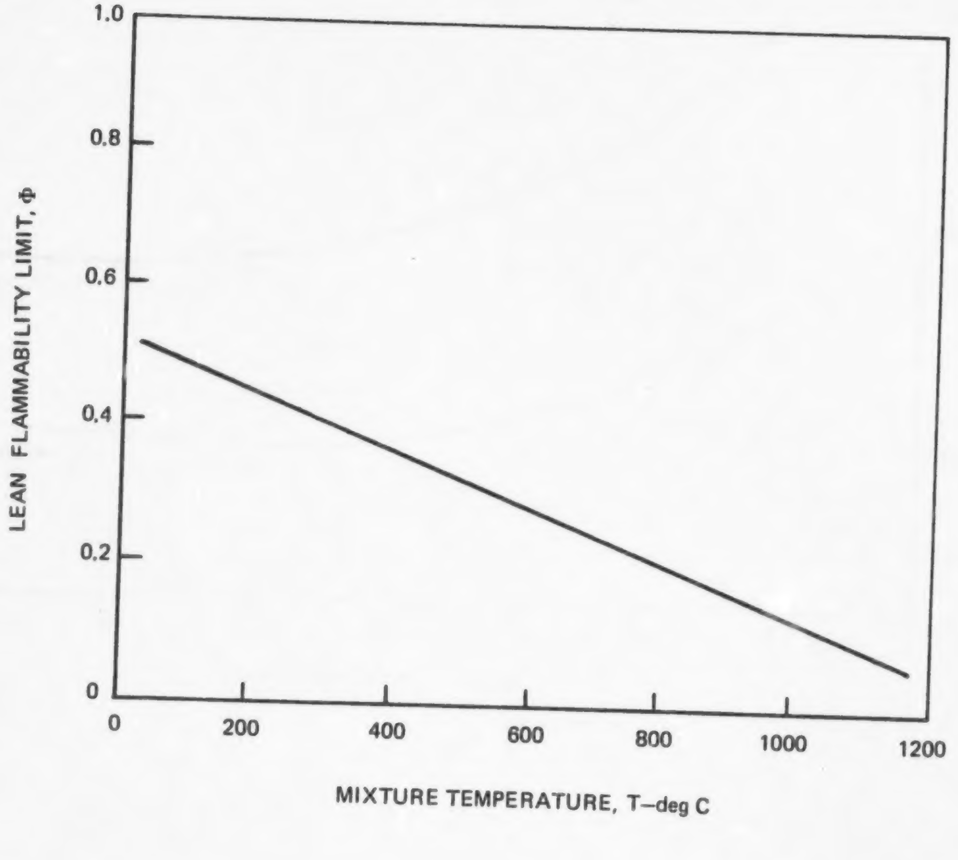

FIG. 7

EFFECT OF GAS SPACE VELOCITY ON IGNITION TEMPERATURE OF PROPANE–AIR MIXTURES

C.P. PROPANE

MATTHEY–BISHOP CATALYST, 1 IN. THICK

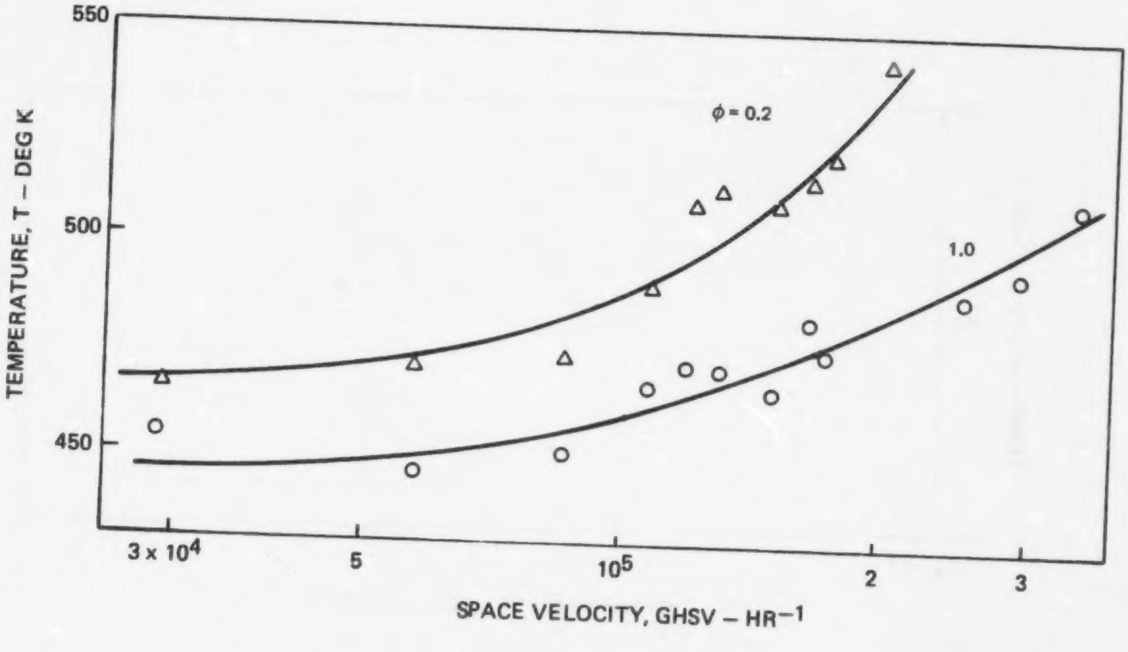

FIG. 8

EFFECT OF NITROGEN ADDITION ON IGNITION TEMPERATURE OF PROPANE–AIR MIXTURES

C.P. PROPANE

MATTHEY–BISHOP CATALYST, 1 IN. THICK

EQUIVALENCE RATIO, $\phi = 1.0$

NITROGEN ADDED:

○ 25 PERCENT
◇ 50
□ 100

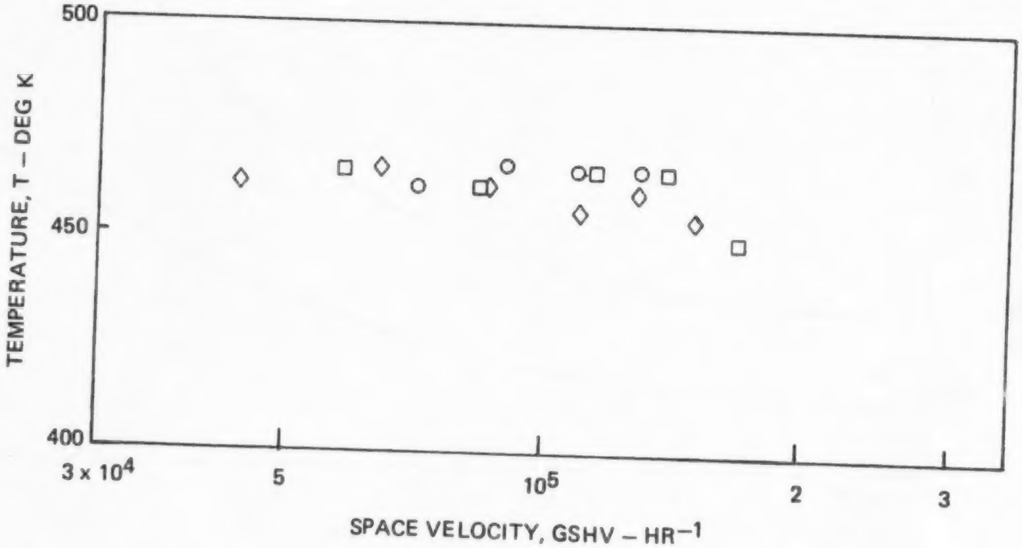

FIG. 9

VARIATION OF HETEROGENEOUS RATE WITH TEMPERATURE

$K = \alpha \exp -E/RT$

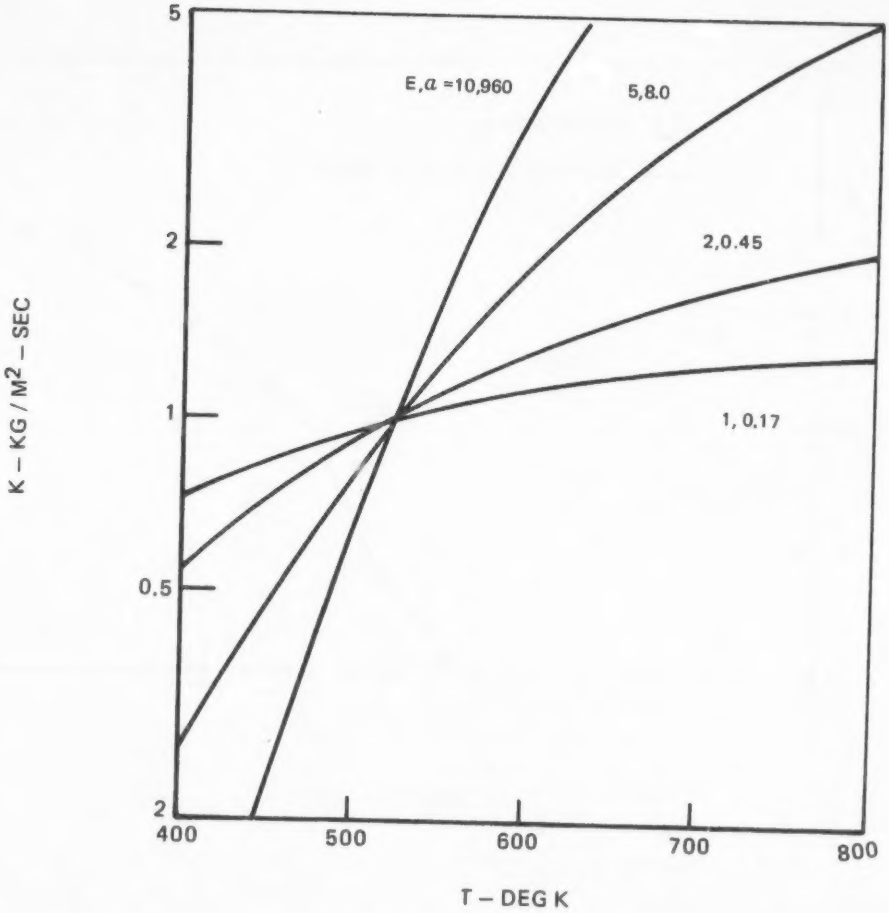

FIG. 10

COMBUSTION EFFICIENCY IN ISOTHERMAL TESTS

FUEL– C.P. PROPANE

CATALYST–MATTHEY BISHOP HONEYCOMB, 1 IN. THICK

EQUIVALENCE RATIO – 1.0

DILUENT ARGON 20/1

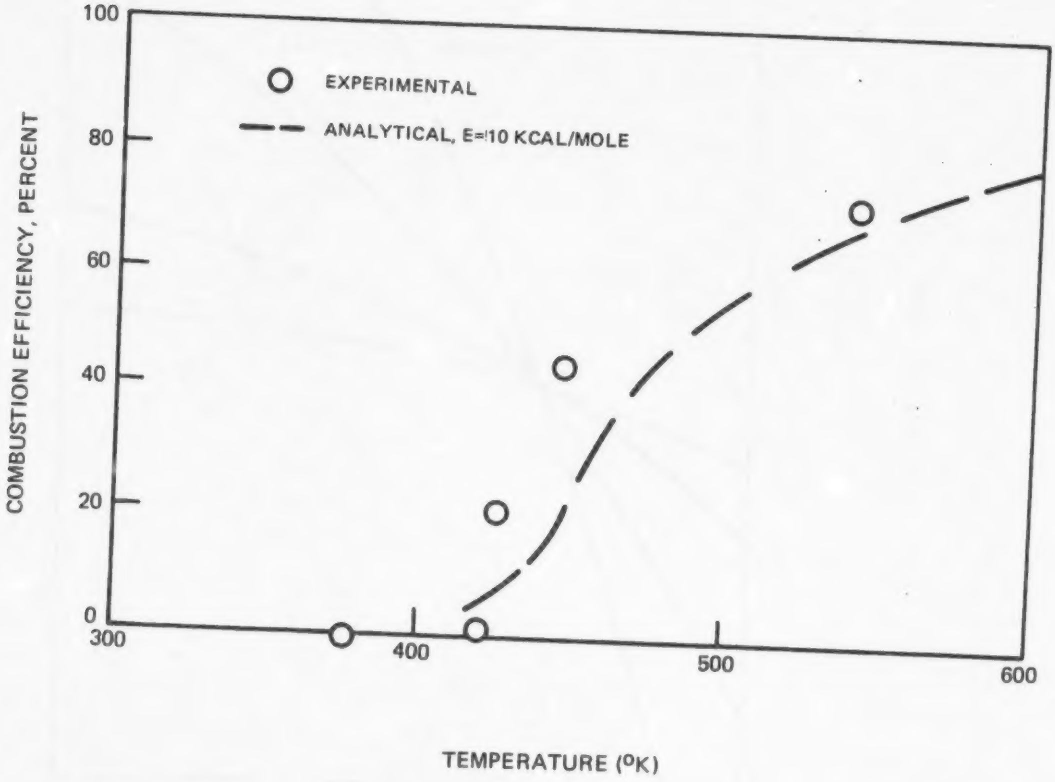

DEPENDENCE OF CO_2 AND CO CONCENTRATION ON EQUIVALENCE RATIO

BURNER INLET MIXTURE: Pr/O_2/Ar 20/1 DILUTION

INLET TEMPERATURE: 673 K

OUTLET TEMPERATURE: 925 K

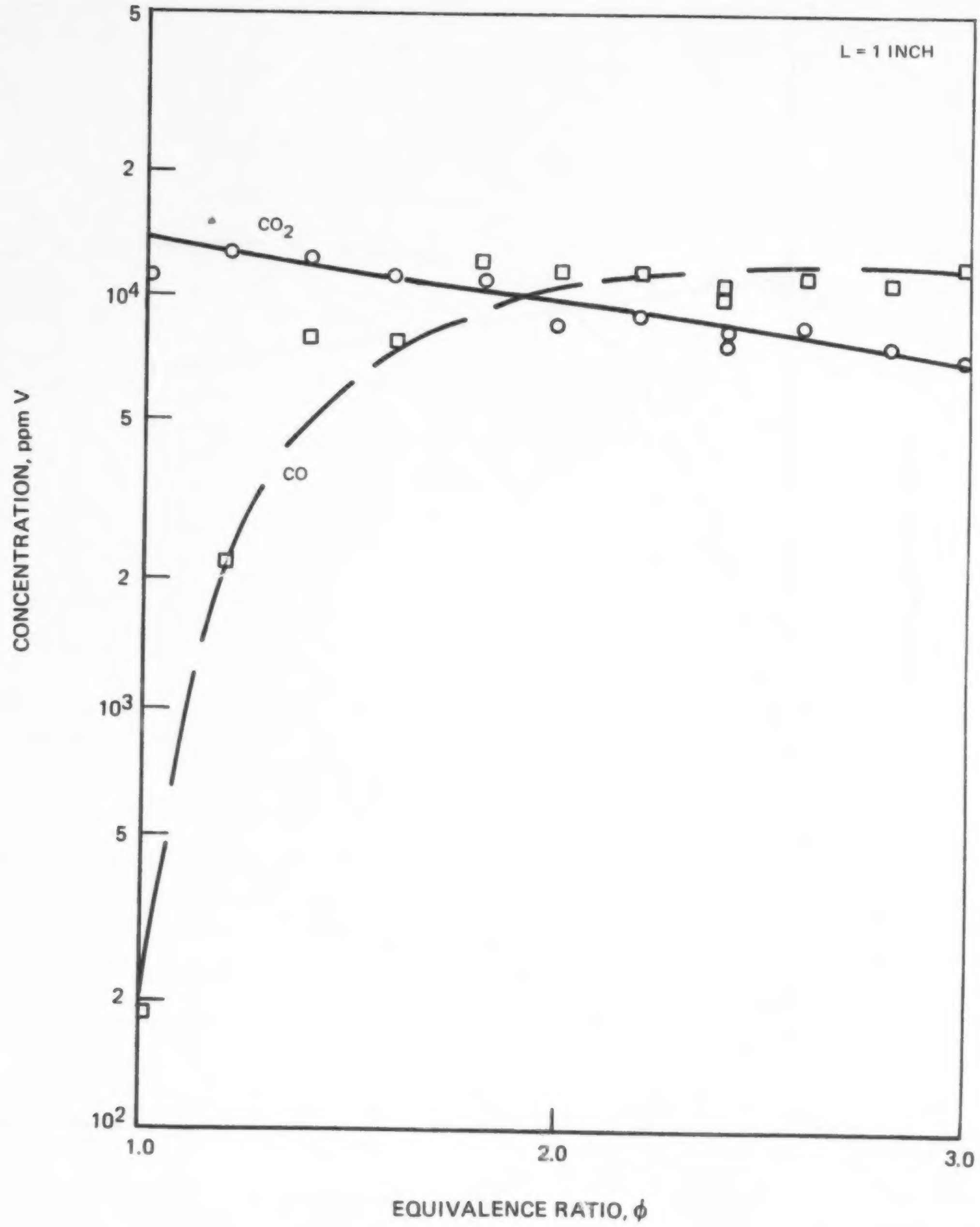

FIG 12

DEPENDENCE OF MEASURED CONCENTRATIONS OF CO_2 AND CO ON EQUIVALENCE RATIO

BURNER INLET MIXTURE: Pr/O_2/Ar, 20/1 DILUTION

INLET TEMPERATURE: 673 K

EXHAUST TEMPERATURE: 875 K

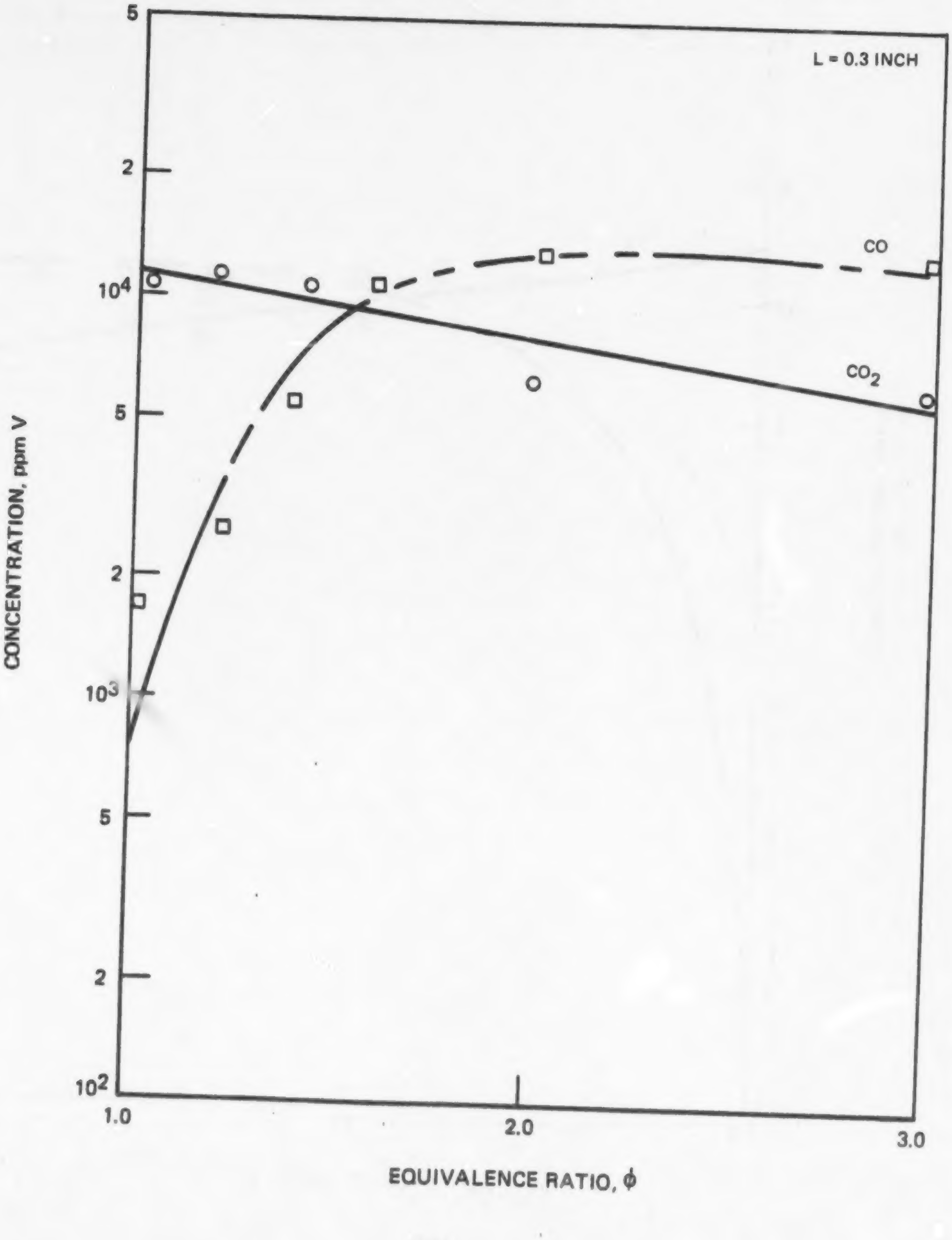

FIG 13

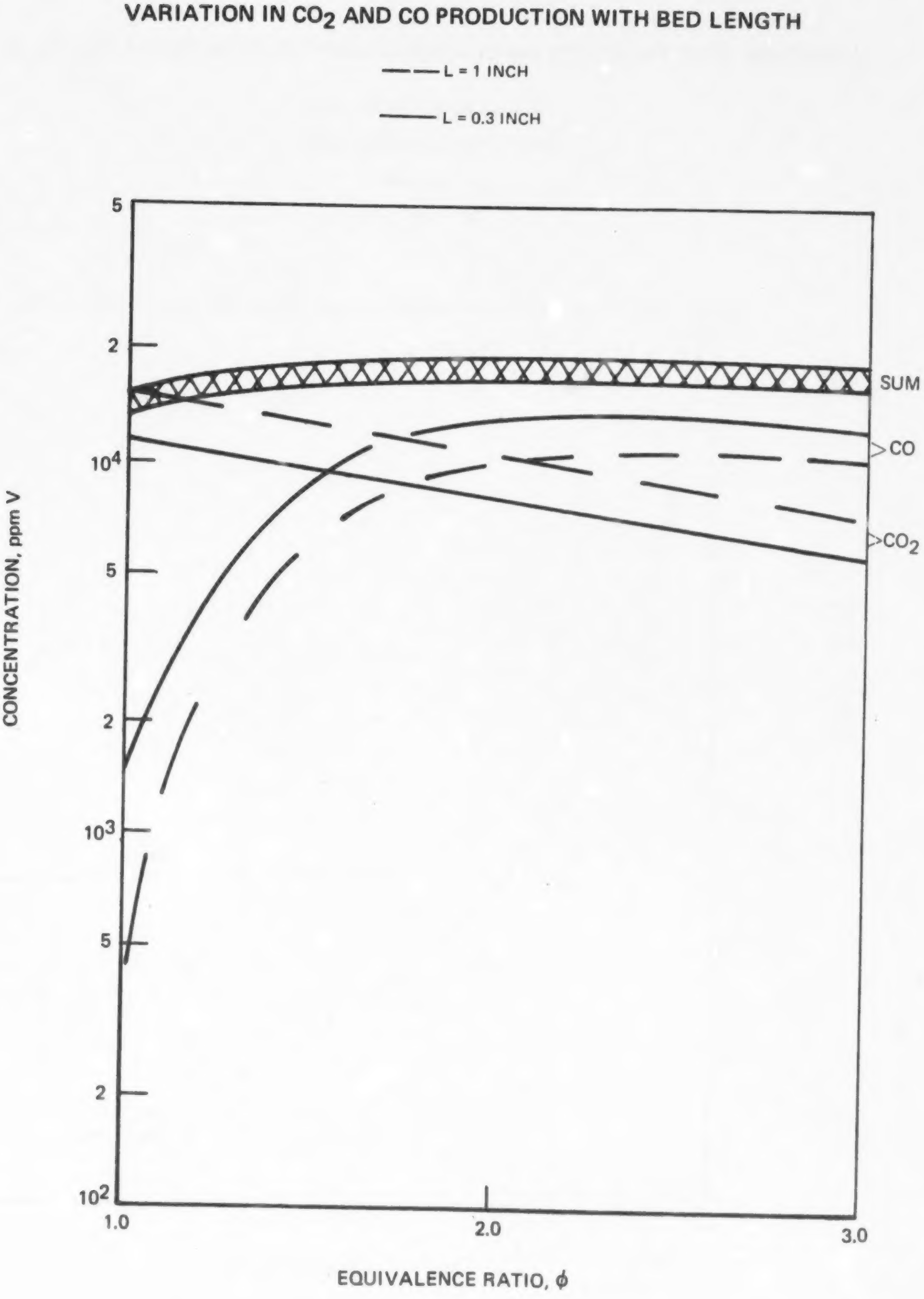
VARIATION IN CO_2 AND CO PRODUCTION WITH BED LENGTH
L = 1 INCH
L = 0.3 INCH
5
2
10^4
5
2
10^3
5
2
10^2
1.0
2.0
3.0
CONCENTRATION, ppm V
EQUIVALENCE RATIO, ϕ
SUM
CO
CO_2

FIG 14

EFFECT OF STOICHIOMETRY ON MEASURED AND CALCULATED RATIO CO_2/CO

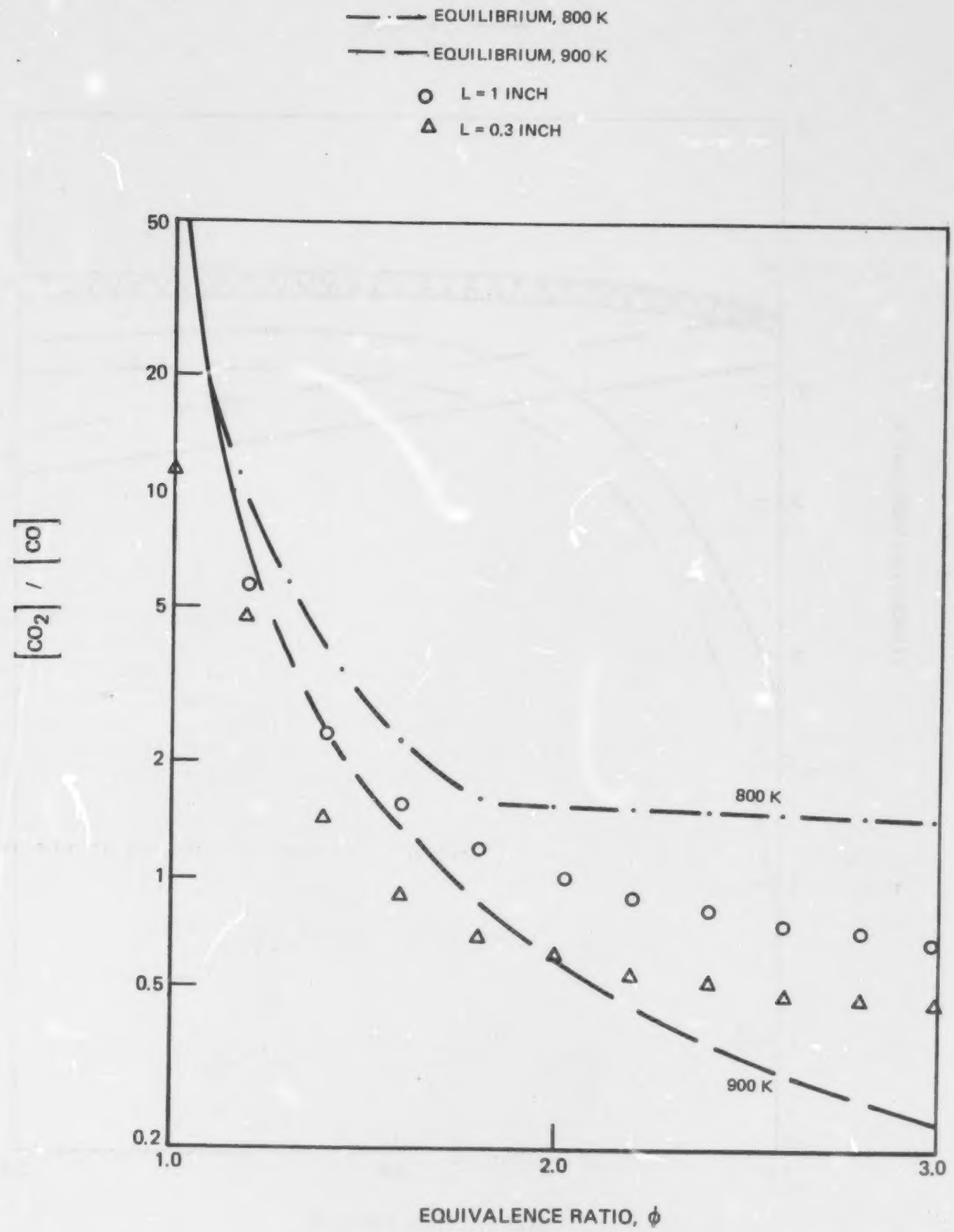

APPENDIX

STEADY-STATE ANALYSIS OF THE USE OF CATALYZED SURFACE REACTORS TO PROMOTE COMBUSTION

The analysis of a catalyzed surface reactor to promote hydrocarbon combustion pertains to a monolithic structure containing uniformly distributed parallel flow passages of arbitrary cross section. The walls of the flow passages are impregnated with catalytic materials. Fuel and air flowing through the passages diffuse normal to the flow and are taken to react at the catalyzed surface.* Combustion products and the heat generated by catalytic reaction are transported from the walls to the interstitial fluid. As the fluid moves downstream it is also heated by homogeneous gas phase reaction to a temperature which exceeds the temperature of the structure. From this point to the end of the reactor the fluid loses heat to the surface by convection. The heat gained by the structure in the downstream end of the reaction chamber is conducted back upstream.

In developing a steady-state model of this system, the bed temperature and the temperature and reactant concentrations in the interstitial fluid are assumed to vary only with axial distance along the reactor. The axial diffusion of heat and mass in the fluid is neglected. In applying the model to the analysis of low temperature experiments designed to extract information on rates of catalytic reaction, radiation heat transfer can be neglected. Mass transfer coefficients and heat convection coefficients relating heat transfer between the interstitial fluid stream and either the reactor bed or surroundings are permitted to vary with axial distance along the reactor.

The general equations describing the rates of change with axial distance of the weight fractions of each of the chemical species in the interstitial phase are:

$$\frac{dw_F}{dz} = -\frac{1}{G}\left\{r_{hom}\delta + k_c^F A_s\left[\rho_F - (\rho_F)_s\right]\right\} \tag{1}$$

$$\frac{dw_{O_2}}{dz} = -\frac{1}{G}\left\{r_{hom}\delta \frac{M_{O_2}}{M_F}\gamma_{O_2} + k_c^{O_2} A_s\left[\rho_{O_2} - (\rho_{O_2})_s\right]\right\} \tag{2}$$

---

*Diffusion of reactant molecules within the pores of the substrate is not considered.

$$\frac{dw_{H_2O}}{dz} = \frac{1}{G}\left\{r_{hom}\,\delta\,\frac{M_{H_2O}}{M_F}\,\gamma_{H_2O} - k_c^{H_2O}\,A_s\left[\rho_{H_2O} - (\rho_{H_2O})_s\right]\right\} \qquad (3)$$

$$\frac{dw_{CO_2}}{dz} = \frac{1}{G}\left\{r_{hom}\,\delta\,\frac{M_{CO_2}}{M_F}\,\gamma_{CO_2} - k_c^{CO_2}\,A_s\left[\rho_{CO_2} - (\rho_{CO_2})_s\right]\right\} \qquad (4)$$

$$\frac{dw_{inert}}{dz} = 0 \qquad (5)$$

The rates of change of species concentrations with axial distance are then given by

$$\frac{d\rho_J}{dz} = \rho\,\frac{dw_J}{dz} + w_J\,\frac{d\rho}{dz} \qquad (6)$$

where

$$\frac{1}{\rho}\frac{d\rho}{dz} = \frac{1}{P}\frac{dP}{dz} + \frac{1}{\overline{M}}\frac{d\overline{M}}{dz} - \frac{1}{T_i}\frac{dT_i}{dz} \qquad (7)$$

and

$$\frac{1}{\overline{M}}\frac{d\overline{M}}{dz} = -\left[\frac{\sum_J \frac{dw_J}{dz}\Big/M_J}{\sum_J \frac{w_J}{M_J}}\right] \qquad (8)$$

Empirical correlations used to represent heat and mass transfer coefficients and pressure drop as functions of the flow regime in the reaction chamber.

Rates of homogeneous gas phase reaction can normally be written as global functions of reactant concentrations and temperature

$$r_{hom} = f(\rho_F, \rho_{O_2}, T_i). \qquad (9)$$

Surface concentration of reactants and products can be related to the rate of catalytic reaction by

$$r_{het} = k_c^F \left[\rho_F - (\rho_F)_s\right] = \frac{M_F}{M_{O_2}} \frac{k_c^{O_2}}{\gamma_{O_2}} \left[\rho_{O_2} - (\rho_{O_2})_s\right]$$

$$= \frac{M_F}{M_{H_2O}} \frac{k_c^{H_2O}}{\gamma_{H_2O}} \left[(\rho_{H_2O})_s - \rho_{H_2O}\right] = \frac{M_F}{M_{CO_2}} \frac{k_c^{CO_2}}{\gamma_{CO_2}} \left[(\rho_{CO_2})_s - \rho_{CO_2}\right] \qquad (10)$$

where

$$r_{het} = f \left[(\rho_F)_s, (\rho_{O_2})_s, (\rho_{H_2O})_s, (\rho_{CO_2})_s, T_s\right]. \qquad (11)$$

The change in enthalpy of the interstitial fluid with position is related to the temperature of the structure by

$$G \frac{dh_i}{dz} - h A_s (T_s - T_i) + \frac{h_a p}{A_x} (T_i - T_a) + r_{hom} H \delta = 0. \qquad (12)$$

Assuming structural thicknesses normal to the flow direction are small enough so that the temperature at all points of a cross section can be taken as the same, the equation describing heat conduction in the bed may be written as

$$(1-\delta) k \frac{d^2 T_s}{dz^2} = h A_s (T_s - T_i) + A_s H r_{het} \qquad (13)$$

where the thermal conductivity of the monolithic structure is taken as constant.

If the heat transfer coefficient in Eq. (13) is a function of axial position, it is often desirable to express it in the form

$$h(z) = h_0 + a(z). \qquad (14)$$

The boundary conditions for Eq. (13) are

$$\frac{dT_s}{dz} = 0 \quad \text{at} \quad z = 0 \tag{15}$$

$$\frac{dT_s}{dz} = 0 \quad \text{at} \quad z = L \tag{16}$$

providing that heat loss from the ends of the structure is negligible. It should be noted that this condition also implies that all heat transferred from the fluid to the bed in the downstream section of the chamber is transferred back to the fluid in the upstream section, i.e.,

$$\int_0^L \left(\hbar(z) \left[T_s(z) - T_i(z) \right] + Hr_{het} \right) dz = 0. \tag{17}$$

With the knowledge of variation in fluid properties with temperature and extent of reaction, the system is completely defined. The simultaneous solution of these equations can be simplified greatly by converting Eq. (13), together with the boundary conditions given by Eqs. (15) and (16), into integral form (Refs. A-1 and A-2) as

$$\begin{aligned} T_s(z) = {} & \frac{\cosh\theta(L-z)}{\theta\sinh\theta L} \int_0^z \left[\alpha(\xi)(T_i - T_s) - Hr_{het} + h_o T_i \right] \frac{A_s}{(1-\delta)k} \cosh\theta\xi \, d\xi \\ & + \frac{\cosh\theta z}{\theta\sinh\theta L} \int_z^L \left[\alpha(\xi)(T_i - T_s) - Hr_{het} + h_o T_i \right] \frac{A_s}{(1-\delta)k} \cosh\theta(L-\xi) \, d\xi \end{aligned} \tag{18}$$

where

$$\theta = \sqrt{\frac{\hbar_0 A_s}{(1-\delta)k}}$$

Equation (18) is an implicit integral equation which can be solved numerically to determine the temperature at any point in the bed in terms of the surface concentrations and the temperature in the interstitial fluid. By solving this equation simultaneously with Eqs. (1) through (12), both the fluid and the surface concentration and temperature profiles can be determined. Numerical methods have been developed to accomplish this. The computational scheme consists generally of assuming a bed temperature profile, computing the fluid temperatures and concentrations corresponding to this assumed profile using finite difference representations of Eqs. (1) through (12), and then using Eq. (18) to compute a new bed temperature profile. The next assumed bed temperature profile is then computed from the calculated profile by adjusting the latter to satisfy Eq. (17), i.e.,

$$\left[T_s(z)\right]_{\text{assumed}} = \left\{ T_s(z) - \frac{\int_0^L \left(h(z)\left[T_s(z) - T_i(z)\right] + Hr_{\text{het}} \right) dz}{\int_0^L h(z)\, dz} \right\}_{\text{calculated}} \qquad (19)$$

Iteration continues until successive assumed and calculated profiles converge within a fixed tolerance.

REFERENCES

A-1. Kesten, A. S.: An Integral Equation Method for Evaluating the Effects of Film and Pore Diffusion of Heat and Mass on Reaction Rates in Porous Catalyst Particles. AIChE Journal 15, pp. 128-131, January 1969.

A-2. Kesten, A. S., J. J. Sangiovanni and L. S. Bender: The Use of Axial Heat Combustion as a Mechanism for Promoting Exothermic Chemical Reactions in Packed-Bed Reactors. Proceedings of the Fourth International Heat Transfer Conference, Vol. VII, Paris, France, September 1970.

PROTOTYPE SURFACE COMBUSTION FURNACE EVALUATION

by

G. Blair Martin
Combustion Research Branch
Energy Assessment and Control Division
U. S. Environmental Protection Agency
Research Triangle Park, North Carolina 27711

ABSTRACT

Prototype Surface Combustion Furnace Evaluation

by G. Blair Martin

The emissions characteristics of a prototype surface combustion residential furnace have been evaluated using both propane and natural gas. The combustion of premixed fuel and air takes place on a refractory surface without a visible flame. Heat is transferred from the surface to an air cooled firebox wall by radiation. This maintains a relatively low surface temperature and reduces the oxides of nitrogen (NO_x).

The furnace was operated over a range of excess air from 5 to 45% and with heat input from 16,000 to 24,000 watts. For a nominal operating point for natural gas at 10% excess air, NO_x emissions were less than 15 ppm (as measured). CO and HC emissions were also low. Furnace efficiency calculated from flue losses was greater than 80%. Performance on propane was similar.

INTRODUCTION

The Combustion Research Branch (CRB) of the EPA's Industrial Environmental Research Laboratory at Research Triangle Park, N.C., has the responsibility for carrying out a combustion modification R&D program directed toward control of nitrogen oxides and other pollutants from stationary combustion sources. In addition to pollutant emission control it appears that the technology can also lead to equal or improved efficiency of energy utilization compared to current practice. The majority of the R&D is carried out under EPA contracts initiated and directed by CRB and performed by private organizations. However, CRB also maintains an in-house research program in a number of areas. This in-house activity provides direct project officer expertise in combustion research and provides the capability for initial evaluation of potential control techniques or promising novel concepts applicable to combustion systems. The results of many of these studies are well documented.

A continuing activity is the evaluation of novel combustion devices which may have the potential for very low pollutant emissions. One such device is a prototype of a residential gas fired furnace using surface combustion to promote fuel oxidation. The purpose of this paper is to describe the performance of that prototype.

BACKGROUND

Stationary combustion equipment used in residential heating can be classified as area sources. Pollutant emissions from an individual unit are relatively small, the discharge into the atmosphere is near ground level in populated areas, the emissions are concentrated in the heating season and the number of sources is large (i.e., about 55 X 10^6 units).

Preceding page blank

Although the residential sources contribute only about 3% of the mass emissions of nitrogen oxides (NO_x), the environmental impact may be much more significant. In addition, these sources require relatively clean fuels (e.g., natural gas and distillate oil) and account for over 10% of the stationary source energy usage (ref. 1). In 1974, residential warm air furnaces used over 4.5 X 10^{12} kJ of fuel with natural gas and propane providing about 60% and fuel oil providing the balance. Based on these factors, it appears that both emission control and energy conservation in this source class are required. The emission levels for distillate oil fired residential furnaces have been characterized (ref. 2) and there has been some technology development for reducing emissions and increasing efficiencies (ref. 3). Much less work has been done on gas fired residential furnaces because of less flexibility in adjusting operating conditions and relatively simpler equipment design. The normal residential gas furnace does not have a "burner" as such, but rather relies on natural draft to provide combustion air and to accomplish fuel and air mixing. The available gas pressure is used to entrain some air and to form a primary air and fuel mixture that is admitted to the combustion chamber through one or more log manifolds. Secondary air to complete combustion is admitted to the combustion chamber around the manifolds. Although the primary air can be controlled to a degree, there is essentially no way to control secondary air. Therefore, the overall excess air cannot be controlled to a significant degree.

The available emission data on gas fired furnaces are very limited. Hall (ref. 3) reported data for three gas furnaces with NO_x emissions ranging from 0.084 to 0.115 gm of NO_x (as NO) per 10^6 cal [i.e., 0.32 to 0.42 kg NO_x (as NO_2) per 10^{10} J]. Any given furnace could only be operated over a narrow range of excess air; however, the three different designs operated at levels in the range of 20 to 60% excess air. The emissions of carbon monoxide (CO) and hydrocarbon (HC) were low for all three furnaces at the normal operating point. DeWerth (ref. 4) measured emissions from 38 forced warm air gas furnaces in the AGA laboratory and reports an average NO_x value of 0.097 lb NO_x (as NO_2) per 10^6 Btu [i.e., 0.415 kg NO_x (as NO_2) per 10^{10} J] with a small effect of furnace design. Decreasing the primary air setting to the point of yellow flame operation decreased the NO_x level by about 10%; however, CO emissions increased by a factor of 20 and the NO_2 component increased from about 5% of the total NO_x to the range of 10 to 17%. Data for other gas appliances and for modified furnace design also showed high fractions of NO_2 associated with higher CO levels. Several modifications of furnace design were examined with the most successful one achieving 37 ppm of NO_x [i.e., 0.172 kg NO_x (as NO_2) per 10^{10} J] at low CO levels by putting a screen in the flame zone to increase radiant heat transfer. Finally, Brookman (ref. 5) performed field measurements on 50 residential gas fired furnaces and boilers and reported average NO_x emissions of 112 lb (as NO_2) per 10^6 ft^3 of gas [i.e., about 0.455 kg NO_x (as NO_2) per 10^{10} J].

The efficiency of the furnace is dependent on the extent of heat loss from the system by various avenues. The predominant energy losses are the following:

1. Latent heat of vaporization of the water formed during combustion which cannot be recovered without a condensing heat exchanger. About 10% of the gross heat input of natural gas is irretrievably lost in this form using current technology.

2. Sensible heat in the combustion products which is dependent on the amount of excess air used for combustion, the amount of dilution air and the temperature of the gas in the flue. This loss can be reduced by low excess air operation, elimination of dilution air and/or reduction of stack temperature.

3. Draft losses, which remove residual heat from the firebox during the off-cycle. This loss can be reduced by minimizing or eliminating air flow through the furnace during off-cycle.

4. Miscellaneous casing losses. These losses are normally held to a minimum by proper insulation of the furnace enclosure.

The significant features of these losses are discussed for fuel oil in reference 3. The general discussion also holds for natural gas, although differences in latent heat losses and system design will change the quantitative levels. DeWerth (ref. 4) reported that the average of furnaces tested in the AGA Lab had 5.8% CO_2 in the flue products (approximately 100% excess air); however, no flue temperatures were given. Flue losses for two units tested were reported to be 20.1 and 26.6%, based on steady state operation. The cycle average efficiency will be further reduced by the draft and casing losses.

EXPERIMENTAL APPROACH

This section provides information on several aspects of the experimental approach including: 1) the fuel supply system; 2) the Bratko* prototype furnace; 3) the analytical instrumentation; and 4) the range of variables examined.

Fuel Supply

Natural gas was provided from a laboratory gas line at a pressure of 3.45×10^4 pascal gage [5 psig]. Propane was provided from a pressurized gas bottle and the line pressure was controlled at 4.83×10^4 pascal gage [7 psig]. The gas supply was passed through a dry gas meter to obtain a volumetric flow rate. Following this the pressure was regulated to 3.45×10^3 pascal gage [0.5 psig] and the gas passed through an ASTM orifice meter. The pressure drop across the orifice was used to adjust the gas flow to a constant value during a test series. The gas supply was connected to the fuel inlet system of the furnace.

Bratko Prototype Furnace

The furnace tested was a prototype of a surface combustion concept for use in residential gas furnaces. The concept is based on combustion of premixed fuel and air on the surface of a refractory matrix without

---

(*) Bratko Corp., 10714 Harvard Ave., Cleveland, OH 44105 visible flame. The glowing refractory surface radiates to a surrounding air cooled combustion chamber and, thereby, maintains the surface temperature at a relatively low value (i.e., below about 1250 K). A schematic of the surface combustor and firebox is shown in Figure 1. The combustion chamber was enclosed in a conventional upright furnace body and used a three speed circulating air fan to pass air over the heat exchange surface. The speed of the fan increased stepwise as the pressure drop across the system increased.

The combustion air was supplied by an external centrifugal fan that was considerably oversized in capacity, but was necessary to supply the required pressure. [This arrangement would not be practical in a production furnace; however, Bratko stated that a small fan with the necessary pressure capability has been developed (ref. 6)]. A regulator drops the natural gas supply pressure to 3450 pascals gage (0.5 psig), then the gas is piped through solenoid valves to both a pilot burner and the main furnace. The pilot burner premixes the gas with part of the combustion air and the mixture is ignited with a spark. A flame rod is used to prove the pilot flame prior to the burner gas solenoid valve opening. The burner gas supply is premixed with combustion air with a mixing device (in the prototype furnace the amounts of both air and fuel could be controlled independently, although in practice, relatively fixed flow rates would be expected). The premixed gas and air is fed to a plenum inside the surface combustor at a pressure of about 895 pascals gage (0.13 psig) and is forced through the refractory pad to burn on the surface. The refractory is selected to be sufficiently insulating that the plenum temperature remains essentially at ambient, thereby eliminating preignition due to heat feedback.

Analytical Instrumentation

The gas sample for analysis was withdrawn from the flue after the gas had been cooled to 422-475 K in the convective pass of the heat exchanger. The samples are conditioned and analyzed with a similar system to that described earlier (ref. 7). To summarize, the analytical instruments are: 1) oxygen by paramagnetic resonance; 2) CO and CO_2 by non-dispersive infrared (NDIR); 3) hydrocarbon by flame ionization detector; 4) NO by a long path NDIR; and 5) NO and NO_x by chemiluminescence analyzer. The temperature of the flue gas was measured with a dial thermometer and cross checked with a thermocouple.

Range of Variables

The tests were planned to screen the furnace combustion and emission performance over the permissible range of operation. The two variables were fuel flow and excess air level. Since there was some interaction between fuel and air flow in the mixer it was not possible to attain completely comparable input levels. Therefore, three nominal values were used: 16,000, 19,000 and 22,000 watts (55,000, 65,000, and 75,000 Btu/hr, respectively). The excess air range for the first two fuel flows was from 45% down to the point where excessive CO (i.e., > 200 ppm) was formed. For the highest rate the maximum excess air was 25%.

In addition a limited number of tests were run with propane to establish the multifuel capability of the unit.

EXPERIMENTAL RESULTS

This section presents a discussion of two specific aspects of the results: 1) emission; and 2) efficiency.

Emissions Measurements

The primary evaluation of the furnace performance was based on measurements of pollutant species in the flue gases as a function of operating condition. To fully characterize the operating range the excess air level was varied from a high value (i.e., > 25%) down to the point that excessive

CO (i.e., > 200 ppm) was being emitted. No hydrocarbons or smoke were observed during the test. The effects of excess air and fuel input are discussed below.

Excess Air. The effect of excess air level on emissions is shown in Figure 2 for a thermal input of 16,000 watts (55,000 Btu/hr). The data shown here were obtained during five different experimental periods covering 4 months and the small scatter in the points shows that the performance was quite repeatable. At 40% excess air, the CO emissions are quite low (i.e., 20-30 ppm) and remain low as the excess air is reduced to 10%. When the excess air is reduced below 10% the CO begins to rise sharply and at 5% excess air is greater than 1500 ppm. The results for oxides of nitrogen are shown as measured for both NO and NO_x and corrected to zero % excess air for both NO and NO_x. The NO_x concentration to zero % excess air gives a direct indication of the trend of mass emissions as a function of excess air and will be used as the primary basis of discussion. The NO_x is low (i.e., 7.5 ppm) at 40% excess air and rises slowly to 10 ppm as excess air is decreased to about 15%. Then as excess air is reduced further, the NO_x rises sharply to about 19 ppm at 7.5% excess air. Comparison of the as measured values of NO and NO_x (where the difference is interpreted as being NO_2) shows that the amount of NO_2 increases as the excess air is decreased; however, the ratio of NO_2 to NO is approximately constant. This holds true even when high CO levels are observed.

Fuel Input. The effect of fuel input on emission performance was examined. The furnace design condition was taken as a nominal 16,000 watts (55,000 Btu/hr) and two higher levels were evaluated: 19,000 and 22,000 watts (65,000 and 75,000 Btu/hr, respectively). The data for these higher levels are shown in Figures 3 and 4. The emission trends are essentially the same as the baseline case with only small changes. The point at which CO emissions increase sharply is moved down to 5% excess air for both higher heat inputs. The NO_x emissions are increased slightly as heat input increases for excess air levels of 10 to 30%; however, the ends of the range do show minor differences. Finally, the ratio of NO_2 to NO decreases as the heat input increases.

Fuel Type. A limited series of runs were performed using propane as the fuel. In general, the effect of excess air on emissions was similar to that for natural gas, except that the onset of excessive CO occurred at somewhat higher excess air (i.e., 10-15%). A run with propane at a nominal 26,000 watts (90,000 Btu/hr) heat input gave a different trend as shown in Figure 5. The onset of CO formation occurs at a higher excess air and, of more interest, the ratio of NO_2 to NO increases significantly as the CO begins to increase.

Thermal Efficiency

The data gathered for evaluation of the furnace emission performance can also be used to gain some insight into the thermal efficiency of the furnace. In addition, several measurements of furnace warm air output were made. These two indications of the furnace thermal performance are discussed.

Stack Heat Loss. The main energy loss from a furnace is in the sensible and latent heat associated with the flue gas components, principally N_2, CO_2, O_2 and H_2O. The latent heat loss is determined by the carbon to hydrogen ratio of the fuel and is irretrievable unless a condensing heat exchanger is used. It should be noted that condensing heat exchangers for this application are not currently available. For natural gas the latent heat is equivalent to about 10% of the gross heating value. The sensible heat losses can be minimized by low excess air operation and the lowest stack temperature consistent with avoiding condensation (i.e., about 180 K net). A generalized plot of efficiency versus excess air with stack temperature as a parameter is shown in Figure 6 for natural gas.

The flue gas temperature taken during the experimental runs was relatively independent of excess air for a given firing rate; however, the temperatures increased with increased firing rate. The average flue gas temperatures were 447, 475 and 498 K, at 16,000, 19,000 and 22,000 watts, respectively. An operating excess air of 15% is selected based on the emission curves, giving steady state furnace efficiencies for the three firing rates of 83.4, 82, and 81%, respectively. When the casing losses are taken into consideration, the actual heat loss would be about 2% greater. At the low firing rate, the stack temperature was below the value required to prevent condensation and a production furnace would require less convective heat transfer surface. For the high firing rate, the stack temperature potentially could be reduced by about 22 K. If heat exchanger design was changed to achieve a 475 K stack temperature for each firing rate, the theoretical efficiencies would be the same as that for the 19,000-watt heat input. However, a given furnace is normally designed to be capable of a range of firing rates, and the existing design represents a reasonable compromise for input over 19,000 watts.

Some measurements of output air velocity and temperature rise were made at the output of the plenum on top of the furnace. As an extended duct run was not used to smooth the flow, the stratification of flow due to the heat exchanger was significant. Measured exit velocities were 1.25 to 11.5 m per sec (250 to 2300 ft/min) across the exit face of the plenum, and low temperature rises were normally associated with low velocity areas. These stratifications also strongly influence the accuracy of the measurements; however, they can be taken as semi-quantitative. The warm air flow was about 0.45 m^3/sec for two firing rates, with average temperature rises of 24 and 31 K for heat inputs of 19,000 and 24,000 watts, respectively.

Discussion of Results

Examination of the experimental results raises several points that merit further discussion. It is obvious that some additional measurements within the combustion chamber would greatly assist in explanation of the phenomena involved; however, the fact that the furnace was a prototype inhibited making the modifications required for sampling.

Operating Principle. The inventor of the furnace stated (ref. 6) that the furnace was designed to operate with a hot refractory surface as a means of increasing the radiative heat transfer to the heat exchanger. The use of radiative heat transfer for combustion zone heat removal is a common feature of large conventional boilers with diffusion flame burners (especially the water-tube type); however, in general residential systems do not have heat transfer surface in the combustion zone. It appears that the key features of the design are: 1) the insulating properties of the refractory used to form the surface combustor; and 2) the use of radiative heat transfer to reduce the refractory surface temperature to a level where degradation does not occur. The refractory material was selected to have a low thermal conductivity and, therefore, a very slow soakback of heat from the reacting surface to the plenum containing the premixed fuel and air. It appears that this has a twofold benefit: 1) the heat release is maintained in a thin zone close to the outside of the refractory surface; and 2) radiative heat transfer reduces the refractory surface temperature to a level where degradation does not occur. The degradation of the refractory with time, and the attendant increase in probability of autoignition, needs to be evaluated.

The use of radiative heat transfer allows a high rate of energy removal and apparently maintains the surface temperature well below the adiabatic temperature for the fuel and air stoichiometry being used. This allows the use of fuel/air ratios near stoichiometric where the adiabatic temperature is about 2200 K (3500° F), and yet the reaction zone temperature is maintained below the level where degradation of the refractory would occur. In addition, the temperature is low enough to reduce thermal NO formation.

The observations of the effect of heat input on combustor performance indicate that some increase in surface temperature may occur with increased fuel input as indicated by the lower excess air capability. This is a relatively small effect that may be associated with either the temperature or the thickness of the heat release zone. The small increase in NO_x level suggests that the change is relatively small. It appears that the increased heat release is balanced by increased radiative transfer and/or an increased convective removal of energy due to the larger volume of combustion gases at a given excess air level. The effects could be explained either on the basis of complete reaction of the fuel within the surface or on the basis of partial reaction in the surface with oxidation being completed by homogeneous reactions in the space between the surface and the firebox wall. To answer these questions fully would require measurement of: 1) surface temperatures for the heat exchanger and the refractory material; 2) gas temperature at the firebox exit; and 3) gas phase species measurements within the firebox.

Based on the foregoing discussion and operating experience with two different combustor and firebox configurations in Bratko prototype furnaces, it appears that proper matching of the combustor and radiative heat transfer surface does significantly influence the performance.

NO_2 Emissions. As noted in the background section, above, instances where the NO_2 is greater than 25% of the NO_x have been observed by several investigators for natural gas combustion under conditions where CO levels are high. This same trend was observed for an earlier version of the Bratko prototype tested for both methane and propane at low excess air (i.e., $< 20\%$). Due to the fuel/air mixer configuration of the earlier furnace, excess air was changed by increasing fuel flow at a relatively constant air flow. With the new furnace, propane at a high fuel rate exhibited a high NO_2 to NO ratio at low excess air. This effect was not noted with the new furnace burning methane even at relatively high firing rates; however, the excess air level at which CO increased was significantly lower (i.e., $< 6\%$). Although there is some disagreement with his interpretation, Merryman (ref. 8) has reported "flame front NO_2" for flat flames. His data show conditions within the reaction zone where NO_2 is a large percentage of the NO_x. This is also the zone in which significant amounts of CO were present. Although a flat flame is difficult to relate directly to a surface combustor, these results give a possible basis for explaning the furnace data. It can be postulated that, for a given combustor surface and heat exchanger area, total oxidation occurs in or very near the surface until some critical fuel flow rate is reached and the final oxidation of fuel fragments (e.g., CO) begins to occur in the gas phase above the surface. At low excess air levels, the combustion may not be completed fast enough by these gas phase reactions, thereby allowing some pockets of gases containing CO and high NO_2 to NO ratios to escape and be quenched before the NO_2 can relax back to NO. If this is the case, the data would tend to indicate that this phenomenon is sensitive to the relationship between the surface combustor and the radiant heat exchanger firebox.

Efficiency. Although the furnace efficiency is good for all the cases tested, the potential exists for optimizing the furnace for each heat input value by fine tuning the convective section of the heat exchanger to get minimum allowable stack temperature. Other features of the furnace may provide an increase of cycle average efficiency, particularly by reducing or eliminating off-cycle losses. One source of such loss is the continued flow of draft air through the firebox during the off-cycle. This not only removes accumulated heat from the furnace components, but may also cause a loss of heated air from the furnace space. The Bratko design provides a positive air shut off, which should reduce off-cycle losses significantly.

CONCLUSIONS

Based on the furnace evaluation the following conclusions can be drawn:

1. The surface combustion concept shows clear potential for NO_x emissions significantly below previously reported values, while also giving low levels of CO and HC.

2. The Bratko furnace represents an application of surface combustion to a practical system once a satisfactory combustion air source is incorporated.

3. The low excess air capability gives the potential for high efficiency. Other furnace features which limit off-cycle losses also have the potential for increasing cycle average efficiencies.
4. The concept appears to lend itself to a wide range of firing rates. In fact, performance improved with natural gas at the higher firing rates tested.

REFERENCES

1. Barrett, R. E., S. E. Miller, and D. W. Locklin, "Field Investigation of Emissions from Combustion Equipment for Space Heating," Battelle Columbus Laboratories, EPA-R2-73-084a, NTIS No. PB 223-148, June 1973.

2. Combs, L. P., and A. S. Okuda, "Residential Oil Furnace System Optimization - Phase II," Rockwell International, EPA-600/2-77-028, NTIS No. PB 264-202/AS, January 1977.

3. Hall, R. E., J. H. Wasser, and E. E. Berkau, "A Study of Air Pollutant Emissions from Residential Heating Systems," U. S. EPA, ORD, Control Systems Laboratory, EPA-650/2-74-003, NTIS No. PB 229-697/AS, January 1974.

4. DeWerth, D. W., and R. L. Himmel, "An Investigation of Emissions from Domestic Natural Gas-Fired Appliances." Presented at the 67th APCA Annual Meeting, June 14, 1974, Denver, Colorado.

5. Brookman, G. T., and P. W. Kalika, "Measuring the Environmental Impact of Domestic Gas-Fired Heating Systems." Presented at the 67th APCA Annual Meeting, June 14, 1974, Denver, Colorado.

6. R. Bratko, Bratko Corporation, Cleveland, Ohio, private communication, August 1976.

7. Pershing, D. W., J. W. Brown, and E. E. Berkau, "Relationship of Burner Design to the Control of NO_x Emissions Through Combustion Modification." In Proceedings, Coal Combustion Seminar, EPA-650/2-73-021, NTIS No. PB 224-210/AS, September 1973.

8. Merryman, E. L., and A. Levy, "Nitrogen Oxide Formation in Flames: The Roles of NO_2 and Fuel Nitrogen," 15th Symposium (International) on Combustion, Tokyo, Japan, August 1974.

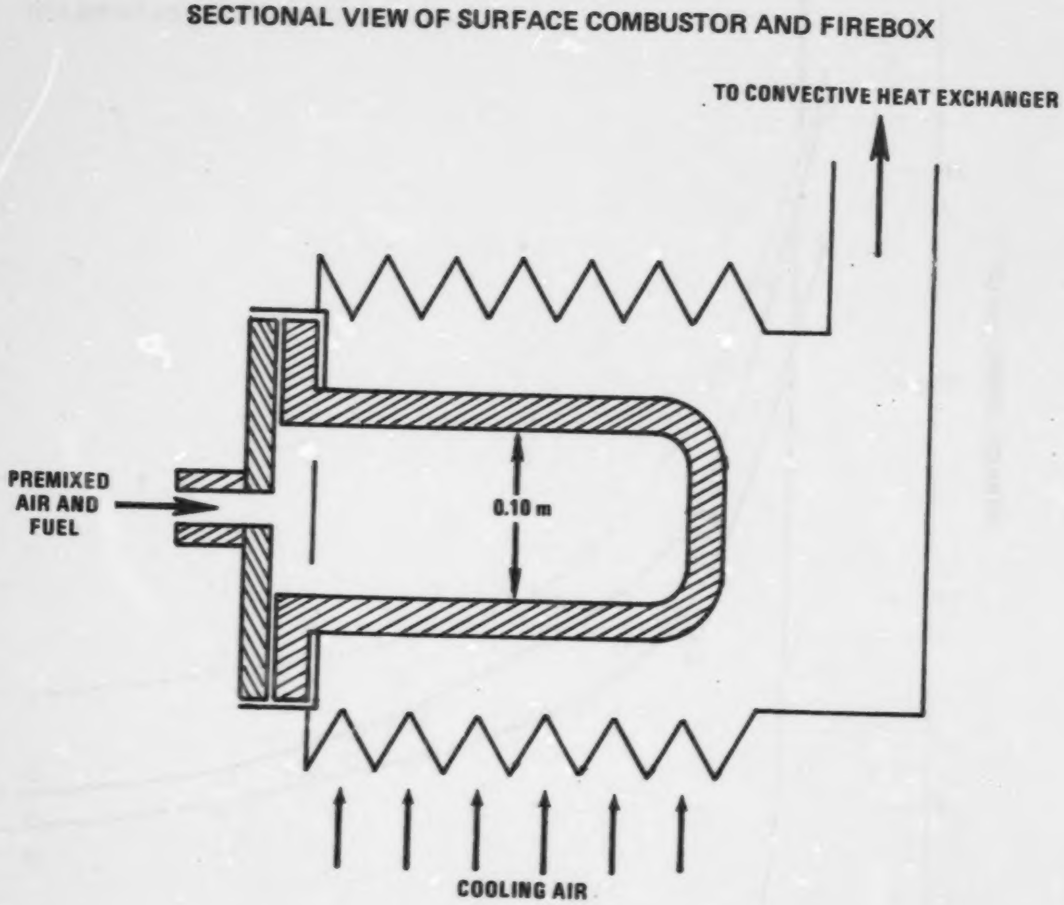
SECTIONAL VIEW OF SURFACE COMBUSTOR AND FIREBOX
TO CONVECTIVE HEAT EXCHANGER
PREMIXED AIR AND FUEL
0.10 m
COOLING AIR

Figure 1. Sectional view of surface combustor and firebox.

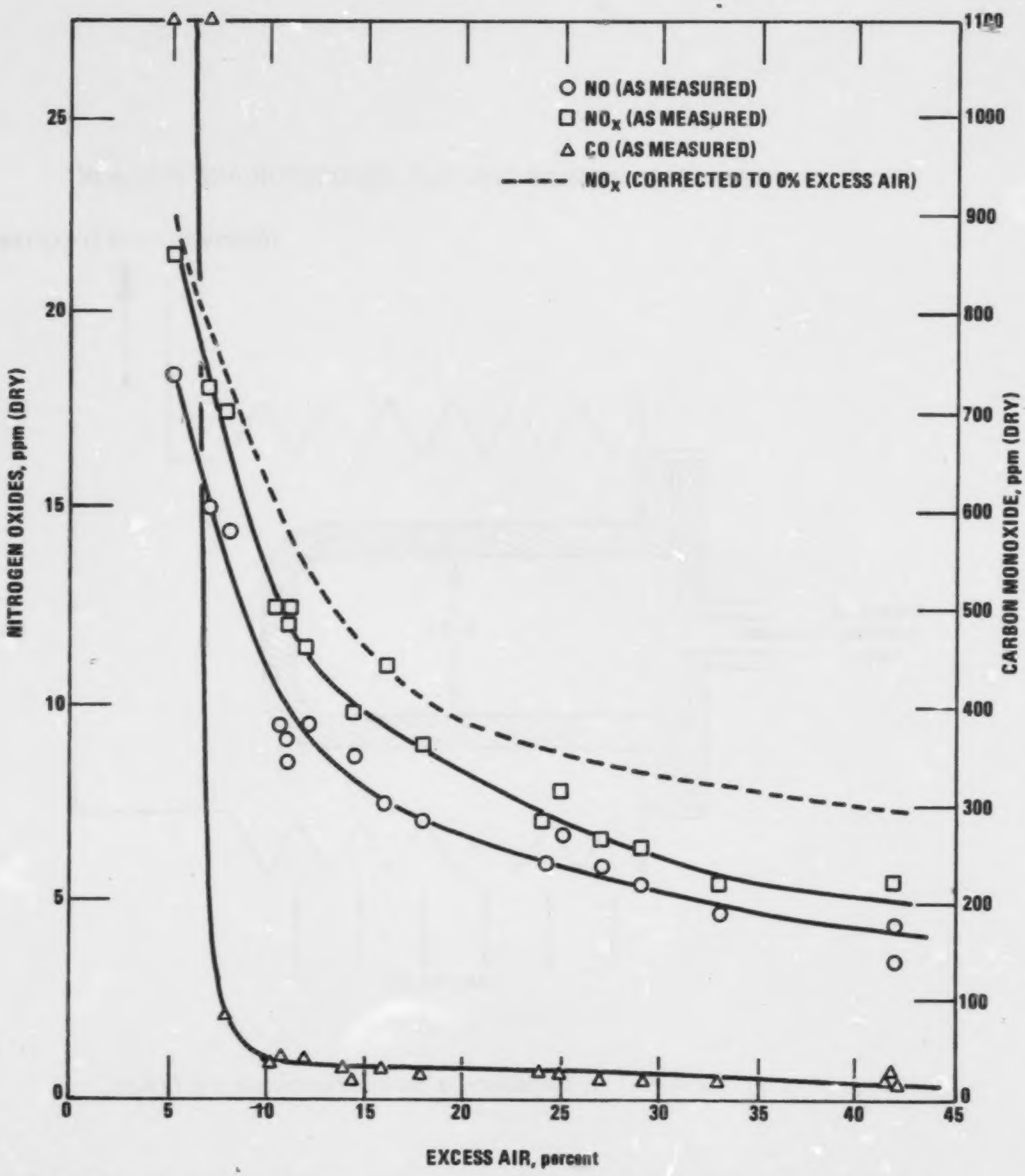
EMISSIONS CHARACTERISTICS AT A NOMINAL HEAT INPUT OF 16,000 WATTS OF NATURAL GAS

Figure 2. Emissions characteristics at a nominal heat input of 16,000 watts of natural gas.

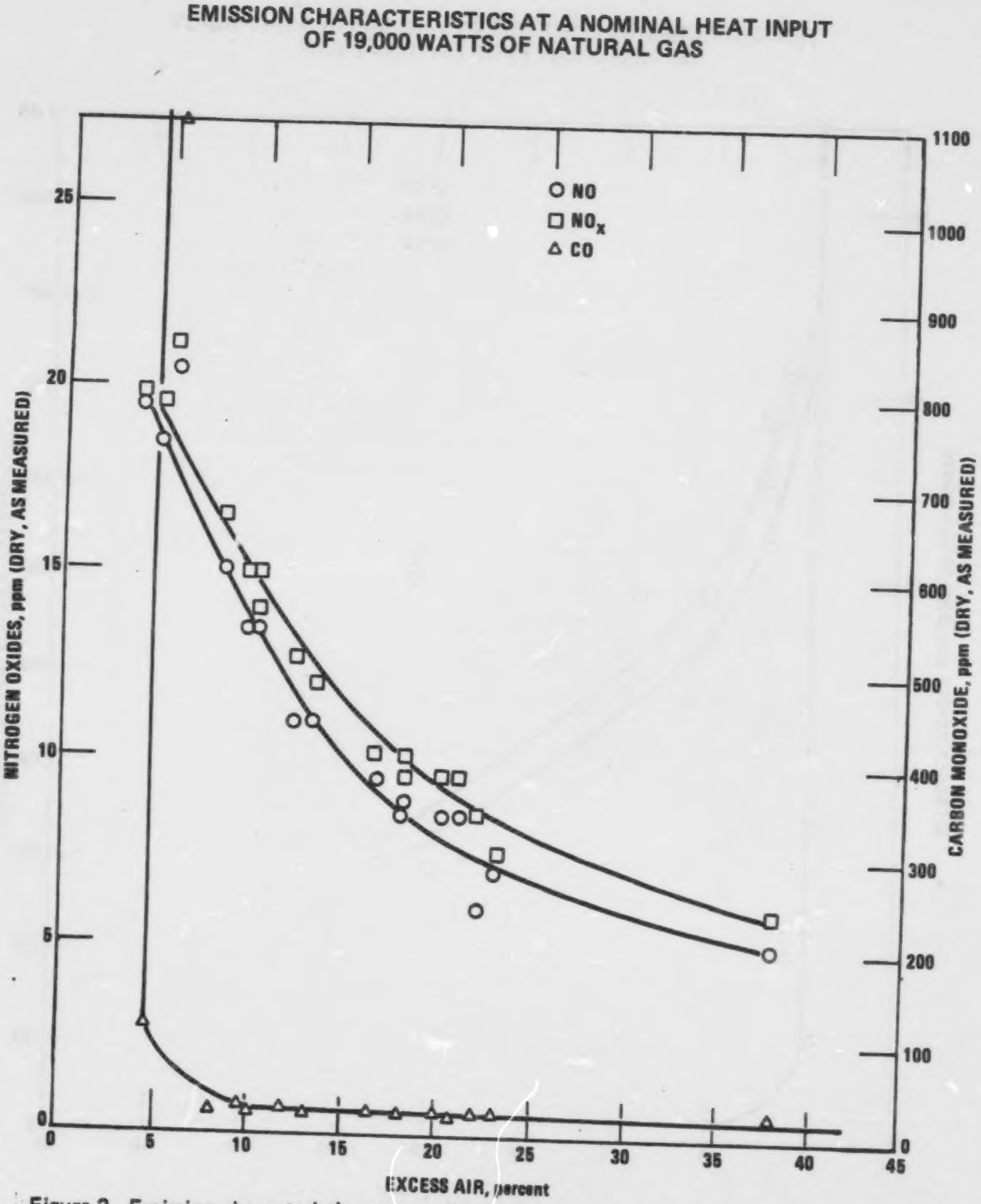

Figure 3. Emission characteristics at a nominal heat input of 19,000 watts of natural gas.

EMISSION CHARACTERISTICS AT A NOMINAL HEAT INPUT OF 22,000 WATTS OF NATURAL GAS

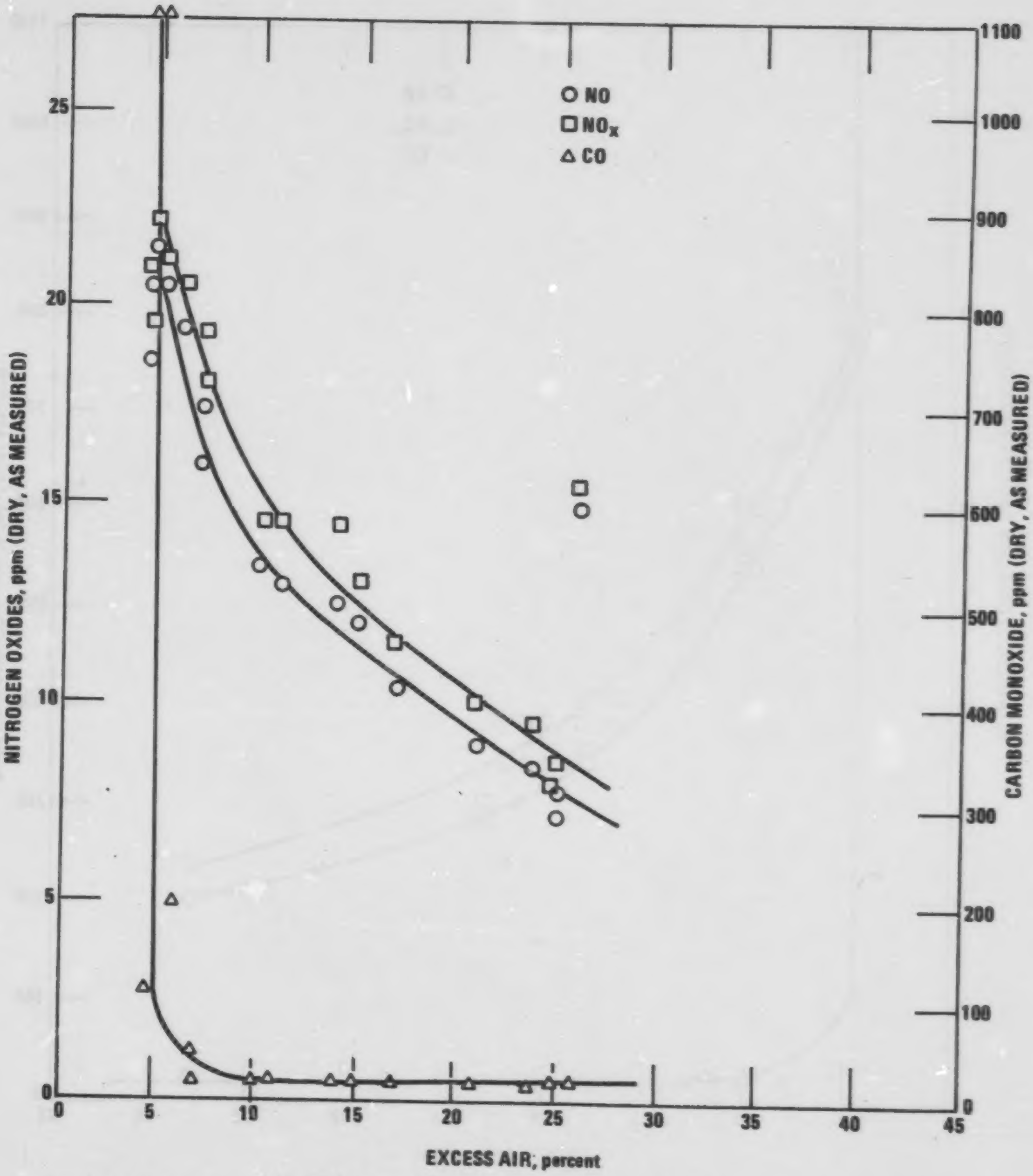

Figure 4. Emission characteristics at a nominal heat input of 22,000 watts of natural gas.

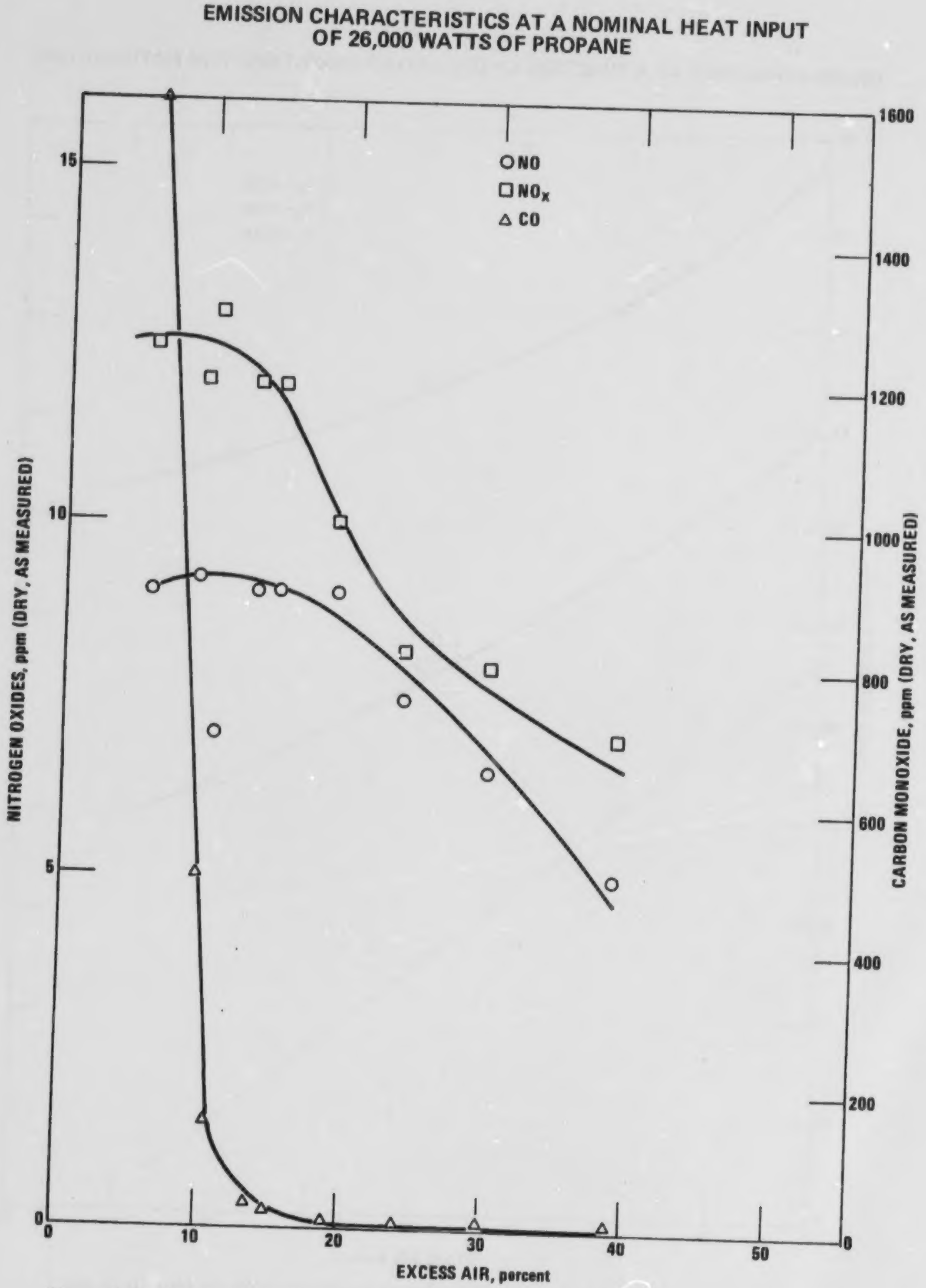

Figure 5. Emission characteristics at a nominal heat input of 26,000 watts of propane.

GROSS EFFICIENCY AS A FUNCTION OF OPERATING CONDITIONS FOR NATURAL GAS

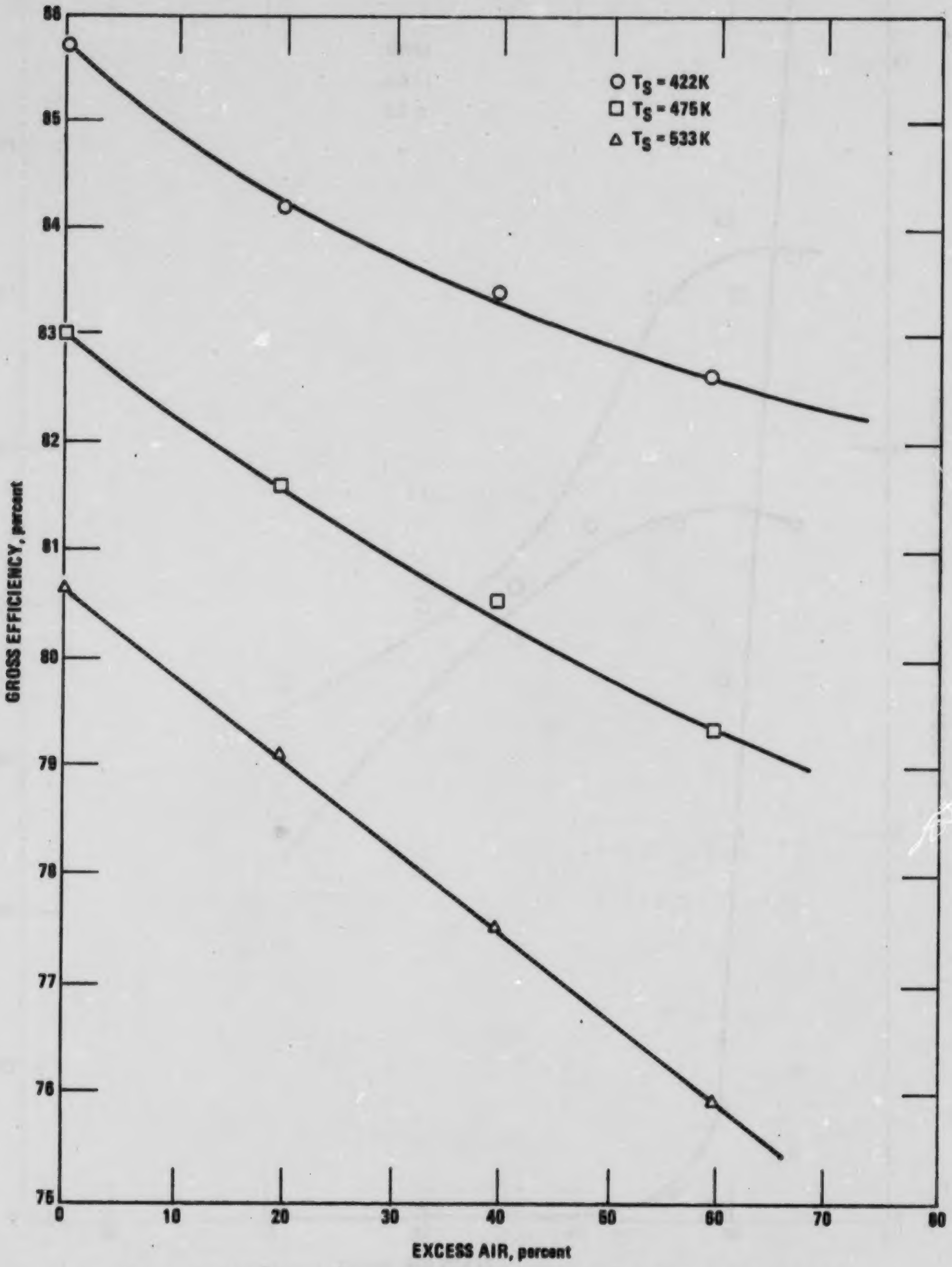

Figure 6. Gross efficiency as a function of operating conditions for natural gas.

AN ANALYSIS OF CATALYTIC COMBUSTION IN MONOLITHIC HONEYCOMB BEDS

By:

Robert M. Kendall, John T. Kelly, Edward K. Chu, and
John P. Kesselring
Acurex Corporation/Energy & Environmental Division
485 Clyde Avenue
Mountain View, California 94042

ABSTRACT

An analysis of catalytic combustion in monolithic catalyst beds is developed. This analysis serves as a basis for the PROF-HET computer code set. The HET code treats the critical phenomena associated with "blowout" of catalytic combustors by performing complex energy and species mass balances along the catalyst surfaces. The PROF code treats the phenomena associated with ignition and sustenance of the homogenous gas phase reactions. The code accurately treats the axial feedback of chain carrying species and energy. This feedback is required to maintain the flame-like gas phase combustion process, and thus avoid "breakthrough".

Based on a series of HET computer simulations of catalytic combustor performances the benefits of large cells, high preheat, and high adiabatic flame temperature are qualitatively related to increases in the maximum mass throughput at blowout. In a similar manner simulations with PROF indicate the degree of surface combustion required before the system will sustain homogeneous combustion reactions. These simulations have led to catalytic combustor designs with greatly improved performance.

Preceding page blank

LIST OF SYMBOLS

A	cross sectional area
C_H	Nusselt number divided by Reynolds and Prandtl numbers (Stanton number)
C_m	dimensionless mass transfer coefficient defined by Equation (8) (Sherwood number)
C_p	specific heat
C_w	circumference of bounding tube
D_{ij}	binary diffusion coefficient
$\overline{D}$	diffusion constant defined by Equation (17)
E	activation energy for kinetic reaction
F_i	diffusion factor of species i
h	enthalpy
J	species flux
k	thermal conductivity
K	channel segment radiative heat transfer view factors
K_p	equilibrium constant
Le	Lewis number
$\dot{m}$	mass rate of gas
M	molecular weight
p	pressure
Pr	Prandtl number
q	heat flux
R	gas constant
Re	Reynolds number
s	distance along flame axis

LIST OF SYMBOLS (Concluded)

T	temperature
W	chemcial production rate
X	mole fraction
Y	mass fraction
ε	wall emissivity
ρ	density
σ	Stefan-Boltzmann constant

Superscripts

P	reaction products
R	reaction reactants

Subscripts

i	denotes species
m	denotes reaction
o	inlet conditions
r	radiation
$r1$	upstream reservoir
$r2$	downstream reservoir
s	solid bed material
w	wall

INTRODUCTION

Catalytic combustion in a honeycomb monolith is a complex process which involves the interaction of several physical and chemical phenomena. Of primary importance are (1) radial heat and mass transport between the gas and wall, (2) axial heat and mass transport in the gas, (3) axial radiative and conductive wall heat transfer, (4) heterogeneous surface and bulk gas phase chemical kinetic reactions. The interaction of these phenomena determines the maximum mass throughput and fuel conversion efficiency of the catalytic bed.

In this paper, the analysis of a catalytic combustor is discussed with regard to:

- Fundamentals of operation, where a simplified version of the catalytic combustion process is described and the important system implications are introduced,
- The PROF-HET computer code, which models all of the important physical phenomena occurring within monolithic catalytic combustors and verifies some of the conclusions of the simplified model,
- Conclusions and recommendations regarding major system impacts and further analytical requirements.

The following discussion provides the information needed to understand the operation of the catalytic combustion system.

FUNDAMENTALS OF OPERATION

Catalytic combustion in a monolith bed includes the interaction of chemical reactions (surface and gas phase), diffusive heat and mass transport

Preceding page blank

(laminar or turbulent), convection, bed conduction, and radiation. These phenomena are depicted schematically in Figure 1. During steady operation, the catalytic combustion process can be described as follows:

- Premixed fuel and air are introduced into the combustor.
- These gases diffuse to the catalyst-coated surface of the combustor and react on the active sites at and within the surface. Near the cell entrance, where most of the gas is at low temperature, gas-phase chemical reactions are unimportant.
- At the entrance, heat release is controlled by catalytic wall chemical reactions. This heat is transferred by conduction, radiation, and convection. Further down the channel, where the gas has been preheated to a high temperature, gas-phase reactions become active. In this region fuel is rapidly consumed by a "flame type" phenomenon which controls the amount of unburned hydrocarbon emissions that escape the system.
- Surface reaction products diffuse back to the main flow of gases and are carried downstream.

Under normal operating conditions, wall and gas phase reactions are active and very little unburned hydrocarbon escapes the bed for lean and stoichiometric initial mixture ratios. However, it has been experimentally observed that above a certain mass flow limit, small increases in flow rate cause an abrupt rise in unburned hydrocarbon emissions. The abruptness of the increase indicates that a "flame type" phenomenon has been extinguished. This condition, called breakthrough, represents an upper mass throughput for low unburned hydrocarbon emissions.

Increasing the mass throughput in a catalytic bed to levels much above the breakthrough point can cause the front of the bed to become cool. It has been experimentally found that small increases in mass throughput, once the front end of the bed has become cool, can cause the cool region to spread downstream. At this point, all wall reactions are extinguished and the entire bed becomes cold. This condition, called blowout, represents the maximum mass throughput for hot bed operation. It is very important to know when this blowout condition occurs for a given catalyst system.

For the purpose of understanding system characteristics, considerable simplification of the catalytic combustion process can be made if it is assumed that:

- No conductive or radiative heat transfer occurs
- The Lewis number is unity for all species
- The combustion reaction is a single global reaction described by an Arrhenius law equation

Once these assumptions are made, it is possible to perform a simple mass balance on the lean reactant at the wall of the monolith bed; that is, the mass of lean reactant transported to the wall is equal to the mass of lean reactant consumed at the wall. In equation form this can be written as

$$\dot{m} = \mathrm{Nu}\,\frac{\rho \mathcal{D}}{D}\,(K_E - K_W) = AK_W e^{-\Delta E/RT_W}$$

where $\dot{m}$ = mass of lean reactant transported to and consumed at the wall, per unit area

Nu = Nusselt number for mass transfer (Sherwood number)

ρ = gas density

$\mathcal{D}$ = diffusion coefficient

D = diameter of one channel of monolith bed

K_E = mass fraction of lean reactant at boundary layer edge

K_W = mass fraction of lean reactant at monolith wall

A = preexponential factor

ΔE = activation energy

R = universal gas constant

T_A = adiabatic flame temperature of fuel/oxidizer

T_W = temperature at monolith wall*

T_P = preheat temperature of fuel/oxidizer

---

*Based on the assumptions, this temperature can be related to the residual concentration of lean reactant at the surface, K_W.

$$T_W = T_P + \frac{K_W}{K_E}\,(T_A - T_P)$$

Each of these expressions for the mass flux can be shown graphically by plotting the mass flux vs. the mass fraction of lean reactant at the monolith wall (i.e., plot $\dot{m}$ vs. K_W). This is shown in Figure 2.

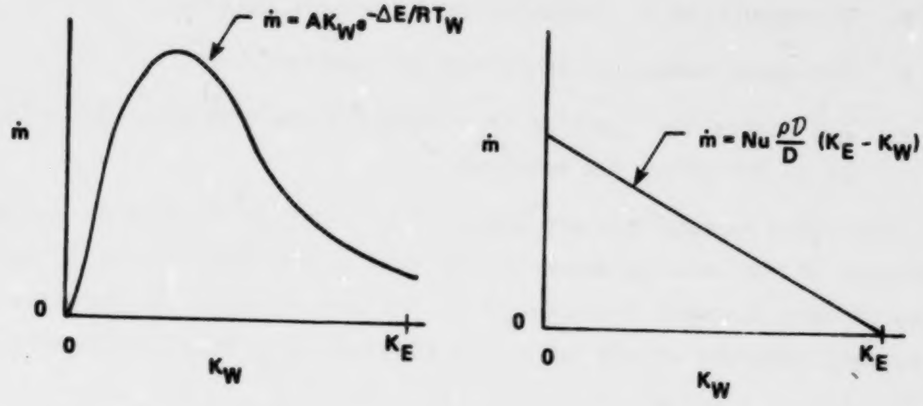

Figure 2. Mass flux as a function of mass fraction of lean reactant at the monolith wall.

By combining the two curves on a single graph, solutions to the problem may be identified as intersections of the two curves. The blowout condition may also be identified from this graphical solution. As shown in Figure 3, there are generally three solutions that can exist: a hot stable solution, an unstable solution, and a cold stable solution. Only the hot stable solution is of interest here. The blowout point can be considered as that value of $\dot{m}$ where the hot stable solution and the unstable solution coincide; any increase in mass throughput above this value will cause the combustion reaction to be extinguished, i.e., the reaction is "blown out." A large value of $\dot{m}$ at blowout is desirable; it allows the monolith bed to operate at a large value of volumetric heat release rate, thereby minimizing the combustion volume required. As shown in Figure 3, to avoid blowout the intercept $Nu(\rho\mathcal{D}/D)K_E$ should be low. For a given surface activity of the monolith, blowout can therefore be avoided by:

- Using large diameter cells in the bed
- Operating at a small value of Nusselt number
- Operating at higher preheat or adiabatic flame temperature (increases T_W at given K_W and thus increases Arrhenius factor)

The simplest of these to implement is the use of large diameter cells. These large cells operate at a low transfer coefficient and should be effective for both lightoff and sustained operation.

However, using large cells throughout the bed would result in poor surface conversion of combustibles to products. The amount of surface conversion is directly related to the number of transfer units in the bed, where the length of each transfer unit is equal to

$$\frac{Pr \cdot Re}{4\ Nu} \cdot D,$$

where P_r = Prandtl number

Re = Reynolds number

Nu = Nusselt number

D = cell diameter

Thus, to get complete conversion on the catalyst surface, it is necessary to have many transfer units available by minimizing the length of each transfer unit. This suggests use of small diameter cells. The small cells will also accelerate gas phase reactions, which are helpful for full conversion.

As a consequence of these operational fundamentals, it appears that a catalytic monolith bed used for the purpose of combustion should use large diameter cells at the front of the bed to prevent blowout, and small diameter cells at the back of the bed to maximize the number of transfer units in a given length of bed. Therefore, for a given catalyst, it was postulated that superior performance can be obtained by using the catalyst in a graded cell configuration, with large cells at the front end, small cells at the back end, and perhaps one or more intermediate sized cells between. A complete discussion of the model used to support these conclusions is given in the following section.

THE PROF-HET COMPUTER CODE

The PROF-HET computer code models the important physical phenomena occurring within monolithic catalytic combustors. An efficient numerical technique which includes axial and radial heat and mass transport, axial radiative and conductive wall heat transfer, and heterogeneous surface and bulk gas phase chemical kinetic reactions has been developed to establish how performance varies with bed operating and design parameters. In this technique, matrix procedures are used to solve the finite difference form of the governing differential equations. The axial distribution of both wall and bulk gas properties, as well as wall temperature, are output by the code. The solution procedure is reliable and stable for the range of input parameters used to date.

The PROF-HET model differs from previous models in that it can handle the high-temperature effects of catalytic combustion, where bed radiative heat transfer and "flame type" phenomena are important. Most of the models constructed to date have focused on catalytic cleanup devices (e.g., automotive catalytic mufflers, and industrial process exhaust cleanup devices for sludge drying, PVC processing, foodstuff processing, etc.) where the temperature rise due to catalytic oxidation is small compared to that which occurs during combustion. For example, Votruba et al. (Reference 1) published an analytical study on the heat and mass transfer in monolithic catalysts. In their model, the heat and mass transfer normal to the channel walls was treated by a transfer coefficient approach where the detailed distribution of properties across the channels need not be known. This reduced an essentially two- or three-dimensional (for noncircular channels) problem to one dimension. Equations for the variation of wall temperature and gas conditions as a function of distance along the channel were developed. Calculations made using this model are more economical than higher dimensional models. Illustrative predictions for catalytic monoliths where the wall temperature rise was both low and high were given. These predictions showed that monolithic structures give more stable operation and less pressure drop than packed beds. However, since radiative heat transfer and gas phase reactions were ignored and only fully developed heat transfer parameters utilized, the model cannot be accurately applied to catalytic combustors.

Cerkanowicz et al. (Reference 2) presented results generated using a catalytic combustor model similar to Votruba's model, except for the inclusion of a gas phase chemical reaction. As with Votruba, only constant fully developed heat transfer coefficient values were utilized in the model. Also, the gas phase chemical reaction was assumed to be a one-step process. This approach is useful for illustrative predictions to show global effects due to gas phase reactions. However, the method is not sufficiently fundamental for exploring the types of "flame" phenomena and pollutant formation processes which occur in catalytic combustors.

Young and Finlayson (Reference 3) developed one-, two-, and three-dimensional models for monolithic catalytic converters. Their two- and three-dimensional models treated heat and mass transfer perpendicular to the wall by an orthogonal collocation method which determines the detailed distribution of properties across the tube. As in Votruba's model, bed radiative transfer and gas phase reactions were not included, making applications to catalytic combustors limited. Young and Finlayson's predictions showed that three-dimensional effects associated with peripheral temperature and concentration variations are not important to overall bed operation. They also showed that holding transfer coefficients constant over the bed length is not an adequate approach.

Heck (Reference 4), using a finite difference procedure, compared one- and two-dimensional catalytic converter model predictions. Like Finlayson, Heck concluded that one-dimensional constant heat transfer solutions were not adequate. However, he showed that if the transfer coefficients are allowed to be functions of distance and wall temperature, characteristic of developing boundary layers, predictions comparable to the two-dimensional results could be achieved at a fraction of the cost.

Following Heck, this study employs a one-dimensional model with transfer coefficients given as functions of distance, wall temperature, initial gas temperature, and inlet flow conditions. In addition to including wall reactions and bed heat conduction, the present model also includes bed radiative heat transfer and gas phase chemical reactions and axial diffusion.

The important bed operating characteristic of blowout is controlled by events occurring near the combustor inlet. At this location, the bulk gases are relatively cool and heat release due to gas phase chemical reactions is small. Heat release in this zone is solely due to wall surface chemical reactions. The heat produced by these reactions is carried away by radial transport of heat to the bulk gases, heat conduction towards the front of the bed, and radiative transfer towards the front of the bed and into the upstream reservoir. Because the thermal boundary layer is developing in this region, the heat transfer coefficient is large. Above a certain limiting mass flow, the heat transfer coefficient for the developing boundary layer becomes so large that the radial convective heat loss plus the radiative heat loss exceeds the heat produced by wall reactions. The wall reactions are then extinguished and the bed becomes cold. To model this blowout state, the following phenomena must be treated:

- Heterogeneous surface chemical reactions
- Radial heat and mass transport
- Axial convection
- Axial bed conductive and radiative heat transfer

Unlike blowout, breakthrough and certain emissions phenomena are controlled by processes which occur away from the front of the bed where the bulk gases are hot. Breakthrough occurs when there is insufficient preheat of the bulk gases by the wall reactions to "light off" gas phase "flame type" phenomena. Since breakthrough is believed to be flamelike in nature, in addition to the above phenomena, the following phenomena must be treated:

- Homogeneous gas phase chemical reactions
- Axial gas phase heat and mass transport

Since the controlling regions for blowout and breakthrough are spatially separated, two compatible models, optimized for their respective regions, have been developed to treat blowout and breakthrough. The HET numerical model is employed to determine blowout and the PROF code is used to predict breakthrough and emissions. Both codes employ compatible thermal, transport, and chemical reaction data and formulations. They differ primarily in the amount of detail included in their respective regions of application.

The HET code governing equations are developed by integrating the steady two-dimensional gas phase species, mass, and energy equations across a plane perpendicular to the axis of a channel. This results in a set of quasi-one-dimensional equations which can be written in terms of bulk gas properties and wall heat and mass fluxes. As previously indicated, wall fluxes are treated by a transfer coefficient approach where the fluxes are directly proportional to bulk and wall gas states. The proportionality factor varies over the bed length and is a function of channel diameter, distance down the channel, inlet gas temperature, wall temperature distribution, and flow Reynolds and Prandtl numbers. The use of transfer coefficients permits the application of efficient one-dimensional solution procedures to a two-dimensional problem. Heat transport in the bed is determined by heat conduction in the solid and radiative transfer within the channel and outside into the upstream and downstream reservoirs. The radiative transfer is modeled through a view factor approach, in which all sections of the channel are able to radiatively communicate with each other and with the upstream and downstream reservoirs.

The quasi-one-dimensional governing equations are:

Species balance in the gas phase

$$\dot{m}\,\frac{dY_i}{ds} = AW_i - C_w J_{w_i} \tag{1}$$

Species balance at the wall

$$J_{w_i} = W_{w_i} \tag{2}$$

Energy balance in the gas phase

$$\dot{m}\,\frac{dh}{ds} = -C_w q_w \tag{3}$$

Overall energy balance

$$\dot{m}\,\frac{dh}{ds} = A_s \frac{d}{ds}\left(k_s \frac{dT_w}{ds}\right) - C_w q_r \tag{4}$$

Global continuity has been incorporated into these equations, and the momentum equation has been replaced by an assignment of fixed pressure. This assignment is usually reasonable for the flow rates and channel dimensions of interest.

Applying the transfer coefficient approach, wall species flux, J_{w_i}, becomes

$$J_{w_i} = \frac{\dot{m}}{A} C_{m_i} \left(Y_i - Y_{w_i}\right) \tag{5}$$

Similarly, wall heat flux, q_w, including a term due to chemical reaction between the bulk and wall gas, becomes

$$q_w = \frac{\dot{m}}{A} C_H \left[(h - h_w) + \sum_i \frac{C_{m_i}}{C_H} h_i^{T_w} \left(Y_i - Y_{w_i}\right) \right] \tag{6}$$

The heat transfer coefficient formulation, taken from Kays (Reference 5), is applicable to circular channels with variable surface temperature, and is given by:

$$C_H = \frac{1}{RePr} \left[\frac{b - 8b \sum_n \left(\frac{G_n}{\lambda_n^2}\right) e^{-\lambda_n^2 X^+} + 8a \sum_n G_n \, e^{-\lambda_n^2 X^+}}{16b \sum_n \frac{G_n}{\lambda_n^4} - 16b \sum_n \left(\frac{G_n}{\lambda_n^4}\right) e^{-\lambda_n^2 X^+} + 16a \sum_n \left(\frac{G_n}{\lambda_n^2}\right) e^{-\lambda_n^2 X^+}} \right] \tag{7}$$

where

$$X^+ = \frac{2x/D}{RePr}, \quad b = \frac{dT_w}{dX^+}, \quad a = T_w - T_o$$

and G_n and λ_n are constants and eigenvalues whose magnitudes (given in Reference 5) depend on whether the flow is laminar or turbulent. This expression is valid for flows with fully developed velocity profiles and developing thermal profiles and is assumed to be adequate for the problem of interest. Entrance effects due to channel web thickness and developing velocity profiles are not considered in the code, except to define a limiting heat transfer coefficient at the channel entrance. The limiting value is based on stagnating flow on the channel web.

The mass transfer coefficient C_{m_i} is developed from the heat transfer coefficient by:

$$C_{m_i} = C_H \, (Le_i)^{2/3} \qquad (8)$$

Wall reactions are given by

$$W_{w_i} = k_{w_f} \, X^{\ell}_{w_f} \, X^{m}_{w_o} \qquad (9)$$

where $k_{w_f} = A_w e^{-E_w/RT}$ and ℓ and m are arbitrary exponents on fuel and oxidizer concentrations at the wall.

Bulk gas phase reactions are given by

$$W_i = M_i \sum_m \left(\mu^P_{im} - \mu^R_{im} \right) R_m \qquad (10)$$

where μ_i are the stoichiometric coefficients of the reaction m, and R_m is given by

$$R_m = k_{fm} \left[e^{\sum_i \mu^R_{im} \ln p_i} - e^{\sum_i \mu^P_{im} \ln p_i - \ln Kp_m} \right] \qquad (11)$$

and k_{f_m} has the Arrhenius form $k_{f_m} = aT^b e^{-E/RT}$

The wall radiative heat flux q_r at station j is given by:

$$q_{r_j} = \varepsilon\sigma \left[\left(1 - K_{ij} \right) T^4_{w_j} - \sum_k K_{kj} T^4_{w_k} - K_{jr1} T^4_{r1} - K_{jr2} T^4_{r2} \right] \qquad (12)$$

where K is the channel segment view factor, k denotes all other stations except j and r1, r2 denote upstream and downstream reservoirs.

Completing the definition of the problem, the boundary conditions for equations (1) through (4) are:

$$s = 0 \qquad Y_i = Y_{oi},\ h = h_o,\ \left.\frac{dT_w}{ds}\right|_o = 0,\ T_{r1}$$

$$s = L \qquad \left.\frac{dT_w}{ds}\right|_L = 0,\ T_{r2} \tag{13}$$

Applying a straightforward linear finite differencing technique, the differential equations 1 through 4 are reduced to algebraic form. The resulting algebraic equations are solved by a Newton-Raphson matrix procedure which includes a predictor-linearized corrector step. Very briefly:

1. Initial values are guessed for T_w at all grid points
2. By applying known upstream conditions and the initial guessed T_w's, grid point values for Y_i, T, h, Y_{w_i}, T_w, h_w, etc. are found through Newton-Raphson solution procedures
3. Using the derivatives obtained from the solutions at each grid point, the rate of change of wall temperatures with respect to initially guessed wall temperatures at each grid point is constructed
4. Assuming the system is linear, corrections to all T_w's are made by applying the derivatives from step 3
5. Using the corrected T_w's as new guesses, steps 2 through 4 are repeated until guessed T_w's equal corrected T_w's

The PRemixed One-dimensional Flame (PROF) code has been described in detail elsewhere (Reference 6). Very briefly, the two-dimensional governing equations are integrated across the channel, producing a set of quasi-one-dimensional equations similar to the HET model formulation. These equations are:

Species

$$\dot{m}\frac{dY_i}{ds} = A\,W_i - \frac{d}{ds}(AJ_i) - C_w J_{w_i} \tag{14}$$

$$\dot{m}\frac{dh}{ds} = AQ - \frac{d}{ds}\left(\sum_i AJ_i h_i + Ak\frac{dT}{ds}\right) - C_w q_w \tag{15}$$

They differ from the HET equations by the addition of axial gas phase diffusion, J_i, and heat conduction $\sum_i J_i h_i + k\,(dT/ds)$ terms, where J_i is given by

$$J_i = -\frac{\rho\bar{D}}{\mu_1 F_i}\left[\frac{dY_i}{ds} + \frac{Y_i}{M}\left(\frac{dM}{ds} - F_i\,\frac{d\mu_2}{ds}\right)\right] \tag{16}$$

where the binary diffusion coefficient, D_{ij}, is replaced by the bifurcation approximation (Reference 6)

$$D_{ij} = \frac{\bar{D}}{F_i F_j} \tag{17}$$

and

$$\mu_1 = \sum X_i F_i,\ \mu_2 = M \sum Y_i/F_i$$

The development of Equation (16) is given in Reference 6.

The inclusion of the axial diffusion terms makes the PROF model a multivariable (Y_i,T) boundary value problem. A difference between the PROF and HET models is the assignment of wall state (Y_{w_i}, T_w) in the PROF model, whereas in the HET model the wall state is calculated as part of the solution. For PROF calculations, the wall state is found by running the HET code for the same inlet flow conditions. The predicted wall state is then input as a boundary condition into the PROF code. Additional boundary conditions for PROF calculations are the initial gas composition, pressure, and temperature; and the condition of no heat and mass diffusion at the downstream boundary.

The PROF code can handle many chemical species, including those which model detailed combustion and pollutant formation mechanisms. As discussed in Reference 6, solving the species equations, including chemical production terms, R_m, is difficult. The PROF code has been optimized so that chemical reaction rates -- from nearly equilibrated to inactive -- can be handled reliably, accurately, and efficiently. This has been demonstrated by comparison of detailed free flame species predictions and data in Reference 9.

Also, a favorable comparison in Reference 9 of PROF predictions of flame quench in small diameter tubes and data demonstrates the accuracy of the code when applied to confined flame problems such as catalytic combustors.

To reduce the PROF differential equations to algebraic form, straightforward linear finite differencing is used. The resulting system of simultaneous equations are solved by a predictor-linearized corrector solution procedure which consists of the following steps:

1. Initial values are selected for Y_i, T, h at all grid points. These may be output from a prior run or may be generated by a linear interpolation between initial and guessed final values.
2. By applying known upstream conditions and the initial guessed downstream values, grid point values for Y_i, h, T, etc., are found through matrix solution of the equation set
3. When the downstream boundary is reached, the no-diffusion boundary condition is applied.
4. Using the derivatives of Y_i obtained from chemistry solutions at all grid points, the rates of change of all Y_i's with respect to initially guessed Y_i's at each grid point are constructed
5. Assuming the system is linear, corrections to all Y_i's are made by applying the derivatives from Step 4
6. Using the corrected Y_i's as new guesses, Steps 2 through 5 are repeated until the guessed Y_i equals the corrected Y_i

HET code predictions illustrating the effect of bed channel diameter, preheat gas temperature, mixture ratio, conductivity (and/or void fraction) and surface activity on the important bed operating characteristics of blowout are presented. Also, PROF code predictions which show the effect of channel diameter and preheat gas temperature on the important bed operating characteristic of breakthrough are given. These results have significant system design implications for achieving catalytic combustors with high heat release (high blowout limit) and low emissions (high breakthrough limit).

Numerical results presented in Figures 4 through 9 use a surface reaction rate based on an assumed activation energy and an experimentally found blowout condition. Methane fuel and air are assigned as initial reactants in all of the calculations. For methane fuel on a platinum catalyst, Anderson (Reference 7) experimentally found an activation energy of 96 kj/mole. This value of activation energy was used in all of the calculations. The pre-exponential factor was obtained by matching predicted blowout mass flowrates to experimentally found values for a bed operating on methane fuel with 0.00635 m diameter channels, initial gas preheat of 672 K and 193 percent excess air. The preexponential factor, A_w, found using this approach is 6.5×10^6 mole/m^2/sec for l and m in Equation 9 assumed to be one and two, respectively. This preexponential rate factor incorporates effects of surface area, catalyst dispersion, catalyst activity, etc. and is a global rate for the experimental support/catalyst system. All calculations presented below are for a pressure of 101.325 KPa.

Figure 4 gives the HET code predicted distribution of wall and bulk gas fuel concentration and temperature through a monolith bed. Initial gas conditions and bed geometrical and material properties are listed on the figure. These results are typical of catalytic combustor operation at high mass throughput and graphically illustrate how blowout occurs.

Close to the channel entrance radial heat transport and radiative heat losses are large, causing the surface temperature to be much lower than the adiabatic flame temperature. Due to the low wall temperature, surface reactions are much slower than the radial transport of fuel and oxidizer to the wall, and fuel concentration at the wall is a substantial fraction of the bulk gas value. The wall reactions are controlling heat release in this case and the front of the bed is said to be kinetically controlled. Further down the channel, heat losses decrease and the wall temperature rises. This drives the wall reaction rate to much higher levels than the radial mass transport which is now controlling heat release. This region of the bed is said to be mass transfer controlled and any fuel reaching the wall is rapidly consumed giving low values of fuel concentration at the wall. As the mass flow through the channel is increased, the heat transfer coefficient and radial heat transport away from the wall is increased and a greater portion of the front of the bed becomes kinetically controlled. This is illustrated in Figure 5 where wall fuel concentration distributions are given for several bed mass throughputs. These results show that the kinetically controlled region spreads downstream as mass throughput increases. The wall then becomes cooler and the surface chemical reactions are extinguished.

In this study, blowout is defined as the condition where the kinetically controlled region sweeps down the bed and the wall reactions are extinguished. It should be noted that the movement of the kinetically controlled region to locations downstream where the channel flow is more hydrodynamically developed does not ease the problem of the extinguishing of wall chemical reactions. This is due to the thermal boundary layer initiation point moving concurrently with the kinetically controlled region, resulting in locally high values of heat transfer coefficient which can extinguish wall reactions.

Predictions of blowout mass throughput as a function of channel diameter are presented in Figure 6. The upper curve in Figure 6 is for a preheat temperature of 672 K and the lower curve is for a preheat temperature of 550 K. The parameters held constant for these calculations are listed on the figure. These include mixture ratio, flow area, wall conductivity (or product of conductivity and wall solid cross sectional area) and surface emissivity. The dashed curve at the top of the figure is a constant Reynolds number of 2,000 line. For fully developed pipe flow, this curve represents an approximate upper limit for purely laminar flow. Between Reynolds numbers of roughly 2,000 and 10,000 is a transitional flow regime where part of the tube flow is laminar and part is turbulent. If the length-to-diameter ratio of the channel is less than 50, entrance effects and the transition of laminar to turbulent flow in the developing boundary layer must be considered.

The point of transition to turbulent flow within the channel depends on the entering freestream turbulence level, disturbances due to entrance geometry, rate of wall heating and roughness of tube wall. If the channel length is short and disturbances due to entrance effects and roughness are not severe, laminar flow can be maintained within the entire channel for values of Reynolds numbers based on channel diameter much above the fully developed 2,000 value. For the geometries and flowrates of interest, fully developed flow is never achieved in the channel and Reynolds numbers do not exceed the 2,000 limit by a large amount. Therefore, laminar flow should prevail for most of our cases of interest.

The mass throughput curves in Figure 6 show that blowout increases almost linearly as tube diameter increases for both the 550 K and 672 K preheat cases. This is primarily the result of the heat transfer coefficient, for fixed mass throughput, decreasing with increases in diameter of the cells and in thickness of the web. Increasing the channel diameter permits more mass to pass through the channel before blowout occurs. However, increasing diameter also decreases the mass transfer coefficient which reduces fuel conversion efficiency. A longer bed is then required to convert all of the fuel to combustion products. Comparison of the two curves shows that preheat has a very strong influence on blowout. This is even more dramatically demonstrated in Figure 7 where the channel diameter is held constant at 0.003175 meters along with all the other parameters and gas preheat temperature is varied. These predictions show that preheat has a very strong influence on blowout with higher preheat producing more than a proportionate increase in blowout mass throughput. This is due to the "activation" nature of the wall reaction rate, which is an exponential function of wall temperature. These results indicate that, for maximum heat release, beds should be operated at as high a temperature as is compatible with the degradation of the catalyst or is acceptable from an NO emissions point of view.

Figure 8 shows the effect of mixture ratio on blowout. The upper curve is for a preheat temperature of 672 K and the lower a preheat of 550 K. Numerical values of the other parameters held fixed during the calculations are listed on the figure. Both curves show a rapid rise in blowout mass flowrate as the amount of excess air is decreased. In Figure 8, the parameter controlling the high blowout mass throughput rates is surface temperature. For low excess air levels and no wall cooling, surface temperatures (~2200 K at 0 percent excess air) are very high, exceeding present bed material operating limits. These high temperatures drive the surface chemical reaction rates to very high levels which far exceed radial (and radiative) heat losses under laminar flow conditions. Large mass flowrates are needed to produce blowout at these conditions. Once again, the strong influence of wall temperature on blowout is evident.

For the 50 percent excess air, 550 K preheat case, the blowout Reynolds number based on tube diameter is in the transitional flow regime. To investigate the effect of fully turbulent flow on blowout, the HET turbulent developing boundary layer heat transfer coefficient model was activated for the 50 percent excess air case. These predictions show that the high turbulent heat transfer coefficient forces the blowout mass throughput down to very low values where laminar flow would prevail. From these results, it may be conjectured that as mass throughput approaches a value such that the developing channel boundary layer transists from laminar to turbulent flow within the channel, the surface reactions in the downstream turbulent flow portion of the tube could be extinguished.

Figure 9 gives the effect of bed material conductivity on blowout. Since the solid cross sectional area enters the governing equations coupled with conductivity, the variation of blowout with conductivity can also be interpreted as blowout variation with solid cross sectional area for fixed conductivity. The blowout trends in Figure 9 show that the blowout mass throughput varies almost linearly with conductivity. However, at low values of conductivity, the blowout limit levels off and reaches a constant value for no wall conductivity. It should be noted that radiative heat transfer is included in these calculations and, therefore, the zero conductivity calculation does not represent adiabatic conditions.

Figure 10 gives the effect of wall activity on blowout. Variations in wall activity model the effect of increasing surface area, catalyst loading and dispersion on blowout. Since the exponential factor in the catalyst rate expression was held fixed during these calculations, the results represent a single catalyst whose amount and distribution on a monolith bed has been varied. Results in Figure 10 show that the effect of surface activity on blowout is nearly linear.

The results of the parametric blowout calculations are summarized in Table 1. These results indicate that for maximum mass throughput, surface temperature should be as high as is compatible with the support/catalyst material combination and the channel diameter should be large. However, large diameter channels also have poor fuel conversion performance and long beds are needed to convert all the fuel to combustion products by wall chemical reactions. This dilemma of high mass throughput but poor fuel conversion for large diameter channels can be solved by adding additional beds behind the first bed to efficiently convert the remaining fuel. Blowout should not be a severe problem for these additional beds because the entering gases are highly preheated. The next section addresses the fuel conversion or breakthrough problem.

TABLE 1. EFFECT OF PARAMETER CHANGES ON BLOWOUT

Parameter	Effect of Increase on Blowout	Comments
Channel diameter	Linear increase	
Gas inlet temperature	Exponential increase	
Initial fuel/air mixture ratio	Exponential increase in lean systems	Same type of behavior as temperature
Conductivity	Linear increase	No variation as conductivity goes to zero
Surface activity	Linear increase	

Breakthrough

As indicated previously, large diameter channels increase blowout mass throughput but decrease fuel conversion by wall chemical reactions. Therefore, small diameter channels should be used to minimize unburned fuel emissions. However, blowout, channel mechanical forming, and pressure drop considerations limit the minimum channel diameter that can be applied.

Complete fuel conversion by wall chemical reactions in channels of practical size requires long beds. To minimize bed length, homogeneous chemical reactions must be activated to rapidly consume any fuel remaining in the bed.

As discussed previously, homogeneous gas phase reduction of fuel is postulated as "flame-like" in nature. The PROF predictions in Figures 11 and 12 support this postulate by illustrating the importance of upstream diffusion of reactive chemical species and heat on homogeneous reactions. Boundary conditions for these calculations are listed on the figures, and Table II gives the elementary chemical kinetic reactions and associated rates applied in the calculations. The prediction represented by the dashed curve in Figure 11 includes both diffusion and chemical reactions. This prediction shows a rapid decay of fuel concentration, indicative of "flame-type" phenomena. In Figure 11, predictions represented by the solid line and circular symbols include only chemical reactions or diffusion, respectively. These predictions show the less rapid fuel decay characteristic of wall reactions only. The effect of including both diffusion and chemical reactions can also be seen in Figure 12. This figure shows that predictions which include both diffusion and chemical reaction have a rapid rise in temperature indicative of "flame-type" phenomena whereas other calculations show a much slower rise to the final temperature, indicative of wall reactions. The "flame-type" nature of the homogeneous fuel concentration reduction is further shown in Figure 13, which presents detailed species concentrations through the channel. From this figure it can be seen that the rapid decay of CH_4 is accompanied by an increase in free radicals (O atoms for example) and production of CO and H_2. The CO and H_2 are subsequently oxidized to CO_2 and H_2O. This sequence of events is very similar to those which occur in free methane/air flames, and demonstrates the "flame-type" nature of the processes occurring within the catalytic combustor. It may be concluded that, to accurately predict breakthrough, the analytical model must include the effects of axial heat and mass diffusion, as well as homogeneous chemical kinetic reactions.

PROF code predictions demonstrating the effect of channel diameter on breakthrough are given in Figure 14. Axial heat and mass diffusion, as well as chemical kinetic reactions, are included in these and all subsequent calculations. The boundary conditions for this case are listed on the figure and chemical kinetic reactions and rates are given in Table II. Figure 14 shows that, as channel diameter is decreased, the rapid fuel decay region associated with "flame-type" phenomena moves towards the front of the bed. This is due to the acceleration of bulk gas heating through the increase in heat transfer coefficient which accompanies reductions in channel diameter. Examining detailed computer printout shows that for this 100-percent excess air case, the "flame-type" phenomena is initiated at a channel bulk gas temperature of approximately 1400 K. These results show that wall reactions play an important role in preheating the gases to temperatures sufficiently high to light off the "flame-type" phenomenon. The importance of gas preheat is shown in Figure 15, where predictions of fuel concentrations for a fixed channel diameter and several inlet bulk gas mixture temperatures are presented. As can be seen, preheating the inlet gas to higher temperatures causes the "flame-type" rapid fuel decay region to approach the front of the bed. For these cases the "flame-type" phenomenon is initiated at a bulk gas temperature of approximately 1400 K.

In summary, the parametric breakthrough calculations show that initiation of "flame-type" phenomena in catalytic combustors requires high channel bulk gas temperatures. These temperatures can be achieved by a combination of wall reaction heating, which is a function of channel diameter, and/or inlet gas preheat. Once the "flame-type" phenomena are active, rapid decay of fuel and fuel fragments, characteristic of free flame behavior, is achieved. If "flame-type" phenomena are active, only short bed lengths are needed to reduce unburned fuel and fuel fragments to extremely low concentrations.

CONCLUSIONS

The PROF and HET codes have been successfully used to characterize catalytic combustor performance. HET code predictions indicate that blowout mass throughput increases roughly linearly with increases in channel diameter, conductivity, and catalyst/support surface activity. Also, blowout increases roughly exponentially with increases in inlet mixture preheat temperature and fuel/air ratio for lean operation. Therefore, for maximum catalytic combustor mass throughput, surface temperature should be as high as is compatible with the support/catalyst material combination and channel diameter should be large. Maximum channel diameter, however, is limited by fuel conversion requirements.

PROF code predictions show that homogeneous chemical kinetic phenomena in catalytic combustors are "flame-like" in nature and proper modeling of this effect requires treatment of axial heat and mass diffusion as well as homogeneous chemical kinetic reactions. Predictions which include axial diffusion indicate that the rapid decay of fuel, associated with "flame-type" phenomena, moves towards the front of the bed as channel diameter is decreased and initial preheat temperature is increased. These results show that high gas temperatures, produced by either wall reaction heating or high preheat, are needed to "light off" the "flame-type" phenomena in catalytic combustors.

Predictions suggest that a catalytic combustor system which has high mass throughput (high blowout limit) and low emissions (no breakthrough) could be constructed by joining two or more bed segments in series. The first segment would have channels large enough to prevent blowout and yet small enough to convert sufficient fuel to meet the preheat/blowout requirement of the second bed segment. The second segment would have smaller diameter channels to convert more of the fuel to products and further heat the gases. The last segment would have very small diameter channels and the entering gas preheat would be sufficient to "light off" homogeneous "flame-type" phenomena. Any fuel remaining in this segment would be rapidly consumed by homogeneous reactions. This system design, called the graded cell concept, is described in Reference 8, where tests have shown this system to have very high mass throughputs and heat release while maintaining very low unburned hydrocarbon, CO, and NO_x emissions.

REFERENCES

1. Votruba, J., Sinkule, J., Hlavacek, V. and Skrivanek, J., "Heat and Mass Transfer in Monolithic Honeycomb Catalysts-I.", Chemical Engineering Science, 1975, Vol. 30, pp. 117-123, Pergamon Press, Great Britain.

2. Cerkanowicz, A. E., Cole, R. B. and Stevens, J. G. "Catalytic Combustion Modeling; Comparisons with Experimental Data," ASME paper 77-GT-85, presented at the ASME Gas Turbine Conference, Philadelphia, Pennsylvania, March 27-31, 1977.

3. Young, L. C., and Finlayson, B. A., "Mathematical Models of the Monolith Catalytic Convertor; Part II. Application to Automobile Exhaust," AIChE Journal, Vol. 22, No. 2, pp. 343-353, March 1976.

4. Heck, R. H., Wei, J., and Katzer, J. R., "Mathematical Modeling of Monolithic Catalysts," AIChE Journal, Vol. 22, No. 3, pp. 477-484.

5. Kays, W. M., Convective Heat and Mass Transfer, McGraw Hill, New York, 1966.

6. Kelly, J. T., and Kendall, R. M., "Premixed One-Dimensional Flame (PROF) Code Development and Application," Proceedings of the 2nd EPA Stationary Source Combustion Symposium, Volume IV, EPA-600/7-77-073d, July 1977.

7. Anderson, R. B., Stein, K. C., Feenan, J. J. and Hofer, L.J.E., "Catalytic Oxidation of Methane," Industrial and Engineering Chemistry, Vol. 53, No. 10, pp. 809-812, October 1961.

8. Kesselring, J. P., Krill, W. V., and Kendall, R. M., "Design Criteria for Stationary Source Catalytic Combustors," Western States Section/The Combustion Institute Fall Meeting on Catalytic and Fluidized Bed Combustion, Paper Number 77-32, Stanford, California, 17-18 October 1977.

9. Kendall, R. M., and Kelly, J. T., "Premixed One-Dimensional Flame Code (PROF) - Its Formulation, Manipulation, and Evaluation," Aerotherm Report TR-75-158, July 1975.

TABLE 2. CH_4 COMBUSTION CHEMICAL KINETIC REACTIONS AND RATES

```
KINETIC REACTION DATA

     NUMBER OF REACTIONS= 28

          REACTION                    PRE EXP FACTOR    TEMP EXP  ACTIVATION ENERGY    INDIVIDUAL THIRD BODY EFFIC.

  1   CH4 +OH   +     -->   CH3 +H2O      .1000+14        .000        6.0000                  .000      .000
  2   CH4 +H    +     -->   CH3 +H2       .2000+15        .000       11.9000                  .000      .000
  3   CH4 +O    +     -->   CH3 +OH       .2000+14        .000        6.9000                  .000      .000
  4   CH3 +O    +     -->   CH2O+H        .3500+14        .000        3.3000                  .000      .000
  5   CH3 +O2   +     -->   CH2O+OH       .1000+13        .000       15.0000                  .000      .000
  6   CH2O+     +M    -->   CO  +H2       .2000+17        .000       35.0000                  .000      .000
  7   CH2O+OH   +     -->   CHO +H2O      .2500+14        .000        1.0000                  .000      .000
  8   CH2O+O    +     -->   CHO +OH       .3000+14        .000         .0000                  .000      .000
  9   CH2O+H    +     -->   CHO +H2       .1700+14        .000        3.0000                  .000      .000
 10   CHO +O2   +     -->   CO  +HO2      .3000+14        .000         .0000                  .000      .000
 11   CHO +OH   +     -->   CO  +H2O      .1000+15        .000         .0000                  .000      .000
 12   CHO +O    +     -->   CO  +OH       .5400+12        .500         .0000                  .000      .000
 13   CHO +     +M    -->   CO  +H        .2000+13        .500       28.8000                  .000      .030
 14   CO  +OH   +     -->   CO2 +H        .5500+12        .000        1.0800                  .000      .000
 15   CO  +O    +M    -->   CO2 +         .3600+19      -1.000        2.5000                  .000      .000
 16   HO2 +O    +     -->   O2  +OH       .2500+14        .000         .0000                  .000      .000
 17   HO2 +OH   +     -->   O2  +H2O      .2500+14        .000         .0000                  .000      .000
 18   HO2 +H    +     -->   OH  +OH       .2500+15        .000        2.0000                  .000      .000
 19   HO2 +H    +     -->   O2  +H2       .2500+14        .000         .0000                  .000      .000
 20   H   +O2   +M    -->   HO2 +         .2000+16        .000         .8700    H2O         20.000      .000
 21   H   +O2   +     -->   OH  +O        .2200+15        .000       16.8000                  .000      .000
 22   O   +H2   +     -->   OH  +H        .1700+14        .000        9.4600                  .000      .000
 23   OH  +H2   +     -->   H2O +H        .2200+14        .000        5.2000                  .000      .000
 24   OH  +OH   +     -->   H2O +O        .6000+13        .000         .7800                  .000      .000
 25   H   +OH   +M    -->   H2O +         .7000+20      -1.000         .0000                  .000      .000
 26   O   +H    +M    -->   OH  +         .4000+19      -1.000         .0000                  .000      .000
 27   H   +H    +M    -->   H2  +         .2000+20      -1.000         .0000                  .000      .000
 28   O   +O    +M    -->   O2  +         .4000+19      -1.000         .0000                  .000      .000
```

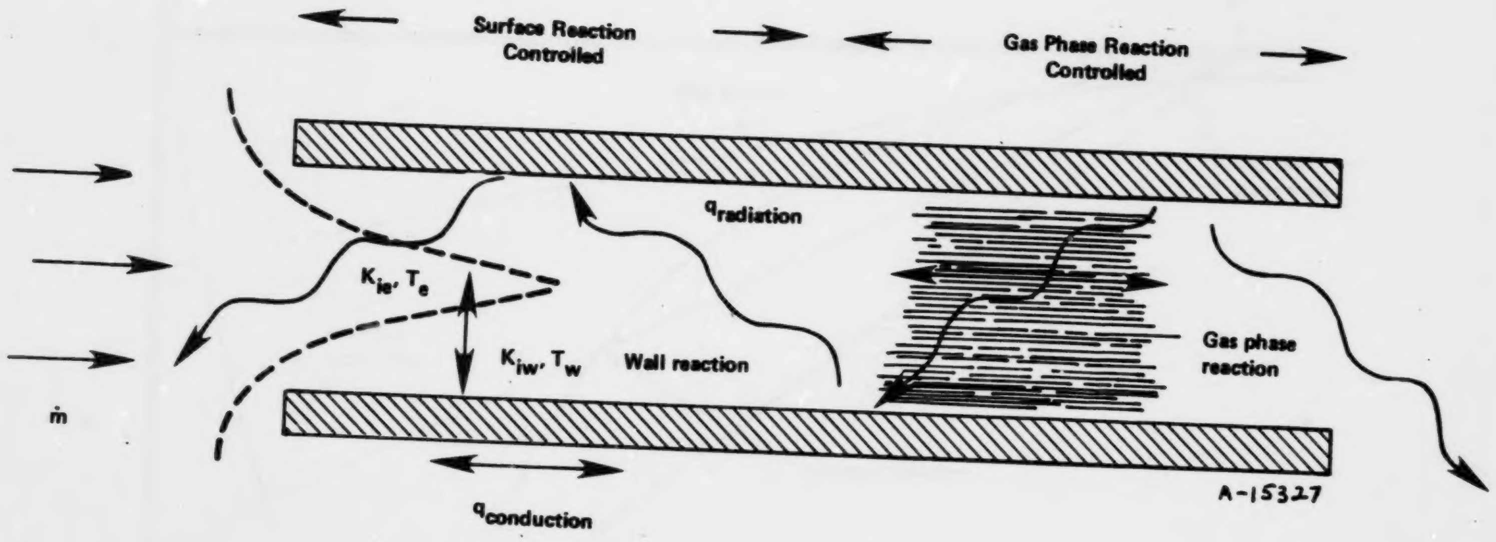

Figure 1. Physical events in a monolith cell.

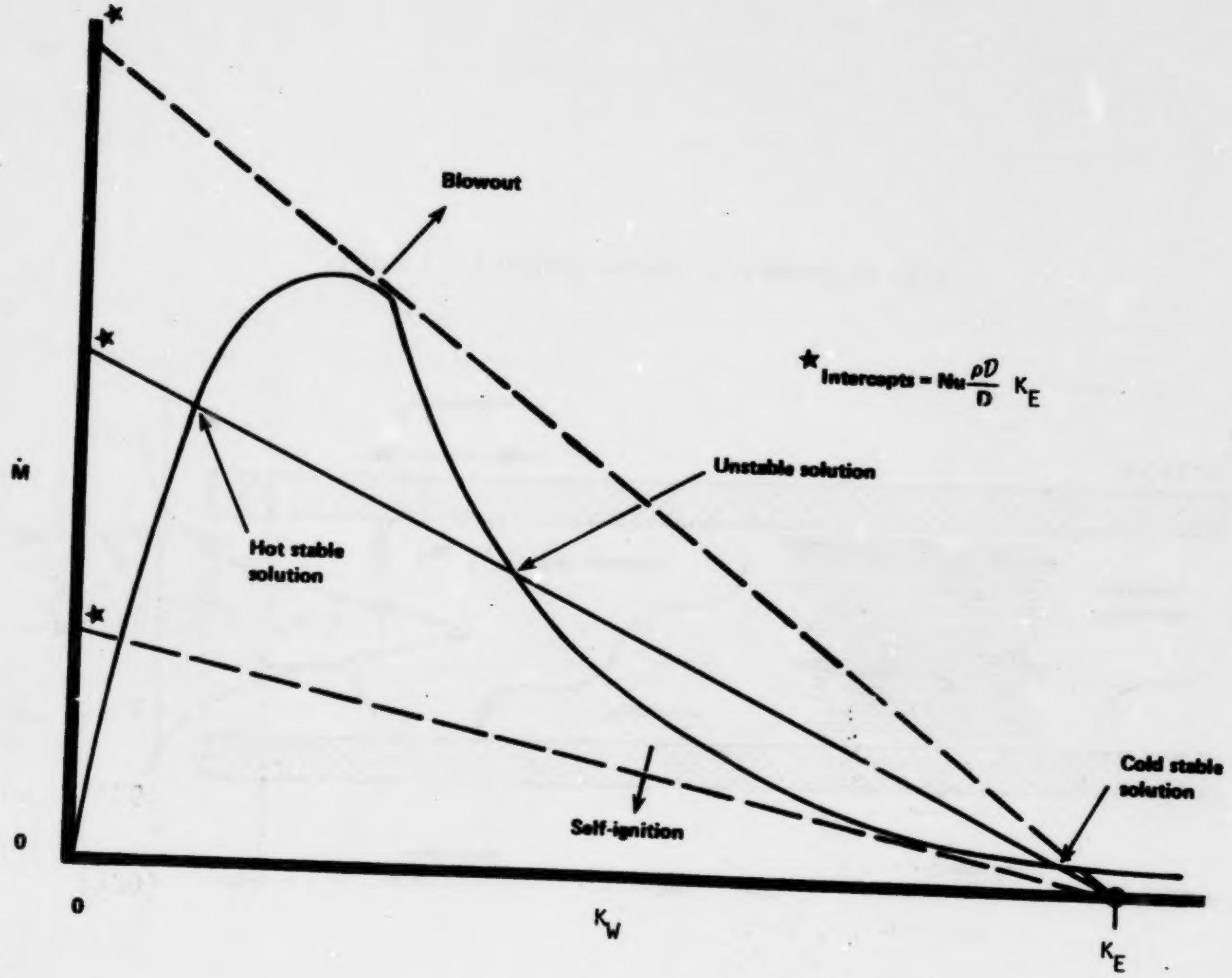

Figure 3. Simplified mass balance solution for catalytic combustion in a monolith bed.

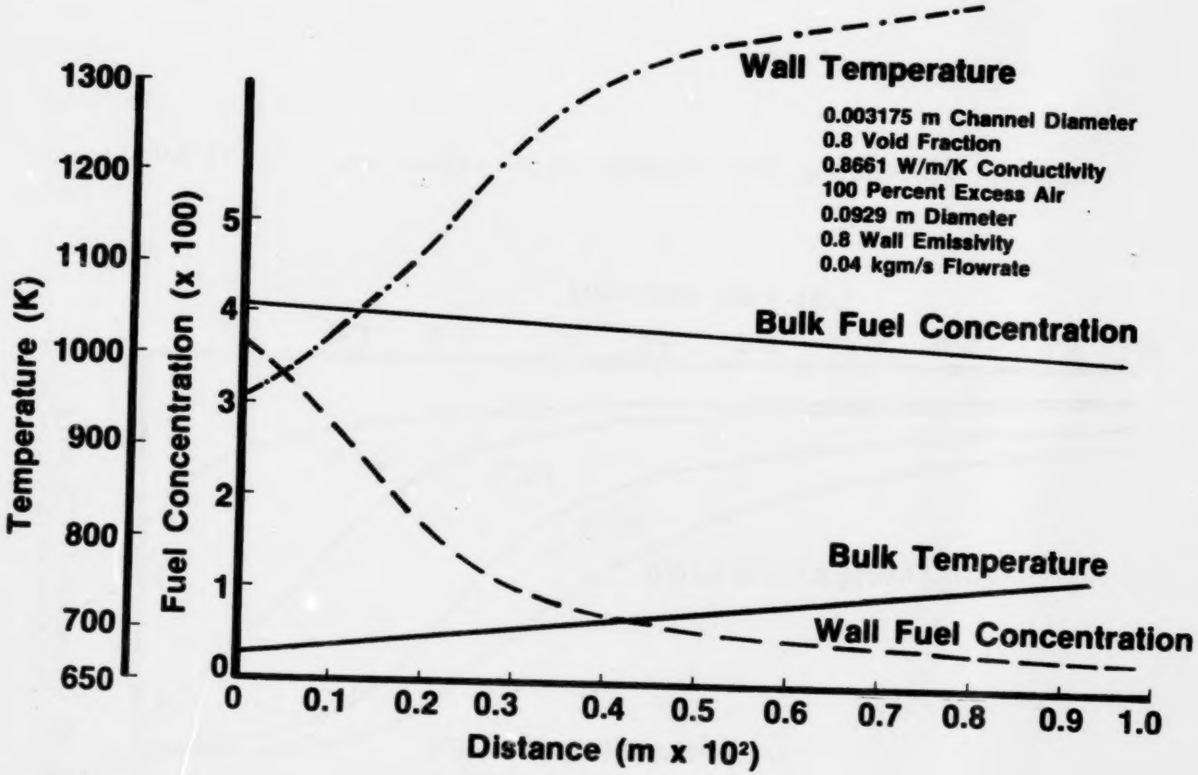

Figure 4. Wall and bulk gas temperature and fuel concentration through bed.

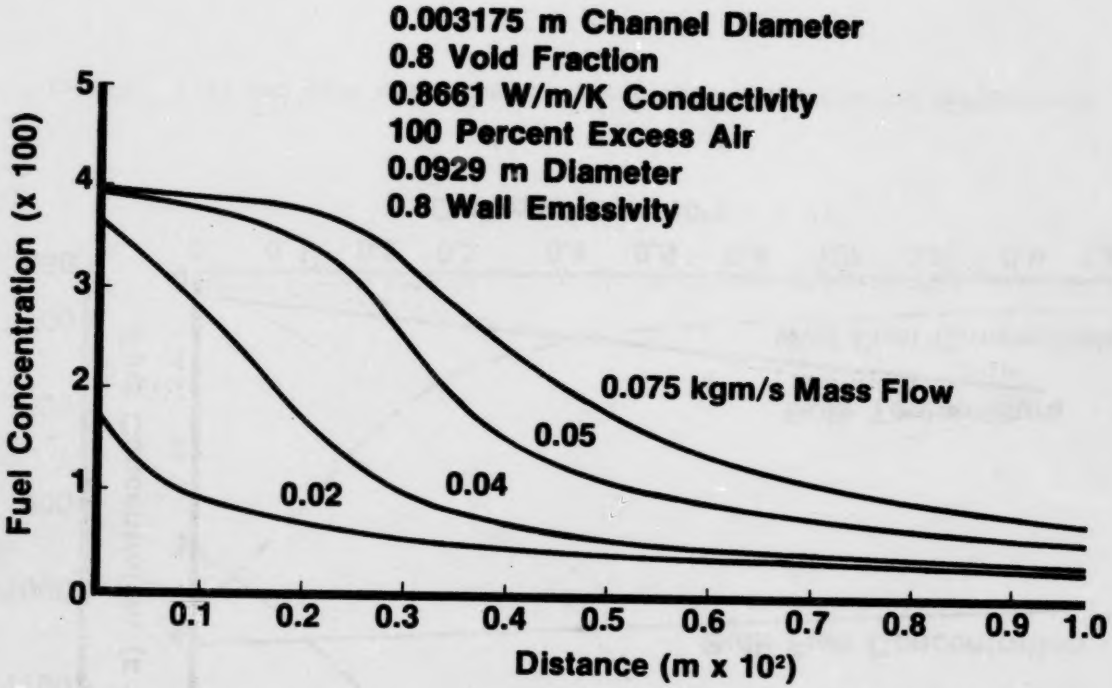

Figure 5. Wall fuel concentration distributions for several flowrates.

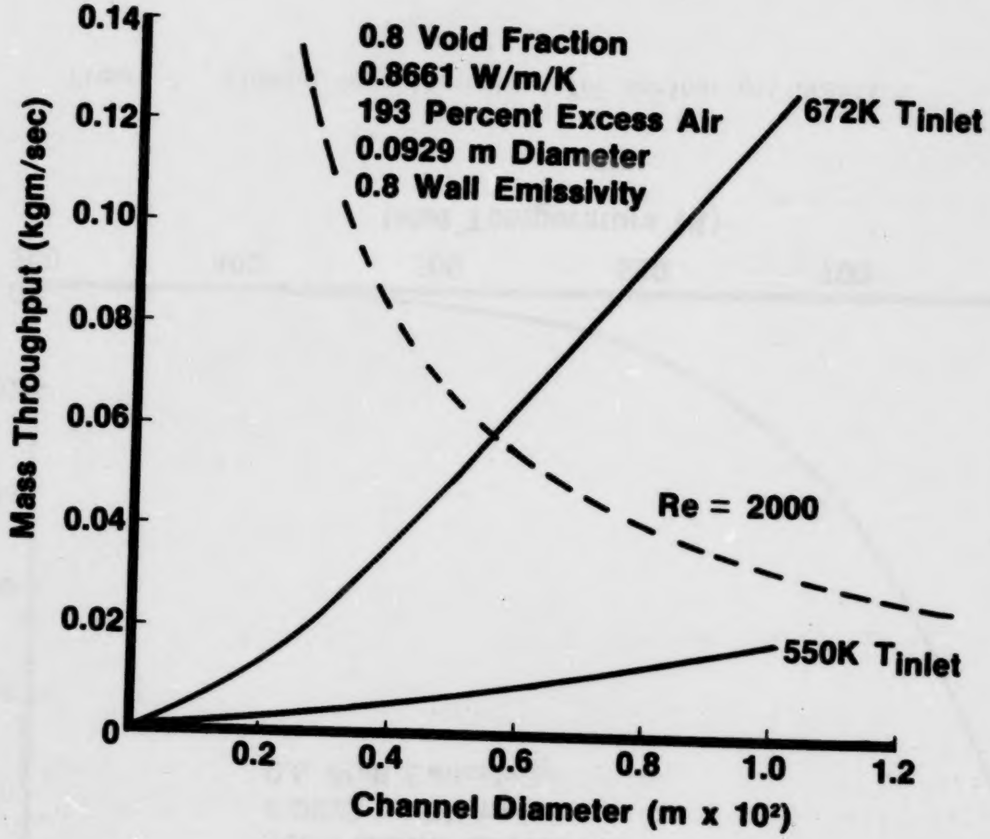

Figure 6. Blowout mass throughput for various channel diameters.

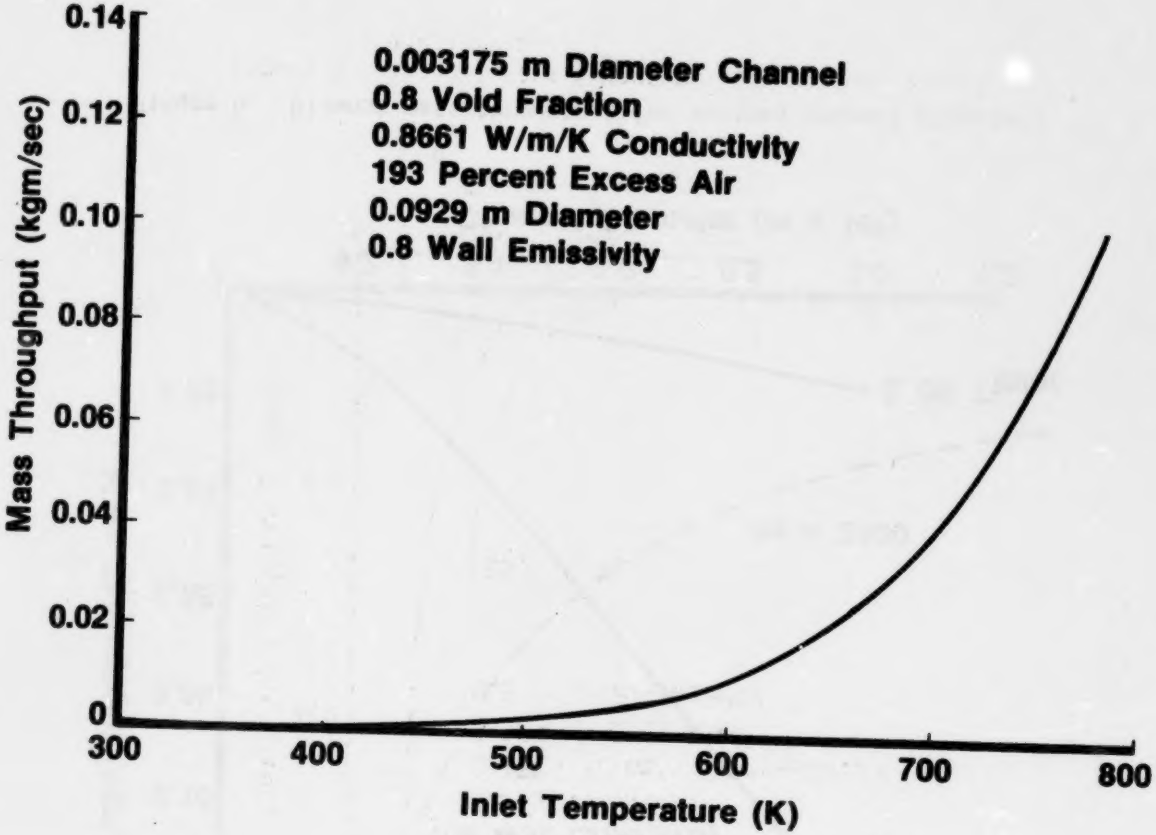

Figure 7. Blowout mass throughput for various gas preheats.

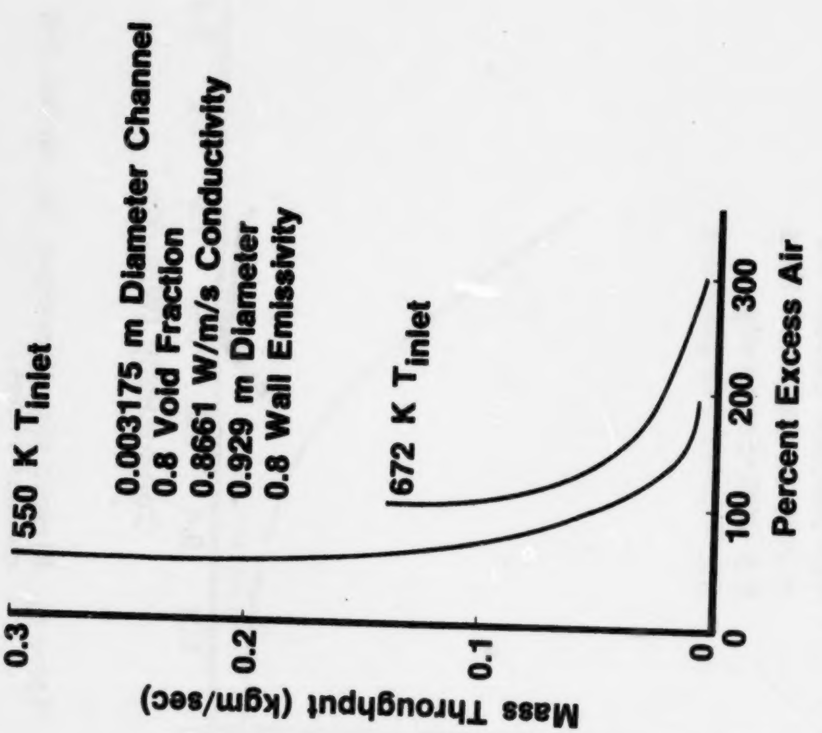

Figure 8. Blowout mass throughput for various excess air levels.

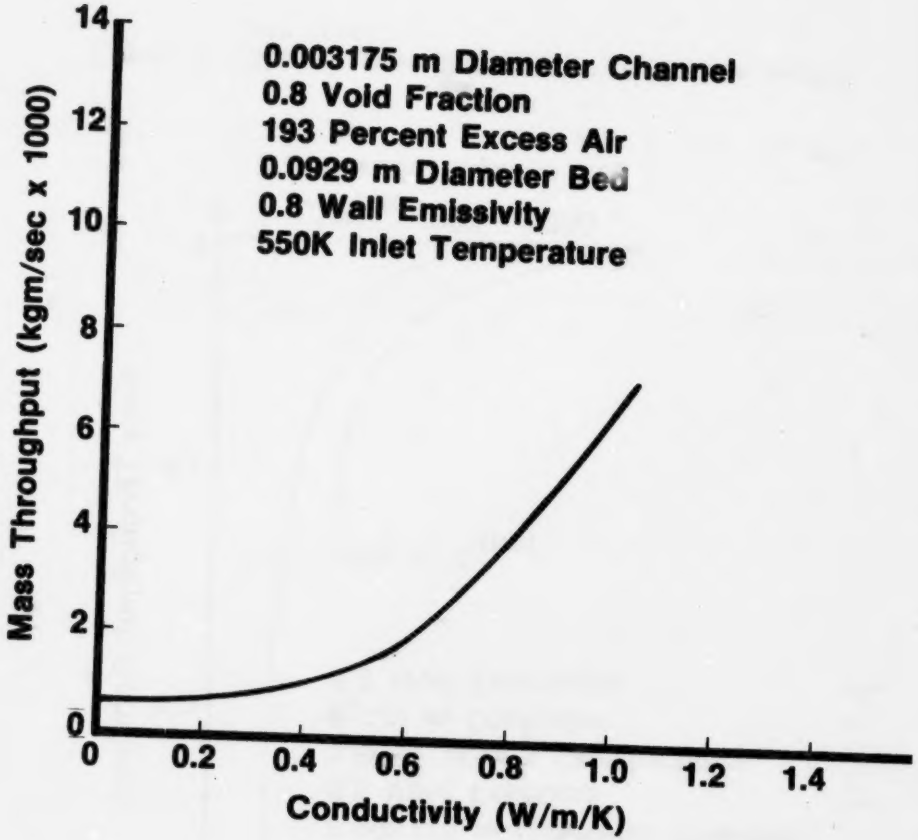

Figure 9. Blowout mass throughput for various bed conductivities.

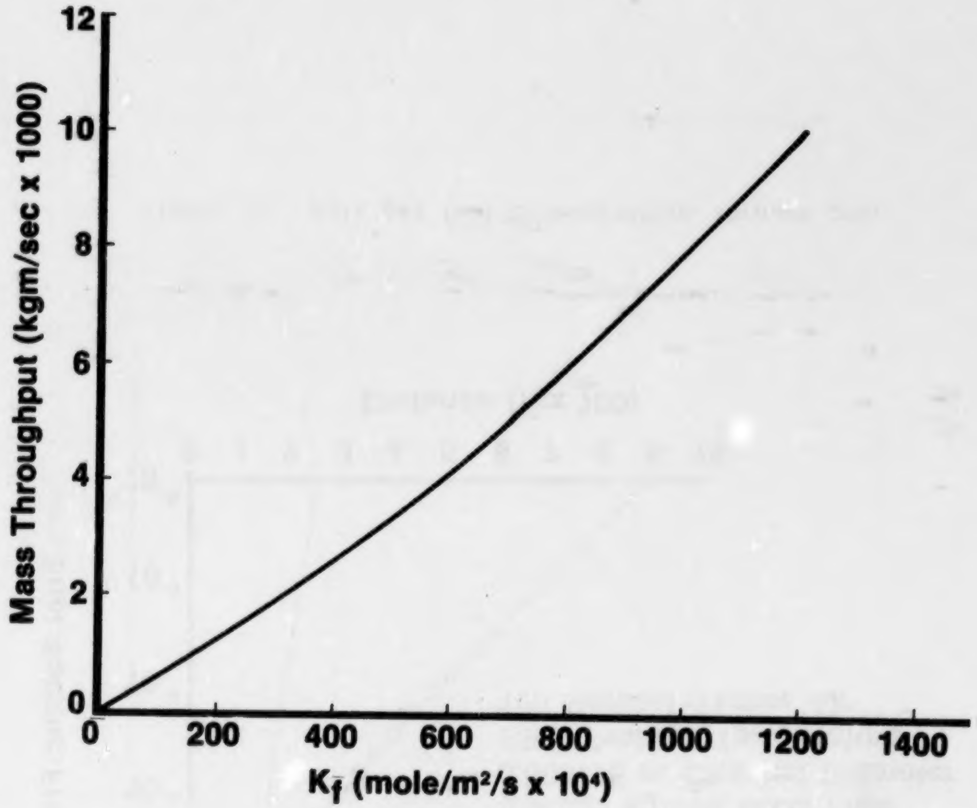

Figure 10. Blowout mass throughput for various surface reaction activities.

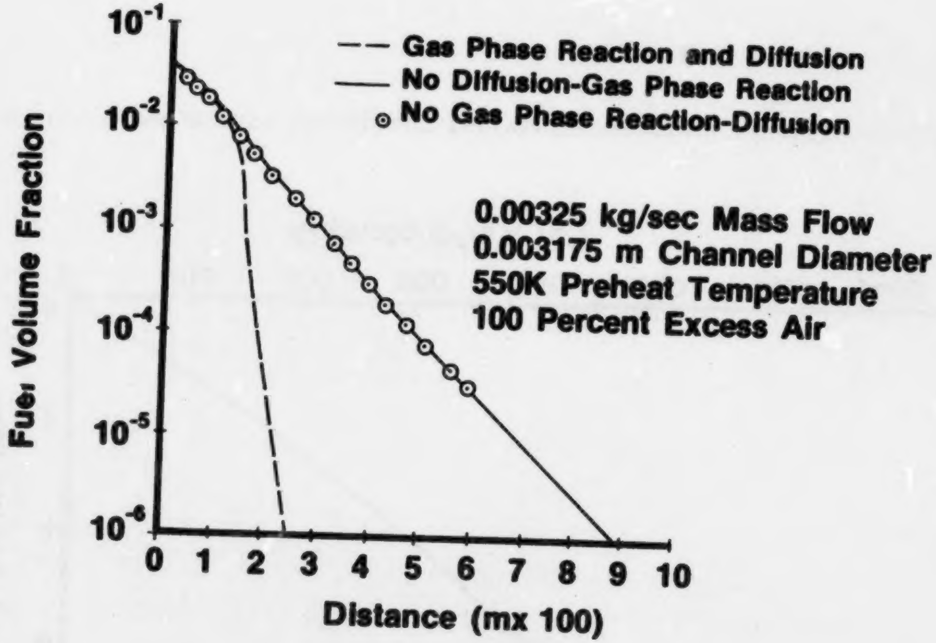

Figure 11. Bulk gas fuel concentration through bed.

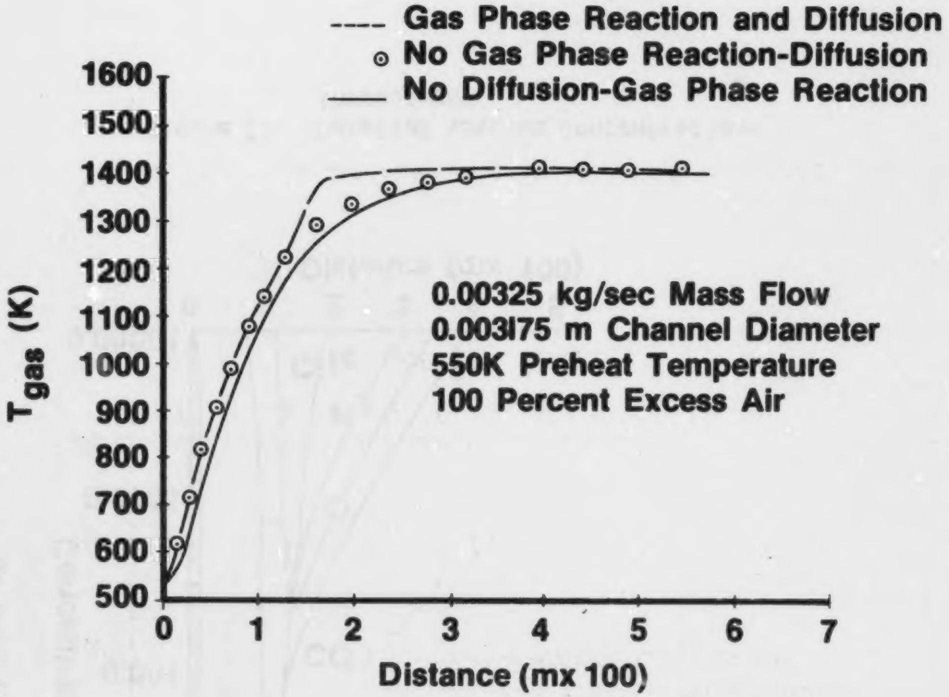

Figure 12. Bulk gas temperature through bed.

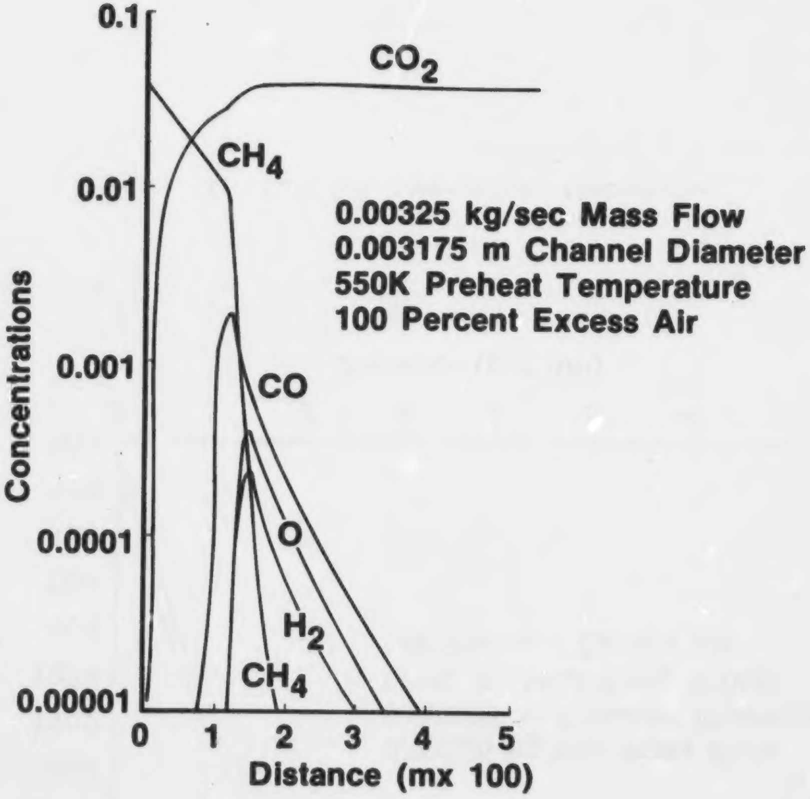

Figure 13. Detailed species concentrations through bed.

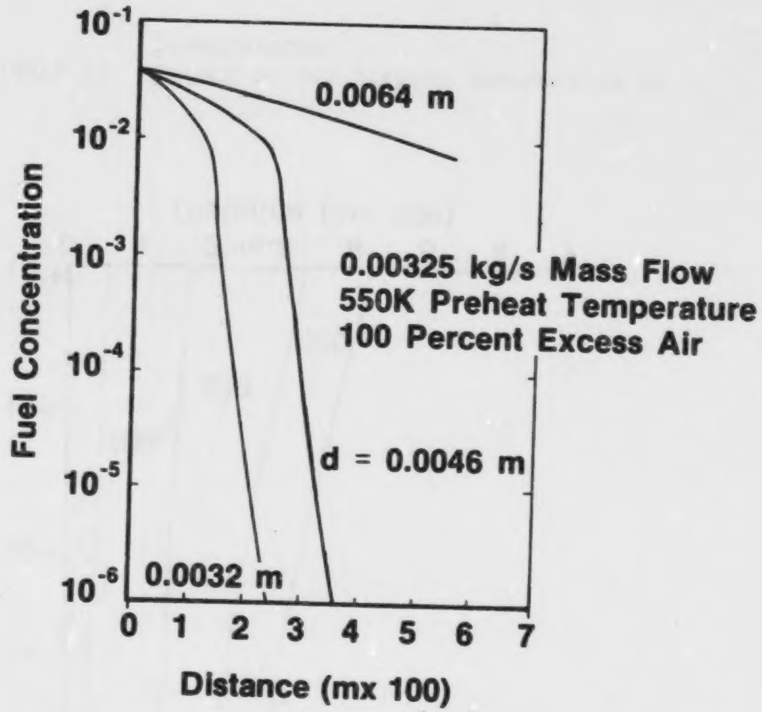

Figure 14. Effect of channel diameter on breakthrough.

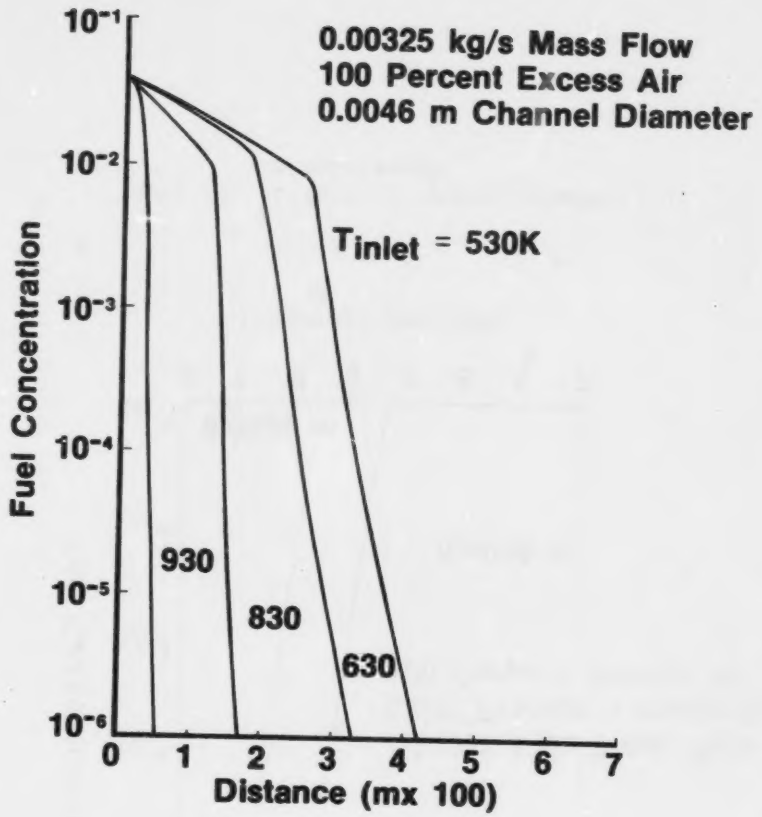

Figure 15. Effect of gas preheat temperature on breakthrough.

THE DEVELOPMENT OF CATALYTIC COMBUSTORS FOR STATIONARY SOURCE APPLICATIONS

By:

W.V. Krill and J.P. Kesselring
Acurex Corporation
Mountain View, California 94042

ABSTRACT

An experimental program has been conducted for the Environmental Protection Agency to develop design criteria for catalytic combustors as applied to stationary systems. The program included catalyst screening tests from which the graded cell concept was developed. The graded cell catalyst exhibits greatly enhanced combustion characteristics in terms of increased maximum throughput. Advanced testing of the graded cell catalysts showed high heat release rate capabilities with low emissions of CO, HC, and thermal NO_x. Operation of the catalysts under fuel-rich conditions showed capability to control fuel NO_x emissions. Additional criteria for system scaleup and operation under varying preheat and pressure conditions were also generated.

Catalysts developed during the program were incorporated into three small-scale systems with heat extraction. A radiative catalyst/watertube system, utilizing direct heat removal from the catalyst, was devised and tested. The concept has potential application to watertube boilers. A model gas turbine combustor was tested at pressures between .101 and 1.01 MPa (1 to 10 atmospheres) to investigate operating characteristics and fuel nitrogen conversion to NO_x. The final system, a two-stage combustor, was constructed to utilize fuel-rich first stage combustion for fuel NO_x control. Measured emission results make the concept attractive for a variety of future system applications.

Preceding page blank

INTRODUCTION

Catalytic combustors have been shown to reduce the levels of CO, HC, and NO_x emissions over those of conventional burners in laboratory tests with both clean and nitrogen-doped fuels. The operating conditions for these catalytic combustors are limited by the catalyst temperature capability. Since the temperature obtained through normal one-stage, low excess air operation (necessary for high system efficiency) is outside the temperature capability of current catalyst systems, system techniques to control temperature are required. The development of combustors for boiler, furnace, and gas turbine systems depends on establishing design criteria for system temperature control and related system parameters. The EPA catalytic combustion program has focused on determining these criteria for stationary source combustors.

System design criteria include information on the catalyst/washcoat/substrate combination and its operational life, preheat requirement, heat release capability, and pressure and temperature limitations. This information was developed through the preparation of varying catalyst combinations and comparison of the catalysts through combustion screening. Developed catalysts were then incorporated into small-scale systems for demonstration of energy release and heat extraction concepts. Additional criteria were developed to operate these systems at low emission levels with the highest achievable efficiency. The following summarizes results for the catalyst screening and system configuration tests conducted under EPA Contract 68-02-2116.

CATALYST DEVELOPMENT

Preliminary Screening Tests

An initial combustion test series was conducted at the Jet Propulsion Laboratory in Pasadena, California on systems with monolithic catalyst supports. This test series identified the most suitable combustion characteristics for catalysts as follows:

Preceding page blank

- Low ignition temperature
- Low preheat requirements for sustained combustion
- Combustion uniformity throughout the bed
- High heat release capability
- High combustion efficiency
- Low pollutant emissions
- High operating temperature
- Fuel flexibility
- Long life.

Catalyst models tested included variations in substrate, washcoat, and catalyst materials -- as well as substrate geometry and preparation techniques.

Catalysts developed in the screening test series showed greatly enhanced combustion characteristics over those initially tested. Specifically, performance was improved by:

1. Increased catalyst loading, resulting in lower initial lightoff temperatures, higher mass throughputs, and increased lifetime at 1367K (2000°F).
2. Increased cell size, allowing higher possible mass throughputs at the expense of increased hydrocarbon emissions.
4. Heavier hydrocarbon fuels which promote lightoff at lower ignition temperatures.
5. Hydrogen sulfide (H_2S) fixation of platinum catalysts to promote retention of platinum surface area.
6. Presintering of catalyst washcoats which reduces burying of active catalyst below the surface during combustion.
7. Stabilization of γ-Al_2O_3 washcoats with cesium oxide (Cs_2O) up to 5 weight percent increased surface area. Stabilization of alumina washcoats with ceria up to 5 weight percent had a negative effect on surface area.

8. Decreased cell size to significantly reduce unburned hydrocarbon and carbon monoxide emissions.
9. Catalyst beds of combined large cell and small cell monoliths also significantly increase throughput (at a given preheat temperature) and overall catalyst life with low emissions.
10. Bed temperature uniformity was increased by operation at higher temperatures.

Catalysts with combined large and small cell segments represent the best concept developed by the test series. This graded cell concept (three segments shown in Figure 1) was further developed through predictions of the PROF-HET catalytic combustion computer code (Reference 1). Finally, preliminary data with ammonia-doped natural gas indicated a potential for control of fuel nitrogen compounds to NO_x under lean conditions.

Graded Cell Catalyst Tests

Additional catalyst screening tests were conducted at Acurex on the graded cell configuration. The preliminary objective of these tests was to identify the best catalysts for system application. Catalysts were also tested for high temperature capability, system scaleup design criteria, and conversion data of fuel nitrogen to nitrogen oxides under varying operating conditions.

Screening catalysts were obtained from six sources, including W.R. Grace and Company, Universal Oil Products, Inc., William Pfefferle (a private consultant), Matthey Bishop, Inc., Johnson Matthey, and Acurex. Substrate materials were either DuPont alumina or Corning zirconia spinel. Washcoats varied from proprietary preparations with high pretest surface area to no washcoat and a subsequent low pretest surface area. Catalysts were either precious metal, metal oxide, or mixtures. The catalyst loadings and fuels used are listed in Table I.

To support combustion test results, pre- and post-test catalyst physical measurements were made. These measurements included catalyst surface area and dispersion performed in the Acurex catalyst characterization laboratory. Additional scanning electron microscopy (SEM) and energy dispersive analysis by X-ray (EDAX) tests were performed at the Jet Propulsion Laboratory as required.

Table II is presented for reference, and summarizes all surface area and dispersion measurements.

Catalysts were compared by limited aging, maximum throughput, varying stoichiometry, and minimum preheat tests. Some catalysts, primarily precious metals with low loadings, exhibited lifetimes of less than 10 hours, precluding extensive data evaluation. Others were tested to completion in a 20 to 30 hour test sequence. In addition, some catalysts showed preferential activity for either fuel-rich or fuel-lean combustion or [illegible] operation only at higher preheats of 700 to 811K (800 to 1000°F).

The maximum throughput (volumetric heat release rate) capabilities were compared for various graded cell catalysts to indicate relative activity. Catalyst data selected from Table I are compared below.

MAXIMUM THROUGHPUT COMPARISON DATA**

Catalyst Type	Manufacturer	T_{Bed} K	SV, 1/Hr	q''', $\frac{J}{Hr\text{-}Pa\text{-}m^3}$	Bed Uniformity
UOP Proprietary	UOP 2	1522	343,900	3.9×10^6	Excellent
Pt-Ir/Al_2O3	W.R. Grace	1256-1589	327,400	2.8×10^6	Ragged
Stab. Pt/Al_2O3	Matthey Bishop	1611	348,000	5.2×10^6	Ragged
JM Proprietary	Johnson Matthey	1589	603,300	7.2×10^6*	Excellent
Co_2O_3/Al_2O_3	Pfefferle 3	1617	443,100	5.1×10^6*	Excellent
Co_2O_3/Zirconia Spinel	Acurex 3	1644	661,400	7.8×10^6*	Excellent

**All results with natural gas/methane fuel

*Bed not blown out

The first three catalysts, either precious metal or proprietary materials, exhibited volumetric heat release rates (q''') of approximately 3.7×10^6 J/hr-Pa-m^3 (10×10^6 Btu-hr-Atm-ft^3) at blowout conditions. The latter three, either proprietary or cobalt oxide catalysts, reached approximately 7.4×10^6 J/hr-Pa-m^3 (20×10^6 Btu/hr-Atm-ft^3) without blowing out. This heat release rate represented the maximum facility capability in the screening test configuration. It is apparent that the cobalt oxide catalysts are capable of higher heat release rates than the precious metals in the graded cell configuration. The oxides required operation at higher temperature, however, to produce combustion efficiencies comparable to the precious metals at lower temperatures.

During graded cell catalyst testing, operating temperatures were varied from 1367K to over 1978K (2000 to 3100°F). Thermal NOx data were obtained with natural gas as the primary test fuel. A number of the test models are compared in Figure 2. From 1367 to 1644K (2000 to 2500°F), little variation among the NOx emissions with catalyst type is apparent with NO levels below 20 ppm. At 1756 to 1867K (2700 to 2900°F), the NOx production rate begins to increase, as with conventional flame combustion but at a less rapid rate.

In Figure 2, two different catalyst geometries are shown for fuel-lean operation in the 1644 to 1978K (2500 to 3100°F) range. The upper curve is for a two-segment graded cell model (A-029) that acted primarily as a flame holder for downstream gas phase reactions. The lower curve represents data for a three-segment catalyst (A-030) where significantly increased combustion occurs on the surface of the catalyst bed. It is apparent that maximizing the amount of surface reaction occurring in a catalytic combustor minimizes the production of thermal NO_x. These results indicate the importance of the graded cell configuration, particularly for thermal NO_x control in high excess air gas turbine applications.

In addition to baseline catalyst screening tests, selected catalysts were tested to characterize conversion of fuel-bound nitrogen to nitrogen oxides with catalytic combustion. Ammonia was added to natural gas to simulate fuels of varying nitrogen content. Exhaust gas analyses for NO_x by chemiluminescent analyzer and for ammonia (NH_3) and cyanide (HCN) by specific ion electrode were performed.

A nickel oxide/platinum catalyst was prepared at Acurex and tested over a range of stoichiometries from 55 to 200 percent theoretical air at a nominal bed temperature of 2900°F. Fuel dopant concentration ranged from 2500 to 10,000 ppmv NH_3 in the fuel. The results are shown in Figure 3 as the percentage of the incoming NH_3 converted to NH_3, HCN, and NO. The NH_3 conversion to NO increased from zero levels under very fuel-rich conditions to better than

90 percent on the fuel-lean side. NH_3 conversion to HCN showed the opposite trend -- high under rich conditions and decreasing to zero on the lean side. Unconverted ammonia was highest below 70 percent theoretical air and remained at low levels under lean combustion.

The total of these three curves (dashed line and cross symbols) represents all NO_x precursor species for the NiO/Pt catalytic combustor. A distinct minimum occurs between 70 and 80 percent theoretical air, where only 20 percent of the fuel nitrogen is converted to NO_x precursors.

A second graded cell catalyst (cobalt oxide/platinum) was tested with simulated fuel nitrogen. The fuel nitrogen conversion is shown in Figure 4. The ammonia conversion to nitric oxide provided the same characteristic curve as the nickel oxide/platinum catalyst. Differences in the HCN and NH_3 species measured, however, resulted in lower total NO_x precursor ($NO + NH_3 + HCN$) levels under fuel-rich conditions. The minimum occurred at a lower value of theoretical air (60 percent) than that of the previous nickel oxide catalyst (75 percent). The cobalt oxide catalyst could thus be operated fuel rich without dilution to achieve low conversion of fuel-bound nitrogen to nitrogen oxides.

The low fuel nitrogen conversion of these two catalysts at 60 to 80 percent theoretical air has important system implications. Combustors which could operate fuel-rich, possibly with staging, have potential for fuel NO_x control. This characteristic of the catalytic combustor under fuel-rich conditions is the basis for the two-stage catalytic combustor demonstrated under this program.

Design criteria for the graded cell catalyst concept also included scaleup, pressure, and preheat characteristics. Catalyst blowout was again selected to compare activity. Based on the results of small-scale testing, a Universal Oil Products catalyst was selected for scaleup. Analytical modeling predicted that combustion throughput capability would scale proportionately to bed frontal area. Therefore, the bed diameter was increased to provide a 2.7 increase in frontal area over the small-scale model. Bed length remained fixed at 7.6 cm (3.0 inches).

Test data showed that maximum throughput (at blowout) did scale approximately with frontal area. Maximum throughput reported for the small-scale catalyst was 258.5 MJ/hr (245,000 Btu/hr) and 3.42×10^6 J/hr-Pa-m^3 (9.3×10^6 Btu/hr-atm-ft^3) volumetric heat release rate. This compares to a volumetric heat release of 4.38×10^6 J/hr-Pa-m^3 (11.9×10^6 Btu/hr-atm-ft^3) at 926.3 MJ/hr (878,000 Btu/hr) for the scaleup catalyst at 672K preheat.

A series of blowout tests were then conducted to determine the operational mass throughput limit of the catalyst for varying preheat and pressure conditions. The blowout points used are shown below.

BLOWOUT DATA — CATALYST A-041

Data Point	Bed Temp K (°F)	Preheat Temp K (°F)	Max. Fuel Flowrate Kg/hr (lbm/hr)	Pressure MPa (atm)
1	1588 (2400)	608 (635)	15.0 (33.0)	.195 (1.93)
2	1588 (2400)	478 (400)	10.5 (23.1)	.140 (1.39)
3	1588 (2400)	389 (240)	8.4 (18.5)	.134 (1.33)
4	1588 (2400)	603 (625)	22.2 (49.0)	.301 (2.98)

Two things are evident from the data:

- Blowout scales linearly with pressure ($\dot{m}_{fuel\ max} = P_{atm} \times \dot{m}_{fuel\ max,\ 1\ atm}$)
- Blowout for catalyst A-041 was exponential in preheat temperature, although a relatively weak exponential factor is shown.

Operation of the catalyst was, of course, possible at any combination of preheat and fuel flowrate below the blowout limits.

The exponential behavior of preheat temperature and its effect on blowout was shown in PROF-HET code predictions (Reference 1). The blowout data obtained support this prediction and can be employed as design criteria for operation of catalyst A-041 under varying conditions.

The graded cell catalyst screening tests identified the design criteria required for incorporating the graded cell configuration into system applications.

Specifically, these criteria included mass throughput and heat release capabilities, emissions under varying operating conditions and with nitrogen-containing fuels, lightoff requirements, and current lifetime capabilities. In addition, the state of the art in catalyst development has been evaluated, including an understanding of preparation techniques, material capabilities, and material interactions.

SYSTEM CONCEPT TESTING

The design criteria generated for graded cell catalyst configurations were used in the specification of three small-scale systems incorporating heat extraction techniques. A radiative catalyst/watertube system demonstrated a stoichiometric, water-cooled combustor for boiler application. A model gas turbine combustor utilized high excess air for catalyst and exhaust gas temperature control. Finally, a two-stage combustor was constructed to demonstrate fuel nitrogen control with application to either boiler, furnace, or turbine equipment.

Radiative Catalyst/Watertube System

The radiative catalyst/watertube concept is shown in Figure 5. A stoichiometric fuel/air mixture is fed to the radiative section which contains a close-packed array of catalyst elements and watertubes. The mixture is partially combusted by the catalyst which is kept at a low surface temperature by radiation heat loss to the watertubes. The combustion products and remaining unburned fuel and air are then passed to a downstream catalytic adiabatic combustor to complete combustion reactions. A final convective section extracts energy from the fully combusted gases. Both catalyst sections operate well below the maximum use temperature of the catalyst supports -- the radiative section by radiative cooling and the adiabatic section by dilution of the fuel/air mixture with exhaust products from the radiative section. The radiative section was constructed and tested independently of the downstream adiabatic combustor and convective sections.

An initial test series was conducted using a platinum catalyst on Coors alumina cylinders. Stoichiometry was varied from 40 to 219 percent theoretical air and fuel mass rate from 2.1 to 6.7 kg/hr (4.7 to 14.8 lbm/hr) of natural gas.

Preheat conditions were also varied. Figure 6 shows the energy extracted by the cooling tubes out of the total available energy at the bed inlet as a function of theoretical air. The total available energy includes the latent heat of the fuel and the sensible preheat energy. The energy extracted by the watertubes is essentially the same as the fuel energy release since the bed inlet and outlet temperatures were approximately equal. At low theoretical air, the heat extraction is controlled primarily by the catalyst surface temperature, peaking at approximately 100 percent theoretical air. As theoretical air further increases above 100 percent, surface temperature again begins to decrease, decreasing the radiant exchange. The higher mass throughput, however, also increases convective heating of the watertubes such that the energy exchange does not fall off rapidly. Overall combustion efficiency at 100 percent theoretical air was calculated as approximately 37 percent from the data. Significant emissions of CO and HC were measured for the radiative section due to the incomplete combustion. NO_x levels were consistently below 2 ppm as measured.

The radiative section was also tested to evaluate fuel nitrogen conversion characteristics of the system. For those tests, natural gas was doped with ammonia and stoichiometry was varied from 52 to 120 percent theoretical air.

Figure 7 shows the fuel nitrogen conversion characteristics of the radiative system for natural gas doped with 2000 ppm of ammonia. Low NO_x and high NH_3 values above 100 percent theoretical air are consistent with the incomplete combustion characteristics of the radiative section. The low point in the total NO_x precursor curve (NH_3 + HCN + NO_x) at 60 percent theoretical air is similar to those obtained for metal oxide graded cell catalysts.

The actual measured heat release of the radiative catalyst/watertube system was not as high as that predicted at the nominal 4.3 Kg/hr (9.5 lbm/hr) methane flowrate design condition. Therefore, the radiant section as tested is not fully suited for complete system development. The addition of the downstream adiabatic catalytic combustor results in too high a temperature in that region at stoichiometric conditions since combustion efficiency in the first stage is not as high as expected. The radiative catalyst/watertube section did exhibit excellent performance at stoichiometric conditions with very low levels of NO_x. The potential for control of fuel nitrogen conversion and the extremely stable operation experienced under all test conditions make it attractive for future boiler applications.

Model Gas Turbine Combustor

Since the graded cell catalyst was demonstrated to have the low preheat, high heat release, and pressure capabilities required for gas turbine applications, a 1055.1 MJ/hr (10^6 Btu/hr) model turbine can and fuel injection system was constructed. The system and catalyst are shown in Figure 8. Testing was performed at Acurex and Pratt and Whitney Aircraft (West Palm Beach, Florida) facilities. Acurex and UOP catalysts were prepared on either DuPont alumina or Corning zirconia spinel support materials of varying configurations.

The model gas turbine combustor was first tested at Acurex with propane at pressures between .101 and .354 MPa (1 and 3.5 atmospheres). A heat release rate of 263.8 MJ/hr (250,000 Btu/hr) at 1478K (2200°F) bed temperature was run as the nominal test condition. No significant emissions of NO_x or CO were obtained.

Pratt and Whitney test data were obtained with propane, No. 2 oil, and No. 2 oil with 0.5 weight percent nitrogen as fuels. Heat release rates to 844 MJ/hr (800,000 Btu/hr) were achieved with low NO_x emissions for both propane and No. 2 oil. Some difficulty was encountered with flashback and flameholding on the fuel nozzles when running No. 2 oil. High CO and unburned hydrocarbon emissions resulted from operating at low bed temperatures (near the breakthrough limit) to avoid flameholding. Variations in pressure were not found to affect emission levels. Tests run with pyridine-doped No. 2 fuel oil, however, increased the NO_x emission levels, representing percentage conversions of fuel nitrogen to NO_x of 100, 61, and 55 percent for test pressures of .303, .505, and .707 MPa, respectively.

Subsequent inspection of the test hardware showed that low liquid fuel inlet velocities due to a fabrication error were responsible for the flashback and flameholding.

A final test series was conducted at Acurex (after the test hardware had been reworked) with natural gas, natural gas doped with ammonia, and No. 2 oil. Pressures from .101 to .808 MPa (1 to 8 atm) with natural gas and .101 to .505 MPa (1 to 5 atm) with fuel oil were included. A decrease in ammonia converted to NO_x with pressure was observed. These results are consistent with those obtained at Pratt and Whitney with pyridine-doped No. 2 fuel oil. Maximum throughput for the catalyst at .303 MPa, 1422K (3 atm, 2100°F) pressure and bed temperature, and 561K (550°F) preheat temperature was also investigated. At space velocities near 200,000 per hour, the catalyst began to break through with increasing CO and unburned hydrocarbon emissions. Nitrogen oxide emissions remained at near zero levels throughout the test. Full blowout was not achieved as control of catalyst temperature during breakthrough produced difficulties in system control. The maximum heat release obtained was 615 MJ/hr (583,000 Btu/hr).

Final tests were conducted with diesel fuel to compare emissions with those from natural gas. An increased bed temperature was maintained for the oil tests to maintain uniform bed conditions and suppress soot formation. The NO_x levels were higher than for natural gas (15 ppm compared to 3 ppm) due primarily to higher average bed temperatures.

The results of the model gas turbine testing demonstrated the application of the graded cell concept in a system similar to current turbine combustor designs. High mass flowrates were achieved in a relatively small volume combustor. Overall pressure drop for the combustor and fuel injector were measured at less than one percent at .303 MPa (3 atmospheres) test pressure.

Two-Stage Combustor

The two-stage catalytic combustor is attractive for two reasons. First, it allows control of bed temperatures to those compatible with the support material without large excess air requirements. Second, the first stage can be operated fuel-rich, which has been shown to be advantageous for reduced conversion of fuel nitrogen to nitrogen oxides. A two-stage combustor was designed and constructed to demonstrate these concepts.

The two-stage combustor is shown schematically in Figure 9. A fuel-rich mixture is introduced into the primary stage which contains a graded cell catalyst bed. The fuel is partially combusted, and the released energy is removed by an interstage heat exchanger. Sufficient secondary air is then injected into the combustion products to complete combustion of the remaining fuel in the second stage. The full system combustor would also include a second heat exchanger to remove the combustion energy released in the second stage.

The two-stage combustor containing two cobalt oxide catalysts was tested with natural gas at .101 MPa and .202 MPa pressures (1 and 2 atmospheres).

Lightoff and steady-state operation presented no unusual control problems. Some thermal and fluid dynamic interactions between stages were apparent, however. The combustor was tested at an overall stoichiometry varying from 70 to 150 percent theoretical air at a nominal fuel flowrate equivalent to 211 MJ/hr (200,000 Btu/hr) heat release rate. The first stage stoichiometry was varied from 40 to 70 percent theoretical air. Ammonia was added to the natural gas fuel at a rate of 0.2 to 0.4 percent.

Bed temperatures ranged from 1256K to 1660K for a relatively constant preheat of 617K (650°F). The energy extracted in the interstage heat exchanger represents 50 to 60 percent of the combustion energy generated in the first stage.

The results of the fuel nitrogen conversion data are shown in Figure 10 as a function of overall combustor stoichiometry. The data show that when operating above 100 percent theoretical air, only nitrogen oxides are normally present. Under overall fuel-rich conditions, fractions of ammonia and cyanide were also present. These results are consistent with fuel nitrogen data obtained on the single cobalt oxide catalyst (model A-037, Figure 4). The data in Figure 10 show a nominal 30 percent conversion rate of fuel nitrogen to NO_x precursors with a value of approximately 27 percent near overall stoichiometric conditions. A slight decrease in conversion was noted at .202 MPa (2 atm) pressure.

The data shown in Figure 10 at approximately 10 percent conversion levels varied in test conditions from the other data in two respects:

1. The first stage was operated at higher values of theoretical air (75 percent) compared with 50 percent for the initial data, and
2. The first stage catalyst had experienced some sooting by later test times when the data were taken, causing the catalyst to operate at lower temperatures with incomplete combustion.

The first stage sooting of the cobalt catalyst proved to be a limiting factor in the test life of the system. The incomplete combustion occurring at later test times was evident by increasing measured carbon monoxide levels.

The demonstration of the two-stage catalytic combustor showed a number of important results:

1. The two-stage combustor is effective in controlling conversion of fuel nitrogen to nitrogen oxides under stoichiometric and fuel-lean conditions.
2. A slight decrease in nitrogen conversion was found at .202 MPa (2 atmospheres) pressure.
3. The variation of first stage stoichiometry impacts overall fuel nitrogen conversion.
4. First stage sooting of the cobalt oxide catalyst was a limiting factor in combustor operating life.

Application of the concept to both boiler and turbine systems is possible. Convective heat exchangers downstream of each catalyst stage would provide for steam raising in boiler applications. Interstage cooling would not be required for gas turbine systems where high excess air in the second stage could be used to control the catalyst and exhaust gas temperatures. Further work is required for optimization of the system and catalyst elements for specific applications.

CONCLUSIONS

As a result of this research and development program, significant progress has been made toward developing a practical catalytic combustion system. Before the step to demonstration can be taken, however, additional work relating to the integration of the catalytic combustor into the total combustion system must be performed.

Based upon the analysis and test results of this program, the design, fabrication, and operation of catalytic combustors with high volumetric heat release rates and low emissions have been demonstrated. Both precious metal and oxide catalysts have been tested over a wide operating temperature range. The precious metal catalysts should be limited to temperatures below 1589K (2400°F) for catalyst life considerations, while oxide catalysts can be operated for long periods at temperatures above 1644K (2500°F). Catalyst performance has been greatly enhanced through the use of graded cell monoliths and higher catalyst loadings.

Catalytic combustors have been shown to be effective in controlling both thermal and fuel NO_x emissions. The thermal NO_x control appears to result from maximizing surface reactions in the combustor, while fuel NO_x can be minimized by operating at a rich fuel/air ratio which minimizes the formation of NH_3, HCN, and NO, with complete combustion of CO and HC at a later time.

The maximum throughput of a catalytic combustor is a linear function of pressure and an exponential function of preheat. Thus, for a given preheat, the catalyst is face velocity limited in throughput ability.

Small-scale catalytic combustion system configurations have been tested and demonstrate the feasibility of direct radiative removal of bed heat for temperature control, two-stage catalytic combustion for temperature and fuel NO_x control, simulated exhaust gas recirculation through the use of nitrogen diluent for temperature control, and high excess air operation. The combustion system concepts that have been operated show that it is possible to operate near stoichiometric conditions with less than 10 ppm NO_x and CO in a natural gas-fired catalytic combustor.

A number of areas in catalytic combustion need to be addressed to capitalize on the progress to date. Additional testing of simple and mixed oxide catalysts for combustion and fuel nitrogen conversion abilities is needed, along with life testing of selected catalysts to 1000 hours at various pressures.

Exploratory work with heavy fuel oils (Nos. 4, 5 and 6) and pulverized coal should be conducted to determine system feasibility and fuel preparation problems. The potential of catalytic combustion in controlling NO_x emissions from the combustion of these fuels is great and needs early experimental verification.

Development of auxiliary systems required to interface with the catalytic combustor is also needed. This includes lightoff systems, temperature control systems, and fuel and air introduction systems. In addition, further testing of the radiative catalyst/watertube, two-stage combustor, and gas turbine combustor systems is needed to more thoroughly define operating ranges with a variety of fuels.

Finally, the design, fabrication, and operation of a demonstration unit should be undertaken when the above work is completed. The demonstration unit would be operated as a laboratory device for several months prior to the initiation of field demonstration tests.

REFERENCES

1. Kelly, J.T., _et_ _al_., "Development and Application of the PROF-HET Catalytic Combustor Code," Paper No. 77-33 presented at the Western States Section of the Combustion Institute, October 1977.

2. Kesselring, J.P., _et_ _al_., "Design Criteria for Stationary Source Catalytic Combustion Systems," Acurex Final Report 78-278, March 1978.

TABLE I. GRADED CELL CATALYST MODEL S

Sample No.	No. of TC	Substrate Manu.	Substrate Type	Washcoat Manu.	Washcoat Type	Catalyst Manu.	Catalyst Type	Wt. %	Gas	Dates Tested	Fuel	Test Purpose
AERO-025	9	DuPont	Alumina	Grace	Rare earth stabilized alumina 10-18 Wt. %	Grace	Pt/Ir	0.6-1.0	.47/.76/.80	4/25 – 4/29/77	Nat. Gas	Screen Grace Pt/Ir catalyst
AERO-026	6	DuPont	Alumina	UOP	Proprietary	UOP	Proprietary	–	–	6/24 – 6/29/77	Nat. Gas	Screen UOP catalyst
AERO-027	6	DuPont	Thoria impregnated alumina	None	–	W. Pfefferle	Pt/Ir/Os	0.29	.36/.24/.17	6/30 – 7/1/77	Nat. Gas	Determine effects of high melting point precious metals and catalyst without washcoat
AERO-028	–	DuPont	Zirconia impregnated alumina	None	–	W. Pfefferle	Pt/Ir/Os	0.29	.52/.08/.08	–	–	Not to be tested based on results of A-027.
AERO-029	6	Corning	Zirconia spinel	None	–	W. Pfefferle	NiO/Pt	0.29-0 Pt .29/.46/ 2.9 NiO	0.5/.31/0 .5/.8/5.0	7/10 – 7/11/77	Nat. Gas	Investigate metal oxide catalyst capabilities (no washcoat). Perform high temp. operation (3100°F).
AERO-030	6	Corning	Zirconia spinel	None	–	Aero	Co_2O_3/Pt	2.4-0 Pt 5.4-7.8 Co_2O_3	4.1/0/0	7/14 – 7/21/77	Nat. Gas	Metal oxide comparison, extensive evaluation
AERO-031	6	DuPont	Alumina	Matthey Bishop	Proprietary	Matthey Bishop A	Stab. Pt	.33-.76	–	8/2 – 8/10/77	Nat. Gas	Compare to A-032
AERO-032	6	DuPont	Alumina	Matthey Bishop	Proprietary	Matthey Bishop B	Stab. Pt	.86-1.09	–	7/26 – 7/29/77	Nat. Gas	Screen Matthey Bishop catalyst
AERO-033	7	Corning	Zirconia spinel	None	–	Aero	NiO/Pt-Pd	.67-0 Pt 2.2/.94/ 2.0 NiO	15/0.7/0 Pt 5.0/2.1/ 4.5 NiO	9/14 – 9/20/77	Nat. Gas	Fuel nitrogen and pressure testing Test difficulties precluded data results
AERO-034	7	Corning	Zirconia spinel	Oxy-Catalyst	γ-Alumina 4 Wt. %	Aero	Co_2O_3/Pt	2.2-0 Pt 9.3/5.6/ 4.3 Co_2O_3	3.0/0/0 Pt 7.7/9.9/ 20.8 Co_2O_3	9/22 – 9/27/77	Nat. Gas	Comparison to A-033
AERO-035	7	DuPont	Alumina	Matthey Bishop	Proprietary	Matthey Bishop C	Stab. Pt	1.96/1.2/ 0.9	–	10/1 – 10/6/77	Nat. Gas	Screening comparison
AERO-036	7	Corning	Zirconia spinel	Aero	Zirconia Magnesia .8-1.0 Wt. %	Aero	NiO/Pt	1.8/2.1/ 2.1 NiO 1.2/0.9/ 0 Pt	3.0/3.2/ 4.0 NiO 2.0/1.4/ 0 Pt	10/10 – 10/12/77	Nat. Gas	Fuel nitrogen testing
AERO-037	4	Corning	Zirconia spinel	None	–	Aero	Co_2O_3/Pt	2.7/2.8/ 3.4 Co_2O_3 4.0/0/0 Pt	4.5/4.5/ 10.1 Co_2O_3 6.7/0/0 Pt	12/5 – 12/23/77	Nat. Gas & Methane	Fuel nitrogen and pressure testing
AERO-038	5	DuPont	Alumina	None	–	W.Pfefferle	Co_2O_3	15.9/4.1/5.8	10.3/2.9/8.8	12/28 – 12/29/77	Nat. Gas	Investigate catalyst-support interactions
AERO-040	5	DuPont	Alumina	Johnson Matthey	Proprietary	Johnson Matthey	Proprietary	–	–	1/25 – 2/6/78	Nat. Gas	Screen Johnson Matthey catalyst
AERO-041	4	DuPont	Alumina	UOP	Proprietary	UOP	Proprietary	–	–	12/30/77 – 1/3/78	Nat. Gas	Catalyst scaleup, 6.06-inch diameter

TABLE II. SURFACE AREA AND DISPERSION MEASUREMENTS ON GRADED CELL CATALYSTS

T-637

Sample No.	Surface Area m²/g Pretest	Surface Area m²/g Post-test	Dispersion % Pretest	Dispersion % Post-test	Catalyst	SEM/EDAX Results and Comments
AERO-025	1.55-2.49	0	1.5-4.9	0	Pt/Ir	No Pt or Ir found on back two segments by SEM/EDAX
AERO-026	5.94	0	—	—	Proprietary	
AERO-027	0.44	—	20.64	—	Pt/Ir/Os	
AERO-028	0.06	—	8.33	—	Pt/Ir/Os	Not combustion tested
AERO-029	0.60	0	—	—	NiO/Pt	
AERO-030	0.15	.01	—	—	Co_2O_3/Pt	
AERO-031	24.38	0	36.16	0	Stab. Pt	
AERO-032	11.99	0	9.11	0.20	Stab. Pt	
AERO-033	—	—	—	—	NiO/Pt-Pd	Invalid test data
AERO-034	—	—	—	—	Co_2O_3/Pt	Invalid test data
AERO-035	5.17	0.09	4.09	0	Stab. Pt	
AERO-036	—	—	—	—	NiO/Pt	
AERO-037	—	—	—	—	Co_2O_3/Pt	Zero surface area on each segment
AERO-038	0	—	—	—	Co_2O_3	
AERO-040	4.00	0	—	—	Proprietary	
AERO-041	6.37	0.50	—	—	Proprietary	

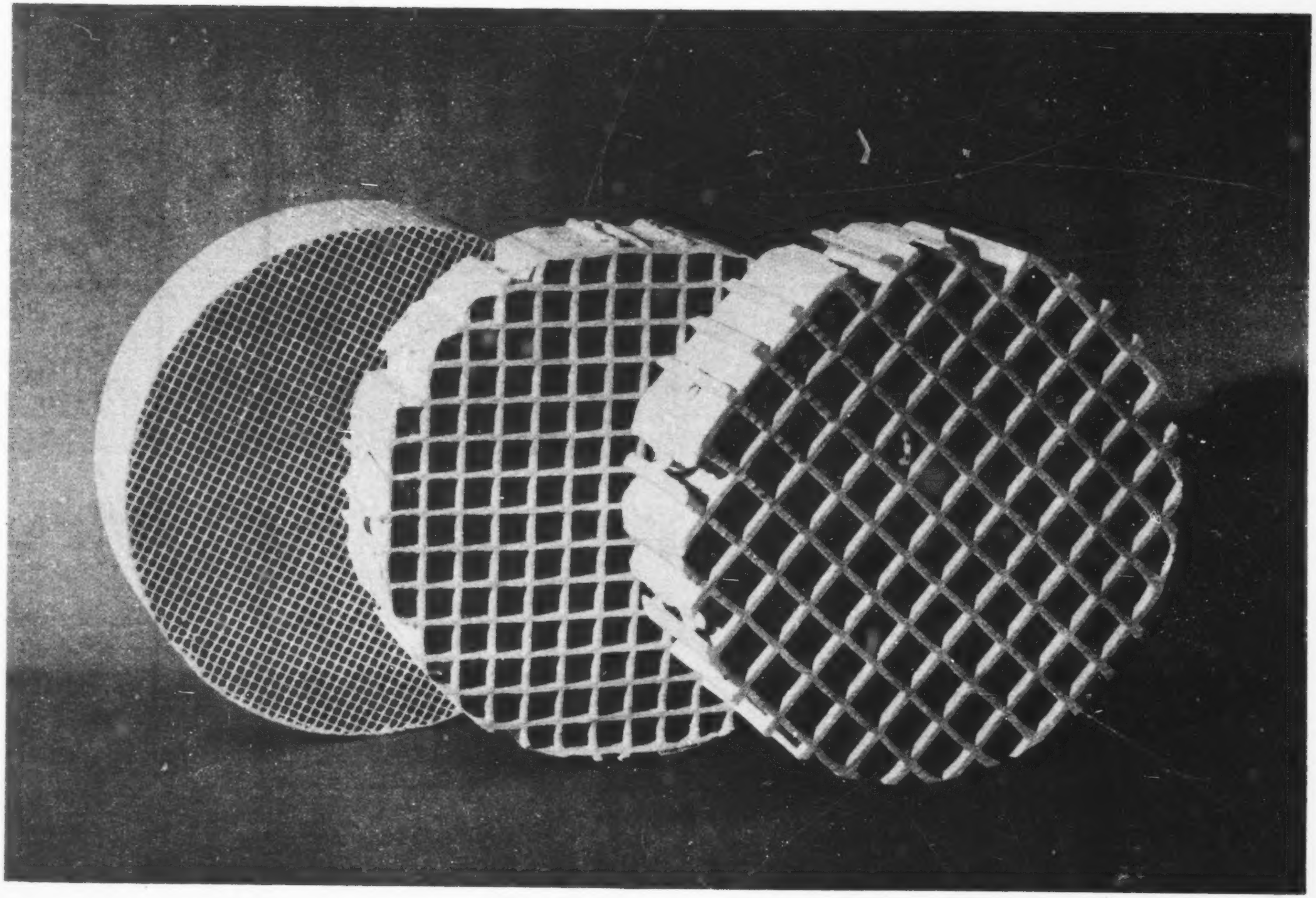

Figure 1. Corning square-celled extruded monolith structures.

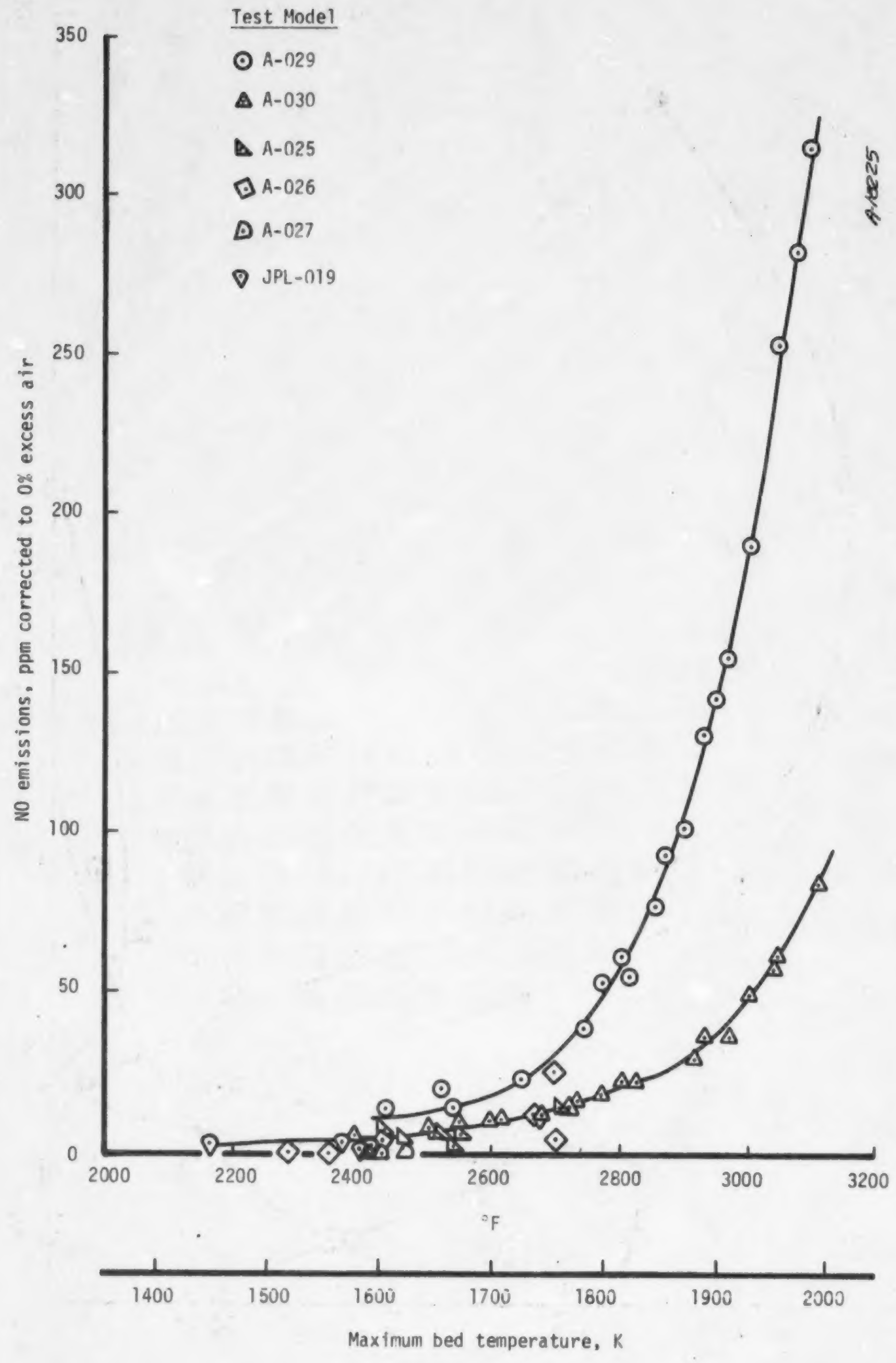

Figure 2. NO_x comparison corrected to 0-percent excess air.

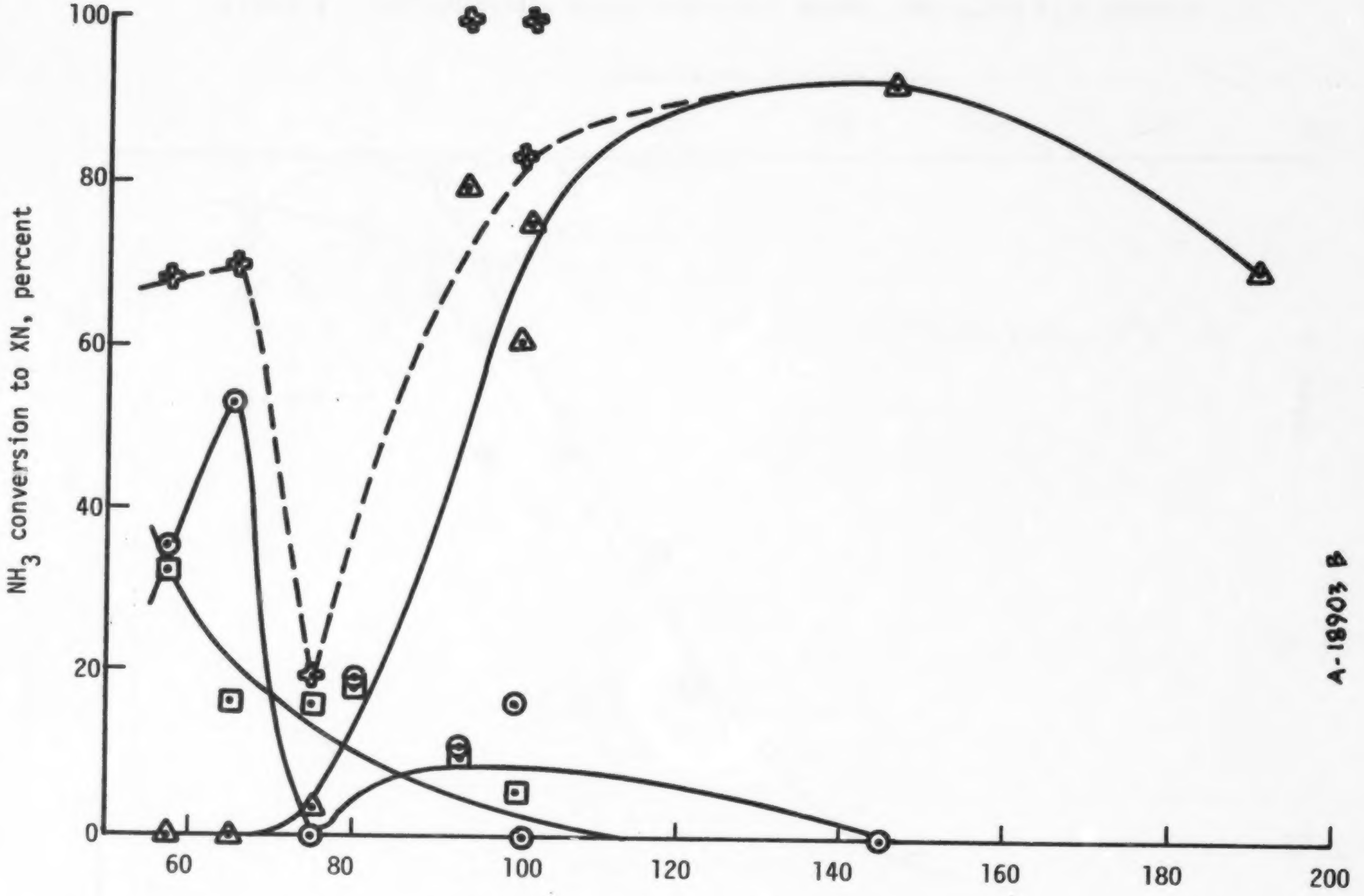

Figure 3. Theoretical air, percent.

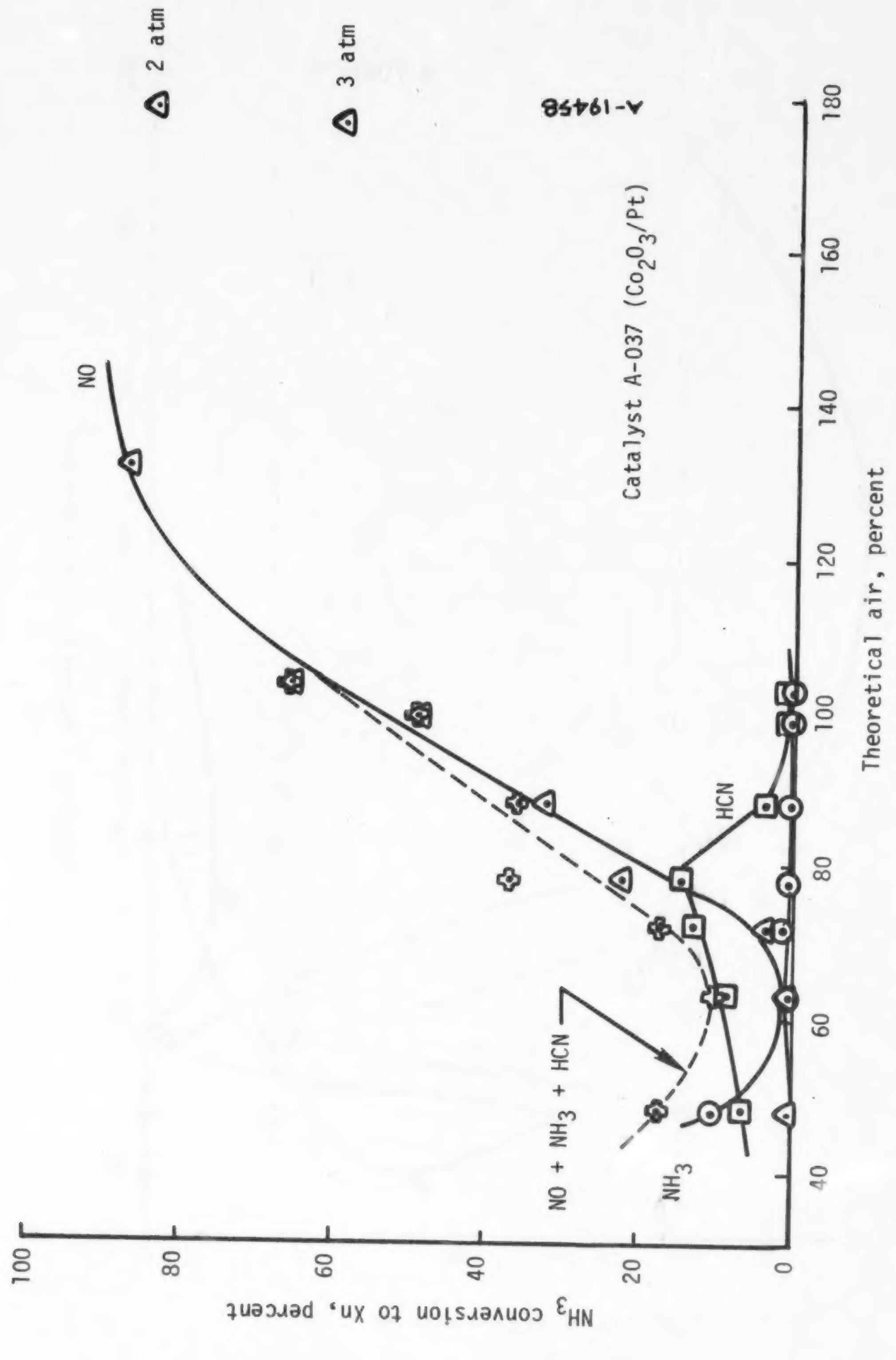

Figure 4. NH_3 conversion characteristics, natural gas doped with ammonia Co_2O_3/Pt catalyst.

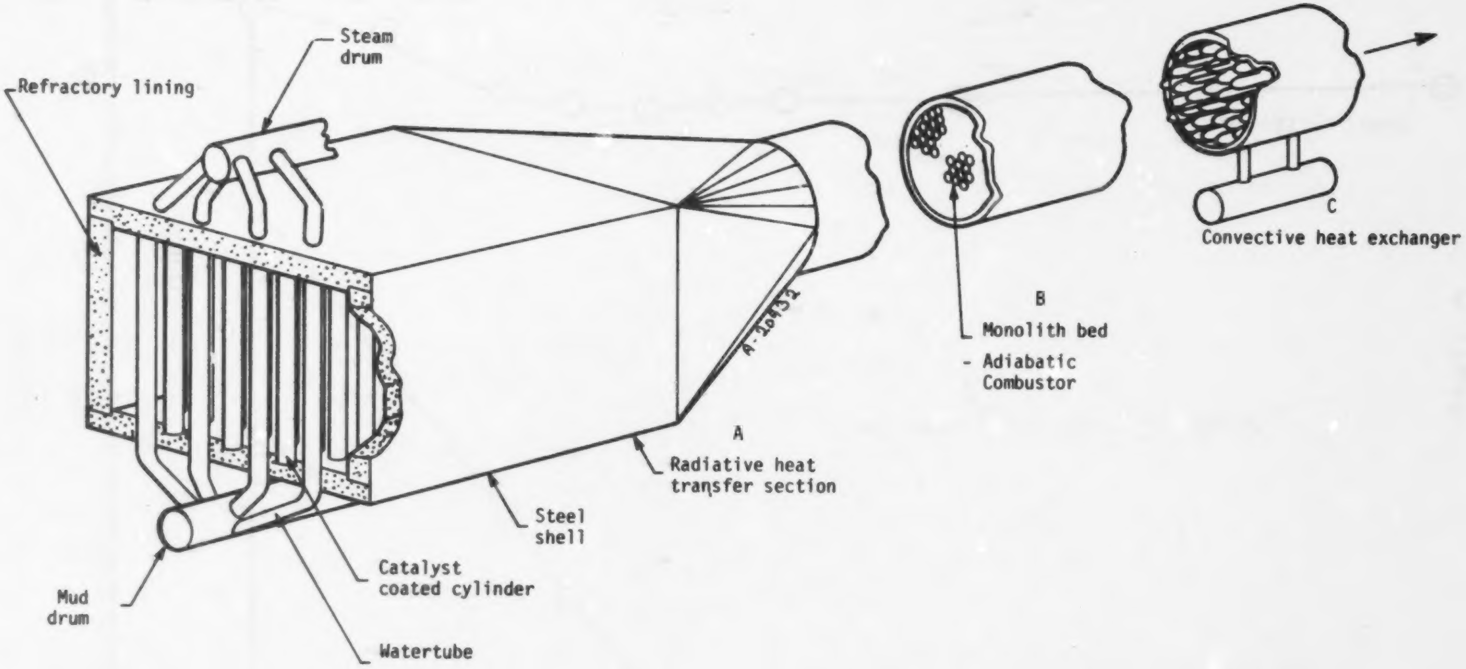

Figure 5. Radiative watertube boiler concept.

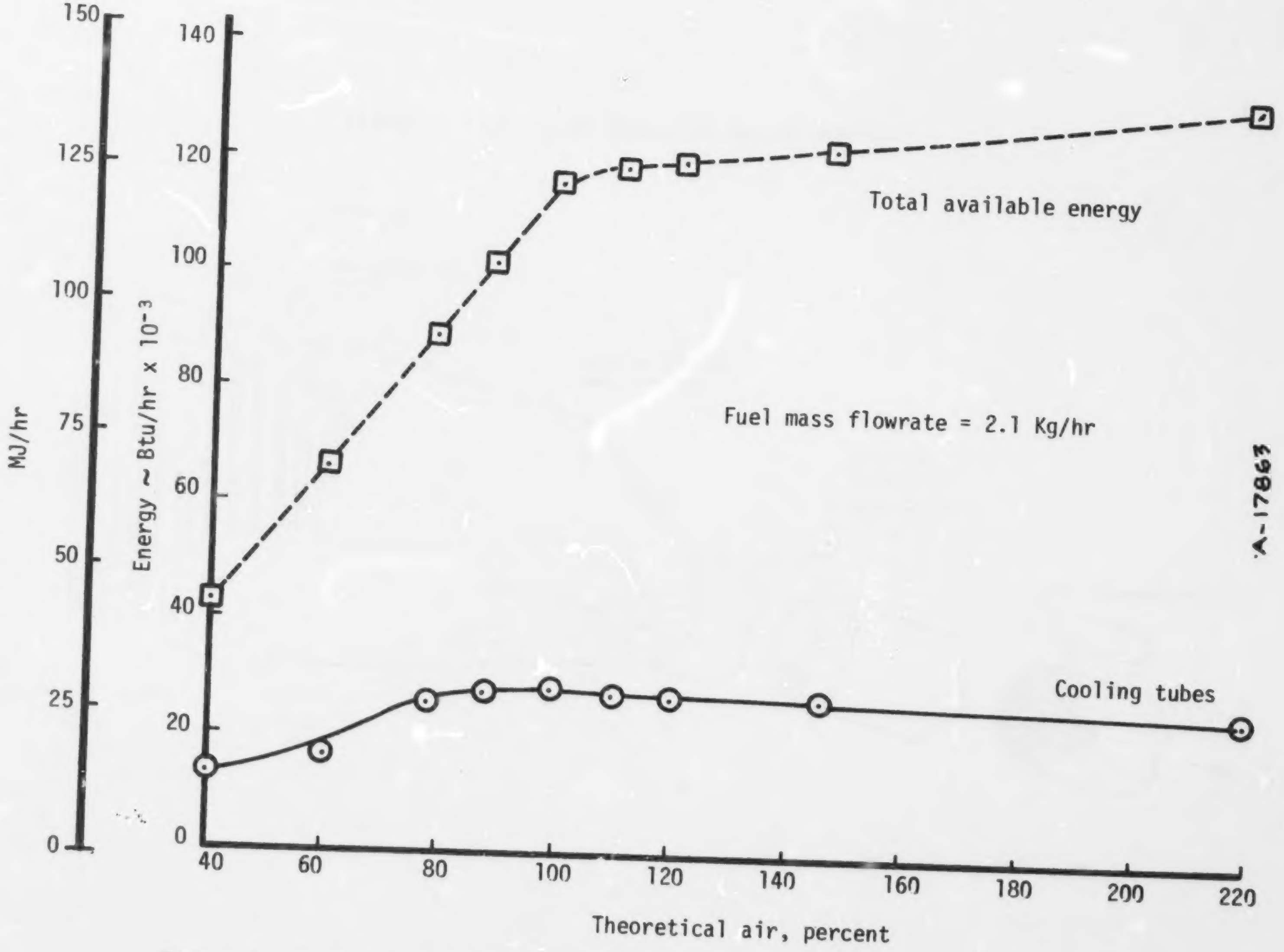

Figure 6. Radiative catalyst/watertube system energy release vs. theoretical air.

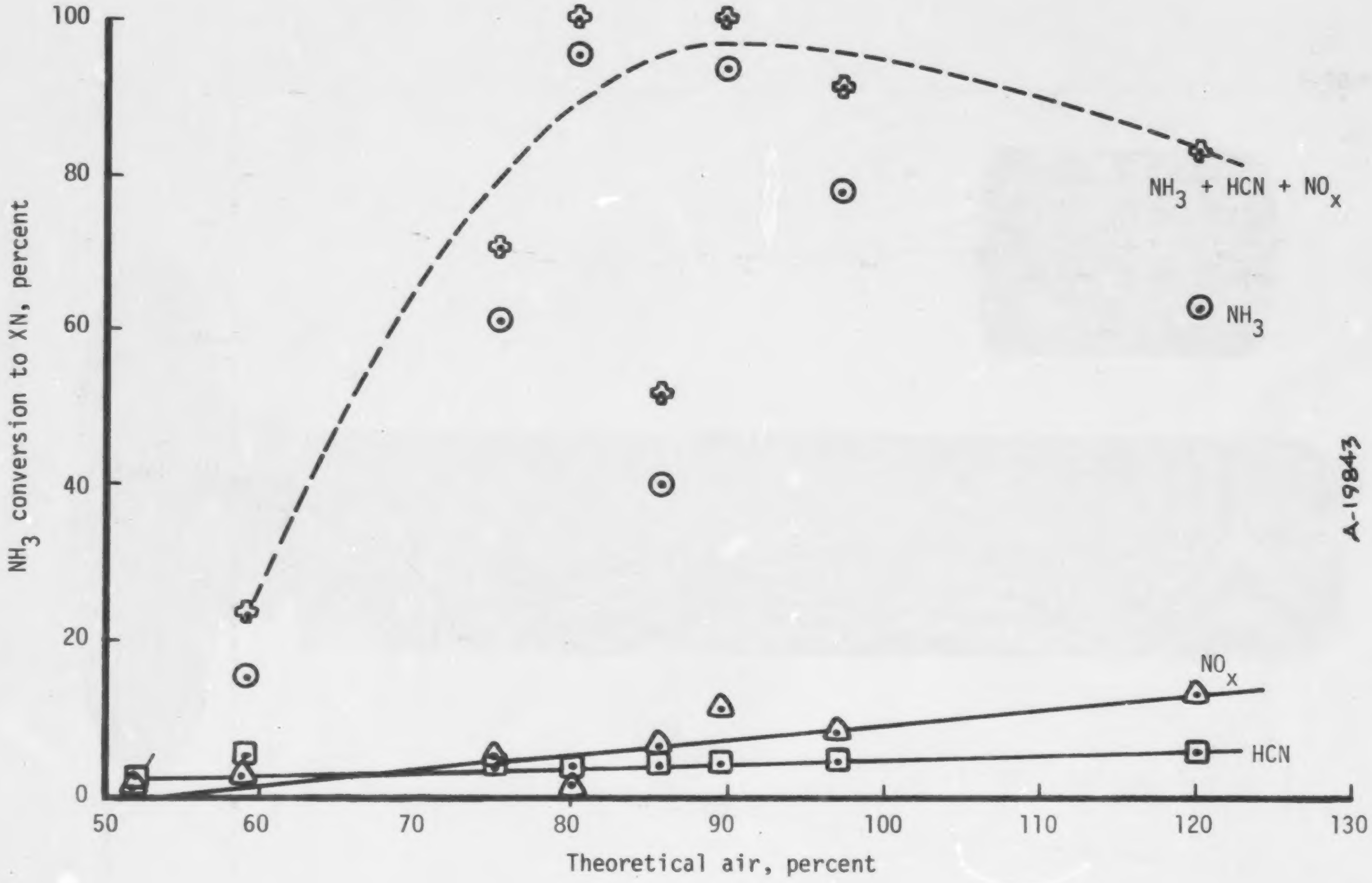

Figure 7. Radiative catalyst/watertube system, fuel nitrogen conversion

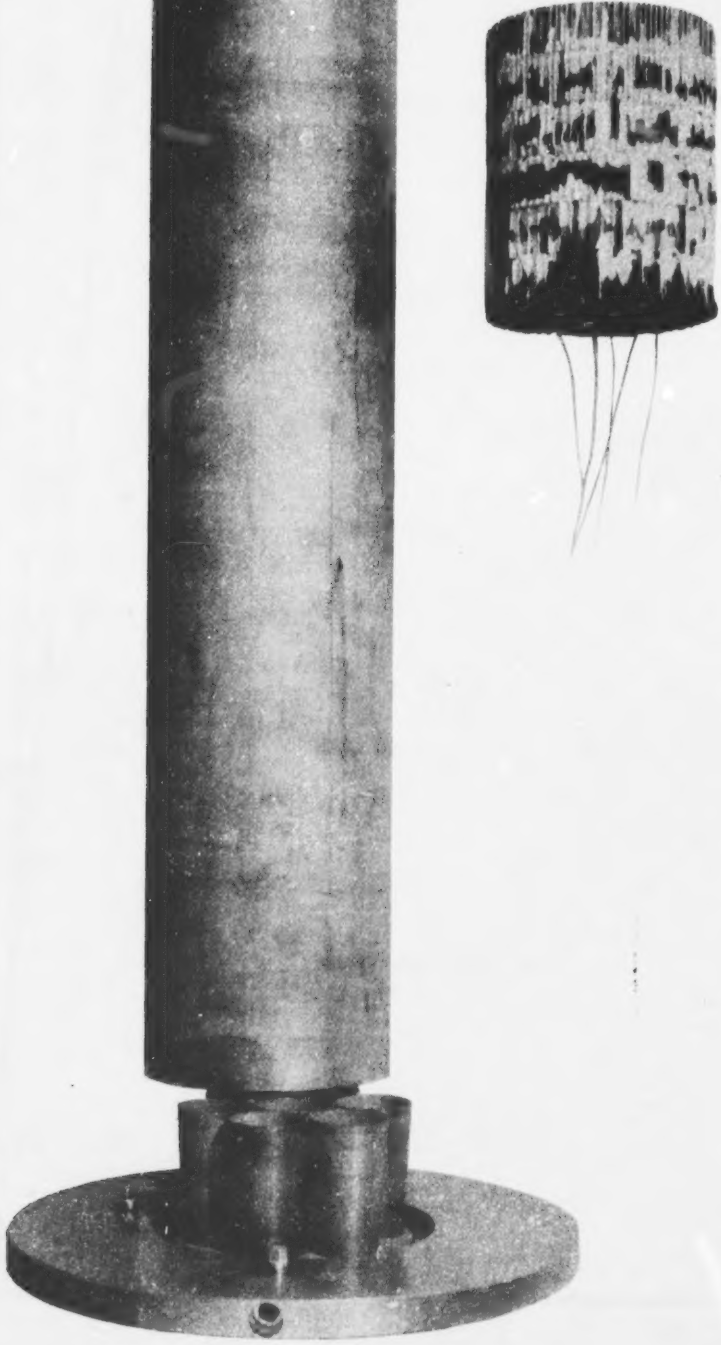

Figure 8. Model gas turbine combustor.

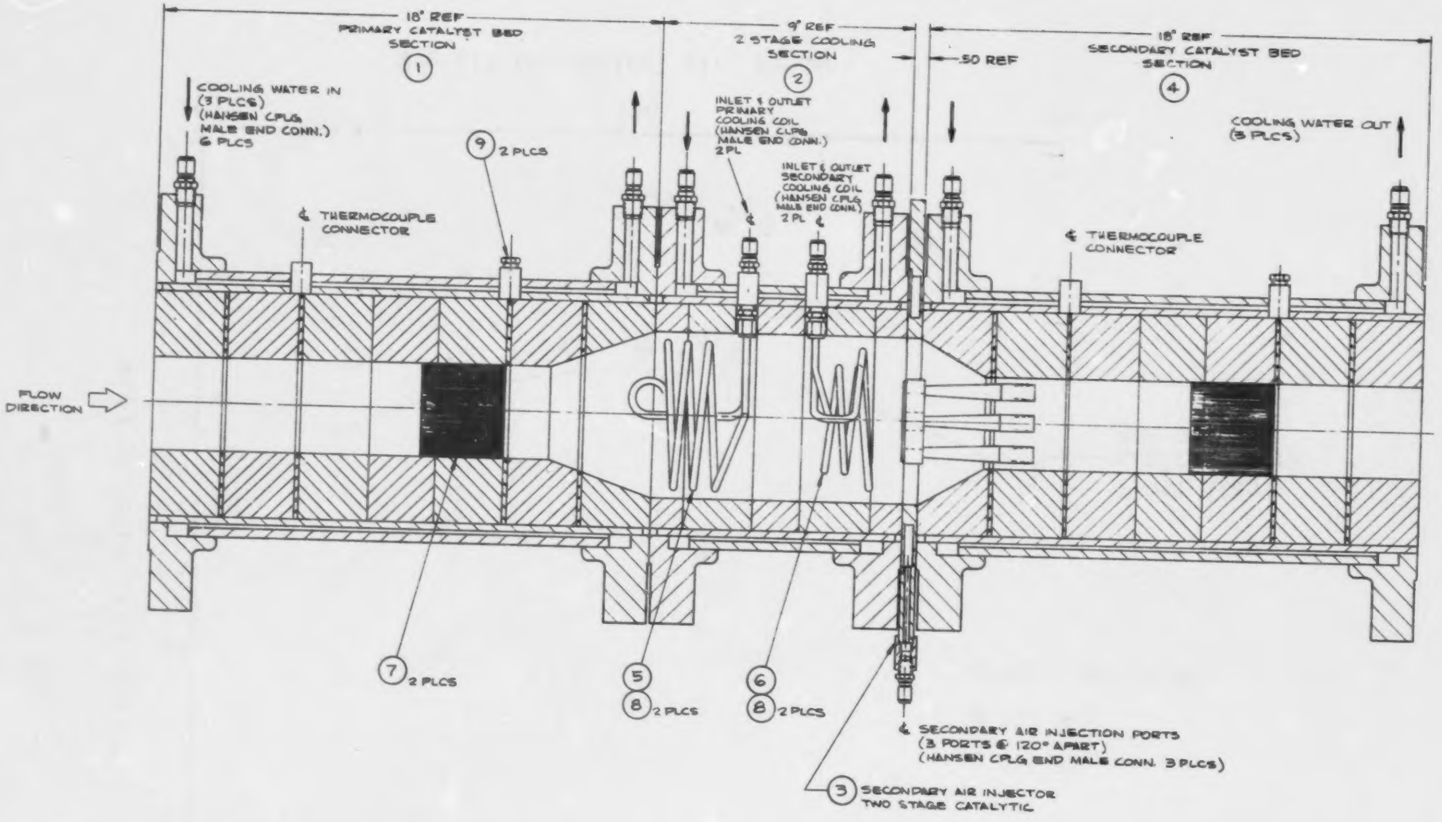
18" REF
PRIMARY CATALYST BED SECTION
①
9" REF
2 STAGE COOLING SECTION
②
.50 REF
18" REF
SECONDARY CATALYST BED SECTION
④
COOLING WATER IN (3 PLCS) (HANSEN CPLG MALE END CONN.) 6 PLCS
⑨ 2 PLCS
℄ THERMOCOUPLE CONNECTOR
INLET & OUTLET PRIMARY COOLING COIL (HANSEN CLPG MALE END CONN.) 2 PL ℄
INLET & OUTLET SECONDARY COOLING COIL (HANSEN CPLG MALE END CONN.) 2 PL ℄
℄ THERMOCOUPLE CONNECTOR
COOLING WATER OUT (3 PLCS)
FLOW DIRECTION
⑦ 2 PLCS
⑤ ⑧ 2 PLCS
⑥ ⑧ 2 PLCS
℄ SECONDARY AIR INJECTION PORTS (3 PORTS @ 120° APART) (HANSEN CPLG END MALE CONN. 3 PLCS)
③ SECONDARY AIR INJECTOR TWO STAGE CATALYTIC

Figure 9. Two stage catalytic arrangement.

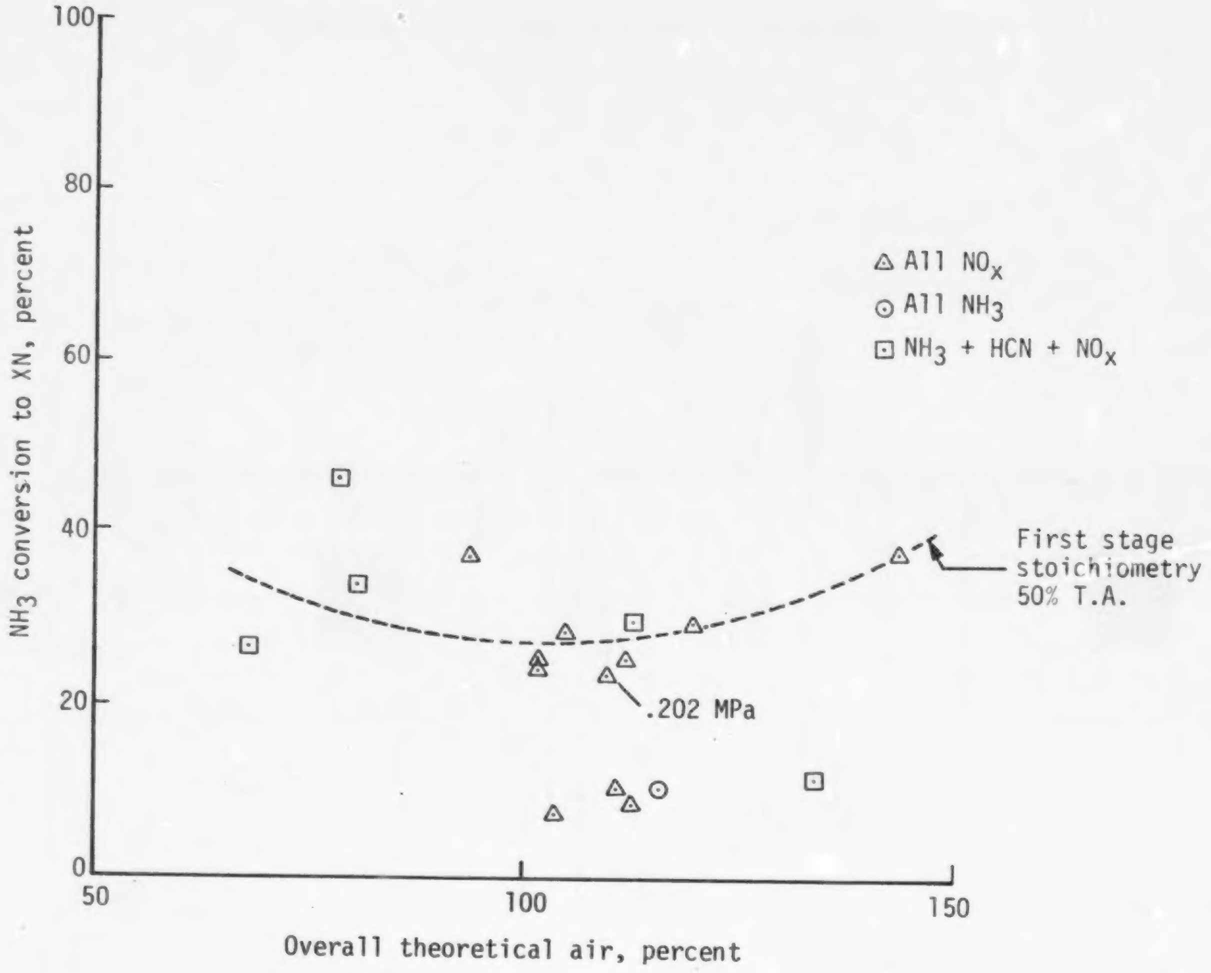

Figure 10. Two-stage combustor fuel nitrogen conversion.

FUEL NO_x CONTROL BY CATALYTIC COMBUSTION

BY

Edward K. Chu and John P. Kesselring
Acurex Corporation/Energy & Environmental Division
485 Clyde Avenue
Mountain View, California 94042

Work performed under EPA Contract 68-02-2611, Task 11.

ABSTRACT

The use of catalytic combustion in controlling fuel NO_x was evaluated experimentally. Screening tests of three different catalysts were conducted over a range of stoichiometries from rich to lean, to determine the effect of theoretical air, bed temperature, mass throughput, fuel type, and fuel bound nitrogen type and concentration on the conversion of fuel bound nitrogen to NO_x or NO_x precursors. Minimum fuel NO_x conditions were then determined. Since these minima occur at fuel-rich conditions, the use of a two-stage catalytic combustor for control of fuel NO_x appears promising.

Detailed studies of the chemical reactions occurring in catalytic combustion were made to determine what nitrogenous species are formed. The experiments were performed using an oxygen/argon mixture as the oxidant in order to eliminate thermal NO_x reactions from the system. The results showed that N_2, NO, NH_3, and HCN are the major products of the fuel bound nitrogen conversion process. Further, the data tended to agree with the reaction mechanism proposed for homogeneous reactions; i.e.,

$$HCN \rightarrow NH_i \begin{array}{l} \nearrow NO \\ \underset{NO}{\searrow} N_2 \end{array}$$

The reaction, however, takes place on the catalytic surface rather than in the gas phase.

Preceding page blank

INTRODUCTION

An emerging technology which shows promise in controlling both thermal and fuel NO_x emissions is that of catalytic combustion. As reported in Reference 1, catalytic combustors have been tested at temperatures to 2000 K (3140°F) with thermal NO_x emissions less than 90 ppm corrected to 0 percent excess air. Fuel NO_x control through the use of a two-stage catalytic combustion system is also reported in Reference 1, with NH_3-doped natural gas used to simulate a nitrogen-containing fuel. Conversions of bound nitrogen to NO_x of only 11 percent were measured for this system.

The subject of fuel nitrogen conversion in catalytic combustion systems has been examined by Matthews and Sawyer (Reference 2). Trace amounts of either nitric oxide or ammonia were added to propane/oxygen/argon mixtures and combusted on a platinum catalyst under rich, stoichiometric, and lean combustion conditions. Conversion of the two model fuel nitrogen compounds to nitric oxide was measured as a function of equivalence ratio, adiabatic flame temperature, and fuel nitrogen concentration. Since the monolithic catalyst bed was uninsulated during operation, the measured bed temperatures were much lower than the corresponding adiabatic flame temperatures. For this operational mode, the conversion of fuel nitrogen to NO_x was found to be strongly dependent on equivalence ratio, weakly dependent on calculated adiabatic flame temperature, and moderately dependent on fuel nitrogen concentration. The precise fate of the fuel nitrogen was not determined.

The current study was conducted under EPA Contract 68-02-2611 to achieve two objectives. First, the study was to define operating conditions for catalytic combustors giving low levels of NO_x emissions. Second, the study was to conduct a systematic experimental determination of the fate of fuel nitrogen during catalytic combustion.

PROGRAM OBJECTIVES

This study had two primary objectives. The first objective, discussed in Screening Test Results, was to evaluate the parameters which affect the conversion of fuel bound nitrogen to NO_x during catalytic combustion, and to

Preceding page blank

define conditions yielding low NO_x emissions. Specifically, the following parameters were examined:

- Catalyst type
- Percent theoretical air
- Mass throughput (or heating rate)
- Reaction temperature
- Fuel bound nitrogen type and content

The second objective, described in Detailed Test Results, was to determine the fate of fuel bound nitrogen during catalytic combustion with and without the coexistence of fuel sulfur. Nitrogenous species measured include: NO, NO_x, N_2, N_2O, NH_3, and HCN.

EXPERIMENTAL APPARATUS

Figure 1 illustrates the experimental apparatus. For simplicity, the equipment can be divided into the following five categories:

- Flow metering and measurement systems
- Preheating system
- Combustor and housing
- Probe and sample transfer system
- Analytical equipment

As illustrated in Figure 1, the following components of the reactive mixtures can be metered in the system:

$$\left.\begin{array}{l} \bullet\ C_3H_8/CH_4 \\ \bullet\ NH_3/CH_3NH_2 \\ \bullet\ H_2S \end{array}\right\}\ \text{Fuel}$$

$$\left.\begin{array}{l} \bullet\ \text{Air/Argon} \\ \bullet\ N_2/O_2 \end{array}\right\}\ \text{Oxidant}$$

The oxidant is allowed to pass through the main heater, which consists of a series of six 6000-Watt exposed-element heaters (GTE Sylvania Model 138825, Style A). Within this main heater, the gas mixture can be heated to as high as 811°K (1000°F) depending on the preselected preheat temperature.

The fuel, however, bypasses the main heater to avoid preignition hazards within the main heater, and passes through a flame arrester before mixing with the oxidant. The fuel/oxidant mixture then passes through the mixing chamber and flow straightener before arriving at the catalytic combustor. During this time, the preheat temperature of the gas mixture is maintained by an auxiliary heater jacketted around the exterior of the mixing chamber.

The combustor consisted of three 0.025m (1 inch) segments of graded cell catalyst. Table 1 lists the four different catalysts tested and gives information on the cell sizes used. Two UOP catalysts were required when performance changes were noted on UOP-1 after several hours of testing. As noted in Table 1, UOP-2 used only intermediate and small cells. The combustor was mounted inside a 0.0457m (1.8 inch) I.D. fused quartz tube. A thickness of six inches of insulation was applied to the exterior of the quartz tube housing to minimize heat losses from the combustor.

TABLE 1. CATALYST TYPE AND GEOMETRIC CONFIGURATIONS

Catalyst Type	Large Cell Diam, m (in)	Intermediate Cell Diam, m (in)	Small Cell Diam, m (in)
UOP-1 Proprietary catalyst on DuPont alumina	6.35×10^{-3} (0.25)	4.76×10^{-3} (0.1875)	1.59×10^{-3} (0.0625)
UOP-2 Proprietary catalyst on DuPont alumina	4.76×10^{-3} (0.1875)	4.76×10^{-3} (0.1875)	1.59×10^{-3} (0.0625)
Acurex Pt/NiO 2.5 wt % Pt on large cells; 6 wt % NiO on DuPont alumina	6.35×10^{-3} (0.25)	4.76×10^{-3} (0.1875)	1.59×10^{-3} (0.0625)
Acurex Pt 5 wt % Pt on DuPont alumina	6.35×10^{-3} (0.25)	4.76×10^{-3} (0.1875)	1.59×10^{-3} (0.0625)

Five K-type thermocouples were placed in the combustor at various locations to monitor in-depth combustion temperatures. In addition to these five thermocouples, a thermocouple located at the combustor exit measured the exhaust gas temperature.

A water-cooled stainless steel sample probe was used in this experiment. This probe was selected because of its durability in a hostile environment. The probe, however, is capable of reducing NO_2 to NO catalytically unless the probe is sufficiently quenched by water. For this reason, the actual measurement of NO and NO_2 may not be completely reliable. Nevertheless, from studies of homogeneous combustion (Reference 3), NO_2 exists only in the flame zone. In the near-postflame region the concentration of NO_2 is generally low as a result of rapid conversion from NO_2 to NO. If the same analogy were drawn, NO_2 concentration should also be low in this study.

Chemical species measured in this experiment include: CO, CO_2, O_2, UHC, NO, NO_x, N_2, N_2O, NH_3, and HCN. The list of the analytical equipment used and the corresponding chemical species measured is shown in Table 2.

SCREENING TEST RESULTS

In this section, the results of the screening tests are presented and discussed. For convenience of discussion, the emission characteristics of each catalyst will be discussed independently prior to comparison with each other.

Figures 2 to 5 show the effect of bed temperatures on the conversion of chemically bound nitrogen for the UOP catalyst. In Figures 2 and 3, natural gas was fired at a heating rate of 42.2 MJ/hr (40,000 Btu/hr) and with a chemically bound nitrogen content of 0.3 percent by weight of the fuel. The bed temperatures were 1367 K (2000°F) and 1478 K (2200°F), respectively. As may be seen from the figures, an increase in NO_x yield over the entire range of theoretical airs was observed with increased bed temperature. The same effect was observed in Figures 4 and 5, although the heating rate was reduced to 25.32 MJ/hr (24,000 Btu/hr) and the chemically bound nitrogen content was increased to 0.5 percent by weight of the fuel.

Figures 4 and 5 also show the percent of NH_3 and HCN yield under fuel-rich conditions. Both figures show that these two species rapidly diminish as stoichiometric proportions are approached. The disappearance of NH_3 and HCN is largely a result of these species being oxidized to NO_x, as evidenced by the increasing level of NO_x. In the fuel-rich condition, however, some of these species were presumably converted to N_2, as is the case in homogeneous combustion. By summing the percent yields of NH_3, HCN, and NO_x in fuel-rich conditions and plotting them on the figure, the condition which yields the highest percent of N_2 can be determined. Figures 4 and 5 show that this condition occurs somewhere between 85 and 95 percent theoretical air with the UOP catalyst.

The effect of heating rate (or mass throughput) on chemically bound nitrogen conversion can be assessed by comparing both Figures 2 and 4 with Figures 3 and 5. In the case of Figures 2 and 4, the bed temperature of the combustor was held at 1376 K (2000°F). At this bed temperature, the low heating rate yielded slightly lower NO_x emissions than the higher heating rate for both rich and lean conditions. When the bed temperature was increased to 1478 K (2200°F) (see Figures 3 and 5), this behavior was observed only for fuel-rich conditions. For fuel-lean conditions, the opposite behavior was observed. A similar NO_x emission characteristic with respect to heating rates at a bed temperature of 1478 K was also observed in Figures 6 and 7 when propane was used as fuel instead of natural gas. Duplicating this result substantiated that a higher heating rate can in fact suppress fuel NO_x formation in the fuel-lean condition at a bed temperature of 1478 K.

An explanation of the above phenomenon is not available at this time. However, it is believed that this phenomenon was closely associated with the occurrence of homogeneous combustion in the combustor. In the case of the lower bed temperature, i.e., 1367 K, the contribution of homogeneous combustion to the overall combustion was expected to be insignificant at both heating rates, since the bed temperature was not hot enough to initiate significant homogeneous reactions. On the other hand, the mass transfer rate of NH_3 increases as the heating rate (or mass throughput) increases. Thus, more fuel NO_x was formed at the higher heating rate than at the lower one.

In the case of higher bed temperature, i.e., 1478 K, the bed temperature was insufficient to initiate homogeneous combustion under fuel-rich conditions, and the same behavior as the lower bed temperature cases is noted. However, for fuel-lean conditions, homogeneous combustion may become significant. Since the lower heating rate case has a longer residence time than the higher heating rate case, the contribution of homogeneous combustion to the lower heating rate was therefore more important. As a result, the lower heating rate yielded a higher NO_x yield than the higher heating rate.

The effect of fuel type on the chemically bound nitrogen conversion can be assessed by comparing Figure 3 with Figure 7 and Figure 5 with Figure 6. These figures show that the emission characteristics for both fuels doped with NH_3 are very similar qualitatively as well as quantitatively. These results indicated that the combustion process was weakly coupled to the chemically bound nitrogen conversion at the bed temperature of 1478 K (2200°F).

The effect of chemically bound nitrogen content is shown in Figure 8. Similar to homogeneous combustion, the NO_x yield decreases as the chemically bound nitrogen content increases. This result indicates that the following self-destruction reactions also occur during catalytic combustion when the chemically bound nitrogen concentration is abundant in the reactive gas mixture.

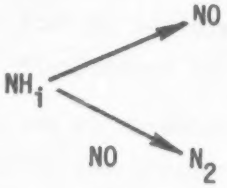

This result, however, contradicts the results of Matthews and Sawyer (Reference 2). Their results show the opposite behavior. It is believed that the discrepancy is due to the difference in bed operating temperatures. The data for this study were obtained at bed temperatures of 1367 and 1478 K, whereas the data of Matthews and Sawyer were obtained at much lower temperatures.

The effect of chemically bound nitrogen type is shown in Figure 9. Methylamine and ammonia were used as the model chemically bound nitrogen compounds in this study. The results shows almost no discrepancy between emissions for the two compounds. This indicates that the pyrolysis kinetics of chemically bound nitrogen is not the controlling process in the conversion of chemically bound nitrogen to NO_x.

Figure 9 also shows the effect of bed temperature on the chemically bound nitrogen conversion. The NO_x yield was weakly dependent on bed temperature when the bed temperature was higher than 1400 K. As the bed temperature was reduced below 1400 K, the NO_x yield gradually became strongly dependent on bed temperature.

The above results confirm that the chemically bound nitrogen conversion process is likely to occur at the surface rather than in the gas phase. At bed temperatures above 1400 K, the reaction rate of the conversion process was so fast that it was controlled by diffusion. Thus, the NO_x yield was weakly dependent on the bed temperature. As the bed temperature was reduced below 1400°K, the reaction rate was no longer controlled by diffusion, but instead controlled by the surface kinetics. Since the reaction rate of the conversion process was slower at these temperatures, it allowed the self destruction reaction, as described previously, to become more significant and thereby convert more NO to N_2.

Screening test results of the Acurex platinum catalyst, showing the effect of bed temperatures, is presented in Figures 10 and 11. The bed temperatures were 1367 K (2000°F) and 1478 K (2200°F). Both results show that 100 percent NO_x yields were observed under fuel-lean conditions.

Under fuel-rich and near-stoichiometric conditions, significant differences were noted for the two temperatures. The NO_x yield was higher for the lower bed temperature than the higher one, and the opposite effect was noted for the NH_3 and HCN yields. These results indicate that the fuel oxidation reaction and the chemically bound nitrogen oxidation reaction were competing with each other for oxygen at these conditions. Apparently, the chemically bound nitrogen oxidation reaction was dominant at 1367 K, resulting in a higher NO_x yield and lower NH_3 and HCN yields. When the bed temperature was increased to 1478 K, most of the free oxygen was consumed by the fuel and hence was unavailable for the chemically bound nitrogen.

The screening test results of the Acurex NiO/Pt catalyst, indicating the effect of heating rates, are shown in Figures 12 and 13. Since NiO is a base-metal catalyst, it requires a minimum of 1589 K (2400°F) bed temperature for satisfactory combustion efficiency. At this bed temperature, the NO_x yield was almost independent of heating rates (see Figures 12 and 13).

However, significant variations in terms of NH_3 and HCN yields were observed under fuel-rich conditions. The NH_3 yield was higher at the lower heating rate than the higher one, and the opposite was true for the HCN yield. It is of interest to note that the same variation was also observed with the UOP catalyst (see Figures 4 and 5).

Since the conversion of chemically bound nitrogen is likely to occur at the surface rather than in the gas phase, as discussed previously, the type of catalyst can have significant effects on the conversion of chemically bound nitrogen. Some of these effects may be seen in Figures 11 and 13, where the emission characteristics of the Acurex Pt catalyst and the Acurex NiO/Pt catalyst are shown, respectively. The Acurex Pt catalyst has a highly reactive surface, and as a result it not only completely oxidized the fuel but also converted all NH_3 to NO_x under fuel-lean conditions. At the temperature tested (1478 K), no selective catalytic reaction was exhibited by the Acurex Pt catalyst. On the other hand, the Acurex NiO/Pt catalyst has a less reactive surface. Consequently, a higher operating temperature (1589 K) was required. For fuel-lean conditions, some selective catalytic reaction capabilities were demonstrated by the NiO/Pt catalyst. It exhibited good combustion efficiency (though not as good as the Pt catalyst), and concurrently lowered the NH_3 conversion from 100 percent to 80 percent.

The UOP catalyst showed better performance than the NiO/Pt catalyst (see Figure 7). It had a combustion efficiency comparable to the Pt catalyst and yet yielded only 75 percent NO_x from NH_3, which was 25 percent better than the Pt catalyst. However, it should be noted that the chemically bound nitrogen contents were not the same in both cases. The chemically bound nitrogen content in the UOP catalyst case was lower than the other two cases. Nevertheless, it was also found that the NO_x yield decreases as the chemically bound nitrogen content increases (see Figure 8) for a percent theoretical air of 310. If the same behavior held true in all fuel-lean conditions, as is the case in homogeneous combustion, the UOP catalyst should yield even less NO_x when the chemically bound nitrogen content increases.

DETAILED TEST RESULTS

The results of detailed tests are presented and discussed in this section. The results include the determination of the fate of chemically bound nitrogen during combustion in the UOP catalyst under the following conditions:

- Variable percent theoretical air under fuel-rich and stoichiometric conditions at a fuel nitrogen content of 3 percent by weight of the fuel
- Same conditions as above but with variable NH_3 concentration
- Same conditions and the same NH_3 concentration as above but tested with an aged UOP catalyst

The Acurex Pt and the Acurex NiO/Pt catalysts were also tested in this experimental series, but on a less extensive scale. Only two test conditions were performed with these two catalysts. The first condition was selected at 75 percent theoretical air where N_2 is presumably the major product from the chemically bound nitrogen conversion process. For the other condition, the Acurex Pt catalyst was tested near the stoichiometric condition where the competing reactions between the hydrocarbon oxidation and the chemically bound nitrogen conversion occurred; and the Acurex NiO/Pt catalyst was tested at 200 percent theoretical air to verify that the selective catalytic reaction had in fact occurred in the fuel-lean condition.

To assure that the nitrogen species NO_x, N_2, N_2O, HCN, and NH_3 were the dominant products of the chemically bound nitrogen conversion process, a nitrogen mass balance was performed for each test condition. Since the emission data were taken on a dry basis, the following equation was used to account for the water content in the combustion products:

$$Y_{N_0} = \left(\sum_j N_j\right) \times \left(1 - K_{H_2O}\right) \times 14.007 \times 10^{-6} \Big/ \overline{MW}$$

where Y_{N_0} is the total mass fraction of elemental nitrogen in the combustion products, N_j is the ppm of the jth nitrogen species, K_{H_2O} is the mole fraction of water vapor, and $\overline{MW}$ is the mean molecular weight of the combustion products. K_{H_2O} and $\overline{MW}$ are estimated from chemical equilibrium calculations.

The results of the chemically bound nitrogen mass balance are shown in Table 3. As may be seen, a maximum deviation of ±12 percent between the input fuel nitrogen content and the measured nitrogen species in the combustion products was obtained, except for two data points. N_2O was not detetted for any test condition. Under fuel-rich conditions, as was expected, N_2 was the dominant product of the chemically bound nitrogen conversion process. Under a fuel-lean condition of 200 percent theoretical air, a conversion of 13 percent NH_3 to N_2 was noted for the NiO/Pt catalyst.

Figure 14 shows the variations of the nitrogen species concentrations as a function of percent theoretical air. A reaction mechanism similar to that for homogeneous reactions, i.e.,

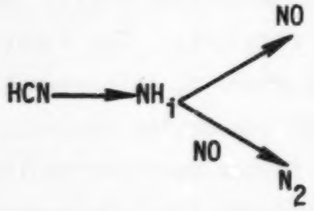

can be used to interpret the data presented in Figure 14. At 75 percent theoretical air or below, the N_2 formation reaction apparently was the dominant reaction, and consequently very low levels of NO, HCN, and NH_3 concentrations were observed. Above 75 percent theoretical air, the N_2 formation reaction became less important. The slow-down of the N_2 formation reaction combined with the unavailability of oxygen led to a rapid buildup of NH_3 and a gradual increase of NO at conditions between 75 and 90 percent theoretical air. However, as the precent theoretical air exceeded 90, NO was quickly formed with a simultaneous decrease of NH_3.

Figure 15 shows the effect of the chemically bound nitrogen content on N_2 yield under fuel-rich conditions. It was shown that the percent N_2 yield increases as the chemically bound nitrogen content increases, which is the same behavior noted in the screening test results under fuel-lean conditions (see Figure 8). Also of interest is that all but the 75 percent theoretical air data exhibited the same slope. However, it should be noted that one of the 75 percent theoretical air data points was associated with a significant error in the nitrogen mass balance (see Table 3). If the N_2 concentration were corrected for this error, a similar slope was observed in comparison with the other data (shown by the dashed line in Figure 15).

Two of the test conditions under the 3 percent chemically bound nitrogen content test series were repeated to evaluate the effect of an aged catalyst on the conversion of chemically bound nitrogen. As may be seen from Table 3, the aging of a catalyst was demonstrated by the lesser requirement of diluent argon than that of the active catalyst for the same bed operating temperature. As for the nitrogen species emissions, the aged UOP catalyst yielded 30 percent or more less N_2 than that of the active UOP catalyst, depending on the theoretical air level. In return, higher concentrations of NO, NH_3, and HCN were emitted by the aged catalyst than the active one. This result, again, confirmed that the chemically bound nitrogen conversion process is a surface event.

H_2S EFFECTS ON CHEMICALLY BOUND NITROGEN CONVERSION

Current flat flame studies show that under fuel-rich conditions, the presence of fuel sulfur can have a radical effect on the fuel NO formation mechanism. Both enhancement and inhibition of fuel NO have been observed, depending on the stoichiometric ratio, the residence time, and (probably) the model fuel-bound nitrogen compound. DeSoete (Reference 4) observed significant enhancement of NH_3 conversion to NO due to the presence of H_2S in his experiment. Wendt et al., (Reference 5), on the other hand, observed both enhancement and inhibition of fuel NO due to the presence of H_2S, depending on the stoichiometric ratio. However, measurements made in the work of Wendt et al., were over much longer residence times, and these experiments involved both lower nitrogen and sulfur levels and higher flame temperatures than those of DeSoete. Furthermore, DeSoete used NH_3 as the model fuel-bound nitrogen compound, while Wendt et al. used C_2N_2.

As part of the detailed tests, the effect of H_2S on the chemically bound nitrogen conversion during catalytic combustion under fuel-rich conditions was evaluated. The results of this study are shown in Figure 16 in terms of percent NO and N_2 yields as a function of percent theoretical air. Also shown in the same figure are the results with the same test conditions but without H_2S dopant. Figure 16 shows that the addition of H_2S enhanced NO formation and suppressed N_2 formation under fuel-rich conditions, which is in agreement with DeSoete's results. However, at the stoichiometric condition, the addition of H_2S inhibited NO formation. A similar trend was also observed by Wendt et al., although their data were taken at conditions between 46 and 70 percent theoretical air.

Additional evidence showing that the addition of H_2S can inhibit N_2 formation can be seen from the gas chromatograph measurements taken before and after the H_2S flowrate was turned off. These two measurements are shown in Figure 17. As may be seen, the N_2 concentration in the case with H_2S dopant is significantly lower than the case without. Also, it is of interest to note that the combustor bed temperature increased more than 367 K after the H_2S flowrate was turned off, indicating that the existence of H_2S also inhibited combustion.

Attempts to perform nitrogen mass balances with the H_2S dopant data have not been successful (see Table 3). With the measured nitrogen species, i.e., NO, N_2O, N_2, HCN, and NH_3, it was found that the sum of these species was consistently lower than the amount of nitrogen input to the system. Also, there was a trend showing that the percent error decreases as the percent theoretical air increases. This trend implies that either there may be some nitrogen species existing only under fuel-rich conditions, which were not accounted for in the current study, or erroneous measurements were induced by the existence of H_2S under fuel-rich conditions.

CONCLUSIONS

Based upon the results of the screening tests, the bed operating temperature was shown to affect the fuel NO_x formation, depending on the temperature range and the reactivity of the catalyst. For the UOP catalyst, at bed temperatures below 1478 K the amount of fuel NO_x formed decreases as the bed temperature decreases. At bed temperatures above 1478 K, the formation of fuel NO_x was found to be insensitive to bed temperatures. For the Pt catalyst, fuel NO_x was insensitive to bed temperatures, even at 1367 K. Based on this data, the formation of fuel NO_x is a surface event. Depending on whether the surface reaction is in the kinetic regime or in the diffusion regime, fuel NO_x formation may be sensitive to bed temperatures. In terms of low NO_x operating conditions for the catalytic combustor, a low bed temperature is recommended within the constraint of satisfactory combustion efficiency. This approach seems ideal for gas turbine applications. However, for boiler applications, this approach is unacceptable because boilers require a high flame temperature and hence a different approach should be used.

The mass throughput (or heating rate) appears to be an effective approach for controlling fuel NO_x for the UOP catalyst. Increasing the mass throughput tends to maximize the surface reactions and minimize the homogeneous reactions within the combustor, and therefore lowers the fuel NO_x formation. For the NiO/Pt catalyst, since it is a less reactive catalyst, the bed operating temperature remains the dominant parameter, and therefore fuel NO_x formation was unaffected by the variation of mass throughput. However, if the bed temperature were increased further, a similar result to the UOP catalyst is anticipated.

Under fuel-rich conditions, the fuel NO_x emission levels were low for all three types of catalyst. Also, there appeared to be a condition where NO, HCN, and NH_3 concentrations reach minimum levels. However, this condition varies with the mass throughput. It is vital that this condition be determined as a function of mass throughput prior to the development of the two-stage catalytic combustion system.

The molecular structure of both fuel and chemically bound nitrogen compounds have been found to be insensitive to fuel NO_x formation. These results indicate that the results of the current study can be extrapolated to the combustion of heavier fuels, such as residual oil, with reasonable confidence provided that the fuel is in the vapor state prior to entering the combustor.

The chemically bound nitrogen content has been found to inversely affect the formation of fuel NO_x. This is because of the self-destruction reaction prompted by the excess NH_3.

Based upon the results of the detailed tests, it was verified that NO, N_2, NH_3, and HCN are the dominant products of the chemically bound nitrogen conversion process. N_2O was not detected in any condition tested.

With the addition of H_2S to the reactive mixture, the formation of fuel NO has been enhanced under fuel-rich conditions and inhibited at the stoichiometric condition. A nitrogen balance within reasonable accuracy was not obtained with H_2S addition. This indicated that either additional nitrogen species should be included in the experiment or the measurement techniques employed were adversely affected by the existence of H_2S. The actual cause of the imbalance, however, remains to be determined in future efforts.

In summary, there is a striking similarity between catalytic combustion and homogeneous combustion in terms of fuel NO_x formation. However, the similarity is somewhat expected since the role of the catalyst is to accelerate the reaction rate towards equilibrium rather than to alter the chemical nature of a given reactive mixture. Current results show that there are great potentials for catalytic combustion in controlling fuel NO_x, one of the proven concepts being the two-stage catalytic combustion system. The use of a one-stage catalyst for fuel NO_x control, however, requires further development, since a "real" selective oxidation catalyst has not yet been found. However, such a system may be possible through use of the graded cell concept (see Reference 1). For example, one can easily design the first segment of the graded cell catalyst to achieve the condition where the NO_x self-destruction reaction is maximized. Then, by using a reduction catalyst as the second segment, fuel NO_x can be eliminated in this region. The last segment of the graded cell catalyst would again be an oxidative catalyst designed primarily to complete the combustion.

REFERENCES

1. Kesselring, J. P., et al., "Design Criteria for Stationary Source Catalytic Combustion Systems," Acurex Final Report 78-278, March, 1978.

2. Matthews, R. D., and Sawyer, R. F., "Fuel Nitrogen Conversion and Catalytic Combustion," University of California/Berkeley, Energy and Environment Division Report LBL-6396, October, 1977.

3. Bowman, C. T., "Kinetics of Pollutant Formation and Destruction in Combustion," Prog. Energy Combustion Science, Vol. 1, 1975.

4. DeSoete, G., "La Formation des Exyde D'Azote Dans La Zone d'Oxydation des Flammes d'Hydrocarbures," Institute Français du Petrole, Final Report No. 23309, Ruiell Malmaison, France, June, 1975.

5. Wendt, J. O. L., Corley, T. L., and Morcomb, J. T., "Interactions Between Sulfur Oxides and Nitrogen Oxides in Combustion Process," Proceedings of the Second Stationary Source Combustion Symposium, Vol. IV, EPA-600/7-77-073d, July, 1977.

TABLE 2. ANALYTICAL EQUIPMENT USED

Chemical Species	Method	Detection Range	Equipment Model
NH_3	Absorbed in 0.005 N H_2SO_4		Orion 951000
	Ammonia -- Sensing Electrode	2-10 ppm	
	Direct Nesslerization (Colorimetric)	>10 ppm	
HCN	Absorbed in 0.2 N NaOH		Chemtrix Cn1015 M
	Cyanide Ion-Selective Electrode	<10 ppm	
	Titrimetric -- Silver Nitrate Solution	>10 ppm	
N_2	G.C: Silica Gel & Molecular Sieve 5A Columns	>50 ppm	Carle G.C. 8700
N_2O	G.C: Poropac Q Column	>50 ppm	Carle G.C. 8700
CO	Infrared Absorption	0-2000 ppm	Hartman & Braun Uras 2T/CO
CO_2	Infrared Absorption	0-20%	Hartman & Braun Uras 2T/CO_2
O_2	Paramagnetic Detection	0-21%	Hartman & Braun Magnos 5T
UHC	Flame Ionization	0-100,000 ppm	Beckman Model 400 HC Analyzer
NO, NO_x	Optical Detector (Chemiluminescent)	0-10,000 ppm	Air Monitoring Inc. Model 32 C

TABLE 3. FUEL NITROGEN BALANCE

Run No.	Catalyst Type	H_2S Additive	Fuel-N Content (Wt. % of Fuel)	Theoretical Air (%)	Percent Conversion of Nitrogenous Species In the Combustion Products					Error (%)
					NO_x	N_2	NH_3	HCN	N_2O	
1	Pt	No	2.0	98	76.00	15.97	8.12	1.22	0	1.00
2	Pt			77	0.83	79.05	18.07	1.51		-0.56
3	NiO/Pt			200	80.57	13.19	1.81	1.21		-3.21
4	NiO/Pt			75	9.63	58.94	41.20	3.09		12.86
5	UOP		3.0	100	34.13	71.54	4.77	1.52		11.97
6				90	1.06	58.93	44.11	2.96		6.81
7				80	0.58	79.29	25.17	2.03		7.07
8				75	0.29	98.68	4.49	2.59		6.05
9				70	1.00	74.86	4.29	2.95		-16.91
10			2.4	100	23.77	68.20	5.90	0.72		-1.43
11			2.0	75	0.25	74.01	5.36	2.33		-18.02
12			3.6	90	0.68	61.50	42.34	4.71		9.23
13			3.0	80	3.28	54.68	37.92	16.79		12.66
14			3.0	70	2.47	45.60	41.91	7.00		-3.02
15		Yes	3.0	100	22.97	34.46	8.53	8.50		-25.54
16			4.0	90	7.55	44.44	31.12	7.01		-9.88
17			3.0	80	2.44	31.76	23.80	9.28		-32.72
18			3.0	75	0.89	18.59	27.99	10.14		-42.39
19			3.0	70	0.21	8.98	20.24	11.68		-58.89

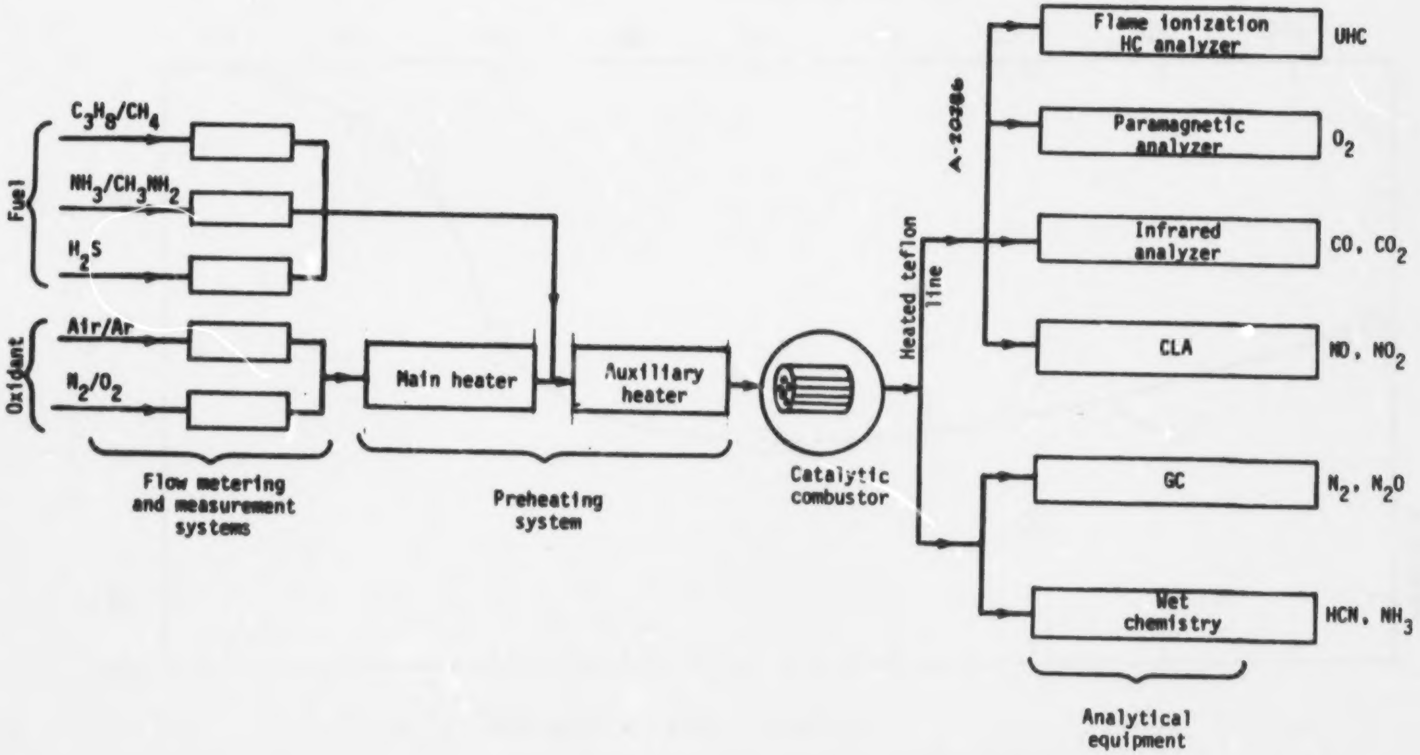

Figure 1. Experimental apparatus.

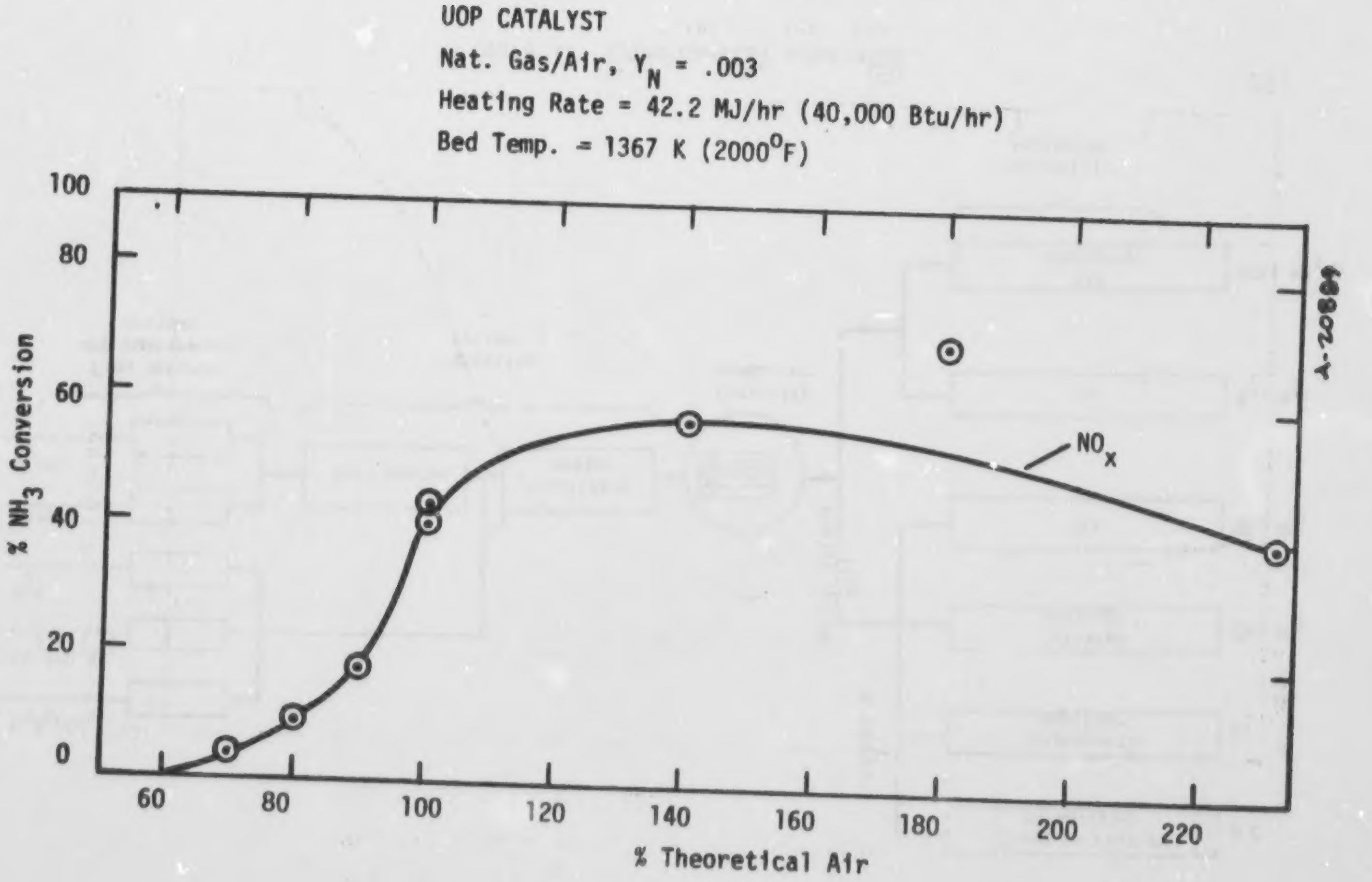

Figure 2. NH_3 conversion at 1367 K — UOP catalyst.

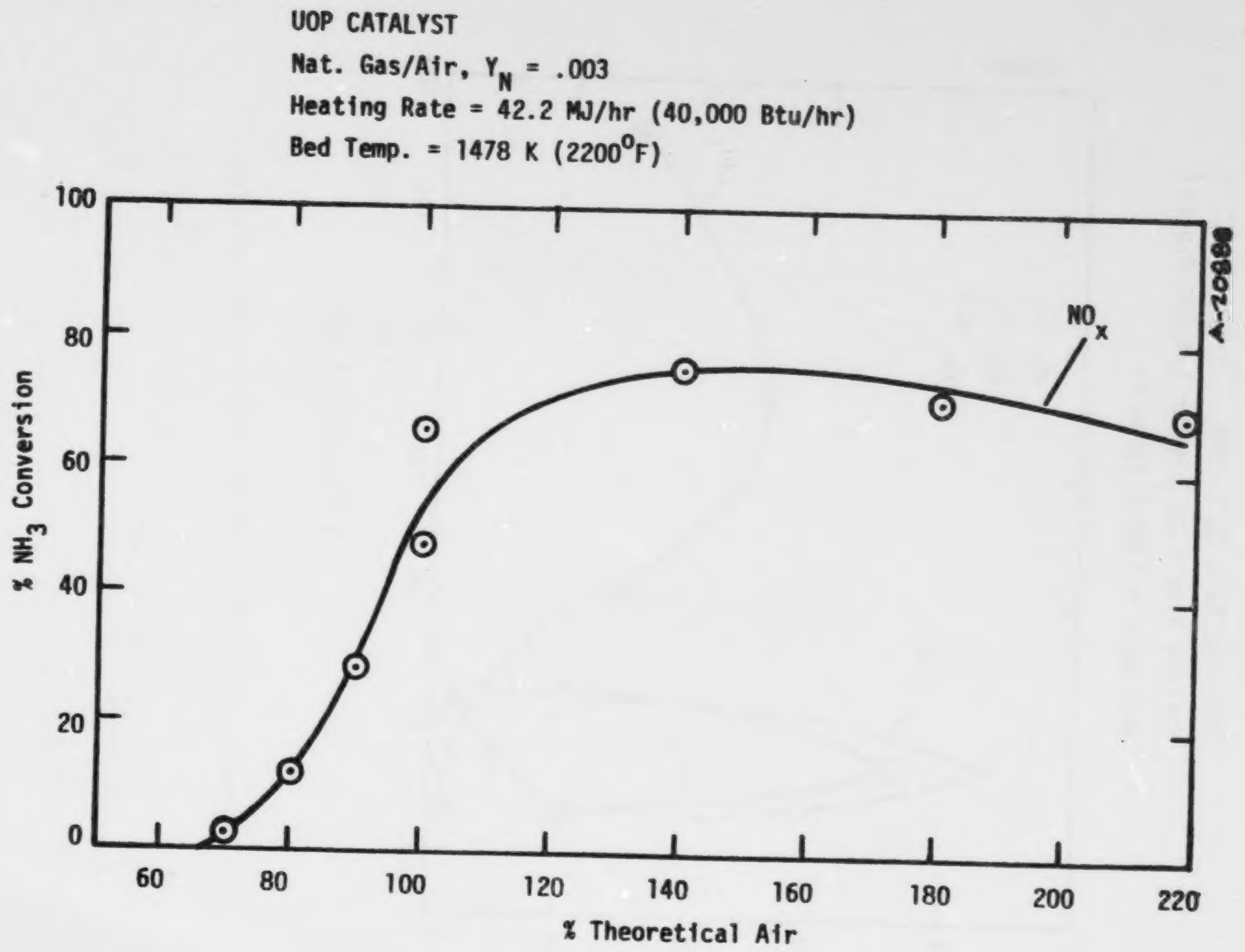

Figure 3. NH_3 conversion at 1478 K — UOP catalyst.

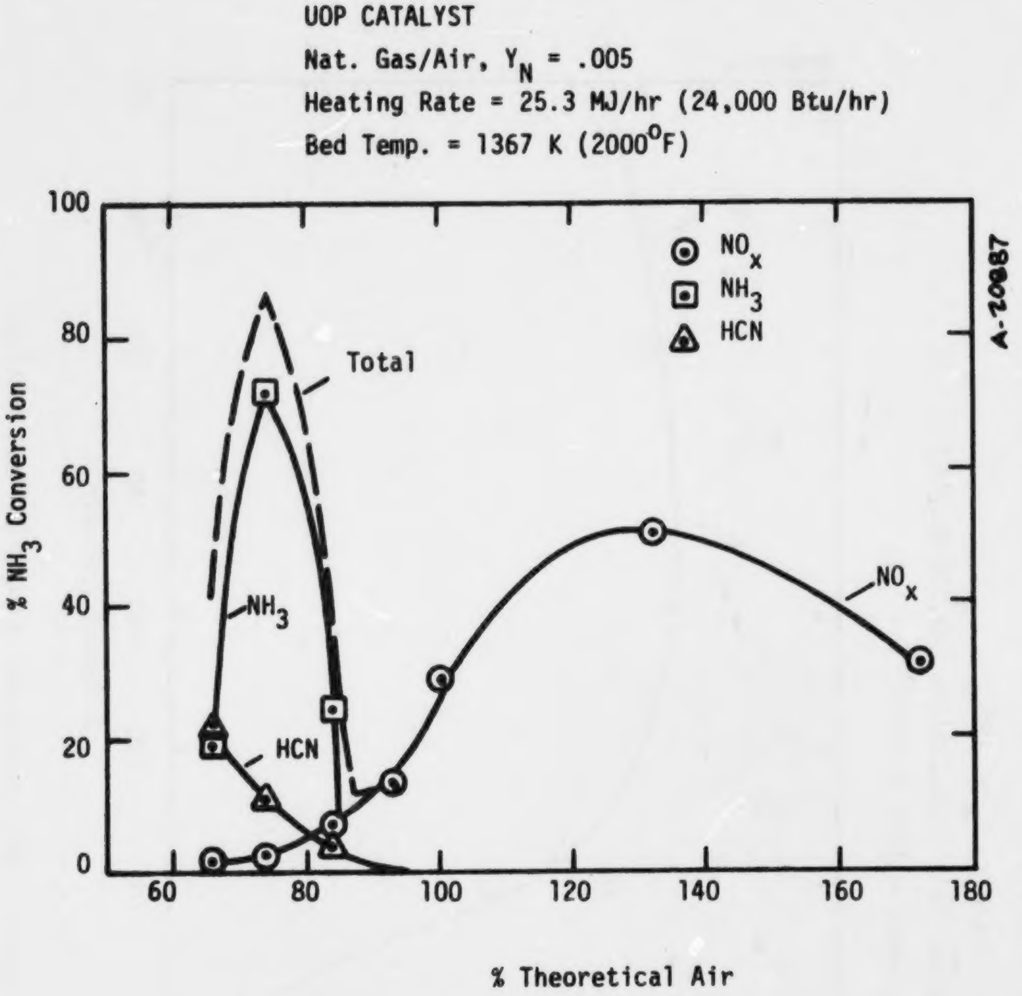

Figure 4. NH_3 conversion at 1367 K — UOP catalyst.

UOP CATALYST
Nat. Gas/Air, Y_N = .005
Heating Rate = 25.3 MJ/hr (24,000 Btu/hr)
Bed Temp. = 1478 K (2200^oF)

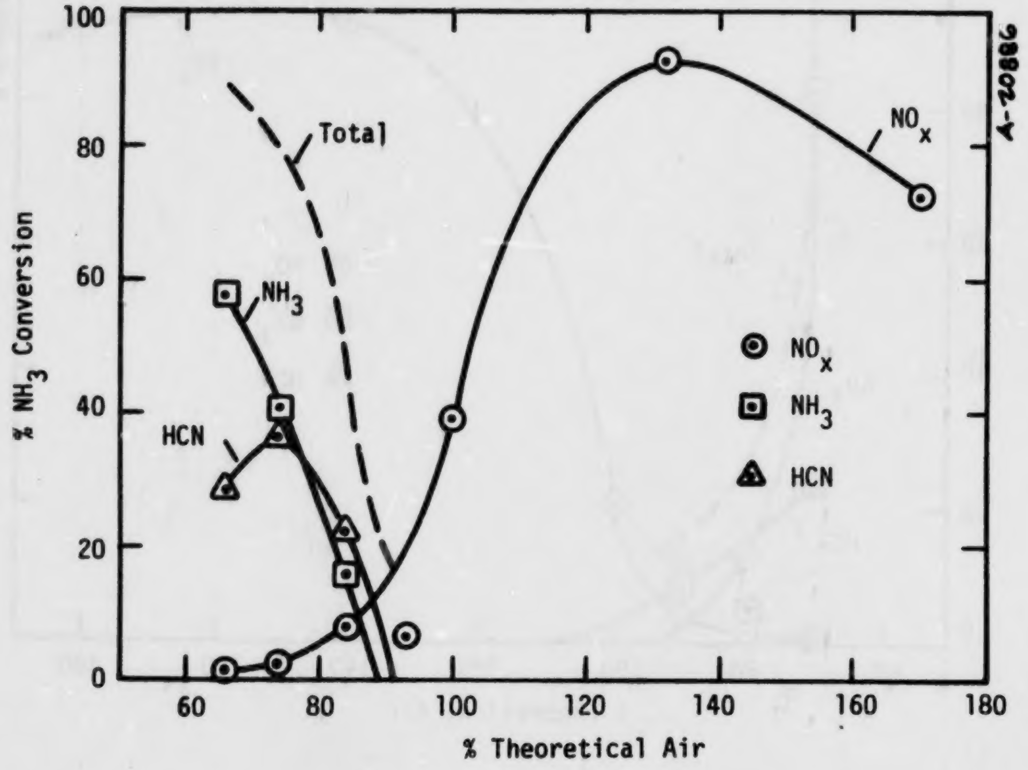

Figure 5. NH_3 conversion at 1478 K — UOP catalyst.

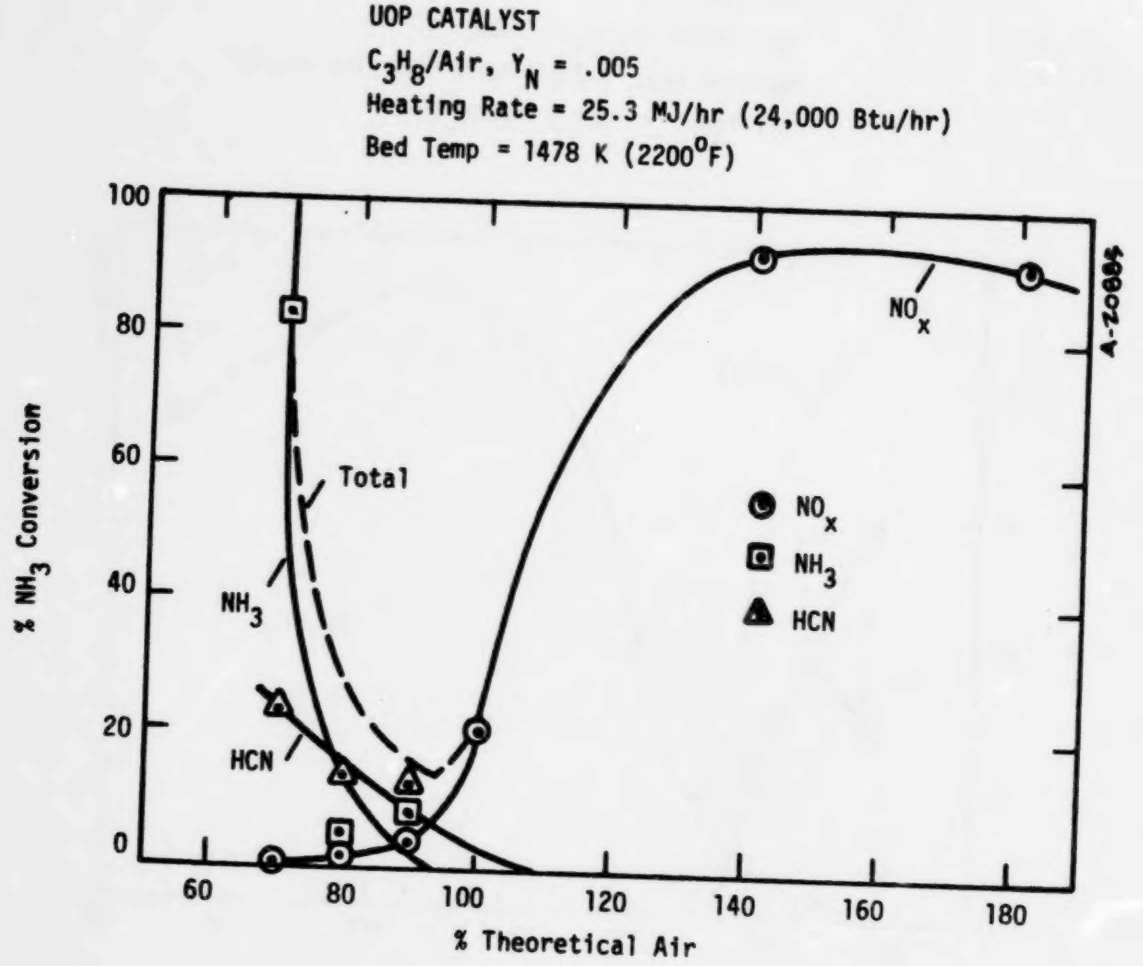

Figure 6. NH_3 conversion at 1478 K — UOP catalyst.

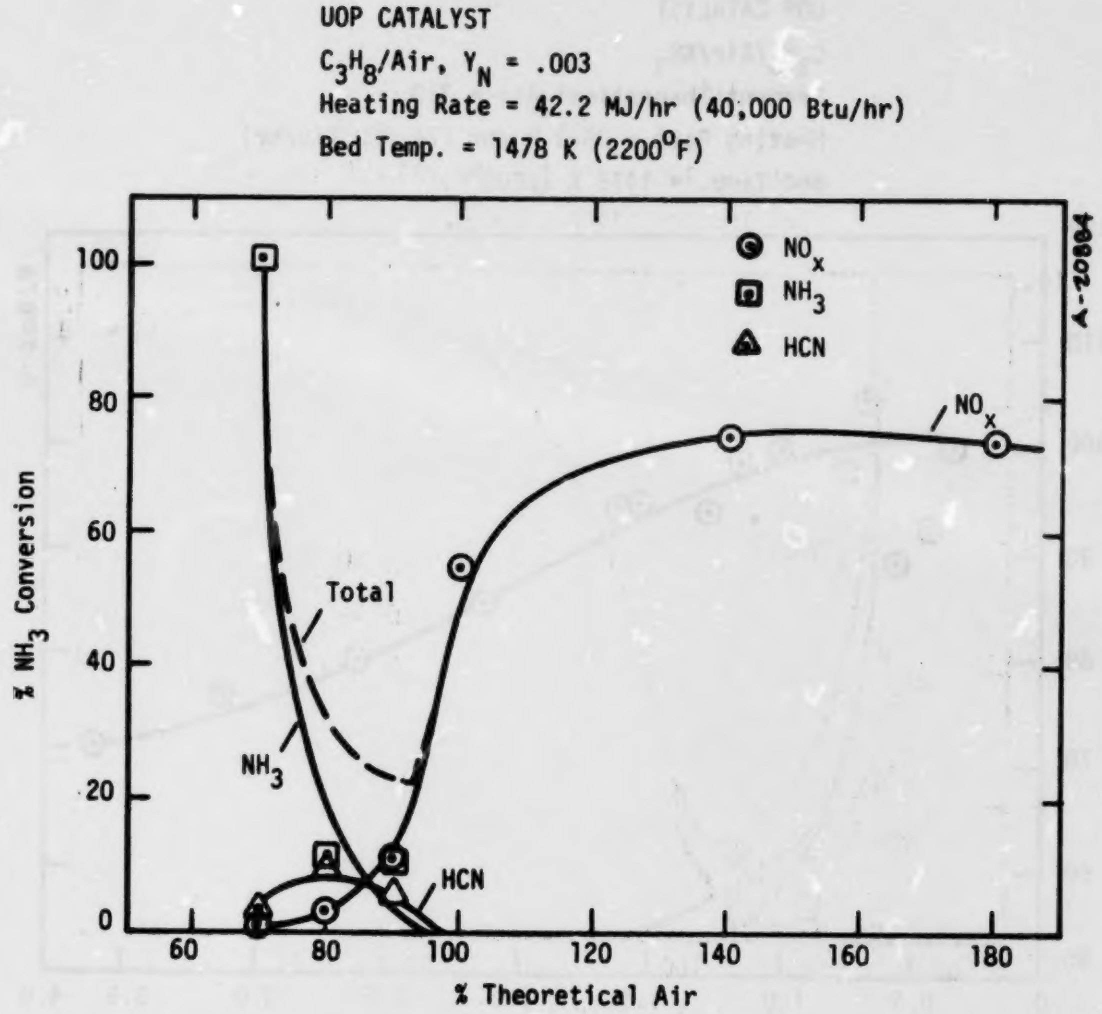

Figure 7. NH_3 conversion at 1478 K — UOP catalyst.

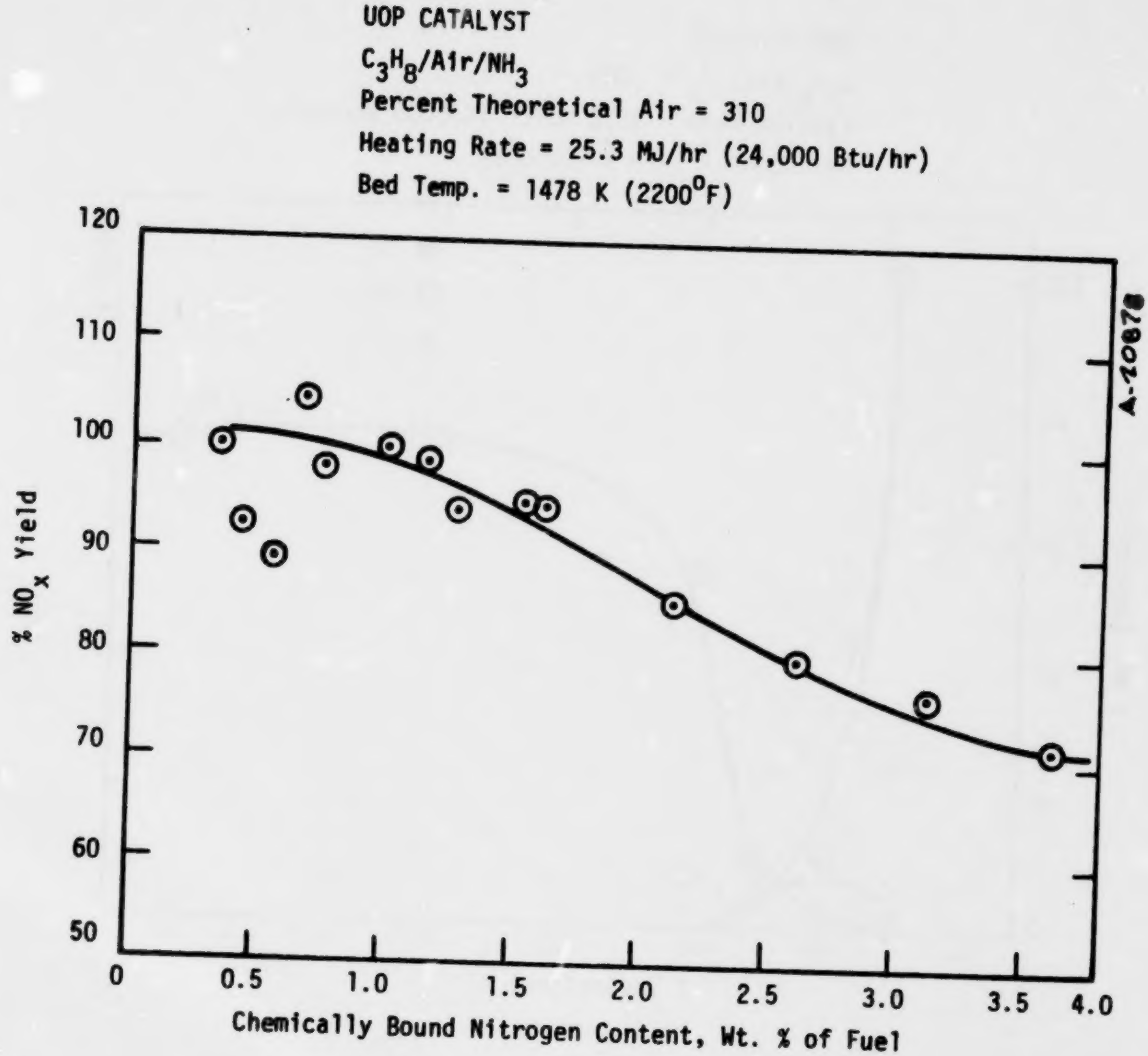

Figure 8. Effect of nitrogen content on NO_x yield — UOP catalyst.

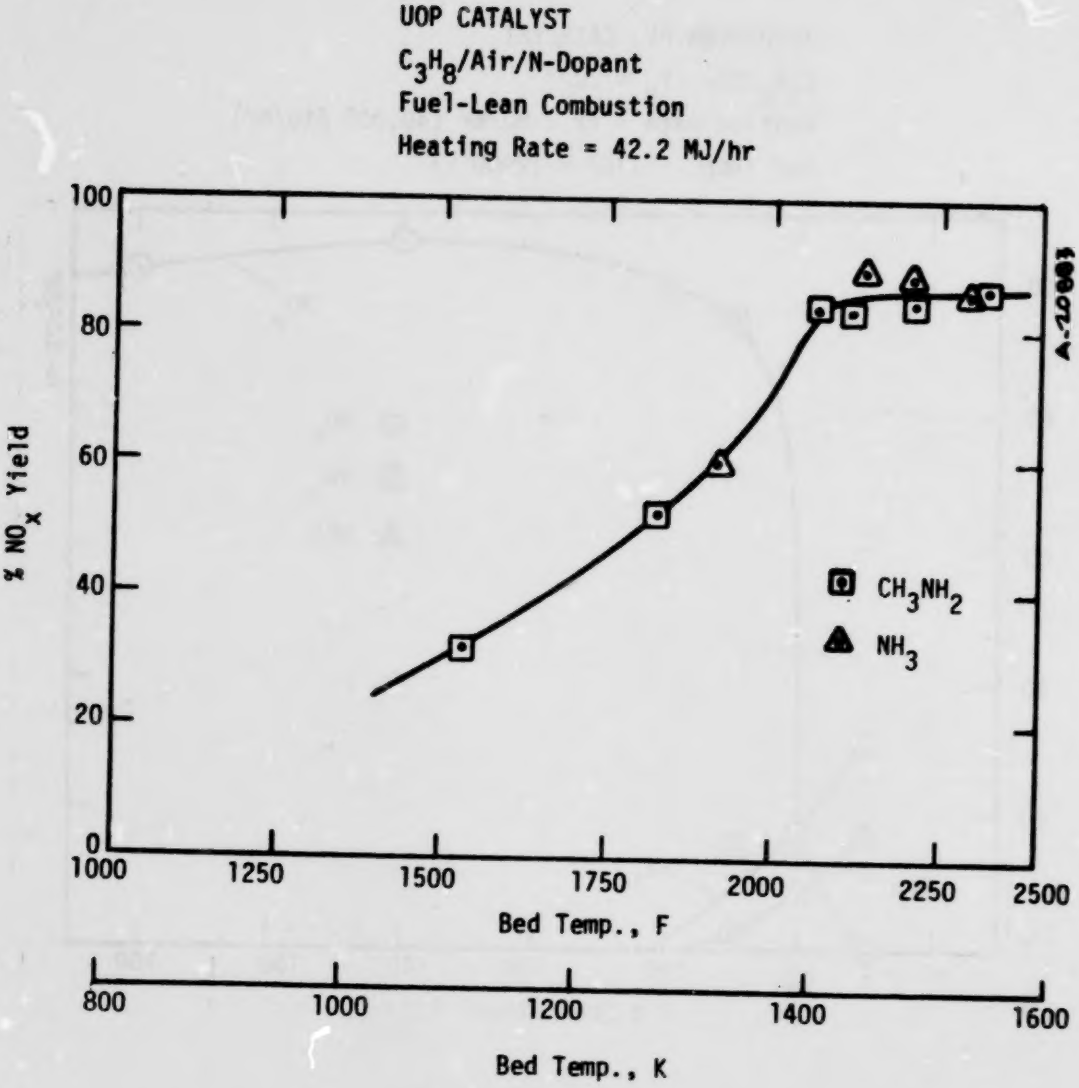
UOP CATALYST
C_3H_8/Air/N-Dopant
Fuel-Lean Combustion
Heating Rate = 42.2 MJ/hr

Figure 9. Effect of dopant type on NO_x emission — UOP catalyst.

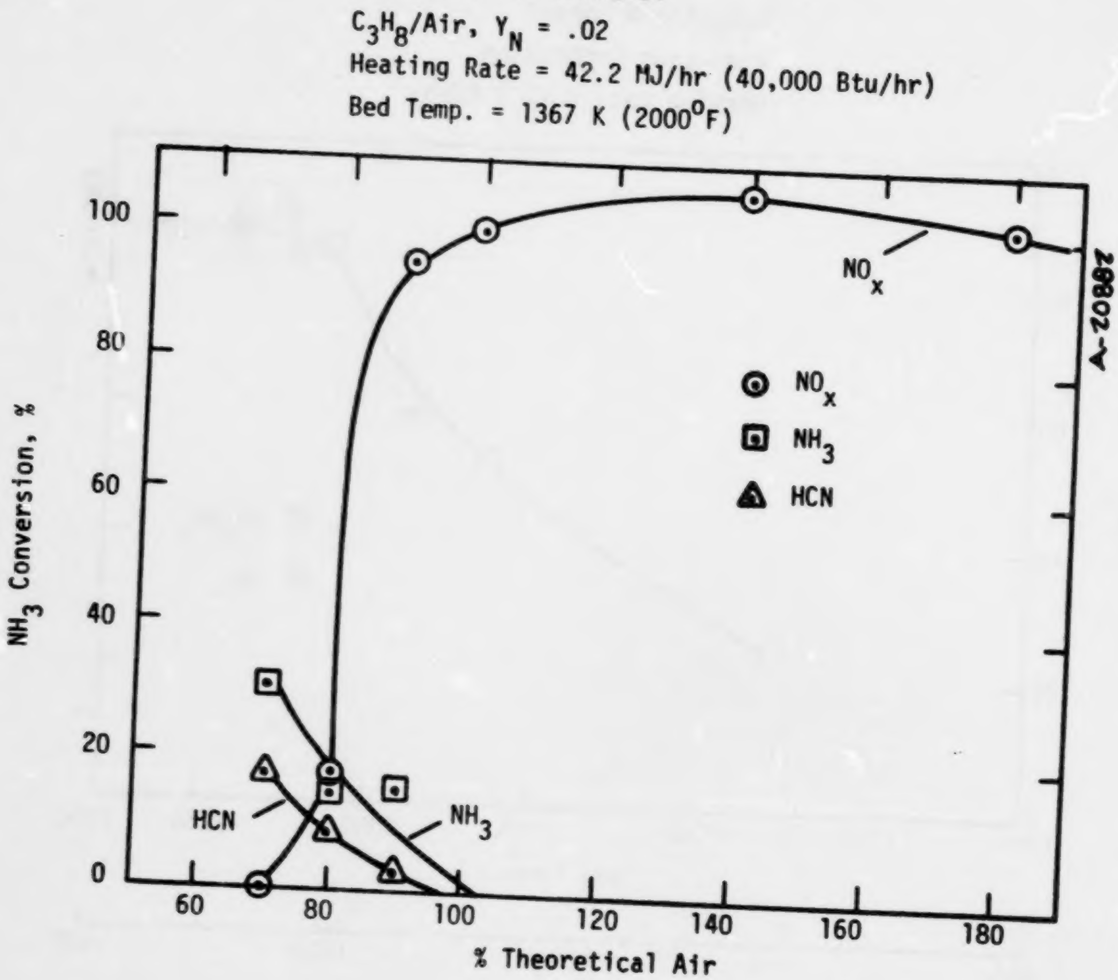

Figure 10. NH_3 conversion at 1367 K — Pt catalyst.

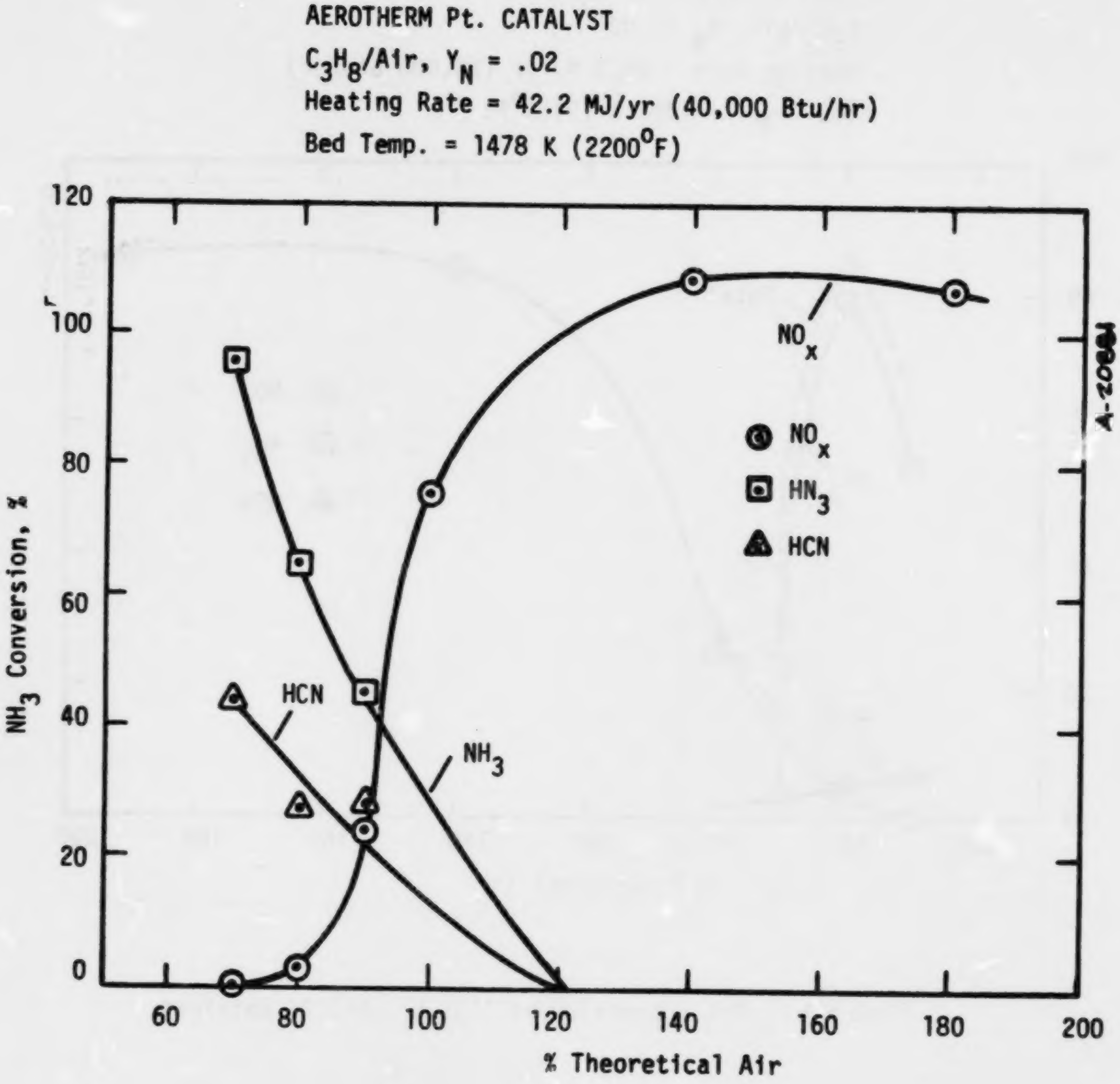

Figure 11. NH_3 conversion at 1478 K – Pt catalyst.

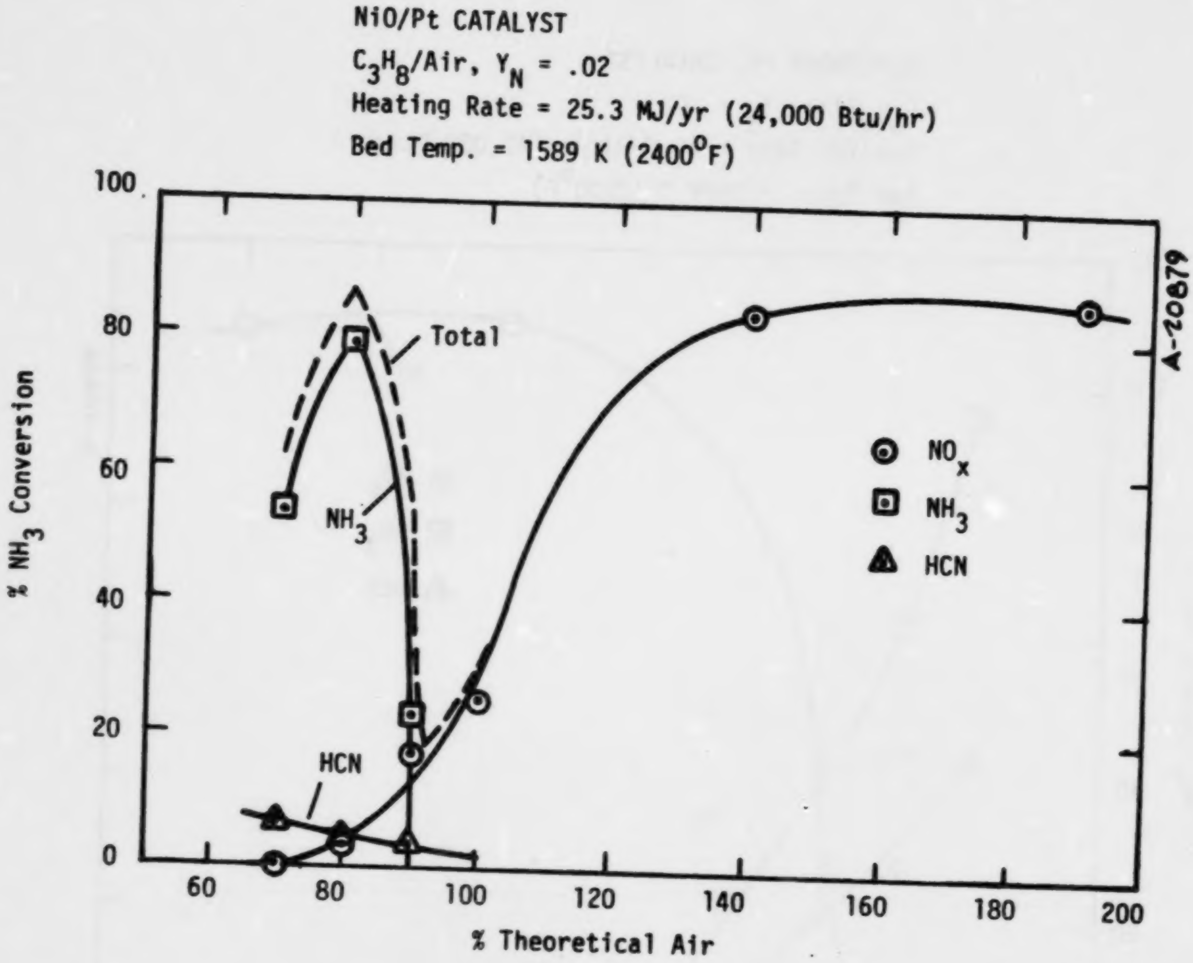

Figure 12. NH_3 conversion at 1589 K — NiO/Pt catalyst.

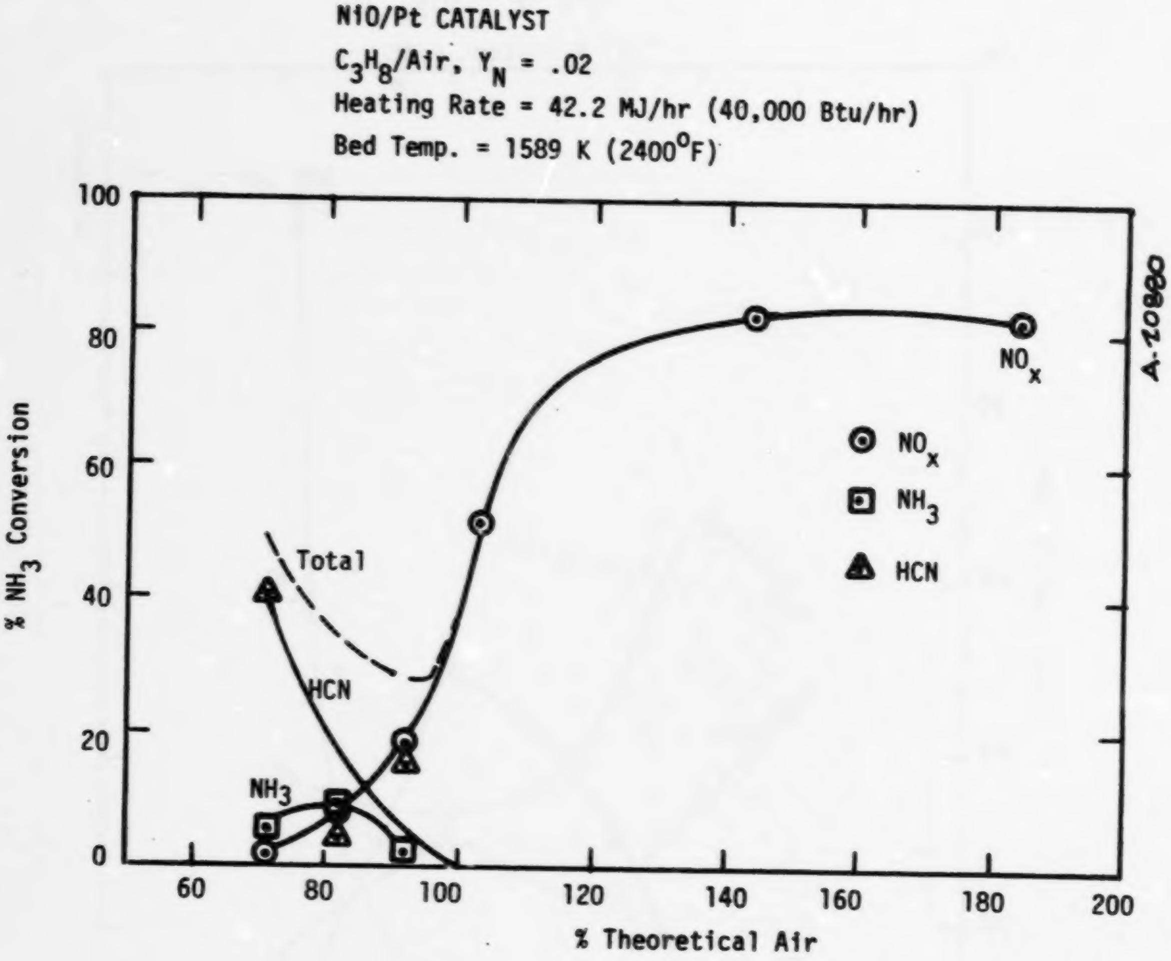

Figure 13. NH_3 conversion at 1589 K — NiO/Pt catalyst.

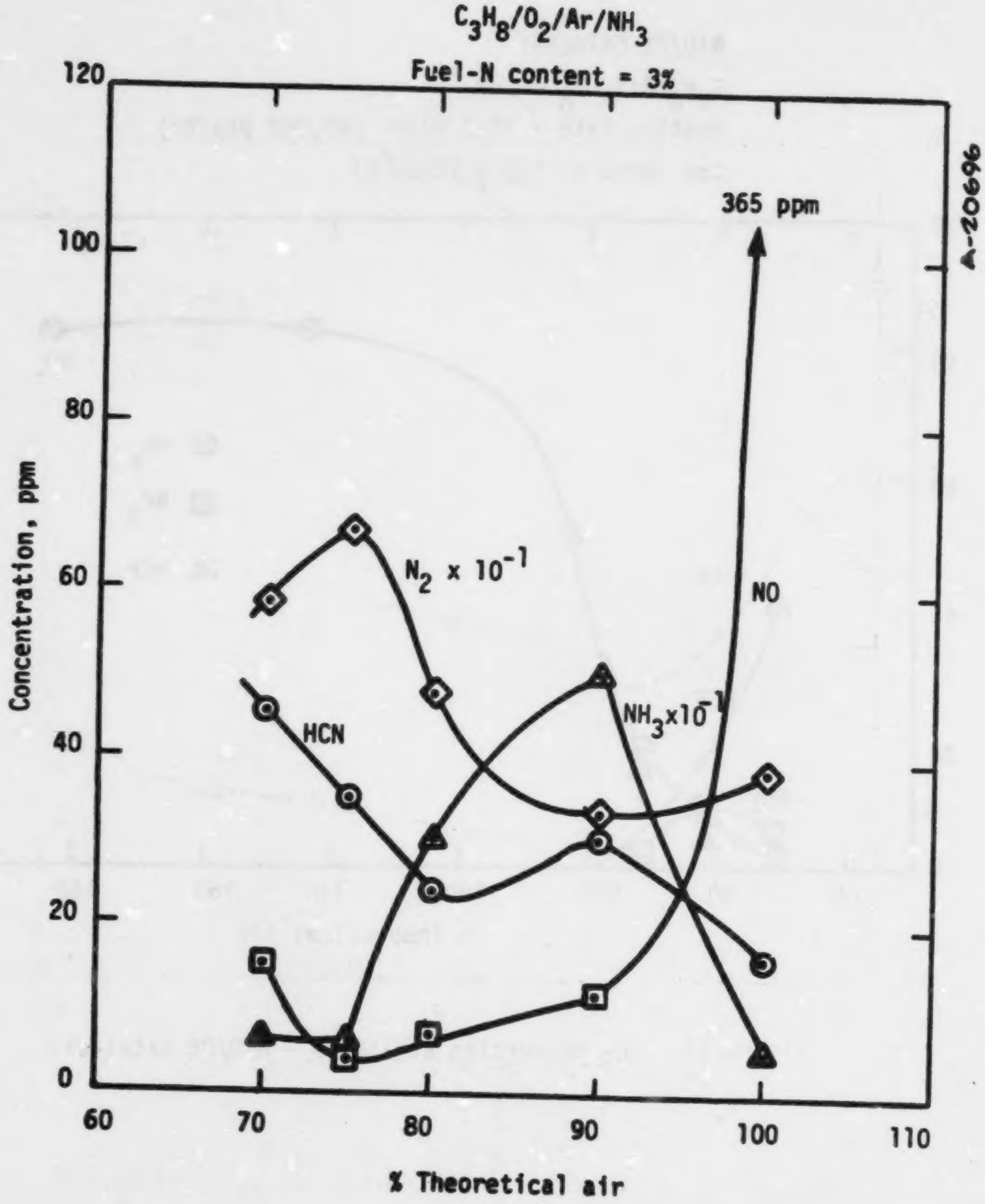

Figure 14. Effects of percent theoretical air on the emissions of nitrogen species under fuel-rich conditions.

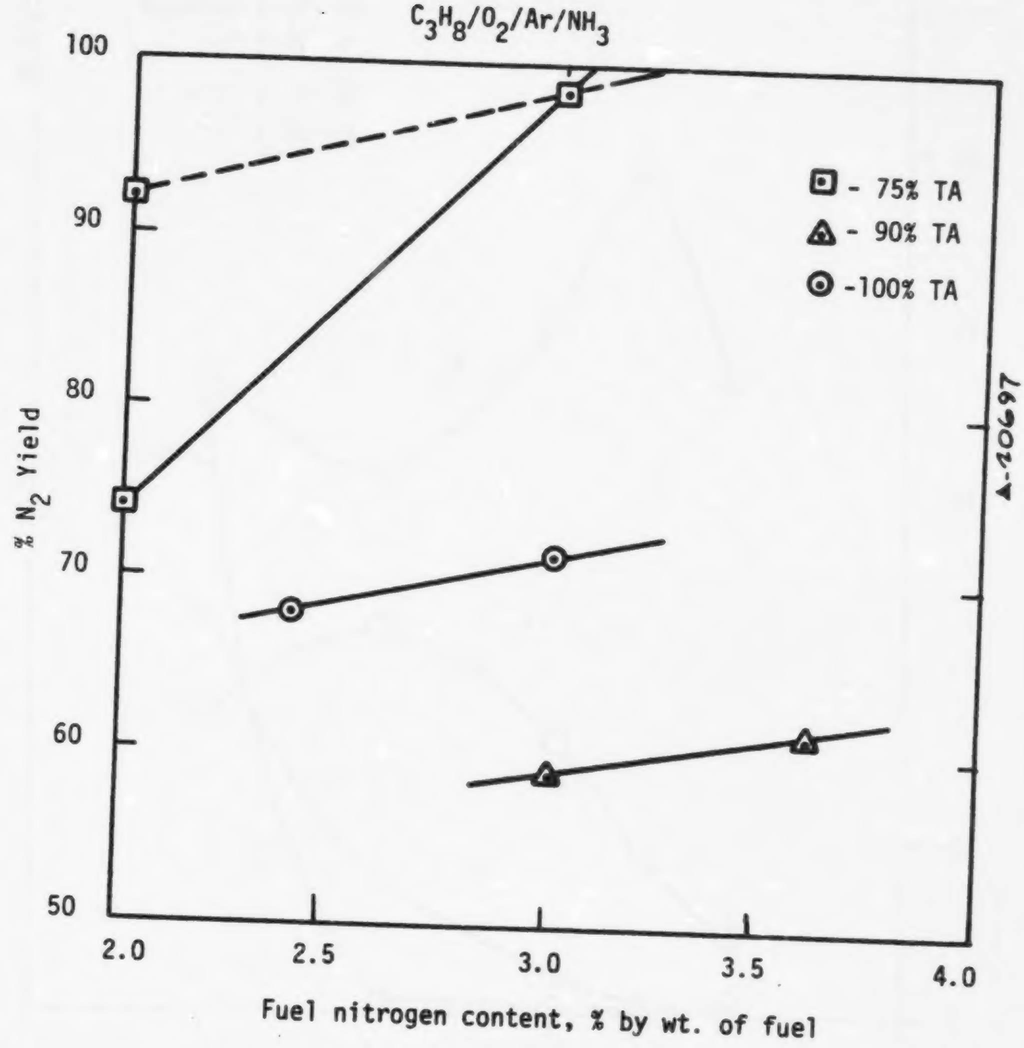

Figure 15. Effects of fuel-N content on N_2 yield under fuel-rich conditions.

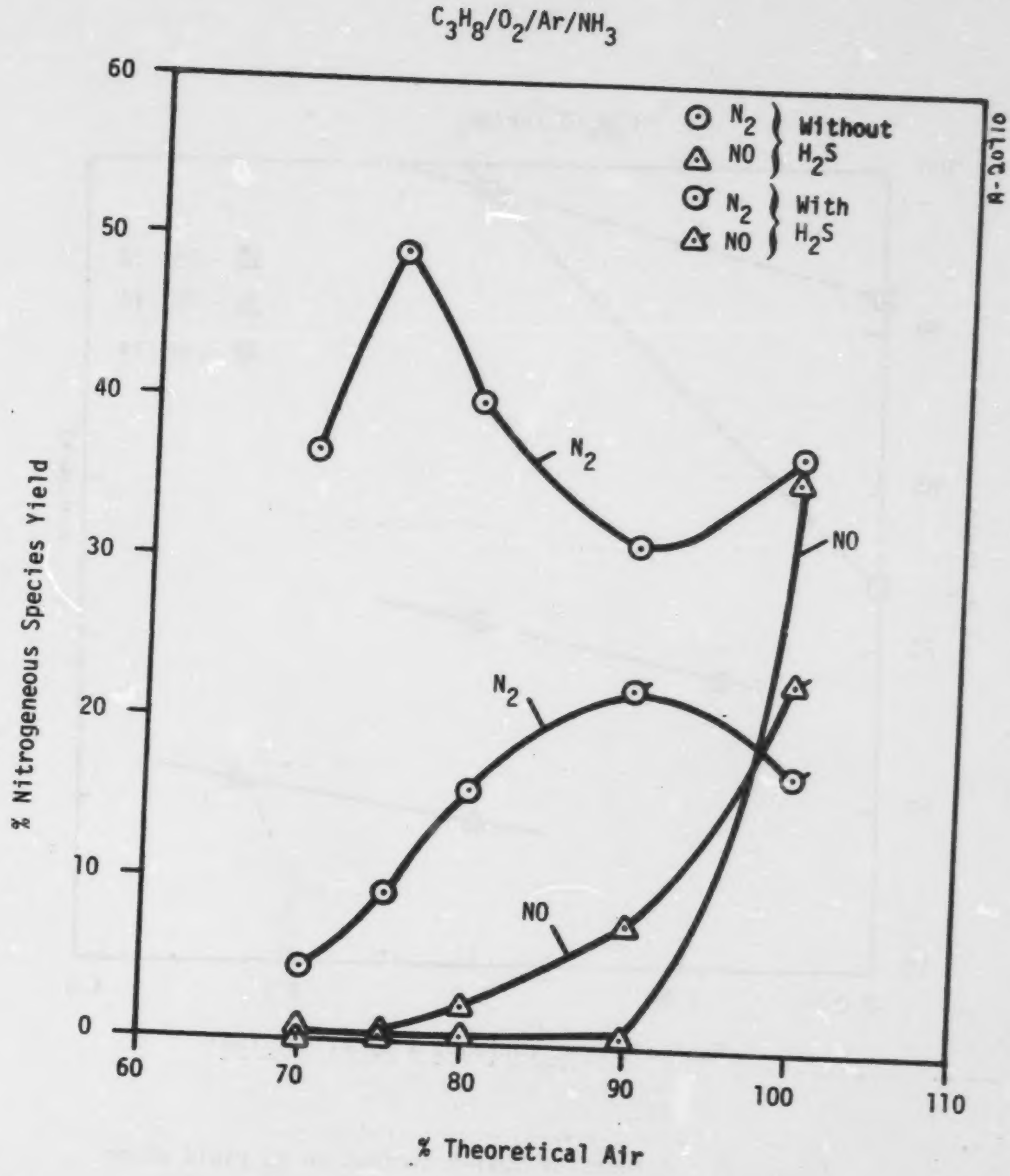

Figure 16. Effects of H_2S on the conversion of chemically bound nitrogen.

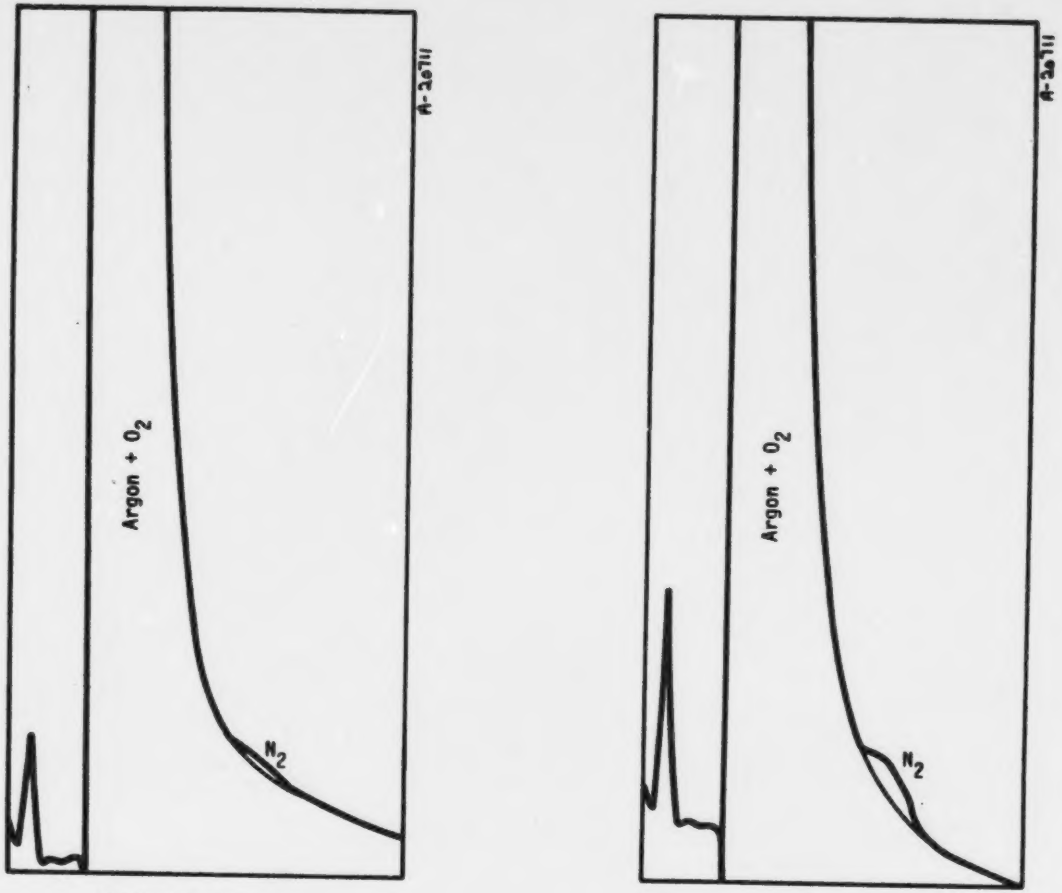

With H_2S dopant

Without H_2S dopant

Figure 17. Comparisons of N_2 concentrations with and without H_2S dopant.

PROSPECTS FOR HIGH-TEMPERATURE CATALYSTS

By

William C. Pfefferle
Consultant
Middletown, N. J. 07748

This work was supported by EPA Contract 68-02-2611, Task 30.

ABSTRACT

The development of the catalytic combustor, a device that not only yields low emissions but fuel savings as well, has created a need for catalysts capable of operating at 1600-1700C for prolonged periods. A high temperature combustor catalyst must be able to withstand the thermal stresses associated with cyclic operation. Materials to be suitable for use in a high temperature combustion catalyst must have a high melting point (above 2000C), a very low vapor pressure at the use conditions, and catalytic activity or compatibility with a suitable high temperature catalytic component. Good thermal shock properties are required but need not be an intrinsic quality of the selected material. Suitable candidate materials include, among others, catalytic alumina spinels such as magnesium cobalt aluminate and stabilized zirconia doped with a catalytic metal such as nickel. Prospects for a durable catalyst capable of 1700C operation appeared to be excellent. Fabrication of a monolithic structure directly from a material incorporating the catalytic component appears to be the best route to a successful high temperature catalyst.

Preceding page blank

INTRODUCTION

In contrast to other catalytic systems, the catalytic combustor requires catalysts capable of both continuous and cyclic operation at very high temperatures, ideally as high as 1600 or 1700C, without degradation of either catalytic or physical properties. It is obvious that this requires the use of high-melting point, low volatility materials. Similarly, very low surface area catalysts are needed, since sintering in use would alter mechanical properties. It is important to recognize that high surface area materials, even a high purity alumina (MP∼2000C), such as is used in reforming catalysts, will sinter badly at temperatures below 600C.

As is the case with any catalytic system, the performance of a catalyst for combustion of fuels depends on many factors besides the intrinsic catalytic activity. Structural, thermal and chemical properties of both the catalytic agents and the support material are important. The important factors include:

Selectivity (No NO_x formation)
Resistance to Poisoning
Mechanical Strength
Thermal Shock Resistance
Attrition Resistance
Chemical Inertness

With combustion catalysts, no selectivity problems are encountered, even at the highest temperatures, with respect to the fixation of atmospheric nitrogen. However, combustion catalysts can convert fuel nitrogen to nitrogen oxides.

Precious metal combustion catalysts are normally resistant to most catalyst poisons at the temperatures of catalytic combustion. Even with base metal oxide catalysts, catalyst poisoning is not a significant problem under catalytic combustor operating conditions since all base metal salts decompose to the corresponding oxides at the temperatures involved.

Mechanical strength is not usually a problem with catalysts since the mechanical load is typically just the weight of the catalyst itself. However, it is important that a catalyst not degrade in use to the point of crumbling. Unlike most catalysts, gas turbine combustor catalysts must maintain structural integrity at very high flow velocities and resist both attrition and thermal shock.

Thermal shock resistance is especially important for combustion catalysts since it is often desirable to light offa combustor as rapidly as possible. A high thermal conductivity and high strength contribute to good thermal shock resistance. Systems with high volume change phase transitions should be avoided.

A good attrition resistance is important for combustor catalysts because of the high flow velocities encountered in many applications. Proper firing conditions are critical. Slip coatings must be well bonded.

Chemical inertness of a catalyst to the process stream is important in many applications. In the case of platinum combustion catalysts, halides in the fuel can cause rapid loss of platinum. The problem is the volatility of the platinum oxyhalides. Similarly, chromia can be stripped off a catalyst at even lower temperatures than can platinum. Chromium oxychloride has a vapor pressure of one atmosphere at 390C. At high temperatures one must also consider the interaction between the support and the catalytic material. For example, cobalt oxide reacts readily with alumina to form the less active cobalt aluminate (Reference 1). Slip Coatings can react with the support and degrade mechanical strength and thermal shock resistance.

BASIS FOR DEVELOPMENT OF HIGH TEMPERATURE CATALYSTS

Prior to the development of a catalytic combustor suitable for gas turbine use, combustion catalysts were limited to an operating temperature of about 800C. Above this temperature catalysts degraded very rapidly. At the second workshop on catalytic combustion in June 1977 catalysts operable at temperatures between 1200 and 1500C were reported. It is believed that higher temperature catalysts capable of operating as high as 1700C are feasible. A basis for the selection of such a high temperature catalyst follows.

1. Only materials with melting points above about 2000C should be considered. Even with low surface area catalysts, grain growth of the structural material must be limited. Ideally, this means the melting point of the material must be about 1.5 times the catalyst operating temperature. For a 1700C operating temperature one would prefer a material that melts no lower than 2700C. Zirconia (MP 2760C) meets this requirement. For a 1500C operating temperature the corresponding requirement for the melting point is about 2385C. Based on data for alumina catalysts, somewhat lower melting points should be allowable. Kesselring (Reference 2) has reported the operation of an alumina (MP 2050C) based on a catalyst at 1500C without apparent catalyst degradation.

2. Low surface area catalysts are preferred. As already noted, sintering of high surface area substrates could lead to degradation of mechanical properties and to undesired solid state interactions. Further, high surface area has already been shown to be unnecessary to good low temperature light off activity. Kesselring (Reference 2) has also shown that a catalyst can give good combustion results with a surface of $0.02M^2/g$ or less.

3. Very low vapor pressure materials are required. Because of the high volumetric flows which a combustor must handle, many refractories which might be suitable in a non-flow environment will have an unacceptably large weight loss in a combustion system. Beryllia, an excellent ceramic material with very good thermal shock resistance, is unacceptable in a combustor environment because beryllia suffers severe weight loss in air at temperatures over 1100C if as little as 0.5% water vapor is present. Obviously, materials must be selected with care with this consideration in mind.

4. Base metal oxide catalysts are required. This is because precious metals are much too volatile under catalytic combustor operating conditions. At 1400C, platinum (MP 1773C) exhibits a vapor pressure in air equivalent to a weight loss of about 56 grams of platinum per 100,000 cubic feet of air (Reference 3). For a combustor with a throughput of 1.1 pounds per second, this would represent less than two hours operation. It is obvious why platinum catalysts can degrade so rapidly at high temperatures. On the other hand, many high melting, low vapor pressure base metal oxide compounds exist. Many are catalytically active or can be made so by proper doping. Cobalt aluminate is an example of a catalytically active oxide compound (Reference 1).

5. Slip coated catalysts should be avoided. Although in principle it should be possible to make a high temperature slip coated catalyst the requirement for tight, reliable bonding of the slip to the substrate would appear to require both a very high firing temperature and careful selection of slip and substrate materials for compatibility. Inasmuch as even conventional auto exhaust catalysts lose significant amounts of slip in use, slip coated catalysts would not appear to be the preferred choice, at least for gas turbine applications. Preferrably, a high temperature combustion catalyst should be made by forming a catalytic composite into a desired structure and then firing, a procedure already used with many low temperature commercial catalysts.

MATERIALS OF INTEREST

As previously noted, a number of oxide compounds exist which meet the basic requirements for a high temperature combustion catalyst. It is important to note that refractories are presently used at even higher temperatures than those contemplated for combustor catalysts. Alumina has even been used at temperatures as high as 1900C (Reference 4). Of course, an alumina catalyst for operation at even 1500 or 1600C can not be expected to maintain much surface area. It is fortunate that high surface area is not required for combustor combustor catalysts.

Of the materials which might be considered for combustor catalysts, those based on zirconia or alumina are of most interest. This is primarily because there is more data available for these materials and because systems based on these materials could be readily produced commercially.

The highest melting oxides available are thoria (MP 3220C), urania (MP 2876C), hafnia (MP 2837) and zirconia (MP 2760). Of these thoria is reported to be one of the most stable of the refractory oxides (Reference 5). However, it is radioactive and therefore is not a prime candidate material. Zirconia, on the other hand, is readily available and there is a great deal of data on its use.

ZIRCONIAS

Although zirconia is not catalytically active, it should be readily possible to dope zirconia with say cobalt or nickel. A calcium stabilized zirconia with nickel replacing some of the calcium should make a very good candidate material.

Another zirconia candidate is zirconia-spinel. As reported by Corning at the last Catalytic Combustion Workshop, a zirconia-spinel honeycomb is suitable for operation at 1700C. If some of the magnesium in the spinel is replaced by nickel, one has suitable catalytic honeycomb. Many other catalytic materials could be utilized with zirconia. Any spinel with catalytic properties would be a good possibility since most spinels melt at about the same temperature.

The major drawback to zirconias is poor thermal shock resistance. However, considerable toughening can be achieved by various techniques such as the introduction of microcracks. Nevertheless, a flexible structure such as Corning's flexible cell design would seem to be important.

ALUMINAS

Alumina is perhaps the most widely used of the refractory oxides. Although alumina has a melting point of only 2000C, most alumina spinels melt somewhat higher (~ 2100C). Inasmuch as alumina can be used at least for short periods at 1900C, 1600 or 1700C does not appear out of reach for alumina spinel type catalysts. As is the case with zirconia, pure alumina is not a good catalyst. However, a number of catalytically active spinels are known, e.g. cobalt aluminate. Many doping possibilities exist.

Although better than zirconia, alumina has relatively poor thermal shock properties. Also as with zirconia, toughening techniques exist. Chromium alumina composites, for example, can survive many hundreds of thermal shock cycles of a severity which destroys pure alumina samples in the first cycle. Further, the resistance to oxidation at 1500C of a 30%Cr - 70%Al_2O_3 composite is reported to be excellent (Reference 6). Chromium of course is catalytically active.

CATALYTIC COMPONENTS

Lanthanum chrome is not only catalytically active (Reference 7), but is also a good high melting refractory with good mechanical properties. This material is presently being studied for use in MHD electrodes.

A large number of catalytically active oxide compounds exist (Reference 7). Although many have relatively low melting points, others such as lanthanum chrome have high melting points. Even the lower melting compounds could be used as dopants in higher melting systems.

Ideally, however, the catalytic material should have good structural as well as good catalytic properties, as is the case with lanthanum chrome. Another such material is magnesium chrome spinel. As with lanthanum chrome, magnesium chrome spinel is being considered for use as a high temperature MHD electrode material (Reference 8).

CONCLUSIONS

Prospects for the development of durable combustion catalysts for operation at 1600-1700C appear to be excellent. A number of readily available materials meet the basic requirements for such a catalyst. Fabrication into a suitable structure of a selected matrix material incorporating the catalytic component avoids the difficulties associated with slip coated catalysts. Such an approach permits catalysts with optimal mechanical as well as catalytic properties.

Base metal oxides are required as the catalytic component inasmuch as platinum metals have a high vapor pressure at combustor operating conditions. In general, the choice of materials is dictated much more by considerations such as melting point, chemical stability, and vapor pressure than by catalytic properties. At the high temperature conditions contemplated for catalytic combustor operation, solid state reactions are rapid and materials must be chosen on the basis of their behavior as ceramics. Suitable materials include stabilized zirconias, spinels, zirconia spinels and lanthanum chrome.

Although suitable materials can now be specified, much work remains in developing formulations which optimize both structural and catalytic properties. A program to develop thermal shock resistant high temperature catalytic structures for combustion catalysts is warranted.

REFERENCES

1. Schachner, H. Cobalt Oxides as Catalysts. COBALT, December 1960.
2. Kesselring, J. P., W. V. Krill, and R. M. Kendall. Design Criteria for Stationary Source Catalytic Combustors. Second Workshop on Catalytic Combustion, Raleigh, North Carolina, 1977.
3. Alcock, C. B., and G. W. Hooper. Thermodynamics of the Gaseous Oxides of the Platinum - Group Metals. Proc. Royal Society (London) A, 254: 551-561, 1960.
4. Campbell, I. E. High Temperature Technology. John Wiley and Sons, New York, 1957.
5. Ryshkewitch, E. Oxide Ceramics: Physical Chemistry and Technology. Academic Press, New York, 1960.
6. Shevlin, Thomas S. Oxide-Base Cermets - Chromium-Alumina. In: Cermets, J. R. Tinklebaugh and W. B. Crandall, eds. Reinhold, New York, 1960. Chapter V pp. 97-109.
7. Voorhoeve, R. J. H., J. P. Remeika, and L. E. Trimble. Defect Chemistry and Catalysis in Oxidation and Reduction over Perovskite-type Oxides. Annals of the N. Y. Acad. of Sci., 272: 3-21. 1976.

7. Negas, T. Private communication.

ENVIRONMENTAL ASPECTS
OF
LOW BTU GAS-FIRED
CATALYTIC COMBUSTION

By:

B.A. Folsom, C.Courtney
and M.P. Heap
Energy and Environmental Research Corporation
8001 Irvine Boulevard
Santa Ana, California 92705

ABSTRACT

One alternative to the economic and efficiency penalties of stack gas sulfur removal from conventional coal-fired power plants is to gasify the coal, remove the sulfur products from the fuel gas and fire the essentially sulfur-free gas in a high-efficiency combined gas turbine-steam turbine power cycle.

The low Btu gases produced in these systems can contain high levels of ammonia and nitrogen oxide emissions could be a problem if the ammonia is oxidized to NO in the combustion process.

This paper presents some preliminary data on the processing of nitrogenous compounds in low Btu gas-fired catalytic combustors. Three experiments are discussed. In the first experiment an ammonia-containing low Btu gas was fired in a catalytic combustor. Nearly all of the NH_3 was oxidized to NO under lean conditions, but approximately half was reduced to N_2 under rich conditions. The second experiment was designed to simulate the operation of a reheat combustor firing low Btu gas in an oxidant-containing NO. Under rich conditions up to 85 percent of the NO was reduced to N_2. Methane doped with ammonia was the fuel in the third experiment and the results obtained here were found to be similar to results obtained by other investigators.

Preceding page blank

ACKNOWLEDGMENT

The work upon which this publication is based was prepared under Contract No. 68-02-2196 with the Environmental Protection Agency. The authors wish to express their appreciation to Messrs. J. Johnson and J. Keene of Energy and Environmental Research Corporation, Dr. J. Kesselring of Accurex Corporation, and Mr. G.B. Martin for their assistance in various portions of the work.

SECTION 1

INTRODUCTION

This paper addresses the catalytic combustion of low Btu gas (LBG) in combined gas turbine-steam turbine power cycles. The rising demand for electrical power coupled with the limited availability of petroleum mandates the construction of many alternate fuel-based power plants by 1985-1990. These power plants must have high overall efficiency, low net cost of electricity and must be environmentally acceptable. Since these plants will commence operation in the future when environmental restrictions are projected to be much more restrictive than at present, the environmental design goals should be to minimize emissions rather than to meet current New Source Performance Standards.

Several advanced coal-based power cycles are currently being developed for this application (1,2,3,4). The integrated gasifier LBG-fired combined gas turbine-steam turbine cycle is one of these alternatives. The primary advantage of this cycle is the potential for low emission of sulfur products without the economic and efficiency penalties associated with stack gas sulfur removal (5,6). Since the coal gasification process operates fuel-rich, the sulfur in the coal is converted mainly to H_2S* in the low Btu offgas which can be removed (potentially) more easily than SO_2. Furthermore, the H_2S concentration is high and the total volume of gas to be processed is small in comparison with total stack gas. Energy losses associated with the gasification and cleanup processes can amount to as much as 30 percent of the coal's heating value. However, if the clean LBG is fired in a gas turbine combustor as part of a combined cycle power plant the gains in overall power plant performance, when compared to conventional steam cycles, may more than offset the losses in the gasification and cleanup processes.

---

*COS is the second principal LBG sulfur product.

Figure 1 is a simplified schematic diagram of a LBG-fired gas turbine-steam turbine combined cycle power plant with integrated gasifier. Only the major heat, work and mass flow paths have been shown for clarity. The system consists of a gas turbine topping cycle with exhaust heat transferred to a steam turbine bottoming cycle through a waste heat recovery boiler. Low Btu gas is produced in a gasifier supplied with coal, compressed air from the gas turbine air compressor, and steam from the bottoming cycle. This "integration" with other cycle components significantly reduces the energy losses attributable to the gasification process.

"Raw" LBG exits the gasifier at temperatures as high as 1370 K depending upon gasifier design and operation containing three pollutant precursors:

- Sulfur compounds which can be oxidized to SO_x in the combustor,
- Particulates including carbon, tars and ash which may damage turbine blades and may be emitted to the atmosphere,
- Ammonia which may be oxidized to NO_x in the combustion process.

Raw LBG is processed through a gas cleanup system to reduce the concentrations of these materials prior to combustion. Several gas cleanup systems have been developed or are under development for this application. Hot gas cleanup systems process the LBG without significantly reducing its temperature and remove a majority of sulfur products and particulates. Cold gas cleanup systems require cooling the LBG to near ambient temperature (400 K), and they remove a majority of the sulfur products and particulates and may also remove a substantial portion of the ammonia. The sensible heat removed from the LBG may be used for a variety of purposes, but it effectively bypasses the gas turbine topping cycle and contributes to reduced efficiency.

The thermodynamic trade-offs in hot and cold gas cleanup processes have recently been investigated (7,8,9). Figure 2 shows the effects of LBG intercooling on the efficiencies of the individual gas and steam turbine subcycles and the overall cycle. The configuration considered was a 1366 K (2000 F) turbine inlet temperature, 12.0 pressure ratio gas turbine with integrated gasifier and a nonreheat steam bottoming cycle optimized for the gas turbine waste heat (other cycle parameters are listed in Ref. 8). Three uses for the LBG sensible heat are considered: dumping the heat into the environment, raising steam and injecting it into the gasifier, and raising steam to operate a separate high-efficiency steam cycle. Since LBG gasifier offgas temperatures are usually well in excess of 900 K, dumping this sensible heat is clearly wasteful. A more economical alternative is to generate steam either for gasifier injection or to operate a separate steam cycle. Figure 2 shows that all three alternatives reduce overall cycle efficiency. Depending upon gasifier design and operating parameters, the sensible heat in LBG offgas can amount to as much as 20 percent of the total heat release and the losses due to intercooling the LBG with a cold gas cleanup system can be substantial.

From a combustor design point of view, the choice of a hot gas cleanup system as opposed to a cold system could well have two important effects:

- Higher adiabatic flame temperature
- Higher NH_3 concentration

The sensible heat in the LBG contributes directly to the adiabatic flame temperature. For typical LBG compositions, cooling the gas by 400 K will decrease the adiabatic flame temperature at stoichiometric conditions by about 200 K thus reducing the potential for thermal NO_x formation. Cooling the LBG will also require an increased LBG flow rate and reduced stoichiometry (percent theoretical air) to achieve the same turbine inlet temperature.

The concentration of NH_3 in raw LBG depends upon gasifier design and operating parameters and may be as high as 0.38 percent (6). With hot gas cleanup systems no NH_3 is removed, and the entire amount will enter the gas turbine combustor and could be oxidized to NO_x. A concentration of 0.38 percent NH_3 in the LBG will produce approximately 3.2 lb $NO_2/10^6$ Btu if all NH_3 is converted to NO_2. This is far in excess of the current New Source Performance Standard, 0.7 lb $NO_2/10^6$ Btu.* Thus, one important challenge to the combustor designer is to minimize the conversion of NH_3 to NO_x.

---

*This is the current New Source Performance Standard for solid fossil fuel-fired steam generators with greater than 250 x 10^6 Btu/hr heat input. The comparable standard for a gaseous fuel is 0.2 lb $NO_2/10^6$ Btu.

If a low temperature cleanup process is employed, a substantial portion of the NH_3 may be removed — NH_3 levels from 100 to 400 ppm have been reported (3,4). While these levels are sufficiently low to meet current New Source Performance Standards even with full conversion, further NO_x control may be necessary to meet future standards.

Most proposed LBG-fired combined cycles utilize the basic cycle configuration illustrated in Figure 1. However, a recent study of several alternative cycle arrangements has shown the potential for significantly improved performance (7,8). One very promising alternative cycle is the reheat cycle shown in Figure 3. In this cycle the hot combustion products from the main gas turbine combustor are partially expanded in a high pressure turbine and then reheated in a second combustor before being expanded to atmosphere. The reheat combustor could be fired with LBG from the main high pressure gasifier throttled to the proper pressure, or (more efficiently) from a second midpressure gasifier as shown in Figure 3. The performances of a reheat cycle with 1366 K (2000 F) turbine inlet temperatures and a basic cycle with the same turbine inlet temperature are shown in Figure 4. Reheating increases the gas turbine subcycle efficiency, particularly at high pressure ratios. It also increases the steam bottoming cycle efficiency by increasing the turbine exhaust temperature, thus allowing higher temperature steam to be generated. The result is a substantial increase in overall cycle performance. The reheat combustor also provides the opportunity to reprocess the NO_x formed in the main combustor through a second reaction zone.

The design and operation of low NO_x combustors for LBG-fired combined cycle power plants has been considered by several investigators (3,4,7,8,11, 12). The development of low NO_x combustors for LBG-fired combined cycle power plants is the subject of EPA Contract 68-02-2196. Several alternative combustor designs are being investigated analytically and experimentally in a search for the lower bounds of pollutant emissions limited by chemistry and practical mixing constraints (12,13). Catalytically supported combustion is one of the concepts being considered.

The remainder of this paper discusses some recent measurements of nitrogenous specie processing in an atmospheric pressure LBG-fired catalytic reactor. Three experiments are discussed. In the first experiment a LBG with NH_3 concentration comparable to that obtained from a cold gas cleanup system was fired over a range of stoichiometries. The oxidant was air diluted with N_2 to maintain the equilibrium adiabatic flame temperature at 1473 K. In the second experiment the NH_3 was replaced by an equal amount of NO to simulate a reheat combustor reprocessing NO_x from a high pressure combustor. The third experiment utilized CH_4 doped with NH_3 as the fuel, and was included to compare results from this catalytic reactor with those of prevoius investigations firing CH_4 in other reactor designs.

SECTION 2

EXPERIMENTAL APPARATUS

CATALYTIC REACTOR

The catalyst used in these tests was a platinum coated graded cell monolith supplied by the Acurex Corporation. The desirable features of the graded cell catalyst have been discussed previously (14) and include:

- Consistent low temperature light-off
- High throughput without blowout
- Low CO emissions

The catalyst used for these tests was 25 mm (1.0 in.) diameter and included three 25 mm (1.0 in.) long segments of varying cell sizes. Each segment consisted of a hexagonal cell Du Pont alumina monolith washcoated with Du Pont alpha alumina and subsequently loaded with platinum. The cell sizes and platinum loadings were as follows:

Axial Position	Cellsize mm	Platinum Loading wt %
Upstream	7	6.3 - 6.4
Center	5	5.2 - 5.4
Downstream	3	2.1

The maximum recommended temperature for this catalyst is 1588 K (2400 F). Type K thermocouples were cemented in two of the cells in the downstream segment to monitor maximum monolith temperature.

The 25 mm (1.0 in.) monolith diameter was chosen to be compatible with the characteristics of the LBG synthesizing system described in the next section. This relatively small diameter raises two important questions:

- Is the system dominated by edge effects?
- Will heat loss from the periphery be significant and prevent the attainment of near-adiabatic conditions?

The gas passages near the center are bounded on all sides by platinum-coated monolith surfaces. In contrast, the outermost gas passages are partially bounded by the surrounding supporting material. The reactants passing through the outer passages will thus encounter a reduced amount of catalytically active surface area and may process the reactants differently. This "edge effect" is aggravated by large cell sizes and small overall monolith diameters such as the upstream segment of the monolith tested here. The ratio of surrounding tube surface area to monolith surface area is an index of the magnitude of edge effects. It can be shown that this ratio is approximately 0.5 d/D where D is the monolith outside diameter and d is the hexagonal cell size. For the catalyst segments utilized here, these ratios were 0.14, 0.10 and 0.06. Thus, the surface area presented by the surrounding tube surface was small compared to monolith surface area.

To minimize heat losses and approximate adiabatic conditions, the catalyst was mounted in a refractory tube and electrically backheated. The catalyst and its housing are shown schematically in Figure 5. The temperature between the refractory tube and the heating element was measured with a thermocouple and the heating power was controlled to maintain this temperature near the equilibrium adiabatic flame temperature of the reactants.

The reactants passed through a sintered stainless steel disc immediately upstream of the catalyst. This disc had three functions:

- Flame arresting in the event of flashback
- Velocity profile smoothing
- Temperature profile smoothing

A thermocouple downstream of the disc measured reactant temperature. Flashback was observed as a rapid rise in this temperature as a flame front moved toward the disc.

The combustion products discharged into a 100 mm (4.0 in.) exhaust stack and a water-cooled stainless steel sample probe was installed to measure combustion product concentrations. The outside diameter of the probe was 9.4 mm (3/8 in.) and the probe tip was 44 mm (1-3/4 in.) from the downstream catalyst face.

FLOW SYSTEM AND INSTRUMENTATION

The flow system and instrumentation utilized in these experiments are shown in Figure 6. LBG was synthesized by blending together high purity gases from cylinders. All gases were high purity grade (99.97 percent or better) with the exception of CO (99.0 percent). NH_3 and NO were supplied as custom grade mixtures (±2 percent accuracy) to facilitate metering: 1.0 percent NH_3 in CH_4 and 8570 ppm NO in N_2. Oxidant was supplied as dry air in pressurized cylinders. Oxygen concentration ranged from 19.9 to 23.1 percent and was adjusted by nitrogen addition to the concentration required to achieve the desired flame temperature.

All gases were metered with sapphire jewel critical orifices. Pressures upstream of the orifices were measured with high accuracy (±0.11 percent full-scale) variable capacitance pressure transducers and the downstream pressures were maintained constant. All transducers were calibrated weekly against a common laboratory reference. The flow rate through each orifice was calibrated by filling an evacuated tank. The total inaccuracy in each gas flow rate was less than 0.5 percent.

Reactants were preheated electrically to a maximum of 773 K. The reactant temperature was monitored with the thermocouple downstream of the sintered disc and the preheat power was adjusted to achieve the desired temperature.

Combustion products were sampled with a water-cooled stainless steel probe and analyzed for O_2, CO_2, CO, NO, NO_x, NH_3 and HCN. The sample train components were constructed entirely of stainless steel, glass and Teflon. NH_3 and HCN were measured by bubbling known volumes of combustion products through three water baths in series. The NH_3 and HCN were absorbed in the water and measured with Orion specific ion instrumentation. The accuracy of this procedure was checked by synthesizing known concentrations of NH_3 and HCN in air and processing the mixtures as combustion products. Agreement between calculated and measured concentrations was consistently within 10 percent.

The other product species were monitored continuously. The sample was dried to 273 K dewpoint in a cyclone water trap located as close as possible to the sample probe. Residence time between probe and trap was less than 0.5 sec. Residence time between trap and instruments was less than 2.0 sec. The chemiluminescent analyzer was a Thermo Electron Model 10 A equipped with a stainless steel NO_x converter operated at 1073 K. CO and CO_2 were measured with Beckman NDIR analyzers and the O_2 was measured with a Taylor paramagnetic instrument. These readings were used to calculate combustion efficiency and close the carbon balance.

SECTION 3

EXPERIMENTAL RESULTS

LBG TESTS

The term low Btu gas does not refer to a specific gas composition, but rather to a family of fuel gases produced by reforming coal with air and steam. The composition of LBG depend upon:

- Coal composition
- Gasifier design and operating conditions
- Air and steam flow rates
- Product gas cleanup system

The heating value of LBG may range from 16,000 to 41,000 J/m^3 (80 to 200 Btu/ft^3) and the primary combustible specie are CO and H_2. The ratio of CO to H_2 concentrations ranges from 0.5 to 2. Hydrocarbon fuel gases (normally CH_4) may also be present in quantities up to 10 percent, and nitrogen is the primary diluent comprising 35 to 55 percent of the fuel gas with the remaining diluents being CO_2 and H_2O. Trace amounts of H_2S, COS and NH_3 may also be present, since these specie are not entirely removed from the product gas by the gas cleanup system.

The relationship between LBG composition and combustor performance is currently under investigation as part of EPA Contract 68-02-2196 (13). For the experiments reported in this paper the following LBG composition was synthesized using the metering system described earlier:

CO = 20 percent
H_2 = 20 percent
CH_4 = 5 percent
N_2 = 55 percent

The higher heating value of this synthesized LBG is 37,200 J/m^3 (182 Btu/ft^3) and the adiabatic equilibrium flame temperature at stoichiometric conditions is 2135 K. Since this temperature is higher than the maximum acceptable catalyst temperature of 1588 K, it was necessary to dilute the reactants with nitrogen to ensure that this temperature was never exceeded within the catalyst bed.

An initial test series was carried out to select suitable catalyst operating parameters for troublefree operation. This LBG composition was found to light-off consistently at room temperatures under a wide range of both fuel-rich and fuel-lean conditions. Under fuel-lean conditions with adiabatic equilibrium temperatures in excess of 1273 K and back heating the catalytic reactor to control heat loss, the catalyst temperatures rose to essentially adiabatic equilibrium flame temperatures. Measured exhaust CO concentrations were less than 50 ppm (often less than 5 ppm). Measured concentrations of CO_2 and O_2 confirmed complete combustion within the limits of experimental error. Under similar but fuel-rich conditions the catalyst temperature also reached adiabatic equilibrium flame temperature. When excess catalyst heat loss or low adiabatic equilibrium flame temperatures prevented the attainment of 1273 K exhaust CO concentrations rose substantially, indicating incomplete combustion.

Maximum turbine inlet temperatures (TIT) for state-of-the-art stationary gas turbines are in the range of 1400 to 1500 K (2000 to 2200 F). As turbine cooling technology improves, the maximum TIT is expected to increase and 1700 K (2600 F) has been projected for the next generation of gas turbines for utility use (6). An adiabatic equilibrium flame temperature of 1473 K (2200 F) was selected for the experimental investigation based upon the information on TITs and the operating characteristics of the catalyst.

The catalytic reactor operates with premixed reactants, and it is possible for a flame front to propagate upstream through the reactants from an ignition source on the catalyst under certain conditions. It is not sufficient that the average reactant velocity be greater than the mixture flame speed since flashback can occur in the boundary layer along the tube wall or in other low velocity regions. In these experiments the average reactant velocity was maintained at 3.0 m/sec (10.0 ft/sec) and this was sufficient to prevent flashback. This corresponds to a space velocity of 1.4×10^5/hr and an average catalyst residence time of 13 msec. The heat release rate was 3.9×10^6 J/hr (3700 Btu/hr) or 1.0×10^{11} J/m^3 (2.7×10^6 Btu/ft^3).

Ammonia Processing

An LBG cleaned with a cold sulfur removal process contains low concentrations of ammonia typically in the range of 100 to 500 ppm. The LBG composition discussed above was doped with 471 ppm NH_3 and mixed with air and nitrogen to adjust the adiabatic equilibrium flame temperature before passing to the catalytic reactor. Figure 7 shows the measured concentrations of NO, NO_x, NH_3 and HCN as ppm dry and the calculated percentage conversion of the input ammonia to the various XN specie. For lean mixtures complete conversion of the input ammonia is constant due to the nitrogen dilution, but under rich conditions complete conversion increases because the LBG fraction of the reactants increases.

Under fuel-lean conditions approximately 90 percent of the input ammonia is converted to NO_x. As the stoichiometry is reduced below 100 percent of the theoretical air required for complete combustion, the fraction of NH_3 converted to NO decreases rapidly to essentially zero at 52 percent theoretical air. As the stoichiometry is reduced, the fraction of ammonia passing through the reactor increases from near zero at 100 percent theoretical air to over 50 percent at 44 percent theoretical air. HCN is produced at stoichiometries less than 80 percent theoretical air, and at 44 percent theoretical air the HCN concentration corresponds to almost 50 percent conversion of the NH_3 in the original reactants.

A low NO_x combustor might well consist of a staged heat release system in which the products of a fuel-rich primary zone are burned out in a lean secondary zone. The challenge to the combustor designer is to minimize the conversion or retention of the NO, NH_3 or HCN in the primary zone products to NO_x in the lean burnout zone. It has been shown that under certain conditions large portions of these nitrogenous compounds can be converted to NO_x in lean combustion zones (13). Consequently, it is of considerable interest to minimize the total XN specie exiting the rich primary zone. The percentage of input ammonia converted to ΣXN specie is plotted in Figure 8 as a function of percentage theoretical air. Under rich conditions

ΣXN was calculated as the sum of NO, NH_3 and HCN, and under fuel-lean conditions it was assumed to be entirely NO_x. It can be seen that for a range of stoichiometries between 60 and 100 percent theoretical air the ΣXN is minimized. It should be noted that the operation of the catalyst in this range requires the addition of substantial amounts of diluents (in this instance nitrogen) to reduce flame temperatures. In practical systems flame temperatures could be limited either by the recirculation of combustion products or by radiantly cooling the primary section in a similar manner to that proposed by Kesselring (14). Adiabatic combustion of this LBG in air without temperature control requires stoichiometries richer than 40 or leaner than 230 percent theoretical air to avoid temperatures in excess of 1473 K. Under both conditions ΣXN is essentially 100 percent.

Nitric Oxide Processing

A reheat combustor incorporated in a combined cycle power plant would utilize the partially vitiated lean combustion products exiting the high pressure turbine as oxidant and additional LBG as fuel. The NO produced in the high pressure combustor would be reprocessed through a second reaction zone and could be partially reduced to N_2. Thus, the reheat combustor offers the potential for both NO_x control as well as a gain in overall cycle efficiency. As a first order simulation of an LBG-fired reheat combustor the LBG composition referred to previously was doped with 471 ppm NO and fired in the catalytic reactor under the same conditions as those described for the ammonia doping tests. Since no NH_3 was present in the reactants, this experiment simulates the combustion of an LBG with all the NH_3 removed. It could be speculated that if the premixing occurred under the correct temperature conditions that the ammonia present in an LBG gas could homogeneously reduce the NO produced in the high pressure combustor.

Figure 9 presents the results of the experiments involving NO doping in the same format as Figure 7. Combustion products were analyzed for ammonia and HCN at all stoichiometries richer than 120 percent theoretical air. However, concentrations were found to be zero within in the limits of the experimental techniques. Under fuel-lean conditions essentially all of the NO entering with the reactants exited as NO_x. However, under rich conditions the catalytic reactor was an effective method of reducing NO. Between 60 and 80 percent theoretical air 78 to 85 percent of the NO was removed and at stoichiometric conditions only 50 percent of the input NO was retained in the exit stream.

METHANE TESTS

Several investigators have tested catalytic reactors firing hydrocarbon fuels doped with NH_3 (14,15), and it is of interest to operate the catalytic reactor tested here with similar fuels to provide a comparison with other investigations. Consequently, the catalytic reactor was fired with CH_4 doped with NH_3 to give a concentration of 9417 ppm NH_3 in CH_4, and the reactants were diluted with N_2 as before to adjust the adiabatic equilibrium flame temperature. Similar test runs were conducted with methane as those described earlier for LBG to identify suitable catalyst operating parameters. With LBG light-off occurred consistently at room temperatures. However, it was found necessary to preheat the methane mixtures to between 573 and 673 K in order to sustain ignition. With LBG the reactant velocity (space velocity) was required to be high to avoid flashback. If the catalytic reactor was operated at similar velocities with methane, blowout occurred and it was found necessary to reduce the space velocity to 4.7×10^4/hr for sustained ignition. Flashback was not a problem with the methane mixtures.

Measured nitrogenous specie concentrations are presented in Figures 10 and 11 in the same format as those described earlier. In comparison with the LBG data, the actual concentrations are much higher due to the higher concentration of ammonia in the reactants. However, the percentage of ammonia converted to the various XN specie to the various nitrogenous specie are similar. The ΣXN also exhibit the same broad minimum over the range 70 to 100 percent theoretical air.

SECTION 4

DISCUSSION

The results presented in this paper are part of a more general study to develop low emission combustors for application to advanced power systems (8). The approach being taken in this study involves both numerical and experimental investigations to define combustor design parameters to minimize NO_x production from simulated LBG gases containing trace quantities of NH_3 and H_2S. It is generally recognized that the most cost-effective technique for controlling NO_x emissions from stationary sources is to modify the combustion process in such a way as to prevent NO formation. For fuels containing nitrogen species (other than N_2) this normally involves dividing the total heat release process into two zones. Since it is known that fuel nitrogen conversion to NO is minimized under fuel-rich conditions, the fuel is caused to react in the first zone with less than the stoichiometric air requirement. The remainder of the air is provided in the second zone to complete the heat release process. Minimum NO_x emissions require that:

- The rich combustion products formed in the initial zone contain minimum quantities of nitrogen specie such as NO, NH_3 or HCN.
- The rich combustion products are burned in such a way to prevent thermal NO production (oxidation of molecular nitrogen) and to maximize N_2 production from the NO, NH_3 and HCN which might be present in the reactants exiting from the first zone prior to second stage burnout.

Thermal NO production can be essentially eliminated in the second heat release zone if peak temperatures never exceed 1800 K (2800 F). Consequently, the investigation to define combustor design parameters for minimum NO_x

emissions are concentrating upon the minimization of XN specie in rich combustion products and those factors which maximize N_2 production during the burnout of these products.

Thermodynamic calculations indicate that equilibrium ΣXN concentration in rich combustion products of fossil fuels and air is less than 10 ppm under optimum conditions. This provides a target emission level for advanced combustors; however, typical emission levels far exceed this level suggesting that the process of N_2 production is kinetically limited. Two competing reaction paths (16) occur under combustion conditions which account for the production of N_2 or NO. These are:

$$NX + Oxidant \rightarrow NO + \ldots\ldots \underline{A}$$

$$NX + NY \rightarrow N_2 + \ldots\ldots \underline{B}$$

The precise details of Path B which predominates under fuel-rich conditions are open to question. When ammonia is the initial fuel nitrogen specie, it will break down to give NH_i which will then produce N_2 via Path B. For high temperature flames Morley (17) has shown that regardless of their nature, nitrogen compounds are quantatively converted to HCN in the reaction zone of premixed rich hydrocarbon flames. Two possible mechanisms for HCN formation are:

$$CH_3 + NO \rightarrow NH_3NO \rightarrow CH_2NOH \rightarrow HCN \qquad (1)$$

or

$$CH + NO \rightarrow HCN + O \qquad (2)$$

The subsequent oxidation of HCN via NCO as a possible intermediate would then allow interconversion of the three major stable nitrogenous specie via

$$HCN + OH \rightleftarrows CN + H_2O \qquad (3)$$

$$CN + OH \rightleftarrows NCO + H \qquad (4)$$

$$NCO + H \rightleftarrows NH + CO \qquad (5)$$

$$NH_i + H \rightleftarrows NH_{i-1} + H_2 \qquad (6)$$

$$N + OH \rightleftarrows NO + H \qquad (7)$$

$$N + NO \rightleftarrows N_2 + O \qquad (8)$$

If hydrocarbon specie are present other reactions are possible sources of HCN, such as

$$CH + N_2 \rightleftarrows HCN + N \tag{9}$$

or

$$CH_2 + N_2 \rightleftarrows HCN + NH \tag{10}$$

Fuels containing bound nitrogen normally contain sulfur compounds and Wendt (18) and co-workers have shown that the presence of sulfur specie may affect the interconversion of nitrogenous specie in rich combustion products.

The combustor designer is faced with practical constraints such as size, pressure drop, construction cost and maintainability, but the basic design parameters controlling ΣXN emission from the rich first stage are the method of fuel/air contacting, and the time, temperature, and stoichiometric history of the reactants. Numerical investigations (19) associated with a search for the lower bounds of fuel nitrogen conversion involving ideal fuel/air contacting have indicated several potentially promising combustor concepts. Two of these concepts are illustrated in Figure 12. If the conversion of NH_3, NO and HCN to N_2 in rich products is kinetically limited, then the rate of this conversion can be accelerated by increasing the temperature of the reactants (20). An idealized combustor design (see Figure 12a) which relies upon heat transfer feedback in the first stage zone is one method of achieving this effect while ensuring that the second stage temperatures are too low to allow thermal NO production. The rate of ΣXN decay in rich combustion products is not only dependent upon temperature, but also upon stoichiometry and the optimum primary reactor might well include distributed air addition to vary stoichiometry as a function of time (see Figure 12b).

The idealized combustor concepts illustrated in Figure 12 do not indicate how the fuel and air are mixed or how ignition stability is achieved. The experimental results presented in this paper concern one method of fuel/air contacting — the use of a catalytic reactor. Results are presented which show the stable nitrogenous specie produced as a function of reactant stoichiometry for a constant adiabatic flame temperature when a simulated LBG and methane were doped with NH_3 and when the LBG was doped with NO. The results with ammonia doping are consistent with the kinetic mechanisms described above and are similar to results obtained with premixed flat flames. However, it is somewhat surprising that no HCN or ammonia was observed with NO doping.

Under fuel-rich conditions Path B predominates and N_2 is produced, resulting in low NO emissions. However, if the reactants are too rich those reactions involving HCN oxidation predominate and although NO is no longer produced, the NH_3 present in the original reactants either does not decompose or produces HCN. The ratio of NH_3 to HCN will depend upon reactant temperature as well as stoichiometry. It can be speculated that the failure to form either HCN or NH_3 when LBG is doped with NO may be associated with the low reactant temperature or the influence of the catalyzed heterogenous reactions.

Recognizing the preliminary nature of the results, it appears that a catalytic reactor offers considerable promise for utilization in low emission combustors firing LBG. Future effort will concentrate upon determining the effect of LBG composition on NH_3 and NO processing in catalytic reactors since it has been shown that fuel composition has a significant effect upon fuel NO production in diffusion flames (13). Investigations are currently underway to couple a catalytic reactor to a second stage burnout reactor to investigate its potential for application in the combustor concepts shown in Figure 12.

REFERENCES

1. Evaluation of Phase 2 Conceptual Designs and Implementation Assessment Resulting from the Energy Conversion Alternatives Study (ECAS), prepared under Interagency Agreement E(49-18)-1751, NASA Report No. TM X-73515.

2. Shaw, H., Cerkanowicz, A.E., and Tung, S.E. Environmental Assessment of Advanced Energy Conversion Technologies - Interim Report, Vol. 1, State-of-the-art. Contract No. 68-02-2146, U.S. Environmental Protection Agency, Cincinnati, Ohio, 1977.

3. Harris, L.P., and Shah, R.P. Energy Conversion Alternatives Study (ECAS), General Electric Phase II Final Report: Vol. II, Advanced Energy Conversion Systems - Conceptual Designs: Part 3, Open Cycle Gas Turbines and Open Cycle MHD, General Electric Report No. SRD-76-064-2, NASA Report No. NASA CR-134949, 1976.

4. Beecher, D.T., et. al. Energy Conversion Alternative Study (ECAS), Westinghouse Phase II Final Report: Vol. II - Combined Gas-Steam Turbine Plant Using Coal-Derived Fuel, Westinghouse Report No. 76-9E9-ECAS-R2v.2, NASA Report No. NASA CR-134942, 1976.

5. Fluor Engineers and Constructors, Inc. Gasification-Combined-Cycle Power Plants. EPRI Journal, July/August, 1978. p. 43

6. Robson, F.L., Blecher, W.A., and Giramonti, A.J. Combined-Cycle Power Systems. EPA-600/2-76-149, U.S. Environmental Protection Agency, Washington, DC, 1976. p. 359

7. Tyson, T.J., Heap, M.P., Kau, C.J., Folsom, B.A., and Brown, N.D. Low NO_x Combustion Concepts for Advanced Power Generation Systems Firing Low-Btu Gas. EPA-600/2-77-235, U.S. Environmental Protection Agency, Washington, D.C., 1977.

8. Folsom, B.A., Corley, T.L., Lobell, M.H., Kau, C.J., Heap, M.P., and Tyson, T.J. Evaluation of Combustor Design Concepts for Advanced Energy Conversion Systems. In: Proceedings of the Second Stationary Source Combustion Symposium, v.5, Addendum, EPA-600/7-77-073, July, 1977.

9. Myerson, A.L. The Reduction of Nitric Oxide in Simulated Combustion Effluents by Hydrocarbon-Oxygen Mixtures. In: 15th Symposium (International) on Combustion, The Combustion Institute, Pittsburgh, Pennsylvania, 1975.

10. Muzio, L.J., Arano, J.K., and Teixeira, D.P. Gas Phase Decomposition of Nitric Oxide in Combustion Products. In: 16th Symposium on Combustion, The Combustion Institute, 1977. p. 199

11. Martin, G.B. NO_x Considerations in Alternate Fuel Combustion. EPA-600/1-76-149, U.S. Environmental Protection Agency, Washington, DC, 1976. p. 373

12. Heap, M.P., et al. Environmental Aspects of Low Btu Gas Combustion. In: 16th Symposium on Combustion, The Combustion Institute, 1977. p. 535

13. Folsom, B.A., Courtney, C.W., Heap, M.P., and Martin, G.B. The Effect of LBG Composition and Combustor Characteristics on Fuel NO_x Formation. In: 14th Annual International Gas Turbine Conference, A.S.M.E., Gas Turbine Division, March 1979.

14. Kesselring, J.P., Krill, W.V., Kendall, R.M. Design Criteria for Stationary Source Catalytic Combustors. EPA-600/7-77-073c, U.S. Environmental Protection Agency, Washington, DC. July 1977. p 193

15. Matthews, R.D., and Sawyer, R.F. Fuel Nitrogen Conversion and Catalytic Combustion. Presented at the Western States Section, The Combustion Institute, Paper No. 77-40, LBL-6396, Fall Meeting, Palo Alto, CA, October, 1977.

16. De Soete, G. La Formation Des Oxydes D'Azote Dans La Zone D'Oxydation Des Flammes D'Hydrocarbures. No. 23 309, June 1975, Institut Francais De Petrole, France.

17. Morley, C. The Formation and Destruction of Hydrogen Cyanide from Atmospheric and Fuel Nitrogen in Rich Atmospheric-Pressure Flames. Combustion and Flame, Vol. 27, 1976. pp. 189-204

18. Wendt, J.O.L., Corley, T.L., Morcomb, J.T. Interactions Between Sulfur Oxides and Nitrogen Oxides in Combustion Processes. In: Proceedings of the Second Stationary Source Combustion Symposium, Vol. IV., Fundamental Combustion Research. EPA-600/7-77-073d, July 1977. p 101

19. Tyson, T.J., Heap, M.P., Corley, T.L., and Kau, C.J. Fundamental Combustion Research Applied to Pollutant Control. First Annual Report, EPA Contract 68-02-2631. In preparation.

20. Sarofim, A.F., Pohl, J.H., Taylor, B.R. Mechanisms and Kinetics of NO_x Formation Recent Developments. Paper presented at 69th Annual Meeting AIChE, Chicago. November, 1976.

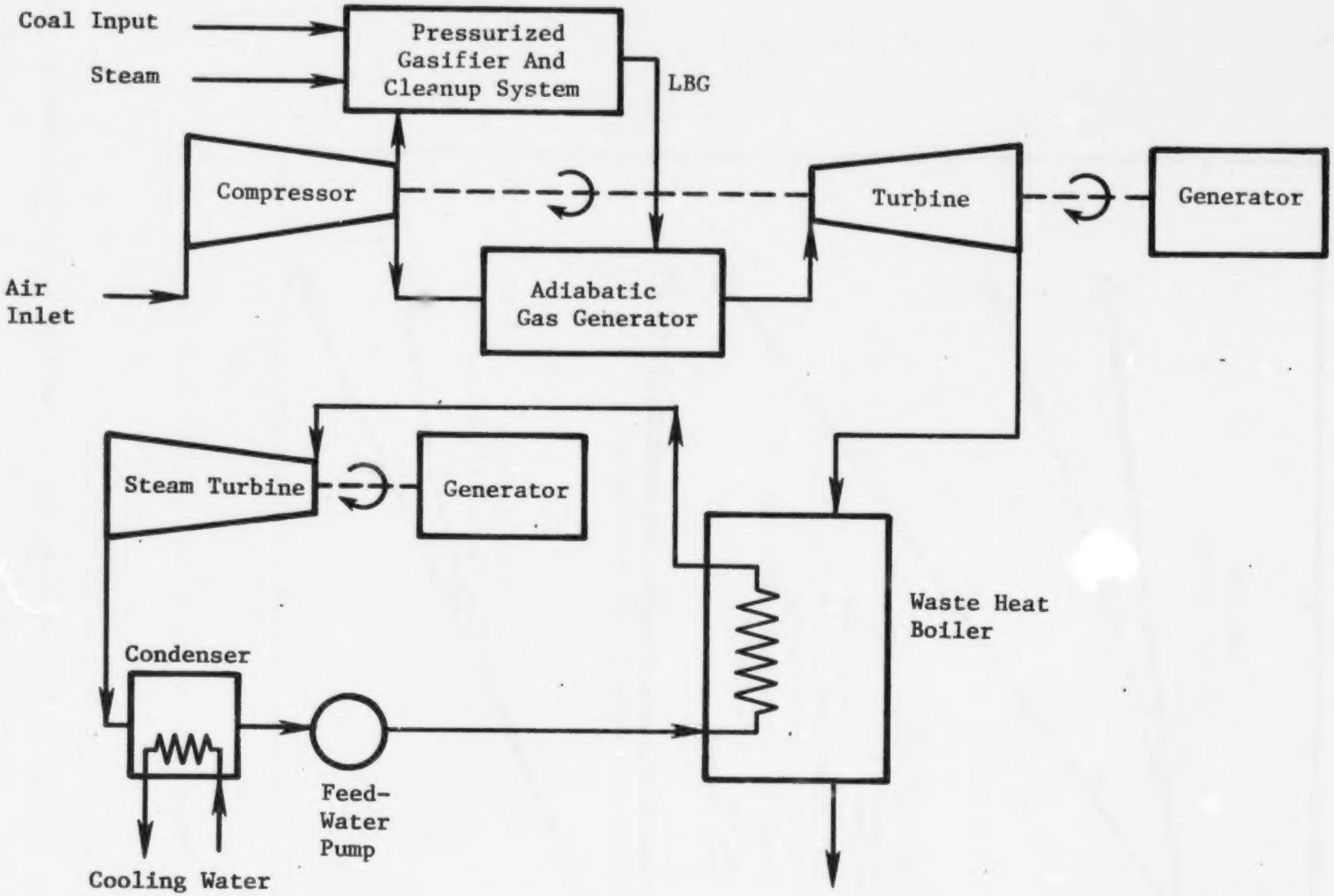

Figure 1. Simplified Schematic of Basic LBG-Fired Combined Cycle

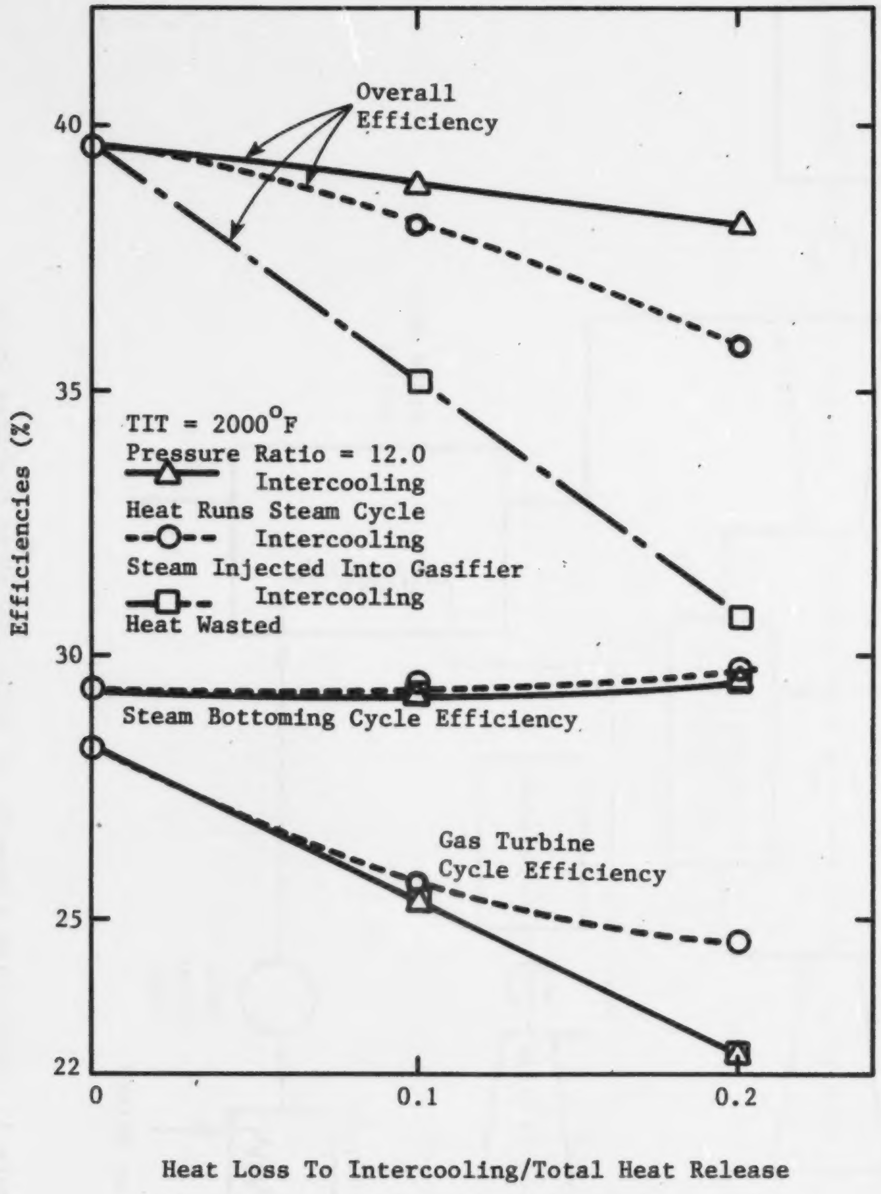

Figure 2. Effect of LBG Intercooling on Combined Cycle Performance

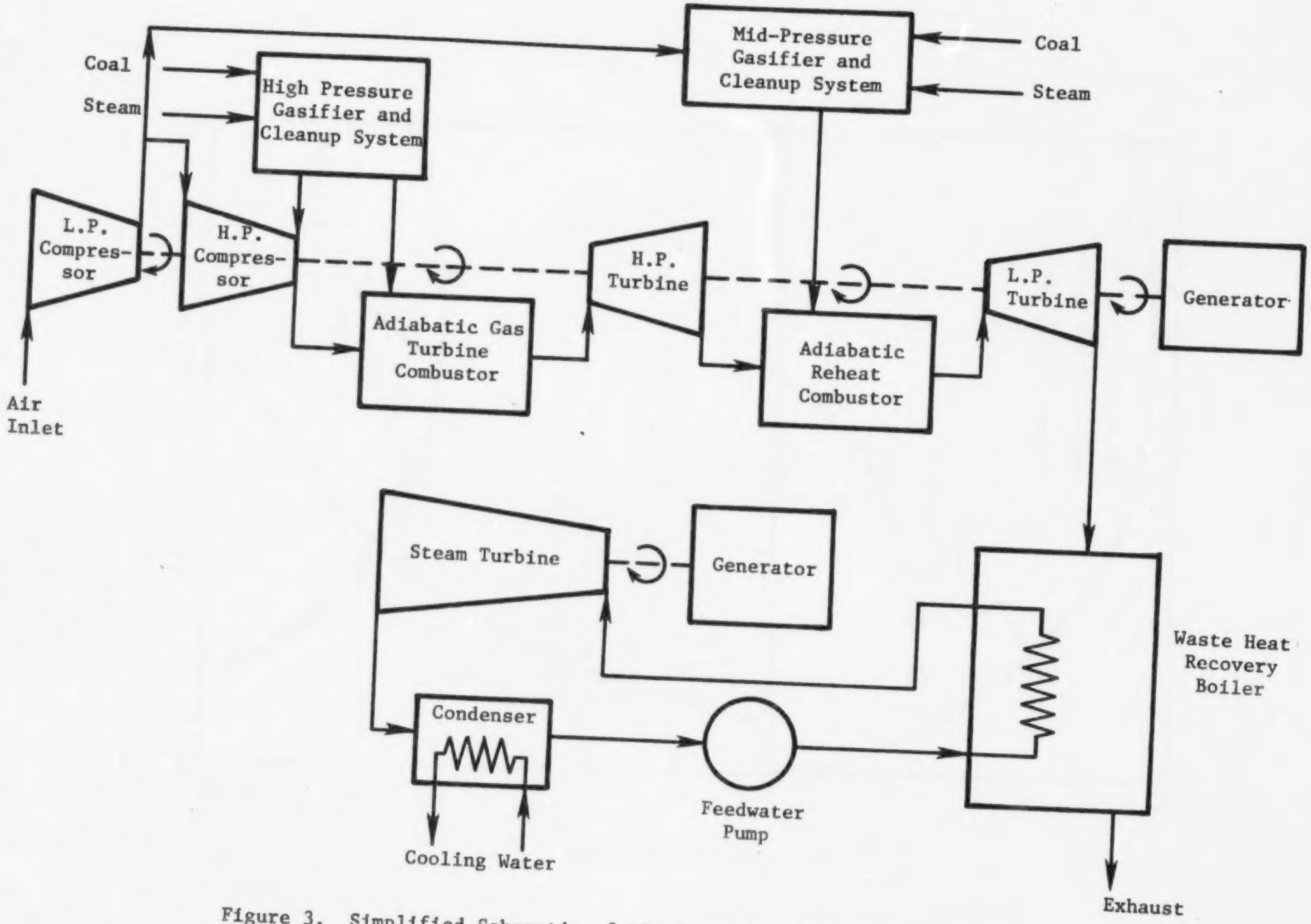
Mid-Pressure Gasifier and Cleanup System
Coal
Steam
Coal
Steam
High Pressure Gasifier and Cleanup System
L.P. Compres-sor
H.P. Compres-sor
H.P. Turbine
L.P. Turbine
Generator
Adiabatic Gas Turbine Combustor
Adiabatic Reheat Combustor
Air Inlet
Steam Turbine
Generator
Waste Heat Recovery Boiler
Condenser
Feedwater Pump
Cooling Water
Exhaust

Figure 3. Simplified Schematic of LBG-Fired Combined Cycle With Reheat

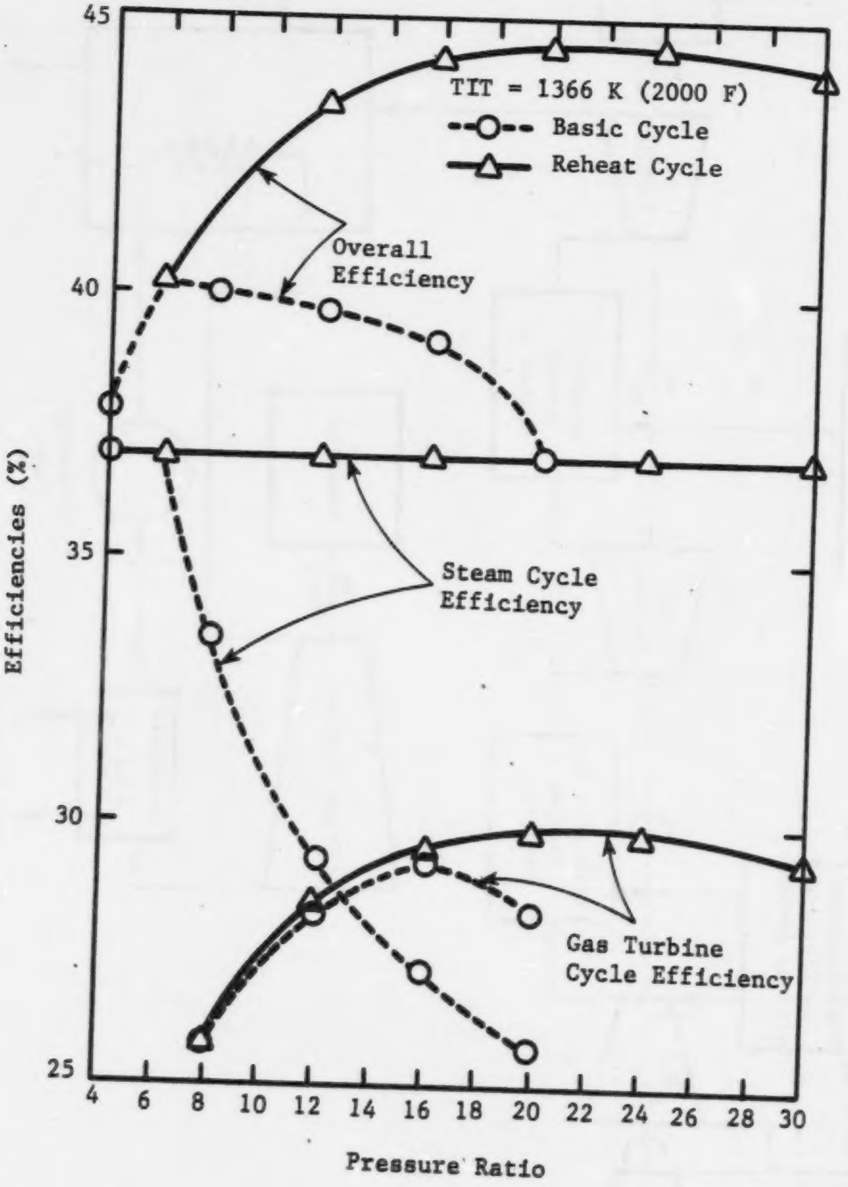

Figure 4. LBG-Fired Combined Cycle: Basic Cycle Versus Reheat

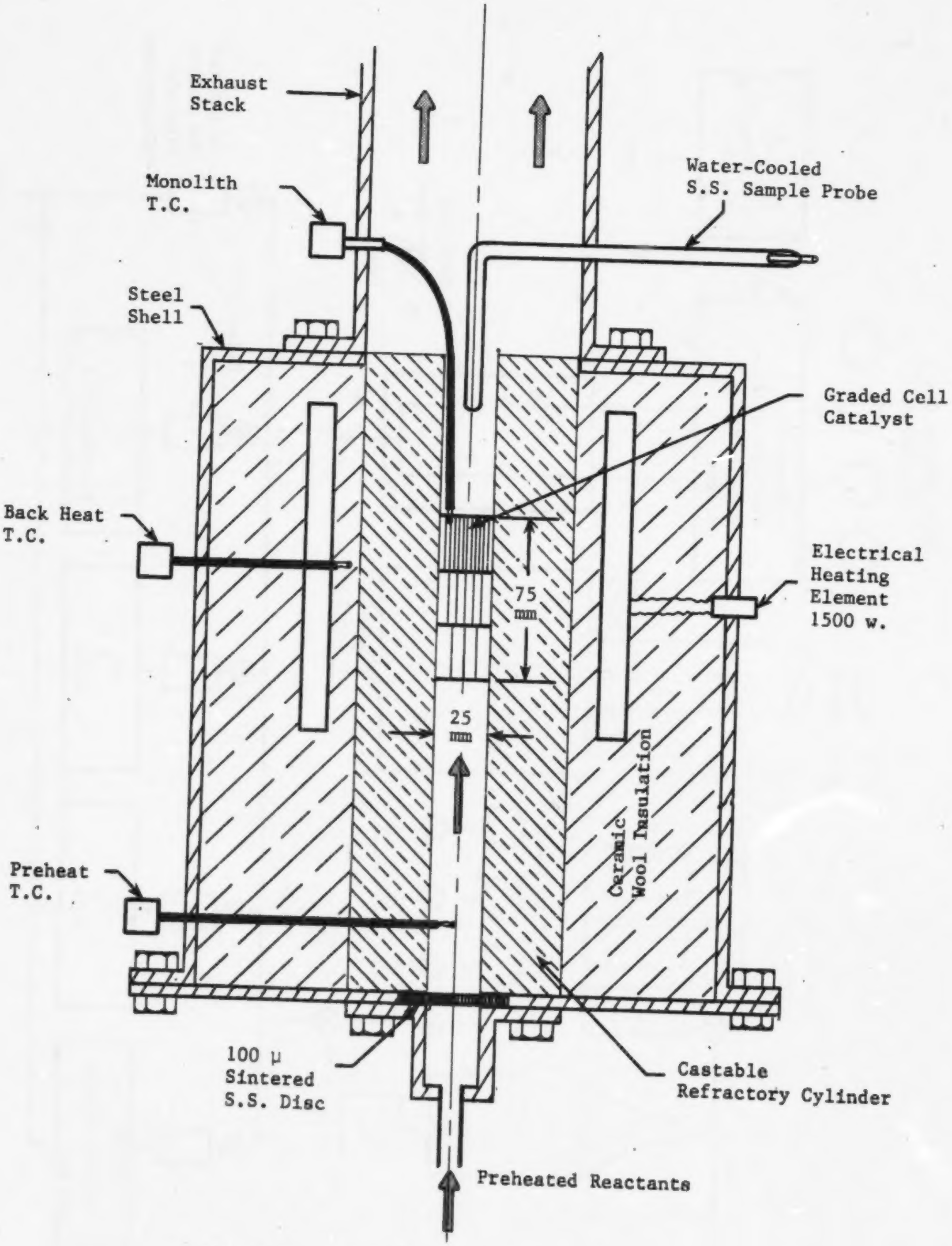

Figure 5. Catalytic Reactor and Housing

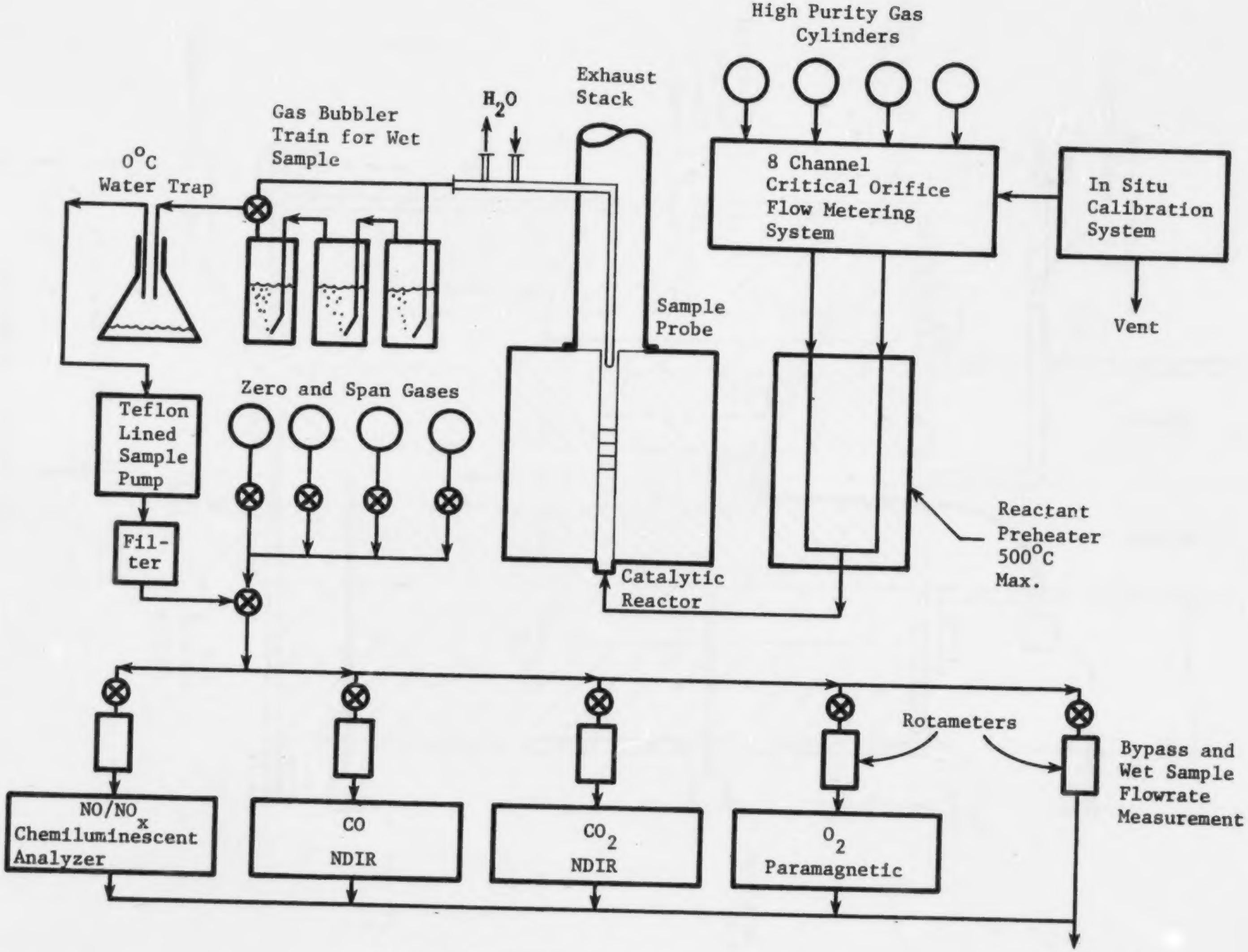
High Purity Gas Cylinders
8 Channel Critical Orifice Flow Metering System
In Situ Calibration System
Vent
Exhaust Stack
H_2O
Gas Bubbler Train for Wet Sample
0°C Water Trap
Sample Probe
Reactant Preheater 500°C Max.
Catalytic Reactor
Zero and Span Gases
Teflon Lined Sample Pump
Fil-ter
Rotameters
Bypass and Wet Sample Flowrate Measurement
NO/NO_x Chemiluminescent Analyzer
CO NDIR
CO_2 NDIR
O_2 Paramagnetic
Vent

Figure 6. Flow System and Instrumentation

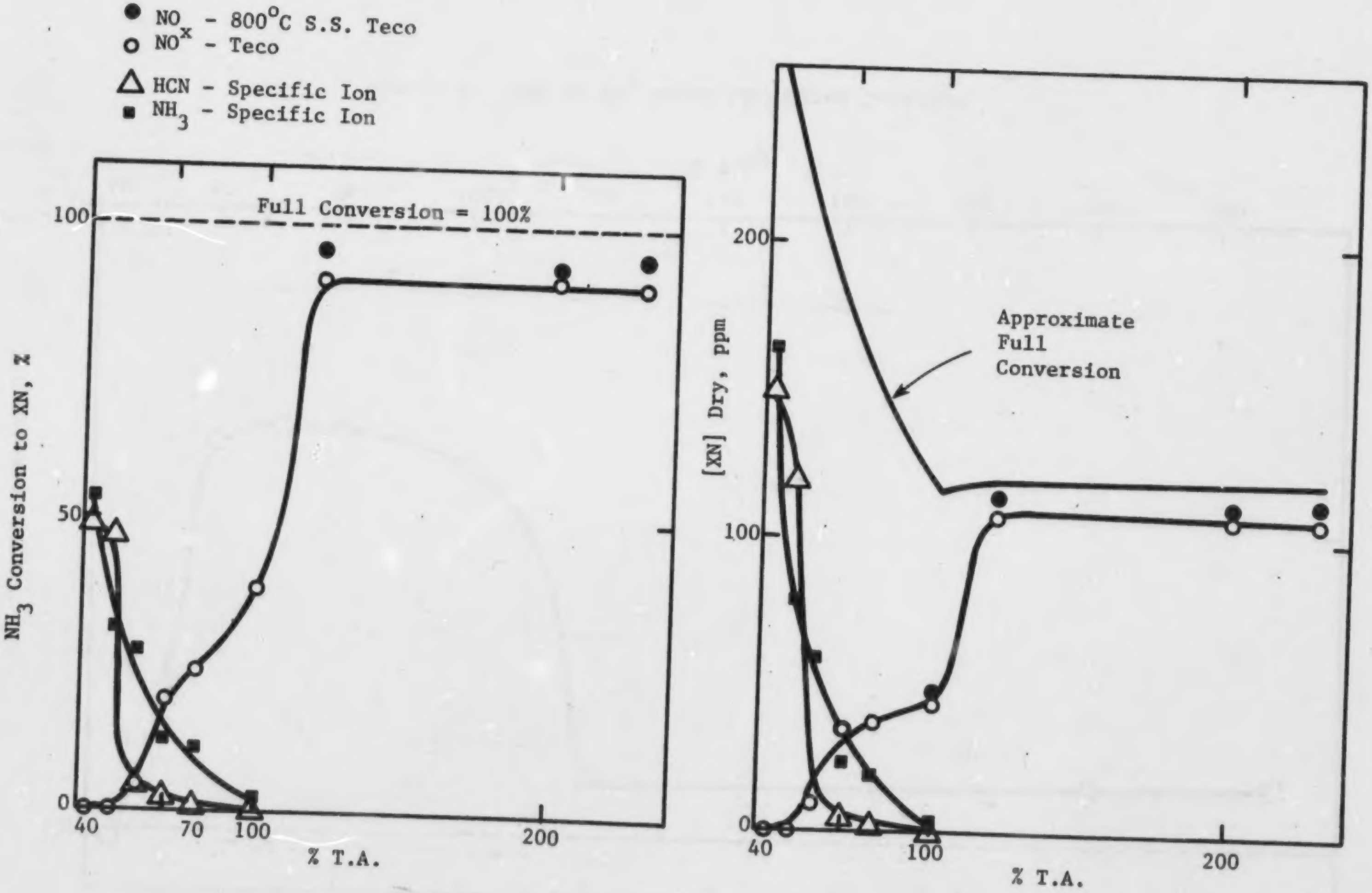

Figure 7. NH$_3$ Processing in LBG-Fired Catalyst

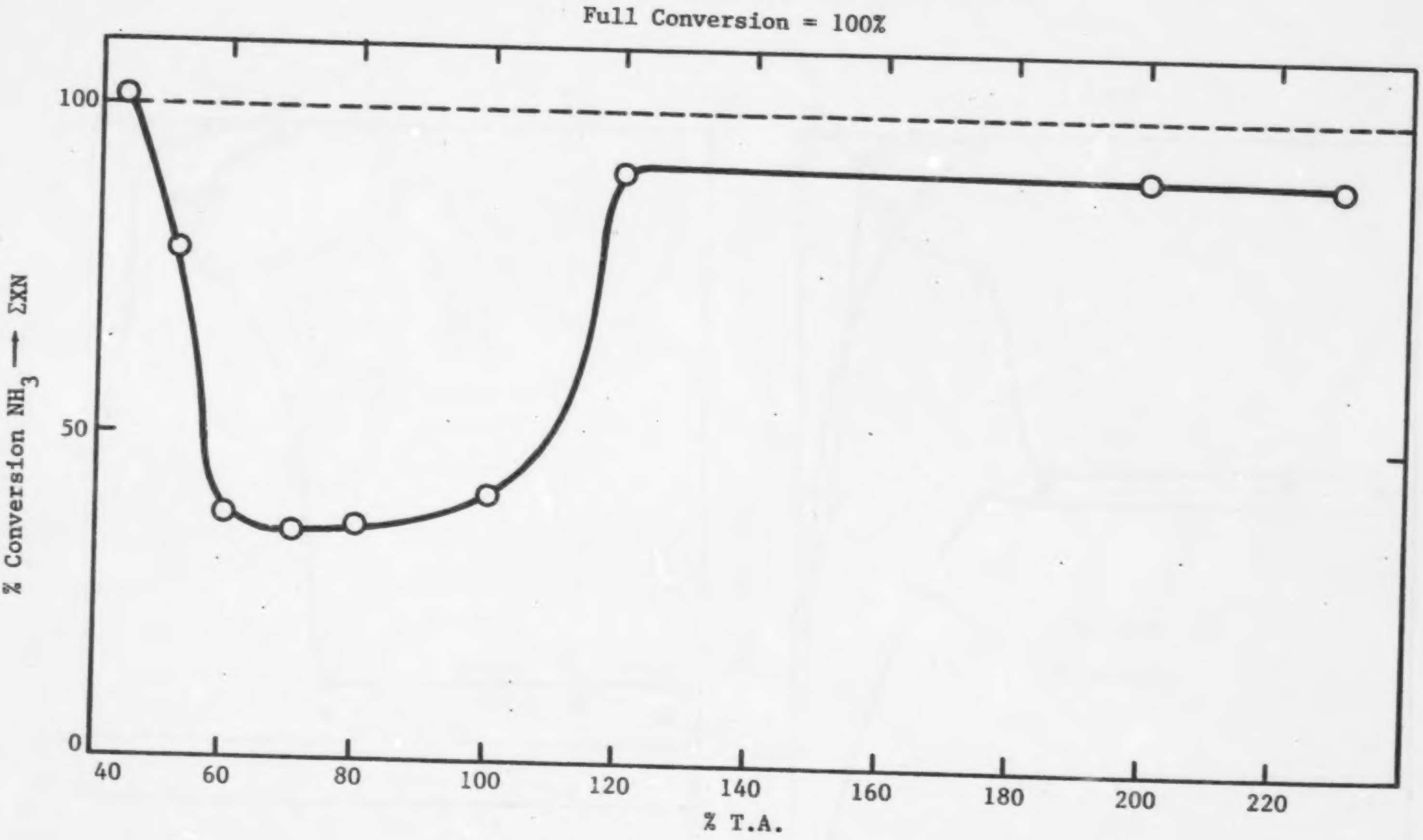

Figure 8. ΣXN in NH_3 Doped LBG-Fired Catalyst.

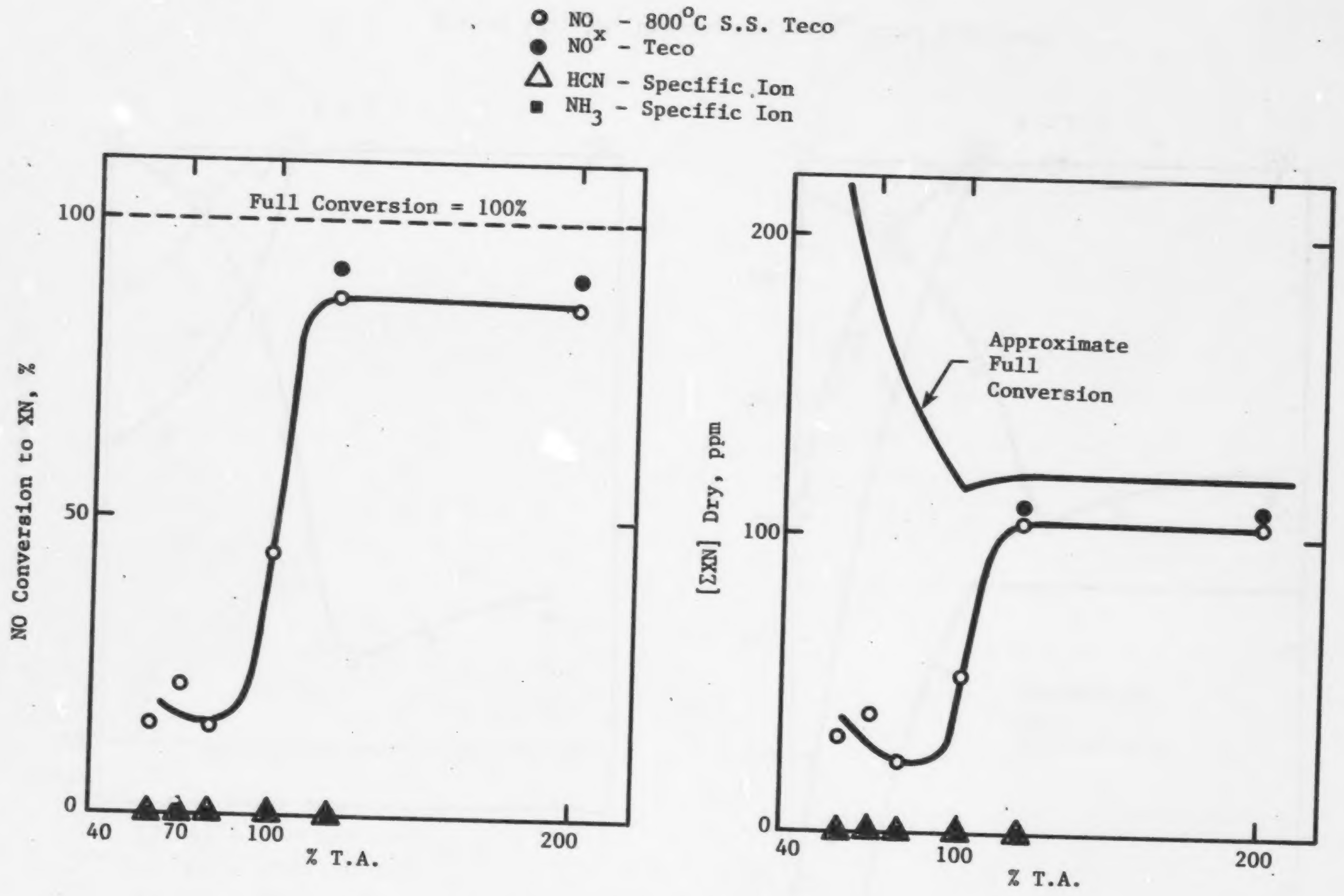

Figure 9. NO Processing in LBG-Fired Catalyst

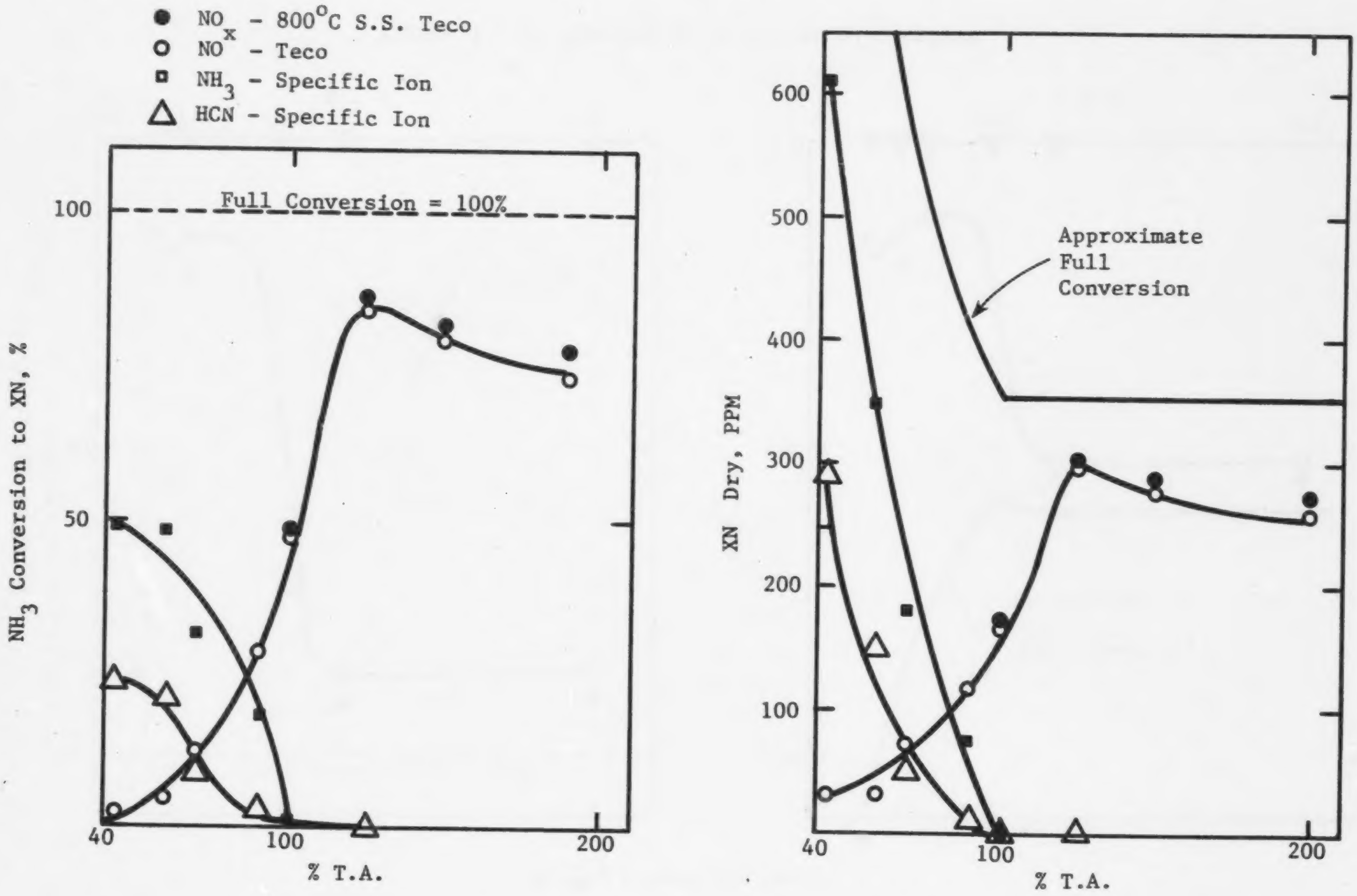

Figure 10. NH_3 Processing In CH_4-Fired Catalyst

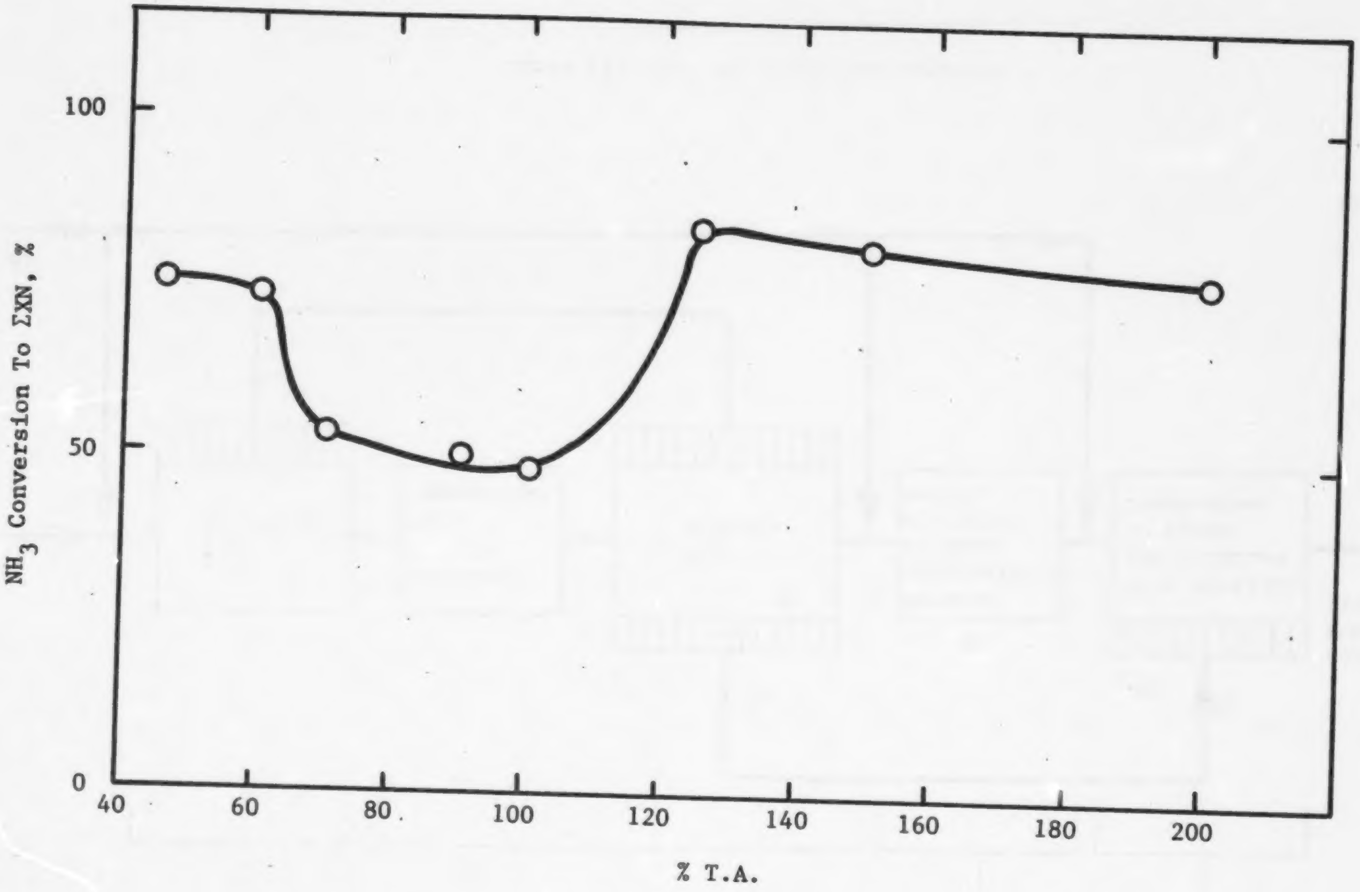

Figure 11. ΣXN in CH$_4$-Fired Catalyst

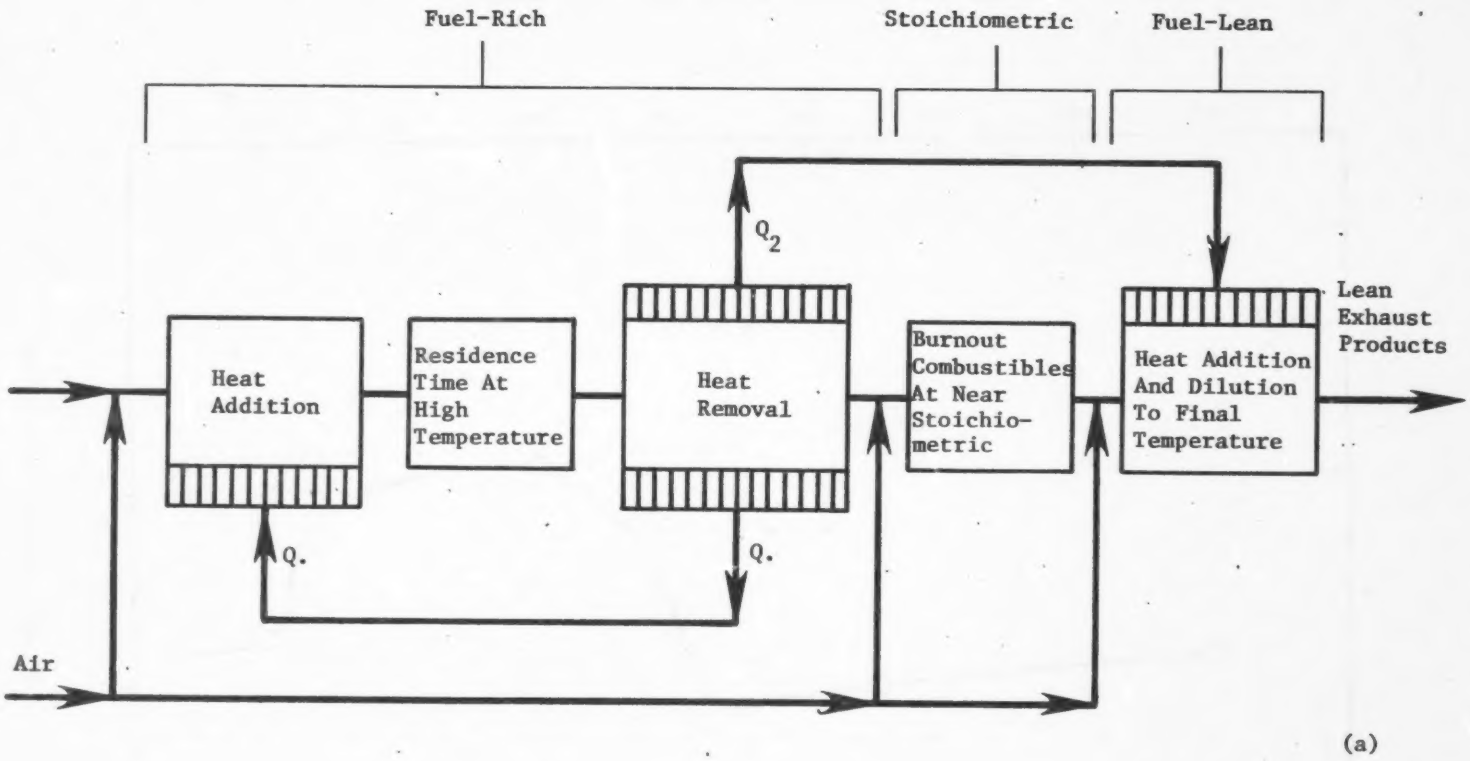
Fuel-Rich
Stoichiometric
Fuel-Lean
Q_2
Heat Addition
Residence Time At High Temperature
Heat Removal
Burnout Combustibles At Near Stoichiometric
Heat Addition And Dilution To Final Temperature
Lean Exhaust Products
Q.
Q.
Air
(a)

Figure 12. Low NO_x Combustor Concepts

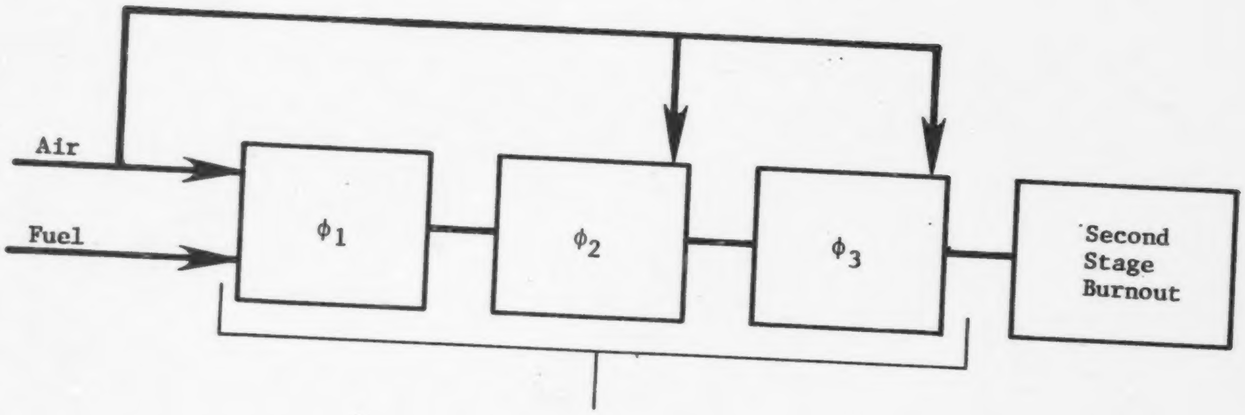

Figure 12b. Fuel-rich primary $\phi_1 > \phi_2 > \phi_3$

THE ADVANCED LOW - EMISSIONS
CATALYTIC -COMBUSTOR PROGRAM
PHASE I - DESCRIPTION AND STATUS

By:
Andrew J. Szaniszlo
NASA - Lewis Research Center

Preceding page blank

THE ADVANCED LOW-EMISSIONS CATALYTIC-COMBUSTOR PROGRAM

PHASE I - DESCRIPTION AND STATUS

by Andrew J. Szaniszlo

NASA - Lewis Research Center

ABSTRACT

The Advanced Low-Emissions Catalytic-Combustor Program is an ongoing three-phase contract effort with the primary objective of evolving the technology required for incorporating catalytic combustors into advanced aircraft gas-turbine engines. Phase I is currently in progress. At the present time, analytical evaluation is being conducted on advanced catalytic-combustor concepts - including variable geometry - with their known inherent potential advantages of low-level pollutant emissions, improved operational stability, reduced specific fuel consumption, and reduced pattern factor for longer turbine life. Phase II and III consist of experimental development.

Preceding page blank

CATALYST-COATED FLAMEHOLDER FOR LEAN STABILITY IMPROVEMENT

By:

E. J. Szetela
J. B. McVey
United Technologies Research Center
East Hartford, Connecticut 06108

ABSTRACT

A program is being carried out at United Technologies Research Center to improve lean stability in premixed, prevaporized combustor concepts designed for reducing gas turbine pollutant emissions. Among the techniques being investigated is the use of a catalyst-coated flameholder similar in principal to a perforated plate. The flameholder consists of a multitude of coated cylindrical passages which terminate at the combustor inlet. A mixture of fuel and air is flowed through the passages and at the discharge end in the combustor, recirculation regions are produced between the ports. The recirculation regions extend the residence time of a portion of the mixture and form a pilot for the flame. The catalyst-coated passages were designed to produce a heated boundary layer that enters the recirculation region and extends the piloting capability of the flameholder to leaner mixtures.

Preceding page blank

CONTENTS

Introduction 395

Program Goals 395

Approach 396

Planned Experiment 398

References 399

LIST OF FIGURES

		Page
Figure 1	Flame Stabilization Process	400
Figure 2	Catalyzed Tube Performance	401
Figure 3	Catalyzed Flameholder	402

LIST OF SYMBOLS

A - Area, ft^2

C - Concentration, lb/ft^3

d - Diameter, ft

D - Diffusion Coefficient, ft^2/hr

G - Mass Velocity, $lb/hr\text{-}ft^2$

$\dot{M}$ - Mass Flow Rate, lb/hr

$\dot{q}$ - Heat Transfer Rate, BTU/hr

μ - Absolute Viscosity, lb/hr-ft

ρ - Density, lb/ft^3

Subscripts

D - Diffusion

F - Fuel

r - Recirculation

S - Surface

INTRODUCTION

The operating characteristics of the combustors in current aircraft gas turbines result in the emission of objectionable quantities of air pollutants over a large part of the engine operating cycle. Considerable effort has been devoted to reduction of pollutant emissions by modifying conventional concepts (Ref. 1-3). Current emission regulations are concerned with emissions generated during the takeoff-landing phase of aircraft operation. There is also a concern that pollutants emitted during stratospheric cruise may prove to be a serious environmental problem. Several NASA studies (Ref. 4) are being carried out to develop approaches to the solution of the stratospheric cruise emissions problem. One such investigation is the Lean Stability Augmentation Program that is being conducted at United Technologies Research Center with sponsorship by NASA Lewis Research Center under Contract NAS3-20804.

The concept that is being explored in this program is the combustion of lean, uniform gaseous fuel and air mixtures in a low temperature zone with low residence time. The key element in this concept is bluff-body flame stabilizer that is composed of a large number of circular passages and is commonly called a perforated plate flameholder. Although it can produce combustion products with low emissions, its natural operating range does not satisfy the requirements of a gas turbine engine because the engine equivalence ratio covers a range beyond the lean extinction limit of the flameholder.

A large number of methods and variations for augmenting the lean stability of a perforated plate flameholder were considered in this program. After study and evaluation of predicted performance, initial cost, and maintenance cost, the list was reduced to three main methods. Among these is the catalyst-coated flameholder. The other two involved addition of fuel downstream of the flameholder and geometric variations of the flameholder design.

PROGRAM GOALS

The goals of the program are defined by the emissions index, EI (grams per kilogram of fuel), which is specified as follows:

EI_{NO_X} 1.0 at design

3.0 over specified operating range

EI_{CO} 10 at design

EI_{UHC} 1 at design

These values are consistent with the specified combustion efficiency which is 99% over a range of equivalence ratio of 0.3 to 0.6. The operating conditions for the flameholder are specified in terms of inlet conditions as shown below:

Pressure - 10 atm
Inlet Temperature - 600 to 800 K
Equivalence Ratio - 0.25 to 0.6
Reference (approach) Velocity - 25 m/sec

The program goals are accompanied by a number of constraints on the methods and variations that are employed in the program in order to avoid duplication of the work being done elsewhere. For instance, the use of a catalytic combustor as a substitute for the flameholder is not permitted. The use of a number of stages with catalytic combustors in some of the stages is also not permitted. These constraints led to the use of catalytic effects in a manner that augments the lean stability of a flameholder by a reduction of its natural lean extinction limit.

APPROACH

The merit of using a catalytic surface to extend the lean extinction limit of a flameholder was examined in relation to a model of the bluff body flame stabilization process. The model (Ref. 5) is based on a heat balance between heat generated at the flame front and the heat transferred to the incoming mixture as shown in Fig. 1. It can be seen that sudden expansion of the incoming gases forms a recirculation zone which consists primarily of combustion products. Heat is transferred from this region by direct mixing of recirculated products ($\dot{M}_r$) with the incoming mixture and by convection to the wall of the bluff body. Burning is possible only when the flow of heat out of the recirculation zone is limited to an acceptable level. A reduction in the equivalence ratio results in a reduction in the temperature of the recirculation zone. When the temperature falls below a minimum level, the flame is extinguished.

An increase in the temperature of the incoming mixture near the wall results in an increase in the temperature of the recirculation region. A higher temperature should produce a reduction in the lean extinction limit of the burner. One method of heating the layer at the wall is the initiation of local combustion reactions by catalyzing the surface. It has been estimated from the data contained in Ref. 6 that approximately 5% of the incoming mixture enters the recirculation zone. Therefore, it is felt that the catalyzed wall should be designed to produce a reaction of close to 5% of the fuel in the gas mixture.

DESIGN OF CATALYZED WALL

The reaction of fuel at the wall of the gas passage was estimated by assuming that diffusion of fuel to the wall is the controlling mechanism. The mass transfer rate can be expressed by an analogy to heat transfer in a manner described in Ref. 7 as shown below:

$$W_F/A_S = h_D (C_\infty - C_W)$$

The mass transfer coefficient, h_D, is described in the Sherwood No., N_{SH}, as follows:

$$N_{SH} = \frac{h_D d}{D}$$

For fully developed turbulent flow, Sherwood No. can be related to the Reynolds No. and Schmidt No. as shown below:

$$N_{SH} = 0.023 (N_{Re})^{0.83} (N_{SC})^{0.44}$$

where

$$N_{Re} = \frac{Gd}{\mu}$$

and

$$N_{SC} = \frac{\mu}{\rho D}$$

For laminar flow in a tube, Sherwood No. is a constant with an approximate value of 4.

These equations were used after making two important simplifying assumptions as follows:

1. Jet A fuel can be described as a pure hydrocarbon with a molecular weight of 150.

2. Reaction of fuel at the wall is instantaneous.

For the case of the flameholder, the calculated value of reacted fuel flow is shown in Fig. 2. From these results, it can be seen that 4% of the fuel will be reacted after the mixture flows through a 2 in. long circular passage. This result is very conservative because fully developed flow only occurs near the end of the passage. When corrected for entrance effects, the calculated value of reacted fuel flow can be expected to reach close to 5%.

To verify this analysis, the calculation was repeated using a monolithic catalytic combustor based on a substrate having a cell density of 35 cells/cm^2 where the flow was assumed to be laminar. The results indicated that approximately 50% of the flow will be reacted in a 2 in. long monolith. The data of Ref. 8, which were obtained with propane-air mixtures, showed that approximately 40% of the fuel was reacted in the first two inches of a similar combustor operating at an equivalence ratio of 0.3 and a reference velocity of 20 m/sec.

PLANNED EXPERIMENT

An experiment will be run to measure the effect of a catalyzed flameholder on the lean extinction limit. The flameholder consists of a group of 22 discharge ports in a circular plate. The open area of the ports is 25% of the total area. Each port is fed from an individual tube as shown in Fig. 3. The tube has an internal diameter of 0.47 in. and a catalyzed length of 3.5 in. The tube material is AISI 321. The internal surface of each tube and the downstream face of the plate have been catalyzed by Oxy-Catalyst of West Chester, Pennsylvania. To apply the catalyst, the surface was first grit-blasted for adherence of a coating of alumina. The alumina was next applied at a loading of 5-10 mg/in.^{2}. A final application of Pt-Rh catalyst was added to the alumina surface at a loading of 2-3% of the alumina loading.

The external surface of the tubes will be cooled by a crossflow of cooling air. A second cooling stream will be used to control the temperature of the circular plate. Thermocouples will be used to monitor the wall temperatures during the test.

The test of the flameholder will consist of the determination of the lean extinction limit at the specified inlet temperature, pressure, and velocity. Following this, the downstream face of the flameholder will be scraped to remove the catalyst and the extinction limit will be again determined. Finally, the internal surface of the forward two inches of the tubes will be scraped to remove the catalyst and thereby to determine the sensitivity of extinction limit behavior to catalyzed tube length.

REFERENCES

1. Roberts, R., A. Peduzzi, and G. E. Vitti: Experimental Clean Combustor Program. Alternate Fuels Addendum. PWA-5370. NASA CR-134970. July, 1976.

2. Gleason, C. C. and D. W. Bahr: Experimental Clean Combustor Program. Alternate Fuels Addendum. GE R76 AEG 268. NASA CR-134972. January, 1976.

3. Jones, R. E.: Emissions Reduction Technology Program. NASA Conference Publication 2021. May, 1977.

4. Diehl, L. A., G. M. Reck, C. J. Marek, A. J. Szaniszlo: Stratospheric Cruise Emission Reduction Program. NASA Conference Publication 2021. May, 1977.

5. Cheng, S. I. and A. A. Kovitz: Theory of Flame Stabilization by a Bluff Body. Seventh International Symposium on Combustion. Butterworth's Scientific Publications, pp. 681-691. 1959.

6. Ozawa, R. I.: Survey of Basic Data on Flame Stabilization and Propagation for High Speed Combustion Systems. The Marquardt Co. Technical Report AFAPL-TR-70-81. January, 1971.

7. Rohsenow, W. M. and H. Choi: Heat, Mass and Momentum Transfer. Prentice-Hall, Inc. 1961.

8. Anderson, D. N.: Preliminary Results from Screening Tests of Commercial Catalysts with Potential Use in Gas Turbine Combustors. NASA TMX-73412. May, 1976.

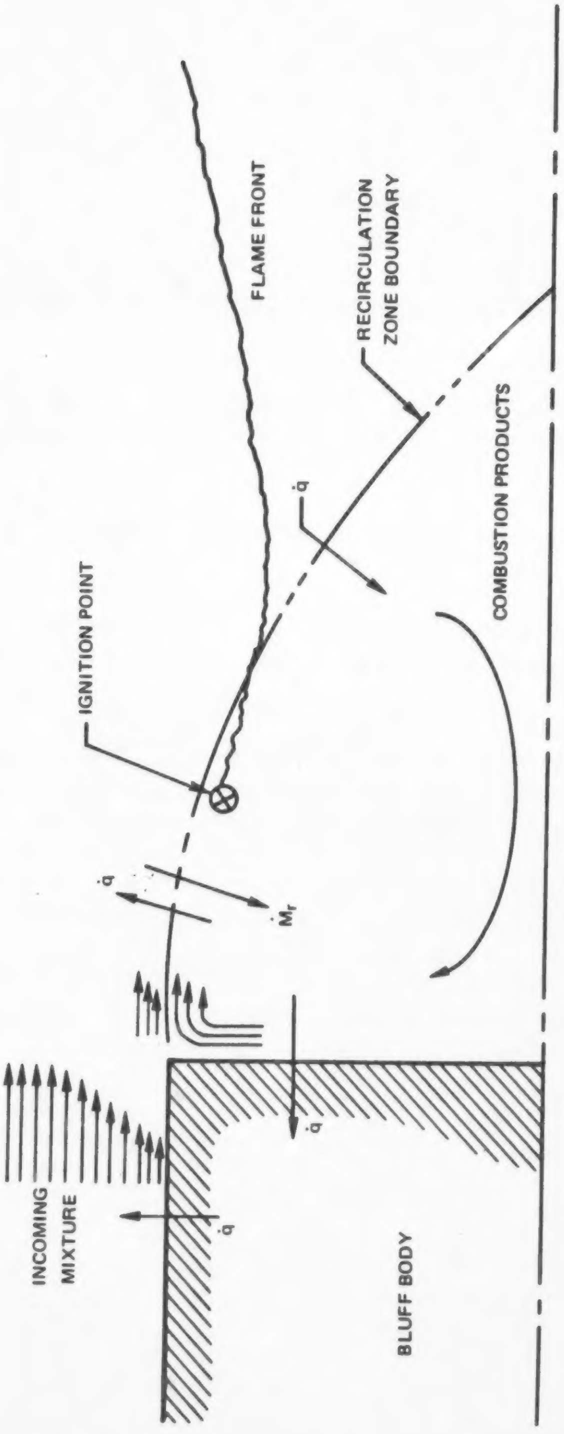

Figure 1. Flame stabilization process.

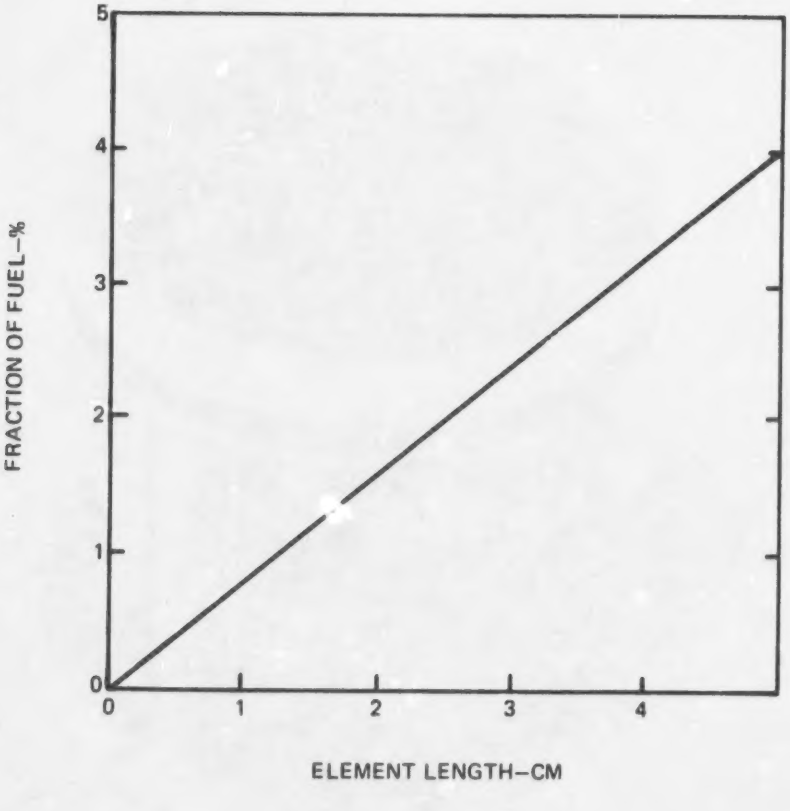

Figure 2. Catalyzed tube performance - fraction of fuel contacting surface.

Figure 2. Catalyzed tube performance - fraction of fuel contacting surface.

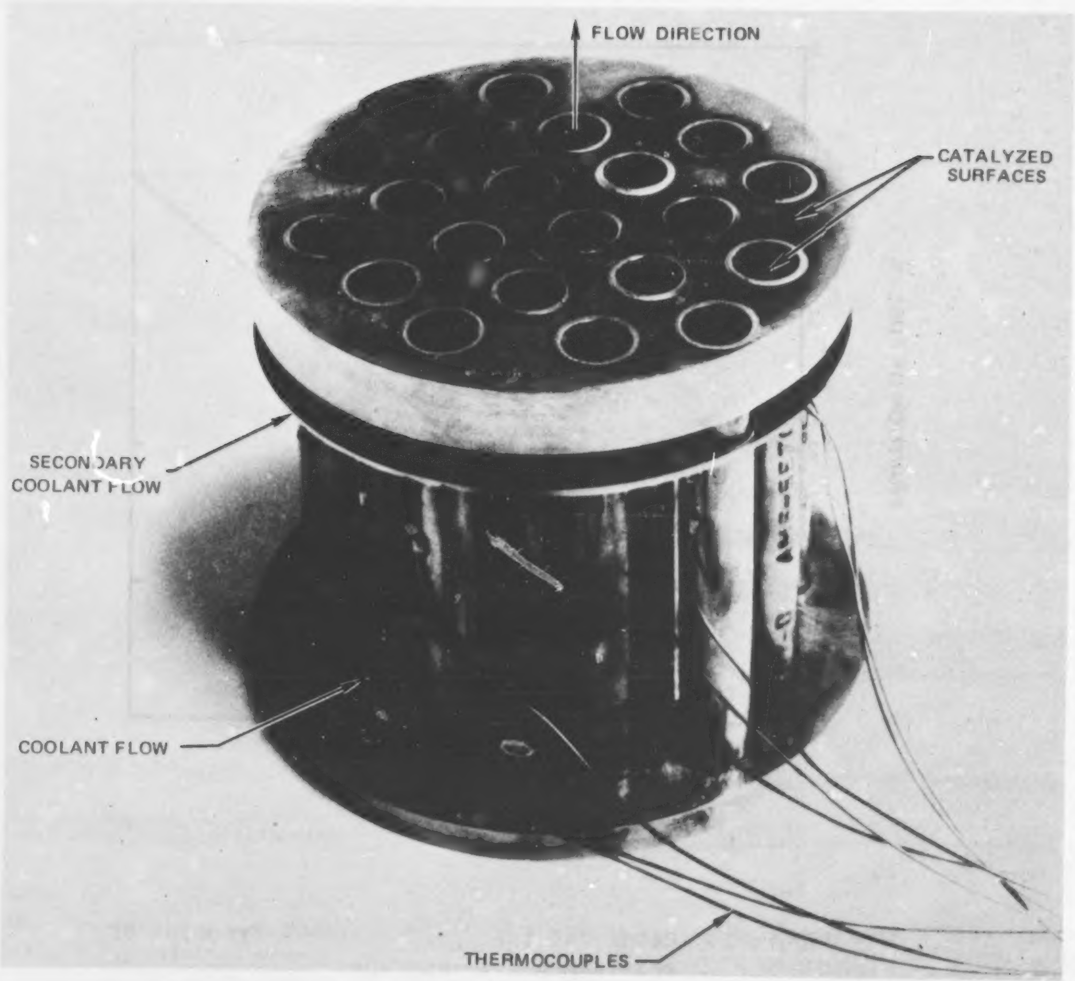

FIGURE 3. CATALYZED FLAME HOLDER

78-08-84-3

EFFECT OF INLET TEMPERATURE ON THE PERFORMANCE OF A CATALYTIC REACTOR

by

David N. Anderson
NASA-Lewis Research Center
Cleveland, Ohio 44135

EFFECT OF INLET TEMPERATURE ON THE PERFORMANCE OF A CATALYTIC REACTOR

by David N. Anderson
National Aeronautics and Space Administration
Lewis Research Center
Cleveland, Ohio 44135

ABSTRACT

A 12-cm diameter by 15-cm long catalytic reactor was tested with No. 2 diesel fuel in a combustion test rig at inlet temperatures of 700, 800, 900, and 1000 K. Other test conditions included pressures of 3 and 6×10^5 Pa, reference velocities of 10, 15, and 20 m/s, and adiabatic combustion temperatures in the range 1100 to 1400 K. The combustion efficiency was calculated from measurements of carbon monoxide and unburned hydrocarbon emissions. Nitrogen oxide emissions and reactor pressure drop were also measured. At a reference velocity of 10 m/s, the CO and unburned hydrocarbons emissions, and, therefore, the combustion efficiency, were independent of inlet temperature. At an inlet temperature of 1000 K, they were independent of reference velocity. Nitrogen oxides emissions resulted from conversion of the small amount (135 ppm) of fuel-bound nitrogen in the fuel. Up to 90 percent conversion was observed with no apparent effect of any of the test variables. For typical gas turbine operating conditions, all three pollutants were below levels which would permit the most stringent proposed automotive emissions standards to be met. The pressure drop increased linearly with reference velocity and decreased slightly as the inlet temperature was raised. Pressure drop increased linearly with velocity to a maximum value of 1.5 percent at a reference velocity of 20 m/s.

INTRODUCTION

Probably the most important aspect of catalytic combustion is the produc-

Preceding page blank

tion of extremely low concentrations of thermal NO_x. Because of this feature, evaluations are being made of catalytic combustion for aircraft (refs. 1 to 3), stationary (refs. 4 to 6), and automotive applications.

Catalytic combustion is being studied at the NASA-Lewis Research Center for the Gas Turbine Highway Vehicle Systems Project which is supported by the Department of Energy. The goal of this project is to demonstrate the technology for an automotive gas turbine engine which would improve the thermal efficiency over current spark-ignition piston engines. This improved gas turbine is presently being defined by each of the four major American automobile manufacturers under development contracts to the DOE. The engine is expected to operate with a turbine inlet temperature of about 1300 K and with combustor inlet temperatures which will decrease from 1200 K at idle to 1000 K at full speed (ref. 7).

Combustor work in support of this Project involves studies of fuel-air premixing/prevaporizing systems (refs. 8 and 9), and the evaluation of catalytic reactors (refs. 10 and 11). Monolithic catalytic reactors have been tested at steady-state conditions which simulated those of the improved engine combustor except that the maximum test section inlet temperature was only 800 K. Several studies (refs. 1, 10, and 12) have shown that an increase in inlet temperature results in an improvement in catalyst performance; however, none of those studies reported results for temperatures higher than 800 K.

The present study was made with test section inlet temperatures as high as 1000 K. While this temperature matches the improved gas turbine combustor inlet at full speed, it is 200 K lower than the idle inlet temperature. To provide a basis for extrapolation of results to the idle condition, reactor performance was determined at inlet temperatures of 700, 800, and 900 K as well. Other test conditions included pressures of 3 and 6×10^5 Pa, reference velocities (catalytic reactor inlet velocities) of 10, 15, and 20 m/s, and a range of adiabatic combustion temperatures of 1100 to 1400 K. The catalytic reactor was 12 cm in diameter and 15 cm long. No. 2 diesel fuel was used for all tests.

EXPERIMENTAL DETAILS

The test rig is described in figure 1(a). All ducting was made from 15.2-cm (6-in. nominal) diameter stainless steel pipe with 12 cm ID by 15.2 cm

OD Carborundum T30R Fiberfrax tube insulation inserted inside the pipe to give a flow diameter of 12 cm.

Test section inlet air was indirectly preheated to temperatures in the range of 700 to 1000 K. The inlet temperature was measured before fuel injection at a plane 40 cm upstream of the catalytic reactor. Twelve Chromel-Alumel thermocouples were positioned in this plane at the centers of equal duct cross-sectional areas. In previous studies at Lewis (refs. 7 and 11), the inlet fuel-air mixture temperatures were measured nearer the reactor inlet plane to avoid cooling errors associated with the poorly insulated pipes used in those tests. The difference between the inlet air temperature and the inlet fuel-air mixture temperature depends on the fuel-air ratio, but should be no more than 15 to 20 K for the conditions of these tests.

A multiple conical tube fuel injector was located 15 cm downstream of the inlet thermocouple plane and 25 cm upstream of the catalytic reactor. This fuel injector was of the same type developed by Tacina (refs. 8 and 9); it is pictured in figure 1(b). Two separate sets of 21 equal-length fuel tubes introduced fuel at the small-diameter (high-air-velocity), upstream end of the conical airflow tubes. The large-diameter (1.6 mm) fuel tubes were for propane which was not used in this study, and the small-diameter (0.5 mm) were for the No. 2 diesel fuel used in this study. Tests with this injector type have shown that, 24 cm downstream of the fuel injector inlet, the fuel-air ratio and the velocity varied by less than ±10 percent over the duct cross-section (ref. 8). With an inlet air temperature of 700 K or greater, fuel vaporization approached 100 percent at a distance of 17.8 cm (ref. 9). Therefore, at 25 cm the fuel should be fully vaporized and mixed. The pressure drop reported in reference 13 for this type of fuel injector was about 0.25 percent at a reference velocity of 10 m/s, increasing to 1 percent at 20 m/s.

The reactor inlet pressure was measured at a tap 13 cm upstream of the catalytic reactor. At the same location a single Chromel-Alumel thermocouple was used to detect burning upstream of the reactor. None was observed.

The catalytic reactor was the same J4 reactor used in two earlier studies (refs. 11 and 14). It consisted of two 12-cm diameter and 7.5-cm long metal-foil monolithic elements placed end to end and separated by a 0.31-cm diameter Pt vs Pt-13 percent Rh thermocouple which measured the temperature at the duct centerline. The elements are described in Table I; they were identical except that the first element used a Pt catalyst and the second Pd. Previous to the start of testing this reactor had been operated for about 30 hours at adiabatic combustion temperatures as high as 1500 K.

An array of 12 Pt vs Pt-13 percent Rh thermocouples were used to measure the temperature at the reactor exit plane (see fig. 1(a)). The reactor pressure drop was measured with a differential pressure transducer which indicated the difference between the inlet static pressure and the static pressure at a tap 7 cm downstream of the reactor.

An array of 11 Pt vs Pt-13 percent Rh thermocouples measured the average temperature at a plane 22 cm downstream of the reactor. At the same plane a sample of the exhaust gas was obtained at the centerline of the duct with a single-point probe. The probe was water-cooled to quench the sample near the entrance port. The quenched gases flowed from the probe through an 18-m length of 0.5-cm diameter electrically heated stainless-steel tubing to the gas analyzers. This sample line was maintained at 410 to 450 K to prevent the condensation of any unburned hydrocarbons in the sample. Concentrations of CO and CO_2 were determined with Beckman Model 315B nondispersive infrared analyzers, unburned hydrocabons with a Beckman Model 402 flame ionization detector, and nitrogen oxides (NO and NO_2) with a Thermo Electron Model 10A chemiluminescent analyzer. Before analyzing for CO, CO_2, or NO_x, water vapor was removed with a Hankinson Series E refrigeration-type dryer. Corrections were made to the measured concentrations to obtain the actual, wet-basis concentrations of these three constituents.

After discharging from the downstream instrumentation section, the exhaust gas passed through a water spray to cool the combustion gases, then through a back-pressure valve for control of rig pressure.

MEASUREMENTS AND COMPUTATIONS

For each setting of inlet airflow, temperature, and pressure, data were obtained at several different fuel flowrates, first with fuel flow increasing, then decreasing. This procedure permitted a check to be made of the repeatability of the data, and to determine if hysteresis effects occurred. The repeatability was excellent and no hysteresis was evident.

The reference velocity was computed from the measured mass flowrate, the average temperature measured at the test section inlet plane, the duct cross-sectional area, and the pressure measured at the test section inlet. Thus, the reference velocity is the same as the reactor inlet velocity.

The emissions were measured as concentrations in ppm by volume and converted to emission indexes using the expression

$$(\mathrm{E.I.})_x = C_x \times 10^{-3} \, \frac{1 + f}{f} \, \frac{M_x}{M_p}$$

where

$(\mathrm{E.I.})_x$	emission index of specie x, g_x/kg_{fuel}
C_x	concentration of specie x, ppm V
f	fuel-air weight ratio, $(kg/s)_{fuel}/(kg/s)_{air}$
M_x	molecular weight of specie x, $g_x/mole_x$
M_p	molecular weight of combustion products, $g_{products}/mole_{products}$

The combustion efficiency was computed from the CO and HC emissions measurements. The difference between the measured and equilibrium values of these two emittants represents available chemical energy which has not been released in the combustion process. Thus, the combustion efficiency in percent is

$$\begin{aligned} \mathrm{EFF} = 100 &- 0.1\left[(\mathrm{E.I.})_{HC} - (\mathrm{E.I.})_{HC,EQ}\right] \\ &- 0.1\left[\frac{(\mathrm{HV})_{CO}}{(\mathrm{HV})_{fuel}}\right]\left[(\mathrm{E.I.})_{CO} - (\mathrm{E.I.})_{CO,EQ}\right] \end{aligned}$$

where

EFF	combustion efficiency, percent
$(\mathrm{HV})_x$	heating value of x, J/kg

The fuel-air ratio was determined both from the metered fuel and air flowrates and by making a carbon balance from the measured concentrations of CO, CO_2, and unburned hydrocarbons. The carbon-balance fuel-air ratio has the advantage that it is the local fuel-air ratio at which the emissions data are obtained. The equilibrium concentrations of each important specie and the adiabatic combustion temperature were obtained using the carbon-balance fuel-air ratio with the computer program of reference 15.

RESULTS AND DISCUSSION

Acceptable carbon-balance fuel-air ratios were between 90 and 112 percent of the fuel-air ratio determined from fuel and airflow measurements. Several data points (8 percent of all data taken) had values below this range and were rejected; none were above. Virtually all of those data rejected were obtained at extremely low fuel flow rates which were difficult to measure accurately. Eighty two percent of the data retained had a carbon-balance fuel-air ratio which was between 94 and 106 percent of the measured fuel-air ratio. Thus, the carbon-balance fuel-air ratio was generally a valid representation of the fuel-air ratio obtained from measured flows.

Combustion Efficiency

The combustion efficiency is shown in figure 2 as a function of the adiabatic combustion temperature. Figure 2(a) gives the results at a reference velocity of 10 m/s and for inlet temperatures of 700 to 1000 K with pressures of 3 and 6×10^5 Pa. For each set of conditions the combustion efficiency increased with adiabatic combustion temperature. At a pressure of 3×10^5 Pa the efficiency was above 99 percent for all inlet temperatures when the adiabatic combustion temperature was higher than 1200 K. At combustion temperatures below 1200 K, the effect of raising the inlet temperature was to improve the combustion efficiency.

The combustion efficiency decreased with an increase in pressure at inlet temperatures of 800 and 900 K, but it increased with pressure at 1000 K. The two different effects of pressure resulted from the relative roles of surface and gas-phase reactions. The surface reation rate is limited by that of mass diffusion, which is inversely proportional to pressure. Surface reactions cannot provide complete combustion, and gas-phase reactions, which increase with pressure, are necessary to achieve high combustion efficiency (refs. 4, 12, and 16). Thus, when the pressure is increased, combustion efficiency may either increase or decrease depending on whether gas-phase reactions become important near the reactor inlet or not until much later.

At reference velocities of 15 and 20 m/s, data were taken only with a pressure of 3×10^5 Pa (see figs. 2(b) and (c)). The effect of inlet temperature on combustion efficiency was much greater than at 10 m/s and 3×10^5 Pa. As the inlet temperature was increased, the combustion efficiency also increased.

Reference 11 reported combustion efficiencies at an inlet temperature of 800 K and a pressure of 3×10^5 Pa for the same reactor tested in this study. Higher combustion temperatures were required in the experiments of reference 11 to achieve the same efficiencies as this study. The primary reason that better performance was obtained in the present study was the elimination of most of the test section heat loss through the use of better insulation. Heat loss was calculated to be less than 2 percent, and measured exit thermocouples agreed with the adiabatic combustion temperatures within a few degrees for the present experiments. Exhaust-gas sampling techniques were different for the two experiments, as well. The single-point probe of this study was located 8 cm farther downstream than the multi-point probe of reference 11. Both of these differences would explain why higher combustion efficiencies were obtained for the present study.

Emissions

Emissions goals for the Gas Turbine Highway Vehicle Systems Project have been established (ref. 17) as 13.6 g CO/kg fuel, 1.64 g HC/kg fuel, and 1.60 g NO_x/kg fuel. These goals are used as reference values to help evaluate the measured emissions.

Carbon Monoxide

The carbon monoxide emission index is plotted as a function of the adiabatic combustion temperature in figures 3(a) to (c). Figure 3(a) gives the emissions at a reference velocity of 10 m/s for pressures of 3 and 6×10^5 Pa. Emissions decreased as the adiabatic combustion temperature increased. Values below the reference level were achieved at a pressure of 3×10^5 Pa when the adiabatic combustion temperature was higher than 1220 K for all four inlet temperatures.

As with the combustion efficiency results, the nature of the pressure effect depended on the inlet temperature. Emissions at an inlet temperature of 1000 K decreased when the pressure was doubled from 3 to 6×10^5 Pa. In contrast, at an inlet temperature of 800 or 900 K, doubling the pressure produced an increase in the CO emission index for adiabatic combustion temperatures below 1250 K, but a decrease in emissions for higher combustion temperatures.

With a reference velocity of 15 m/s (fig. 3(b)) the carbon monoxide emissions decreased with increases in either inlet temperature or adiabatic combustion temperature. The same trends are shown in figure 3(c) for a reference velocity of 20 m/s.

If figures 3(a) to (c) are compared at an inlet temperature of 1000 K it can be seen that there is little difference in the emissions produced at 10, 15, or 20 m/s reference velocities. Overall reaction rates are high enough at this inlet temperature that an increase in residence time (decrease in reference velocity) provided little benefit. Similarly, it was seen in figure 3(a) that at a reference velocity of 10 m/s there was enough residence time that an increase in inlet temperature (i.e., initial reaction rate) had little effect on the CO emissions produced.

Unburned Hydrocarbons

The emission index of unburned hydrocarbons is plotted as a function of the adiabatic combustion temperature in figure 4. Figure 4(a) gives the results at a reference velocity of 10 m/s and shows no significant effect of either inlet temperature or pressure. The temperature required to meet the hydrocarbon emission index goal was 40 K lower than that required to meet the CO emission index goal.

An effect of inlet temperature on hydrocarbon emissions was clearly seen when the reference velocity was increased to 15 m/s (fig. 4(b)). The combustion temperatures required to meet the hydrocarbon emissions goal were 30 to 80 K less than those required to meet the CO goal at this velocity.

Similarly, at 20 m/s (fig. 4(c)) emissions were higher with the lower inlet temperatures. The hydrocarbon emissions goal was achieved at combustion temperatures which were 10 to 95 K lower than those required to meet the CO goal.

As with the CO emissions, the reference velocity had little effect on the hydrocarbons emissions at an inlet temperature of 1000 K, while inlet temperature had little effect at a reference velocity of 10 m/s.

Nitrogen Oxides

The third pollutant of interest in automotive combustion studies is nitrogen oxides. Because of the low temperatures at which catalytic combustion takes place, thermal NO_x emissions are on the order of 1 ppm or less. However, conversion of nitrogen in the fuel can produce significantly higher levels than this.

The fuel used in this study contained 135 ppm of N. Eightly percent of the NO_x emissions data ranged in value from 0.2 to 0.4 g NO_2/kg fuel which represents conversion of from 45 to 90 percent of the fuel N. It should be noted, however, that there is a great deal of uncertainty associated with the measurement of such low levels of NO_x. No effect of inlet temperature, reference velocity, pressure, or adiabatic combustion temperature was apparent within the scatter of the data. The emissions were well below the reference emission index of 1.60 g NO_2/kg fuel for all test conditions.

Minimum Operating Temperature

The minimum operating temperature is the adiabatic combustion temperature above which the reactor must be operated to insure that all three pollutants meet the project goals. In this study, NO_x emissions were below the reference value at all test conditions, and the hydrocarbons goal was met at lower combustion temperatures than the CO goal. Thus, the minimum operating temperature was identical with the minimum adiabatic combustion temperature required to meet the CO goal.

Figure 5 gives the minimum operating temperature as a function of the inlet temperature. As noted in the discussion of the CO emissions, at a reference velocity of 10 m/s and a pressure of 3×10^5 Pa, excess residence time was available so that an increase in inlet temperature (and, thus, initial reaction rate) had no effect on the minimum operating temperature. A shorter reactor would probably perform equally well at these conditions.

When the pressure was increased to 6×10^5 Pa, the adiabatic combustion temperature required to meet the emissions goals increased at 800 and 900 K inlet temperatures but decreased at 1000 K. This result was due to changes in the relative roles of surface and gas-phase reactions as discussed under CO emissions.

At reference velocities of 15 and 20 m/s an increase in inlet temperature produced a decrease in the minimum operating temperature. For inlet temperatures above 1000 K the extrapolated results in figure 5 show that the minimum operating temperature approaches 1220 for all three velocities independent of inlet temperature. Thus, at an inlet temperature of 1220 K, the minimum operating temperature and the inlet temperature will be equal.

Reactor Pressure Drop

In addition to operating with very low emissions, an automotive gas turbine combustor must have minimal pressure losses to permit high cycle efficiencies. In general, the pressure drop for a catalytic reactor includes both friction losses and entry/exit losses. For the reactor and the test conditions of this study, however, friction losses dominated. The Reynolds number was less than 1000 for all flow conditions; thus, the flow through the reactor passages was laminar. For laminar flow, the friction drop over a small element of length, $d\ell$, is

$$\frac{dp}{p} = k \frac{VT^{0.6}}{p} d\ell$$

where

k	a constant
V	local velocity
T	local temperature
p	pressure

The local velocity is equal to the reference velocity V_{ref}, times the ratio of the local to inlet temperature, T/T_{in}. Then the pressure drop over the reactor length, ℓ, is

$$\frac{\Delta p}{p} = \frac{k}{T_{in}} \frac{V_{ref}}{p} \int_0^{\ell} T^{1.6} \, d\ell$$

The pressure drop as a percent of upstream pressure is presented in figure 6 as a function of V_{ref}/p. For an inlet temperature of 700 K the data show a direct proportionality between $\Delta p/p$ and V_{ref}/p. This result suggests that the temperature history, $T = f(\ell)$, does not change appreciably with reference velocity. At higher inlet temperatures, some decrease in pressure drop was observed as would be expected for laminar flow friction loss. For example, at a reference velocity of 10 m/s and a pressure of 3×10^5 Pa

$\left(V_{ref}/p = 3.3\times10^{-5}\ \frac{m/s}{Pa}\right)$, the pressure drop decreased from 0.8[illegible] to 0.66 percent when the inlet temperature was raised from 700 to 1000 K.

The pressure drop data in figure 6 at an inlet temperature of 800 K and a pressure of 3×10^5 Pa were about half the values reported in references 11 and 14 for the same reactor. In those previous studies, however, the thermocouple instrumentation within the reactor housing was more dense than that used for the present study. In addition, the earlier data included the pressure drop across the downstream instrumentation section. For the very low pressure drops at which this reactor operates, these additional instrumentation pressure drops were significant.

CONCLUSIONS

This study of the effect of inlet temperature on the performance of a catalytic reactor has shown that if sufficient residence time was provided, as occurred at a reference velocity of 10 m/s, inlet temperatures in the range 700 to 1000 K had little effect on combustion efficiency or emissions. At 700 K inlet temperature, significantly better performance was achieved at 10 m/s than at higher reference velocities. Thus, for applications with low inlet temperatures, such as the aircraft or stationary gas turbines, long residence times (low reference velocities) must be provided to achieve high combustion efficiencies.

In contrast, the reference velocity had little effect on the combustion efficiency or emissions when the inlet temperature was 1000 K. This result suggests that for combustor applications with high inlet temperature, such as the regenerative automotive gas turbine, the upper limit on reference velocity may be determined by permissible pressure drop rather than combustion efficiency.

The pressure drop in this study resulted primarily from friction loss through the reactor passages. Because the flow was laminar, the percent pressure drop decreased slightly with increasing inlet temperature at a constant adiabatic combustion temperature.

The improved catalyst performance which results from operation at high in-inlet temperatures makes the automotive gas turbine an especially attractive application for catalytic combustion. In this study, at 1000 K inlet temperature, 1300 K exit temperature, and 20 m/s reference velocity, emissions of CO, unburned hydrocarbons, and NO_x were below levels which would permit the stringent automotive standards to be achieved, and pressure drop was only 1.5 percent.

REFERENCES

1. Blazowski, W. S., and D. E. Walsh. Catalytic Combustion: An Important Consideration for Future Applications. Combust. Sci. Technol., 10(5/6) 233-244, 1975.
2. Rosfjord, T. J. Catalytic Combustors for Gas Turbine Engines. AIAA Paper 76-46, 1976.
3. Siminski, V. J., and H. Shaw. Development of a Catalytic Combustor for Aircraft Gas Turbine Engines. EXXON/G.R.U. 1 BFA.76, Exxon Research and Engineering Co., Linden, N. J., 1976. (AFAPL-TR-76-80, AD-A040135.)
4. DeCorso, S. M., S. Mumford, R. Carrubba, and R. Heck. Catalysis for Gas Turbine Combustors - Experimental Test Results. ASME Paper 76-GT-4, 1976.
5. Kesselring, J. P., R. A. Brown, R. J. Schreiber, and C. B. Moyer. Catalytic Oxidation of Fuels for NO_x Control from Area Sources. EPA-600/2-76-037, Environmental Protection Agency, 1976.
6. Kesselring, J. P., W. V. Krill, and R. M. Kendall. Design Criteria for Stationary Source Catalytic Combustors. Paper presented at the 1977 Fall Meeting, Western States Section, Combustion Institute, WSS/CI Paper 77-32.
7. Anderson, D. N., R. R. Tacina, and T. S. Mroz. Catalytic Combustion for the Automotive Gas Turbine Engine. NASA TM X-73589, 1977.
8. Tacina, R. R. Experimental Evaluation of Premixing-Pre-vaporizing Fuel Injection Concepts for a Gas Turbine Catalytic Combustor. NASA TM-73755, 1977.
9. Tacina, R. R. Degree of Vaporization Using an Air-Blast Type Injector for a Premixed-Prevaporized Combustor. NASA TM-78836, 1978.
10. Anderson, D. N., R. R. Tacina, and T. S. Mroz. Performance of a Catalytic Reactor at Simulated Gas Turbine Combustor Operating Conditions. NASA TM X-71747, 1975.
11. Anderson, D. N. Performance and Emissions of a Catalytic Reactor with Propane, Diesel, and Jet A Fuels. NASA TM-73786, 1977.

12. Pfefferle, W. C., R. V. Carrubba, R. M. Heck, and G. W. Roberts. Catathermal® Combustion: A New Process for Low-Emissions Fuel Conversion. ASME Paper 75-WA/Fu-1, 1975.

13. Tacina, R. R. Experimental Evaluation of Fuel Preparation Systems for an Automotive Gas Turbine Catalytic Combustor. NASA TM-78856, 1977.

14. Anderson, D. N. Effect of Catalytic Reactor Length and Cell Density on Performance. Paper presented at the Second Workshop on Catalytic Combustion, Raleigh, N. C., June 21-22, 1977. Sponsored by Environmental Protection Agency.

15. Gordon, S., and B. J. McBride. Computer Program for Calculation of Complex Chemical Equilibrium Compositions, Rocket Performance, Incident and Reflected Shocks, and Chapman-Jouguet Detonations. NASA SP-273, 1971.

16. Wampler, F. B., D. W. Clark, and F. A. Gaines. Catalytic Combustion of C_3H_8 on Pt Coated Monolith. Combust. Sci. Technol., 14,25-31, 1976.

17. Aircraft Engines Emissions, NASA CP 2021, 1977.

TABLE I. - DESCRIPTION OF CATALYST ELEMENTS

Element number	1	2
Element designation	JM1	JM2
Position in reactor	Upstream	Downstream
Manufacturer	Johnson Matthey, Ltd.	Johnson Matthey, Ltd.
Catalyst	Pt	Pd
Loading, kg/m^3	5.3	5.3
Substrate	Metal foil, corrugated and wound into a cylinder	Metal foil, corrugated and wound into a cylinder
Cell density, $cells/cm^2$	62	62
Element diameter, cm	12	12
Element length, cm	7.6	7.6

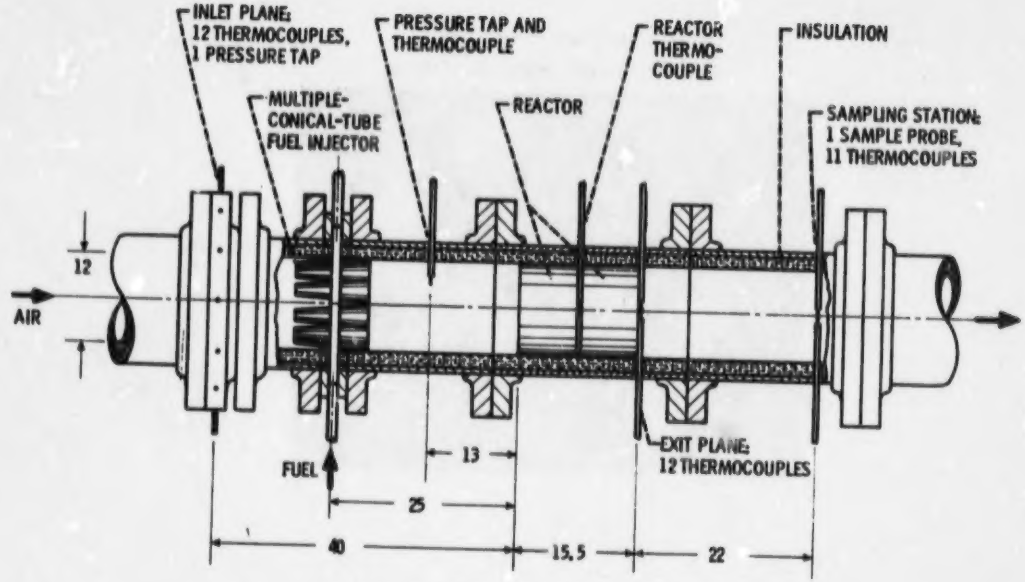

(a) TEST SECTION (DIMENSIONS IN cm).

Figure 1. - Experimental apparatus.

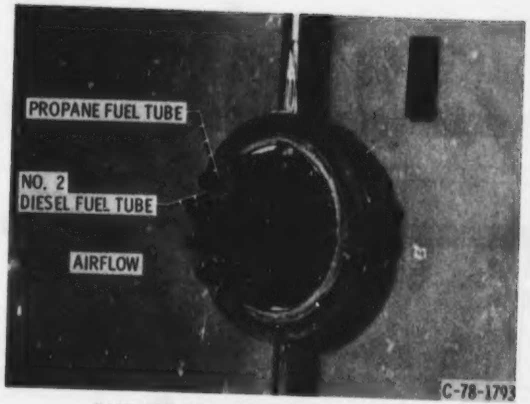

(b) MULTIPLE CONICAL TUBE FUEL INJECTOR.

Figure 1. - Concluded.

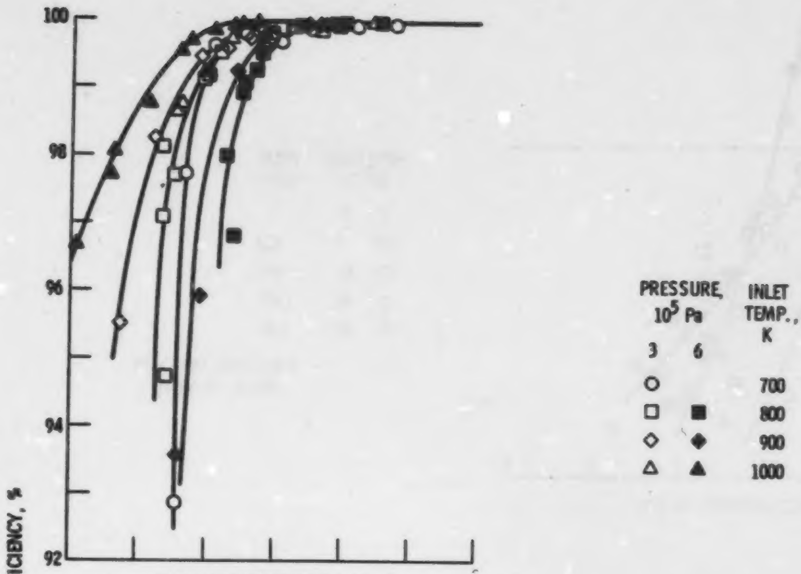

(a) REFERENCE VELOCITY, 10 m/s.

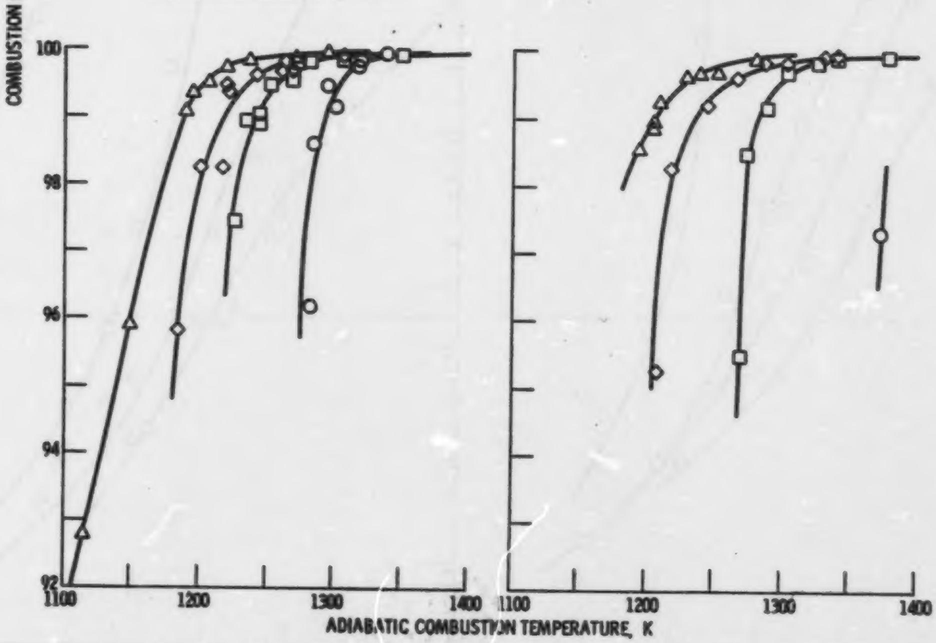

(b) REFERENCE VELOCITY, 15 m/s; PRESSURE, 3×10^5 Pa. (c) REFERENCE VELOCITY, 20 m/s; PRESSURE, 3×10^5 Pa.

Figure 2. - Combustion efficiency.

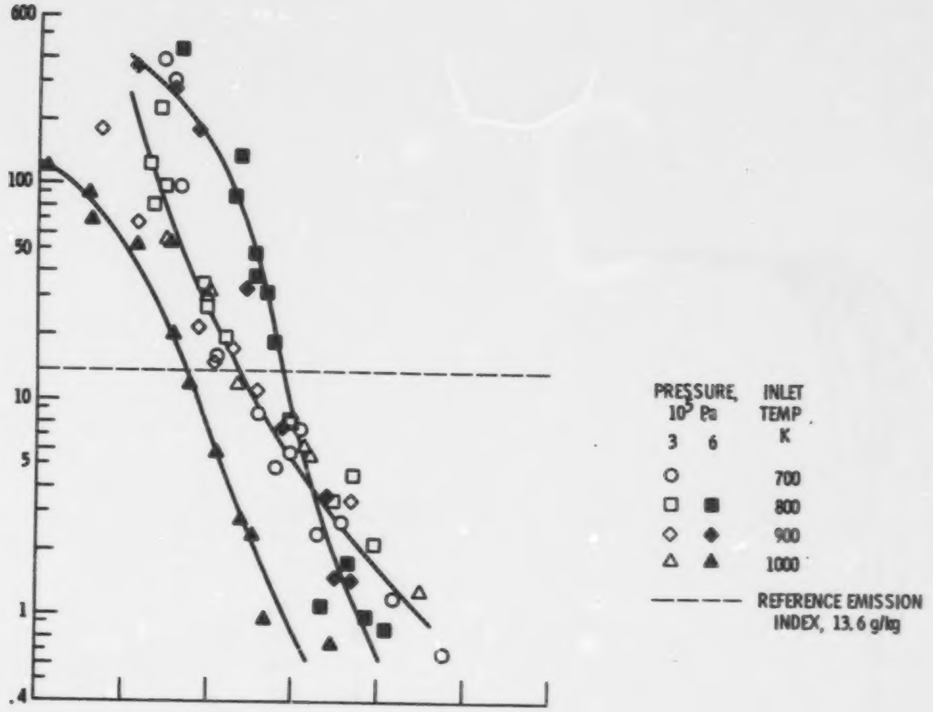

(a) REFERENCE VELOCITY, 10 m/s.

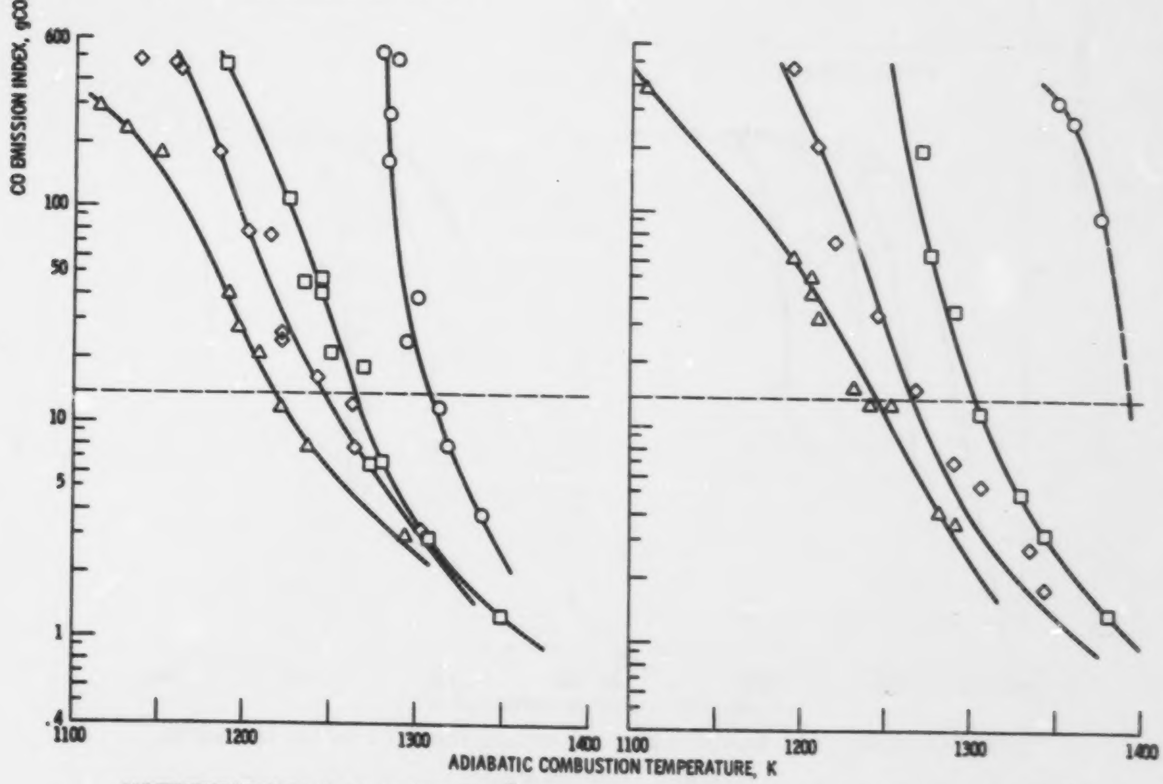

(b) REFERENCE VELOCITY, 15 m/s; PRESSURE, 3×10^5 Pa.

(c) REFERENCE VELOCITY, 20 m/s; PRESSURE, 3×10^5 Pa.

Figure 3. - Carbon monoxide emissions.

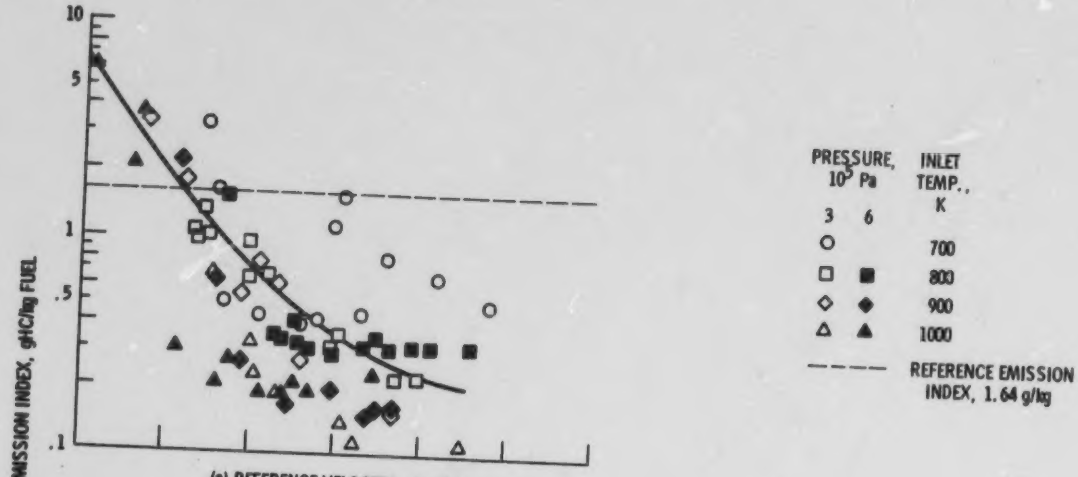

(a) REFERENCE VELOCITY, 10 m/s.

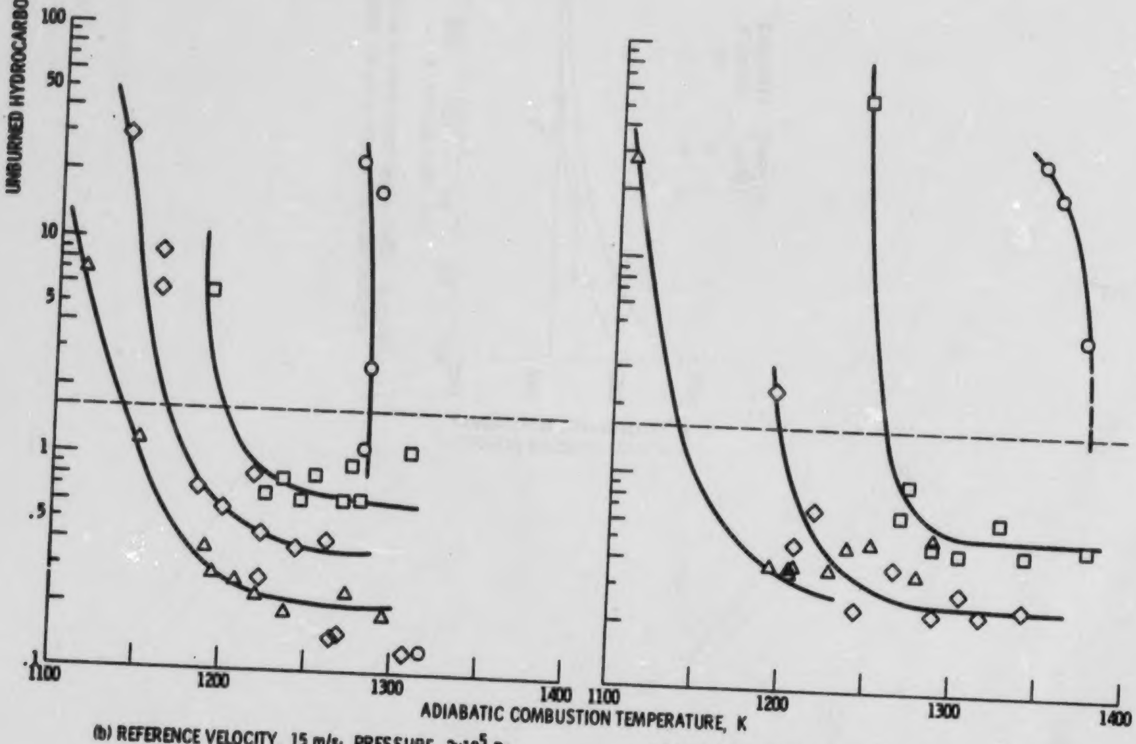

(b) REFERENCE VELOCITY, 15 m/s; PRESSURE, $3x10^5$ Pa.

(c) REFERENCE VELOCITY, 20 m/s; pressure, $3x10^5$ Pa.

Figure 4. - Unburned hydrocarbons emissions.

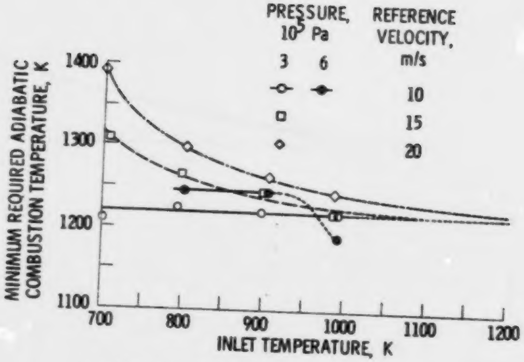

Figure 5. - Effect of inlet temperature on minimum operating temperature required for low emissions.

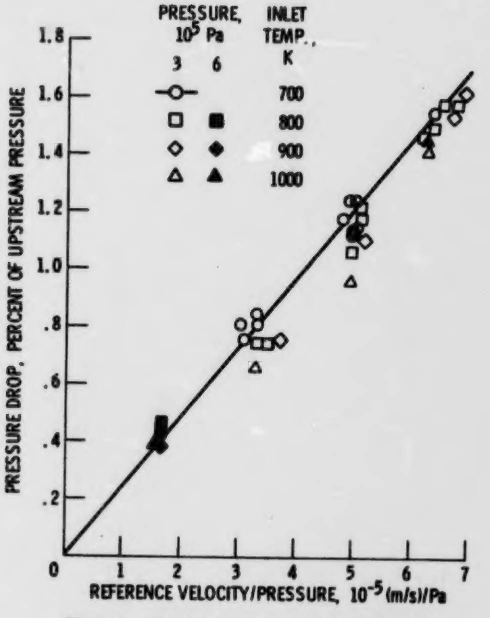

Figure 6. - Reactor pressure drop at an adiabatic combustion temperature of 1300 K.

PERFORMANCE OF MULTIPLE-VENTURI FUEL PREPARATION SYSTEM

by

Robert R. Tacina
NASA-Lewis Research Center
Cleveland, Ohio 44135

Preceding page blank

PERFORMANCE OF MULTIPLE-VENTURI FUEL PREPARATION SYSTEM

by

Robert R. Tacina

NASA Lewis Research Center
Cleveland, Ohio 44135

ABSTRACT

An airblast-type fuel-injection system was evaluated for use with a catalytic reactor in a gas turbine application. Multiple, venturi-type tubes were used to provide high-velocity air for atomization and would also straighten the inlet airflow. Spatial fuel-air distributions, degree of vaporization, and pressure drop were measured 16.5 cm downstream of the fuel injection plane. Tests were performed in a 12 cm tubular duct. Test conditions were: a pressure of 0.3 MPa, inlet air temperatures from 400K to 800K, air velocities of 10 and 20 m/s, and fuel-air ratios of 0.010 and 0.020. The fuel was diesel #2. Spatial fuel-air distributions were within ± 20 percent of the mean at inlet air temperatures above 450K. At an inlet air temperature of 400K, the fuel-air distribution was within ± 30 percent of the mean. No distortion in the fuel-air distribution was measured when a 50 percent blockage plate was placed 9.2 cm upstream of the fuel injection plane to distort the inlet air velocity profiel. Vaporization of the fuel was 50 percent complete at an inlet air temperature of 400K and the percentage increased linearly with temperature to complete vaporization at 600K.

Preceding page blank

CORRELATIONS OF CATALYTIC COMBUSTION PERFORMANCE PARAMETERS

Daniel L. Bulzan
NASA-Lewis Research Center
Cleveland, Ohio

Preceding page blank

ABSTRACT

Performance parameters were correlated for a catalytic combustor. Correlations for combustion efficiency, percentage pressure drop and the minimum required adiabatic reaction temperature necessary to meet emissions goals of 13.6g CO/kg fuel and 1.64g HC/kg fuel are presented. Combustion efficiency was found to be a function of the cell density, cell circumference, reactor length, reference velocity and adiabatic reaction temperature. The percentage pressure drop at an adiabatic reaction temperature of 1450K was found to be proportional to the reference velocity to the 1.5 power. The percentage pressure drop was also found to be proportional to the reactor length and inversely proportional to the pressure, cell hydraulic diameter and fractional open area. The minimum required adiabatic reaction temperature needed to meet the emissions goals was found to increase with reference velocity and decrease with cell circumference, cell density and reactor length. A catalyst factor was introduced into the correlations to account for differences between catalysts. Combustion efficiency, the percentage pressure drop, and the minimum required adiabatic reaction temperature were found to be a function of the catalyst factor. The catalyst factor ranged from .12 to 1.52. The data was from a 12 cm. diameter test rig with noble metal reactors using propane fuel at an inlet temperature of 800K, a pressure of 3×10^5 Pa, and reference velocities from 10 to 20 m/s.

Preceding page blank

CATALYST DESIGN STUDIES IN LOW BTU GAS COMBUSTION

by

R. Carrubba
I. T. Osgerby
Engelhard Industries Division
Edison, New Jersey

This paper was not received in time for publication. Contact the authors for details.

Preceding page blank

CATALYZED COMBUSTION OF H_2/AIR MIXTURES IN A FLAT PLATE BOUNDARY LAYER

By:

R.W. Schefer
F.S. Robben
R.K. Cheng

Lawrence Berkeley Laboratory
University of California
Berkeley, California 94720

*This work was supported by DOE, Division of Conservation Research and Technology

ABSTRACT

A study has been made of the combustion characteristics of lean hydrogen-air mixtures flowing over a heated catalytic platinum plate. The objectives of the investigation are to develop a better understanding of the interaction between fluid mechanics, gas phase combustion, and the surface catalytic reactions in high temperature surface catalyzed combustion.

The experimental system consists of a thin quartz plate with vacuum deposited platinum heating strips mounted over an open atmospheric pressure jet of premixed hydrogen and air. Boundary layer density profiles were measured using differential interferometry for flow visualization studies and Rayleigh scattering for point density measurements. The presence of heat release due to surface reaction was determined from changes in heating strip power inputs with fuel addition.

Results are presented for a range of equivalence ratios from 0.05 to 0.30 and plate surface temperatures from 470K to 1300K. Significant surface heat release was found for all mixtures at plate temperatures as low as 470K. Only at increased equivalence ratios and plate temperatures was heat release due to gas phase reaction present. This was characterized by local increases in temperature across the boundary layer and an increase in thermal boundary layer thickness.

The effect of various surface boundary conditions was studied using a computer program to solve the boundary layer equations for flow over a heated plate with H_2/air combustion. Surface conditions investigated include: 1) a noncatalytic surface; 2) finite rate surface oxidation of H_2; and 3) radical recombination at the plate surface in addition to surface oxidation of H_2. Surface reaction is found to have a strong quenching effect on the initiation of gas phase combustion in the boundary layer due to the removal of H_2 near the plate surface and quenching of radical species generated in the gas phase.

Preceding page blank

SECTION 1

INTRODUCTION

Interest in the use of catalytic surfaces to promote combustion reactions has increased greatly over the past several years. A number of studies have been undertaken which indicate that catalytically supported combustion makes efficient burning of a variety of fuels possible under fuel lean conditions with a substantial reduction in NO_x levels (1,2). While initial emphasis was based on the use of catalytic combustors for aircraft gas turbine application its potential application to stationary power sources has also been studied with favorable results (3).

Much of the work to date has involved parametric investigations of prototype catalytic combustor configurations. The results of such studies are both necessary to the long term development of catalytic combustors and have been very promising. However, such studies are somewhat limited in terms of deriving a more fundamental understanding of catalytically supported combustion. Two such areas where a greater knowledge would be desirable are the role of internal heat and mass transfer in the catalytic combustion process, and the role of homogeneous as opposed to catalytic surface reactions. An understanding of these and related processes is necessary for the optimum evaluation and application of the catalytic concept to practical combustion system design.

The approach of the present investigation has been to examine catalytically supported combustion in a well characterized system in which most of the important physical and chemical processes found in larger scale catalytic combustors are present. The geometry chosen consists of combustion in the boundary layer of heated catalytic flat plate. This system provides a suitable geometry for both experimental and numerical modeling studies. The operation of such a system under a suitably selected range of conditions greatly

Preceding page blank

facilitates determination of the roles of the various processes involved.

The experimental study has concentrated on the use of two optical diagnostic techniques, Rayleigh scattering and differential interferometry, for boundary layer density measurements. Optical diagnostic techniques were used because they are non-perturbing to the flow and provide good spatial resolution. The advantage of a flow visualization method such as interferometry is that a relatively rapid study of boundary layer behavior under combustion conditions is possible. Rayleigh scattering was then used for a more detailed investigation of the boundary layer structure under those conditions of greatest interest.

In Section 2 of this paper the experimental facility and diagnostics are described, and results are presented for the flow of chemically reacting H_2/air mixtures over a heated platinum catalytic surface. The numerical model and procedure are described in Section 3. Results are presented for the combustion of H_2/air at an equivalence ratio of 0.1 over a heated noncatalytic plate with a surface temperature of 1100 K. The model is then extended to include finite rate surface reaction. Two models are formulated to account for catalytic reactions at the plate surface. These are based on: 1) a boundary condition which includes finite rate surface oxidation of H_2 (case 1); and 2) a condition which includes radical recombination at the surface in addition to surface oxidation of H_2 (case 2). Comparisons are made with the experimental results.

SECTION 2

EXPERIMENTAL INVESTIGATION

APPARATUS

Flow System and Plate Design

The experimental configuration consists of a thin quartz plate with vacuum deposited platinum heating strips suspended vertically over an open, atmospheric pressure jet of premixed hydrogen and air. The jet is produced by a stagnation chamber with a converging nozzle at the exit. The stagnation chamber is 20 mm in diameter and is fitted with a 5 cm diameter nozzle at the exit. It has three internal screens and produces a uniform, low turbulence flow of premixed combustible mixture which is directed vertically upwards. Lower flow rates of gases are metered by calibrated rotometers, and larger air flow rates are metered using a standard orifice gauge and water manometer. The house air supply is passed through a dryer and filter combination which eliminates particulate matter. The flat plate and stagnation chamber are mounted on a three-dimensional traverse mechanism (adapted from a milling machine) with a 0.001 cm positioning sensitivity.

Details of the flat plate and holder design are shown in Fig. 1. The plate is made from a 1.5 mm thick, 75 mm square quartz sheet with a sharp leading edge angle of 2°. Five platinum heating strips are vacuum deposited on the plate surface. The central region of the plate is coated to a thickness of 0.3 microns, while the outer edges are coated to approximately three times this thickness. This keeps the outer edges of the plate cool so that gold foil can be used to make electrical contact with the stainless steel fingers. The strips are oriented perpendicular to the flow and are of varying widths to improve temperature control near the plate leading edge. Electrical power is individually controlled to each of these strips and as a result a reasonably uniform plate surface temperature can be maintained.

To reduce the interference of surface scattering of the laser beam with the Rayleigh scattering in the boundary layer, important when measurements are being made close to the plate, it has been found advantageous to have a small bend, about 2°, in the center of the plate. The Rayleigh scattering measurements are made in the shadow of this bend.

Surface temperatures greater than 1000°K are measured using a disappearing filament type optical pyrometer with an emissivity estimate of 0.65 for the platinum surface. For temperatures below 1000°K, the surface temperature is determined from the measured resistivity of the platinum strips.

Optical Diagnostics

Rayleigh Scattering System

Rayleigh scattering refers to the light scattered from gas molecules without any shift in wavelength (4). The intensity is proportional to the gas density and gives approximately the same information as an interferometric measurement of gas density. The principal advantage over interferometric techniques (5) is that it measures the density at a single point rather than integrating along the optical path. The principal disadvantage, compared to an interferometric photograph, is that the density is measured at only one point at a time.

The optical arrangement for the Rayleigh scattering system is shown in Fig. 2. A Spectra Physics argon-ion laser operating at 488 nm with 1 watt power is used in the system. The Rayleigh scattering is measured at right angles to the focused laser beam by a monochrometer and photomultiplier. For measurements close to the plate surface scattering appears as a background signal and thus limits how close measurements can be made. In order to minimize the surface scattering, spatial filters are used to "clean up" the laser beam. A waist diameter of 50 microns was chosen to give good spatial resolution in the boundary layer.

An f/1.2, 55 mm focal length camera lens is used to collect the scattered light. An image of the monochrometer slit, about 100 microns wide and 1 mm long, is then focused on the waist region of the laser beam. The optics and monochrometer (a 0.3 m McPherson) are arranged such that all the rays from the lens fall onto the photomultiplier, an RCA type 1P28. The quantum efficiency of this type of photomultiplier is about 15% at 488 nm. The output current of the photomultiplier is measured using a Keithley electrometer.

As noted previously the slight bend (about 2°) down the middle of the plate effectively shadows the second half of the surface of the plate from the laser beam. This results in a substantial reduction in plate scattered light and makes Rayleigh measurements possible as close as 0.2 mm from the surface.

Differential Interferometer

To study changes in the flow pattern as a function of variations in operating parameters, differential interferometry was used to visualize the flow field. This technique is based on the interference of two beams passing through adjacent points in the test space. Creeden (6) has shown that in this situation, the fringe displacement is proportional to the deflection, Θ, rather than to the index of refraction as in the case of a conventional interferometer. Θ is defined as:

$$\Theta = \int \frac{dn}{dy} dz$$

where n is the index of refraction, z and y are the coordinates along and normal to the optical path respectively. Since the index of refraction is linearly proportional to the density, the fringe displacement is proportional to the density gradient in the test space provided that all other index of refraction fields along the optical path are negligible.

An example of an interferogram is shown in Fig. 3 for a plate surface temperature of 1200 K and an equivalence ratio of 0.3. The distribution of the gradient of the refractive index in the boundary layer is shown by the displacement of the fringes from the undisturbed position. Details of the optical arrangement and analysis procedure can be found in reference (7).

To obtain density or temperature profiles across the boundary layer, the fringe displacement is measured directly from the interferograms. Numerical integration of the area under the fringe displacement curves then gives the difference between the density of the gases in the free stream (ρ_{∞}), and the local gas density. The corresponding temperature profiles are obtained using the ideal gas law.

RESULTS

Differential Interferometer Study

Typical temperature profiles obtained from an analysis of the interferograms are shown in Fig. 4 for a plate temperature of 1270 K and various equivalence ratios. The profiles for equivalence ratios of 0.0 and 0.1 are typical of those with no heat release due to gas phase reaction. Under these conditions the profiles are self-similar. For mixtures with higher equivalence ratios the temperature profiles are significantly different. In this case the heat release rates due to gas phase combustion are considerably greater than at lower equivalence ratios. As a result the local gas temperature increases and the thermal boundary layer becomes thicker.

It should be noted that the temperature profiles obtained from the interferograms are only approximations to the actual profiles measured with Rayleigh scattering and predicted by the numerical calculations. This can be attributed to the various assumptions regarding the refractive surfaces which were necessary for the analysis (7). As shown in Fig. 4 the interferograms do, however, provide the information needed to distinguish between various stages of gas phase reaction. Further analysis of the data over a range of conditions shows that the existence of gas phase combustion in the boundary layer depends on mixture composition, surface temperature, and distance from the leading edge.

Significant surface reaction was also found to occur under certain conditions. This was apparent as an increase in plate surface temperature due to surface energy release as fuel is added to the flow. By decreasing the power input to the individual heating strips when surface reaction was present the plate temperature could be maintained at the desired value.

The conditions under which the various phenomena occur are summarized in Fig. 5. These results are based on an analysis of data taken at a distance of 50 mm downstream from the plate leading edge. At distances greater than this fluctuations in the jet mixing layer become a significant source of disturbance to the boundary layer. Surface reaction was found to occur at temperatures as low as 470 K, the minimum surface temperature at which measurements were taken. At increased temperatures and equivalence ratios a region exists over which both surface reaction and boundary layer combustion occur simultaneously. At the highest temperatures and equivalence ratios the primary heat release, or reaction, zone moves out of the boundary layer and takes on a flame-like structure characterized by a steep temperature gradient and an approximately constant temperature region extending to the plate surface.

Rayleigh Scattering Study

Based on the results of the differential interferometer study a set of conditions was chosen for Rayleigh scattering measurements in which various stages of gas phase reaction were present. The set of conditions at which Rayleigh scattering measurements were taken is indicated in Fig. 5. These measurements, in addition to providing a better understanding of boundary layer behavior under combustion conditions, also provide a set of data upon which the development of the numerical model can be based.

Density profiles at a distance of 30 mm downstream from the plate leading edge are shown in Fig. 6 for a surface temperature of 1170 K and various equivalence ratios. Also shown as a solid line is the corresponding density profile obtained from the numerical calculations for the case of no combustion. At equivalence ratios less than 0.15 good agreement exists between the experimental and predicted profiles, indicating that no significant heat release due to gas phase reaction occurs under these conditions. At increased equivalence ratios the thermal boundary layer becomes considerably thicker due to gas phase heat release and a region of approximately constant density exists across much of the boundary layer.

The effect of plate surface temperature on thermal boundary layer thickness is shown in Fig. 7 for an equivalence ratio of 0.20. The thermal boundary layer thickness, δ_T, is defined here as the point at which $\rho/\rho_\infty = 0.5$. The corresponding results from numerical calculations for the case of no combustion are indicated by solid lines. At a plate temperature of 1070 K the agreement between experimental and predicted profiles is excellent. From this it is concluded that no gas phase combustion is present under these conditions. At temperatures of 1170 K and 1270 K a noticeable increase in δ_T occurs between 15 mm and 20 mm from the leading edge. Farther downstream the thermal boundary layer growth rates again become comparable for the two plate temperatures.

SECTION 3

NUMBERICAL INVESTIGATION

NUMERICAL MODEL

Governing Equations

The governing differential equations for laminar boundary layer flow of a chemically reacting mixture of gases over a heated flat plate are the conservation of mass, the conservation of momentum, the conservation of energy, and the species conservation equations. Introducing the similarity variables

$$\xi(x) = (\rho\mu)_\infty U_\infty X$$

$$\eta(x,y) = \frac{U_\infty}{\eta_e\sqrt{2\xi}} \int_o^y \rho dy$$

these conservation equations can be written as follows:

Continuity equation

$$2\xi\frac{\partial f'}{\partial\xi} + \frac{1}{\eta_e}\frac{\partial f'}{\partial\eta} + f' = 0 \qquad (1)$$

Momentum equation

$$2\xi f'\frac{\partial f'}{\partial\xi} + (V - \ell')\frac{1}{\eta_e^2}\frac{\partial f'}{\partial\eta} = \frac{1}{\eta_e^2}\frac{\partial^2 f'}{\partial\eta^2} + \frac{e}{U_\infty} g\beta(T - T_\infty) \qquad (2)$$

Energy equation

$$2\xi f'\frac{\partial h}{\partial\xi} + (V - \frac{\bar{c}'}{c_p})\frac{1}{\eta_e}\frac{\partial h}{\partial\eta} - \frac{\ell U_\infty^2}{\eta_e^2}(\frac{\partial f'}{\partial\eta})^2 - \frac{\bar{c}}{\eta_e c_p}(\frac{\partial^2 h}{\partial\eta^2}) \qquad (3)$$

$$= \frac{1}{(\rho\mu)_\infty\eta_c^2}\frac{\partial}{\partial\eta}\left[\frac{k\rho}{c_p}\sum_i (Lc_i - 1)h_i\frac{\partial\sigma_i}{\partial\eta}\right]$$

Species equation

$$2\xi f'\frac{\partial\sigma_i}{\partial\xi} + (V - b_i')\frac{1}{\eta_e}\frac{\partial\sigma_i}{\partial\eta} - \frac{b_i}{\eta_e^2}\frac{\partial^2\sigma_i}{\partial\eta^2} - \frac{e}{\rho}S_{\sigma_i} = 0 \quad , \qquad (4)$$

In the above equations the following dimensionless quantities have been introduced

$$V = \frac{2\xi}{(\rho\mu)_\infty U_\infty}\left(f'\frac{\partial\eta}{\partial x} + \frac{\rho v}{\sqrt{2\xi}}\right) \quad ; \quad f' = \frac{u}{U_\infty}$$

$$\bar{c} = \frac{\ell c_p}{Pr} \quad ; \quad b_i = \frac{\ell Le_i}{Pr} \quad ; \quad e = \frac{2\xi}{U_\infty(\frac{d}{dx})}$$

$$\ell = \frac{\rho\mu}{(\rho\mu)_\infty} \quad ; \quad \bar{c}' = \frac{1}{\eta_e}\frac{\partial\bar{c}}{\partial\eta} \quad ; \quad b_i' = \frac{1}{\eta_e}\frac{\partial b_i}{\partial\eta}$$

η_e represents the value of η at the outer edge of the boundary layer. The chemical kinetic source term S_{σ_i} in the species equation is defined as

$$S_{\sigma_i} = -\sum_{j=1}^{JJ}(\alpha'_{ij} - \alpha''_{ij})(R_j - R_{-j})$$

where R_j and R_{-j} are the forward and reverse rates of reaction j respectively, and α_{ij} is the stoiciometric coefficient for the ith species in the jth reaction as defined in the general reaction expression

$$\sum_{i=1}^{JJ}\alpha'_{ij}\,\sigma_i + \bar{\alpha}_j\,M = \sum_{i=1}^{NR}\alpha''_{ij}\,\sigma_i + \bar{\alpha}_j\,M \qquad j = 1,2,\ldots,JJ.$$

An additional relation is provided by the ideal gas equation of state

$$\rho = \frac{p}{RT}$$

The mixture viscosity and thermal conductivity are calculated from single component transport properties using the semi-empirical expressions of Wilke (8). Since the principle constituent in the present system is N_2, trace diffusion coefficients for the ith species in N_2 were used to simplify the calculations. Single component properties and the binary diffusion coefficients, D_{ij}, were calculated from the Chapmen-Enskog theory with molecular parameters evaluated using a Lennard Jones potential model (8). Thermodynamic data for specific heat and enthalpy were calculated from JANAF data using a formlism based on the NASA Complex Chemical Equilibrium Code (9).

Boundary Conditions

Boundary conditions for the above equations are required at the plate surface and at the outer edge of the boundary layer. In the present case the veloicty is zero at the plate surface (no slip condition) and the surface temperature is specified. These conditions can be written

$$f'(\xi,0) = 0; \quad h(\xi,0) = h_w(x) \tag{5}$$

The general form of the species boundary condition is given by

$$-\frac{\mu}{Pr} Le_i \frac{\rho\, u_\infty}{\eta_e (2\xi)^{\frac{1}{2}}} \frac{\partial \sigma_i}{\partial \eta} \Big|_s = R_s \tag{6}$$

where R_s is the surface reaction rate per unit area. In the case of a non-catalytic wall the surface reaction rate is equal to zero. At the outer edge of the boundary layer

$$\begin{gathered} f'(\xi,\eta_e) = 1 \,; \quad h(\xi,\eta_e) = h_\infty \\ \sigma_i(\xi,\eta_e) = \sigma_{i\infty} \end{gathered} \tag{7}$$

where the free stream conditions are assumed to be constant along the plate.

Surface Reaction Model

While the general role of a catalyst in promoting chemical reaction is well known, there is considerable uncertainty in many systems concerning the kinetic mechanisms involved. This is particularly true at the high temperatures and pressures encountered in combustion systems. Experimental results presented in Section 2 and in a previous report (7) indicate the existence of significant surface reaction for H_2/air mixtures flowing over a platinum surface at plate temperatures as low as 470 C. This was modeled as a one step surface reaction in which H_2 is oxidized to form H_2O as a product (7)

$$H_2 + 1/2\ O_2 \xrightarrow{\text{SURFACE}} H_2O$$

The resulting surface energy release rates were found to correlate well with an Arrhenius type rate expression given by

$$R_s = 1.4\ (n_{H_2})_S\ \exp(-3850/RT) \frac{\text{moles}}{\text{cm}^2\text{sec}} \tag{8}$$

where $(n_{H_2})_S$ is the concentration of H_2 at the surface.

An additional effect which must be considered is that of the plate surface on radical concentrations. It is likely that radical recombination will be important at the plate surface for the relatively low surface temperatures being considered. To include this effect in the calculations radical recombination at the surface was modeled by the set of reactions shown in Table I where the individual reaction rate expressions are of the form

$$R_S = (n_i)_S\ k_S = \frac{\gamma (n_i)_S C_i}{4}\ (\text{mole/cm}^2\text{sec}) \tag{9}$$

γ is the reaction probability per collision, $(n_i)_S$ is the concentration of species i at the plate surface and C_i is the molecular velocity. The quantity $n_i C_i/4$ thus represents the collision frequency of the i^{th} specie with the plate surface. Substitution of the surface reaction rate expressions (8) and (9) into Eq. (8) provides the necessary species boundary conditions.

TABLE I. Radical Recombination Surface Reactions

Reaction	Rate Constant, k_s
$O + S \rightarrow 1/2\ O_2 + S$	$\gamma_O C_O/4$
$H + S \rightarrow 1/2\ H_2 + S$	$\gamma_H C_H/4$
$OH + S \rightarrow 1/2\ H_2 + 1/2\ O_2 + S$	$\gamma_{OH} C_{OH}/4$
$HO_2 + S \rightarrow 1/2\ H + O_2 + S$	$\gamma_{HO_2} C_{HO_2}/4$

To assess the relative importance of surface oxidation of H_2 and radical recombination, the calculations were carried out for two models of catalytic wall reaction. In case 1 only the surface oxidation of H_2 is considered. In case 2 surface radical recombination is considered in addition to surface oxidation of H_2. To determine the maximum possible influence of radical recombination a reaction probability of unity ($\gamma=1$) was used in the latter case. The plate surface was considered noncatalytic (i.e. $R_s = 0$) for all species not undergoing surface reaction.

Gas Phase Kinetics

The forward and reverse reaction rates of the i^{th} reaction can be written

$$R_j = k_j (\rho\sigma_m)^{\overline{\alpha}_j} \prod_{i=1}^{NS} (\rho\sigma_i)^{\alpha'_{ij}} \quad , \quad j = 1,2...J$$

$$R_{-j} = k_{-j} (\rho\sigma_m)^{\overline{\alpha}_j} \prod_{i=1}^{NS} (\rho\sigma_i)^{\alpha''_{ij}} \quad , \quad j = 1,2...J$$

where k_j is an Arrhenius rate coefficient of the form

$$k_j = 10^{B_j} T^{N_j} \exp(-E_j/RT).$$

Reverse rate coefficients were assumed to be related to the forward rate constant through the equilibrium constant K_{cj}

$$k_{-j} = \frac{k_j}{K_{cj}}$$

The reaction mechanism chosen for H_2/air combustion consists of 13 reactions 8 chemical species. These are shown in Table II.

Numerical Procedure

The above system of equations was solved using an implicit finite difference procedure. The resulting difference equations and the boundary conditions form a system of equations of the tridiagonal type. The approach of the present investigation was to use a standard tridiagonal matrix solution algorithm to solve the hydrodynamic equations for conservation of mass and momentum (16).

The coupled energy and species conservation equations were then solved using a Newton Raphson correctional scheme developed by Pratt (17).

For the results presented a grid consisting of 50 points across the boundary layer between $\eta = 0$ and $\eta_e = 9.0$ was found to be sufficient. To improve accuracy near the wall where the steepest gradients occur a nonuniform grid was used with $\Delta\eta$ given by Eq. (10) with $k = 1.07$.

$$\Delta\eta_{N=1}\frac{k - 1}{(k^{NMAX-1} - 1)}\ ; \quad \Delta\eta_N = \Delta\eta_{N-1} \cdot k \qquad (10)$$

Step size in the streamwise direction, $\Delta\xi$, was adjusted continuously to meet the desired accuracy of 5%. Minimum step size corresponded to a time step on the order of 10^{-7} sec.

RESULTS

Noncatalytic Plate Surface

The results of the numerical calculations for the case of H_2/air flow over a noncatalytic heated plate with combustion at an equivalence ratio of 0.1 are shown in Figs. 8-10. In the case presented the surface temperature was assumed constant at 1100^oK and the free stream velocity and temperature were 3.17m/s and 293^oK respectively.

Temperature profiles are plotted against the nondimensional boundary layer coordinate η in Fig. 8 for several distances downstream of the plate leading edge. The temperature profiles remain self similar until a distance of approximately 0.6 mm along the plate. Upstream of this location little heat release due to chemical reaction has occurred. At x = 1.89 mm combustion is apparent near the surface as can be seen by the peak in the temperature profile. A short distance downstream (x = 2.00 mm) the heat release has become significant with the temperature reaching a maximum of 1470^oK. Combustion has also spread farther out into the boundary layer. At x = 2.80 mm the heat release rate has decreased in regions near the plate surface as H_2 is used up and heat transfer to the plate has resulted in a decrease in gas temperature. Combustion of incoming reactants continues to occur farther out in the boundary layer but at a decreasing rate due to the lower temperatures.

Typical species concentration profiles for several distances downstream from the plate leading edge are shown in Figs. 9 and 10. Profiles at x = 1.35 mm correspond to the region before any heat release due to chemical reaction has occurred. O, H, OH, and HO_2 radical concentrations are rapidly increasing in the high temperature region near the plate surface and the H_2O concentration, while comparable to the radical concentrations, is still quite low. H_2 has undergone little reaction at this point.

At x = 1.89 mm a small amount of chemical heat release has occurred in the boundary layer (the corresponding temperature profile is shown in Fig. 8). This release corresponds to the reaction of H_2 and O_2 near the plate surface, and the formation of relatively large amounts of H_2O. Radical concentrations of H, O, and OH have attained their peak values near the plate and are beginning to decrease as recombination reactions become important.

Catalytic Plate Surface

The effect of including surface oxidation of H_2 on boundary layer combustion (case 1) is shown in Fig. 11 and 12. As can be seen from Fig. 11 surface oxidation of H_2 effectively inhibits the onset of heat release due to gas phase combustion. In this case no significant heat release is found to occur prior to a distance of 4.0 mm from the leading edge. Farther downstream gas phase combustion once again results in local increases in temperature across the boundary layer. The heat release rate is, however, considerably lower than that obtained with the noncatalytic plate. Temperature increases are limited to a maximum of approximately 100 K and only a relatively small increase in thermal boundary layer thickness occurs (compare Fig. 8 for a noncatalytic plate).

The reason for the reduced gas phase heat release rates can be seen in Fig. 12 where H_2 and OH concentration profiles are shown for case 1. Surface oxidation directly results in a reduction in H_2 concentration near the plate surface where maximum heat release was found to occur in the case of the noncatalytic plate. Since less H_2 is available for reaction in this region the overall gas phase heat release rate is significantly reduced. In addition, the onset of gas phase combustion is delayed until farther downstream due to a slower increase in radical concentrations near the leading edge.

The effect of adding surface radical recombination in case 2 is shown in Fig. 13 where the H_2 and OH concentration profiles are shown for several distances downstream of the plate leading edge. With both the noncatalytic plate and case 1 maximum radical concentrations were found to occur in the high temperature region near the plate surface. As can be seen from Fig. 13 radical recombination results in a rapid decrease in OH concentration in this region and a slower initial radical buildup.

The predicted thermal boundary layer thickness, δ_T, is shown as a function of distance from the plate leading edge in Fig. 14 for the surface boundary conditions considered above. Also shown for comparison are results for a heated plate with no combustion. In the case of a noncatalytic plate, the high gas phase heat release rate results in a rapid increase in δ_T at approximately 2 mm downstream from the leading edge. With a catalytic surface the increase in δ_T is only about 30 percent greater than for the case of no combustion at a distance of 20 mm downstream, with the difference between cases 1 and 2 being relatively small. In case 1 gas phase heat release is first apparent at a distance of 4 mm downstream from the leading edge. In case 2 radical recombination at the surface results in boundary layer combustion being delayed until approximately 10 mm downstream.

COMPARISON WITH EXPERIMENT

The above study of surface boundary condition effects indicates that both models for surface reaction predict a relatively small increase in δ_T over that obtained with no combustion. This behavior agrees well with the experimental results shown in Fig. 7. Since it is likely that both radical recombination and surface oxidation of H_2 are important in the present system, this was chosen as the most realistic boundary condition to apply in the case of a catalytic surface and the calculations were repeated for a set of conditions at which Rayleigh data were taken. An equivalence ratio of 0.2, a plate temperature of 1170 K, and a free stream velocity of 1.5 m/s was chosen.

The resulting thermal boundary layer profile is shown with the experimental results for comparison in Fig. 15. It can be seen that the predicted increase in thickness is much more abrupt and occurs farther upstream (approximately 2 mm from the leading edge) than is found experimentally. Since good agreement was obtained between predicted and experimental results when no combustion was present, it would appear that the discrepancy in boundary layer thickness is due either to the kinetic mechanism used or to the model employed for surface reaction. The rate expression used for surface oxidation of H_2 was based on surface heat release rates measured in the present system under similar operating conditions and thus is expected to provide a good model for H_2 oxidation. Since a reaction probability of unity was used in the surface radical recombination rates the calculations should reflect the maximum possible influence of radical recombination on the combustion process. Therefore it appears that the most likely cause of the observed discrepancy is the gas phase reaction mechanism employed.

It would be difficult at this time to conclude which reaction rates are the primary cause of the discrepancy since the occurrence of combustion is a function of both the initial radical buildup rate and energy release rates in the primary combustion zone. A preliminary examination of reaction rates during the combustion process shows that initial radical buildup is controlled by the bimolecular branching reactions (1), (2), and (3), and reaction (13) involving HO_2 (Table II), whereas energy release is due primarily to reactions (2) and (8). Rates for the bimolecular branching reactions (1) through (3) are relatively well known, for the most part to within 30%. Expected uncertainty in rates for the three body recombination reactions is somewhat greater, but these reactions were found to be relatively unimportant to the combustion process (except for reaction (8) involving HO_2). The greatest uncertainty in the present kinetic mechanism appears to exist in the HO_2 reactions, the two most important being reactions (8f) and (13r). A more detailed study of the reaction mechanism is currently being made to determine if the above uncertainties in reaction rate constants could account for the observed discrepancy.

SECTION 4

SUMMARY

A study of boundary layer combustion for lean H_2/air mixtures flowing over a heated platinum plate indicated the presence of significant surface heat release for all mixture ratios at plate temperatures as low as 470 K. At the maximum equivalence ratio studied ($\phi = 0.3$) stable boundary layer combustion was observed for plate surface temperatures between 1070 K and 1170 K. At temperatures greater than 1170 K combustion was apparent very near the plate leading edge and the primary reaction zone took on a flame like structure characterized by a steep temperature gradient which extended well out into the free stream. For lower equivalence ratios the plate surface temperature needed to maintain gas phase combustion increased significantly.

Numerical calculations for a lean ($\phi = 0.1$) H_2/air mixture flowing over a heated noncatalytic plate with a wall temperature of 1100 K indicated the existence of several stages of boundary layer combustion. These included an upstream region in which radical concentrations increased with little associated heat release and a downstream region in which heat release due to the reaction of H_2 became appreciable. In the upstream region temperature profiles were approximately similar and boundary layer thickness corresponded to that for no combustion. Heat release due to gas phase combustion resulted in a significant increase in thermal boundary thickness and gas temperatures greater than the wall temperature were achieved.

The effect of surface reaction on the combustion process was investigated using boundary conditions for a catalytic surface based on 1) a condition which includes finite rate surface oxidation of H_2 and 2) a condition which includes radical recombination at the plate surface in addition to surface oxidation of H_2. Surface reaction was found to have a strong quenching effect on the initiation of gas phase combustion in the boundary layer. This was due to the depletion of H_2 near the plate surface and quenching of radical species generated in the gas phase.

A comparison between experimental results and numerical calculations utilizing condition 2) above showed poor agreement. The predicted increase in thermal boundary layer thickness was more abrupt and occurred farther upstream than was found experimentally. This discrepancy was attributed to uncertainties in the gas phase kinetic mechanism since condition 2) should result in the maximum possible surface quenching of gas phase combustion.

REFERENCES

1. Blazowski, W.S. and Walsh, D.E., Combust. Sci. Technol. 10, p. 233 (1975).

2. Pfefferle, W.C., Carrubba, R.V., Heck, R.M. and Roberts, G.W., "Catathermal Combustion: A New Process for Low Emissions Fuel Conversion," ASME Paper 75-WA/FU-1 (Dec. 1975).

3. Kesselring, J.P., Brown, R.A., Schreiber, R.J., and Moyer, C.B., "Catalytic Oxidation of Fuels for NO_x Control from Area Sources," Environmental Protection Agency Report EPA-600/2-76-037 (February, 1976).

4. Jenkins, F.A. and White, H.E., Fundamentals of Optics, McGraw-Hill, New York, p. 462 (1957).

5. Weinberg, F.J., Optics of Flames, Butterworths, London (1963).

6. Creeden, J.E., Fistrom, R.M., Grunfelder, C. and Weinberg, F.J., J. Phys. D, 5, 1063 (1972).

7. Schefer, R., Cheng, R., Robben, F., and Brown, N., "Catalyzed Combustion of H_2/Air Mixtures on a Heated Platinum Plate," presented at the Western States Section/The Combustion Institute, Boulder, CO (1978).

8. Bird, R.B., Stewart, W.E. and Lightfoot, E.N. Transport Phenomena, John Wiley and Sons, New York (1960).

9. Gordon, S. and McBride, B., "Computer Program for Calculation of Complex Chemical Equilibrium Composition," NASA SP-273 (1971).

10. Baulch, D.L., Drysdale, D.D., and Horne, D.G., Fourteenth Symposium (International) on Combustion, The Combustion Institute, Pittsburgh, 107 (1973).

11. Wilson, W.E., Jr., J. Chem. Ref. Data 1, 535 (1972).

12. Baulch, D.L., Drysdale, D.D., Horne, D.G., and Lloyd, A.C., Evaluated Kinetic Data for High Temperature Reactions, Butterworths, London, Vol. 1 (1972).

13. Myerson, A.L. and Watt, W.D., J. Chem. Phys. 49, 425 (1968).

14. Johnston, H.S., "Gas Phase Reaction Kinetics of Neutral Oxygen Species," NSRDS-NBS 20 (1968).

15. Lloyd, A.C., Int. J. Chem. Kinetics 6, 169 (1974).

16. Blottner, F.G., Johnson, M. and Ellis, M., "Chemically Reacting Viscous Flow Program for Multi-Component Gas Mixtures," Sandia Laboratories Report SC-RR-70-754 (1971).

17. Pratt, D.T., and Wormeck, J.J., "CREK - a computer Program for Calculation of Combustion Reaction Equilibrium and Kinetics in Laminar or Turbulent Flow," Washington State University Report WSU-ME-TEL-76-1 (1976).

TABLE I

H_2 - Air Reaction Mechanism

	Reaction	k	Ref.
1.	$O + H_2 \rightleftarrows OH + H$	$10^{7.255}T^{1.0}\exp(-4479.0/T)$	10
2.	$H_2 + OH \rightleftarrows H_2O + H$	$10^{10.35}\exp(-2617.0/T)$	11
3.	$H + O_2 \rightleftarrows O + OH$	$10^{11.342}\exp(-8450.0/T)$	12
4.	$OH + OH \rightleftarrows H_2O + O$	$10^{9.800}\exp(-550.0/T)$	12
5.	$H_2 + M \rightleftarrows H + H + M$	$10^{9.348}\ T^{0.5}\exp(-48414.0/T)$	13
6.	$H + OH + M \rightleftarrows H_2O + M$	$10^{16.342}\ T^{-2.0}$	12
7.	$O + O + M \rightleftarrows O_2 + M$	$10^{11.410}\ T^{-1.0}\exp(-171.5/T)$	14
8.	$H + O_2 + M \rightleftarrows HO_2 + M$	$10^{9.350}\exp(500.0/T)$	12
9.	$HO_2 + H \rightleftarrows OH + OH$	$10^{11.400}\exp(-950.0/T)$	12
10.	$HO_2 + OH \rightleftarrows H_2O + O_2$	$10^{10.699}\exp(-503.3/T)$	15
11.	$HO_2 + O \rightleftarrows OH + O_2$	$10^{10.699}\exp(-503.3/T)$	15
12.	$HO_2 + H \rightleftarrows H_2O + O$	$10^{10.699}\exp(-503.3/T)$	15
13.	$HO_2 + H \rightleftarrows H_2 + O_2$	$10^{10.398}\exp(-350.0/T)$	15

*Units - k : $(m^3\ kg\ mole^{-1})^{n-1} sec^{-1}$ where n is reaction order
T : ^{o}K

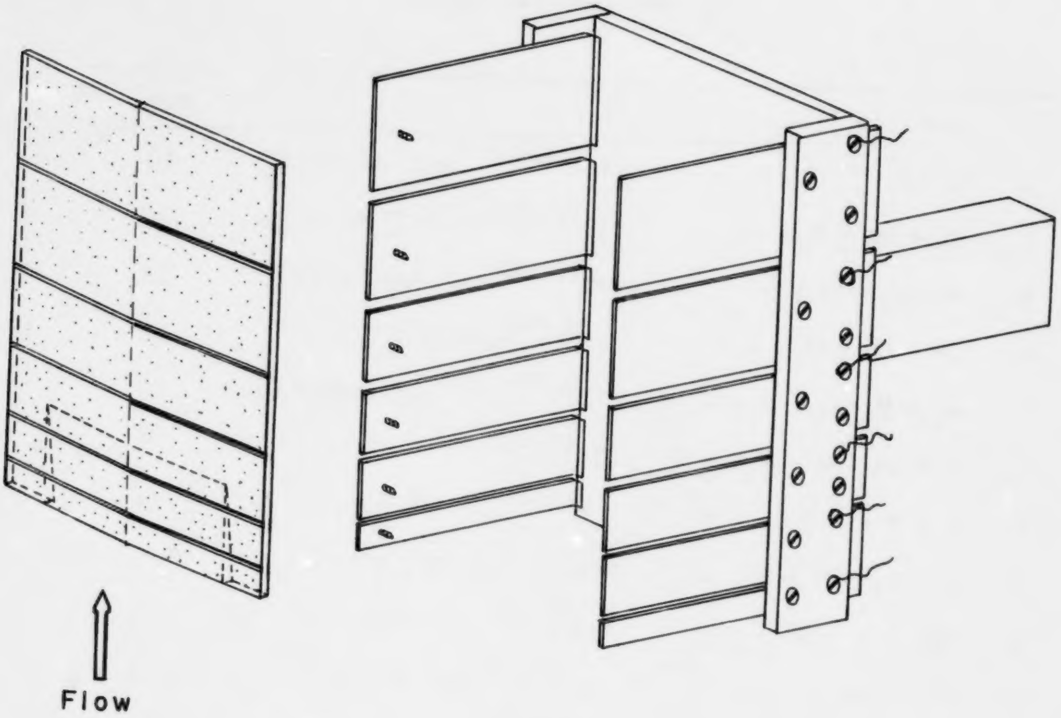

XBL 771-127

Figure 1. Design of the quartz flat plate and the holder.

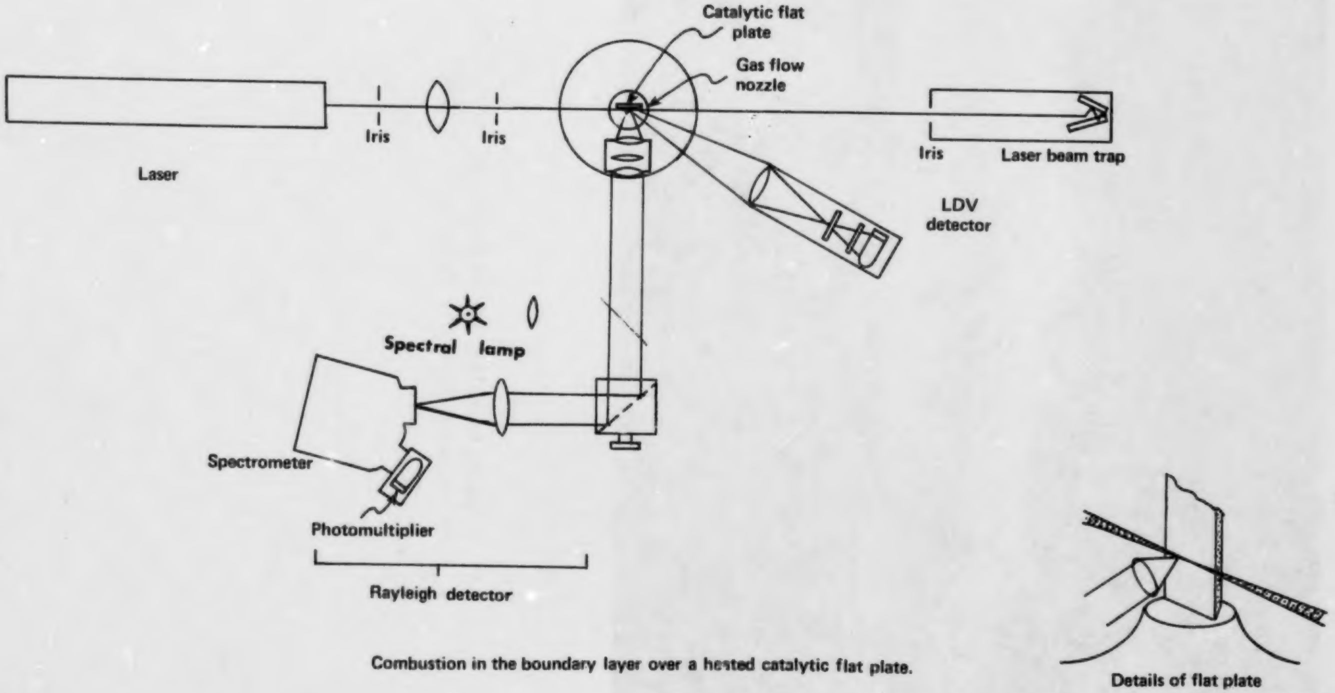

Combustion in the boundary layer over a heated catalytic flat plate.

XBL 764-2757A

Figure 2. Schematic of the experimental apparatus for measurement of velocity and density boundary layer profiles over a flat plate.

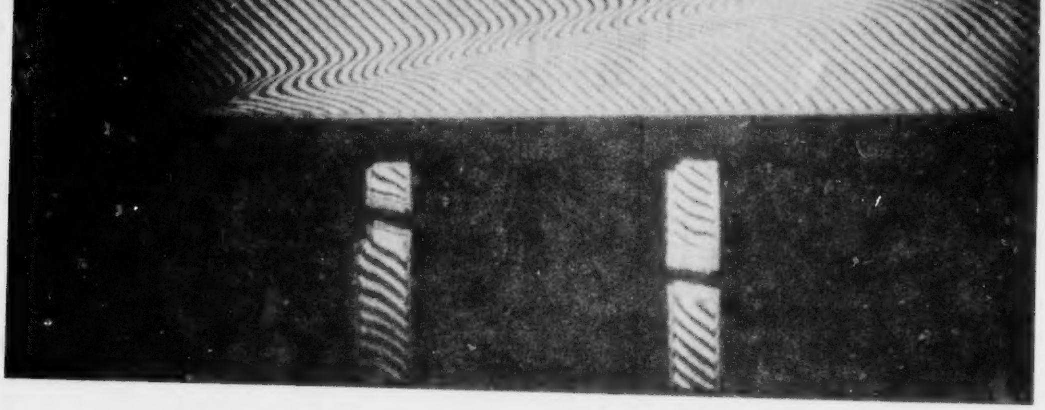

Figure 3. Deflection mapping photograph of the flat plate boundary layer. H_2/air combustion. $\phi = 0.3$, $T_s = 1200$ K, $U_\infty = 1.5$ m/s, $T_\infty = 293$ K.

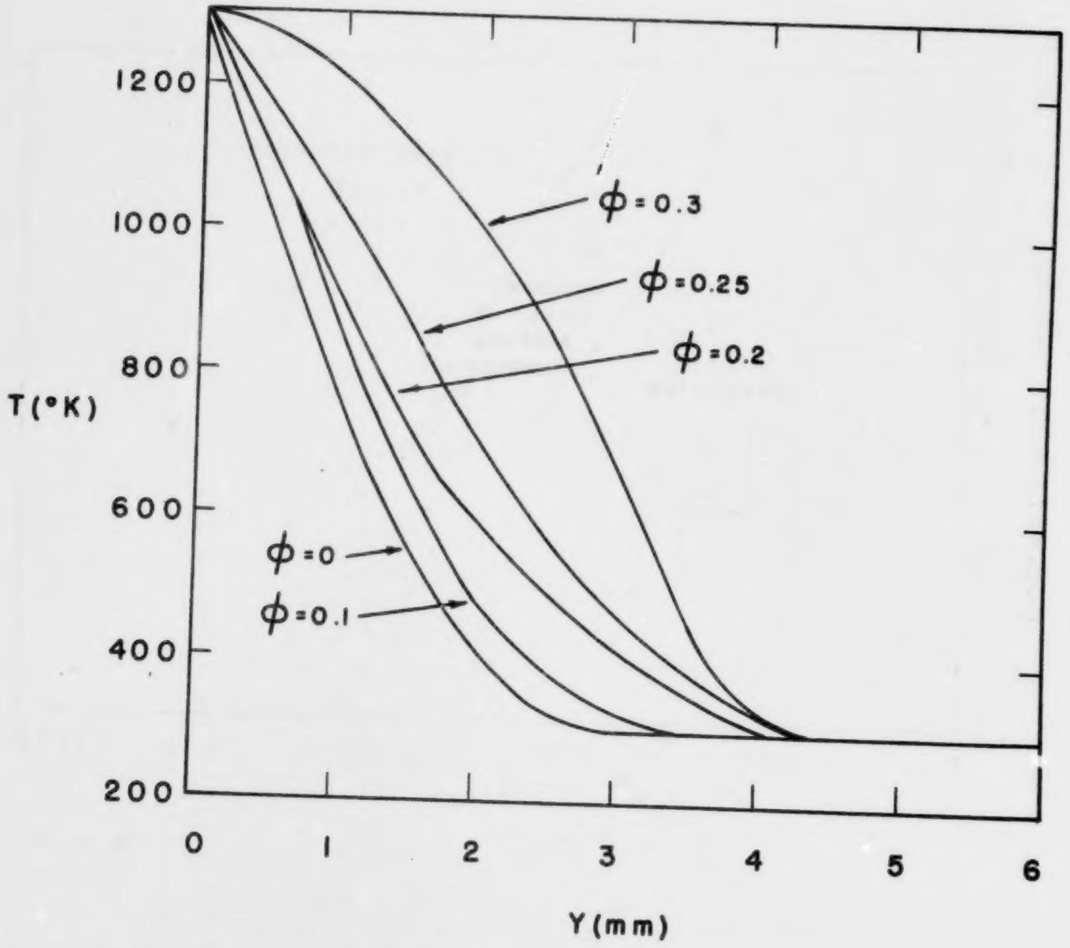

XBL 784-7919

Figure 4. Temperature distribution as a function of distance above the plate. Temperatures are based on differential interferometer measurements. H_2/air combustion. T_s = 1270 K, U_∞ = 1.5 m/s, T_∞ = 293 K.

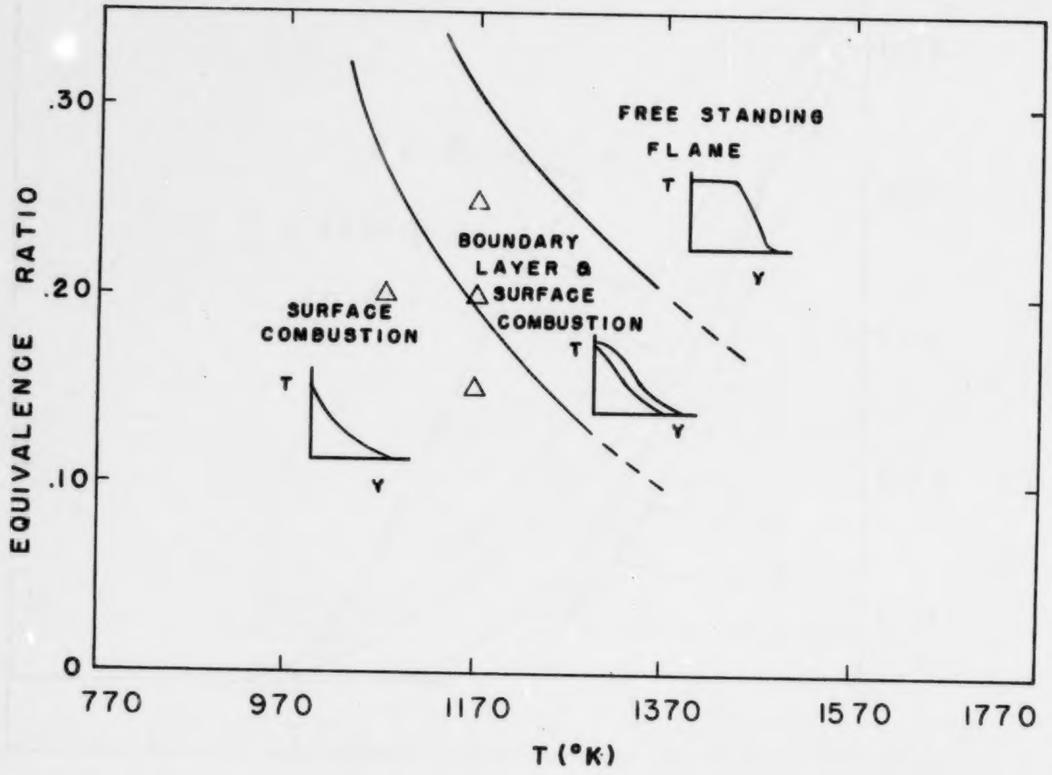

XBL 784-7918A

Figure 5. Combustion regions for H_2/air mixtures over a heated platinum plate. $U_\infty = 1.5$ m/s, $T_\infty = 293$ K. Δ indicates a point at which Rayleigh data was taken.

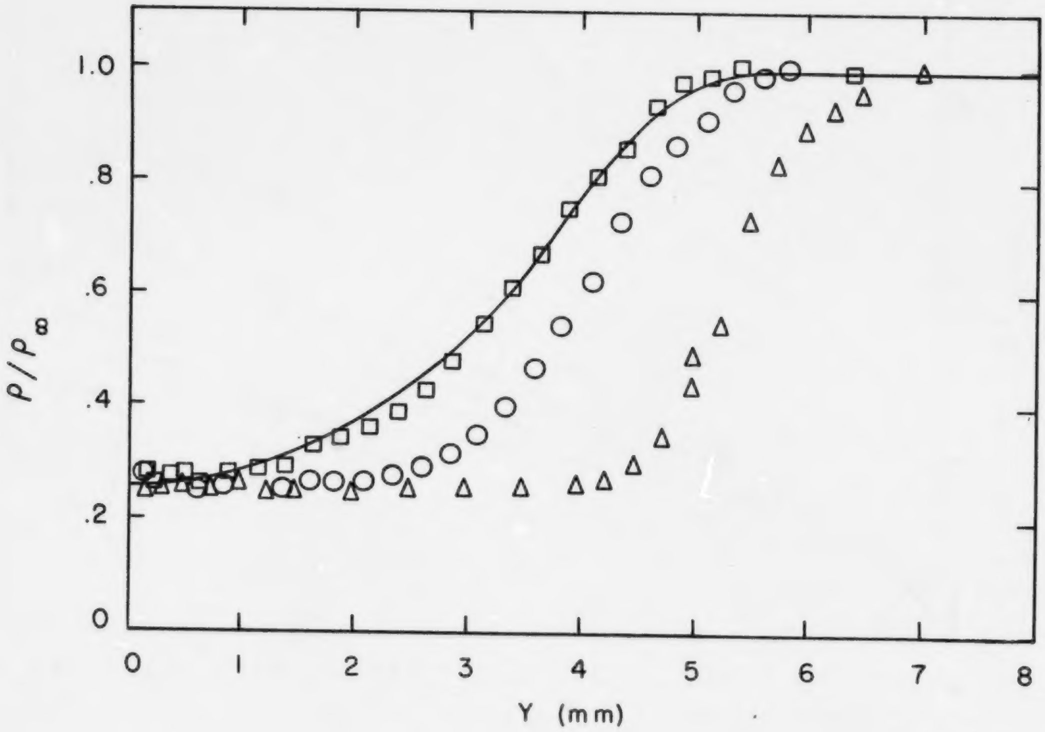

XBL 788-10512

Figure 6. Normalized density profiles over a heated platinum plate at a distance of 30 mm from the leading edge. H_2/air combustion T_s = 1170 K, U_∞ = 1.5 m/s, T_∞ = 293 K, X, ϕ = 0.15; 0, ϕ = 0.20; Δ, ϕ = 0.25. Solid line indicates numerical results for no combustion.

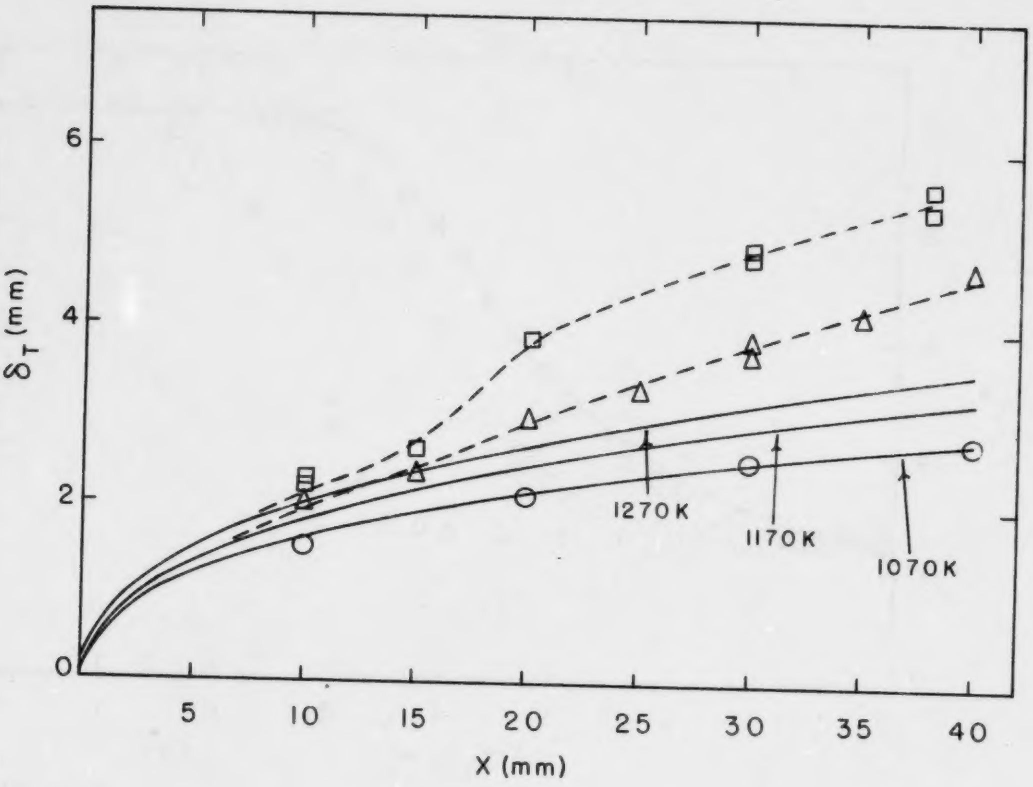

XBL 788-10509

Figure 7. Effect of plate surface temperature on thermal boundary layer thickness ($\rho/\rho_\infty = 0.5$) for flow over a heated platinum plate. H_2/air combustion. $\phi = 0.20$, $U_\infty = 1.5$ m/s. Solid lines indicate numerical results for no combustion.

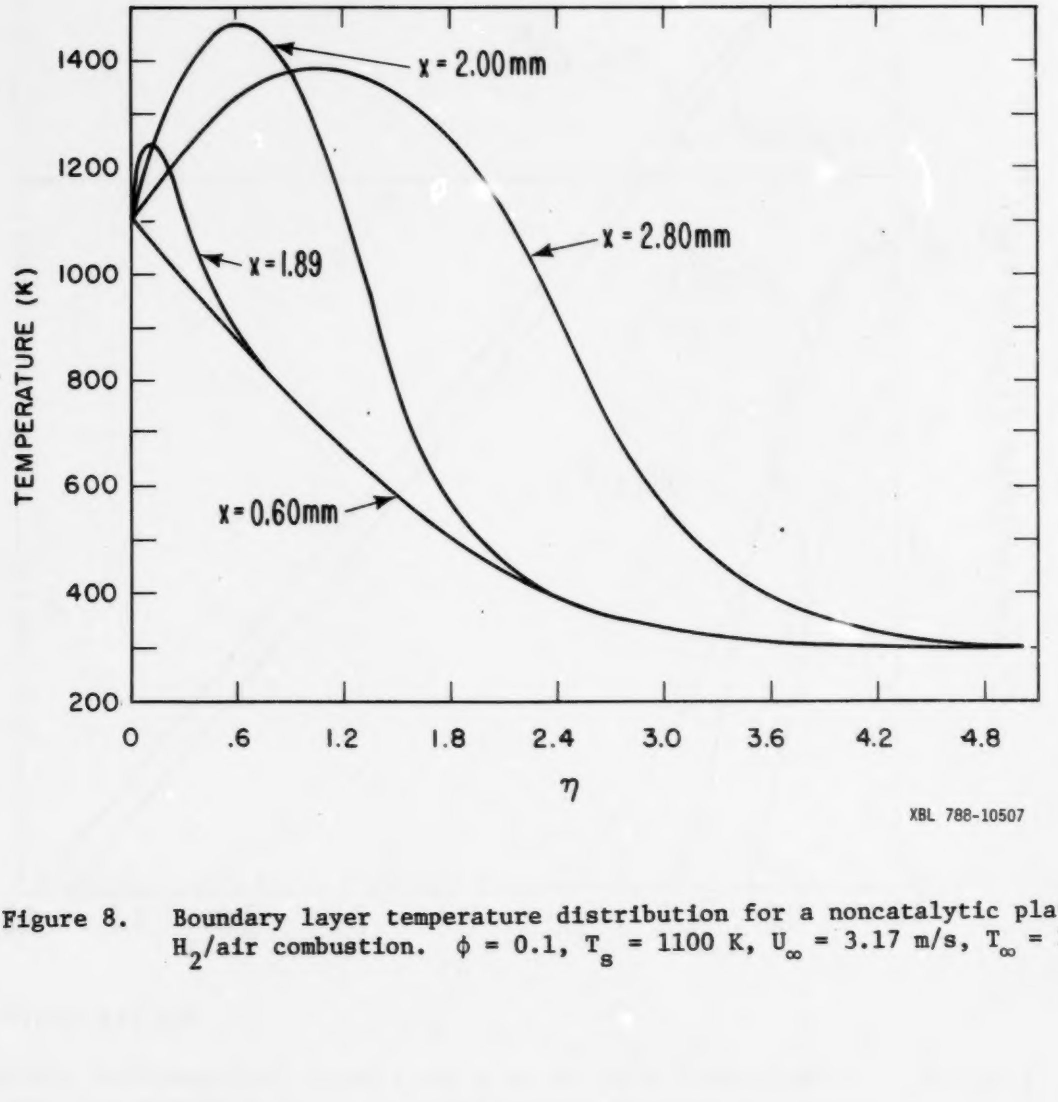

Figure 8. Boundary layer temperature distribution for a noncatalytic plate. H_2/air combustion. $\phi = 0.1$, $T_s = 1100$ K, $U_\infty = 3.17$ m/s, $T_\infty = 293$ K.

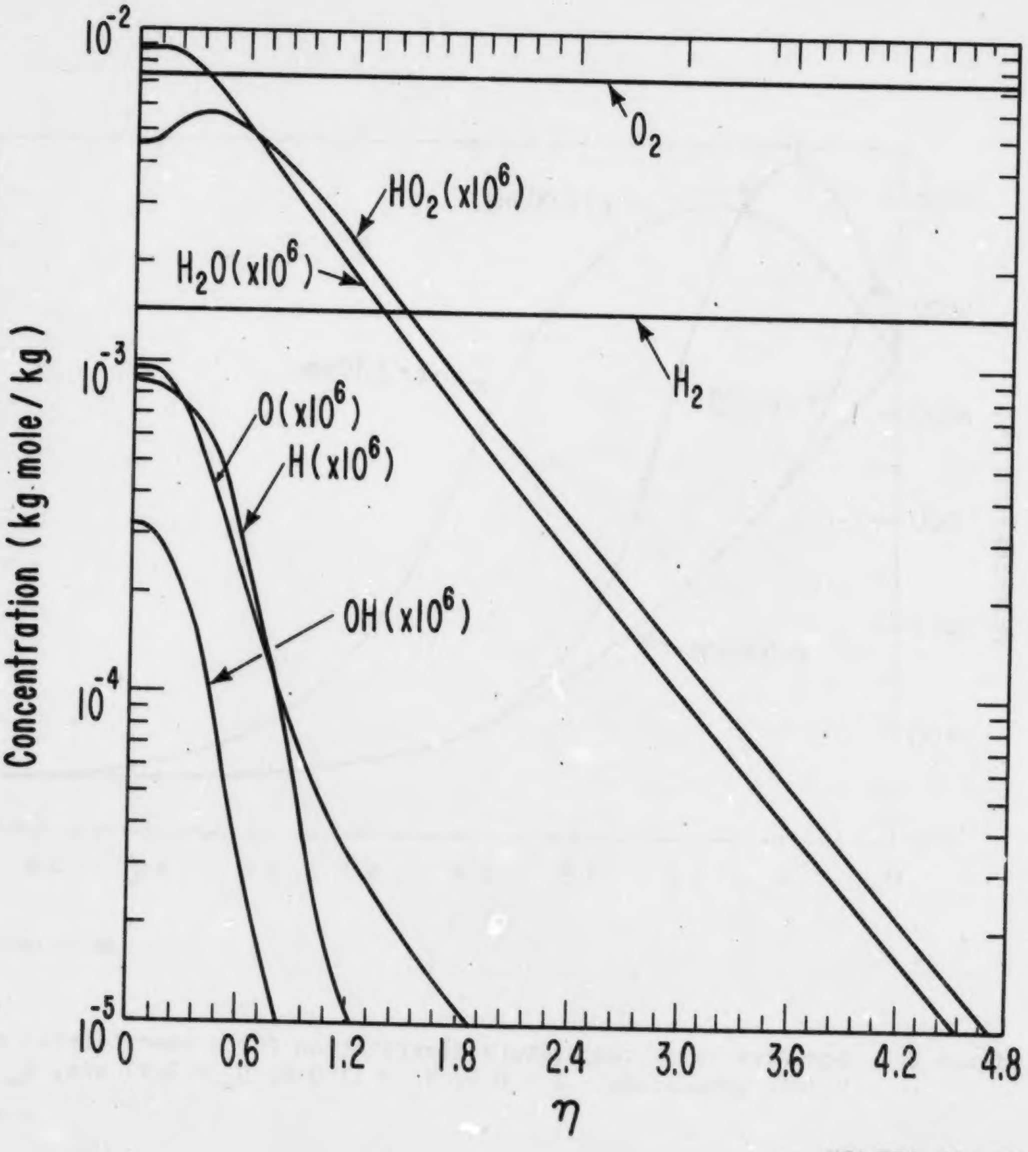

XBL 779-2007A

Figure 9. Concentration profiles as a function of nondimensional distance above plate for a noncatalytic plate. x = 1.35 mm downstream from leading edge. H_2/air combustion. $\phi = 0.10$, T_S = 1100 K, U_∞ = 3.17 m/s.

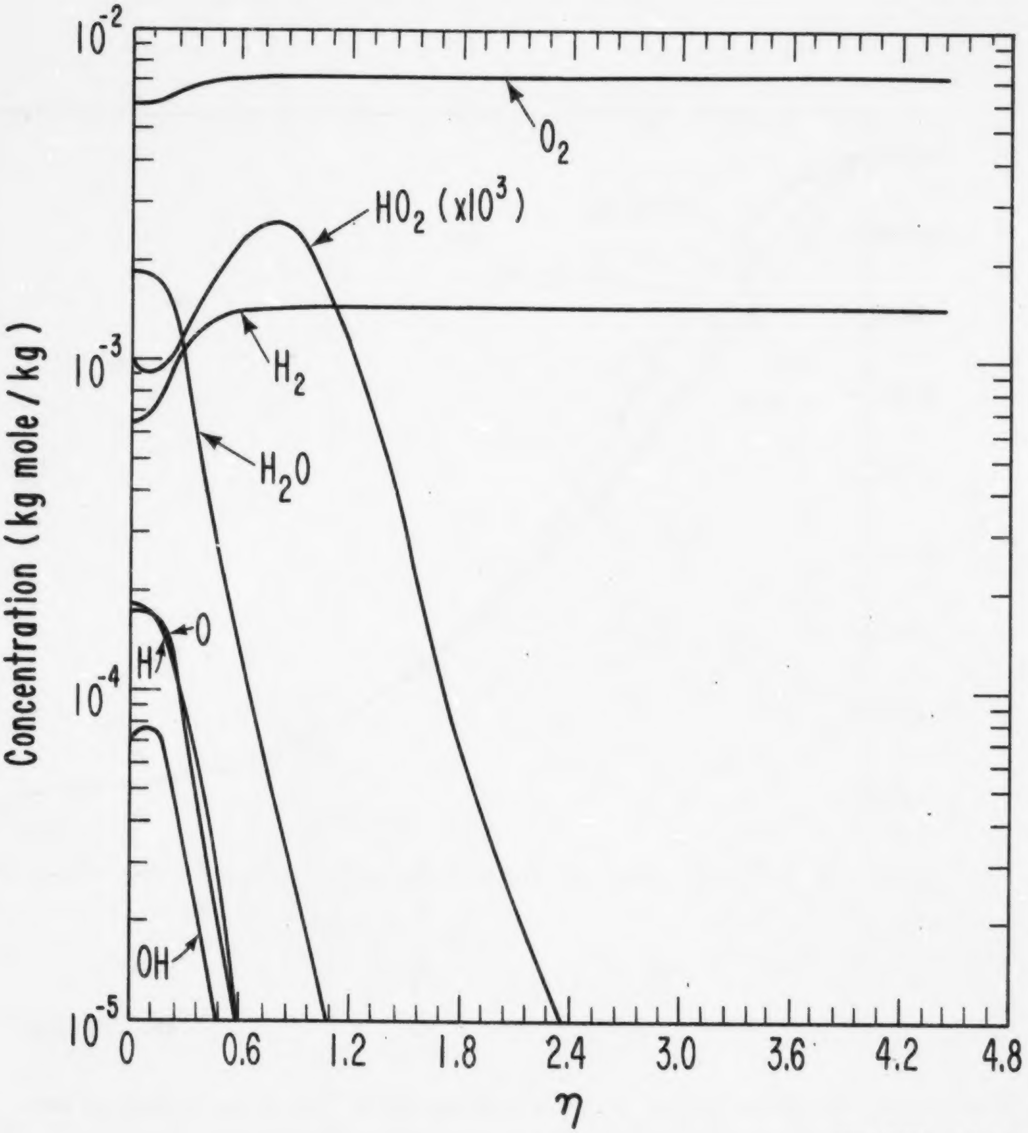

XBL 779-2006A

Figure 10. Concentration profiles as a function of nondimensional distance above plate for a noncatalytic plate. x = 1.89 mm from leading edge. H_2/air combustion. $\phi = 0.1$, $T_S = 1100$ K, $U_\infty = 3.17$ m/s.

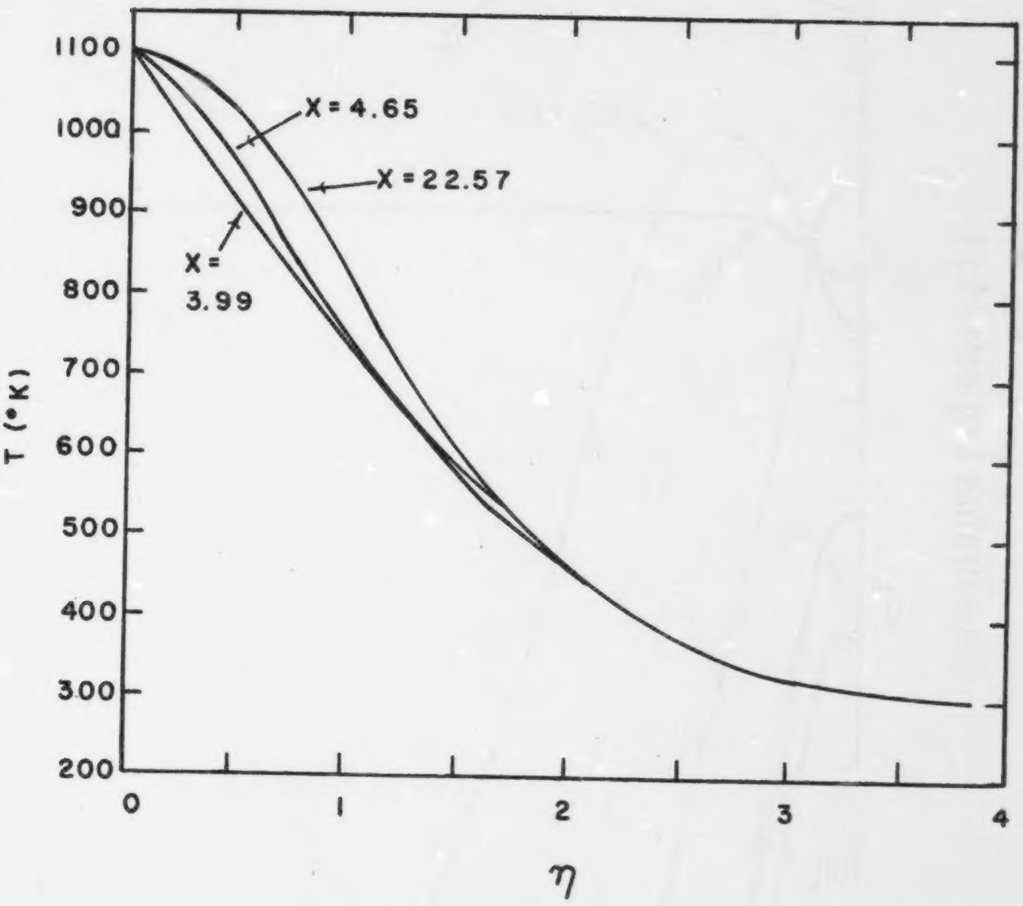

XBL 788-10504

Figure 11. Boundary layer temperature profiles for a catalytic plate. Case 1. Surface oxidation of H_2. H_2/air combustion. $\phi = 0.1$, $T_S = 1100$ K, $U_\infty = 3.17$ m/s, $T_\infty = 293$ K.

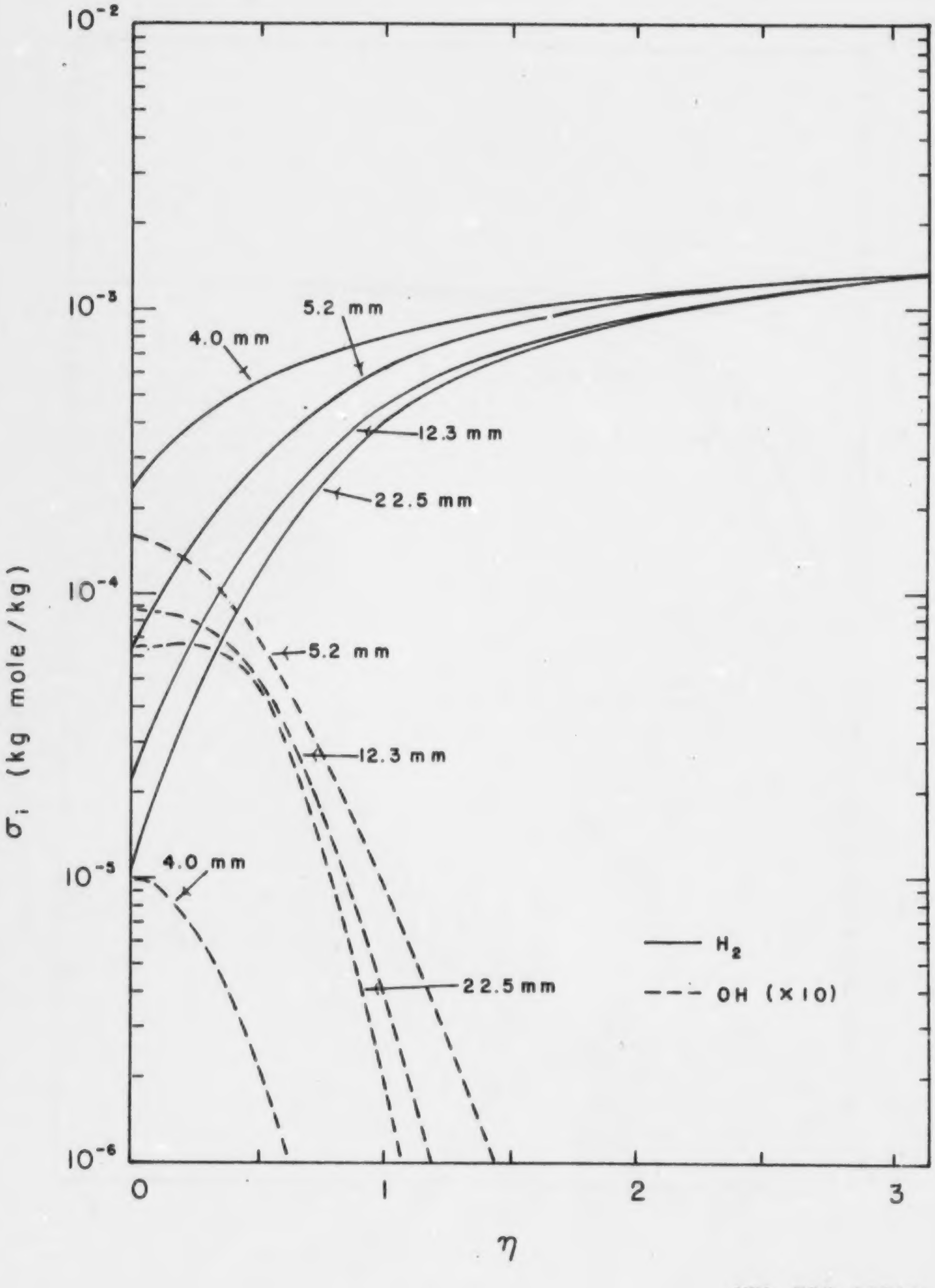

XBL 788-10513

Figure 12. H_2 and OH concentration profiles as a function of nondimensional distance above plate surface for a catalytic plate. Case 1. Surface oxidation of H_2. H_2/air combustion. $\phi = 0.1$, $T_S = 1100$ K, $U_\infty = 3.17$ m/s, $T_\infty = 293$K. ——, σ_{H_2}; ---, σ_{OH}.

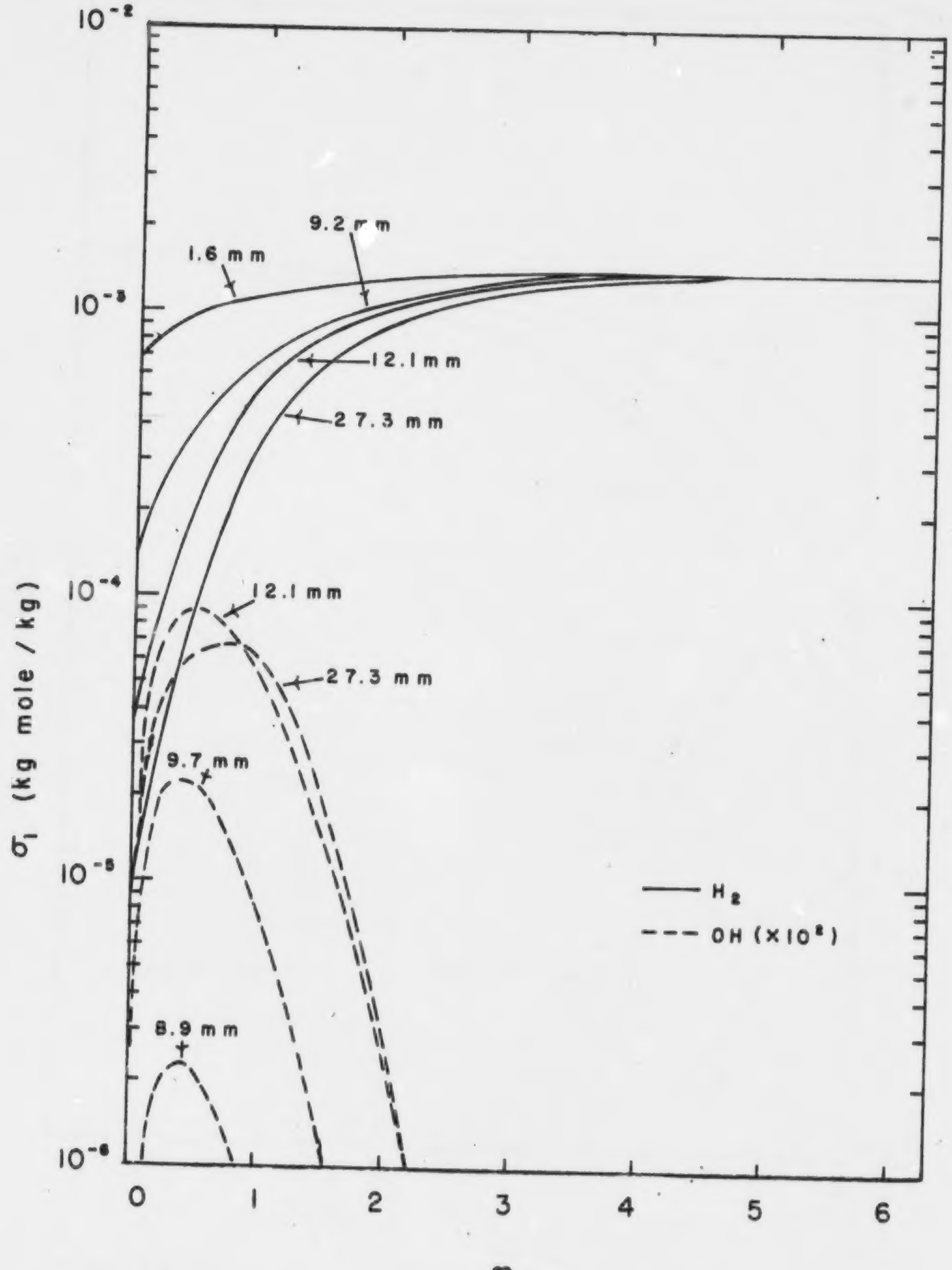

Figure 13. H_2 and OH concentration profiles as a function of nondimensional distance above plate surface of a catalytic plate. Case 2. Surface oxidation of H_2 with radical recombination. H_2/air combustion. $\phi = 0.1$, $T_S = 1100$ K, $U_\infty = 3.17$ m/s, $T_\infty = 293$ K. ——, σ_{H_2}; ---, σ_{OH}.

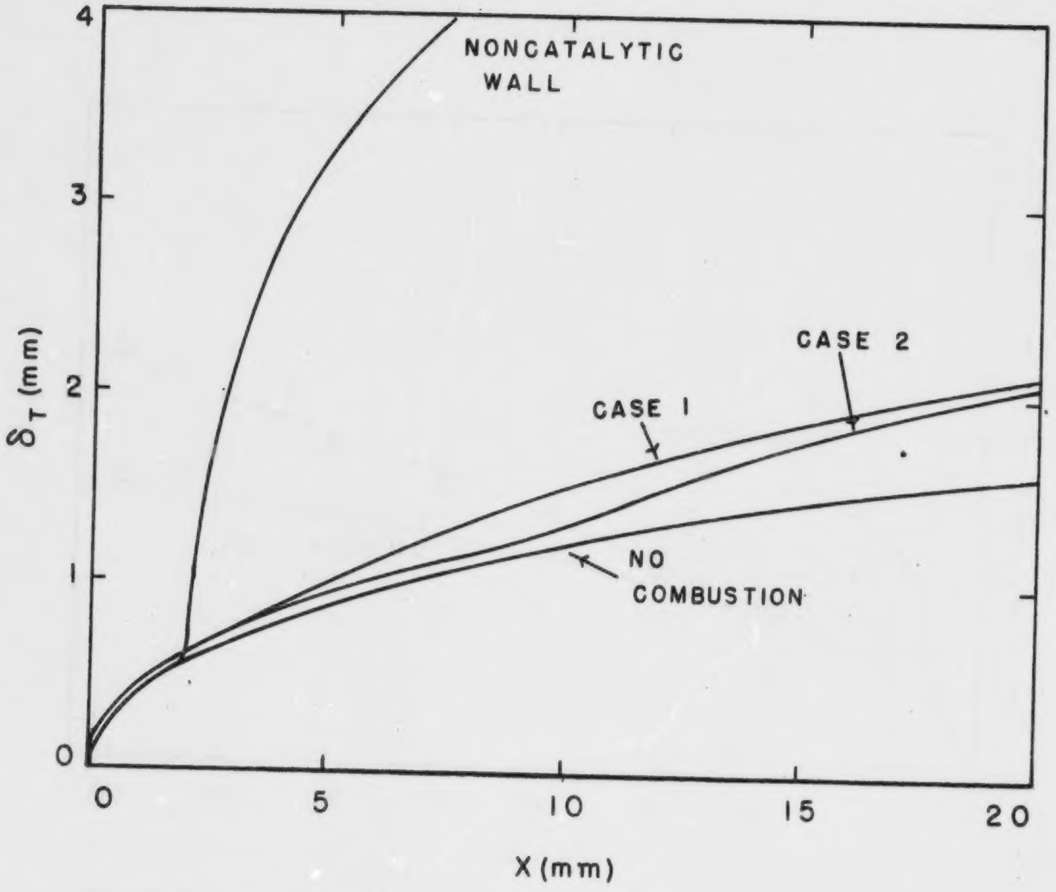

XBL 788-10506

Figure 14. The effect of surface boundary condition on thermal boundary layer thickness. H_2/air combustion. $\phi = 0.1$, $T_S = 1100$ K, $U_\infty = 3.17$ m/s, $T_\infty = 293$ K.

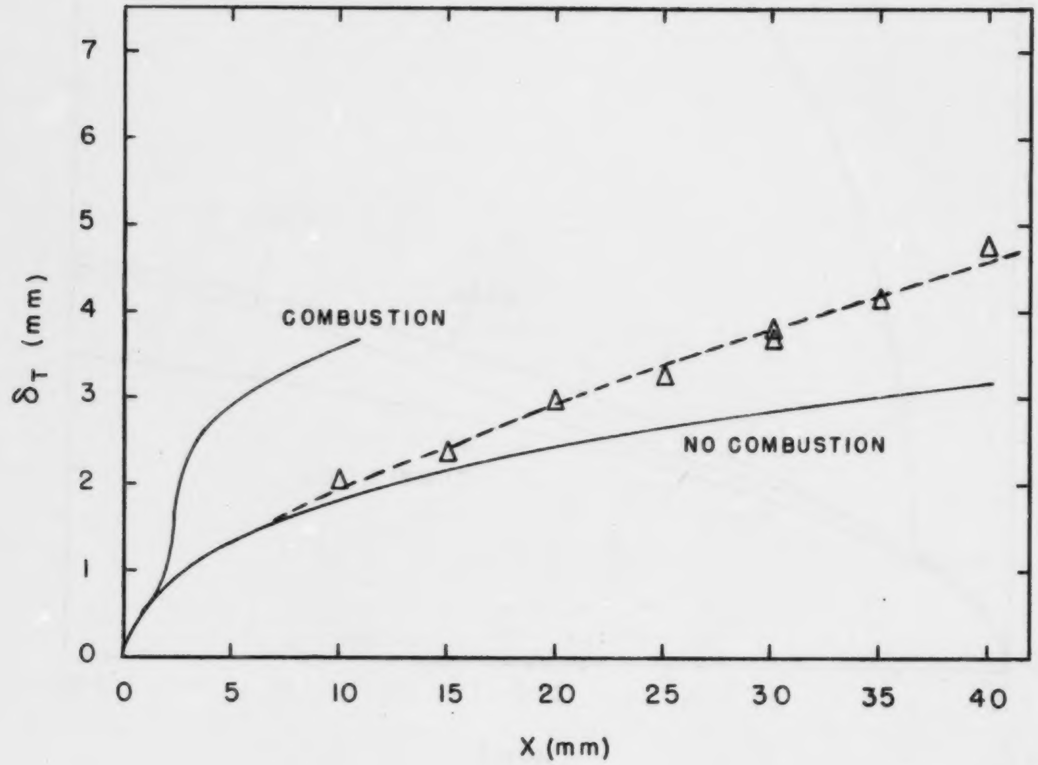

XBL 788-10505

Figure 15. Comparison of experimental and predicted thermal boundary layer thickness profiles for a heated platinum plate. H_2/air combustion. $\phi = 0.20$, $T_S = 1170$ K, $U_\infty = 1.5$ m/s.

APPLICATION OF RICH CATALYTIC COMBUSTION TO AIRCRAFT ENGINES

by:

G. E. Voecks

D. J. Cerini

Jet Propulsion Laboratory
California Institute of Technology
4800 Oak Grove Drive
Pasadena, CA 91103

ABSTRACT

This program was aimed at evaluating the hydrogen enriched operation of an aircraft piston engine as a means of safely operating the engine at a lean air/fuel ratio during cruise mode. An earlier demonstration of this approach to automobile operation indicated a gain in economy and it was expected that most of the same technology and procedures could be transferred to the aircraft. The hydrogen generator utilizes a catalytic rich combustion process to produce a gaseous mixture of hydrogen, carbon monoxide and nitrogen from liquid fuels and air. The hydrogen generator was expected to involve little modifications from the preceding system. However, constraints peculiar to the aircraft application required a series of modifications in the generator (or combustor) design. To meet the aircraft system requirements, a generator scale-up, a change in catalyst support, an inlet design change, a different start-up approach, and a modified generator configuration were implemented. Optimization of each modification was not pursued because of the program constraints concerning the generator development. Use of a monolith catalyst was shown to be superior to the pelleted catalyst used in the previous automotive program in performance and in solving the problem of generating "fines" resulting from vibration. Both electrical and hot gas start-up modes were implemented. A successful operation of the rich combustor with liquid fuel over a range of fuel feeds from 4.2 lb/hr. to 25 lb/hr. at an air-fuel ratio of 5.4 was achieved. The resulting catalytic reactor was operated on the aircraft in the final phase of the program. This application constitutes but one segment of staged combustion in which catalysts will ultimately contribute greatly.

Preceding page blank

SECTION 1

APPLICATION OF RICH CATALYTIC COMBUSTION TO AIRCRAFT ENGINES

INTRODUCTION

The concept of operating a piston engine at equivalence ratios leaner than the lean burn limit of the fuel in order to reduce the NO_x levels in the emission has recently been demonstrated$^{(1)}$. This was achieved by generating hydrogen on-board a vehicle and subsequently mixing the hydrogen with the gasoline/air mixture. The method chosen for generating hydrogen which was deemed most compatible with a vehicle was catalytic partial oxidation, i.e., rich combustion; $(-CH_2- + \frac{1}{2}O_2(\text{air}) \longrightarrow CO + H_2)$

During the past year, a joint NASA/Lycoming/Beech/JPL effort was undertaken to evaluate the application of this concept to piston driven aircraft. Since the current engines are operated constantly at rich equivalence ratios, it was anticipated that the engine could be operated leaner than stoichiometric to extend the range of operation while simultaneously not produce excessive NO_x emissions. During this program an aircraft was successfully operated at lean conditions with liquid fuel and liquid fuel/gaseous hydrogen mixtures$^{(2)}$. The catalytic hydrogen generator constructed for this purpose provided several advances in the area of rich catalytic combustion. The unit constructed will be discussed in the following text.

Although this catalytic partial oxidation or rich combustion unit was installed as a hydrogen generating device on transportation vehicles, the concept is the same as two-stage combustion in stationary applications. By catalytically generating hydrogen (and carbon monoxide) from a liquid fuel and air mixture, the ensuing mixture with more air and fuel can be completely combusted (as in the combustion chamber of the piston engine) for driving turbines or heating boilers at temperatures below the NO_x formation linit. Stationary installations, however, would appear to place somewhat less stringent requirements on the first stage combustor design than were encountered during the aircraft project.

Preceding page blank

SECTION 2

DESCRIPTION OF THE CATALYTIC PARTIAL OXIDATION AIRCRAFT GENERATOR

The decision to use catalytic partial oxidation to generate hydrogen on-board the aircraft was based on the previous assessment made during the NASA sponsored Low Pollution Engine Program for automobile implementation. Earlier efforts to partially oxidize the fuel thermally (i.e., no catalyst), whereby controls and operation would be even simpler, were unsuccessful. This was due to the formation of soot. Catalytically, however, rich combustion can be maintained near the equilibrium soot limit where the hydrogen yield is maximized (Figure 1) without soot production.

In addition to the non-soot/high hydrogen yield requirement, the aircraft application demanded several other specific design considerations for successful operation. Because of the limited space within the engine housing only a volume of 2.5 ft.^{3} was available for the entire reactor. This included the fuel vaporizer, air-fuel mixer, pre-heat, control valves and mounting fixtures.

With respect to the reactor itself, the high conversion efficiency had to be maintained over a range of 0.5 lb/hr. to 3.0 lb/hr. of hydrogen. Based on the fuels used [Indolene (Federal Register specified gasoline) and aviation fuel], 8.3 lb/hr. reacting with 45.2 lb/hr. air (air/fuel ratio = 5.4 to 5.5) would generate one lb/hr. of hydrogen. The resulting space velocity variation for the generator operation in the final analysis was 2,700 to 16,200 hr^{-1}. This constituted a two-fold increase in both maximum flow and turn down ratio over which the generator had previously been constructed for the automobile program.

Two other constraints peculiar to this application were imposed on the rich combustor: two modes of start-up were requested, and the catalyst and reactor would have to withstand the high vibration intensities and frequencies which the engine created during operation.

Start-up had previously been accomplished by pre-heating the catalyst bed to the light-off temperature with a flow of hot air. In the aircraft application the exhaust gas from the engine (which started in the normal rich mode) was routed through the reactor to heat the catalyst. The second method for starting, which was to be a backup approach, was to pass an electric current through wires coiled within the front section of the catalyst bed. With no air flow through the generator, the batteries on-board the aircraft were more than adequate for bringing the inlet section of the catalyst to light-off temperature, typically 1000°F.

Assessing the vibration problem was difficult initially because the combined testing of the engine and generator was completed with the engine in a test dynomoeter and the gearator mounted separately. The severity of the problem was realized during testing in which the generator was mounted on the engine.

Catalyst Description

Initial tests were conducted with the commercial pellet catalyst type employed during the automotive hydrogen enrichment program; a nickel reforming catalyst. This catalyst was 25 wt% nickel oxide coprecipitated with alumina and had an initial surface area of 60 m^2/g. A nickel catalyst had been chosen for the rich combustion because it maintained good activity with various fuels and because a non-noble metal was preferred. Although monolithic catalysts had been tested under rich and lean conditions previously at JPL, none had actually been used in a generator prior to this program. Two distinct advantages were shown to favor the monolith catalyst compared to the pellet catalyst. During the aircraft engine dynomometer tests with the generator installed on the engine, the pellet catalyst produced fines which were carried into the engine resulting in mechanical damage. By proper packing, the 300 $cell/in^2$ Corning cordierite monoliths (5.63 in diameter) eliminated this problem. Nickel oxide was also used as the catalyst on the monoliths to provide a closer comparison to the pellets. The nickel oxide, applied on the washcoat, was nominally 12 wt% and had a surface area of approximately 22 m^2/g. The hydrogen adsorption measurement of the nickel on a fresh catalyst was 3.8 m^2/g. Catalytica Associates achieved the high nickel loading by multiple applications of nickel salts. In Figure 2 the variation of hydrogen yield is shown for both pellet and monolith catalysts as a function of air to fuel ratio. In Figure 3 the catalyst temperatures during start-up and operation are compared between the monolith and pellet catalysts. The monolith catalyst demonstrated this superior performance throughout testing.

The generator size constraints required a different length to diameter ratio than had previously been used for automotive use in order to provide enough catalyst for operating over the entire range of air and fuel throughputs. Scale-up from a 3.66 in. diameter to 5.63 in. diameter and from 6 in catalyst bed length to 8 in. was found to be appropriate.

Use of the electric preheat with the monolith catalysts was accomplished by sectioning the first monolith into segments. The coils of heater wire were placed between the segments in the upper half of the catalyst bed. The reactor with an expanded view of the monolith before installation is shown in Figure 4.

The mounting site constraints also inhibited the length of the mixing and preheat sections, and required a redesigning of the inlet system to maintain uniform flow through the monoliths. Figure 5 shows a cutaway illustration of the rich combustor. Air is preheated by the heat from the reaction when passing through the spiral vanes surrounding the inside wall of the reactor. The preheated air then passes through the atomized fuel inlet, proceeds through an air/fuel mixer and is expanded into an outer manifold prior to entering the inlet of the reactor. The air/fuel mixture is then introduced through a ring of holes above a diffuser at the top of the monolith catalyst.

Summary

Use of a rich combustion reactor to generate hydrogen for two-stage combustion was successfully implemented with a piston engine on an aircraft. The peculiar problems involved in this application were (1) use of a catalyst which with proper packing would maintain adequate heat transfer, match the expansion of the reactor and maintain shock and attrition resistance, (2) scale-up a reactor disproportionately to meet size constraints, and (3) design inlet conditions for a wide range of air-fuel flows and maintain uniform distribution through the monolith catalyst. Application of staged combustion to turbines and boilers with the use of a catalyst used in the rich combustion stage would offer the same advantages realized in the aircraft and automobile applications, i.e., high hydrogen yield, no soot. Second stage combustion could be achieved either thermally (as in the piston engines) or catalytically to meet whatever heat realease, temperature, emission, or geometrical requirements which may be imposed by the application. The scale-up achieved in the work reported here is but one step toward realizing larger industrial utilization of the same principle.

References

1. Houseman, J., and Cerini, D. J., "On Board Hydrogen Generator for a Partial Hydrogen Injection Internal Combustion Engine," SAE - 740600, 1974.
2. Chirivella, J. E., Duke, L. A., and Menard, W. A., "High Fuel Economy in an Aircraft Piston Engine When Operating Ultralean," SAE-770488, 1977.

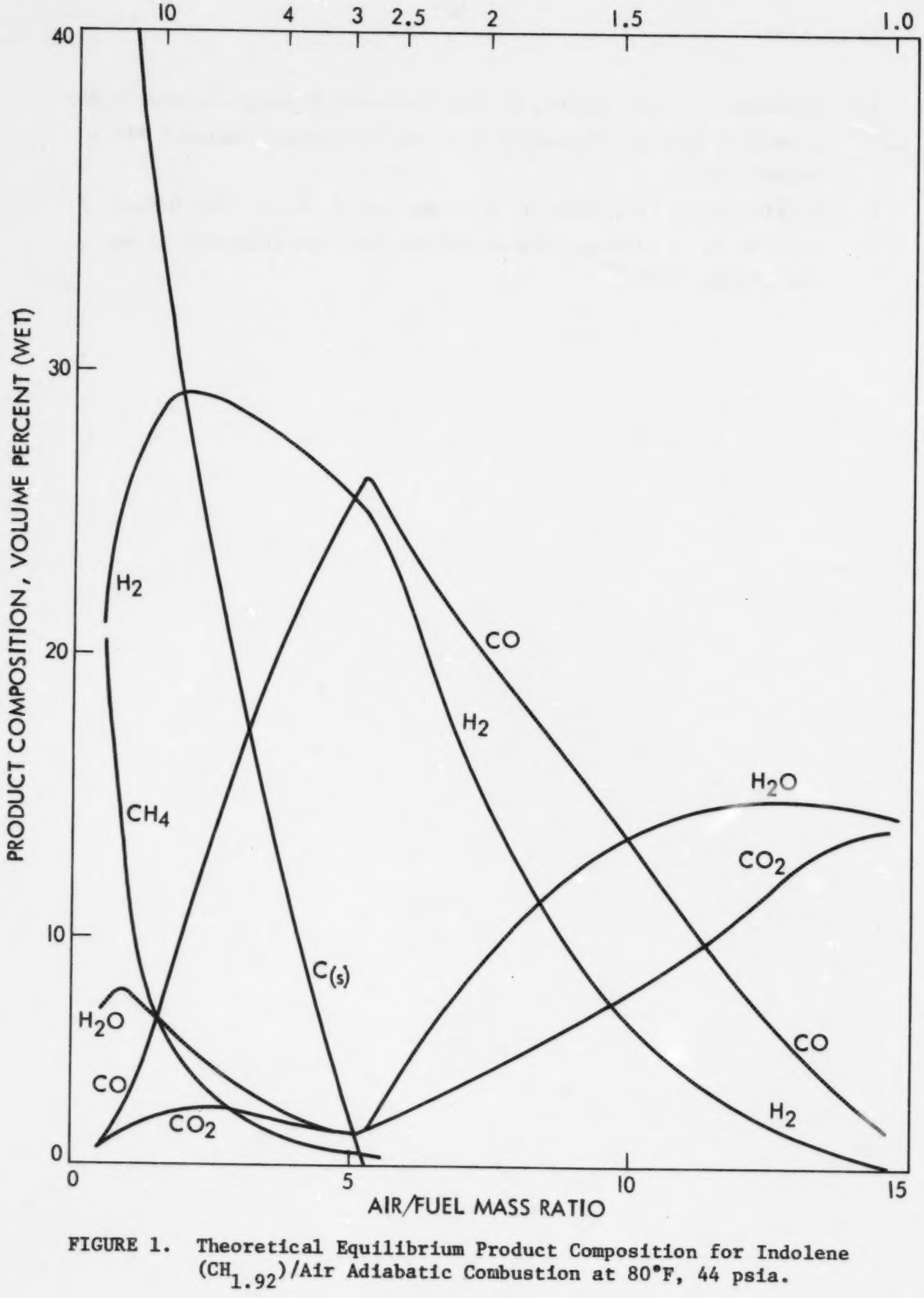

FIGURE 1. Theoretical Equilibrium Product Composition for Indolene ($CH_{1.92}$)/Air Adiabatic Combustion at 80°F, 44 psia.

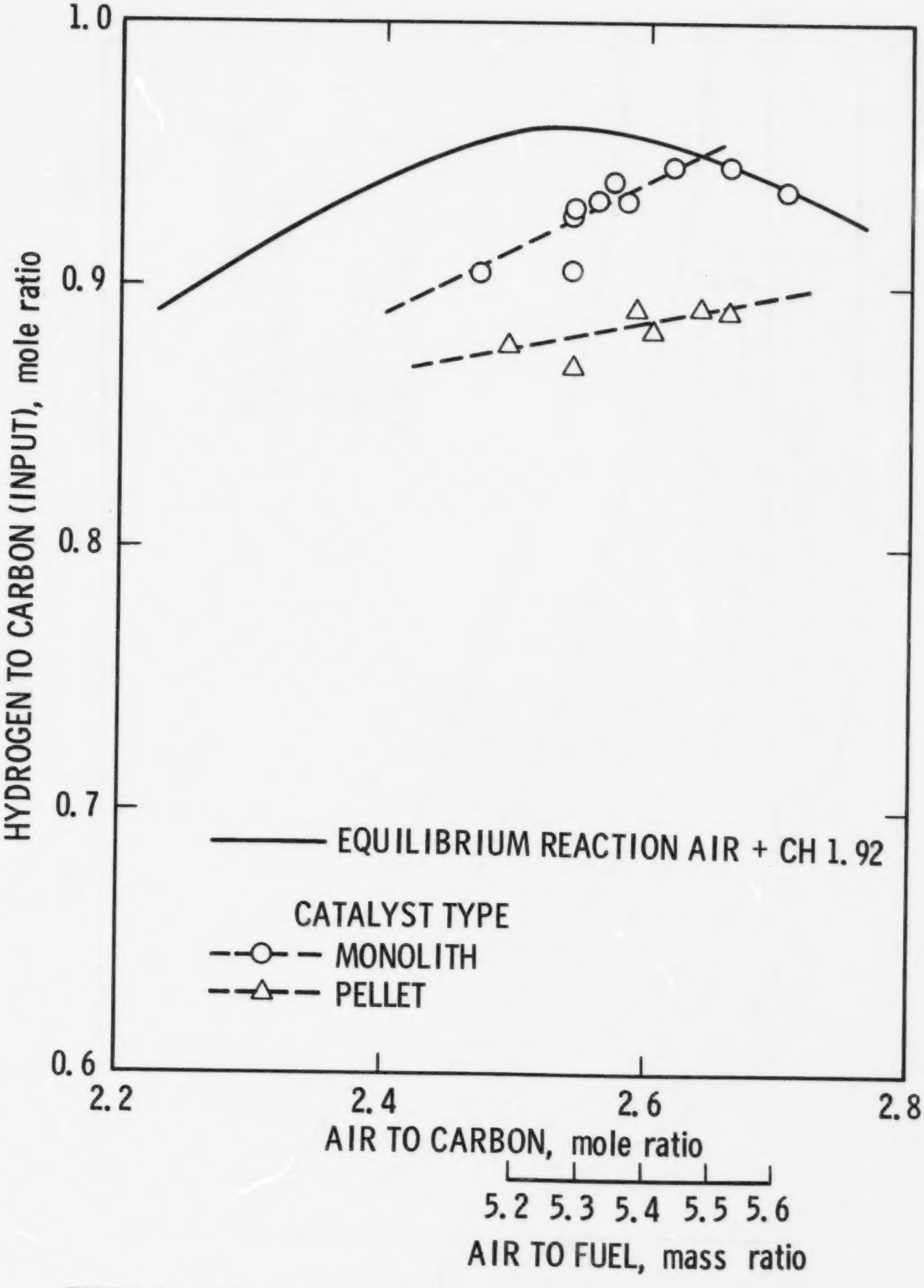

FIGURE 2. Molar Ratio of Hydrogen Produced to Fuel Carbon Input as a Function of Air to Carbon Molar Ratio for the Monolith and Pellet Catalysts.

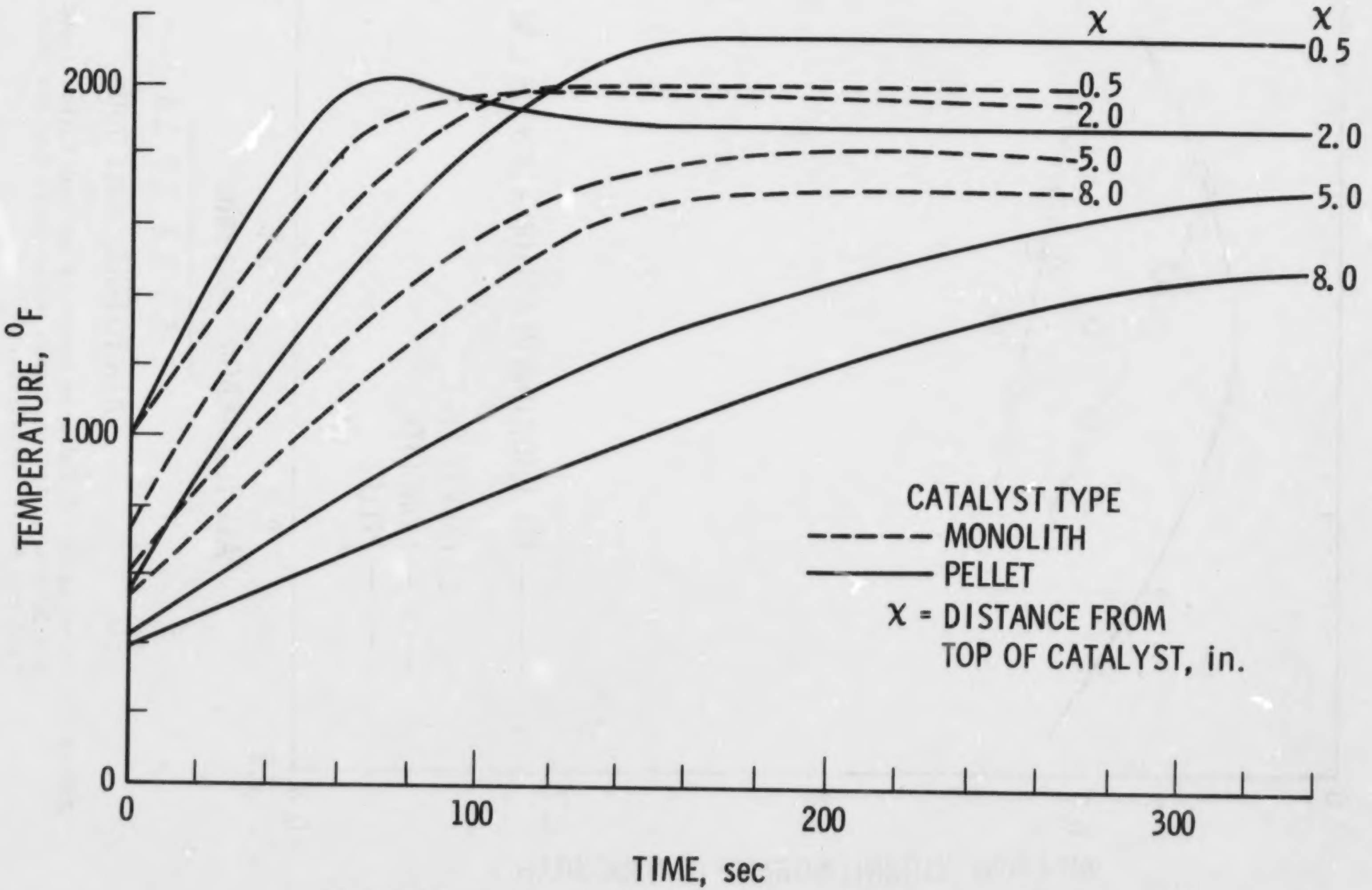

FIGURE 3. Bed Temperature Profile of the Monolith and Pellet Catalyst During Light-Off and Steady State Operation.

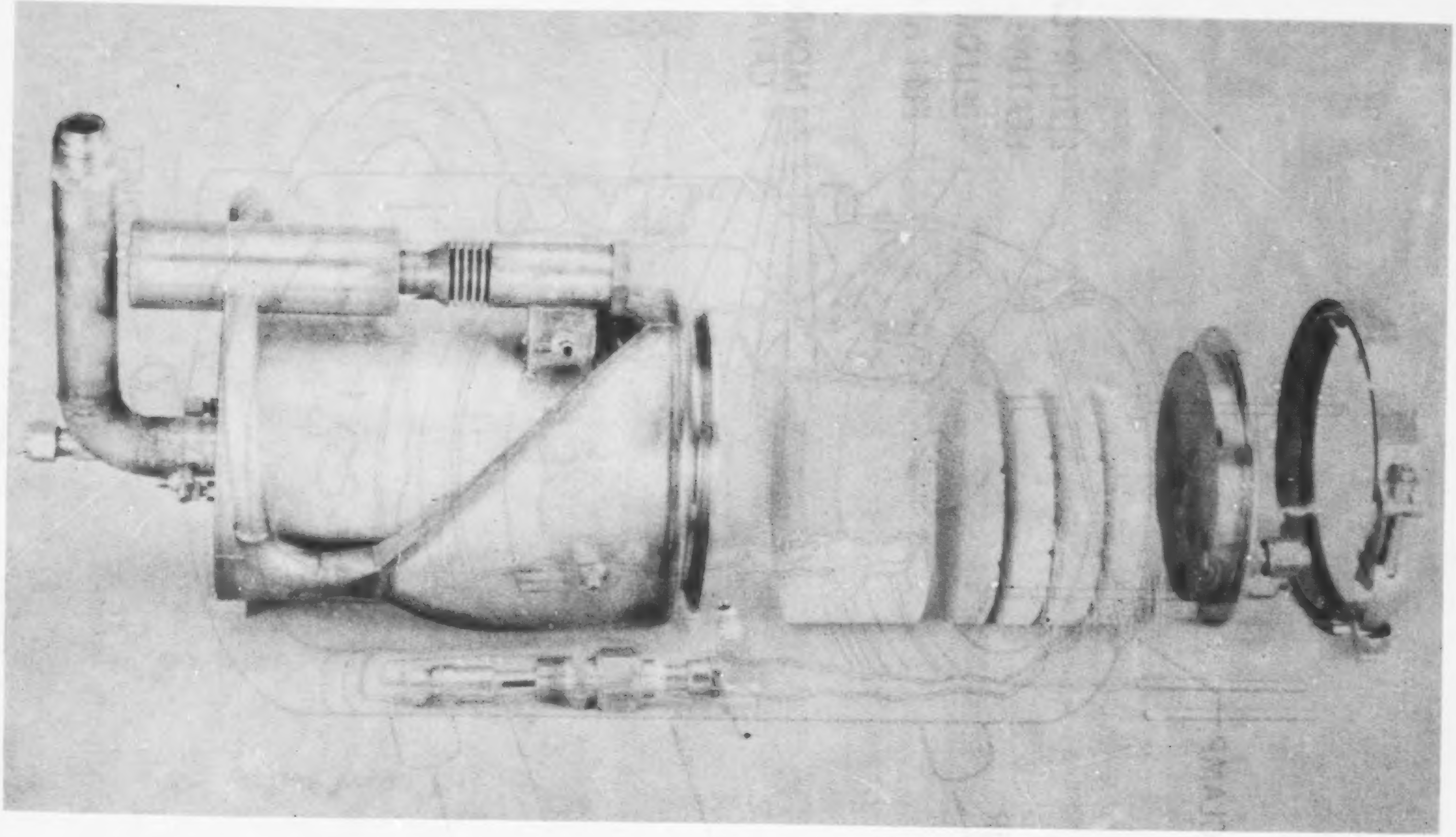

Figure 4. Aircraft generator with expanded catalyst bed.

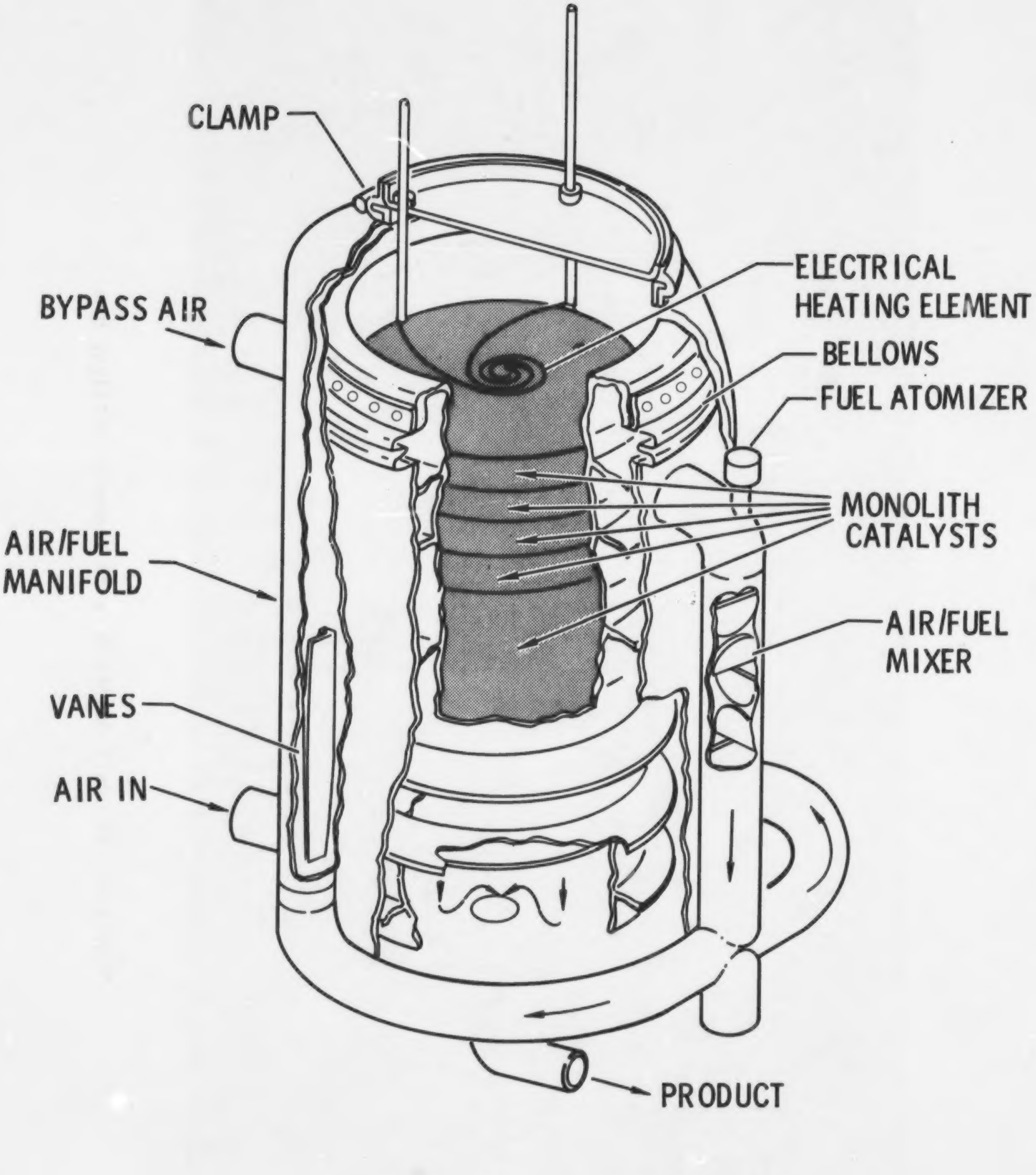

FIGURE 5. Cutaway of Aircraft Generator

CATALYTIC COMBUSTION IN ACTUAL ENGINES

A summary of Engine and Rig tests

By:

B.E. Enga

Johnson Matthey Research Centre
Reading, Berkshire, England.

ABSTRACT

This paper outlines work carried out at JMRC over a period of years into the application of catalytic combustion to gas turbine engines.

The technique adopted consists of examination of the requrements of an actual gas turbine followed by rig and computor experimental work to solve each problem.

A brief outline of the problems of the flow and thermal transients together with start up considerations is given.

An account of the preliminary series of tests carried out on a 65 BHP gas turbine is included together with recorded emissions from this engine.

The system designed to run this engine and overcome the problems experienced is described and attention drawn to the fact that a system is required to ensure efficient use of the concept. It is not sufficient to simply place a catalyst in a combustor.

Preceding page blank

Introduction

At Johnson Matthey Research Centre we have been studying catalytic combustion phenomena for some years. Based upon many series of tests and rig evaluation very accurate computer simulation models of JM catalyst systems were developed for catalytic combustion and thus the basic parameters of the catalyst-support are rapidly computable for any given flow and fuelling system.

In parallel with this work the required catalyst system to power various applications were determine from the engineering point of view.

A TARGET GAS TURBINE:

1. Theoretical considerations

The simple gas turbine cycle comprises the compression of the working fluid, energy addition at constant pressure and expansion of the working fluid. The loss incurred in the system must include compression and expansion inefficiencies, pressure losses through system, and above atmospheric pressure - work lost in the exhaust annulus. Thus the overall thermal efficiency of the system may be stated as:

$$\mathrm{Eff}_a = \frac{\text{EXPANSION Work - Compressor Work}}{\text{Energy Supplied}} \qquad -(1)$$

This can now be resolved into its component form.

$$\mathrm{Eff}_a = \eta_f \left[\frac{(1+f)\,C_{p_f}\eta_t T_3 \left[\dfrac{\left(\dfrac{P_2-\Delta P_c}{P_1+\Delta P_t}\right)^{\frac{\gamma_t-1}{\gamma_t}} - 1}{\left(\dfrac{P_2-\Delta P_c}{P_1+\Delta P_t}\right)^{\frac{\gamma_t-1}{\gamma_t}}} \right] - \dfrac{C_{p_c} T_1}{\eta_c}\left[\left(\dfrac{P_2}{P_1}\right)^{\frac{\gamma_c-1}{\gamma_c}} - 1\right]}{C_{p_f}\left[T_3 - \dfrac{T_1}{\eta_c}\left[\left(\dfrac{P_2}{P_1}\right)^{\frac{\gamma_c-1}{\gamma_c}} - 1 - \eta_c\right]\right]} \right] \qquad -(2)$$

Where

Effa = Overall thermal efficiency
η_f = Combustion efficiency
η_t = Turbine isentropic efficiency
η_c = Compressor isentropic efficiency
f = Fuel/air ratio
Cp_e = Mean specific heat at constant pressure during expansion
Cp_c = Mean specific heat at constant pressure during compression
Cp_f = Mean specific heat at constant pressure during combustion
γ_t = Mean ratio of specific heats during expansion
γ_c = Mean ratio of specific heats during compression
P_1 = Delivery pressure
Δ Pc = Pressure loss through combustion chamber as % inlet P
Δ Pt = Pressure loss in power turbine annulus as % inlet P
T_1 = Inlet temperature
T_2 = Compressor delivery temperature
T_3 = Gas generator turbine inlet temperature
T_4 = Gas generator turbine exit temperature
T_5 = Power turbine exhaust annulus temperature

From equation 2 it can easily be seen that for a standard engine working at any given settings the only factors that the combustion process affects are η_f, the combustion efficiency which by definition must be ideal for a theoretically acceptable engine and can thus be taken as constant for conventional engines and catalytic combustion engines, and Δ Pc, the pressure loss through the combustion chamber.

Thus a change to catalytic combustion from flame combustion requires that the pressure drop through the combustor is minimal.

2. Engine Application

A typical British gas turbine was selected after consultation with the manufacturers and the effects of the change in combustor pressure drop determined with the following results:

This thus served to give the area of ΔP that we were to work in.

B CATALYST SUPPORT

Having determined the importance of pressure drop many forms of support material were then tested on our 10 lbs/sec flow rig.

From this work it was concluded that for a given cell density and cell shape the overriding parameter is the open area. As this is easily variable with metal support system the concept was then scaled up.

1. Target Engine flow

There are two systems of catalyst that can be applied to our target engine, an annular combustor and multi canular combustors. Scale down test runs of the two systems gave the following results:

Annular Combustor $0.617m^2$ x 0.355m long target size

	Open Area 0.8	Open Area 0.9	Open Area 0.96
Reynolds No	3,430	3,049	2,859
Δ P psi	5	4.3	3.97
Δ P % inlet	3.06	2.63	2.43

8 canular combustors, $0.4257\ m^2$ x 0.355 m long target size

	Open Area 0.8	Open Area 0.9	Open Area 0.96
Reynolds No	4,971	4,419	4,144
Δ P Psi	9.69	6.98	6.39
Δ P %	5.95	4.68	3.92

The 0.9 open area support corresponds to the JM 400 cell metal support and the 0.96 open area corresponds to the JM 200 cell metal support.

Pressure drop evaluation was continued at approach reference velocity of up to 90 metres/sec and mass flows of up to 100 $Kgs/m^2/sec$ and from this it became apparent that no simple relationship with exterior parameters was present. Test results for the 400 cells and 200 cell materials are give in Figure 1-4.

Compressor isentropic efficiency	0.82
Turbine isentropic efficiency	0.85
Combustion efficiency	1.00
Standard ΔPc	4.0%
Intake Pressure	1.0137 bar
Intake Temperature	288^{o} K
Final exhaust pressure	1.0344 bar
Gas generator exhaust annulus diameter	622.3 mm

4.0% Δ Pc	LOAD		
	Emergency	Design	Base
T_4 ^{o}K	923	886	823
LP Compressor speed rpm	6550	6340	5950
Exhaust man flow rate Kg/S	107.72	104.54	96.36
P_2 Bar	10.344	9.862	8.793
T_3 ^{o}K	1192	1157	1080
T_2 ^{o}K	605	595	574
Fuel/air ratio	0.0163	0.01536	0.0136
T_5 ^{o}K	745.9	730	690
Expansion work KW/Kg	512.1	488.4	435.1
Compression work KW/Kg	328.3	319.0	298.1
Energy supplied KW/Kg	677.3	645.6	570.2

Thus the following can be related

Δ Pc	Effect on performance	LOAD		
		Emergency	Design	Base
4.0%	Overall thermal efficiency %	27.14	26.23	24.02
6.0%	Power loss %	2.013	2.007	2.48
	Overall thermal efficiency %	26.58	25.7	23.44
10.0%	Power loss %	6.935	6.434	7.44
	Overall thermal efficiency %	25.48	24.55	22.25
15.0%	Power loss %	11.42	12.1	14.12
	Overall thermal efficiency	24.04	23.06	20.06

The following guide lines were established.

1. Δ P in the turbulent zone in proportional to the approach velocity squared.
2. Δ P% of upstream pressure appeared to decrease proportionally with the reciprocal of upstream pressure squared.
3. The pressure drop of a combination of supports is not the sum of the Δ P across each support.
4. The friction factor for the support in the turbulent zone becomes constant and is a direct function of washcoat type. This friction factor differs radically from established published friction factors for example a 200 cell type II profile metal support 7.62 cm long, at a Reynolds number 18600, has a constant friction factor of 0.0312 for type 6 washcoat.

c START UP TRANSIENTS

The consideration of start up problems led to a series of experimental runs and computer simulations. A typical computer simulation is shown in Figure 5.

Under the mass flow conditions that are normal with gas turbines and the relatively low flows on start up the phenomenon of kinetic limited support surface temperature effects were studied.

This can be stated roughly as the effect that under inlet flow conditions such that the catalysts is obtaining 50% conversion of the fuel delivered during a transient condition then it can be shown that the surface temperature approimates to twice the gas temperature.

This ball park rule is simply modelled and the controlling parameters are found to be approach velocity, inlet pressure and cell density.

Experimental runs under fuel-on conditions gave the following results:

Inlet 200° C 1 Bar, adiabatic fuelling to give 850°C

Time Sec.	Catalyst Exit T°C	Catalyst Surface T°C
0	200.0	200.0
1.28	227.0	329.8
6.40	540.0	819.8
8.51	675.3	1100.4
21.76	849.4	851.3
28.16	851.2	851.2
43.5	851.1	851.3
0	200.3	200.1
2.56	295.9	421.4
3.84	520.4	852.5
7.68	635.0	1121.4
8.96	749.4	1290.4
10.80	847.2	913.4
11.54	852.5	854.4
12.74	852.6	852.6

This test was repeated nine times for each support. A range of ceramic supports was also tested.

It was observed that the activity of the catalyst as measured by the light off temperature on a separate rig decreased with each start up test, this decrease was vastly more than the decrease observed after many hours of constant running after a start up.

In addition it was observed that the ceramic supports exhibited a wide range of thermal shock failures to the point where no ceramic support withstood 20 start ups. Based upon this it was decided not to reconsider ceramic systems.

Cold Starting:

For a practical engine, the ability to start up under cold conditions rapidly and reliably is essential. With the problem that catalyst light off is in the region 200°C and above it is not possible on cranking to obtain compressor air at this temperature.

A variety of systems were considered.

1. Start up fuel

The addition of small amounts of H_2 to the delivered air enables the catalyst to start up i.e. light off instantly. This however, requires a large amount of additional hardware and also an additional expensive fuel.

2. Start up combustor

A small combustor designed to flame fire up the engine until the engine is running and the catalyst system can take over. This however, requires hardware and presents redundancy problems especially in terms of fluid flow control.

The system adopted consists of a pre-burner burning a small amount of fuel up stream of the catalyst. The main flow air is then dumped into the burner flow to quench the flame and pre-heat the feed air to the catalyst. The main power fuel is then added and the heated pre-mixed fuel is then passed through the catalyst as in Fig. 6.

E ENGINE TESTS

The Rover 65 BHP automotive and air-craft auxiliary generator engine was selected as suitable for the engine tests of this system.

A typical data plot and emissions output from this engine was taken and is shown in Table I.

The combustor shown in Fig. 7 was then constructed and the engine test undertaken.

The standard test equipment on the Rover gas turbine was employed. The load and speed were measured by a Heenan and Froude Ĝ type dynamometer and tachometer. Pressures were taken to record impellor tip and compressor delivery pressure, water manometers and mercury manometer were used to take air flow and pressure drop.

At full power the mark one system exhibited problems with fuel preparation but even so the NOx emissions were 0.44 ppm despite rather high CO figures.

A series of test result emission indices were then taken:

STANDARD ENGINE:

Equivalence Ratio	CO gm/Kg Fuel	HC gm/ICs Fuel	NOx gm/Kg Fuel
0.2319	107.39	38.88	2.68
0.2658	9.82	17.68	2.58
0.327	5.17	11.99	3.76
0.380	4.91	9.21	4.18
0.225	119.46	41.35	2.26
CATALYST SYSTEM: 400 cell			
0.35168	0.099	1.86	0.032
0.335	0.099	1.87	0.033
0.349	0.096	1.78	0.031
0.377	0.075	1.46	0.029
0.384	0.039	0.91	0.029
CATALYST SYSTEM: 200 cell			
0.353	7.43	2.22	0.030
0.337	7.45	2.24	0.033
0.40	0.04	1.05	0.056

1. The size of catalyst used was 101.6 mm diameter by 76.2 mm long.
2. The reference velocity to the catalyst 60 metres/sec.
3. Pressure drops 4.2%.
4. By-pass to main flow split for working fluid
   68% main 32% by-pass
5. Pre burner delivery temperature 420°C.

Fuel Variations:

Many variations of fuel specification have been run; the standard fuel used is diesel oil but test runs have been carried out using wide cut gasoline, "washed" number 6, Avcat and Avtur kerosines, high smoke point kerosine, natural gas, propane and low BTU mixtures, including H_2/CH_4, CO/H_2, CO/CH_3 amd various nitrogen diluted mixtures.

No unanticipated problems occurred with these fuel changes and apart from the problems of oinjecting the Number 6 oil and prevention of auto ignition with the wide cut gasoline, the catalysts performed well and the only adjustments required were to the preheater burner output.

Low BTU Fuels:

The throughput on diesel being in the range of 44 litres/hr, thus creates difficulties due to the extreme bulk of low BTU fuel required to produce the same output.

It was found very difficult to thermally combust some of the very low BTU fuels with high nitrogen dilutant, however catalytic combustion of these fuels readily took place and it would seem that for these fuels catalytic combustion presents the best solution.

Combustor Exit Temperatures:

Analysis of required exit temperatures is complicated by variation of by-pass air, however the range of metal and metalloid supports fabricated for the test programme fell into two classes:

a) Type I, a low cost support capable of continuous running at 1200°K; the majority of test work has been carried out using this system which is adequate for the majority of industrial engines.

b) Type II, an expensive high technology support which has a continuous running temperature of 1700°K. This support and material was developed to provide the flexibility to power advanced technology engines.

1500°K exit temperature tests:

Two series of tests were run on the blowing rig: The first series used the ultra high temperature support by itself with a stabilisec high temperature platinum catalyst. The performance of the unit was as per the normal supported catalyst but with the ability to run up to high exit temperatures without damage. This support was also found to be very tolerant to premix fuel quality and suffered no damage when fed a fine spray instead of vaporized fuel.

The second series of tests involved running a standard catalyst unit to provide an exit gas of 1100^{o}K continuous and adding further fuel before passing through an extremely small high temperature support. In this mode the high temperature support was essentially acting as a 'bluff body' and the text book phenomenon of hot body ignition could be observed. However, this hot body ignition led to an interesting series of experiments.

TABLE I. BASE LINE TEST ON ROVER GAS TURBINE

Base Line Test on Rover Gas Turbine

Barometric pressure 775.5mm Hg

Test No.		1	2	3	4	5
RPM	N	3000	3000	3000	3000	3000
Brake load	P	10	40	70	95.2	10
Impeller tip pressure - psig	P_2	3.4	3.6	3.7	3.8	3.5
Compressor delivery pressure - psig	P_3	26	26.6	27.9	28.1	26
" " " - abs	P_3	41.0	41.6	42.9	43.1	41.0
Pressure drop in combustion chamber - cm Hg	hc	15.5	15.7	14.4	14.0	15.7
Exhaust pressure - cm paraffin	P_5	5.3	3.2	2.0	-2.3	4.3
Air venture depression - mm paraffin	h	24.6	22.4	22.0	20.5	24.5
Air intake temperature ^{o}K	T_1	293	293	293	293	293
Compressor delivery temperature (Measured) ^{o}K	T_3	433	-	-	4930	433
Jet Pipe temperature	T_5	628	726	808	867	651
Time for 2000 cm^3 fuel	t	230	201	167	145	230
Compressor delivery temperature (Calc.)^{o}K	T_2	433	434	434.1	435.1	433
Air flow rate Kg/s	M	.667	.637	.6311	.609	.666
Fuel flowrate Kg/s	F	.00735	.00841	.0101	.0117	.00735
Air/fuel ratio	f	90.7/1	75.7/1	62.5/1	52/1	90.6/1
Brake power kW	P_b	5.06	20.23	35.4	48.15	5.06
Specific fuel consumption Kg/kW h	SFC	5.23	1.497	1.027	0.8750	5.23
Brake thermal efficiency	η_B	1.56	5.45	7.7	9.04	1.56
Combustion efficiency	η_{Comb}	74.3	86.2	89.3	86.3	74.2
Compression ratio	R	2.733	2.773	2.86	2.873	2.733
Turbine inlet temperature	T_4	762	882	985	1065	762
Turbine inlet pressure (p.s.i.abs)	P_4	33.4	33.9	35.8	36.2	33.3
Expansion ratio P_4/P_5	E	2.22	2.25	23.8	2.42	2.23

Exhaust Gas Analysis

	1	2	3	4	5
HC ppm	350	180	150	140	360
No ppm	13	22	33	44	17
NO_x ppm	22	24	42	58	18
CO ppm	1450	150	97	112	1560
CO_2 %	2.5	3	3.7	4.5	2.4
O_2 %	18	17.5	16.7	15.7	18.2

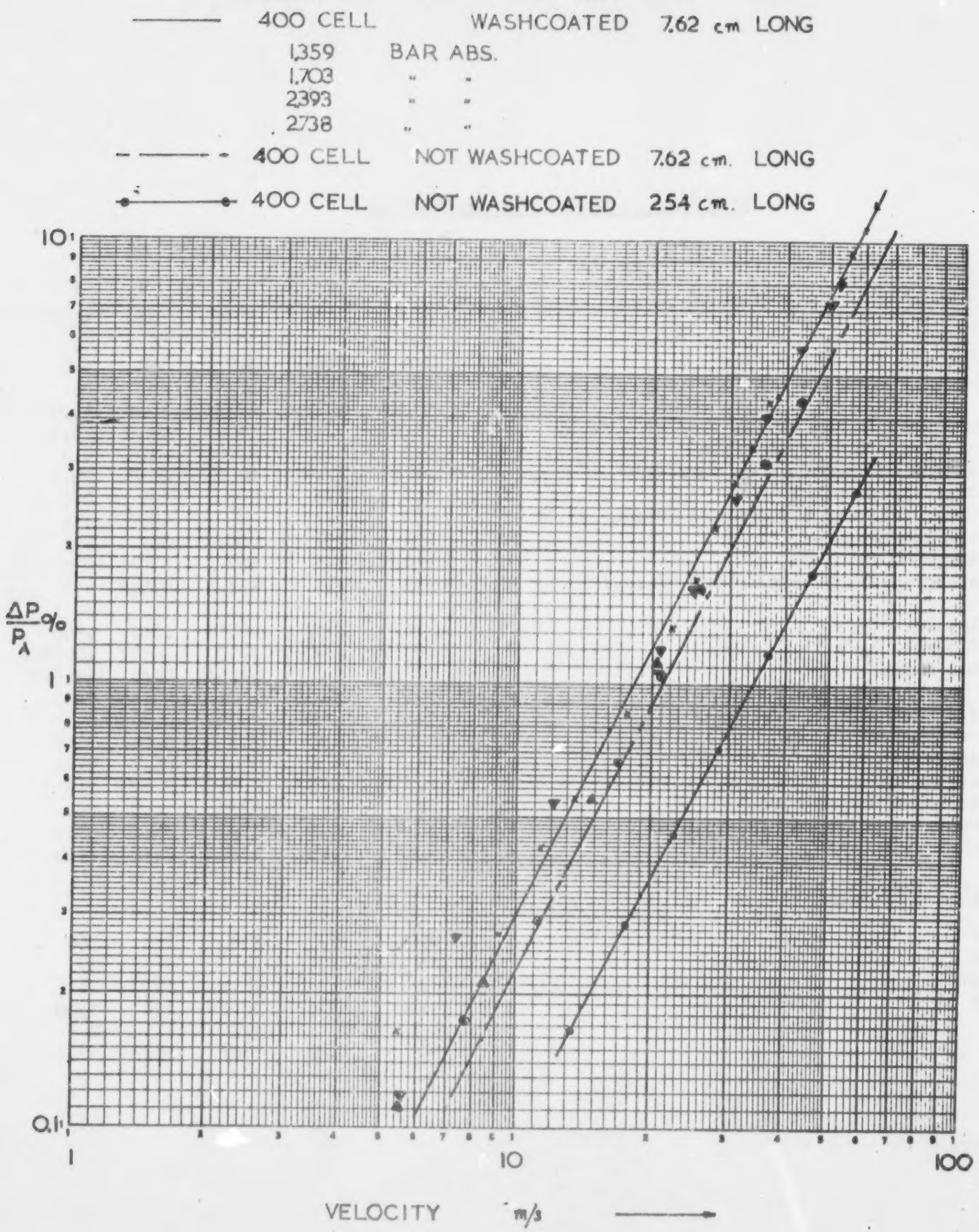

Figure 1. ΔP/PA vs. velocity for 400 cell washcoated support.

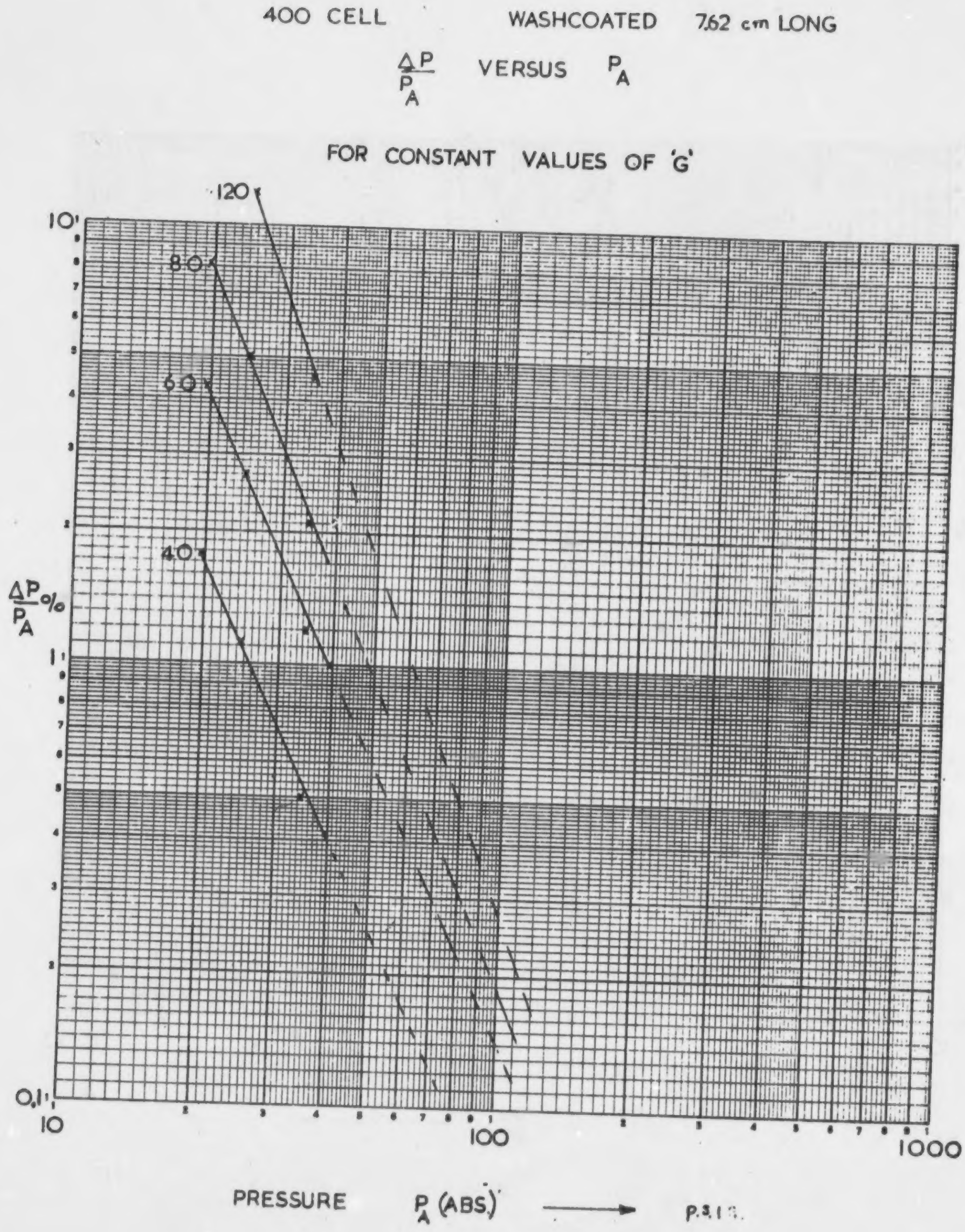

Figure 2. ΔP/PA vs. PA for 400 cell washcoated support.

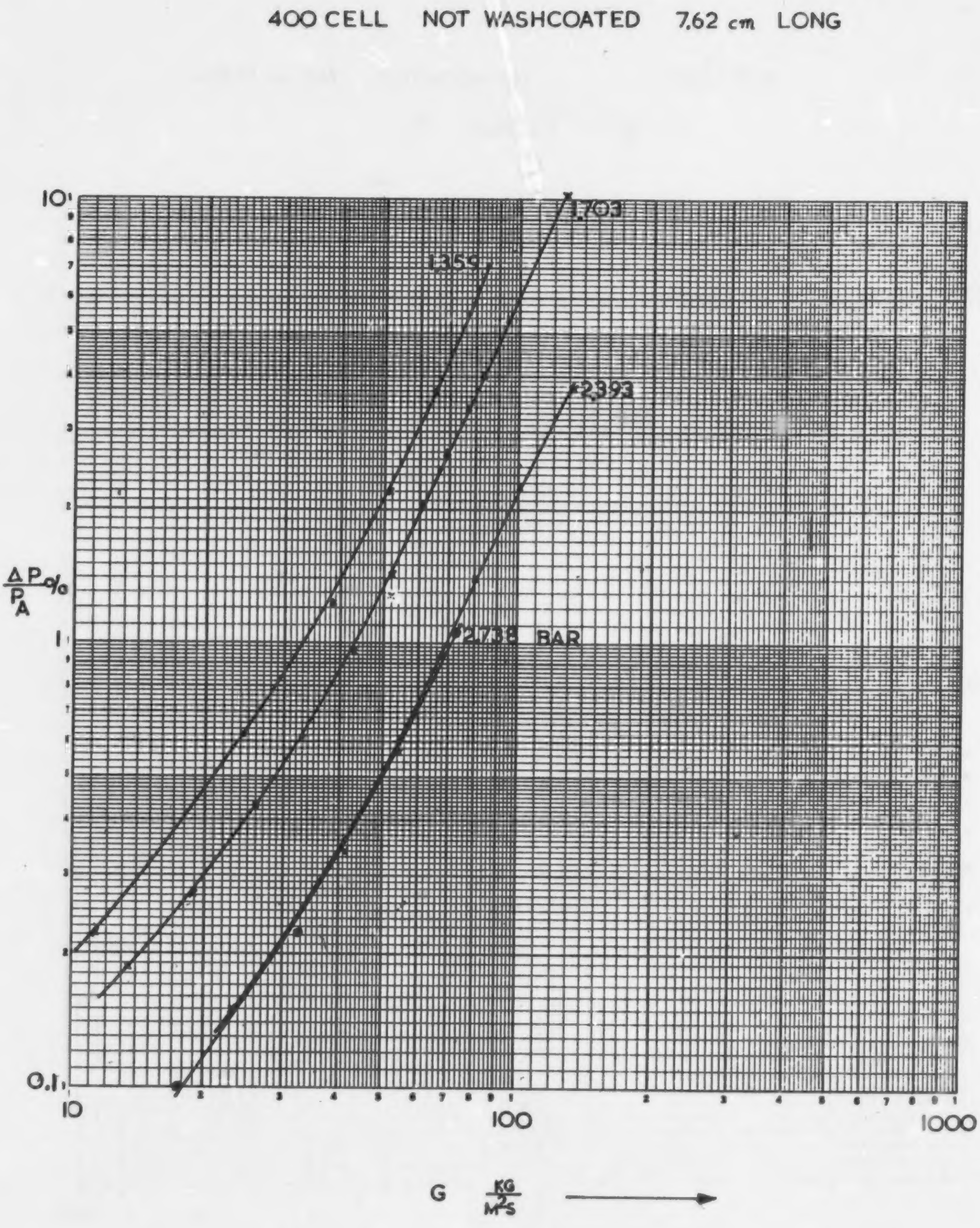

Figure 3. $\frac{\Delta P}{PA}$ vs. G for 400 cell washcoated support.

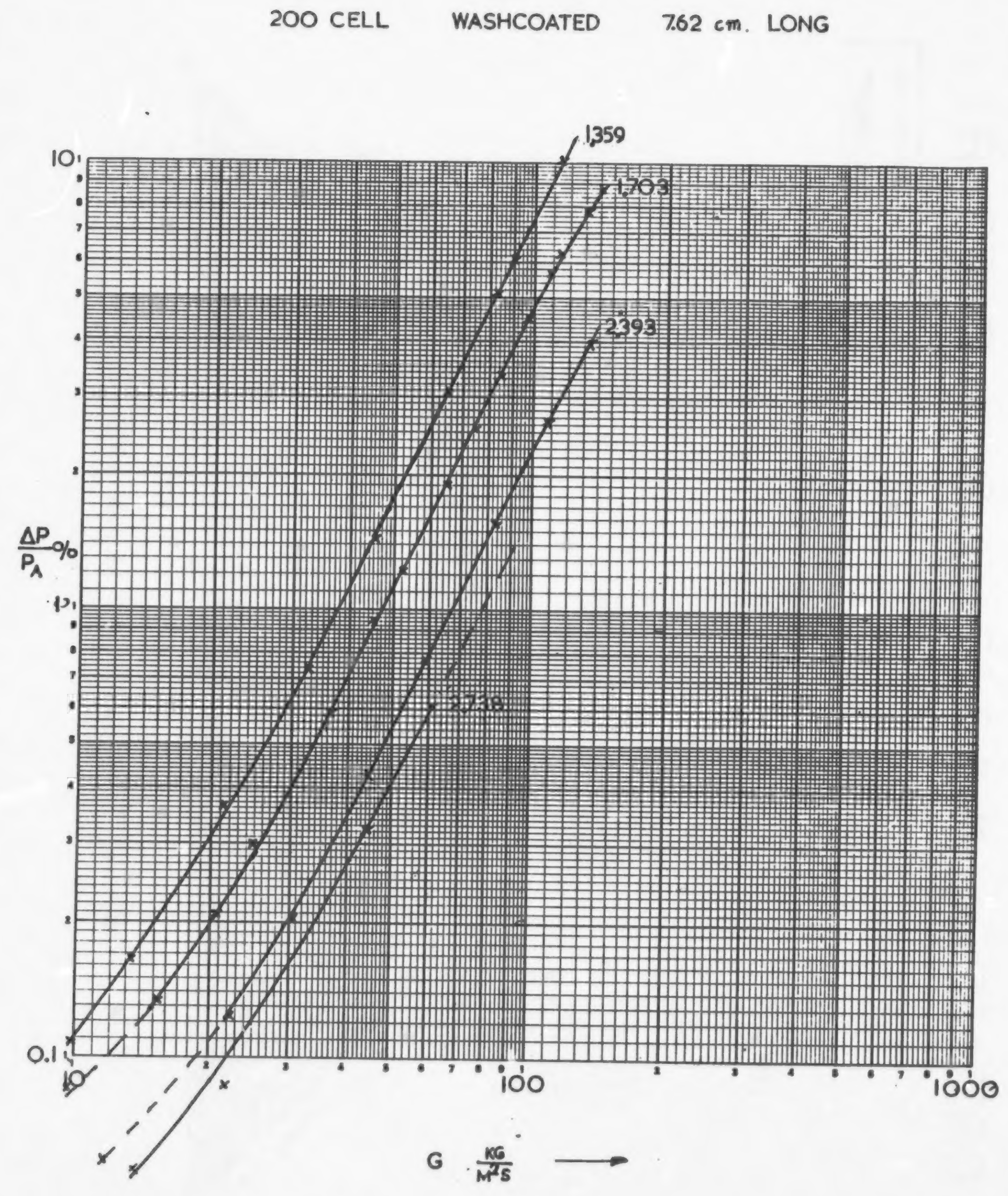

Figure 4. $\frac{\Delta P}{PA}$ vs G for 200 cell support.

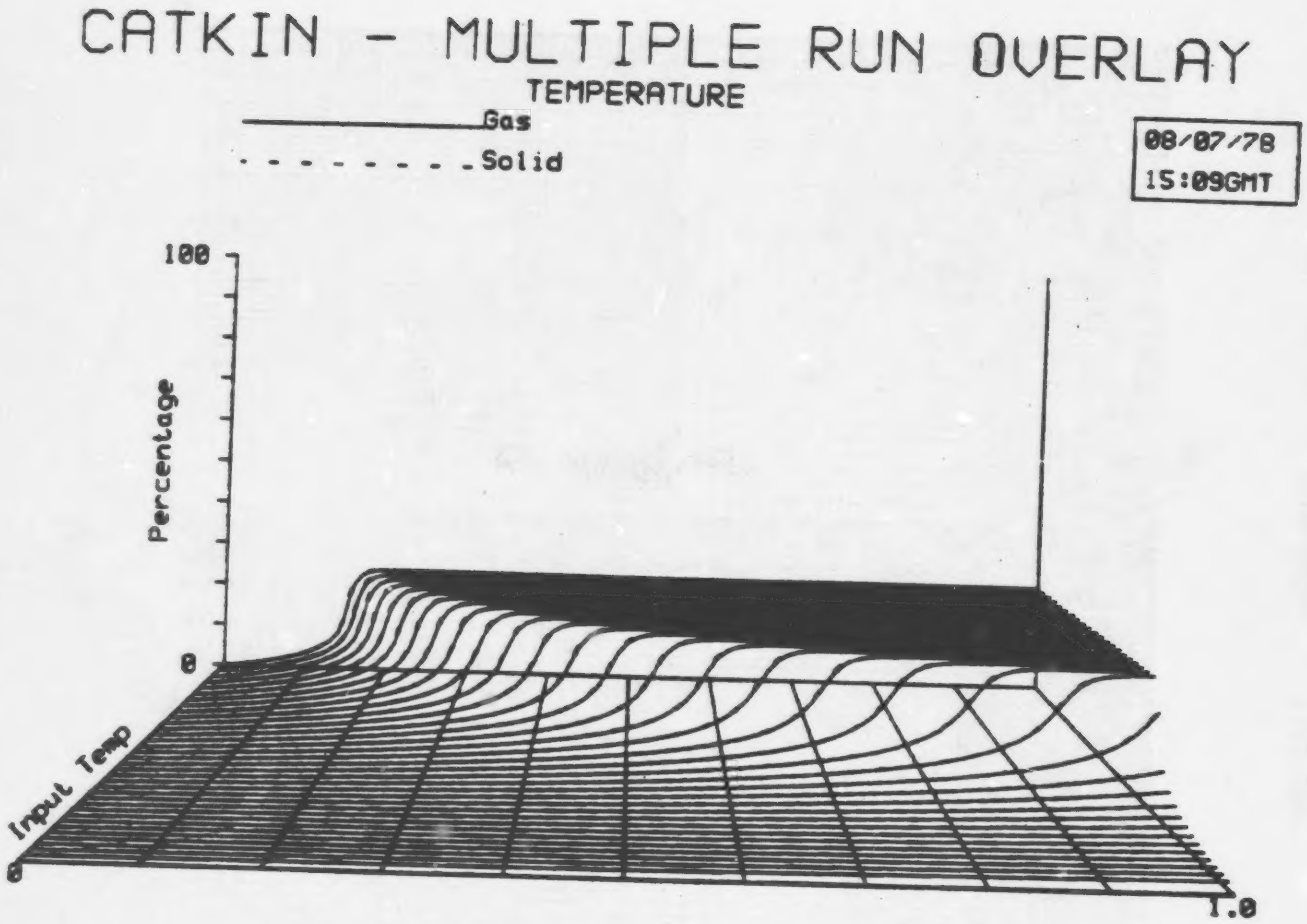

Figure 5. Relative distance through catalyst.

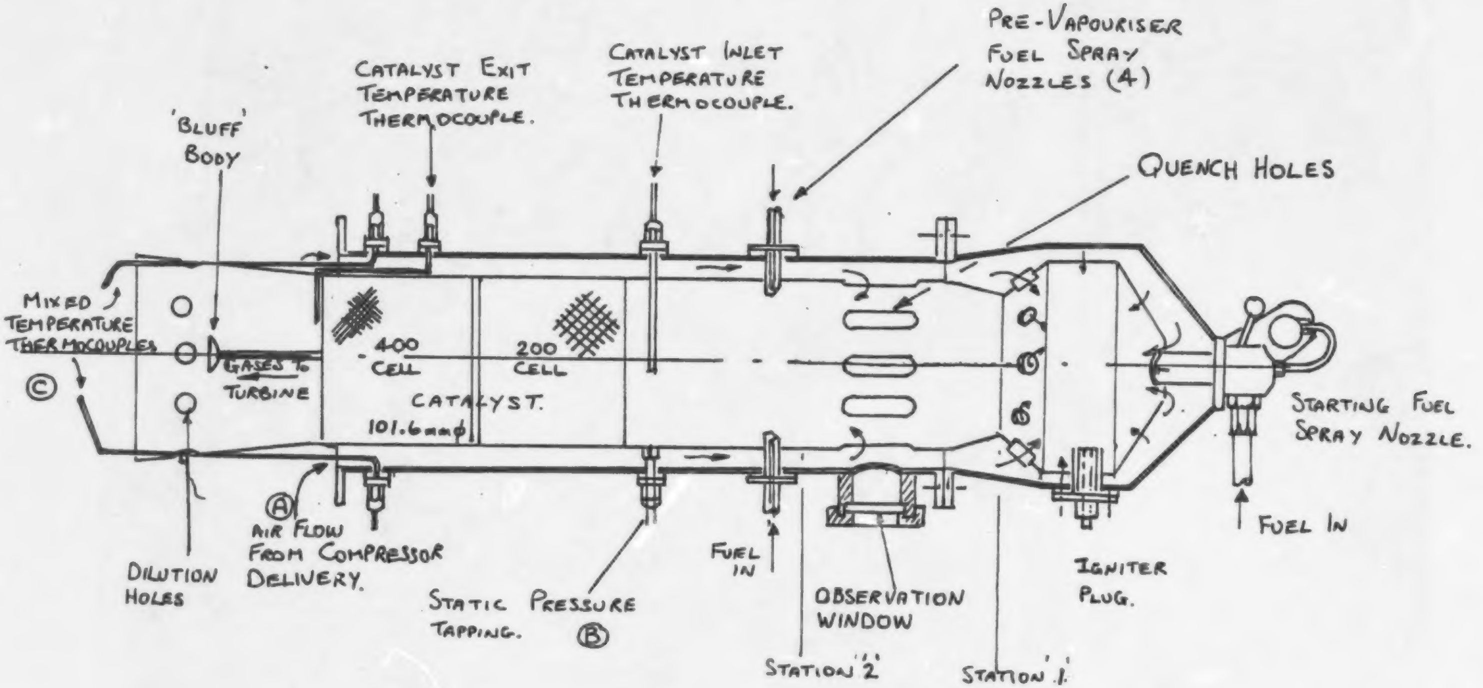
Pre-Vapouriser Fuel Spray Nozzles (4)
Catalyst Exit Temperature Thermocouple.
Catalyst Inlet Temperature Thermocouple.
'Bluff' Body
Quench Holes
Mixed Temperature Thermocouples
©
400 Cell
200 Cell
Catalyst. 101.6mmϕ
Gases to Turbine
Starting Fuel Spray Nozzle.
Ⓐ Air Flow From Compressor Delivery.
Dilution Holes
Static Pressure Tapping.
Ⓑ
Fuel In
Observation Window
Station '2'
Station '1'
Igniter Plug.
Fuel In

Figure 6. Schematic diagram of comubstion chamber.

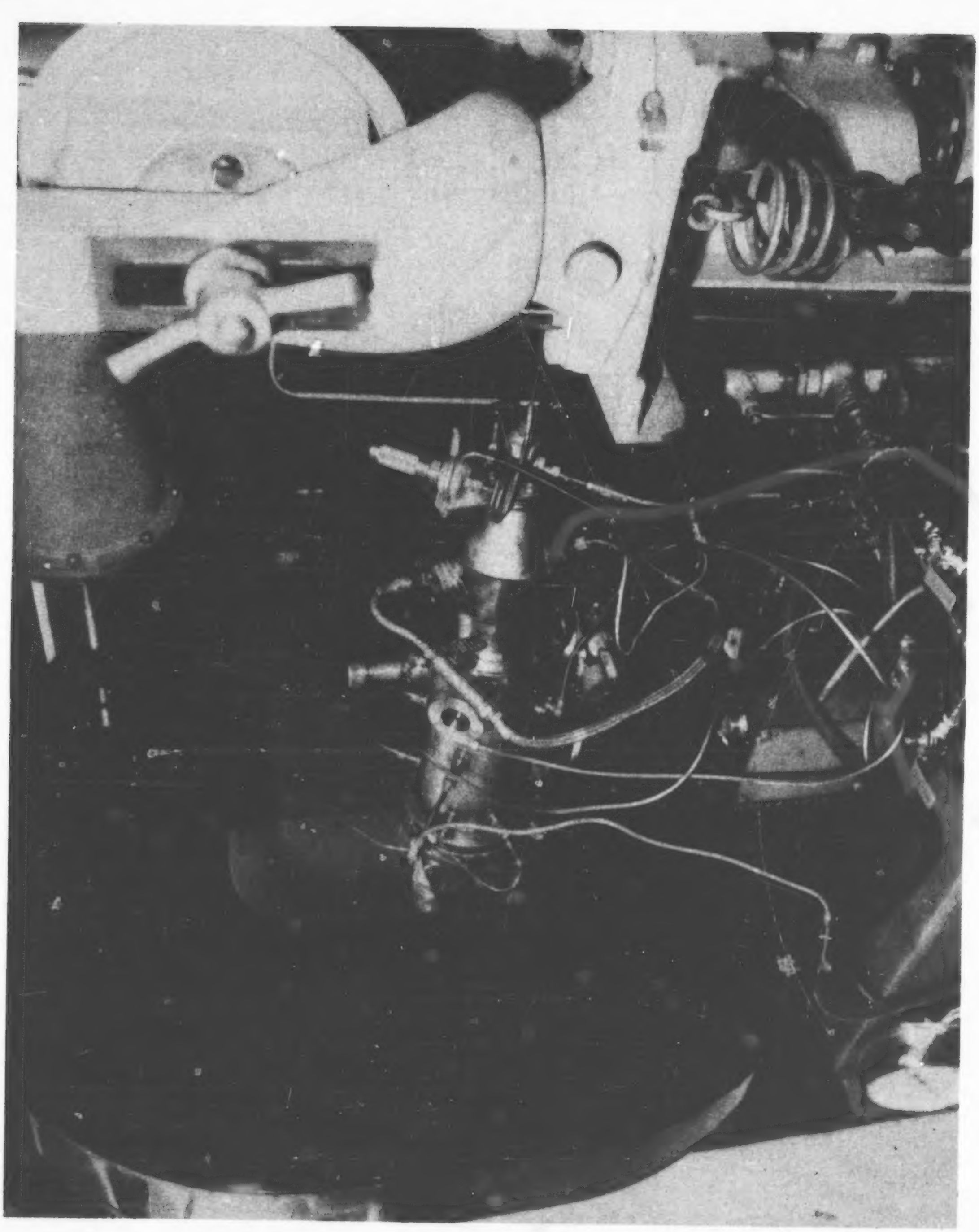

Figure 7. Experimental engine test setup.

HIGH COMBUSTION EFFICIENCY AND LOW POLLUTANT EMISSION BY CATALYTIC AND OTHER MEANS

By:

K. C. Salooja
Esso Research Centre
Abingdon, Oxfordshire, U.K.

ABSTRACT

Much effort is being expended these days to maximize combustion efficiency while ensuring low levels of pollutant emission. We have now achieved these objectives using a staged combustion system where particular attention was paid to the choice of burner, the design of the combustion chamber, and the use of non-volatile, non-dischargeable, catalysts in different combustion stages. Combustion of fuel oil was carried out under almost stoichiometric conditions with negligible smoke and virtually no CO, or unburned hydrocarbons, and with very low emission of NO_x and SO_3.

Preceding page blank

HIGH COMBUSTION EFFICIENCY AND LOW POLLUTANT EMISSION BY CATALYTIC AND OTHER MEANS

INTRODUCTION

The growing concern about both energy conservation and atmospheric pollution requires that combustion systems should be opreated with maximum efficiency and with pollutant emissions controlled to within environmentally acceptable limits. The two goals, however, are not readily compatible since any reduction in excess air to promote combustion efficiency increases smoke, carbon monoxide, unburned hydrocarbons, and often also oxides of nitrogen.

We have now developed a system where both objectives can be achieved. The system, basically, is a staged combustion set-up where particular attention has been given to the choice of the burner, the design of the combustion chamber and the use of non-volatile, non-dischargeable, catalysts within the combustion chamber.

METHOD

Preliminary studies were carried out in a combustion rig of conventional design using a Hamworthy Mark 6A medium pressure burner of 1 M BTU/hr rating firing into a refractory lined water-cooled combustion chamber, 24 in. I.D. and 48 in. long. This system produced such large amounts of carbon even under stoichiometric conditions that for staged combustion a high intensity Hygrotherm R 10 burner was used. A new combustion chamber, which is described later, had to be designed to further greatly minimize production of undesirable products.

Preceding page blank

Temperatures of fuel and air to the burner, of cooling water inlet and outlet, and of the flue gas were monitored. Pressures of the fuel and air were also determined. The fuel firing rate was checked by periodically monitoring the weight of the feed drum.

Flue gas was analyzed continuously for O_2, CO, CO_2, H_2, unburned hydrocarbons (HC), NO_x and smoke. For analysis of O_2, CO, CO_2 and H_2 the gas drawn from the stack was filtered and passed through a refrigerator and then through a column of dry silica gel to remove particulate matter and moisture. CO and CO_2 were analyzed by non-dispersive infra-red analyzers (Maihak 'Unor 2'), O_2 by a paramagnetic analyzer (Servomex 'OA 137'), and H_2 by a thermal conductivity analyzer (Hartmann and Braun 'Caldos 2').

HC were anlayzed by a flame ionization detector (manufactured by Curzon Technical Supplies), and smoke by a von Brand analyzer.

NO_x were analyzed by a chemiluminescent analyzer (Thermo Electron Model 10A). Flue gas sample was drawn through a quartz tube, which was frequently replaced since the deposits that gradually build up affected the readings.

A sensitive technique was developed for SO_3 analysis. This has been described elsewhere (Reference 1).

All the gas analyzers were regularly calibrated with standard gas samples.

Tests were carried out using fuel oil #2 and #5. Both these were doped with pyridine to increase their nitrogen content as high as 0.76% to verify how well the system could curb NO_x even under such exceptional condition.

RESULTS AND DISCUSSION

Pollutant control becomes increasingly difficult when, in the interest of energy conservation, combustion is carried out closer to the stoichiometric condition. Of the various undesirable products, CO, HC and H_2 are not so difficult to control as solid carbon and NO_x (and also SO_3, when sulphur is present in the fuel). Our efforts at the outset were therefore largely directed towards the control of carbon and NO_x. Amongst the various NO_x control techniques hitherto developed staged combustion is considered highly satisfactory since it alone can control both thermal and fuel NO_x (Reference 2). However, even with this technique attempts to reduce NO_x substantially present serious problems with the control of carbon. This is because the effectiveness of NO_x control mainly depends on the degree of fuel-richness of the first stage, but the richer the first stage, the greater is the formation of carbon and the other products of incomplete combustion. Whilst the gaseous combustible products can be effectively burned in the second stage, carbon is notoriously difficult to burn within a practical system. Apart from the combustion difficulties, excessive carbon formation can seriously interfere with additional control measures. The success of the system, therefore, largely depends on how well carbon formation is curbed in the first stage.

The results in Figure 1 typify the severity of carbon formation with a conventional burner even under normal single stage condition. We, therefore, tested a variety of burners, and found that the Hygrotherm burner - which recycles a considerable proportion of the flame products - produces markedly less carbon and also, unlike several other burners, produce less NO_x (Figure 1).

Although the 24 in. I.D. combustion chamber used in the above experiment was adequate for the conventional burner, it was far too wide for the Hygrotherm flame, barely 4 to 7 in. in diameter. One could not therefore attempt a further reduction in carbon and NO_x by further promoting mixing and recriculation of products in the main body of the flame and/or provide a convenient means of treating the combustion medium with catalysts. Studies were, therefore, carried out with narrow combustion chambers. These proved far more amenable to the control of all the undesirable products. The influence of the chamber length was next investigated. Attempts were then made to increase recirculation of combustion gases by inserting baffles in the chamber. Next design studies on the second stage burner (air injector) were carried out. Finally the application of catalysts was investigated. The various developments, together, helped to produce a system which could operate with maximum combustion efficiency (without any excess air) and with exceptionally low pollutants.

INFLUENCE OF COMBUSTION CHAMBER DIAMETER

Comparative performance of Hygrotherm burner in 24 in. I.D. chamber and an 8 in. I.D. chamber, both of the same length, is shown in Figure 2. In the narrower chamber carbon formation was far less, although more NO_x was formed. These effects are, obviously, due to improved mixing and interaction of the flame products, and higher wall temperatures.

Attempts to use a still narrower chamber (5 in. I.D.) showed that now impracticably long length was necessary to effect complete combustion. So most of the further development was carried out with the 8 in. I.D. chamber.

INFLUENCE OF CHAMBER LENGTH

Carbon forming tendency was reduced as the chamber length was increased from 50 in. to 75 in., and then to 90 in.; although NO formation was slightly increased. The magnitude of both these effects, however, was far less than with changing the chamber diameter.

With #2 fuel oil, the combined effect of reduced chamber diameter (8 in. I.D.) and increased length (90 in.) was such that virtually smoke-free combustion could be carried out with barely 56% of the stoichiometric air. The system, therefore, is capable of generating reducing atmospheres of a quality such as hitherto been achieved mainly with gaseous fuels.

INFLUENCE OF BAFFLES

Baffles were introduced into the combustion chamber to

- explore if carbon formation can be further reduced and the more readily combustible CO and H_2 increased,
- find if their use can help reduce chamber length,
- check what effects can arise on the insertion of perforated refractory blocks as catalyst support.

Three refractory baffles, each with a 2.5 in. hole in the centre, were spaced in the combustion chamber at 16 in., 30 in. and 48 in. from the burner. Their presence, as shown in Figure 3, considerably reduced carbon formation, increased CO and H_2 and reduced CO_2. NO was not much affected; its concentration, with air 50-60% of the stoichiometric, was less than 3 ppm. The baffles entailed only slight - ca 1 in. w.g. - pressure drop.

It is thus clear that the insertion of baffles, and hence also of catalyst supports of similar design, is mainly beneficial.

SECOND STAGE BURNER

The principal requirement of the second stage burner - air injector - is that it should cause the air and the hot products from the first stage to mix well quickly in a short space. Several air injectors were designed, but their performance showed little difference. Far greater effect, mainly on carbon formation, was that of its distance from the first burner. The closer it was to the upstream burner, the less the carbon formed. The effect on NO_x, CO, HC and H_2 was much less.

VARIATIONS IN PRIMARY TO SECONDARY AIR RATIO

Whereas according to previous studies NOx reduction increased as the proportion of the primary air is reduced, (Reference 2), our studies show that the reduction reaches a maximum when the primary air is reduced to ca 60% of the stoichiometric. A further reduction in primary air to ca 50% of the stoichiometric increased rather than reduced NO. This reversal in effect is most probably caused by less complete degradation of the organic nitrogen species in the first stage, and their subsequent oxidation in the second stage.

INFLUENCE OF FUEL-NITROGEN CONTENT

The influence of increasing the nitrogen content of fuel, by doping it with pyridine, was studied with the medium pressure burner firing into the 24 in. I.D. combustion chamber, and also with the Hygrotherm burner firing into the 8 in. I.D. chamber. The results showed that whilst NO increases with increasing nitrogen content, the increase is not directly proportional to the nitrogen content. The nature of the combustion system and the air to fuel ratio also affect it. The latter factor has a particularly pronounced effect under sub-stoichiometric conditions. Here the more fuel rich the combustion, the smaller is the conversion factor. This is understandable since the more fuel rich the combustion the more intense are the reducing conditions, and hence the less the NO that can form or survive reduction.

INFLUENCE OF FUEL FIRING RATE

It has been previously established that a decrease in fuel firing rate reduces NO_x (Reference 3, 4). To verify the extent of the effect under our experimental conditions, the influence of changing the firing rate from 2 to 3 gph was examined. Under excess air firing conditions overall, and with the first stage operating with ca 80% of the stoichiometric air, NO indeed decreased as the firing rate was reduced. However, under stoichiometric firing conditions overall, and the first stage operating with considerably less than 80% of the stoichiometric air, increased firing rate produced less, rather than more, NO. There was nothing else unusual about the combustion process: higher firing rate produced more CO, HC and H_2, and the variation in the proportion of CO_2 to CO followed the expected pattern. Obviously, the higher firing rate produces more severe reducing conditions and this gives rise to less NO.

INFLUENCE OF CATALYSTS

We have previously shown how NO_x formation can be markedly reduced by placing catalysts in the flame (Reference 5). In a staged combustion system, the two flames, as well as the interstage zone of a highly reducing nature, should all be readily amenable to NO_x destruction by catalysts. This possibility was explored with following results.

Our previous study, with several catalysts, has shown that Fe/Cr is a highly effective catalyst. This was again found to be the case in the present study and the results presented here are mainly with this catalyst. The catalyst was supported on alumina/silica refractory capable of withstanding temperatures up to 1650°C. For its use in the interstage zone, the refractory block was 3 in. thick and had numerous 1/2 in. diameter channels across it. Catalysts were applied to the block by coating it with an aqueous solution of the nitrates of the metals and then firing it till the nitrates decomposed.

Catalysts in the Interstage Zone

The catalyst block was placed in turn at 40 in., 52 in. and 66 in. from the first stage burner at positions where the temperature with fuel oil#5, firing at 2.5 gph rate, and air 75% of the stoichiometric, was respectively 1260°, 1180° and 1050°. The catalyst reduced NO, the effect being greater the more fuel rich the combustion (curves 1 and 2, Figure 4). With the catalyst 52 in. from the burner and air 75% of the stoichiometric NO was reduced from 300 pm to 130 ppm (57% reduction). The NO reduction was less (46%) with the catalyst 40 in. from the burner, but more (64%) when it was 66 in. from the burner. Whilst NO was thus markedly reduced by the catalyst, carbon formation was somewhat increased. However, no difficultly was experienced in curbing this in the second stage.

The second stage opeation (with the air injector 3 in. downstream of the catalyst) maintained the marked reduction effected by the interstage catalyst. With the primary air 73% of the stoichiometric, and the overall air input stoichiometric, NO emission was 140 ppm (curve 4, Figure 4). Without the interstage catalyst, staged combustion under these conditions produced 380 ppm NO (curve 3, Figure 4).

Catalysts in the Second Stage Flame

An Fe/Cr treated refractory block, similar to the interstage catalyst, but only half its thickness (1.5 in.), was placed ca 3 in. downstream of the air injector. This brought about a further reduction in NO (curve 5, Figure 4). With the primary air 73% of the stoichiometric and the overall air input stoichiometric, the second stage catalyst reduced NO from 140 ppm to 120 ppm.

The effect of using the second stage catalyst in the form of an elonaged ellipsoid, ca 6 in. and 2 in. in axes, supported ca 2 in. from the burner along its central axis was also studied. This had virtually the same effect as the perforated block catalyst.

Catalyst in the First Stage Flame

The use of the catalyst in the first stage, by mere treatment of the burner throat wherefrom the flame emerges into the combustion chamber, brought about a further substantial reduction in NO. The NO concentration in the flue gas, with the system operating with stoichiometric air overall, was now 95 ppm.

The first stage catalyst did cause a slight increase in smoke, but its emission in the stack gas was still fairly low - below 3 Bacharach number. CO, HC and H_2 were hardly detectable.

SO_3 CONTROL

SO_3 formation from fuels containing sulphur is, of course, highly undesirable. The factors which are responsible for NO formation also promote SO_3 formation. Hence the techniques developed for NO_x control should also help reduce SO_3. In our studies with fuel oil #5 containing 2.5% sulphur, SO_3 emission from the conventional system, operating with 2.1% excess oxygen was 44 ppm. In the staged combustion system, at the same firing rate and with the same excess air, SO_3 emission was 26 ppm. The use of catalysts reduced this to 18 ppm. Since the staged set-up, unlike the conventional system, could be operated smoke-free under almost stoichiometric condition - and SO_3 formation is strongly curbed by curtailment of excess air - SO_3 was reduced to only 5 ppm.

CONCLUSIONS

This study demonstrates a combustion system which can be operated with maximum efficiency (with no excess air) and with very low emission of pollutants. Fuels which, under conventional combustion conditions, generate ca 950 ppm of NO, now give rise to only 95 ppm. Moreover, despite the fact that the system is operating without any excess air, CO, HC and H_2 concentrations are negligible and that of smoke is below the visible level. SO_3 formation, when sulphur is present in the fuel, has also been greatly reduced. Whilst conventional combustion conditions generate 44 ppm of SO_3, the new system produces barely 5 ppm.

This study has included examination of fuels with very high nitrogen content (0.76%). Normal fuels, with nitrogen concentrations ranging from 0.1 to 0.4% produce less NO and with these the present system could give rise to very low NO emission. One NO control technique which has been studied in the past but not incorporated in this investigation - interstage cooling (Reference 2) - could, if needed, help to reduce NO even further.

The staged combustion system adopted has been developed to generate very low concentrations of carbon. This capability is reflected by the fact that fuel oil #2 can be fired virtually smoke-free with barely 56%

of the stoichiometric air. In conventional systems, in contrast, smoke-free operation would require air considerably in excess of the stoichiometric.

The exceptionally low emissions of NO_x and SO_3 that have now been achieved arise primarily through the use of catalyst in the different zones of staged combustion. The effective catalyst (Fe/Cr) as well as the catalyst support (Al_2O_3/SiO_2 refractory) are inexpensive materials which can well withstand the furnace temperatures involved in staged combustion, and they do not give rise to secondary pollution problem through loss from the system.

REFERENCES

1. Salooja, K.C., "Some serious errors in SO_3 determination in flue gases", Energy World, March 1974, 10.

2. Siegmund, C.W. and Turner, D.W., "Influence of combustion modification and fuel nitrogen content on nitrogen oxides emissions from fuel oil combustion", Combustion, August 1972, p.21; "NO_x emissions from industrial boilers: potential control methods", Combustion, October 1973.

3. Bartok, W., "Status of EPA-sponsored studies of stationary NO_x control at Esso Research & Engineering Co.", ASME Meeting, November 28-December 2, 1971, Washington D.C.

4. Blakeslee, C.E. and Burbach, H.E., "Controlling NO_x emissions from steam generators", J. Air Poll. Control Assoc. 23: 37 (1973).

5. Salooja, K.C., "Combustion control by novel catalyst means", Nature, 240: 350 (1972).

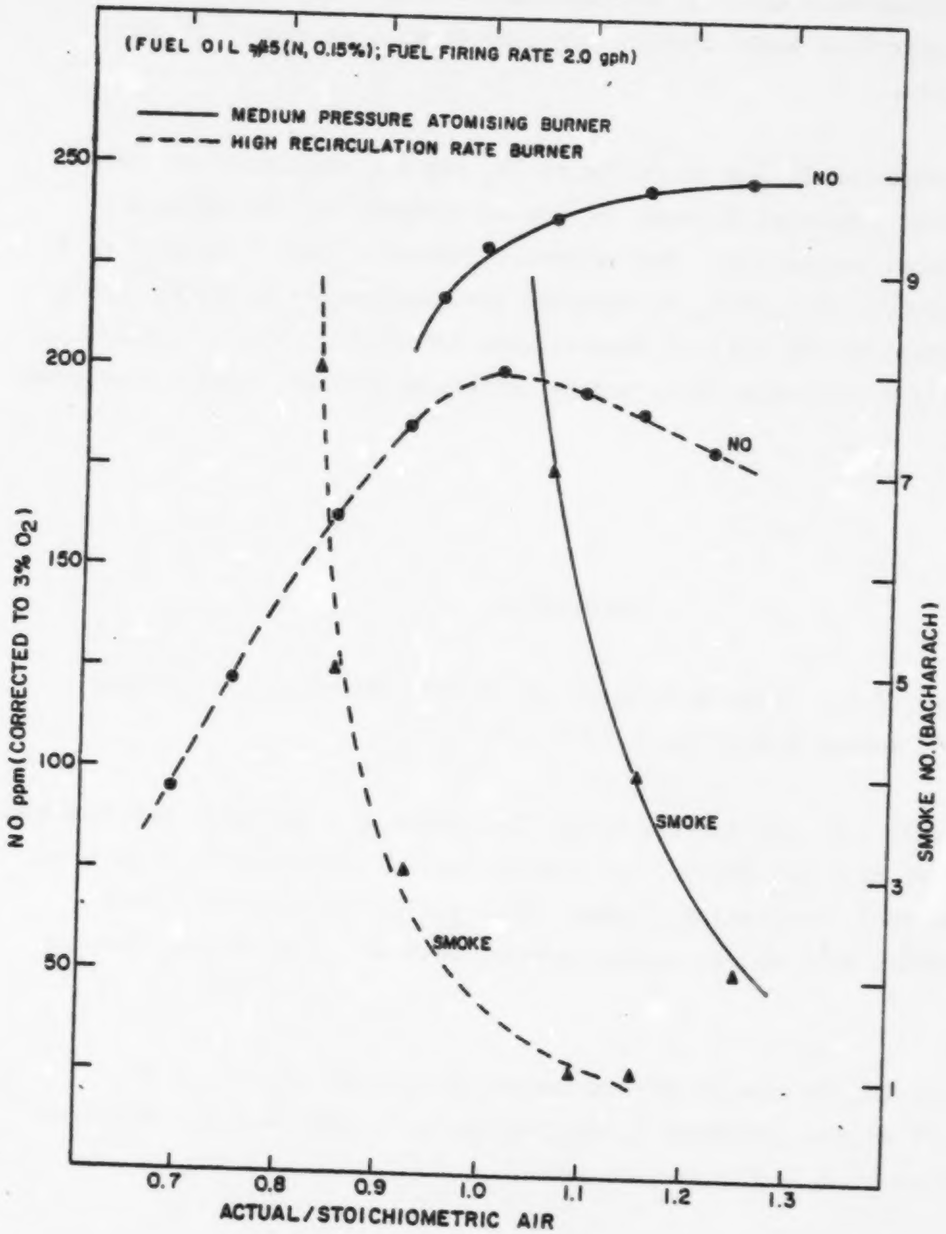

Figure 1. Smoke and NO emission performance of a high recirculation rate burner and a medium pressure atomising burner in a conventional, unstaged system.

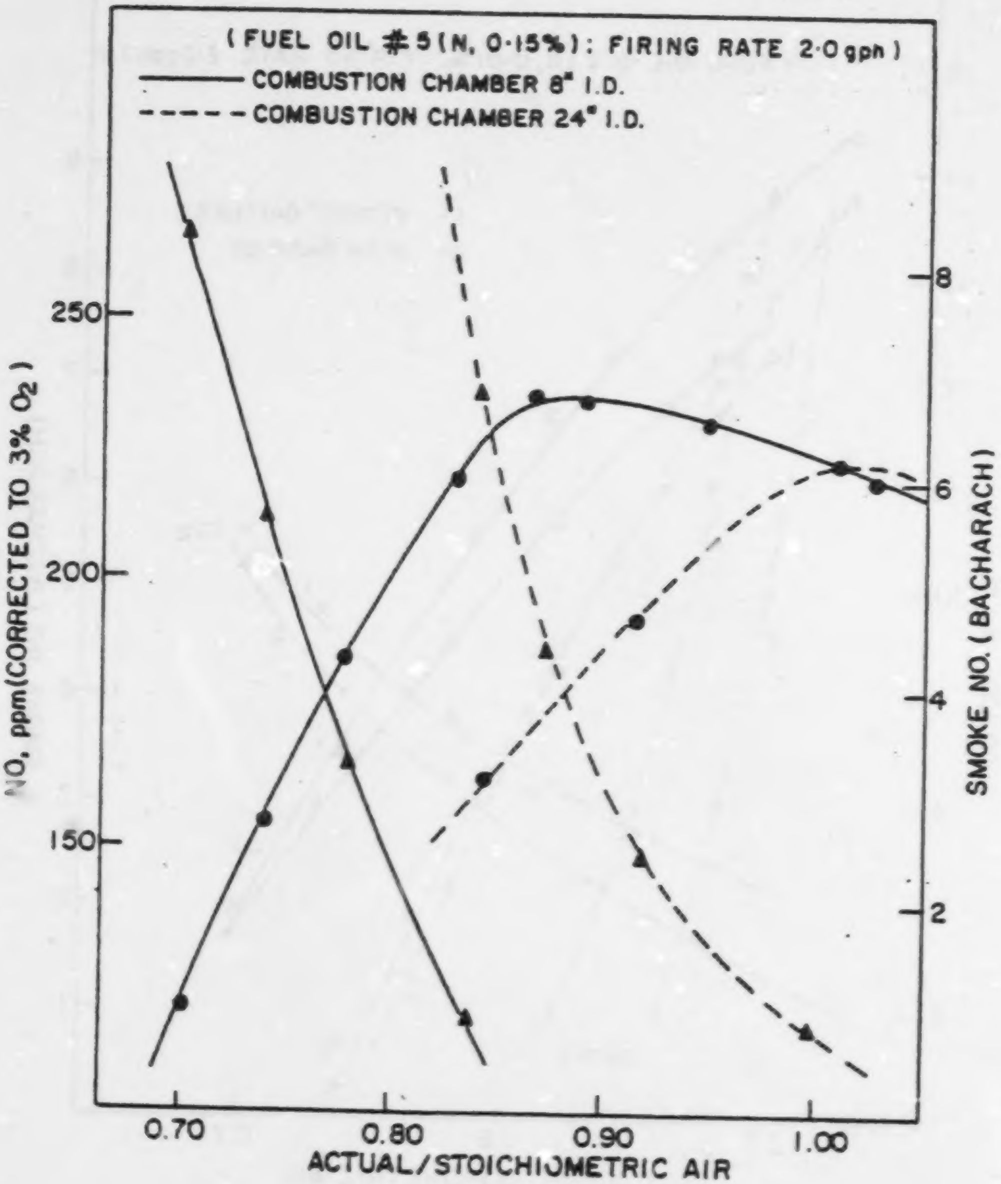

Figure 2. Smoke and NO emissions with high recirculation rate burner in combustion chambers with different internal dimensions.

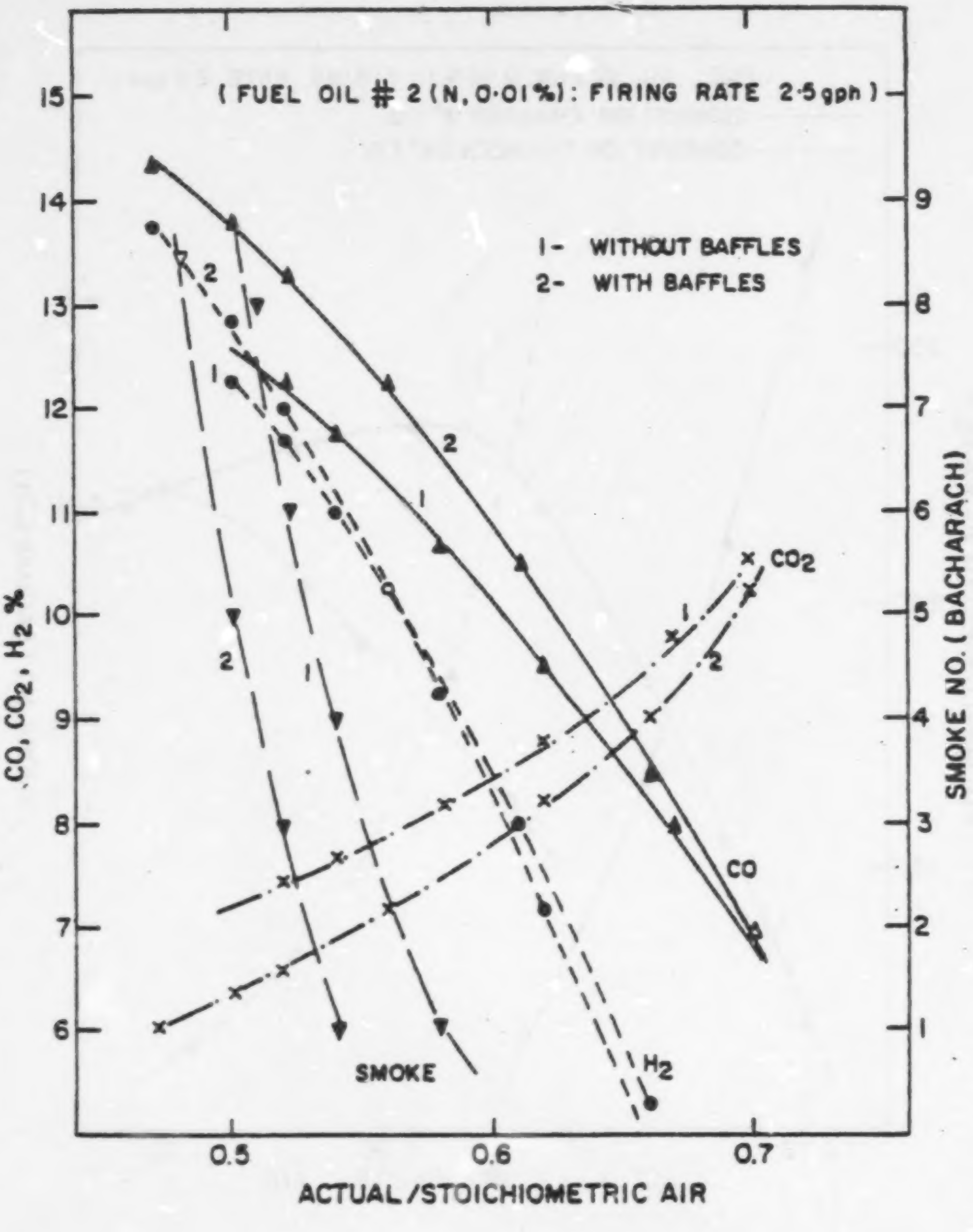

Figure 3. Influence of baffles in combustion chamber on smoke, CO, CO_2 and H_2.

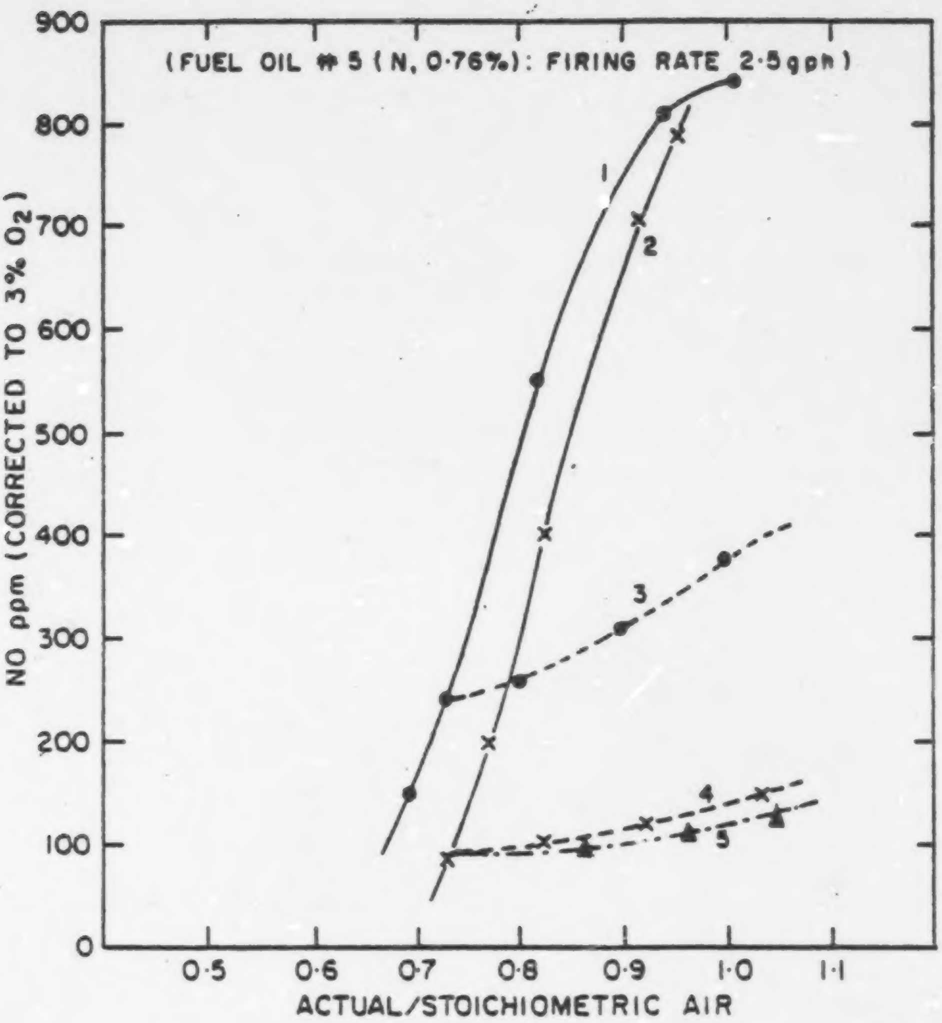

Figure 4. Influence of catalysts on NO emission (1 - unstaged combustion without catalyst; 2 - unstaged combustion with catalyst 52 in. from the burner; 3 - staged combustion without catalyst; 4 - staged combustion with interstage catalyst as in (2); 5 - staged combustion with interstage catalyst as in (4) and second stage catalyst 3 in. downstream of air injector).

APPENDIX A

Summaries

First and Second Workshops on Catalytic Combustion

SUMMARY

SECOND WORKSHOP ON CATALYTIC COMBUSTION

The Plantation Inn
Raleigh, North Carolina

June 21-22, 1977

Sponsored by the U.S. Environmental Protection Agency

Summary prepared by J. P. Kesselring, Acurex Corporation/Aerotherm Division

---

The Second Workshop on Catalytic Combustion was held in Raleigh, North Carolina on June 21-22, 1977. Forty-three people, representing various governmental, industrial, and academic organizations, attended the workshop; a list of attendees is given at the end of this summary. The purpose of the workshop, sponsored by the U.S. Environmental Protection Agency and organized by the Aerotherm Division of Acurex Corporation, was to provide an overall summary of the current state of the art of catalytic combustion. This was accomplished by bringing catalytic combustion research people together for the exchange of results obtained since the first workshop was held in May 1976.

The meeting began on June 21 with introductory remarks by Mr. G. B. Martin of the Environmental Protection Agency. Mr. Martin emphasized the potential role of catalytic combustion in the control of NO_x emissions. For conventional combustion systems, significant amounts of thermal NO_x are produced at temperatures above 2800 °F, and large fuel NO_x emissions are found in lean systems. Analytical and very limited experimental results are beginning to show that catalytic combustion systems may be able to minimize NO_x emissions in systems that operate above 2800 °F and use fuels which contain large amounts of bound nitrogen. The importance of system design on the combustor approach used must also be considered. As an example, firetube or watertube boilers operate under different conditions than gas turbines, and knowledge of the operating regime for the system is required to design the combustor. Mr. Martin then introduced Mr. Dale Johnson of the Institute of Gas Technology.

Preceding page blank

Institute of Gas Technology Programs

Mr. Johnson of IGT described work carried out at the Institute of Gas Technology on ventless appliances and catalytic igniters. During 1972 to 1976, under the sponsorship of Southern California Gas Company of Los Angeles, IGT invented and developed several conceptual burners and model ventless appliances for catalytic combustion of hydrogen and steam-reformed natural gas. During 1975, the U.S. Environmental Protection Agency and Southern California Gas Company cofunded a program at IGT to develop a catalytic range-top burner. These model catalytic appliances operate at low combustion temperatures and produce very low emissions of nitrogen oxides ($NO_x < 8.0 \times 10^{-4}$ lb/10^6 Btu). Because of the low emission levels, outside venting of the products of combustion is not required.

Since 1974, IGT has been working on the development of an instantaneous ignition system for gas appliances using hydrogen fuel ignited in air with a platinum catalyst. The hydrogen is stored in the form of a metal hydride, with small quantities of hydrogen released by valving when ignition is required. This catalytic ignition system could become an alternate to standing pilot or electric systems.

Westinghouse Program

Mr. S. M. DeCorso of Westinghouse described efforts conducted by Westinghouse to assess the applicability of catalytic combustors for stationary gas turbines. In order to achieve a significant reduction in NO_x emissions, new combustor technology is needed. Westinghouse has been working in four areas of gas turbine combustion to develop this technology: (1) conventional combustors, (2) premixed, (3) catalytic, and (4) new wall cooling techniques.

The catalytic combustor approach has been identified as one of the major ways to solve the emissions problem. Experimental test results with No. 2 distillate oil and low Btu gas show much lower emissions than the conventional combustor, with NO_x emissions <1 ppm. Pattern factors measured 1 foot downstream of the catalytic combustor exit were excellent, allowing the air requirement normally reserved for the pattern factor to be distributed elsewhere.

Mr. DeCorso presented catalytic combustor development situations for stationary gas turbines based on a program approach emphasizing integration of system design thoughts throughout the program. Application of these combustors would be in both retrofit and new systems, leading to the combustion of coal gas, waste gas, coal liquids, and bound nitrogen fuels with minimal NO_x emissions.

Based on work done at Westinghouse, the catalytic combustor has been shown to have the characteristics required to help solve problems of fuel conservation, emission requirements, and use of new fuels. Development of the catalytic combustor in a total system design is now needed while research efforts on the catalytic components continue.

U.S. Air Force Programs

The U.S. Air Force is sponsoring programs in catalytic combustion through the Aero Propulsion Laboratory and the Air Force Office of Scientific Research. The Aero Propulsion Laboratory programs deal with the application of catalytic combustors to aircraft gas turbine engines and afterburners. The Air Force Office of Scientific Research programs are concerned with catalytic combustion modeling and the initiation of combustion on catalytic surfaces.

Aero Propulsion Laboratory Program

Captain Thomas J. Rosfjord of the AFAPL described the AFAPL in-house program for catalytic combustion application to aircraft systems. The program addresses the use of catalysts in both mainburner and afterburner applications. Mainburner rig testing will cover the following range of conditions:

- $2 < p < 18$ atm
- $400 < T_{inlet} < 800$ K
- $20 < V_{ref} < 40$ m/s
- $0.1 < \phi < 0.4$

Afterburner tests will be focused on the ability of a catalytic combustor to convert fuel energy in an efficient and stable manner.

A honeycomb flameholder consisting of silicon nitride monolith segments coated with Pt/Pd catalyst has been fabricated and will be tested in July. Inlet temperature for this system will be 1300 ^{o}F, with the surface temperature between 2500 and 3000 ^{o}F.

Dr. Henry Shaw of Exxon Research and Engineering discussed work to develop a hybrid catalytic combustor for aircraft turbine applications. This material is discussed in detail in Air Force Aero Propulsion Laboratory Report AFAPL-TR-76-80. The hybrid catalytic combustor minimizes pollution problems associated with unburned hydrocarbons and carbon monoxide in the idle mode, and NO_x and smoke production in the power mode of aircraft gas turbine operation. This combustor consists of a fuel-rich thermal precombustor, secondary air quenching zone, and monolithic catalyst stage which rapidly oxidizes CO and UHC produced in the precombustor.

Noble metal catalysts on various monolithic support materials and geometries were found to be the most active materials for CO and UHC oxidation in the temperature range of 700 to 1200 K. The hybrid catalytic combustor combustion efficiency for JP-4 fuel containing 535 ppm sulfur was found to be 99.8 percent under realistic conditions. Combustor pressure drop was less than 6 percent. For a Johnson Matthey metal-supported Pt catalyst, average emission indices of CO, UHC, and NO_x were 0.95, 0.43, and 1.8 g/kg of fuel, respectively. This catalyst was effective in reducing CO by 86 percent and UHC by 94 percent, while increasing NO_x by 68 percent relative to catalyst inlet values. It was estimated that the hybrid catalytic combustor can meet the 1979 new aircraft emission standards, but must be modified slightly to reduce UHC emissions to meet the 1981 new aircraft emission standards.

Gerald Roffe of General Applied Science Laboratories, Inc., then described work conducted at GASL to develop a fuel preparation system for the catalytic combustor, which would provide uniform velocity and fuel distribution profiles, completely vaporize the fuel, and have a reasonable pressure drop. Operating conditions for the system include flow velocities of 50 to 125 ft/sec, pressures of 100 to 200 psia, temperatures of 700 to 1000 °F, and fuel air ratios of 0.018 to 0.028. The approach taken in developing the fuel preparation system was to design for a limited residence time to prevent autoignition, to provide for adequate exit blockage to prevent flashback, to produce small droplets to get good evaporation, to use a high flow velocity to preclude flame stabilization prior to entering the combustor, and to obtain the best possible initial dispersion of the fuel to enhance mixing. Three candidate designs were tested, consisting of pressure atomization, air blast atomization, and air assist atomization systems. Following testing of these systems and some modifications, an air assist atomization system with an upstream swirl generator was selected as the final design.

Captain Rosfjord then summarized some areas in need of investigation. One obvious area is the physical, chemical, and thermal endurance of a catalytic combustion system. The investigation of an all-catalytic system, rather than a hybrid system, for low power application also needs to be addressed.

Air Force Office of Scientific Research Programs

Dr. B. T. Wolfson of AFOSR then briefly discussed the AFOSR interests in catalytic combustion for air-breathing propulsion systems. Two programs are currently being funded by the AFOSR in catalytic combustion. Dr. F. B. Bracco of Princeton University is performing a theoretical-experimental study of the initiation of combustion on catalytic surfaces, and Dr. C. M. Ablow of Stanford Research Institute is developing a theoretical model for catalytic combustion. In addition to these efforts, advanced diagnostic techniques and other fundamental studies are of interest to the AFOSR.

Joint National Science Foundation/Environmental Protection Agency/Exxon Program

Dr. Anthony E. Cerkanowicz of Exxon Research and Engineering described this jointly-funded effort to develop a practical model of catalytic combustor operating characteristics for analysis of advanced power systems and data analysis. The major physical assumptions of the steady-state model are:

- Uniform gas-phase properties at a cross section
- Catalyst/substrate temperature and fuel concentration are uniform at a cross section
- Conversion of reactants to products can occur at the catalyst surface and in the gas phase
- Axial variations in velocity are allowed
- Axial heat conduction in the substrate is included, but radiation and gas-phase conduction are neglected

The model consists of a variable-order finite-difference method to solve the two-point boundary value problem. Comparisons of catalytic combustor data and model predictions show excellent agreement. When the model is used to examine conversion as a function of gas inlet temperature for typical lean operating conditions with a noble metal catalyst, a sharp catalytic lightoff temperature is predicted, as is a lightoff/extinction hysteresis. At higher temperatures the onset of gas-phase combustion occurs, resulting in complete conversion.

Further work on expanding the model to include internal heat removal, CO kinetics, multiple fuel species, and NO_x kinetics is planned.

U.S. Environmental Protection Agency Program

Mr. G. Blair Martin of the EPA briefly described the goals of the catalytic combustor application to stationary combustion systems. In stationary systems, it is desirable to operate at high system temperatures, at low overall excess air, and at minimum flue gas temperature. It is also desirable to be able to burn fuels containing bound nitrogen without producing excessive NO_x emissions. These are among the areas being addressed in the EPA program.

Acurex Corporation/Aerotherm Division Program

Under EPA sponsorship, the Aerotherm Division of Acurex Corporation is conducting a study to determine design criteria for catalytic combustors with application to stationary sources. Dr. John P. Kesselring of Aerotherm described the program effort aimed at identifying concepts for new combustion systems capable of extremely low emissions performance at the highest system efficiency achievable.

The development of catalytic combustors for systems such as industrial and commercial boilers depends on establishing design criteria for the combustion system. These design criteria include information on the catalyst/washcoat/substrate, the catalyst life, the preheat requirement for combustion air, and the maximum flow velocity and bed temperature that can be achieved in the system. Additional design criteria include the amount of heat extracted from the combustion system for a given extraction mode and catalytic combustor geometry.

The program began with a review of available catalyst materials (precious metals and metal oxides, washcoats, and substrate materials). This review was interfaced with theoretical calculations for heat and mass transfer in a catalyst bed to determine the materials required for the catalyst systems. Catalyst systems were then prepared in-house and obtained from outside suppliers. Prior to testing, all catalyst systems were characterized by total and active (precious metal) surface area measurements. The catalysts were then instrumented with in-depth thermocouples to provide bed temperature distribution measurements. One-atmosphere screening tests were then conducted with up to four fuels (natural gas, propane, indolene, and methanol) for a test time sufficiently long to determine the catalyst performance after the initial rapid degradation was completed and a constant performance level achieved.

A total of thirty-four screening tests were run on a variety of monolith materials, washcoats, and catalysts. Based upon the results of the screening tests, it was found that:

- Alumina was the best high-temperature (2700 °F) monolith
- α-alumina or presintered γ-alumina washcoat enhanced long term combustion performance at low preheat, compared to γ-alumina washcoats
- H_2S treatment of Pt helped stabilize the catalyst at high temperature
- Increasing Pt loading gave significantly greater activity
- Large cell monoliths passed many UHC, but operated at extremely high mass throughputs
- Small cell monoliths provided excellent cleanup of pollutants

Based upon the screening test results, the graded cell catalyst system was developed and tested. This system used a large-cell monolith segment at the front end, a small-cell segment at the back end, and one or more intermediate-sized segments in the middle. Graded cell catalysts have been operated at maximum bed temperatures of 2735 °F, space velocities of 413,000 $(ft^3/hr)gas/ft^3catalyst$, and for tests on individual catalysts of up to 78 hours duration. Limited test data indicates less conversion of NH_3 dopant (a NO_x precursor) to NO_x at low pressure and high velocity under lean conditions than is found in conventional systems.

The first catalytic combustion system to be tested incorporating direct bed cooling used catalyst-coated cylinders surrounded by water tubes. Surface energy removal was accomplished by radiation from the catalyst to the water tube, allowing the catalyst surface to operate at less than 2000 °F temperature, even under stoichiometric conditions. The water tubes remove approximately 25 percent of the available energy in the fuel. For boiler application, the radiative catalytic/water tube system would be followed by a graded cell catalyst to complete combustion and achieve the goal of extremely low emissions and high system efficiency. Further testing of graded cell catalysts and combustion systems is ongoing, with prototype system design to be completed by the end of the year.

Johnson Matthey Research Center Program

Dr. Gary Acres of the Johnson Matthey Research Center described platinum metal crystallite growth at elevated temperature. Test results have shown that catalytic activity is not proportional to crystallite size or metal area, but that the lightoff temperature is a function of the metal crystallite size. Lightoff is a kinetically controlled phenomenon, whereas high conversion of reactants is diffusion controlled. Increasing metal loading, or using promoters, helps increase the kinetic region activity.

The parameters which affect metal sintering are:

- Temperature, with high-temperature catalytic combustion applications always increasing sintering
- Catalyst environment, with inert atmospheres showing slow sintering and oxygen-combustion gas atmospheres exhibiting rapid sintering

The catalyst may move about on the support by vapor transport in the gas phase, by a surface migration of metal atoms from one crystallite to another, by the combining of crystallites, or by metal-ceramic support interactions. Dr. Acres presented a movie of platinum on silica and platinum/rhodium sintering, giving visual confirmation of the migration and sintering of platinum.

United Technologies Research Center Program

The UTRC catalytic combustion program was described by Dr. Pierre Martenay. The program seeks to determine the feasibility of utilizing catalyzed surface reactors in the combustion of multicomponent fuels. The program is currently involved in simple burner experiments using propane fuel and in an analytical study combining heat and mass transfer and homogeneous reactions in the analysis.

The experimental program uses a catalytic burner apparatus to determine ignition temperature, steady-state operating conditions, and species concentrations by varying mixture ratio, temperature, bed length, flow velocity, bed material, and diluent. The combustible mixture is usually oxygen-propane with argon diluent, but helium and nitrogen diluent have also been used. Isothermal experiments are then run to determine ignition temperature.

The modeling program takes into account both heterogeneous and homogeneous reactions, and seeks to fit experimental data over a range of temperatures with single heterogeneous and homogeneous rate constants. Matching of temperature rise and concentration data has been done for propane combustion with argon diluent.

NASA-Lewis Research Center Programs

Dr. David N. Anderson began the meeting on June 22nd with a brief review of NASA's interests in catalytic combustion. The Air Breathing Engines Division of the Emission Technology Branch is pursuing the application of catalytic combustors to aircraft gas turbines, while the Power Generation and Storage Division of the Combustion Power Section is interested in catalytic combustors for automotive gas turbines.

Dr. Anderson then described the catalytic combustion automotive gas turbine program in more detail. The proposed gas turbine operating conditions are:

- o Pressure 1.5 to 4.5 atm
- o Exit temperature 1310 $^{\circ}K$
- o Primary zone temperature 1350 to 1425 $^{\circ}K$
- o Reference velocity 11.4 to 12.9 m/sec
- o Airflow 0.1 to 0.5 kg/sec
- o Inlet temperature 1210 to 970 $^{\circ}K$

The NASA test rig can duplicate all these conditions except the inlet temperature, which is limited to 800 $^{\circ}K$. The goals are to limit emissions from the combustor to half of those required by the most stringent standards, and to keep the total combustor system (fuel preparation plus combustion chamber) pressure drop under 3 percent.

For the fuel preparation system, the program goals are:

- o Spatial fuel distribution within 10 percent of mean
- o 90 percent of fuel vaporized at 800 $^{\circ}K$
- o Velocity distribution within 10 percent of mean
- o No autoignition
- o Less than 1 percent pressure drop

Four different fuel injectors were tested; (1) air assist sonicore injector, (2) splash-groove injector, (3) multiple-jet injector, and (4) multiple conical tube injector. Air swirlers were used with the sonicore and splash-groove injectors to improve spatial fuel-air distributions. The multiple conical tube fuel injector was generally able to meet the program goals if sufficient mixing length was allowed.

In the catalyst evaluation program, the objectives are:

- Emissions
  - 1.6 g NO_2/kg fuel
  - 13.6 g CO/kg fuel
  - 1.64 g HC/kg fuel
- Pressure drop
  - Less than 2 percent

The combustion test rig used has a long mixing section, and the reactor can hold from one to six individual catalyst elements in series. Each element is located between thermocouple arrays. All tests were performed at an inlet temperature of 800°K, pressure of 3×10^5 Pa, and a range of velocities from 10 to 25 m/sec. Adiabatic reaction temperatures from 1100 to 1600°K were obtained by varying fuel-air ratio.

Catalyst elements were obtained from Engelhard Industries, W. R. Grace and Co., Johnson Matthey Corporation, and Oxy-Catalyst, Inc. All elements were 12 cm in diameter. The Johnson Matthey elements used a metal substrate; all other elements used a ceramic substrate. Emissions measurements were then made in combustion tests to determine the minimum exit temperature at which the reactors should be operated to obtain the steady-state emission objectives. Effects of reactor length, cell density, and gas phase reactions were considered.

The feasibility of using a catalytic reactor in an automotive gas turbine engine and meeting both emissions and pressure drop goals was demonstrated in this program. Potential problems for such a system include the loss of catalytic activity with time and transient operation characteristics.

In addition to the automotive work, NASA is pursuing aircraft gas turbine engine emission reduction programs using catalytic combustors. Dr. Edward J. Mularz described this work. The purpose of the experimental program being conducted by General Electric is to evolve jet aircraft engine combustion technology and reduce low-power CO and HC emissions to extremely low levels. Combustor concepts are tested in a 60-degree sector configuration sized to engines of large commercial aircraft. Three design concepts will be screened over a limited range of operating conditions. The three designs include a hot wall combustor, a recuperative combustor, and a catalytic combustor.

A new program, the advanced low emissions catalytic combustor program, will be starting shortly. The purpose of this program is to evaluate the feasibility of employing catalytic combustion technology in the aircraft gas turbine engine field to achieve the control of NO_x emissions for subsonic, stratospheric cruise operation, while retaining or improving system performance. This program is jointly funded by NASA and the Air Force, and will involve three phases: Phase I is a design study, Phase II involves further design with combustion testing, and Phase III will involve full annular or sector combustion testing. This program will begin in October 1977.

Engelhard Industries Program

In addition to in-house research, Engelhard Industries has active externally supported programs in catalytic combustion. Engelhard is a subcontractor to General Electric on the NASA-sponsored low emissions aircraft combustor program, and has also completed a program on catalyst selection and life test durability in No. 2 diesel oil combustion for NASA under ERDA funding.

Dr. Robert V. Carrubba described the work done for G.E. on catalyst design for low power operation of a low emissions aircraft combustor. As was the case with the Exxon program, Engelhard decided to pursue a hybrid combustor design using a preburner followed by a catalytic cleanup of the vitiated air stream. Performance goals for the preburner/catalyst system are 1 ppm HC, 10 ppm CO, and 4 ppm NO_x, with a 5-percent overall pressure drop in the combustor and 3 percent in the catalyst.

Screening tests were carried out to select a perferred catalyst configuration. Test conditions were 2-atm pressure, temperatures of 1000 and 1400 °F, velocities of 80, 100, 120, and 140 ft/sec, and an addition of 200 and 400 ppm by volume of both CO and HC.

From the screening tests it was found that both CO and unburned hydrocarbon conversion were higher than expected, due to thermal reactions. Thus the cleanup mode, with air bypass, was found to be a workable design for low emissions idle mode gas turbine combustors in the laboratory. Further testing of these catalyst systems at General Electric are forthcoming.

Dr. Ronald M. Heck of Engelhard presented the work done on catalyst life testing for NASA-Lewis Research Center. This work was performed in support of the ERDA highway vehicle gas turbine engine program, and the objective was to investigate the durability of two selected proprietary Engelhard catalysts. The test sequence for the two catalysts involves a 24-hour break-in period, a CO activity test, a test with propane to determine the performance range, another CO activity test, a 1000-hour life test with No. 2 diesel fuel (with CO activity tests every 250 hours), and a final propane test to determine performance range changes.

A summary of the test results showed emissions to be the same for both catalysts during the 1000-hour test with No. 2 diesel fuel. One catalyst required a higher inlet temperature to maintain low emissions after 600 hours of testing. The propane parametric studies showed this catalyst had deactivated completely for high efficiency combustion, and the CO activity test showed significant deactivation of both catalysts between 24 and 250 hours of aging.

Emissions with No. 2 diesel fuel after the 1000-hour test were 4 ppm HC, 50 ppm CO, and 4 ppm NO_x. These emissions are well below the 1977 and 1978 automotive standards. Further work to perform life testing at 5-atmosphere pressure is now underway.

Stanford Research Institute Program

Dr. C. M. Ablow of SRI described work now being undertaken at SRI under AFOSR funding. SRI has begun an analytical study to determine the contribution of catalytic wall reactions to combustion initiation. The temperature distribution on the duct wall is found, taking into account wall heat conduction, convective heat transfer, and heat generation and fuel consumption. For Lewis numbers greater than one, the temperature increases with distance down the duct, while for smaller Lewis numbers the temperature passes through a maximum whose value depends on flow speed. This program is just being initiated at this time, but the results should be useful in determining how a catalyst should be distributed for startup and shutdown in a practical system.

Energy Systems Corporation Program

Richard E. LeCompte of Energy Systems Corporation presented work done at ESC on thermal protection equipment using catalytic combustors. Existing products include belt-mounted Arctic ambulatory heater systems, SCUBA diver heaters, hypothermia prevention and treatment systems, casualty evacuation bag heaters, and downed airman power sources.

The downed airman power source system supplies warmth to airmen in life rafts by circulating heated water through turbulated undergarments or blankets. These systems use either propane or propylene fuel combusted on 1-percent Pt on alumina pellets manufactured by Matthey Bishop. Catalyst bed temperatures are between 1200 and 1400 °F. Heat extraction pins or fins conduct heat to a hot plate and finally to the fluid heat exchanger.

ESC is also currently developing a catalytic/thermoelectric SCUBA diver heater for the U.S. Navy. This system will be capable of delivering 500 thermal watts to a diver in 35 °F seawater.

British Gas Corporation Paper

Dr. Robert M. Kendall of Acurex Corporation discussed a paper sent to the workshop by A. Melvin of the British Gas Corporation. This paper summarizes research conducted on the modeling of diffusive catalytic combustion.

Most discussion centered around the conclusions reached in the paper, which states that diffusive catalytic combustion has disadvantages that preclude its extensive use, and that premixed combustion is really impractical in domestic, commercial, and process applications. Dr. Kendall pointed out that it is a delicate control problem to get air to the surface of a diffusive combustion system, but with a good catalyst it should be possible to produce nearly all CO_2 at the surface if the fuel flowrate is controlled. The importance of boundary layer events in the combustion reaction must also be emphasized. Finally, reference was made to the recently developed Bratko furnace, which operates successfully as a premixed diffusive combustor and has emissions of CO and HC < 30 ppm, and NO_x < 15 ppm.

Dr. Kendall then acted as moderator for brief presentations by substrate and catalyst manufacturers.

Substrate Manufacturer Presentations

The monolith manufacturers were represented by Corning Glass Works and 3M's American Lava Corporation.

Corning Glass Works Presentation

Willard A. Boyer of Corning described high-temperature substrates being developed at Corning for catalytic combustion. Materials such as mullite-alumina-titanate and zirconia spinel are being produced to incorporate high use temperature with good thermal shock properties. In addition to materials research, Mr. Boyer described the new extruded ceramic honeycomb cell shape called "flexible rectangles," which allows cell walls to bend in thermal shock and thereby minimize fracture.

American Lava Corporation Presentation

P. A. Coates of American Lava described Thermacomb brand corrugated ceramics and their applications to catalytic combustion applications. Corrugated ceramics are made using conventional paper-making equipment.

Catalyst Manufacturer Presentations

The catalyst manufacturers were represented by Oxy-Catalyst, Inc., Engelhard Industries, Universal Oil Products, Matthey Bishop, Inc., and W. R. Grace and Company.

Oxy-Catalyst, Inc. Presentation

Dr. William B. Retallick of Oxy-Catalyst discussed a current concern; how much washcoat depth can actually be used during the combustion process? A mathematical model was developed to calculate how far the reactants can diffuse into the catalyst during the contact time. Since kinetic constants are unknown, estimations are necessary. Based on this analysis, a significant penetration of the reactants into the washcoat is predicted.

Engelhard Industries Presentation

Dr. Larry Campbell of Engelhard gave an overview of the Engelhard program in catalytic combustion. Engelhard began with automotive monolithic catalysts, and proceeded through the development of catalytically supported thermal combustors to life testing. Special requirements for the materials used include:

- o Monolith
  - -- Thermal shock properties
  - -- Use temperature
  - -- Melting temperature
  - -- Porosity
  - -- Void fraction (pressure drop)
  - -- Geometric surface area
- o Washcoat
  - -- Surface area stability (>20 m^2/g after 1200 ^oC exposure)
  - -- Adherence
  - -- Reactivity
- o Metals
  - -- Activity
  - -- Stability
  - -- Specific fuels

Engelhard has developed high-temperature combustion catalysts, demonstrated those catalysts for over 1000 hours in life tests, and will now be pursuing commercial development of those catalysts in systems.

Universal Oil Products Presentation

Dr. George R. Lester of UOP sees a significant market potential for this area. Clean fuel catalytic combustion has been fairly convincingly demonstrated, and the extension to fuels with bound nitrogen is now of major interest. UOP will be focusing on optimizing catalysts to produce a minimum conversion of bound nitrogen to NO_x.

Matthey Bishop Presentation

Dr. A. S. D'Allessandro of Matthey Bishop described MBI's interest in developing washcoats with the maximum stable surface area while maintaining adherence to precious metals. MBI is also developing high open area, high surface area, high-temperature metal sheets for monolith application. Catalysts have been tested to space velocities of 10^6/hr.

W. R. Grace and Company Presentation

Mr. Philip A. Smith of W. R. Grace described their Poramic monoliths. Ceramic components are fluxed with polyethylene and passed through rollers to form ribs on sheets of material. The sheets are then rolled up and heat-sealed together, and the structure is fired. During firing the polyethylene is removed and the ribs are fixed to the ceramic structure. Annular substrates up to 2.5 feet in diameter can be made in this manner.

Meeting Summary

Blair Martin concluded the workshop with some summary comments.

Good technical progress has been made in the last year in catalytic combustion. The technology is developing rapidly, more data is available, and cooperation has been solidified between the R&D community, the catalyst/substrate manufacturers and, hopefully, the users of this technology.

Clean fuels are getting in shorter supply every day. Use of lower-grade fuels necessitates coping with the bound nitrogen problem. Low Btu gas can give up to 4,000 ppm NH_3, dependent on the H_2S cleanup process, and shale oils can have significant fuel nitrogen volumes. Catalytic reduction of NO with ammonia is possible at low temperatures, and may be possible at high temperatures as well. Thus, it may be possible to control fuel nitrogen, even in lean combustion, without staging. Tailoring of the catalyst to get the minimum conversion of fuel nitrogen to NO_x is definitely of interest.

Combustion of heavier fuels (No. 4, No. 5, No. 6, and shale-derived oils) with catalysts is also of great importance. Even if fuel NO_x can be controlled by proper catalyst system design, some fuel upgrading may be required for particulate formation control. The degree of fuel treatment will strongly influence fuel cost and the minimum treatment possible should be addressed.

Thanks were extended to the authors and presenters, the catalyst and monolith manufacturers, and the attendees for their efforts and interest.

SECOND WORKSHOP ON CATALYTIC COMBUSTION

Attendees

G. Blair Martin	IERL/U.S. Environmental Protection Agency Research Triangle Park, North Carolina
W. Steven Lanier	IERL/U.S. Environmental Protection Agency Research Triangle Park, North Carolina
Dr. David N. Anderson	NASA-Lewis Research Center, Cleveland, Ohio
Dr. Robert M. Kendall	Acurex Corporation, Mountain View, California
Dr. John P. Kesselring	Acurex Corporation/Aerotherm, Mountain View, California
William H. Nurick	Acurex Corporation/Aerotherm, Mountain View, California
Dr. Stanley A. Mosier	Pratt & Whitney Aircraft, West Palm Beach, Florida
Captain Thomas J. Rosfjord	Aero Propulsion Laboratory, Wright-Patterson Air Force Base, Ohio
Dr. Henry Shaw	Exxon Research & Engineering Company, Linden, New Jersey
Dr. Anthony Cerkanowicz	Exxon Research & Engineering Company, Linden, New Jersey
Dr. William B. Retallick	Oxy-Catalyst, Inc., West Chester, Pennsylvania
Dr. George R. Lester	Universal Oil Products, Des Plaines, Illinois
Dr. C. R. Krishna	Brookhaven National Laboratory, Upton, New York
Dr. Larry Campbell	Engelhard Industries, Edison, New Jersey
Dr. Robert V. Carrubba	Engelhard Industries, Edison, New Jersey
Dr. Ronald M. Heck	Engelhard Industries, Edison, New Jersey
Dr. Karl Bastress	Energy Research and Development Administration, Washington, D.C.
Philip A. Smith	W. R. Grace & Co., Baltimore, Maryland

Willard A. Boyer	Corning Glass Works, Corning, New York
Rodney I. Frost	Corning Glass Works, Corning, New York
Phil Coates	3M Company, St. Paul, Minnesota
S. Mario DeCorso	Westinghouse Electric Company, Lester, Pennsylvania
Dr. Pierre J. Marteney	United Technologies Research Center East Hartford, Connecticut
William Cain	U.S. Environmental Protection Agency, Cincinnati, Ohio
Gerald Roffe	General Applied Science Laboratories, Westbury, N.Y.
Dr. C. M. Ablow	Stanford Research Institute, Menlo Park, California
Dr. Thomas Tyson	Energy & Environmental Research, Inc., Irvine, California
R. V. Dumke	Engelhard Industries, Edison, New Jersey
Dr. Edward J. Mularz	NASA-Lewis Research Center, Cleveland, Ohio
Dr. Bernard T. Wolfson	Air Force Office of Scientific Research Washington, D.C.
Dr. William C. Pfefferle	Private Consultant Middletown, New Jersey
Dr. Gerald Voecks	Jet Propulsion Laboratory California Institute of Technology, Pasadena, California
Dr. Frank A. Robben	Lawrence Berkeley Laboratory, Berkeley, California
Dr. G. J. K. Acres	Johnson Matthey Research Centre, Reading, United Kingdom
Dr. A. S. D'Alessandro	Matthey Bishop, Inc., Malvern, Pennsylvania
Walter Jasionowski	Institute of Gas Technology, Chicago, Illinois
Dale Johnson	Institute of Gas Technology, Chicago, Illinois

C. C. Gleason	General Electric Company, Cincinnati, Ohio
William Moore	Energy Research and Development Administration, Washington, D.C.
Eugene Szetela	United Technologies Research Center, East Hartford, Connecticut
Dr. Frediano Bracco	Princeton University, Princeton, New Jersey
Peter Matuschak	Garrett Corp., Phoenix, Arizona
Richard E. LeCompte	Energy Systems Corp., Nashua, New Hampshire

SUMMARY

WORKSHOP ON CATALYTIC COMBUSTION

The Plantation Inn
Raleigh, North Carolina
May 25-26, 1976

Sponsored by the U.S. Environmental Protection Agency

Summary prepared by J. P. Kesselring, Aerotherm/Acurex Corporation

---

The first Workshop on Catalytic Combustion was held in Raleigh, North Carolina on May 25-26, 1976. Forty people, representing various government, industrial, and academic organizations, attended the Workshop; a list of attendees is given at the end of this summary. The purpose of the Workshop, sponsored by the U.S. Environmental Protection Agency and organized by the Aerotherm Division of Acurex Corporation, was to provide an overall summary of the current state-of-the-art of catalytic combustion. This was accomplished by bringing catalytic combustion research people together for the exchange of results and ideas.

The meeting began on May 25 with introductory remarks by Mr. G. B. Martin of the Environmental Protection Agency. Mr. Martin described the two main areas of research in catalytic combustion at this time: the gas turbine research, where high excess air levels are used and low NO_x emissions are found, and the stationary source research, where the goal is a low NO_x emission level but with a different system requirement from the gas turbine. For stationary combustion sources, obtaining high system efficiency is the primary problem, and for these systems it is necessary to minimize excess air and exhaust gas temperature to maximize system efficiency. The need to control the conversion of fuel nitrogen in stationary sources was also described. Mr. Martin then introduced Dr. R. V. Carrubba of the Engelhard Industries Division of Engelhard Minerals and Chemicals Corporation. Engelhard Industries is the acknowledged pioneer in the field of high temperature, high heat release catalytic combustion.

Engelhard Industries Program

Dr. Carrubba discussed the necessity of having both catalytic and thermal combustion processes operating in a high heat release combustor; the purely catalytic combustion processes are mass-transfer limited, and cannot achieve the required high combustion efficiency on their own. The performance range of the catalytically supported thermal combustor is defined by the two processes, with the catalyst determining the minimum inlet temperature and maximum operating temperature for a given fuel, and the thermal reactions determining the minimum flame temperature as defined by the onset of thermal combustion reactions. For propane, a typical operating range with a proprietary Engelhard catalyst is:

- Inlet temperature 300-550°C
- Maximum operating temperature 1500°C (material and catalyst failure becomes a problem above this value)
- Minimum operating temperature 1000°C (below this value, thermal reactions become less significant
- Minimum inlet velocity 3 m/sec (have flashback below this value)
- Maximum inlet velocity 25 m/sec
- Typical emissions
  - UHC : 2 ppmv
  - CO : 30 ppmv
  - NO_x : 1 ppmv

Dr. Carrubba described the Engelhard laboratory test facility, used for life tests and studies on small (1-inch diameter by 6-inches in length) monolith catalyst systems, and showed photographs of larger monolith catalyst systems tested at NASA-Lewis Research Center and the Air Force Aero Propulsion Laboratory. A comparison of data obtained on small catalysts at Engelhard and on larger systems at NASA-Lewis show identical results under fuel-lean conditions, indicating scale-up of catalyst performance is achievable simply in terms of increasing frontal area.

Data was presented for a variety of fuels tested with a single catalyst. The data demonstrated that acceptable performance can be obtained from a single catalyst on a wide range of fuels, and that the typical inlet temperature for low emissions is below the catalytic ignition or "lightoff" temperature. Lean tests with fuels doped with pyridine and ammonia indicated about 80 percent conversion of fuel nitrogen to NO_x, which is typical of premixed noncatalytic systems.

Data describing the pressure drop as a function of reference velocity for 4-atm tests with propane and a typical monolith catalyst showed the pressure drop to be given by the equation

$$\frac{\Delta p}{p}\,(\%) = \frac{V_{ref}}{6}\,(\mathrm{m/sec})$$

for several inlet temperatures and reference velocities between 10 and 25 m/sec. Fuel-injection and mixing pressure drops should be added to the catalyst bed pressure drop to estimate the total combustion pressure loss.

In hardware development, Engelhard has developed complete working catalytic combustors capable of up to 10^6 Btu/hr heat release, gaseous or liquid fuel feed, ambient start-up, good turndown, and low emissions for a variety of relatively clean fuels.

In conclusion, a low emissions capability has been demonstrated for a broad range of gaseous and light distillate fuels. Gaseous fuels of low heating values (60 Btu/ft^3 and up) can be combusted efficiently, and the scale-up to larger size combustors has been demonstrated in field tests. Unpublished results indicate it is feasible to design and fabricate commercially useful gas turbine and atmospheric burners. Detailed work in terms of poisons and potential use with heavier fuels still needs to be done.

Catalyst Manufacturer's Presentations

Dr. Robert M. Kendall, Corporate Chief Scientist of the Acurex Corporation, acted as moderator for presentations from five catalyst manufacturers and one refractory support manufacturer. The presentations centered on the current state-of-the-art of manufacturing combustion catalysts.

Universal Oil Products. Dr. George R. Lester presented considerations for the selection of combustion catalysts. This selection is based upon many parameters of the specific application, such as fuel type, required fuel/air ratio for acceptable NO_x emissions, minimum required ignition temperatures, range of operating linear velocities, acceptable pressure drop, required life, presence of poisons, and cost restraints. By specifying these parameters, the catalyst manufacturer is allowed to use his experience and skill to develop an optimal catalyst for the application.

Dr. Lester also presented data obtained on an experimental UOP catalyst used to combust propane. At an equivalence ratio of 0.321, inlet temperature of 700°F, and inlet velocity of 75 ft/sec, an outlet temperature of 1900°F was achieved with greater than 99.9 percent conversion of hydrocarbons.

Oxy-Catalyst Division, Research-Cottrell. Dr. William B. Retallick presented his design for an isothermal microreactor system used in the screening of oxidation catalysts. Since many catalysts must be screened, the test method must be fast and simple to perform. The tests screen the catalyst for fresh activity and activity after heat aging has occurred. The microeactor system used consists of a quartz tube in which the catalyst is placed. A gas flow of 1 percent CO, 1 percent O_2 in helium is passed over the catalyst, and a sample of the exhaust is sent to a gas chromatograph for analysis. For heat aging tests, a single stainless steel block could hold several microreactors to maximize the screening rate.

W. R. Grace and Co. Dr. James Maselli presented thoughts on the current catalyst systems. Automotive catalysts will soon be surpassed technologically by greatly improved systems currently under development. The materials problem is critical, since the degradation of the support enhances metal sintering. The stability of the monolith material at high temperatures is also a prime consideration. Grace prefers to take a fundamental solid-state chemistry approach to developmental systems, rather than an empirical approach. The new catalysts being developed under this approach will exhibit major improvements in lightoff temperature and resistance to poisons.

Engelhard Minerals and Chemicals Corporation. Dr. George W. Roberts presented some of the thoughts that directed the development of the Catathermal combustion systems. By comparing the catalyst system pressure drop and reaction rate for both particulate and honeycomb supports, the monolithic honeycomb requires significantly less catalyst volume than the particulate in the mass-transfer controlled regime, and is therefore the preferred support. In order to prolong support life, operation should be in the mass-transfer controlled regime, but unstabilized Al_2O_3 washcoat total surface area will change from approximately 240 m^2/g of washcoat to 10 m^2/g after operation at 1200°C. The solution to this problem is to either stabilize the Al_2O_3 washcoat or look at other washcoats in order to maintain a high total surface area.

Typical operating parameters for the Catathermal combustors with propane and #2 diesel oil fuels were reported as adiabatic flame temperature between 1800 and 2800°F, pressure drop between 1 and 6 percent, heat release rates from 10×10^6 to 20×10^6 Btu/hr-atm-ft^3, reference velocities between 25 and 100 ft/sec, and a catalyst life in excess of 1000 hours. These systems are still under development.

E. I. DuPont deNemours and Co. Dr. Donald M. Sowards presented considerations from the point of view of the monolith manufacturer. The monolith manufacturer must do coating in order to learn to make an improved monolith. DuPont has used two different washcoats (γ-alumina, and α-alumina with some other phases) in their work. The α-alumina is thermally stable at 10 m^2/g to 1000°C, and has been thermally and chemically stabilized. It appears to be more adherent than γ-alumina, and serves as a barrier to inhibit migration of silica out of the monolith structure.

Matthey Bishop, Inc. and Johnson Matthey Research Center. Dr. George McGuire of Matthey Bishop introduced Dr. G. J. K. Acres of Johnson Matthey Research Centre. Dr. Acres described work in progress at the Research Center on pollution control for various systems. They have been successful in holding alumina surface area at 100 m^2/g at temperatures of 1100°C, and can hold the metal crystallite size to very small values as well. For turbine system applications, the desire is a catalyst with a surface-to-volume ratio greater than 1000 ft^2/ft^3. This can be done by going to a monolith with 400 cells/in^2, but the pressure drop is now increased and the open area goes down. It appears that a newly-developed platinum catalyst on a metal-based monolith is capable of achieving 90 percent open area and 400 cells/in^2. Preliminary data with kerosene fuel at 60 psig pressure and 250°C inlet temperature are: space velocity = 1.17 x 10^6/hr @ STP, 2 percent pressure drop, 100 percent conversion of hydrocarbons at an equivalence ratio of 0.38. The pressure drop is only half that of 200 cell/in^2 ceramic monoliths for velocities from 2 to 50 ft/sec. The system should have long lifetime at 1100°C, with 1375°C being the maximum use temperature of the iron-chrome metal monolith. The washcoat is alumina, based on the automotive catalyst technology.

Institute of Gas Technology Programs

Dr. Jon B. Pangborn of IGT described work currently in progress at the Institute of Gas Technology. Starting in 1972, IGT has been developing conceptual burners and model ventless appliances for catalytic combustion of hydrogen and reformed natural gas under the sponsorshop of the Southern California Gas Company of Los Angeles. During 1975, the U.S. Environmental Protection Agency and Southern California Gas co-funded a program at IGT to develop a catalytic range-top burner.

The burners designed for catalytic combustion must be self-starting in order to be practical; flame combustion, standing pilot, or electrical ignition systems were not allowed. These burners were developed for hydrogen-rich gas fuel, and the catalyst configurations were to completely combust the fuel in the system configuration. The system was also to be flashback-free. Based on these requirements, IGT has developed burners and two types of hot-water heaters based on catalytic combustion. The instantaneous catalytic hot-water heater, which uses a noble metal catalyst on a specially-treated aluminum surface, is capable of 99+ percent combustion efficiency, 75 - 80 percent thermal efficiency, and a heat-up time (50°F to 150°F) from 30 to 45 seconds for 6 gallons/hour capacity.

In summary, the catalytic combustion systems developed at IGT have several advantages over current systems. These include: minimal pollutants (very low NO_x and CO emissions), less expensive because no venting is required, provide for humidification of the home, high system efficiency, low operating temperature and lower attendant hazard, and self-ignition. The biggest problem to date has been cracking and peeling of the catalyst from the surface; the need to have either a methane reformer or a hydrogen fuel supply is also evident.

NASA Lewis Research Center Program

Dr. David N. Anderson of NASA Lewis Research Center introduced the NASA Lewis program and described the three major research areas: fuel-air preparation system studies, catalyst evaluation program, and catalyst life test program. This work is directed toward finding a catalyst combustor for automative gas turbine applications, and is sponsored by ERDA.

Fuel-Air Preparation System Studies. Robert R. Tacina of NASA Lewis presented information on the fuel preparation and introduction system accomplished to date. Premixed, prevaporized fuel-air systems are required to avoid local rich zones and subsequent NO_x emissions. The goals of the current program are threefold:

1. 90 percent vaporization of the fuel at 1000°F inlet temperature,
2. A spatial fuel distribution ±10% of the mean value across the duct cross-section,
3. No autoignition at 1400°F.

The spatial fuel distribution and degree of vaporization were measured using Jet A fuel. Fuel injectors tested include two types of air blast injectors, a splash-groove injector, and a multiple-jet cross-stream injector. Air swirlers with vane angles of 15° and 30° were used to improve the spatial fuel distribution.

As a result of these tests, it was found that the multiple-jet cross-stream injector and the splash-groove injector with a 30° air swirler had a uniform fuel distribution and a high degree of vaporization with little total pressure drop at the conditions tested. At 800°K inlet air temperature, fuel oxidation reactions were noted. Since the automotive gas turbine will probably encounter higher inlet air temperatures, further work is required for the application of catalytic combustors to automotive gas turbine engines.

Catalyst Evaluation Program. Dr. Anderson described the two elements of the catalyst evaluation program; the furnace screening tests of monoliths and pellets of small size by passing 500 ppm of propane in air over the catalyst, and the combustion tests of monoliths 12 cm in diameter with 800°K inlet temperature and premixed propane in air at equivalence ratios between 0.1 and 0.3. Results from the furnace screening tests are plotted as oxidized fuel fraction versus catalyst temperature, and serve to identify the most suitable catalysts for further testing. The furnace tests have indicated that the most effective catalysts for gas turbine combustor applications will probably be noble metals on monoliths. Based only on catalytic activity, the furnace tests have shown that the optimum cell density should be between 30 and 45 cells/cm². However, most of the catalysts used in the study were developed for use as automobile exhaust emission control reactors, and not for the current application.

The combustion tests were run on catalyst beds consisting of two to four elements of 12-centimeter diameter by 2.5 centimeter long monoliths. Thermocouples at the back end of each monolith element measure the gas phase temperature. Two cell configurations have been used in the combustion tests to date: small square cells in the Grace Poramic 290 cordierite, with a cell density of 45 cells/cm^2, and round cells in General Refractories' Versagrid mullite, with a cell density of 10 cells/cm^2. Catalysts used include platinum, palladium, mixed platinum/palladium, cobalt oxide, and ceria.

Results of the combustion tests are given by combustion efficiency as a function of adiabatic reaction temperature. Results indicate that the temperature rise across catalyst elements decreases as the reference velocity is increased, and that most of the temperature rise (and thus most of the reaction) occurs across the first two elements. A comparison of the Grace Davex 512B catalyst (with small square cells) and the Oxy-Catalyst 4 catalyst (with larger round cells) shows that the Oxy-Cat system required higher temperatures to achieve the same combustion efficiency as the Grace system. A detailed study of cell shape and cell size for optimum performance has not been done, however.

As a result of this program, several potential problem and developmental areas have been determined. The narrow operating range in temperature between the minimum temperature for good efficiency and the maximum temperature for long catalyst life must be addressed. The transient response has not yet been determined, and the loss in activity with test time will require more durable catalysts to be developed. In addition, the possibility of improved combustor performance from variable catalyst system geometry must be explored.

Life Test Studies. Dr. Robert V. Carrubba of Engelhard Industries returned to describe the life testing Engelhard has carried out for NASA Lewis. The objectives of this program were to select combustion catalysts for testing, to construct a catalyst test rig, to demonstrate low emissions combustion using #2 oil for up to 1000 hours, and to compare catalysts using propane in parametric tests. The test rig is capable of testing catalysts one inch in diameter by 6 inches in length with a maximum inlet temperature of 1000°F. The life test conditions used are 1 atm pressure, 680°F inlet temperature, 45 ft/sec reference velocity, and air/fuel ratio of 38 with #2 oil. At these conditions, one catalyst has demonstrated at least 1000 hours life with emissions which exceed Federal requirements for automotive engines based on a single, static rig operating point. The catalyst showed an initial activity decline to 250 hours, with subsequent stable operation to 1000 hours.

Parametric test results with propane show an operating range decline after 1000 hours compared to #2 oil after 1000 hours on the same catalyst. Further experimentation will be done to compare the fuels capability of the catalyst.

Jet Propulsion Laboratory Program

Dr. John Houseman of JPL described the JPL partial oxidation synthetic gas generator program. The objectives of this program are to design and build a partial oxidation syn-gas generator, to package the reactor and controls in separate consoles, and to prepare an operating manual. The syngas generator will be used in EPA studies to generate a simulated low Btu coal gasification product. It has also been used to produce a hydrogen-rich gas stream for combustion in an automotive engine.

The gas generator consists of an igniter and start-up burner to provide a preheat source for the catalyst bed, a start-up combustion zone, and a steady state reaction zone. The steady state reaction zone consists of nickel on alumina pellets, which act as the catalyst. The generator is normally run in the fuel-rich mode, but could run lean as well. At an equivalence ratio of 2.8, the product gas from the generator is approximately 22 percent H_2 and 25 percent CO by volume, when indolene is used as the fuel. Benzene and methane have also been used as fuels.

U.S. Environmental Protection Agency Program

Blair Martin began the workshop on Wednesday, May 26, by describing the need to improve system efficiency in stationary combustion systems. Conventional flame combustion is very efficient in terms of combustion efficiency, but improvements in system efficiency occur when excess air is decreased and stack temperature is reduced. These requirements are not compatible with the capabilities of current one-stage lean catalytic combustors being developed for gas turbines. If stationary heat and steam generators require the use of catalytic combustion to achieve very low emissions of NO_x with high combustion efficiency, alternate approaches to design must be explored. These include staged combustion, flue gas recirculation, and bed heat removal. The EPA program is directed to establishing the technical feasibility of these concepts as applied to stationary sources.

The potential of using two-stage catalytic combustion to suppress fuel NO production was also discussed. Fuel NO increases with an increase in primary stoichiometric ratio, and it appears that 90 percent control of fuel NO is possible with staged combustion.

Aerotherm/Acurex Corporation Program. Under EPA sponsorship, the Aerotherm Division of Acurex Corporation is conducting a study to determine design criteria for catalytic combustors with application to stationary sources. Dr. John P. Kesselring of Aerotherm began the presentation by discussing the program plan to screen experimental small scale catalysts and combustion system concepts, to scale the promising concepts up, both experimentally and theoretically, and to do preliminary prototype design of systems based on the most promising concepts. The operation of a high-temperature catalytic combustor is based on an interaction of fluid mechanics, radiative, convective, and conductive heat transfer, and heterogeneous and homogeneous chemical reactions, and a proper understanding of these phenomena is basic to the development of a successful system.

Dr. Robert M. Kendall of the Acurex Corporation then discussed basic performance and modeling considerations. A simplified treatment of the surface, in which the wall is assumed adiabatic, the enthalpy assumed constant, and an Arrhenius rate law assumed for the consumption of the lean reactant gives certain information about the blowout point. Blowout, defined as that condition where both homogeneous and heterogeneous reactions cease, can be avoided by having large diameter cells, high thermal conductivity of the monolith, and high surface activity. The large diameter cells, however, will have relatively poor conversion characteristics, and it is known that small cells help support homogeneous reactions and complete conversion. Therefore, for a system it appears desirable to have large cells at the front of the catalyst bed to prevent blowout, and small cells at the back of the bed to prevent breakthrough (passing of unburned hydrocarbons).

The screening program performed consists of catalyst preparation and characterization, catalyst instrumentation with in-depth bed thermocouples, combustion screening tests, and post-test characterization and data analysis. The objectives of the screening program are to develop a catalyst which is fully characterized in terms of catalyst properties which is capable of a volumetric heat release rate of 2.5 x 10^6 Btu/hr-atm-ft^3, and can run under rich, lean, or stoichiometric conditions for a minimum of 50 hours.

Dr. James A. Cusumano of Catalytica Associates described the preparation and characterization procedures for combustion catalysts. Catalytica Associates is working on this program under subcontract from Aerotherm.

The catalyst preparation objectives are to produce a catalyst with good light-off and heat release characteristics that is durable at high temperatures. The characterization procedure helps monitor progress in this direction. Use of total surface area and dispersion measurements gives quantification and direction to improvements in catalyst manufacture. The catalyst system can deactivate at high temperatures because of sintering of the active component (e.g., Pt), sintering of the washcoat and subsequent loss in total surface area, and mechanical degradation. Methods used for catalyst stabilization include sulfide pretreatment, washcoat presintering, and metal-support interactions.

In the combustion screening tests, monoliths 3.66 inches in diameter and 3 inches in length have been tested in a variety of materials, cell sizes, and platinum loadings. The operating temperature selected is 2000°F, and methane has been the primary test fuel, with some propane tests being run. Eventually, low Btu gas, hydrogen, #2 diesel, and methanol will also be tested.

Combustion screening tests to date have been run primarily in the existing catalytic combustion test facility at the Jet Propulsion Laboratory, with some tests being run in the recently-completed test facility at Aerotherm. Dr. Gerald E. Voecks of JPL described the combustion testing at JPL.

The objective of the combustion test program is to evaluate the catalyst in its ability to conduct a variety of fuels over a wide range of conditions. The approach has been to determine catalyst activity under rich, stoichiometric, and lean conditions, to determine blowout or breakthrough performance for rich and lean conditions, and to relate catalyst activity to catalyst properties. The JPL reactor is made of quartz, allowing the monolith bed to be observed during a test when the insulating material is removed.

Results of combustion tests to date have shown considerable degradation with time for all catalyst systems. This degradation levels out to a nearly constant activity after several hours, however, and it is this activity which must be determined for system design considerations. Tests run with a 5 percent platinum on alumina first catalyst element with large cells, followed by 0.7 percent platinum on alumina second and third elements with small cells showed excellent performance after several hours of operation in terms of activity and emissions. The testing of this system thus verifies the basic considerations described earlier.

ERDA Considerations

Mr. William E. Moore of the Fossil Energy Administration of ERDA and Mr. Robert Ebeling of Gilbert Associates described some of the needs of the catalytic combustion program from their point of view.

ERDA's advanced turbine development program couples a high turbine inlet termperature requirement (2600°F and up) with emission problems imposed by coal-based fuels. When burning coal-based fuels the emissions are of primary concern due to the large nitrogen and aromatic content of the fuels. The need for advanced combustors to avoid the conversion of fuel nitrogen to NO_x is apparent.

At some point, the cost tradeoff between fuel enhancement and turbine combustor development will dictate what fuel and combustor combination will be most economical to use. The determination of this point is critical.

United Technologies Research Center Program

Dr. Arthur S. Kesten of UTRC described their catalytic combustion program. The UTRC program involves experimental and theoretical studies of the use of catalyzed surfaces to promote hydrocarbon combustion. The ultimate objective of the program is to assess the feasibility of using catalyzed surface reactors to promote the efficient combustion of multicomponent liquid fuels in practical combustion systems where the fuel is only partially prevaporized before entering the reaction chamber. Initial objectives of the program are to extract information on catalytic reaction mechanisms and rates for pure gaseous fuels and monolithic catalyst structures.

The experimental program is studying the effects on reactor behavior of fuel, catalyst type, monolith structure, temperature, stoichiometry, mass flowrate, bed length, and diluent concentration. Catalyst beds one-inch in diameter are tested in the reactor. Propane fuel has been used to investigate the variation in ignition temperature with inlet velocity and equivalence ratio, and the combustion efficiency change with bed temperature. A mathematical model to aid in evaluating the data was also described. This model is a steady-state analysis which assumes axial variations in bed temperature, bulk-gas temperature, and reactant concentration.

U.S. Air Force Programs

The U.S. Air Force is sponsoring two programs dealing with catalytic combustion. The first program, sponsored by the Aero Propulsion Laboratory, deals with the application of catalytic combustion to aircraft gas turbine engines. The second program, sponsored by the Air Force Office of Scientific Research, deals with the initiation of combustion on catalytic surfaces.

Aero Propulsion Laboratory Program. Captain Thomas J. Rosfjord of the AFAPL described current activity in developing the catalytic combustion concept for application to aircraft gas turbine engines. At this time, the program is addressing the use of catalysts in after burners. Two specific applications are of interest: ignitors and flameholders. A more simple system with increased performance can result with successful application of the concept. Previous work done at the AFAPL dealt with the use of catalysts in the main burner of the gas turbine engine.

The aircraft application imposes a great demand for throttling the power level and presents a large variation in combustor inlet temperature as well. The current studies are divided between low power investigations, subcontracted to Exxon initially and to be followed by extensive in-house testing, and high power investigations, being conducted in-house.

Current focus of applications of catalytic combustion is on ignitors or flameholders. The catalytic ignitor can provide a simple, reliable ignition source, with the prime concern being the location of the ignitor. Use as a flameholder can promote an increase in the axial rate of energy release. Flight tests at aircraft approach conditions have shown that the catalytic ignitor alone is unsatisfactory, but with the pilot burner an expansion in relight envelope can be achieved.

The work to develop a catalytic combustor to operate in the engine idle-mode was described by Mr. V. J. Siminski of Exxon. Since modifications to conventional aircraft turbine engine combustors have not been able to meet 1983 EPA standards, and there is low combustion efficiency in the idle-mode, the use of catalytic combustors is attractive. The catalytic combustor can operate efficiently far off stoichiometric, and generate low NO_x at the same time. The objectives of the program are: 1) to conduct a thorough literature review, defining the best catalysts and substrates, 2) to design and fabricate a combustion system, modifying the existing catalytic combustor at Exxon to include the idle operation mode, 3) to evaluate a minimum of 10 catalyst/substrate systems and select the best two candidates, 4) to complete a detailed design of each recommended system and fabricate two copies for delivery.

Important considerations for the catalyst system include activity, lifetime, pressure drop, cost, and poisoning. Catalysts similar to automotive catalysts have been tested, and the following conclusions have been made:

- The hybrid catalytic combustion technique can be used to meet the 1983 aircraft emission standards. In this system the catalyst is operating in the clean-up mode, with low inlet hydrocarbons and CO.
- An overall combustion efficiency of 99.8 percent has been achieved
- Operating conditions are selected to avoid catalyst degradation (<1200K)
- The optimum support surface/volume ratio required is 1500 m^2/m^3
- The hybrid catalytic combustion technique provides stable and efficient combustion over a wide range of fuel-air mixtures.

Air Force Office of Scientific Research Program. Professor F. B. Bracco of Princeton University presented a discussion of work now beginning under AFOSR funding. This program will consist of a theoretical-experimental study of the initiation of combustion on catalytic surfaces. Initially, an isothermal boundary layer will be considered with gas phase and surface reactions of trace species only. Then, the fully reactive two-dimensional flow system will be studied. The experimental program will be carried out with a steady combustor and will include measurement of stable and unstable species by a continuous argon ion laser system.

Exxon-National Science Foundation Program

Dr. Anthony E. Cerkanowicz of Exxon presented the work done under joint Exxon-NSF sponsorship on catalytic combustion modeling. The objective of this program is to develop a usable model of catalytic combustion reactor operation which provides for optimization, design, scaling, and data analysis. The major assumptions in the model are one step global kinetics, first order kinetics, and negligible gas phase reactions and radiant heat transport. Based on the analysis, it has been observed that multiple steady state solutions exist, and that the gas residence time in the reactor is a critical factor for design. Future work will correlate experimental data, include gas phase kinetics, include heat transfer effects, and consider transient operation.

Westinghouse-Engelhard Joint Program

Mr. S. M. DeCorso of Westinghouse described a program conducted jointly by Westinghouse and Engelhard Industries to assess the applicability of catalytic combustors for gas turbines. Test fuels used were #2 distillate oil and low Btu synthetic coal gas. The tests were carried out over a range of pressure, temperature, and mass flow conditions.

Currently, combustors are based on the diffusion flame, are not scaleable, and are emissions and performance limited. The catalytic combustor can avoid NO_x formation, and also avoid the reliability problems of high temperature operation in conventional systems.

Experimental test results were obtained for #2 distillate oil and low Btu gas (126 Btu/ft^3 lower heating value). Pressure, temperature, and mass flowrate were varied during the tests. The joint program began in 1973 and is still going on. A total of 34 tests have been run, with combustor pressure drop varying from 2 to 12 percent as reference velocity increases. The catalyst bed temperature profile at the bed exit was very uniform for low Btu gas, but not as uniform for #2 oil. Exceptionally low emissions (2-3 ppm NO_x, 20-30 ppm CO) were achieved for either fuel, and unburned hydrocarbons were < 1 ppm. The catalytic combustor has shown excellent potential for gas turbines, but much additional systems work is needed before it can be reduced to practice.

University of California Programs

Dr. Frank Robben of the Lawrence Berkeley Laboratory of UC described an ERDA-sponsored program now underway at LBL. The program consists of an experimental and computational study of combustion in the boundary layer of a catalytic flat plate in a premixed fuel-air stream. The velocity, gas density, and degree of reaction in the boundary layer will be measured using laser light scattering techniques. The principal goals of the program are: 1) a fuller understanding of the relation between catalyzed heterogeneous reactions at the wall and homogeneous reactions in the boundary layer, 2) the development of a suitable computational model to enable these processes to be predicted in more complex geometry, and 3) to test and develop suitable catalytic surfaces for combustion.

Dr. Robert F. Sawyer of the Mechanical Engineering Department at UC is beginning a study of catalytic combustion and its role in solving the fuel-nitrogen problem. The desired goal is the conversion of fuel nitrogen to N_2 during the combustion process, but this appears difficult. Since the use of alternate or synthetic fuels will be likely to include those with relatively high organically bound nitrogen content, work on the fate of these compounds in catalytic combustion processes is needed.

There is no indication that the low operating temperatures of catalytic combustion which effectively suppress thermal NO_x formation will similarly favor the conversion of fuel nitrogen to N_2. On the contrary, lean conditions should favor the formation of NO_x and fuel rich conditions may favor the formation of a number of nitrogen compounds.

Meeting Summary

The Workshop presentations give an indication of the current state-of-the-art of catalytic combustion. Research in catalytic combustion at the present time is in the areas of high temperature catalysts, gas turbines, stationary combustion systems, and home appliances.

For almost all applications of catalytic combustion of current interest, higher temperature catalysts are required. In this regard, current automotive catalyst technology needs to be upgraded to obtain catalyst materials that are capable of high temperature (i.e., 2600°F) operation with good activity, resistance to poisoning, long lifetime, and good lightoff characteristics. Scale-up of performance for catalysts is achievable by scaling the frontal area of the catalyst bed. In the bed itself, both heterogeneous and homogeneous reactions are important, and the monolith bed configuration is the preferred substrate. Tailoring of the geometric cell configuration in the bed, by using large cells at the bed inlet to prevent blowout and small cells at the bed exit to achieve cleanup, is postulated to improve catalyst performance for a given catalyst activity. Further work on tailoring of the catalyst in the bed, and the acceptance of some unvaporized fuel in the bed, is needed. An initiation of work aimed at developing a combustor which does not convert fuel nitrogen to NO_x is also needed; rich catalytic combustion may be applicable here.

The use of catalytic combustors for gas turbines has been shown applicable by a variety of test programs. Further development work is needed, however, to answer questions regarding system impacts of catalytic combustors. While the catalyst performance appears scaleable in size, the performance of the fuel preparation and introduction system is not, and much developmental work is needed there. Tests of a hybrid gas turbine system, with the catalytic combustor acting as a low-temperature cleanup stage, have shown that low emissions can be obtained with good efficiency. Further testing is needed to determine if a catalytic combustor can operate effectively over the entire range of conditions that an aircraft gas turbine encounters, or if a hybrid system is needed.

In the field of stationary combustion systems, testing is needed to show the potential of catalytic combustion for obtaining high system efficiency. Experimental work involving various heat removal mechanisms needs to be done to determine system impacts, followed by further catalyst development work. In particular, the effects of coal-derived fuels on various catalysts must be determined.

For home applicances, the use of lower catalyst lightoff temperatures has been possible because of the fuels used (hydrogen and reformed natural gas). The supply of these fuels is somewhat problematic, however, and this work should be extended to other fuels as well.

Thanks were extended to all speakers and participants for making this workshop a success.

WORKSHOP ON CATALYTIC COMBUSTION

Attendees

Name	Organization
G. Blair Martin	IERL/U.S. Environmental Protection Agency Research Triangle Park, North Carolina
W. Steven Lanier	IERL/U.S. Environmental Protection Agency Research Triangle Park, North Carolina
Joshua S. Bowen	IERL/U.S. Environmental Protection Agency Research Triangle Park, North Carolina
Dr. David N. Anderson	NASA Lewis Research Center Cleveland, Ohio
Robert R. Tacina	NASA Lewis Research Center Cleveland, Ohio
Dr. Gerald E. Voecks	Jet Propulsion Laboratory Pasadena, California
Dr. John Houseman	Jet Propulsion Laboratory Pasadena, California
Dr. Stanley A. Mosier	Pratt & Whitney Aircraft West Palm Beach, Florida
Dr. John P. Kesselring	Aerotherm/Acurex Corporation Mountain View, California
Dr. Robert M. Kendall	Acurex Corporation Mountain View, California
Dr. Kimble J. Clark	Aerotherm/Acurex Corporation Mountain View, California
Dr. James A. Cusumano	Catalytica Associates, Inc. Palo Alto, California
Captain Thomas J. Rosfjord	Aero Propulsion Laboratory Wright-Patterson Air Force Base, Ohio
Dr. William B. Retallick	Oxy-Catalyst, Inc. West Chester, Pennsylvania
Vincent Siminski	Exxon Linden, New Jersey
Dr. Henry Shaw	Exxon Linden, New Jersey
Dr. Anthony Cerkanowicz	Exxon Linden, New Jersey
Daniel Kahn	Rocketdyne Div., Rockwell Int'l Corp. Canoga Park, California
Dr. Jon Pangborn	Institute of Gas Technology Chicago, Illinois

Name	Organization
Dr. Arthur Kesten	United Technologies Research Lab. East Hartford, Connecticut
Robert Ebeling	Gilbert Associates Reading, Pennsylvania
Dr. Robert V. Carrubba	Engelhard Industries Edison, New Jersey
Dr. G. W. Roberts	Engelhard Industries Edison, New Jersey
Dr. James Maselli	W. R. Grace Chemical Co. Baltimore, Maryland
Dr. Fred Bracco	Princeton University Princeton, New Jersey
Dr. Bernard T. Wolfson	Air Force Office of Scientific Research Washington, D. C.
Rudolph Bratko	Bratko Corporation Cleveland, Ohio
Dr. C. C. Lee	IERL/U.S. Environmental Protection Agency Cincinnati, Ohio
Dr. George McGuire	Matthey Bishop, Inc. Malvern, Pennsylvania
Dr. Robert Sawyer	University of California Berkeley, California
Dr. Thomas Tyson	Ultrasystems Irvine, California
S. Mario DeCorso	Westinghouse Electric Company Lester, Pennsylvania
Dr. George R. Lester	Universal Oil Products Des Plaines, Illinois
William Williams	ERDA Washington, D.C.
Paul Jensen	ERDA Idaho Falls, Idaho
Dr. David Clark	Detroit Diesel Allison Indianapolis, Indiana
Dr. Frank Robben	Lawrence Berkeley Laboratory Berkeley, California
Dr. Donald M. Sowards	E. I. DuPont deNemours & Co. Wilmington, Delaware
William E. Moore	ERDA, Fossil Energy Administration Washington, D.C.
Dr. G. J. K. Acres	Johnson Matthey Research Centre Reading, England

APPENDIX B

LIST OF ATTENDEES

THIRD WORKSHOP ON CATALYTIC COMBUSTION

ATTENDEES

Dr. Robert V. Carrubba	Engelhard Industries, Menlo Park Edison, New Jersey 08817
G. Blair Martin	MD-65, IERL/U.S. Environmental Protection Agency, Research Triangle Park, N.C. 27711
Dr. John T. Pogson	Acurex Corp. / E&E Division 485 Clyde Ave. Mt. View, CA 94042
Dr. John P. Kesselring	Acurex Corp./E&E Division 485 Clyde Ave. Mt. View, CA 94042
Dr. Robert M. Kendall	Acurex Corp./E&E Division 485 Clyde Ave. Mt. View, CA 94042
Willard A. Boyer	Industrial Products Dept. Ceramic Products Div. Corning Glass Works Corning, N.Y. 14830
Dr. Frank A. Robben	Lawrence Berkeley Laboratory, 70-158 Berkeley, CA 94720
Dr. Robert W. Schefer	Lawrence Berkeley Laboratory, 70-158 Berkeley, CA 94720
Wayne V. Krill	Acurex Corp./E&E Division 485 Clyde Ave. Mt. View, CA 94042
Edward K. Chu	Acurex Corp./E&E Division 485 Clyde Ave. Mt. View, CA 94042
Dr. George R. Lester	Director - Materials Science Universal Oil Products Company Corporate Research Center Ten UOP Plaza Des Plaines, Illinois 60016

Preceding page blank

Dr. Gerald E. Voecks	Jet Propulsion Laboratory California Institute of Technology 4800 Oak Grove Drive Pasedena, California 91103
Dr. Edward J. Mularz	Propulsion Lab, USARTL (AVRADCOM) Mail Stop 60-4 NASA-Lewis Research Center 21000 Brookpark Rd. Cleveland, Ohio 44135
Y. Ishihara	Mgr., Environmental Chemistry Dept. Energy & Environmental Lab Central Research Institute of Electric Power Industry 11-1, Iwato Kita 2 Chome; Komae-Shi, Tokyo 182, Japan
Dr. David N. Anderson	Mail Stop 500-202 NASA-Lewis Research Center 21000 Brookpark Rd. Cleveland, Ohio 44135
Dr. Blair A. Folsom	Energy & Environmental Research Corp. 8001 Irvine Boulevard Santa Ana, CA 92705
Dr. William B. Retallick	Vice President, R&D Oxy-Catalyst E. Biddle Street West Chester, Pennsylvania 19380
Dr. Stanley A. Mosier	Mail Stop E-75 P. O. Box 2691 Pratt & Whitney Aircraft West Palm Beach, Florida 33402
Dr. Pierre J. Marteney	United Technologies Research Center 400 Main Street East Hartford, Connecticut 06108
Robert R. Tacina	Mail Stop 500-202 NASA-Lewis Research Center 21000 Brookpark Road Cleveland, OH 44135
Daniel L. Bulzan	Mail Stop 500-202 NASA-Lewis Research Center 21000 Brookpark Road Cleveland, Ohio 44135

Dr. William C. Pfefferle	51 Woodland Drive Middletown, New Jersey 07748
Leonard C. Angello	AFAPL/SFF Wright-Patterson Air Force Base Ohio 45433
S. Mario DeCorso	Mail Stop A-702 Westinghouse Electric Co. Gas Turbine Division Lester, PA 19113
Albert C. Dolbec	Electric Power Research Institute 3412 Hillview Ave. P. O. Box 10412 Palo Alto, CA 94303
Dr. Anthony Cerkanowicz	Exxon Research & Engineering Co. Government Research Labs P. O. Box 8 Linden, New Jersey 07036
Dr. Victor J. O'Brien	Houdry Division, P&C Air Products and Chemicals, Inc. Chemicals Group P. O. Box 538 Allentown, PA 18105
Dr. Clarence M. Ablow	Stanford Research Institute 333 Ravenswood Avenue Menlo Park, Calif. 94025
Dr. K. C. Salooja	Esso Research Centre Abingdon, Oxfordshire United Kingdom
Frank Zimar	Mechanical Product Development Corning Glass Works Sullivan Science Park Painted Post, New York 14870
Dr. Irwin M. Lachman	Specialty Ceramic Dept. Corning Glass Works Sullivan Science Park Painted Post, New York 14870
Dr. Edmond R. Tucci	Matthey Bishop, Inc. Malvern, PA 19355

Dr. A. S. D'Allessandro
Matthey Bishop, Inc.
Malvern, PA 19355

Michael Bak
Williams Research Corporation
48080 Maple Road
Walled Lake, Michigan 48080

B. E. Enga
Johnson Matthey Research Centre
Blount's Court
Sonning Common
Reading RG4 9NH
United Kingsom

Dr. Geoffrey J. Sturgess
Pratt & Whitney Aircraft
400 Main Street
East Hartford, Conn. 06108

Dr. Frediano A. Bracco
Dept. of Mechanical and Aerospace Engineering
Princeton University
Princeton, New Jersey 08540

Dr. Nancy D. Fitzroy
Bldg. 500, Room 224
GTD
General Electric Company
Schenectady, New York 12345

Walter Jasionowski
Institute of Gas Technology
3424 South State Street
Chicago, Illinois 60616

Andrew J. Szaniszlo
Mail Stop 60-4
NASA-Lewis Research Center
21000 Brookpark Rd.
Cleveland, Ohio 44135

Dr. Donald M. Sowards
Industrial Chemicals Dept.
Chestnut Run Laboratory
E.I. DuPont de Nemours & Co.
Wilmington,Delaware 19898

W. Steven Lanier
MD-65
Industrial Environmental Research Lab.
Environmental Protection Agency
Research Triangle Park, N.C. 27711

Will Dodds
General Electric Company
Cincinnati, Ohio 45215

Warren Bunker	Department of Energy Washington, D.C. 20545
John C. Bonacci	Engelhard Industries Menlo Park Edison, N.J. 08817
Dr. T. J. Rosfjord	Mail Stop 18 United Technologies Research Ctr 400 Main Street East Hartford, Conn. 06108
Dr. Eugene Szetela	United Technologies Research Ctr 400 Main Street East Hartford, Conn. 06108
Dr. Joshua A. Bowen	MD-65 Industrial Environmental Research Lab. Environmental Protection Agency Research Triangle Park, N.C. 27711
Warren P. Richard	East Shore Drive Lake Toxaway, N.C. 28747
Dr. E. A. DeZubay	Westinghouse Research & Development Center Beulah Road Pittsburgh, Pennsylvania 15235
Dr. R. D. Matthews	Dept. of Mechanical & Industrial Engineering University of Illinois at Urbana-Champaign 144 Mechanical Engineering Building Urbana, Ill. 61801

Howard Lowenstein	Industrial Products Dept. Ceramic Products Division Corning Glass Works Corning, N.Y. 14830
Daniel Carl	Westinghouse Electric Co. Gas Turbine Division Lester, PA 19113
Peter Walsh	Dept. of Mechanical & Aerospace Engineering Princeton University Princeton, New Jersey 08540
Richard Sederquist	Power Systems Division, United Technologies P.O. Box 109 South Windsor, Conn. 06074
Ned R. Baker	Institute of Gas Technology 3424 South State Street Chicago, Illinois 60616